CR-161692

UNITED TECHNOLOGIES
RESEARCH CENTER

East Hartford, Connecticut 06108

R81-955343-9

Final Study Report of an Applications Study of Advanced Power Generation Systems Utilizing Coal-Derived Fuels

Volume II - Technical Report

NAS8-33996

DPD No. 593

DR No. 6

Date March 1981

UNITED TECHNOLOGIES
RESEARCH CENTER

East Hartford, Connecticut 06108

R81-9955343-9 – Vol 2

Final Study Report of an Applications Study of Advanced Power Generation Systems Utilizing Coal-Derived Fuels

Volume II - Technical Report

NAS8-33996

DPD No. 593

DR No. 6

Fred. L. Robson
Chief, Utility Power Systems

DATE March 1981

NO. OF PAGES _____

COPY NO. _____

FOREWORD

This application study of advanced power generation systems utilizing coal-derived fuels was performed by United Technologies Research Center with subcontract assistance from Burns and Roe, Inc. The study program has been prepared under Contract NAS8-33996 for Marshall Spare Flight Center of the National Aeronautics and Space Administration. The technical work described herein was initiated in September 1980 and completed in March 1981.

The technical results of this application study are presented in two parts. The first part is an Executive Summary (Volume I) which provides a concise review of all major elements of the study. The second part is a detailed Technical Report (Volume II) describing the technology status of the three advanced power generation systems studied (combined cycle gas turbine, fuel cells, and magnetohydrodynamics) and the performance of these generation systems either utilizing a medium-Btu coal-derived fuel supplied via pipeline from a large central coal gasification facility or integrated with a gasification facility for supplying medium-Btu coal-derived fuel gas.

The United Technologies Research Center provided overall program management and the major contributions to the combined cycle gas turbine and fuel cell power plant evaluation. This effort involved:

Fred L. Robson, Program Manager
Robert D. Lessard, Deputy Program Manager
William A. Blecher
Stewart J. Lehman
W. Richard Davison

Burns and Roe provided the major contributions to the magnetohydrodynamics power plant evaluation. This effort involved:

Albert W. Carlson

The study program was conducted under the general direction of Richard D. Kramer and Robert Giudici of Marshall Space Flight Center.

The support and assistance of all the aforementioned individuals and organizations in contributing to the successful completion of this study program is acknowledged with sincere appreciation.

R81-955343-9

Final Study Report of an Applications Study of Advanced Power Generation Systems Utilizing Coal Derived Fuels

Volume II - Technical Report

TABLE OF CONTENTS

		Page
FOREWORD		i
TABLE OF CONTENTS		ii
LIST OF TABLES		xiii
LIST OF FIGURES		xvii
TECHNICAL REPORT		xxvi
SECTION NO.		
1.1	Assessment of Fuel Cell Power Systems Status	1.1-1
1.1.1	Current Technology Status and Operational Data Base of Fuel Cell Power Systems	1.1-1
1.1.1.1	Phosphoric Acid Fuel Cell Power Systems	1.1-3
	Principles of Operation	1.1-3
	Cell Components	1.1-5
	General Performance Considerations	1.1-5
	Temperature Effects	1.1-9
	Pressure Effects	1.1-9
	Reactant Utilization Effects	1.1-13
	Reactant Composition Effects	1.1-16
	Fuel Processor and Power Conditioner	1.1-18
1.1.1.2	Molten Carbonate Fuel Cell Power Systems	1.1-21
	Principles of Operation	1.1-21
	Cell Components	1.1-23
	General Performance Considerations	1.1-25
	Temperature Effects	1.1-25
	Pressure Effects	1.1-25
	Reactant Utilization Effects	1.1-28
	Reactant Composition Effects	1.1-30

TABLE OF CONTENTS (Cont'd)

SECTION NO.		Page
1.1.2	Future Fuel Cell Development.	1.1-34
1.1.2.1	Fuel Cell Program	1.1-34
	EPRI Program.	1.1-34
	DOE/ANL Program	1.1-34
	TVA Program	1.1-34
	UTC Program	1.1-34
	IGT Program	1.1-35
	GE Program.	1.1-35
	Westinghouse Program.	1.1-35
	ERC Program	1.1-35
1.1.2.2	Program Objectives.	1.1-35
	Phosphoric Acid	1.1-35
	Molten Carbonate.	1.1-36
1.1.2.3	Fuel Cell Development Scenario.	1.1-38
1.1.3	Bibliography.	1.1-42
2.1	Description of Advanced Fuel Cell Power Systems	2.1-1
2.1.1	Operational Characteristics	2.1-1
2.1.1.1	Phosphoric Acid Cell Characteristics.	2.1-1
2.1.1.2	Molten-Carbonate Cell Characteristics	2.1-9
2.1.2	System/Subsystem Designs.	2.1-18
2.1.3	Description of System Baseline Technology	2.1-23
2.1.3.1	Phosphoric Acid Cell Technology	2.1-23
2.1.3.2	Molten-Carbonate Cell Technology.	2.1-29
2.1.4	References.	2.1-35

TABLE OF CONTENTS (Cont'd)

SECTION NO.		Page
3.1	Evaluation of Coal-Derived Fuels for Advanced Fuel Cell Power Systems.	3.1-1
3.1.1	Definition of Fuel Gas Requirements	3.1-1
3.1.2	Identification of Power Generation Facility	3.1-7
3.1.2.1	Phosphoric Acid Cell.	3.1-7
3.1.2.2	Molten Carbonate Cell	3.1-10
3.1.3	References.	3.1-22
4.1	Evaluation of Integrated Gasification Fuel Cell Power Systems	4.1-1
4.1.1	Identification of Fuel Cell Power Plant with Texaco Gasifier.	4.1-1
4.1.2	Identification of Fuel Cell Power Plant with BGC Gasifier .	4.1-3
4.1.3	Comparison of Performance	4.1-17
4.1.4	Off-Design Operation of Gasification/Molten Carbonate Power Plants.	4.1-18
4.1.5	References.	4.1-20

TABLE OF CONTENTS (Cont'd)

SECTION NO.		Page No.
1.2	Assessment of Combined Cycle Systems Technology Status	1.2-1
1.2.1	Assessment of Combined Cycle Technology Readiness Development Status	1.2-1
1.2.1.1	Technology Readiness - Commercially Available Equipment	1.2-3
1.2.1.1	Technology Readiness - State-of-the-Art Gas Turbines	1.2-6
	FT50/GT200	1.2-6
	V84.3	1.2-8
	Other Engines	1.2-12
1.2.1.2	Development Trends in Operating Parameters	1.2-12
	Compressors	1.2-12
	Turbines	1.2-16
	Problems in Advancing Gas Turbine Technology	1.2-18
	Turbine Cooling Techniques	1.2-18
	Air Cooling	1.2-20
	Water Cooling	1.2-27
	Materials	1.2-27
	Coatings	1.2-31
	Ceramics	1.2-32
	Combustors	1.2-33
	Steam System Development	1.2-39
	Current Research and Development Efforts	1.2-43
	DOE Programs	1.2-43
	ARPA Programs	1.2-44
	EPRI Programs	1.2-45
1.2.2	Develop Data Base on Commercial and Demonstration/Pilot Engines	1.2-46
1.2.2.1	Commercially Available Systems	1.2-46
1.2.2.2	Demonstration/Pilot Systems	1.2-46
1.2.3	Evaluate Requirements for Operational System/Subsystem Development and Testing	1.2-46
1.2.3.1	High Temperature Turbine Technology Program	1.2-46
	Curtis Wright	1.2-56
	General Electric	1.2-56
1.2.3.2	High Reliability Gas Turbine Program	1.2-63

TABLE OF CONTENTS (Cont'd)

SECTION NO.		Page No.
1.2.3	Potential Problem Areas.	1.2-69
1.2.4	Bibliography	1.2-74
2.2	Description of Advanced Combined-Cycle Systems	2.2-1
2.2.1	Establish Operational Characteristics	2.2-1
2.2.1.1	Gas Turbine/Combined Cycle Operational Characteristics	2.2-1
2.2.1.2	Fuel Requirements.	2.2-1
2.2.1.3	Emission Standards for Gas Turbines.	2.2-1
2.2.2	Summarize System/Subsystem Design	2.2-6
2.2.3	Describe System Baseline Technology.	2.2-6
2.2.3.1	Compressor	2.2-11
2.2.3.2	Combustor	2.2-11
2.2.3.3	Turbine.	2.2-11
2.2.3.4	Combined Cycle System	2.2-14
3.2	Evaluation of Coal-Derived Fuels for Advanced Combined-Cycle Power Systems	3.2-1
3.2.1	Definition of Fuel Cell Gas Requirements	3.2-1
3.2.2	Identification of Power Generation Facility.	3.2-2
3.2.3	References	3.2-17
4.2	Evaluation of Integrated Gasification Combined-Cycle Power Systems	4.2-1
4.2.1	Identification of IGCC Power Plant with Texaco Gasifier. . . .	4.2-1
4.2.2	Identification of IGCC Power Plant with British Gas Corporation Gasifier	4.2-3

TABLE OF CONTENTS (Cont'd)

SECTION NO.		Page No.
4.2.3	Comparison of Performance.	4.2-17
4.2.4	Off-Design Operation of IGCC Power Plants	4.2-17
4.2.5	References	4.2-21

TABLE OF CONTENTS (Cont'd)

SECTION NO.		Page
1.3	Assessment of MHD Technology Status	1.3-1
1.3.1	Assessment of MHD Technology Readiness and Development Trends	1.3-1
1.3.1.1	Technology Readiness - Earlier Programs	1.3-1
1.3.1.2	Technology Readiness - Projected Commercial Plant	1.3-2
1.3.1.3	Trends in Operating Parameter	1.3-6
	Plasma Properties	1.3-6
	MHD Channel Phenomena	1.3-9
	Channel Construction and Materials	1.3-18
1.3.2	Develop Data Base for MHD Programs	1.3-29
1.3.2.1	Major Test Facilities	1.3-29
1.3.2.2	MHD Channel Technology	1.3-29
1.3.2.3	Superconducting Magnet	1.3-30
1.3.2.4	Inverter Systems	1.3-31
1.3.2.5	Combustors	1.3-31
1.3.2.6	Air Preheater Systems	1.3-32
1.3.2.7	Heat Recovery/Seed Recovery Systems	1.3-32
1.3.2.8	Seed Regeneration Systems	1.3-32
1.3.3	Characteristics of MHD System	1.3-33
1.3.3.1	MHD Power Plant Design Variations	1.3-34
1.3.3.2	Description of Selected MHD Cycles	1.3-34
	Integrated Low-Btu Gasifier Cycle	1.3-34
	Direct Coal Fired Plant with Direct Air Preheating	1.3-39

TABLE OF CONTENTS (Cont'd)

SECTION NO.		Page
	Direct Coal-Fired Plant with Indirect Air Preheating	1.3-39
	Direct Coal-Fired Plant with Oxygen Enrichment	1.3-42
1.3.3.3	Other MHD Configurations	1.3-46
1.3.4	References	1.3-49
2.3	Description of Advanced Combined MHD/Steam Power Plant	2.3-1
2.3.1	Establish Operational Characteristics	2.3-1
2.3.2	Basic MHD Power Plant Configurations	2.3-4
2.3.3	MHD Power Plant Components and Subsystems	2.3-8
2.3.3.1	Coal Processing and Combustion	2.3-10
2.3.3.2	System for Control of Pollutant Emissions	2.3-10
	Nitrogen Oxides	2.3-10
	Particulates	2.3-16
	Sulfur Oxides	2.3-16
	Seed Regeneration	2.3-17
2.3.3.3	Heat Recovery-Seed Recovery System	2.3-18
2.3.3.4	High-Temperature Air Preheating	2.3-20
2.3.3.5	Superconducting Magnet	2.3-20
2.3.3.6	Inverter Systems	2.3-25
2.3.4	Recommendation for Selection of MHD Power Plant Baseline Technology	2.3-25
2.3.5	References	2.3-33

TABLE OF CONTENTS (Cont'd)

SECTION NO.		Page
3.3	Evaluation of Coal-Derived Fuels for MHD Power Generation Systems	3.3-1
3.3.1	Definition of Fuel Gas Requirements	3.3-1
3.3.2	Identification of Power Generation Facility	3.3-5
3.3.3	References	3.3-12
4.3	Evaluation of Integrated Gasification MHD Power Systems	4.3-1
4.3.1	Identification of IG MHD Power Plant with Texaco Gasifier	4.3-1
4.3.2	Identification of IG MHD Power Plant with BGC Gasifier	4.3-5
4.3.3	Comparison of Performance	4.3-5
4.3.4	Load Following Capabilities of IG MHD Power Plants	4.3-10

TABLE OF CONTENTS (Cont'd)

SECTION NO.		Page
A.1	Fuel Cell Electrochemical Fundamentals	A.1-1
A.1.1	Reversible (Equilibrium) Electrode	A.1-1
A.1.2	Non-Equilibrium Electrodes-Polarization	A.1-3
A.1.2.1	Activation Polarization-Tafel Equation	A.1-4
A.1.2.2	Concentration Polarization-The Limiting Current	A.1-4
A.1.2.3	Total Electrode Polarization	A.1-5
A.1.2.4	Ohmic Polarization-iR Losses	A.1-5
A.1.3	Cell Performance	A.1-7
A.1.4	References	A.1-8
B.1	Potential Fuel Cell Power Generation System Advantages	B.1-1
B.1.1	Fuel Cell Efficiency	B.1-1
B.1.2	Environmental Emissions	B.1-3
B.1.3	Response Characteristics	B.1-3
B.1.4	Waste Heat Recovery Potential	B.1-3
B.1.5	Scaling Effects	B.1-5
B.1.6	References	B.1-6
C.1	Fuel Cell Historical Overview	C.1-1
C.1.1	Early UTC Activity	C.1-1
C.1.2	NASA Program History	C.1-1
C.1.3	Other Space and Defense Programs	C.1-2

TABLE OF CONTENTS (Cont'd)

SECTION NO.		Page
C.1.4	Fuel Cell Program for the Gas Utilities.	C.1-2
C.1.5	Fuel Cell Program for the Electric Utilities	C.1-4
C.1.6	Summary.	C.1-4
C.1.7	References	C.1-6
A.2	Theory of Combined-Cycle Operations.	A.2-1

LIST OF TABLES

Table No.		Page
1.1.1.1-1	Estimated Maximum Allowable Impurity Levels - Phosphoric Acid Fuel Cells.	1.1-19
1.1.1.1-2	Fuel Processing Requirements for Different Coal Products in Phosphoric Acid Power Plants.	1.1-20
1.1.1.2-1	Estimated Maximum Allowable Impurity Levels - Molten Carbonate Fuel Cells	1.1-33
2.1.1.2-1	Cell Stack Flow Conditions at Rated Power	2.1-15
2.1.3.2-1	Summary of System Performance for Oxygen-Blown Texaco Gasifier/Molten-Carbonate Fuel Cell	2.1-31
2.1.3.2-1	Fuel Cell Design Parameters	2.1-33
3.1.1-1	Gaseous Fuel Specifications	3.1-2
3.1.1-2	Liquid Fuel Specifications.	3.1-3
3.1.1-3	Alcohol Fuel Specifications	3.1-4
3.1.1-4	Estimated Maximum Allowable Impurity Levels for Phosphoric Acid Fuel Cells	3.1-5
3.1.1-5	Gas Compositions.	3.1-6
3.1.2.1-1	Mass and Energy Balance for Phosphoric Acid Fuel Cell Power System	3.1-9
3.1.2.1-2	Summary of Coal-Derived Fuel Impact	3.1-11
3.1.2.2-1	Performance Summary of Molten Carbonate Power Systems and Medium-Btu Fuel Gas	3.1-13
3.1.2.2-2	Heat and Mass Balance for Molten Carbonate Power System and Texaco Fuel Gas	3.1-14
3.1.2.2-3	Material Balance for Molten Carbonate Power System Using Texaco Fuel Gas	3.1-16

LIST OF TABLES (Cont'd)

Table No.		Page
3.1.2.2-4	Heat and Mass Balance for Molten Carbonate Power System and BGC Fuel Gas.	3.1-18
3.1.2.2-5	Material Balance for Molten Carbonate Power Systems Using BGC Fuel Gas	3.1-19
4.1.1-1	Performance Summary for Integrated Gasifications/Fuel Cell Power Plants.	4.1-4
4.1.1-2	Heat and Mass Balance for Integrated Texaco Gasification/ Fuel Cell Power Plant.	4.1-5
4.1.1-3	Material Balance for Integrated Texaco Gasifier/Fuel Cell Power Plant System.	4.1-7
4.1.2-1	Heat and Mass Balance for Integrated BGC Gasification/ Fuel Cell Power Plant.	4.1-12
4.1.2-2	Steam Compositions for Integrated BGC Gasification/ Fuel Cell Power System	4.1-14
1.2.1.1-1	Performance of Large Industrial Engines.	1.2-13
1.2.2.1-1	Operating Characteristics of Commercially Available Gas Turbines	1.2-47
1.2.2.1-2	Operating Characteristics of Commercially Available Combined Cycles Systems.	1.2-52
1.2.2.2-1	Projected Operating Characteristics of Demonstration Engines.	1.2-55
2.2.1.1-1	Range of Operating Characteristics of Advanced Gas Turbine and Combined Cycle Systems	2.2-2
2.2.1.2-1	Liquid Fuel Specifications	2.2-3
2.2.1.2-2	Gaseous Fuel Specifications.	2.2-4
2.2.1.3-1	Emissions Regulations.	2.2-5

LIST OF TABLES (Cont'd)

Table No.		Page
3.2.1-1	Gas Compositions.	3.2-3
3.2.2-1	Heat and Mass Balance for Combined Cycle Power System Using Texaco Coal-Derived Fuel.	3.2-5
3.2.2-2	Heat and Mass Balance for Combined Cycle Power System Using BGC Coal-Derived Fuel	3.2-6
3.2.2-3	Material Balance for Combined Cycle Power System Using Texaco Coal-Derived Fuel.	3.2-7
3.2.2-4	Material Balance for Combined Cycle Power System Using BGC Coal-Derived Fuel	3.2-11
3.2.2-5	Performance Estimates for Combined-Cycle Systems.	3.2-15
4.2.1-1	Heat and Mass Balance for Gas Turbine Combined Cycle Power Plant Using Texaco Oxygen-Blown Gasification System .	4.2-4
4.2.1-2	Material Balance for Texaco Gasification/Combined Cycle Power Plant	4.2-6
4.2.1-3	Performance Summary of IGCC Power Plants.	4.2-10
4.2.2-1	Heat and Mass Balance for Gas Turbine Combined Cycle Power Plant Using BGC Gasification Systems.	4.2-12
4.2.2-2	Material Balance for BGC Gasification/Combined-Cycle Power Plant	4.2-14
4.2.4-1	Pinch Temperature in Texaco IGCC Power Plants.	4.2-20
1.3.1.2-1	Projected Characteristics of a Commercial-Scale MHD/ Steam Power Plant	1.3-4
1.3.1.2-2	Summary of Projected MHD/Steam Power Plant Performance and Cost Estimates.	1.3-5
1.3.1.3-1	Ionization Potential of Metal Vapors.	1.3-8

LIST OF TABLES (Cont'd)

Table No.		Page
1.3.3.1-1	Variations in MHD Power Plant Configurations.	1.3-35
2.3.4-1	Baseline Technology for MHD Combined Cycle Power Plant. . . .	2.3-32
3.3.1-1	Gas Composition	3.3-3
3.3.1-2	Adiabatic Flame Temperature for Combustion of Medium-Btu Gases	3.3-4
3.3.2-1	Performance Estimates for MHD Systems	3.3-11
4.3.1-1	Performance Estimates for IG MHD Systems.	4.3-6
B.1.2-1	Fuel Cell Power Plant Emissions per Million Btu Input	B.1-4
C.1.6-1	Chronology of UTC Fuel Cell Activities.	C.1-5

LIST OF FIGURES

Figure No.		Page No.
1.1.1-1	Fuel Cell Power System	1.1-2
1.1.1.1-1	Phosphoric Acid Fuel Cell	1.1-4
1.1.1.1-2	Phosphoric Acid Fuel Cell Cross Section	1.1-6
1.1.1.1-3	Phosphoric Acid Fuel Cell Polarization Curves	1.1-7
1.1.1.1-4	Integral Ribbed Substrate Cell Characteristics	1.1-8
1.1.1.1-5	Phosphoric Acid Fuel Cell Polarization Losses	1.1-10
1.1.1.1-6	Baseline Phosphoric Acid Fuel Cell Performance	1.1-11
1.1.1.1-7	Effect of Temperature on Phosphoric Acid Fuel Cell Performance	1.1-12
1.1.1.1-8	Effect of Pressure on Phosphoric Acid Fuel Cell Voltage	1.1-14
1.1.1.1-9	Effect of Reactant Utilization on Phosphoric Acid Fuel Cell Performance	1.1-15
1.1.1.1-10	Effect of Temperature on Phosphoric Acid Fuel Cell Anode CO Tolerance	1.1-17
1.1.1.2-1	Molten Carbonate Fuel Cell	1.1-22
1.1.1.2-2	Molten Carbonate Fuel Cell Cross Section	1.1-24
1.1.1.2-3	Baseline Molten Carbonate Fuel Cell Performance	1.1-26
1.1.1.2-4	Effect of Temperature on Molten Carbonate Fuel Cell Performance	1.1-27
1.1.1.2-5	Effect of Pressure on Molten Carbonate Fuel Cell Performance	1.1-29
1.1.1.2-6	Effect of Reactant Utilization on Molten Carbonate Fuel Cell Performance	1.1-31
1.1.2.2-1	Performance of Cell Stack at Various Operating Conditions	1.1-37

LIST OF FIGURES

Figure No.		Page No.
1.1.2.2-2	Molten Carbonate Cell Performance History	1.1-39
1.1.2.3-1	EPRI Timetable of Fuel Cell Development	1.1-40
2.1-1	Evolution of Integrated Coal Gasifier/Fuel Cell Power Plants	2.1-2
2.1.1.1-1	Initial Performance of 20 Cell, 3.7-ft^2 Ribbed-Substrate Stack	2.1-4
2.1.1.1-2	Performance History of 20 Cell, 3.7-ft^2 Ribbed-Substrate Development Stack	2.1-5
2.1.1.1-3	Fuel Effect on Performance for 20 Cell, 3.7-ft^2 Ribbed Substrate Stack	2.1-6
2.1.1.1-4	Effect of CO Content and Temperature on Anode Performance	2.1-7
2.1.1.2-1	Effect of Pressure on Molten Carbonate Fuel Cell Performance	2.1-10
2.1.1.2-2	Effect of Temperature on Molten Carbonate Fuel Cell Performance	2.1-11
2.1.1.2-3	ECAS Cell Performance	2.1-13
2.1.1.2-4	Molten Carbonate Cell Design Performance	2.1-14
2.1.1.2-5	Cell Performance as a Function of Fuel Utilization	2-1-16
2.1.1.2-6	Effect of Reactant Utilization on Molten Carbonate Fuel Cell Performance	2.1-17
2.1.2-1	Gas Flow Schematic	2.1-19
2.1.2-2	Fuel Cell Operating Pressure Effect Estimated Power Plant Efficiency	2.1-21
2.1.2-3	Fuel Cell Pressure and Performance Level Effect on Overall Power Plant Efficiency	2.1-22

LIST OF FIGURES

Figure No.		Page No.
2.1.2-4	Overall Hz Utilization Effect on Overall Power Plant Efficiency	2.1-24
2.1.2-5	Cell Stack Temperature Gradient Effect on Overall Power Plant Efficiency	2.1-25
2.1.2-6	Recycle Pressure Drop and Cell Operating Pressure Effect on Overall Power Plant Efficiency	2.1-26
2.1.2-7	DC Module System Schematic	2.1-27
2.1.3.2-1	Molten Carbonate Power System	2.1-30
3.1.2.1 1	Phosphoric Acid Fuel Cell Power System	3.1-8
3.1.2.2-1	Molten Carbonate Fuel Cell Power System	3.1-12
4.1.1-1	Texaco Oxygen-Blown Gasifier/Molten Carbonate Fuel Cell.	4.1-2
4.1.2-1	BGC Slagger Gasifier/Molten Carbonate Fuel Cell	4.1-11
1.2.1-1	Temperature-Entropy Diagram for a Brayton Cycle	1.2-2
1.2.1.1-1	Performance of FT4C	1.2-4
1.2.1.1-2	Modular Construction of FT50	1.2-7
1.2.1.1-3	Estimated Output of FT50	1.2-9
1.2.1.1-4	Estimated Heat Rate of FT50	1.2-10
1.2.1.1-5	KWU Gas Turbine and Auxiliaries	1.2-11
1.2.1.2-1	Compresssor Technology Progression	1.2-14
1.2.1.2-2	Turbine Technology Progression	1.2-17
1.2.1.2-3	Parametric Performance	1.2-19
1.2.1.2-4	Vane Convective Cooling	1.2-21
1.2.1.2-5	Convective Impingement Cooling	1.2-22

LIST OF FIGURES

Figure No.		Page No.
1.2.1.2-6	Film Cooling	1.2-23
1.2.1.2-7	Radial Wafer Cooling - Vane	1.2-24
1.2.1.2-8	Radial Wafer Cooling - Blade	1.2-25
1.2.1.2-9	Water Cooling	1.2-28
1.2.1.2-10	Aircraft Materials Temperature Improvements	1.2-29
1.2.1.2-11	Stress-Temperature Relationship	1.2-30
1.2.1.2-12	Typical In-Line Combustor	1.2-34
1.2.1.2-13	Cross-Section of Silo Combustor	1.2-35
1.2.1.2-14	Equivalence Ratio Effect on NO_x Emission	1.2-36
1.2.1.2-15	Premix Combustor Head	1.2-37
1.2.1.2-16	Schematic of Rich-Burn Quick-Quench Combustor	1.2-38
1.2.1.2-17	Combined Cycle Waste-Heat Boiler T-Q Curve for Nonreheat Steam Cycle	1.2-40
1.2.1.2-18	Combined-Cycle Waste-Heat Boiler T-Q Curve for Dual-Pressure Steam Cycle	1.2-41
1.2.1.2-19	Combined-Cycle Waste Heat Boiler T-Q Curve for Reheat Steam Cycle	1.2-42
1.2.3.1-1	Curtis Wright 130-MW Gas Turbine Configuration	1.2-57
1.2.3.1-2	Cooling Configuration for High Temperature Turbine	1.2-58
1.2.3.1-3	Transpiration Air-Cooled Turbine Blade	1.2-59
1.2.3.1-4	Wrap-Around LBG Combustor Configuration	1.2-60
1.2.3.1-5	General Electric High-Temperature Machine Cross-Section.	1.2-61
1.2.3.1-6	Nozzle Cooling Circuits	1.2-62

LIST OF FIGURES

Figure No.		Page No.
1.2.3.1-7	First-Stage Composite Blade Section	1.2-64
1.2.3.1-8	Second-Stage Monolithic Vane Section	1.2-65
1.2.3.1-9	General Electric Low-Btu Gas Sectoral Combustor	1.2-66
1.2.3.2-1	V84.3 Gas Turbine	1.2-67
1.2.3.2-2	First Vane Cooling Configuration	1.2-68
1.2.3.2-3	V84.3 First-Stage Blade Cooling Scheme	1.2-70
1.2.3.2-4	Combustion Chamber Cross Section	1.2-71
1.2.3.3-1	Turbine Inlet Temperature Effect on Performance	1.2-72
2.2.2-1	Typical Waste Heat Combined Gas and Steam Turbine System	2.2-7
2.2.2-2	Front Elevation of V84.3	2.2-8
2.2.2-3	Schematic of Steam Bottoming Cycle	2.2-9
2.2.2-4	Typical Steam Turbine Generator	2.2-10
2.2.3-1	The Rich/Lean Combustor Concept	2.2-12
2.2.3-2	Bonded Airfoil First Vane V84.3 Group Model	2.2-13
2.2.3-3	Overall Plant System Concept	2.2-15
3.2.2-1	Combined Cycle Power System	3.2-4
4.2.1-1	Texaco Oxygen Blown Gasifier/V84.3 Gas Turbine	4.2-2
4.2.2-1	BGC Slagger Gasifier/V84.3 Gas Turbine	4.2-11
4.2.4-1	Part-Load Performance of IGCC Power Plants	4.2-19

LIST OF FIGURES

Figure No.		Page No.
1.3.1.3-1	Generation of DC Electric Power By Magnetohydrodynamic	1.3-7
1.3.1.3-2	Electrical Conductivity of Combustion Gases	1.3-10
1.3.1.3-3	MHD Duct with Continuous Electrodes - No Hull Effect	1.3-11
1.3.1.3-4	MHD Duct With Continuous Electrodes - With Hull Effect	1.3-13
1.3.1.3-5	Segmented Faraday Generator	1.3-15
1.3.1.3-6	Diagonal Generator	1.3-16
1.3.1.3-7	Variation of Parameters Along Axis of MHD Channel	1.3-17
1.3.1.3-8	MHD Channels with Faraday Interconnection and Alternate Insulating Wall Structure	1.3-19
1.3.1.3-9	MHD Channels with Alternate Types of Diagonal Interconnection	1.3-21
1.3.1.3-10	Diagonal MHD Channels with Multiple Loads	1.3-22
1.3.1.3-11	MHD Channels With and Without Maintenance Layers	1.3-24
1.3.1.3-12	Regions of Electrode/Plasma System	1.3-25
1.3.1.3-13	Electrode System Configurations	1.3-26
1.3.1.3-14	Electrode and Peg Wall Design	1.3-27
1.3.1.3-15	Electrode and Bar Wall Design	1.3-28
1.3.3.2-1	MHD Power Plant Cycle with Integrated Low-Btu Gasifier	1.3-37
1.3.3.2-2	Fluidized Bed Gasification Process with High Temperature Sulfur and Particulate Removal	1.3-38
1.3.3.2-3	Simplified Schematic of MHD Power Plant Cycle with Direct-Fired High Temperature Air Preheater	1-3-40

LIST OF FIGURES

Figure No.		Page No.
1.3.3.2-4	MHD Power Plant Cycle with Direct Fired High Temperature Air Preheater	1.3-41
1.3.3.2-5	MHD Power Plant with Separately-Fired High Temperature Air Preheater	1.3-43
1.3.3.2-6	Gasifier System for Separately-Fired High Temperature Air Preheater	1.3-44
1.3.3.2-7	MHD Power Plant Cycle With Oxgyen Enrichment	1.3-45
1.3.3.1-1	MHD Power Plant Cycle with Tail Gasification	1.3-47
2.3.1-1	Method for Achieving High Electrical Conductivity, Velocity and Magnetic Field Strength	2.3-2
2.3.1-2	Adiabatic Flame Temperature	2.3-3
2.3.2-1	Basic MHD Power Generation Systems	2.3-5
2.3.2-2	Basic MHD Power Generation System Utilizing Direct-Fired Air Preheating	2.3-6
2.3.2-3	MHD/Steam Combined-Cycle Power Generation System	2.3-7
2.3.2-4	MHD/Steam Combined-Cycle Power Generation System Including Gas Clean-Up, Seed Recovery and Seed Recycling	2.3-9
2.3.3.1-1	Slag Removal Schemes in Coal-Fired in Coal-Fired MHD Power Plants	2.3-11
2.3.3.1-2	Two-Stage Direct Coal-Fired MHD Combustor Design	2.3-12
2.3.3.1-3	Two-Stage Direct Coal-Fired MHD Combustor	2.3-13
2.3.3.1-4	Single Stage Direct Coal-Fired MHD Combustor	2.3-14
2.3.3.2-1	Control of Nitrogen Oxides in MHD Power Plants	2.3-15
2.3.3.3-1	Typical Heat Recovery System Flow Train Arrangement with Direct-Fired High Temperature Air Heater	2.3-19

LIST OF FIGURES

Figure No.		Page No.
2.3.3.3-2	Alternative Arrangements of High Temperature Air Preheater System	2.3-21
2.3.3.3-3	Condensate, Feedwater and Steam Flow System for MHD/ Steam Power Plant	2.3-22
2.3.3.4-1	Diagram of Regenerative HTAM System	2.3-23
2.3.3.4-2	Section of Regenerative High Temperature Air Heater Vessel and Cored Brick Matrix	2.3-24
2.3.3.5-1	MHD Magnet Saddle Coil Configurations	2-3-26
2.3.3.5-2	Superconducting Magnet Design for MHD Component Development and Integration Facility	2.3-27
2.3.3.5-3	Schematic Diagram of Cryogenic Support System for Superconducting Magnet	2.3-28
2.3.3.6-1	Consolidation Network for 12 Electrodes	2.3-29
2.3.3.6-2	Consolidation Schemes for Faraday and Diagonal Channels	2.3-30
3.3.2-1	Cycle Configuration for Direct Coal-Fired MHD Reference Plant	3.3-6
3.3.2-2	Steam and Feedwater Cycle Configuration for Direct Coal-Fired MHD Reference Power Plant	3.3-7
3.3.2-3	Cycle Configuration for Medium-Btu Gas Fired MHD Power Plant	3.3-9
4.3.1-1	Integrated Texaco Gasification/MHD Power Plant	4.3-2
4.3.1-2	Cycle Configuration for Integrated Texaco Gasification/ MHD Power Plant	4.3-3
4.3.1-3	Steam and Feedwater Cycle Configuration for Integrated Texaco Gasification/MHD Power Plant	4.3-4
4.3.2-1	Integrated BGC Gasification/MHD Power Plant	4.3-7

LIST OF FIGURES

Figure No.		Page No.
4.3.2-2	Cycle Configuration for Integrated BGC Gasification/ MHD Power Plant	4.3-8
4.3.2-3	Steam and Feedwater Cycle Configuration for Integrated BGC Gasification/MHD Power Plant	4.3-9
A.1.2.2-1	Fuel Cell Polarization Curve	A.1-6
B.1.1-1	Comparison of Power System Efficiency	B.1-2

R81-955343-9

Final Study Report of an Applications Study of Advanced Power Generation Systems Utilizing Coal-Derived Fuels

Volume II - Technical Report

One of the most promising methods for utilizing coal for electric power generation is to gasify it and then combust the fuel gas in an advanced technology power generation system. The analysis of gasification/power generation systems has been the subject of numerous studies in recent years. Despite the proliferation of studies it is often difficult to effectively utilize the data generated because of the differing guidelines which have existed among the studies. Consequently, if data were desired for a specific generation system application, it is often necessary to develop the data unique to that application.

Two applications of interest to Marshall Space Flight Center (MSFC) involve power generation systems that either 1) utilize a medium-Btu coal-derived fuel gas supplied via pipeline from a large central coal gasification facility, or 2) are integrated with a gasification facility for supplying medium-Btu coal-derived fuel gas. Although previous studies have considered these applications, the requirement still exists to evaluate the employment of specific power generation systems in these applications, namely, combined-cycle gas turbines, fuel cells, and magnethodydrodynamics (MHD), on a consistent basis. The objectives of this study are to provide 1) descriptions of the state of the art for these conversion systems and projections of future technological advances; and 2) an assessment of the performance of each of these power conversion systems using medium-Btu fuel gas. This document presents the results of Task 1 (Assessment of Systems Technology Status), Task 2 (Description of Advanced Power Systems), Task 3 (Evaluation of Advanced Power System Utilizing Coal-Derived Medium-Btu Gas), and Task 4 (Evaluation of Advanced Power Generation System Integrated with a Coal Gasifier Producing Medium-Btu Fuel Gas).

The work described in this report has been performed at United Technologies Research Center (UTRC) and Burns and Roe, Inc. (B&R) under Contract No. NAS8-33996 with George C. Marshall Space Flight Center of the National Aeronautics and Space Administration (MSFC).

1.1 Assessment of Fuel Cell Power System Status

The objectives of this technology assessment have been to develop a data base reflecting the current status of both phosphoric acid and molten carbonate fuel cell power generation system technology and to provide an appraisal of probable future development of the technology. The scope of this assessment effort included: a literature review of the current status of fuel cell technology; summarization of fuel cell power generation system operational behavior and experience; and a projection of the future course of fuel cell power generation system development with an indication of potential challenges which must be met to fulfill the projections. The objectives of this technology assessment effort as stated above provide the format for the following commentary.

Prior to reviewing the commentary, however, it may be appropriate to first review the three appendices provided as background to the fuel cell assessment. Appendix A.1 includes a development of the electrochemical fundamentals associated with fuel cells and is provided for the purpose of introducing the key fuel cell performance relationships. Appendix B.1 contains a discussion of the potential advantages of a fuel cell power generation system to a utility. Appendix C.1 furnishes a review of the historical development of the fuel cell up to the present programs.

1.1.1 Current Technology Status and Operational Data Base of Fuel Cell Power Systems

A fuel cell power system consists of a fuel processor that produces H_2-rich fuel from raw and primary fuels, a power section that converts the chemical energy in the gaseous feeds to dc power, and a power conditioner that converts dc to ac power (Fig. 1.1.1-1). To utilize the heat rejected from the fuel cell power system, a cogeneration system to supply thermal energy or a bottoming power generation system to provide additional electrical output could be added. A hydrocarbon fuel (natural gas, mined coal, solid waste, refined petroleum products or resids, synthetic natural gas, naphtha, methanol, etc.) plus steam, and heat recycled from the fuel cell section are fed into the fuel processor to generate a gas rich in hydrogen. The fuel processor could be a reformer, a gasifier, or a hydroprocessor, depending on the hydrocarbon fuel used. The hydrogen-rich mixture is then fed to the anode side of the fuel cell power section which is formed by fuel cells connected electrically in series to generate the desired voltage. The dc power obtained is then processed by the power conditioner (at about 95-percent efficiency) to produce the ac power to meet the user requirements.

Fuel cells and fuel cell power systems are usually classified according to the type of electrolyte or ion conducting media used. In the current study effort two fuel cell types are of special interest: the phosphoric acid fuel cell and the molten carbonate fuel cell. The technology of the phosphoric acid fuel cell has been highly developed. As such it is regarded as a

FIG. 1.1.1-1

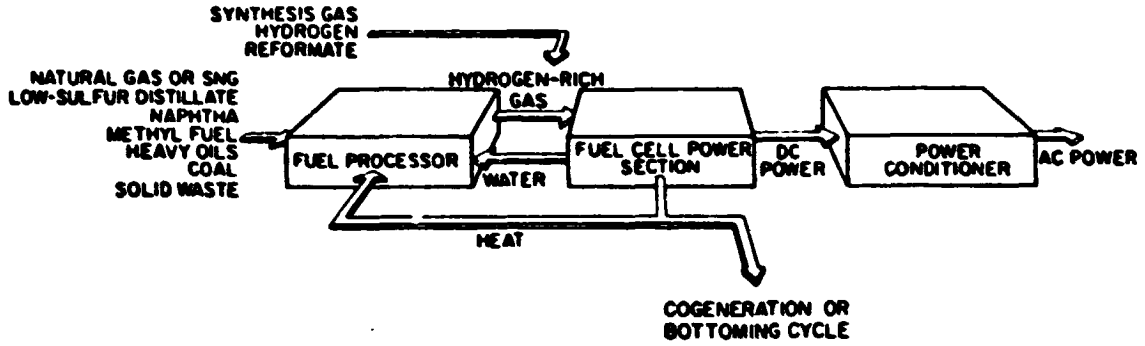

FUEL CELL POWER SYSTEM

first generation fuel cell. Because of the near-term application potential of the phosphoric acid fuel cell, phosphoric acid fuel cell power systems will be discussed first followed by a discussion of the technology of the more long-term, second generation molten carbonate fuel cell power systems.

The topic of the commentary in the following sections is the current status of both phosphoric acid and molten carbonate fuel cell power system. The format for the discussion of these fuel cell power systems will be similar; a brief overview of the principles of operation will be followed by a commentary relating the important parameters which effect performance and identifying the current state of technology which defines these parameters. The material presented has been collected from the recent open literature, a bibliography of which is provided in a later section. One work was especially useful, however, and should be cited and that is (The) Handbook of Fuel Cell Performance prepared under DOE Contract No. EC-77-03-1545 by T. G. Benjamin, E. M. Camara, and L. G. Marianowski.

1.1.1.1 Phosphoric Acid Fuel Cell Power Systems

State-of-the-art phosphoric acid fuel cells operate at 150 to 200 C and 1 to 3 atmospheres. The electrical operating point is 0.55 to 0.65 volts/cell at 100 to 400 mA/cm^2 of electrode area. The present phosphoric acid cell is adequate for utility applications. The fuel cell power system efficiency is 32 to 40 percent which is consistent with reasonable stack costs provided the stacks are made by mass production techniques.

Although small phosphoric acid stacks have operated for extended periods, the desired 40,000 hours has yet to be demonstrated. A 4.8-MW demonstration plant containing all the equipment and facilities necessary to convert fuel into ac electrical necessary to convert fuel into ac electrical power is being constructed and will be operational this year.

Principles of Operation

In the phosphoric acid cell (see Fig. 1.1.1.1-1) gaseous hydrogen in the fuel diffuses through the porous anode to a reaction site at the electrode (solid)/electrolyte (liquid) interface where it is electrochemically oxidized according to:

$$H_2 \rightarrow 2H^+ 2e^- \qquad (1.1.1.1\text{-}1)$$

The electrons are transported through the external circuit, and the hydrogen ions are conducted through the electrolyte to the cathode reaction sites. Oxygen, which has diffused through the cathode, reacts with the hydrogen ions and electrons (Eq. 1.1.1.1-2), and the product water diffuses back out of the cathode:

$$1/2\ O_2 + 2H^+ + 2e^- \rightarrow H_2O(g) \qquad (1.1.1.1\text{-}2)$$

FIG. 1.1.1.1-1

$$H_2 \rightleftharpoons 2H^+ + 2e^-$$

$$1/2 + 2e^- + 2H^+ \rightleftharpoons H_2O$$

$$H_2 + 1/2\ O_2 \rightleftharpoons H_2O$$

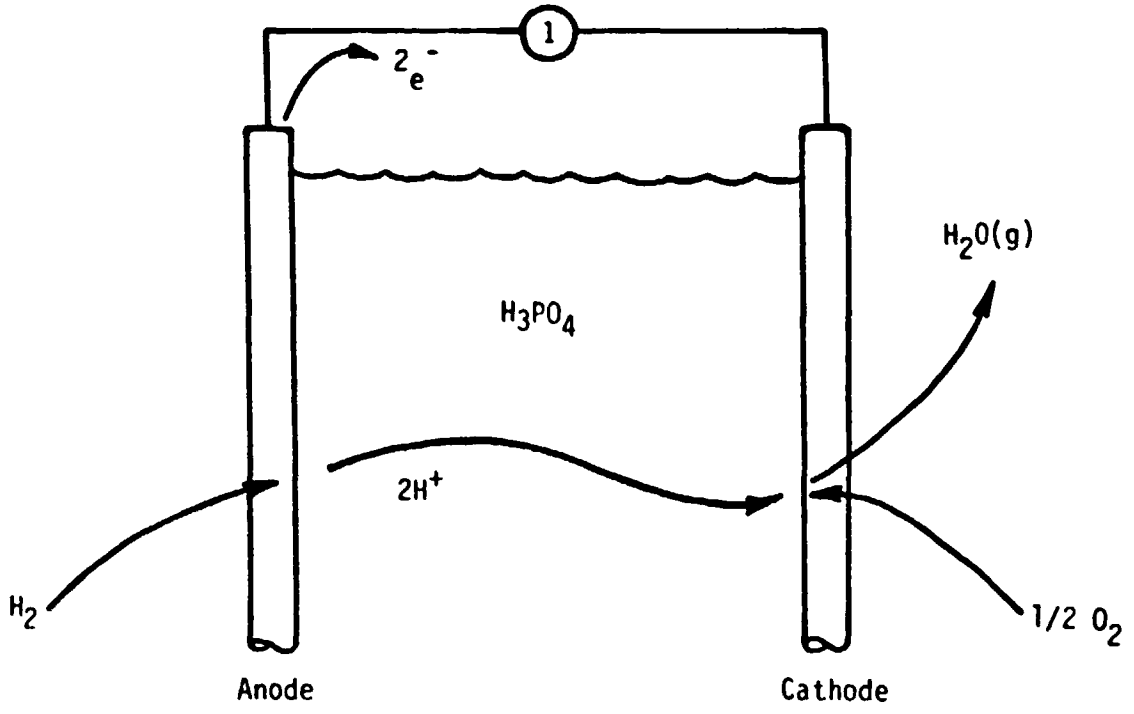

PHOSPHORIC ACID FUEL CELL

The net reaction is:

$$H_2 + 1/2\ O_2 \rightarrow H_2O(g) \qquad (1.1.1.1\text{-}3)$$

Cell Components

A sketch of a conventional phosphoric acid fuel cell is displayed in Fig. 1.1.1.1-2. The cell is composed of a phosphoric acid electrolyte sandwiched between two porous electrodes. The electrolytes are retained by either a thin inert matrix or a thin pad acting as a blotter. The electrodes are porous carbon catalyzed with small amounts of platinum. They are backed with porous conductive support sheets. Sandwiching the entire cell are separator plates which as the name implies separate adjacent cells. The separator plates are ribbed to provide channels for the fuel and oxidant to flow to the anode and cathode, respectively. A large number of these individual cells are then assembled in series to provide the desired output power and voltage. For example, the 4.8-MW demonstrator to be used in Con Edison has fuel stacks with approximately 460 individual cells.

One of the goals of past and current fuel cell programs has been to reduce cell stack cost. One of the most notable achievements has been the reduction of platinum catalyst required in the electrodes. Current cells require less than 4 percent of the platinum used in earlier cells (0.75 mg/cm^2 as compared to 20 mg/cm^2 of active cell area). This has been accomplished with minor effect on cell performance (Fig. 1.1.1.1-3).

Another cell structure advance which promises to reduce fabrication costs is the integral ribbed substrate (Fig. 1.1.1.1-4). This cell concept will also provide increased electrolyte capacity. In part, the cost reduction is brought about by the substitution of a 2-3 day process in place of the conventional 2-week molding and curing process which produces a complex bipolar/separator plate. Aside from being complex, the molded processing method places a limitation on the size of the plate that can be fabricated. Eliminating the size constraint on the cell structure thereby provides the possibility to go to a larger and more cost effective cell.

The unique features of the integral ribbed substrate concept are: 1) replacing with a simple impervious flat plate the complex bipolar/separator (which normally contains a ribbed reactant flow field on either side perpendicular to each other); and 2) transferring the function of each solid ribbed flow field onto a ribbed porous element which, after deposition of catalyst on one side, behaves like an electrode and which is also designed to act as an electrolyte reservoir.

General Performance Considerations

The magnitudes of the anode, the cathode (activation plus concentration), and ohmic polarizations for a typical phosphoric acid fuel cell are shown in

FIG. 1.1.1.1-2

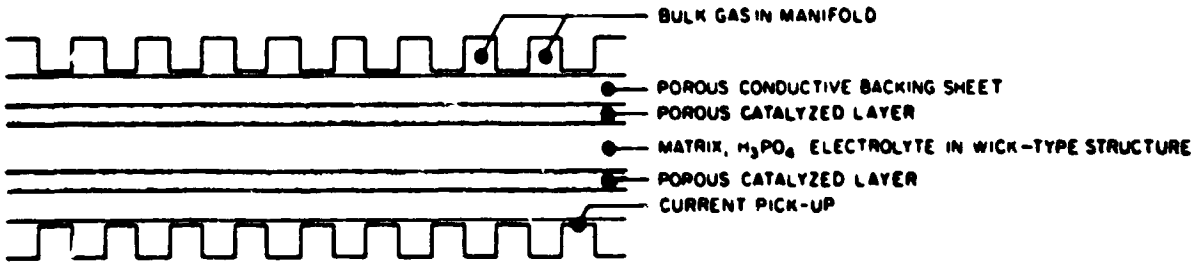

PHOSPHORIC ACID FUEL CELL CROSS SECTION

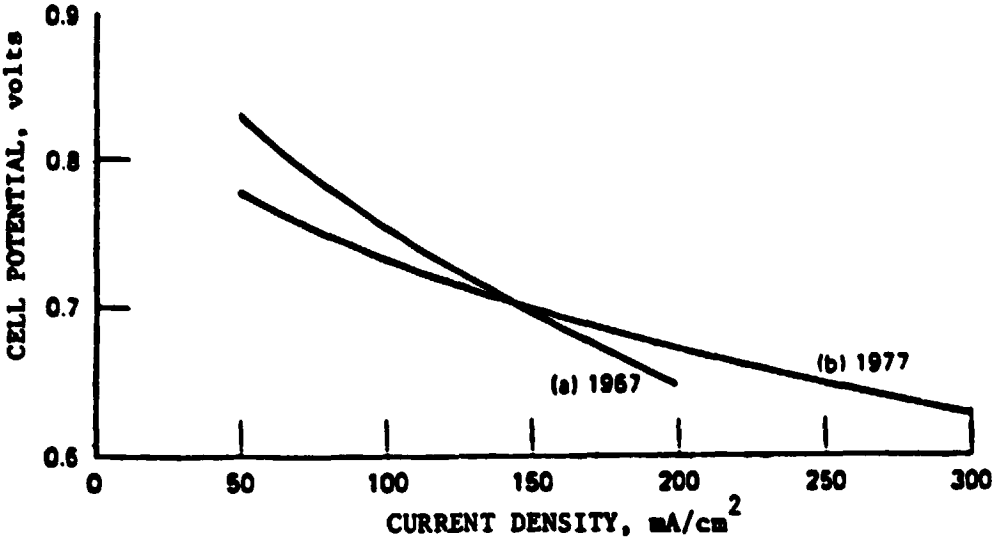

PHOSPHORIC ACID FUEL CELL POLARIZATION CURVES

a) 160°C, 1 Atm, AIR, PLATINUM LOADING OF 20 MG/CM^2, H_2 FUEL
b) 190°C, 3 Atm, AIR, PLATINUM LOADING OF 0.75 MG/CM^2, H_2 FUEL

FIG. 1.1.1.1-4

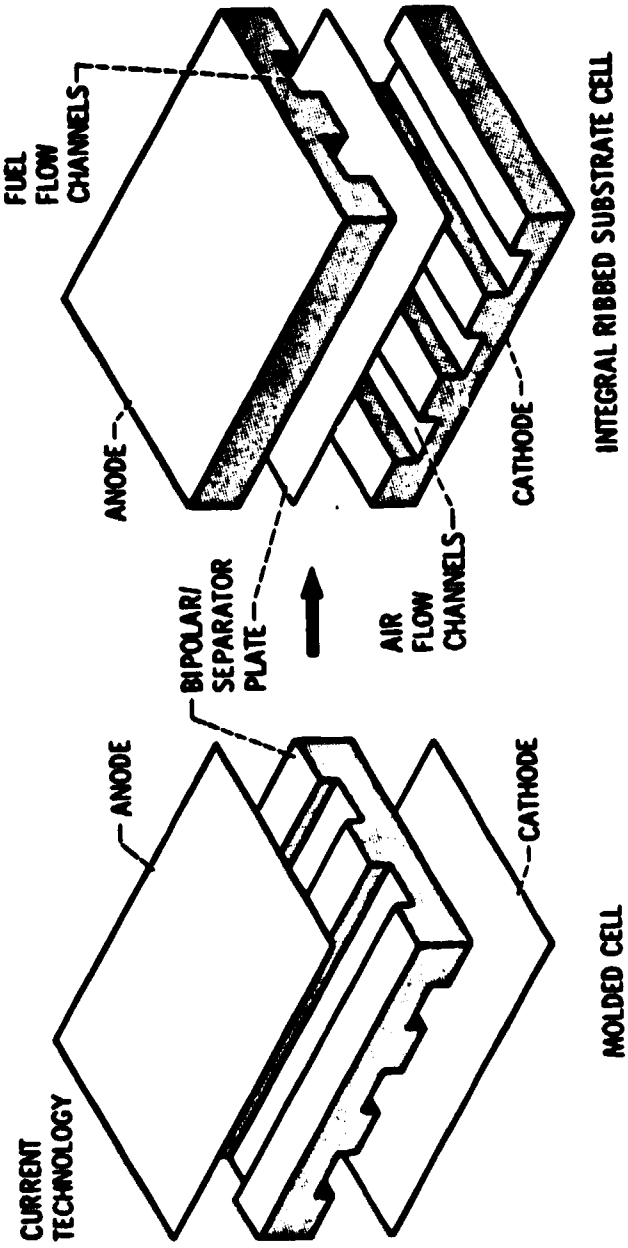

INTEGRAL RIBBED SUBSTRATE CELL CHARACTERISTICS

Fig. 1.1.1.1-5. The upper curve represents the cell performance that could be obtained if ohmic (approximately 15 mV/100 mA/cm^2) and anode (approximately 5 mV/100 mA/cm^2) polarizations were eliminated. It also demonstrates the significant gains possible if the cathode polarization (approximately 400 mV/300 mA/cm^2) could be reduced. The relative magnitudes of the anode and cathode polarizations illustrate why most recent cell electrochemistry research is concentrated on the cathode.

Although the phosphoric acid fuel cell is much more developed than any other fuel cell system, it is difficult to find clear parametric performance data in the open literature. Therefore, in the following discussion on the effects of various performance parameters on fuel cell performance, a baseline system is used to illustrate the effect of parameter variations. The baseline cell operates with H_2 and O_2 at low utilization, atmospheric pressure, and 175 C. Its performance is shown Fig. 1.1.1.1-6.

Temperature Effects

Increasing temperature will enhance mass transfer, increase the reaction rate, and usually decrease cell resistance, thus reducing polarization and increasing cell performance. In the case of the acid cell, the additional benefit of increased CO tolerance at higher temperature is realized. On the other hand, increasing temperature results in increased corrosion, catalyst sintering and recrystallization, and electrolyte loss due to evaporation, so a compromise is required. Current cells operate at 190 C but work is in progress to increase this temperature level.

The increase in cell performance which could be realized by increasing operating temperature is shown in Fig. 1.1.1.1-7 for a cell burning either reformed methane (RM-1) with air, H_2 with air, or H_2 with O_2 all at 50 psia and 300 amp/ft^2 current density. It can be concluded from this illustration that modest temperature increases on the order of 30 C above the current level of 190 C could produce significant (up to 10 percent) performance increases.

Pressure Effects

There are multiple incentives for operating a fuel cell at elevated pressure, including integration with fuel processors, increased reactant partial pressure (Nernst gains), and higher gas solubilities in the electrolyte. There are also problems associated with high-pressure operation such as increased component corrosion resulting from the higher voltage. Phosphoric acid fuel cells operate in the range of 1 to 10 atmospheres.

Increasing cell pressure will result in higher cell performance because of decreased activation polarization at the cathode due to increased oxygen and water partial pressure. The water dilutes the acid resulting in a higher exchange current density (see Appendix A.1). An additional gain is realized in the open circuit potential due to the increased partial pressure of water and oxygen.

FIG. 1.1.1.1-5

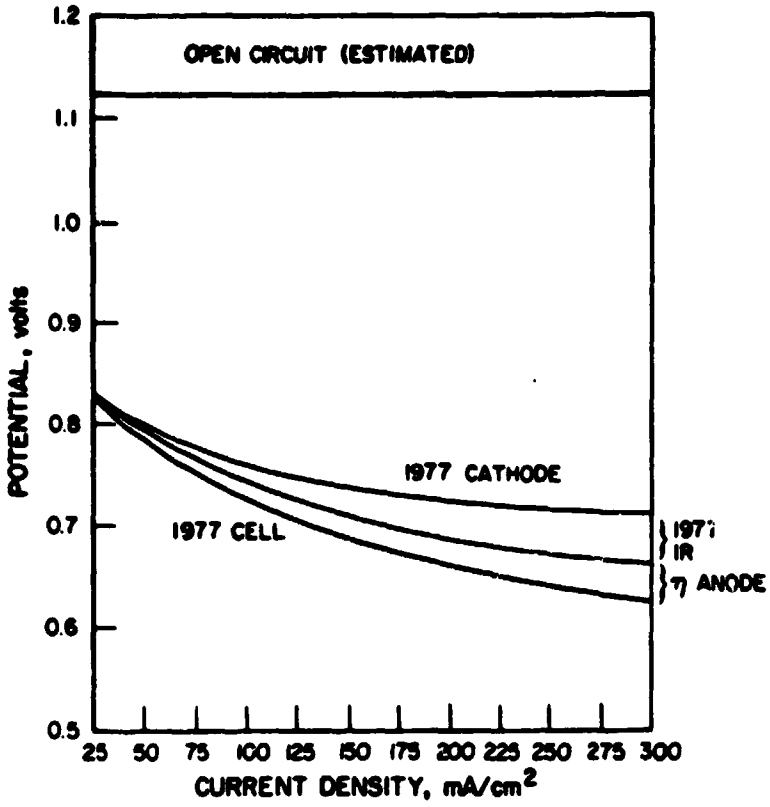

PHOSPHORIC ACID FUEL CELL POLARIZATION LOSSES

190° C, 3 Atm, AIR, PLATINUM LOADING, 0.75 MG/CM^2, H_2 FUEL

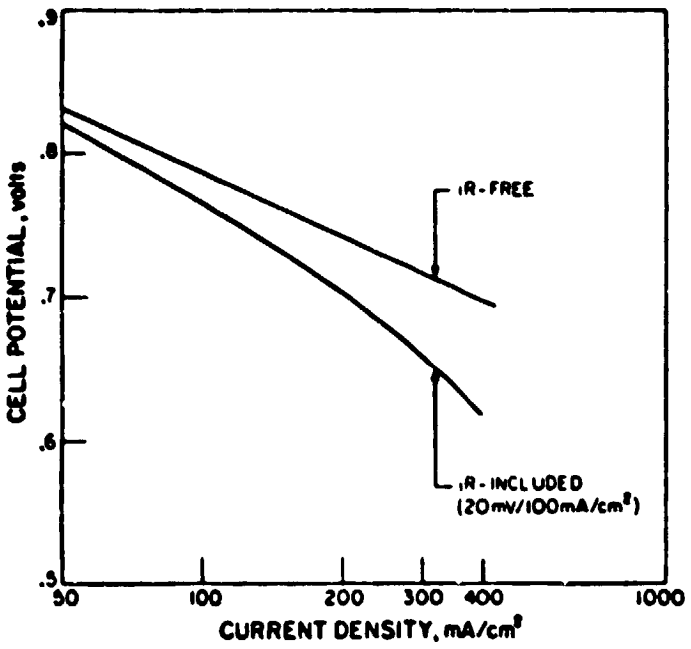

BASELINE PHOSPHORIC ACID FUEL CELL PERFORMANCE

1 Atm, 175°C, H_2 FUEL, O_2 OXIDANT, LOW UTILIZATION

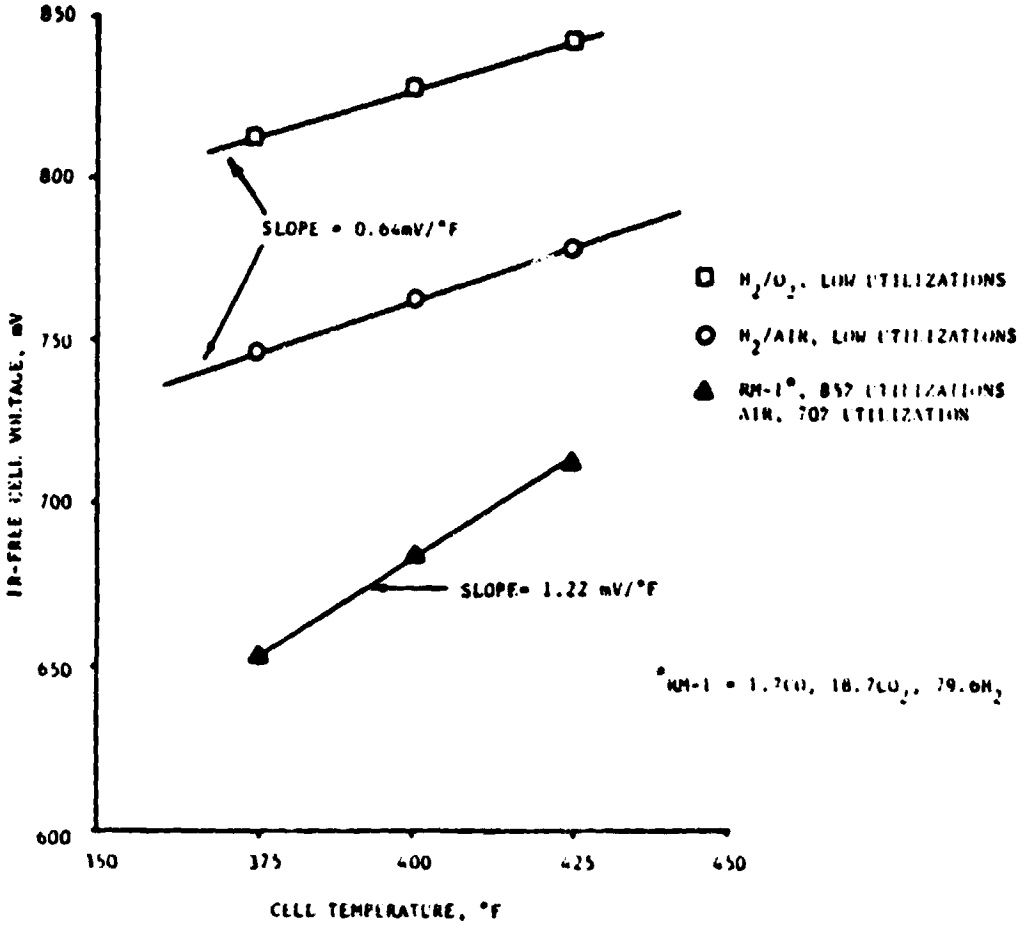

EFFECT OF TEMPERATURE ON PHOSPHORIC ACID FUEL CELL PERFORMANCE

50 PSIA, 300 ASF, 190° F ANODE DEWPOINT

The increase in cell performance resulting from increasing pressure is shown in Fig. 1.1.1.1-8. A correlation describing the relationship between cell voltage change, ΔV, and pressure ratio, P_2/P_1, as shown in Fig. 1.1.1.1-8, is:

$$\Delta V_p = 142 \log (P_2/P_1) \qquad (1.1.1.1\text{-}4)$$

This correlation appears to be valid at least over the range from 190 C to 220 C because the effect of pressure on cell performance is independent of temperature over this range.

Reactant Utilization Effects

High reactant utilization in a fuel cell results in increased concentration polarization, which reduces efficiency. Decreasing reactant utilization or inlet concentration, however, results in decreased cell performance because of increased concentration polarization (diffusion) and Nernst losses. To achieve high system efficienies the reactant must be utilized, either in the fuel cell or elsewhere in the system. For example, in a complete fuel cell system, anode exhaust containing unreacted hydrogen is often burned to supply heat to the fuel processor. Present utilizations are on the order of 70 percent oxidant and 85 percent fuel.

Oxidant

At a constant cathode potential the current varies linearly with oxygen partial pressure. Data on the gains associated with using oxygen at the cathode instead of air are contained in Figs. 1.1.1.1-7 and 1.1.1.1-8. The data in these figures are represented by:

$$\Delta V_{O_2} = 103 \log \frac{(\bar{P}_{O_2})_2}{(\bar{P}_{O_2})_1} \qquad (1.1.1.1\text{-}5)$$

where $(\bar{P}_{O_2})_1$ and $(\bar{P}_{O_2})_2$ are average oxygen partial pressures at the cathode.

Fuel

Because the phosphoric acid fuel cell anode reaction is essentially reversible, the effects of fuel composition and utilization are less critical to cell performance. The available data concerning the effects of fuel composition are more difficult to interpret because of the poisoning effect of carbon monoxide, which is contained in virtually all gaseous fuel cell feeds derived from hydrocarbon (liquid or coal) feedstocks. The cell performance change with respect to hydrogen partial pressure is derived from the data in Fig. 1.1.1.1-9.

FIG. 1.1.1.1-8

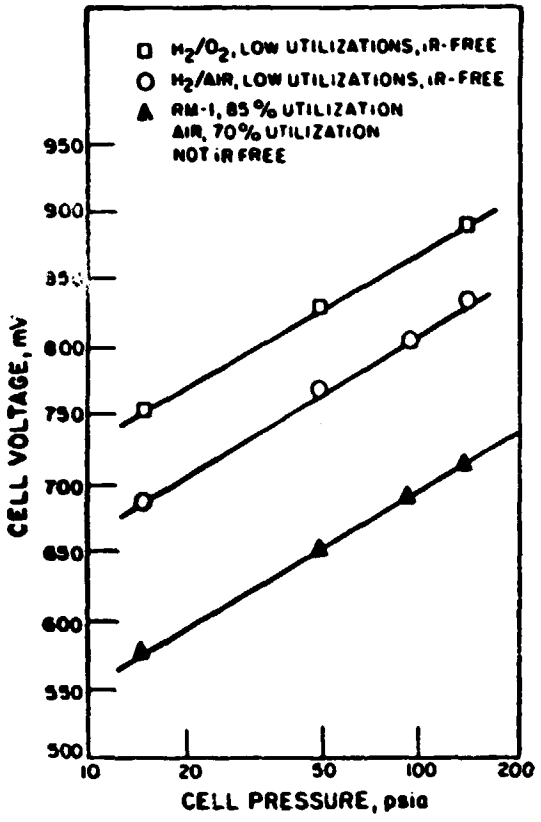

EFFECT OF PRESSURE ON PHOSPHORIC ACID FUEL CELL VOLTAGE

375°F CELL TEMPERATURE , 190°F ANODE DEWPOINT, 300 ASF

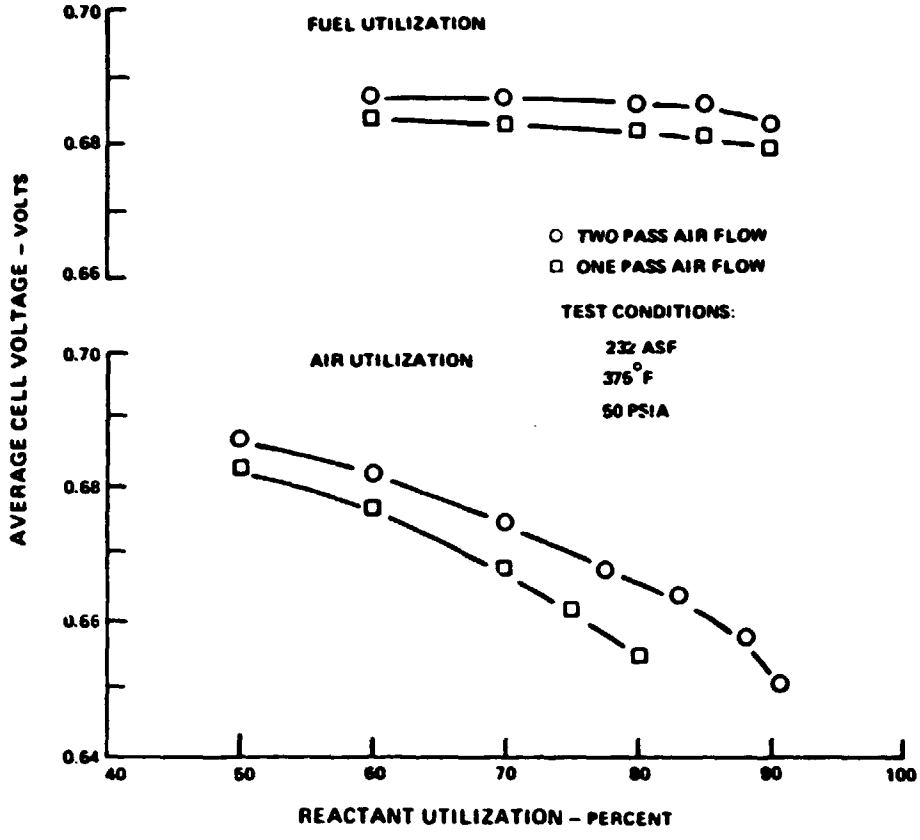

EFFECT OF REACTANT UTILIZATION ON PHOSPHORIC ACID FUEL CELL PERFORMANCE

$$\Delta V_{H_2} \text{ (mV)} = 77 \log \frac{(P_{H_2})_2}{(P_{H_2})_1} \qquad (1.1.1.1\text{-}6)$$

The hydrgoen partial pressures are average values at the anode.

Reactant Utilization

The effect of reactant utilization on a fuel cell is shown in Fig. 1.1.1.1-9. There is a definite increase in cell voltage resulting from high oxidant utilization while the level of fuel utilization has little effect on fuel cell voltage. This data resulted from a test to evaluate a possible approach to achieve high utilization without incurring increased concentration polarization.

Reactant Composition Effects

The ever widening selection of hydrocarbon fuel processing techniques have presented the fuel cell with a wide range of fuels from which hydrogen can be obtained. Knowledge of the various compounds especially the carbon, sulfur, and nitrogen compounds which could effect the fuel cells is important.

Carbon Compounds

Anode feeds derived from hydrocarbons will contain varying amounts of methane, carbon dioxide, and carbon monoxide depending upon the fuel processing techniques used. Both methane and carbon dioxide are inert in the phosphoric acid fuel cell acting as a diluent. Carbon monoxide, however, will poison the platinum catalyst. Consequently, the level of CO in the fuel gas must be controlled. It is possible to mitigate somewhat the effect of CO on the anode by increasing the cell temperature (Fig. 1.1.1.1-10). Although relatively minor temperature increases will extend the acceptable CO level significantly, the reverse is also true, a minor temperature decrease in an operating cell could quickly lead to anode poisoning.

The low CO levels necessary for the operation of the acid fuel cell can be achieved by conventional water-gas shift technology. Utilizing two beds operated at 315-485 C and 175-350 C, respectively, the CO levels can be reduced to 0.05-0.5 percent. With recent developments in sulfur-tolerant shift catalysts, these low concentrations can also be achieved in the presence of H_2S.

Sulfur Compounds

Advanced fuel processors operating on sulfur-containing fuels will produce H_2S that will enter the anode if not first removed. Testing of a fuel cell running on fuel gas containing 130 to 200 ppm H_2S was characterized by long

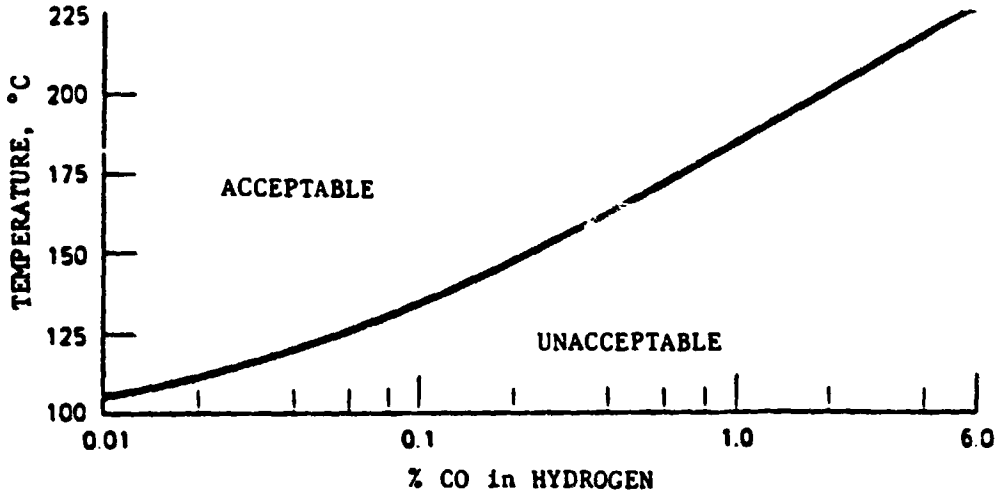

EFFECT OF TEMPERATURE ON PHOSPHORIC ACID FUEL CELL ANODE CO TOLERANCE

periods of stable operation followed by rapid decay. The original performance could be restored by removing either CO or H_2S fron the anode gas, indicating a synergistic effect, or by increasing the cell temperature from 375 to 400 F. The mechanism of H_2S-CO poisoning is not well understood. Post-test analysis of electrodes from shorter term cells showed no observable changes attributable to exposure to H_2S containing anode gas. Work to broaden the understanding of the CO-H_2S interaction in the phosphoric acid fuel cell is continuing.

While the technology for H_2S removal is commercially available, the necessity to remove large amounts of H_2S may cause considerable logistic problems or unrealistic system complexity, particularly with small dispersed power stations.

Nitrogen Compounds

Nitrogen will be present at the cathode of an air-consuming fuel cell, and nitrogen-containing hydrocarbon feedstocks will introduce nitrogen compounds (NH_3, HCN, NO_x) into the anode. In addition, nitrogen compounds can result if nitrogen-free hydrocarbons are processed with air such as in autothermal reforming or coal gasification. The nitrogen in this case will be primarily molecular nitrogen, which acts as a diluent. Data on the interaction of nitrogen compounds other than ammonia have not been found in the literature.

Ammonia reacts with the phosphoric acid electrolyte to form ammonium dihydrogen phosphate (ADHP) according to:

$$H_3PO_4 + NH_3 \rightarrow (NH_4)\ H_2PO_4 \qquad (1.1.1.1\text{-}7)$$

The formation of the ADHP results in a performance loss, possibly by changing the conductivity of the acid or by reducing the activity of the platinum by covering the active sites.

Summary

Data for other possible impurities have not been reported but estimates of maximum allowable levels are summarized in Table 1.1.1.1-1.

Fuel Processor and Power Conditioner

The fuel processor and the power conditioner are the two other subsystems beside the fuel cell power subsystem which comprise a fuel cell power generation system.

Fuel Processor

A number of studies have indicated fuel cell systems could operate efficiently with the potential coal-derived fuels. The principal effect of utilizing different products will be on the amount and complexity of fuel processing equipment required. This is illustrated in Table 1.1.1.1-2.

TABLE 1.1.1.1-1

ESTIMATED MAXIMUM ALLOWABLE IMPURITY LEVELS
PHOSPHORIC ACID FUEL CELLS

Impurity	Maximum Limit
CO_2	diluent
CH_4	diluent
N_2	diluent
CO	Figure 1.1.1.1-10
H_2S, COS	100 ppm
C_2^+	100 ppm
C_1^-	< 1 ppm
NH_3	< 1 ppm
Metal ions (Fe, Cu, etc.)	nil

TABLE 1.1.1.1-2

FUEL PROCESSING EQUIPMENT REQUIREMENTS FOR DIFFERENT COAL PRODUCTS IN PHOSPHORIC ACID POWERPLANTS

Coal Product	Fuel Processing Equipment				
	Reformer	Shift Converters	Water Recovery	Water Conditioning	Steam Generation
High Btu Gas (SNG) 1000 $\frac{BTU}{Ft^2}$	X	X	X	X	X
Medium Btu gas (H_2; CO) 325 $\frac{BTU}{FT^3}$	-	X	X	X	X
Medium Btu Gas (H_2) 325 $\frac{BTU}{Ft^3}$		-	-	-	-
Liquid Product (Naphtha or Methyl Fuel)		X	X	X	X

Alternatives to the steam reforming are being investigated to achieve the capability of processing fuels containing substantial levels of sulfur and unsaturated hydrocarbons. Emphasis is being placed on operation at higher temperature to achieve near complete fuel conversion over suitable catalysts.

Power Conditioner

The power conditioning subsystem converts the dc current from the fuel cell stacks to alternating current and controls its flow into the utility network. This function is accomplished through the use of solid state inverters. The ac voltage output from the inverters is stepped up through transformers to the desired level for utility distribution. Elimination of the power conditioning equipment will result in a dc voltage output which varies from a maximum value at low loads to approximately 75 percent of this voltage at rated power.

The power conditioner now available appears to be satisfactory for current fuel cells and more advanced cells.

1.1.1.2 Molten Carbonate Fuel Cell Power Systems

State-of-the-art molten carbonate cells operate at 650 to 700 C and up to 10 atmospheres. The cell voltage is 0.7 to 0.9 volts/cell at 100 to 150 amps/ft^2. The present molten carbonate fuel cell technology is at least five years behind the phosphoric acid fuel cell technology. A fuel cell power system utilizing a molten carbonate fuel cell could be 45 to 50 percent efficient. It is too early in the development of the molten carbonate fuel cell to accurately predict the final cost for the power system.

The endurance of molten carbonate fuel cells is still under investigation with small-scale cells logging more than 10,000 hours. To date the benchmarks in molten carbonate development have included thermal cycling of a 20-cell stack with 12" x 12" cells and 1000 hours of operation of a 10" x 10" cell.

Principles of Operation

In the molten carbonate cell (see Fig. 1.1.1.2-1) the electrolyte is a mixture of alkali metal carbonates (a molten ionic conductor at the cell operating temperatures of 600 to 700 C) and ceramic particulates that retain the liquid. Fuel enters the anode, and the H_2 reacts* at the anode/electrolyte interface according to:

$$H_2 + CO_3^{=} \rightarrow H_2O + CO_2 + 2e^- \qquad (1.1.1.2\text{-}1)$$

* Carbon monoxide in the fuel can also be oxidized, but a more favorable reaction for the conversion of CO is via conversion to hydrogen by the shift reaction, $CO + H_2O \rightarrow CO_2 + H_2$. The hydrogen formed is then consumed according to 1.1.1.2-1.

FIG. 1.1.1.2-1

$$H_2 + CO_3^{=} \rightleftharpoons H_2O + CO_2 + 2e^-$$

$$CO_2 + 1/2\ O_2 + 2e^- \rightleftharpoons CO_3^{=}$$

$$H_2 + 1/2\ O_2 \rightleftharpoons H_2O$$

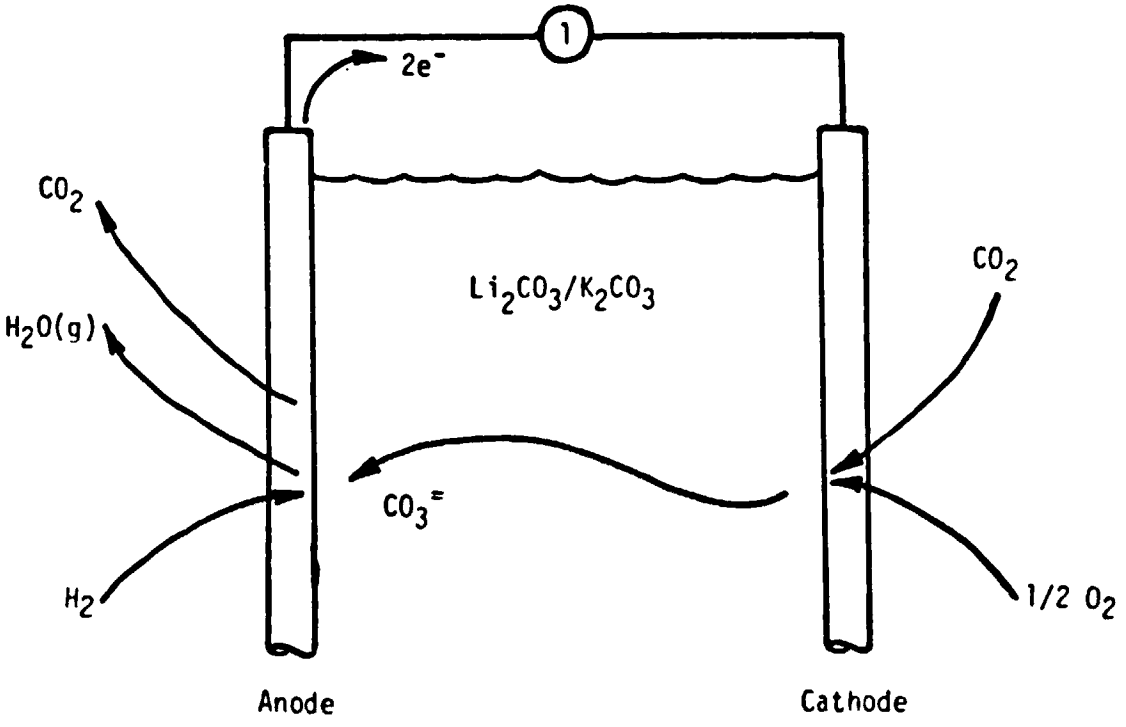

MOLTEN CARBONATE FUEL CELL

The product H_2O and CO_2 diffuse out of the electrode. At the cathode, the following reaction takes place:

$$CO_2 + 1/2\ O_2 + 2e^- \rightarrow CO_3^= \qquad (1.1.1.2\text{-}2)$$

Note that CO_2 is formed at the anode and consumed at the cathode. For an efficient molten carbonate fuel cell system, the CO_2 in the anode effluent must be recycled back to the cathode. This could be accomplished by catalytic combustion of the anode effluent to CO_2 and H_2O plus N_2 in the combustion air), followed by mixing with air to produce the cathode feed.

Cell Components

A schematic of one repeating element in a stack of molten carbonate fuel cells is shown in Fig. 1.1.1.2-2. The electrolyte tile is held in place between the two stainless-steel cell housings that form the anode and cathode cavities. The holding force maintains low-resistance contacts between the electrodes and the stainless steel current collectors and causes the housings to bite into the electrolyte tile, forming a wet-seal that prevents leakage of fuel from the anode chamber and oxidant from the cathode chamber. In a stack of several cells (series connection) the cell separator must be able to withstand both the high-humidity reducing environment of the anode and the oxidizing environment of the cathode.

Carbon dioxide and oxygen diffuse from the bulk gas through the pores of the cathode to a reaction site at the electrode/electrolyte interface. The cathode is 70 percent to 80 percent porous NiO with a mean pore size of about 10 μm, formed by the oxidation of sintered nickel at operating temperatures. The $CO_3^=$ is conducted through the liquid electrolyte (a mixture of alkali carbonates 62 or 50 mole-percent Li_2CO_3 and balance K_2CO_3) molten at cell operating temperatures. The electrolyte is held in place by inert $LiAlO_2$ particles to form the electrolyte tile (40-weight percent inert, 60-weight percent electrolyte). Because iR loss is a function of tile thickness, tiles are kept as thin as possible, 1.0 to 2.5 mm in current cells. The carbonate ions react at the anode/electrolyte interface. The anode is sintered nickel about 60 percent to 70 percent porous with a 5 μm mean pore size. The product H_2O and CO_2 diffuse out of the cell through the porous anode into the gas stream.

One of the major goals of current molten carbonate programs is to fabricate cell stacks containing a large number of cells of sufficient size to produce a significant power level. One of the most notable achievements in molten carbonate fuel cell development has been the extension of current density by a factor of four yet maintaining a promising level of cell endurance. Other improvements are: 1) electrolyte change to the current Li_2CO_3/K_2CO_3 alkali carbonate eutectic which increased initial cell performance; 2) the anode structure was stablized by adding sintering inhibitor to the nickel, and 3) the use of thinner electrolyte tiles reducing iR losses.

FIG. 1.1.1.2-2

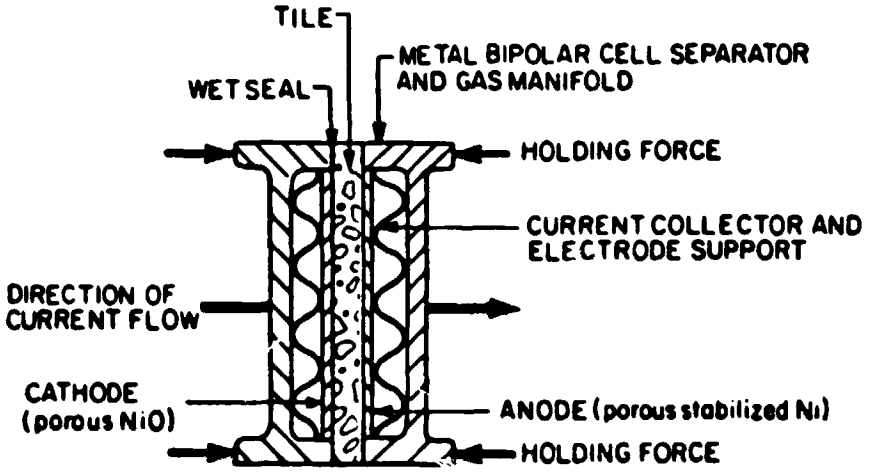

MOLTEN CARBONATE FUEL CELL CROSS SECTION

General Performance Considerations

For a cell operating on reformed natural gas fuel at 75-percent total H_2 utilization and on an oxidant mixture of 70-percent air and 30-percent CO_2 utilization, at 200 mA/cm^2, losses are approximately 68 mV ohmic and 260 mV polarization with anode polarization losses being greater than those at the cathode. Of course, these losses depend on the fuel cell operating variables. Consequently, for the purposes of this discussion, molten carbonate fuel cell performance at atmospheric pressure and 650 C, using a cell operating on simulated reformed methane fuel (the composition is 60 mol % H_2 10 mol % CO, 7.4 mol % CO_2, and 22.6 mol % H_2O) at low utilization and on an oxidant consisting of 67-mole percent CO_2 and 33-mole percent O_2 at low utilization, will be considered as baseline. The electrolyte tile composition is 40-weight percent inert $LiAlO_2$ particles to provide structural integrity and 60-weight percent binery eutectic mixture of Li_2CO_3 and K_2CO_3 as the electrolyte. The baseline performance is shown in Fig. 1.1.1.2-3.

Temperature Effects

As the molten carbonate fuel cell operating temperature is increased through its range of 600 to 700 C, hydrogen is consumed for a gas in water gas shift equilibrium. Because standard cell potential also decreases with increasing temperature, the open-circuit potential decreases as temperature increases: However, ohmic, activation, and concentration polarizations all decrease, more than offsetting the decrease in the open-circuit potential. The net result is an increase in cell performance with the anode being only slightly affected by changes in cell temperature.

A plot illustrating the potential voltage gains is provided in Fig. 1.1.1.2-4. There is a discontinuity in the curve at 650 C with a diminishing gain in performance at temperatures greater than 650 C. This diminishing gain coupled with increased electrolyte loss resulting from evaporation and increased component corrosion, point to an optimum operating temperature of 650 C for molten carbonate fuel cells with an electrolyte tile composed of 40-percent $LiAlO_2$, 28-percent K_2CO_3, and 32-percent $LiCO_3$ by weight.

Pressure Effects

Cell performance increases with pressure because of increased reactant partial pressures, increased reactant solubilities, and increased mass transport rates. Higher pressures tend to favor carbon formation and consumption of CO and H_2 fuel. The addition of water controls carbon formation, because it reduces the amount of CO and methanation. However, strict pressure control is required to prevent reactant leakage through the electrolyte and seals, to provide compatibility with the fuel processor, and to inhibit the possible corrosion of cell components at the higher pressure which molten carbonate fuel cells are expected to operate (1 and 10 atmospheres).

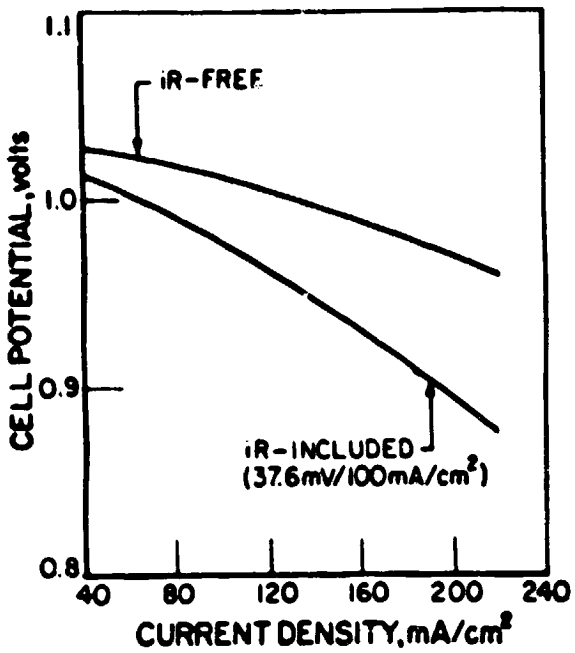

BASELINE MOLTEN CARBONATE FUEL CELL PERFORMANCE

1 Atm, 650° C, 67 Mol % CO_2/33Mol % O_2 OXIDANT AT 15% UTILIZATION, AT 25% UTILIZATION

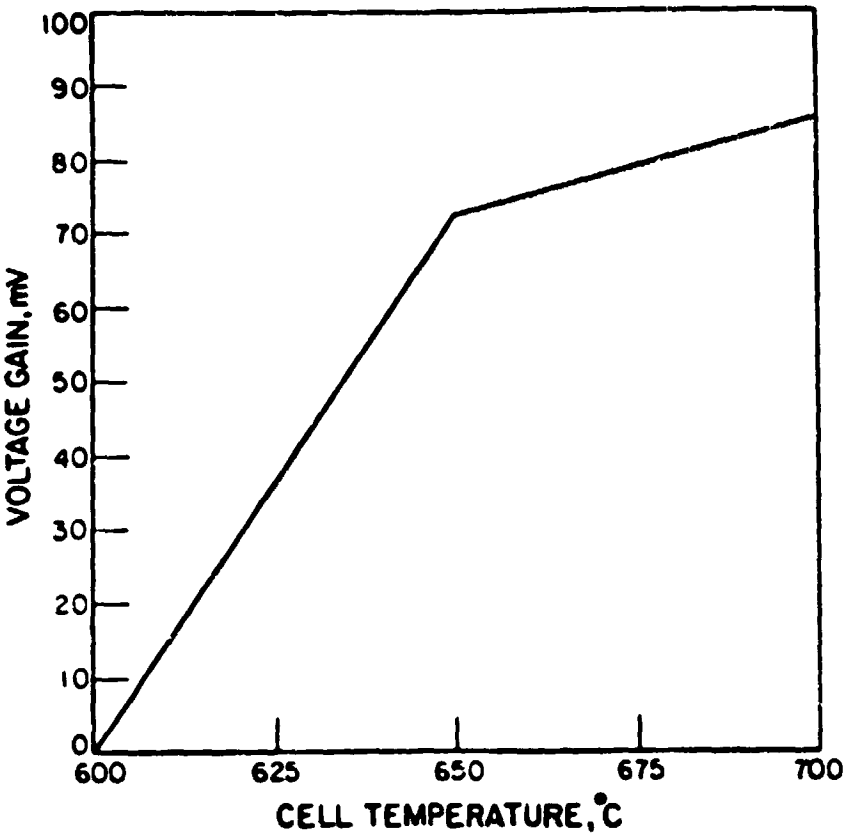

EFFECT OF TEMPERATURE ON MOLTEN CARBONATE FUEL CELL PERFORMANCE

1 Atm, 200 mA/CM^2, 70 Mol % AIR/30 Mol % CO_2 OXIDANT
AT 50 % UTILIZATION ,75 % FUEL UTILIZATION

The effect of cell pressure on cell performance is displayed in Fig. 1.1.1.2-5. For the product gas of an air-blown, low-Btu coal gasifier, the relationship between changes in cell performance and operating pressure in atmospheres is:

$$\Delta V_p(mV) = 70 \log \frac{P_2}{P_1} \qquad (1.1.1.2\text{-}3)$$

and for reformed methane, it is

$$\Delta V_p(mV) = 83 \log \frac{P_2}{P_1} \qquad (1.1.1.2\text{-}4)$$

Because these two cases represent a wide range of gas composition, other fuels should obey the average relationship:

$$\Delta V_p(mV) = 76.5 \log \frac{P_2}{P_1} \qquad (1.1.1.2\text{-}5)$$

Reactant Utilization Effects

The effect of reactant utilization on molten carbonate fuel cell performance is difficult to analyze because of the participation of CO at the anode via the water-gas shift reaction and because of consumption of CO_2 and O_2 at the cathode.

Oxidant

According to the Nernst equation, (see Appendix A.1) performance should be related to oxidant (CO_2 and O_2) partial pressure. However, at low oxidant partial pressure (high utilization), the gains are caused by diminishing mass transfer effects in addition to the Nernst gains. As the partial pressure increases, mass transfer effects become negligible and the gains become governed by Nernst effects.

Fuel

The performance related to the fuel partial pressure is directly related to the Nernst equation.

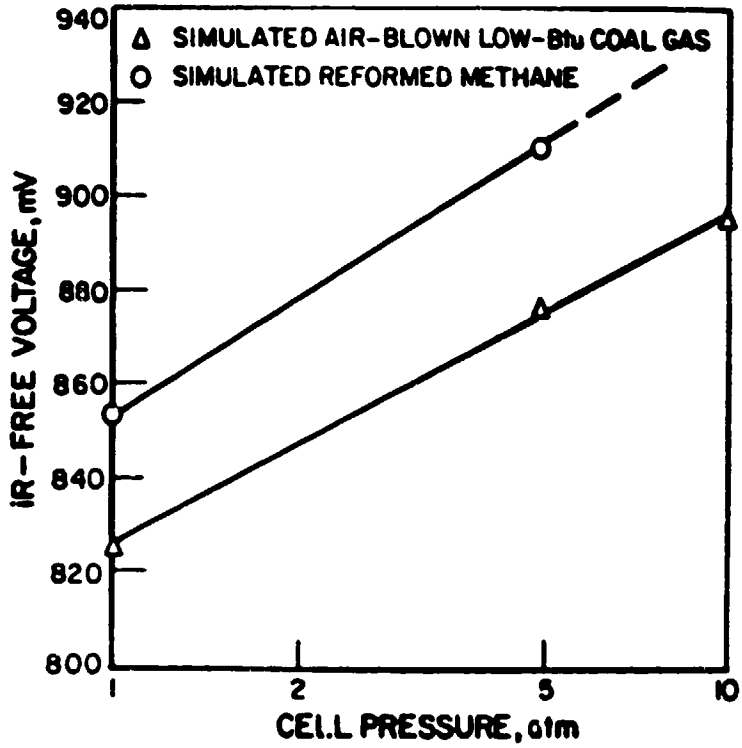

EFFECT OF PRESSURE ON MOLTEN CARBONATE FUEL CELL PERFORMANCE

650° C, 160 mA/CM^2, 70 Mol % AIR/30 % Mol CO_2 OXIDANT
AT 50 % UTILIZATION, 75 % FUEL UTILIZATION

Reactant Utilization

The data of Fig. 1.1.1.2-6 is representative of data published on reactant utilization. The data indicate that increasing oxidant utilization (decreasing oxidant partial pressure) causes less cell potential loss than increases in fuel utilization. Once again a compromise is required, because operating at low fuel utilization increases cell performance but decreases the current efficiency. Current molten carbonate fuel cells commonly run at 75 to 85-percent fuel utilization and 50-percent oxidant utilization.

Reactant Composition Effects

The question of molten carbonate fuel cell tolerance to coal-derived contaminants is inherently complex. One problem is that the identity and concentration of expected contaminants is highly variable and depends upon the particular coal sample and its pretreatment. Further, even when well defined "synthetic" contaminants are to be evaluated -- the effect on the fuel cell may be dependent upon the concentrations of other components in the fuel or oxidant, the degree of fuel/oxidant utilization, the cell voltage, and the cell current density. Finally, experiments with low contaminant concentrations are difficult to carry out and evaluate conclusively.

Many discussions have centered on integrating the molten carbonate fuel cell with advanced fuel processors because of its tolerance to CO at the anode and CO_2 at the cathode. Other compounds likely to be present in the effluent of advanced fuel processors include NH_3, NO_x, SO_x, H_2S and COS.

Carbon Compounds

Solid carbon can form in the cell or in system plumbing. The addition of water prevens carbon deposition by reducing CO concentrations through the water-gas shift reaction. Carbon dioxide present in the anode feed and produced at the anode acts only as a diluent, reducing the hydrogen partial pressure. In fact, a small amount of CO_2 is required to maintain the $LiCO_3/K_2CO_3$ electrolyte composition. Of course, CO_2 is required at the cathode. Although carbon monoxide dilutes the hydrogen, it is also consumed indirectly through the water-gas shift reaction.

Methane at the anode can be reformed to hydrogen by adding sufficient water to the fuel gas. If the methane is not reformed, fuel cell efficiency will decrease; energy in the methane must be recovered elsewhere in the system to maintain the total system efficiency.

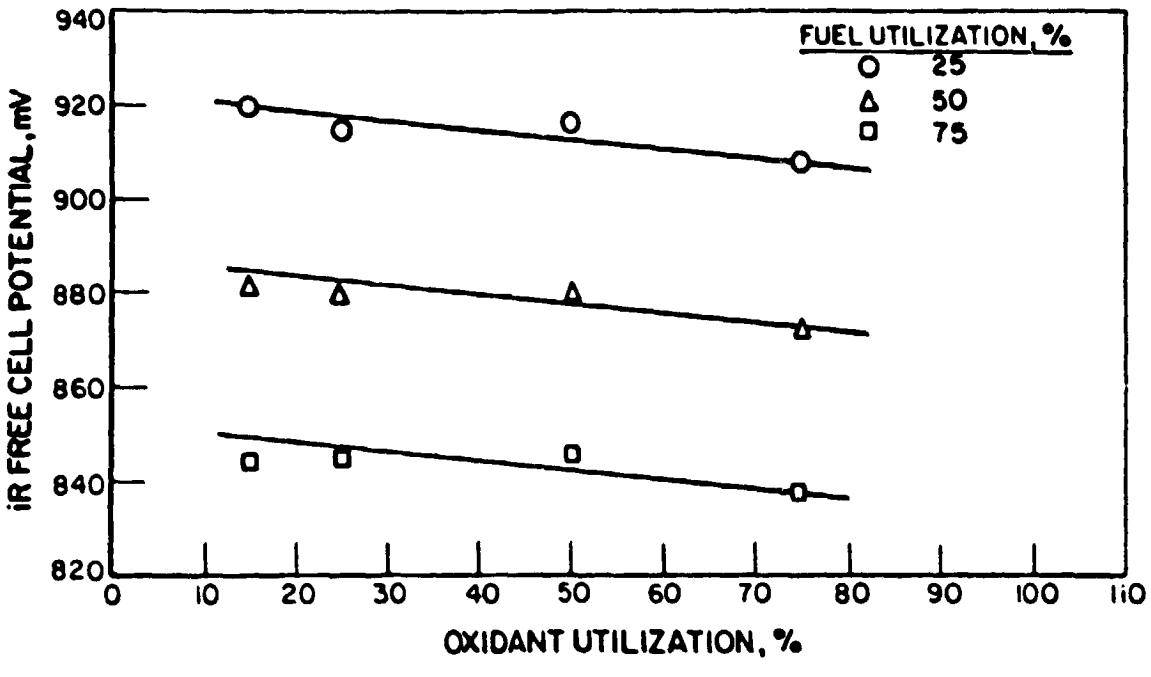

EFFECT OF REACTANT UTILIZATION ON MOLTEN CARBONATE FUEL CELL PERFORMANCE

1 Atm, 650°C, 160 mA/CM^2, 70 Mol % AIR/30 Mol % CO_2 OXIDANT,
SIMULATED REFORMED METHANE FUEL

Sulfur Compounds

Sulfur initially reaches the cathode in the form of SO_2 and SO_3. Sulfur entering the cathode will tend to form $SO_4^=$ ions in the electrolyte. These ions will be transported through the electrolyte along with the predominant $CO_3^=$ ions, reacting at the anode to form additional H_2S and COS. Thus a concentration of sulfur will take place in the cell, reaching some steady state distribution along the cell with the highest sulfur levels at the anode outlet and cathode inlet.

The presence of sulfur in the cell creates several caverns. A first concern would be what effects the sulfur will have on the anode where the sulfur, as predominately H_2S, can sulfidize the nickel electrode, poison the surface of the catalyst by chemisorption, or create a mixed potential by entering into an electron exchange reaction. A second concern is the effect of sulfur on the cathode compartment, where as SO_2 or SO_3 it might cause sulfidation of the electrode. A third concern is the effect of sulfur in the electrolyte where it can affect the transport of the $CO_3^=$ ions, alter the chemistry of the $LiAlO_2$ support material within the electrolyte matrix (tile), and form sulfides, sulfites and sulfates. A final concern is the effect of sulfur on corrosion of cell hardware and system plumbing.

Nitrogen Compounds

Molecular nitrogen at the anode or cathode acts as diluent. The presence of NH_3 and NO_x is also expected at both anode and cathode, but no data on the effect of these impurities on cell performance are available, although the $K_2CO_3/Li_2CO_3/Na_2CO_3$ eutectic is known to absorb NO.

Chlorine Compounds

Like sulfur, chlorine compounds are anticipated in a coal-derived fuel gas. Recent short-term data indicate that anode performance is only slightly affected after 400 hours on a fuel gas containing 100 ppm HCl, but cathode performance is catastrophically affected by 100 ppm HCl in the oxidant gas. Stable cathode performance with 10 ppm HCl has been demonstrated for 120 hours. Although long-term trends have not been established, it appears that the decay results from both hardware corrosion and chlorination of the electrolyte.

Summary

A summary of the estimates for maximum allowable contamination limits is displayed in Table 1.1.1.2-1.

TABLE 1.1.1.2-1

ESTIMATED MAXIMUM ALLOWABLE IMPURITY LEVELS
MOLTEN CARBONATE FUEL CELLS

Impurity	Maximum Limit
CO_2	diluent
CH_4	diluent/fuel
CO	fuel
N_2	diluent
H_2S, SO_2, COS	< 1 ppm
C_2^+	unknown
HCl (anode)	100 ppm
HCl (cathode)	10 ppm
NH_3m NO_x	unknown
Metal ions (Fe, Cu, etc.)	unknown

1.1.2 Future Fuel Cell Development

The course of future fuel cell development has already been charted. Its milestones will be the successful achievement of the goals and the solving of the problems identified in current fuel cell programs. The following section will provide an identification of some of the major fuel cell investigations and an indication of the program objectives associated with the development of phosphoric acid or molten carbonate fuel cells. In addition a scenario of projected fuel cell development will be furnished. The sources for the data provided herein are presented in the accompanying Bibliography (Section 1.1.3).

1.1.2.1 Fuel Cell Programs

The major participants in the fuel cell program for electric utilities are EPRI (Electric Power Research Institute), DOE (Department of Energy), ANL (Argonne National Laboratory), TVA (Tennessee Valley Authority), UTC (United Technologies Corporation), GE (General Electric), IGT (Institute of Gas Technology), Westinghouse, and ERC (Energy Research Corporation).

EPRI Program

EPRI as the electric utility centralized research coordinating organization quite legitimately is playing a major role in fuel cell development. Not only does EPRI sponsor fuel cell programs but also assists in coordinating and guiding utility fuel cell research and development.

DOE/ANL Program

ANL has been assigned as technical manager of the DOE advanced fuel cell program, especially those utilizing carbonate as the electrolyte.

TVA Program

TVA is engaged in evaluating the feasibility of using coal-derived fuel gas as a fuel cell fuel. This evaluation will be carried out in part by actually operating a phosphoric acid fuel cell on coal-derived fuel gas.

UTC Program

UTC is working toward commercializing phosphoric acid fuel cell power plants. This activity includes, among others, participating with EPRI and DOE in the 4.8-MW demonstrator in New York City (see Appendix C.1), evaluation of manufacturing techniques to reduce phosphoric acid fuel cell fabrication costs, investigation of phosphoric acid technology to improve performance and increase lifetime, and development of molten carbonate fuel cells.

IGT Program

IGT is investigating the molten carbonate cell and its utilization with gasified coal.

GE Program

GE is active in molten carbonate cell investigation. Of special interest is the technical and economic problems of developing fuel assemblies and stacks. In conjunction with IGT, GE is evaluating cell lifetime.

Westinghouse Program

Westinghouse is currently involved in the investigation of a unique fuel cell cooling concept called DIGAS. This approach to stack cooling has the potential of improving performance while at the same time increasing endurance.

ERC Program

ERC has been active in phosphoric acid fuel cell development. They have teamed with Westinghouse and DOE to evaluate a 120-kw on-site fuel cell which will provide for electric power and thermal energy.

1.1.2.2 Program Objectives

Because of the different state of development of the phosphoric acid and molten carbonate fuel cells, the program goals differ and will be treated separately.

Phosphoric Acid

Although the phosphoric acid fuel cell system is on the verge of large-scale demonstration, a number of areas for possible improvement are still receiving attention. For example:

1. The platinum catalyst is expensive and suffers a reduction in surface area and performance due to sintering. The CO-poisoning problem mentioned earlier has been somewhat mitigated by operation at higher temperatures, however, increasing the temperature also increases the sintering. CO-tolerant catalysts such as mixtures of Pt, Rh and WO_3 have also been used.

2. Electrolyte is lost because of evaporation. This problem can be alleviated by incorporation of an electrolyte reservoir in the cell. However, this reservoir can increase concentration polarization in the cell, and the evaporated acid condenses downstream of the cell, creating corrosion problems.

3. The most difficult challenge concerns the irreversibility (severe activation polarization) and lack of understanding of the reduction of oxygen at the cathode. This area also offers considerable opportunity for improvement of the phosphoric acid fuel cell performance.

In addition to continued effort in the above areas it also necessary to continue development of the fuel cell system so as to meet the following cost and endurance goals for a commercially acceptable power plant:

1. Implementation of an improved cell stack concept which is necessary to reduce cell stack manufacturing costs and to provide sufficient electrolyte capacity for 40,000 hours of operation.

2. Incorporation of more corrosion resistant and stable materials and supported electrocatalysts in the fuel cell which are necessary to meet performance and life goals (9300 Btu/kWh heat rate for 40,000 hours).

3. Increasing cell operation pressure (to approximately 100 psia) and temperature (by approximately 30°F) to substantially improve power plant performance and reduce cost.

Accomplishment of these goals will produce an evolutionary improvement in technology. An example of such an improvement is shown in Fig. 1.1.2.2-1. The effect of a moderate increase in temperature and an increase in pressure has produced an improvement in performance as compared to the 4.8-MW demonstrator plant.

As a result of this evolutionary advance of technology it is anticipated that a phosphoric acid fuel cell, a decade hence, will not be unlike the current fuel cell.

Molten Carbonate

Although molten carbonate fuel cell technology has made impressive advances in the last decade, a number of questions concerning cell performance and life remain:

1. The sulfur and chlorine tolerance of the cell is only a few parts per million; the tolerance to other impurities has not been defined.

2. Electrolyte losses result in decreases in electrolyte tile strength and bubble pressure, increased tile porosity, and diffusion of reactants across the tile causing decreases in cell voltage and

FIG. 1.1.2.2-1

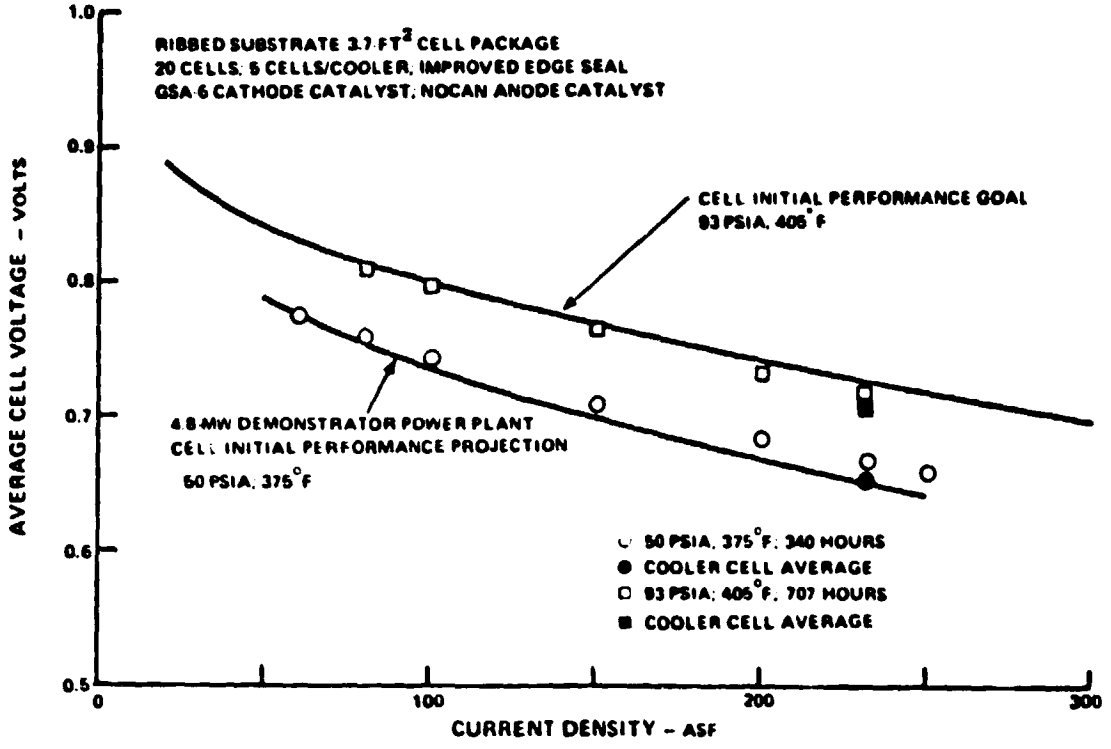

PERFORMANCE OF CELL AT VARIOUS OPERATING CONDITIONS

efficiency. A partial solution to the evaporation problem is the incorporation of a reservoir with enough electrolyte to achieve the design life of 40,000 hours. The electrolyte may not be evenly distributed, however, and redistribution can cause performance loss. In addition, new tile and electrode structures and materials that inhibit carbonate evaporation are being sought.

3. Electrolyte creepage and corrosion result in failure of the wet-seal and leakage of reactants out of the cell. The wet-seal is now protected by aluminizing although it is uncertain whether this approach will be effective for 40,000 hours.

4. Effects of structural changes in the electrolyte support ($LiAlO_2$) on cell performance have not been defined.

5. Cost-effective cell components (tile, electrodes, and hardware) and manufacturing techniques must be identified.

6. Transfer of the CO_2 from the anode to the cathode is desirable with physical separation of the CO_2 from the rest of the anode exhaust preferred. To date studies on the approach to achieving this are incomplete.

Programs are underway addressing these development areas. DOE in its program anticipates development of the molten carbonate fuel cell power plants to a point where 1) operation of a prototype fuel cell stack with simulated coal-derived fuel gas is possible by 1982; 2) operation of a prototype stack occurs in 1983; and 3) operation of an integrated multi-MW test facility is accomplished by mid-1985.

Other goals for the molten carbonate fuel cell include: 1) a power density of 135 mW/cm^2 of active cell area using low-Btu coal-derived gas at a cell voltage of 0.85 volts and 75-percent utilization; 2) an operating time between major overhauls of 40,000 hours; 3) removal of the contaminant H_2S down to the 1-10 ppm level; and 4) development of practical cell stack fabrication techniques.

Attainment of these goals will contiunue the impressive advance of molten carbonate fuel cell technology during the last decade which has seen almost a quadrupling of current density (Fig. 1.1.2.2-2) with potentially long lifetimes.

1.1.2.3 Fuel Cell Development Scenario

One possible scenario of future fuel cell development has been advanced by EPRI (Fig. 1.1.2.3-1). This timetable takes into account the current work being done on both the phosphoric acid and molten carbonate cell. Several assumptions were made in developing the timetable. One of the most important is that it is

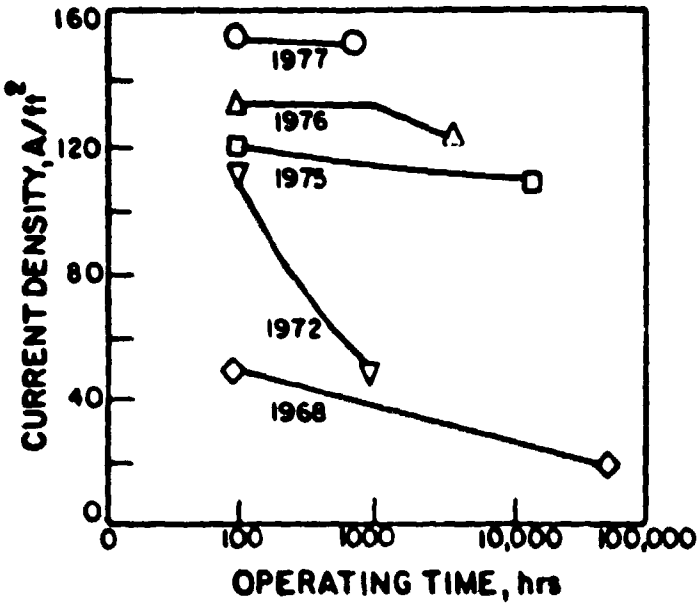

MOLTEN CARBONATE CELL PERFORMANCE HISTORY

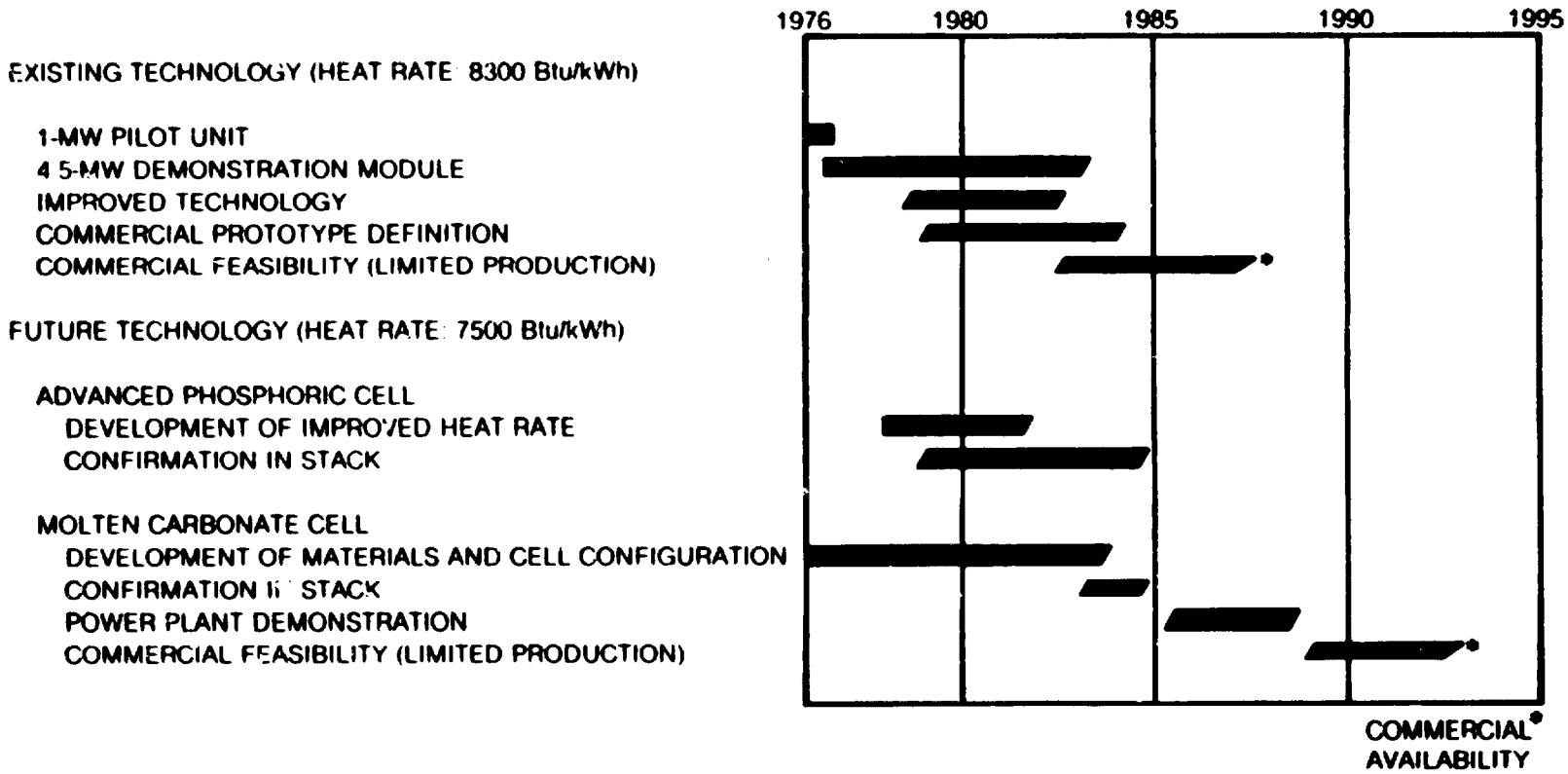

EPRI TIMETABLE OF FUEL CELL DEVELOPMENT

assumed that funding from the Federal government is forthcoming for the commercial prototype definition and commercial feasibility phases. Another equally important assumption is that a market will exit for the fuel cell. These two assumptions deserve further elaboration.

The first fuel cell power plants off the assembly line will not meet the goal of $350/kW, they can be offered at that price only after some 500-1500 MW worth have been mass-produced in a factory. More likely the first unit will cost about $1500/kW, with the cost of subsequent units decreasing by about 15% for each doubling of quantity, following a typical product learning curve. The eighth unit, for instance, should therefore cost $920/kW. However, the worth of these units to an electric utility will be somewhere between $330 and $600/kW, depending on such factors as how severely a utility's siting options are restricted.

Even in the best of times, it is unlikely a utility would invest $1500/kW for the first unit of an as yet immature technology. Nor are manufacturers likely to underwrite the 1500-MW learning curve. Consequently, in the EPRI scenario it is necessary for the federal government to assist the private sector in the commercialization process. Failure to do so could delay the timetable milestones to an unspecified later date.

1.1.3 Bibliography

1.1-1 Appleby, J. A.: Proceedings of the DOE/EPRI Workshop on Molten Carbonate Fuel Cells. EPRI Project WS 78-135, November 1979.

1.1-2 Bell, R. A. and W. A. Messner: Fuel Cells for Electric Utility Use. Proceedings of the 7th Energy Technology Conference, Washington, DC, March 1980.

1.1-3 Benjamin, T. G., E. H. Camara, and L. G. Marianowski: Handbook of Fuel Cell Performance. DOE Contract No. EC-77-C-03-1545, May 1980.

1.1-4 Berman, I. M.: Fuel Cells and Coal Derived Fuel. Power Engineering, October 1980.

1.1-5 Borys, S. S. and J. P. Ackerman: Molten Carbonate Fuel Cell Systems Development Program. Proceedings of the 14th IECEC, Boston, Mass., August 1979.

1.1-6 Breault, R. D., et al: Improved FCG-1 Cell Technology. EPRI Contract No. 842-5, October 1980.

1.1-7 Brownell, L. W., et al.: Development of Molten Carbonate Fuel Cells for Power Generation. DOE Contract No. AC03-77ET11319, April 1978.

1.1-8 Brownell, K. W. and F. N. Mazandray: Development of Molten Carbonate Fuel Cells for Power Generation. Proceedings of the 15th IECEC, Seattle, Washington, August 1980.

1.1-9 Christner, L. G., et al.: Scale-Up of Phosphoris Acid Fuel Cells. Proceedings of the 14th IECEC, August 1979.

1.1-10 Cusomano, J. S. and R. B. Levy: Assessment of Fuel Processing Alternatives for Fuel Cell Power Generation. EPRI Contract No. 919-1, October 1977.

1.1-11 Fickett, A. P.: Clean Power for the Cities. EPRI Journal, November 1978.

1.1-12 Fickett, A. P.: Fuel Cell Power Plants. Scientific American, December 1978.

1.1-13 Fickett, A. P.: Overview of the Electric Utilities Fuel Cell Program. Transaction of American Nuclear Society, June 1979.

1.1.3 Bibliography (Cont'd)

1.1-14 Hahn, K. W., T. E. Tang, and E. M. Camara: Effect of Temperature and Pressure on Molten Carbonate Fuel Cell Fuels and Performance. Proceedings of the 14th IECEC, August 1980.

1.1-15 Handley, L. M., et al.: Advances in Lower Cost Phosphoric Acid Fuel Cells. Proceedings of 13th IECEC, San Diego, Calif., August 1980.

1.1-16 Handley, L. M.: FCG-1 Power Plant Model Specifications. DOE Contract No. EX-76-C-01-2102, March 1980.

1.1-17 Improvement of Fuel Cell Technology Base. DOE Contract No. EY-76-C-03-1169, January 1978.

1.1-18 Khalsa, P. S. and L. Stamets: Commercial Status: Electrical Generation and Non-Generation Technologies. California Energy Commission, September 1979.

1.1-19 King, J. M. et al.: Integrated Coal Gasifier/Molten Carbonate Fuel Cell Powerplant Conceptual Design and Implementation Assessment. NASA Contract No. NAS 3-19586, October 1976.

1.1-20 King, J. M. et al.: Advanced Technology Fuel Cell Program. EPRI Project 114-1, October 1976.

1.1-21 King, J. M., W. E. Haughtby, and R. A. Thompson: Advanced Technology Fuel Cell Program. EPRI Project 114-2, December 1978.

1.1-22 Larson, E.: Fuel Cells in the Gas Industry. Proceedings of the 7th Energy Technology Conference, Washington, DC, March 1980.

1.1-23 Prokospius, P. R., et al.: Commercial Phosphoric and Fuel Cell Technology Development. Proceedings of the 14th IECEC, Boston, Mass., August 1979.

1.1-24 Technical Assessment Guide. EPRI Special Report SP-1201-SR, July 1979.

1.1-25 Venture Analysis Case Study for On-Site Fuel Cell Energy System. DOE Contract No. EA-77-C-01-2684, July 1978.

2.1 Description of Advanced Fuel Cell Power Systems

The two primary types of fuel cell discussed in Task 1 are the phosphoric acid and molten carbonate cells. Their relative performance and development status is shown in Fig. 2.1-1 in which the overall thermal efficiency of a number of integrated coal gasifier/fuel cell power plants are plotted as a function of the application time frame. As shown, it is possible to achieve efficiencies greater than 40 percent for systems integrating a coal gasifier with near-term phosphoric acid electrolyte fuel cells. In these, a gas turbine bottoming cycle was incorporated to recover power from the fuel cell exhaust. Systems studies with molten carbonate cells indicated potential efficiencies in the range of 45 to 60 percent depending on the degree of system integration, the type of bottoming cycle selected for waste heat recovery, and the technology assumed for the coal gasifier and the fuel cell.

The higher power plant efficiencies of molten carbonate systems result because at reasonable power densities, these cells offer higher efficiency than the near-term phosphoric acid cell. Higher cell performance results from reduced activation polarization at high temperature. In addition, since molten carbonate cells operate at high temperature, they derive increased benefit from integration with the bottoming cycle.

In this section, the characteristics of each type will be reviewed briefly, the potential system configurations and optimum operating conditions reviewed, and the resulting candidate systems described.

2.1.1 Operational Characteristics

Probably the most significant characteristic of a fuel cell is the potential that can be developed across the cell and the reduction in that potential with increasing current density. For good efficiency a high cell potential is desired, while for minimum capital cost high current density, hence reduced potential is needed. Other characteristics that are important to system performance and economics are such things as fuel utilization, air utilization, temperature gradient and pressure drop of the cooling gas. Because all of these require optimization on a system level, they are discussed fully in Section 2.1.2 and only the basic cell characteristics are presented here.

2.1.1.1 Phosphoric Acid Cell Characteristics

The acid cell is typified by the 4.8-MW demonstration plant which is intended to expedite the introduction and acceptance of fuel cells for use as dispersed generators. This 4.8-MW unit is currently being installed at a Consolidated Edison Co. site in New York City. While it is generally believed that the performance of that system is typical of future acid cell units, advanced development work is aimed at reducing the manufacturing cost and improving the durability of the cells to make them competitive with other generation methods. That work is being sponsored by Niagra Mohawk Northeast Utilities, TVA, EPRI and DOE (Ref. 2.1-1).

FIG. 2.1-1

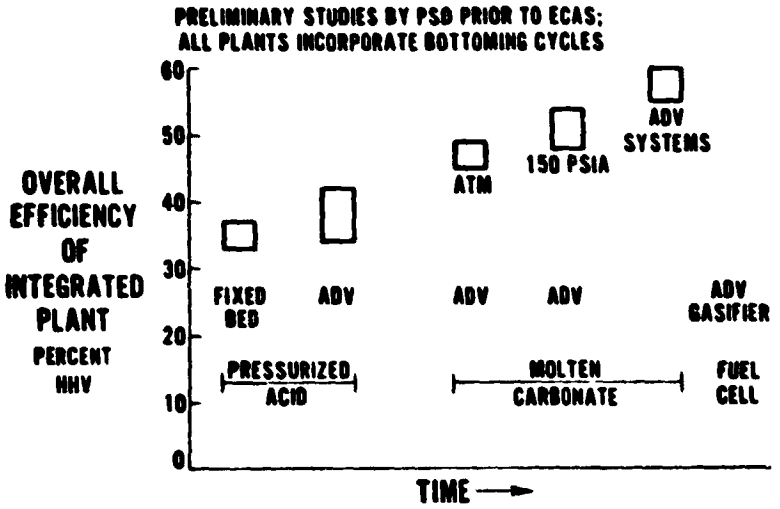

EVOLUTION OF INTEGRATED COAL GASIFIER/FUEL CELL POWER PLANTS

For the acid cell, Fig. 2.1.1.1-1 compares the development cell voltage vs current density for two different operating conditions. It also shows the initial projected performance which correlates closely with the test data.

The cell performance decay characteristics were evaluated at both the estimated rated-power level and the estimated minimum-power level of a power plant. The rated-power level was 232 ASF, 93 psia, 405°F with a cell potential of 0.65 V to 0.70 V. The minimum-power level was at 93 psia, 405°F and a current density that resulted in 0.79 volts per cell average. This minimum-power level condition, which is an overstress condition on the components' electrochemical stability, was found to cause a greater decay rate than when operating at rated-power conditions. The performance diagnostic testing indicates that this greater decay rate is due to both a loss in cathode catalyst activity and an increase in cathode diffusion losses. Figure 2.1.1.1-2 shows the cell performance history and the decay rates experienced in a development stack. Advanced cathode catalyst development activities in small cell tests have identified candidate cathode catalysts which demonstrate lower performance decay rates than the GSA-6 cathode catalyst shown in Fig. 2.1.1.1-2.

The compatibility of acid fuel cell stacks with operation on medium-Btu gaseous fuels is presented in Fig. 2.1.1.1-3. This data provides design analysis information useful for the evaluation of typical fuels available from coal gasification and the impact that such fuel compositions will have on power plant operation.

Another important cell characteristic is fuel and air utilization. Typical curves of reactant and air utilization have been shown in the previous section for both one- and two-pass air flow. Fuel utilization in the mid to high 80 percent range appears feasible. The FCG-1 demonstration unit has a target of 83 percent fuel utilization.

Of particular importance to the integration of the cell with a gasified coal fuel supply system is the tolerance of the cell to impurities in the hydrogen feed. Carbon monoxide, which is a major product of most gasification processes, acts as a poison to the platinum catalyst. The mechanism is believed to be that of a simple site-elimination and results in decreased activity at the anode. The effect on performance is shown in Fig. 2.1.1.1-4 (Ref. 2.1-2). Also shown is the beneficial effect of increased temperature in improving the cell tolerance to CO. It is clear that a relatively efficient shift conversion from CO to H_2 will be required not only to improve fuel utilization, but to avoid cell degradation.

Other carbon compounds, CO_2 and CH_4, common in gasifier off-gas streams, are reported not to be harmful and act only as a diluent. However, as with CO, the methane does represent a performance loss due to incomplete fuel utilization and if present in significant amounts would warrant special consideration.

The effect of sulfur compounds (H_2S and COS) on the cell is not well defined. The current approach for fuels containing more than .05 ppm sulfur is to catalytically hydrogenate the fuel, forming H_2S followed by absorption of the H_2S in

FIG. 2.1.1.1-1

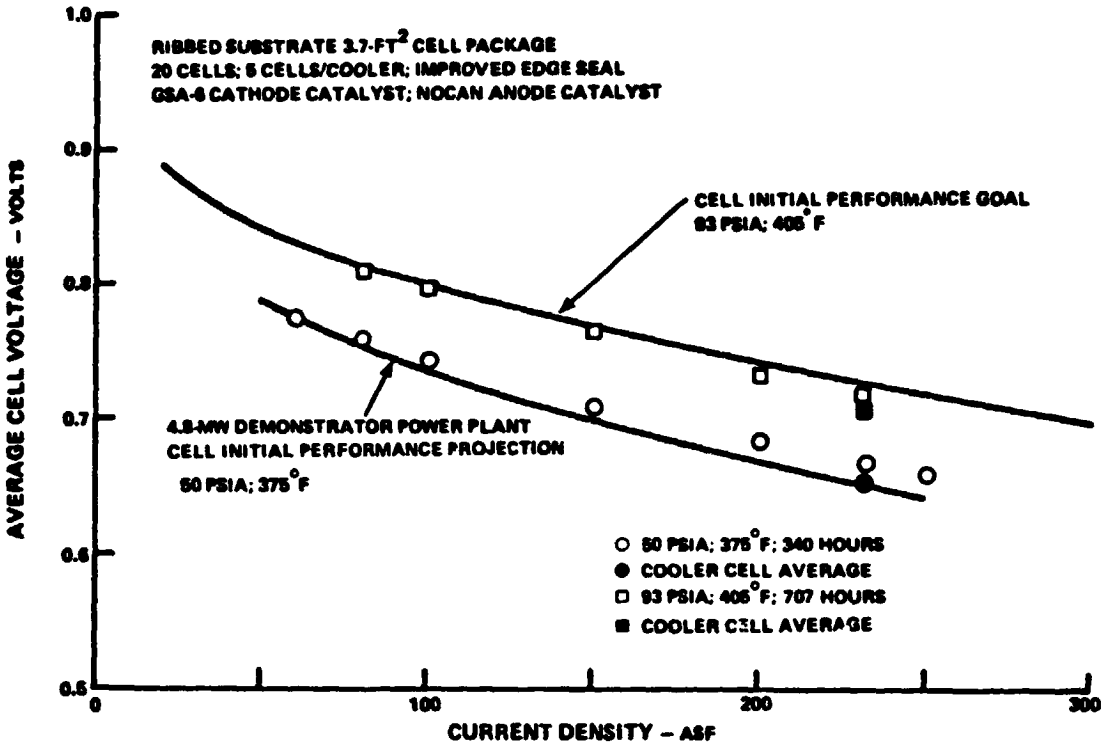

INITIAL PERFORMANCE OF 20-CELL, 3.7-FT^2, RIBBED-SUBSTRATE STACK

FIG. 2.1.1.1-2

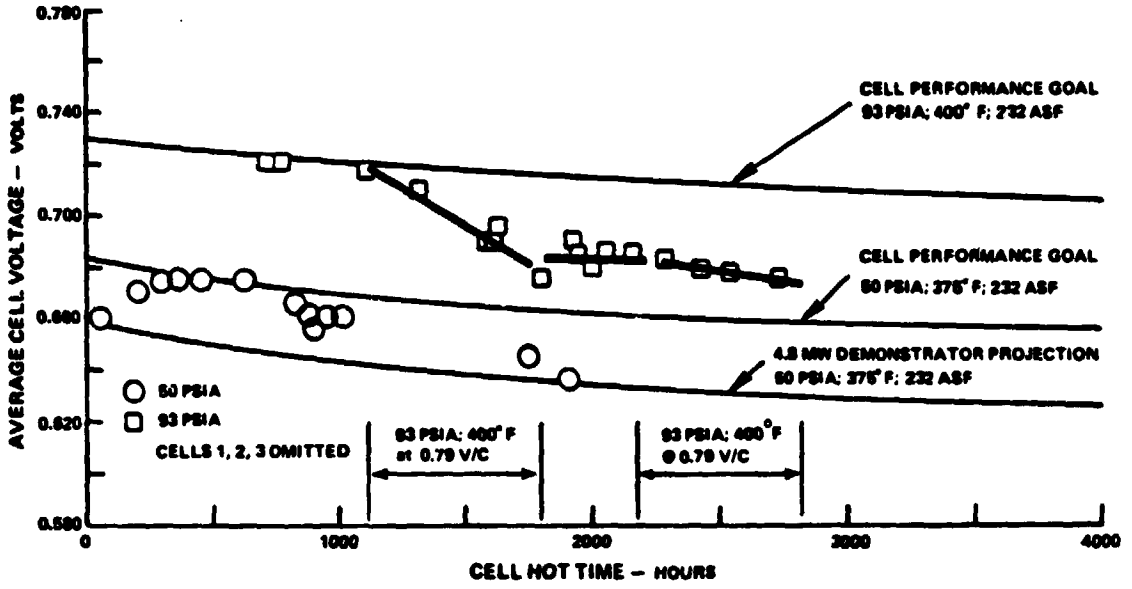

PERFORMANCE HISTORY OF 20-CELL, 3.7-FT^2, RIBBED-SUBSTRATE DEVELOPMENT STACK

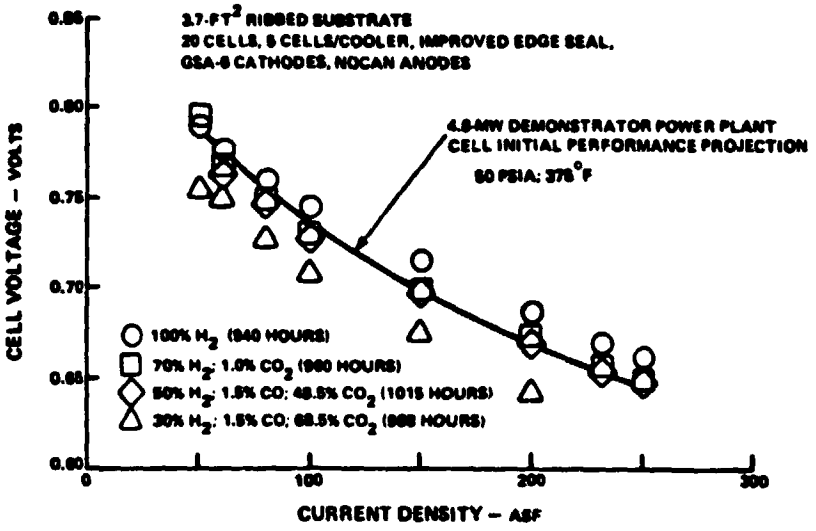

FUEL EFFECT ON PERFORMANCE FOR 20-CELL, 3.7-FT^2 RIBBED-SUBSTRATE STACK

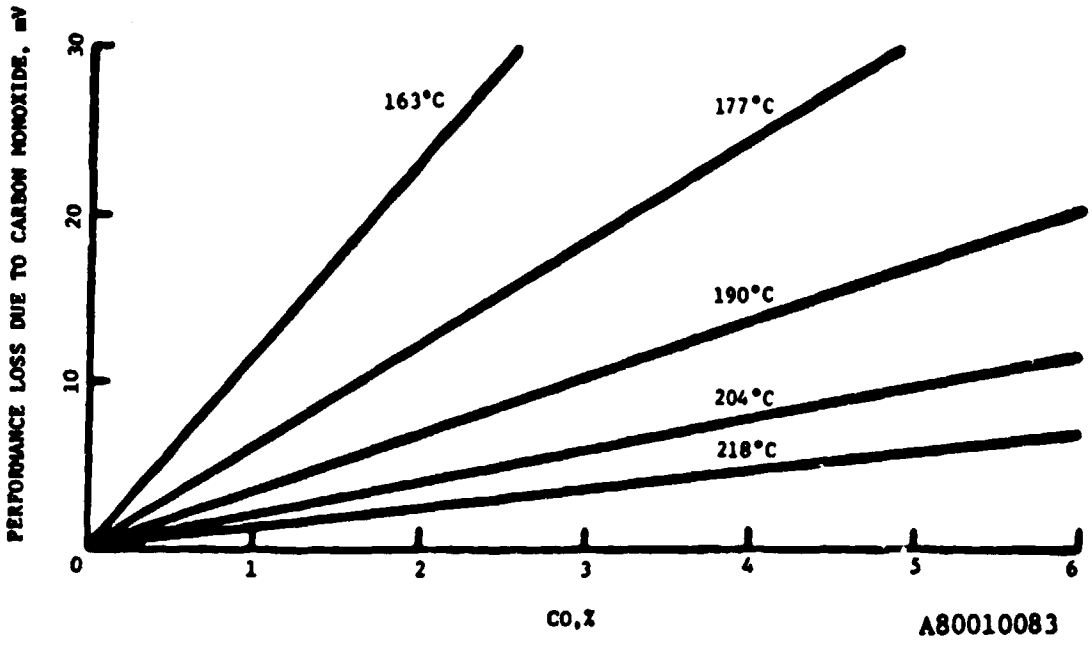

EFFECT OF CO CONTENT AND TEMPERATURE ON ANODE PERFORMANCE

0.35 mg Pt/CM^2,269 mA/CM^2

a bed of zinc oxide. As a result, there is virtually no sulfur in the feed and the catalysts in the fuel processing units and in the cell are not exposed to any significant amount of sulfur.

Subscale two-inch by two-inch cell tests have been carried out at UTC (Ref. 2.1-3) to determine the long term tolerance of phosphoric acid cells to the presence of H_2S in the fuel. One test cell was run for more than 2400 hours with 130 to 200 ppm H_2S added to the fuel. It showed long periods (900 hours) of stable operation followed by rapid performance decay. Performance could be restored by removal of CO from the fuel, removal of H_2S from the fuel, or by raising the cell temperature to 400 F.

The results of that testing are:

1. The long term tolerance of acid cells to H_2S in the fuel is not totally defined although over 2400 hours of operation on H_2S containing fuel has been demonstrated in a 2-inch x 2-inch cell.

2. The cell operated for periods up to 900 hours with 130-200 ppm H_2S in simulated reformer effluent with no decay.

3. Stable operation was followed by abrupt decay.

4. Post-test analyses of catalyst from a cell tested with H_2S added to the fuel showed no identifiable changes resulting from exposure to H_2S.

Ammonia is a common constituent of the gasifier off-gas. It reacts with the phosphoric acid electrolyte to form $(NH_4)\ H_2PO_4$, ammonium dihydrogen phosphate (ADHP). The formation of the ADHP results in a performance loss, possibly by changing the conductivity of the acid or by reducing the activity of the platinum by covering the active sites. Electrolyte conversion must be limited to less than about 0.2 mole percent to avoid unacceptable performance penalties. Diagnostic data on the cells tested indicate that most of the performance loss occurs at the cathode. Approximately 84 percent of the cathode activity is lost by conversion of only 1 percent of the acid to ADHP.

While the consequences of ammonia in the fuel gas appear severe, the resultant performance degradation is not irreversible. Long term tests have shown that the ADHP levels reach a constant value much lower than would be predicted by inlet ammonia concentrations. This, plus the fact that performance is restored when ammonia is removed from the feed, led to the hypothesis that the ammonium ion is oxidized at cell operating conditions. This has been confirmed by measurement of the current associated with the oxidation (Ref. 2.1-4).

In the design of a power system, each of the above characteristics must be considered and the optimum chosen on the basis of not only performance, but other important factors such as reliability and cost.

2.1.1.2 Molten Carbonate Cell Characteristics

A number of development programs are currently in progress or have already been reported on in the development of molten carbonate cell technology (Refs. 2.1-3 through 2.1-11). The questions concerning cell performance and cell life that remain to be investigated are summarized in Ref. 2.1-12.

These problem areas include loss of electrolyte, failure of the wet seal with reactant leakage, effect of structural changes on performance, cost-effective manufacturing techniques and tolerance to impurities such as sulfur and chlorine. The last of these is an important factor in the integration of the fuel cell with a coal gasification and fuel gas cleanup system. While the tolerance to these impurities has not been fully defined, present studies are based on the premise that sulfur removal must be down to a level of less than 1 ppm. In general, this is most economically achieved by a combination of a regenerable removal system followed by a zinc oxide bed.

The basic cell design has been discussed previously. The overall cell reaction is simply the combination of one mole of hydrogen with one-half mole oxygen to produce water, electrical power and heat. Unlike the acid cell, carbon monoxide is not detrimental to performance and, in fact, is utilized by the cell since the water gas shift reaction is catalyzed by the anode ($CO + H_2O \rightleftarrows CO_2 + H_2$). The catalytic qualities are not all beneficial however, and under certain conditions solid carbon may be formed ($2CO \rightleftarrows CO_2 + C$). Additionally, methane which acts as an inert gas in the cell may be formed ($CO + 3H_2 \rightleftarrows CH_4 + H_2O$). Methane formation is harmful to performance since it passes through the cell without reacting.

Both carbon deposition and methane formation are enhanced by increased pressure. Thus, while high pressure operation is desirable from a performance standpoint, Fig. 2.1.1.2-1 (Ref. 2.1-13), care must be taken to eliminate the possibility of carbon formation and minimize methane formation. The humidification of the fuel gas stream has been found to be an effective means of helping achieve both goals.

The addition of water reduces the concentration of CO due to the water gas shift reaction. This is turn, reduces the likelihood of both carbon formation. Methane formation is controlled by the reduced CO concentration and the increased water vapor concentration. Cell operating pressure appears to be optimum at approximately 10 atm as will be discussed in the following section.

Cell operating temperature is based on a trade-off between ideal cell voltage, cell polarization and endurance. The electrolyte, which is comprised of a mixture of alkali metal carbonates in a ceramic matrix, is a solid at room temperature. The cell must be heated above the electrolyte melt temperature to provide the necessary ionic mobility to sustain cell reactions. As the temperature is increased beyond the melt point, the ideal cell voltage drops but the ionic mobility increases resulting in reduced polarization. The operating temperature range of the cell will be between 1100 and 1300°F (866 and 978°K); this permits waste heat to be removed as sensible heat in the cathode gas stream. A curve showing the composite effect of the variables is shown in Fig. 2.1.1.2-2 (Ref. 2.1-13). The knee of the curve, or point of diminishing return occurs at approximately 1200 F, which is the nominal cell operating temperature.

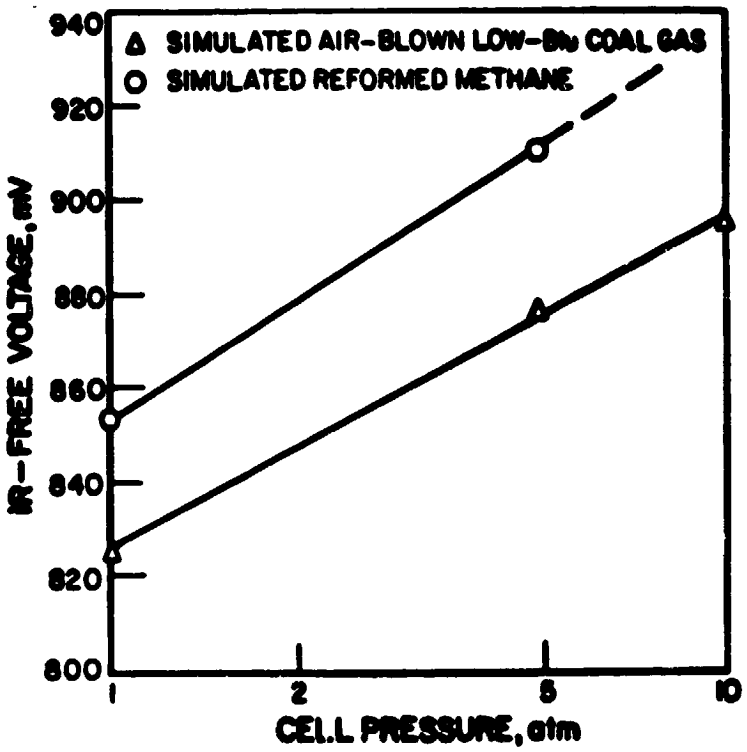

EFFECT OF PRESSURE ON MOLTEN CARBONATE FUEL CELL PERFORMANCE 650°C, 160 mA/CM^2, 70 MOL % AIR/30 % MOL CO_2 OXIDANT AT 50% UTILIZATION

75% FUEL UTILIZATION

FIG. 2.1.1.2-2

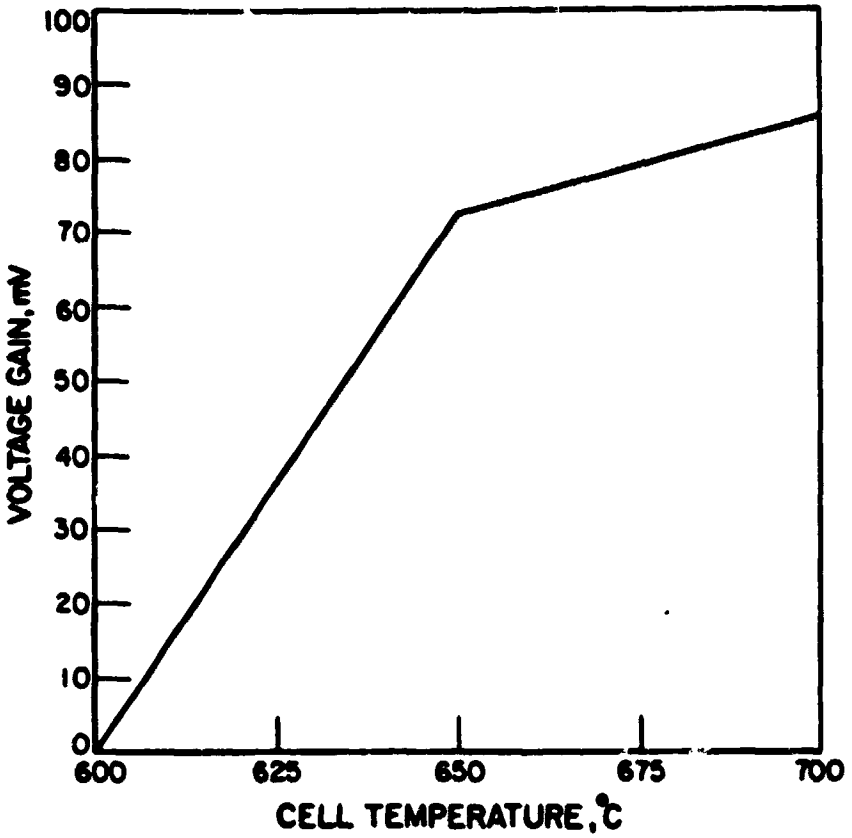

EFFECT OF TEMPERATURE ON MOLTEN CARBONATE FUEL CELL PERFORMANCE
1 atm, 200 mA/cm^2, 70 mol % AIR/30 mol % CO_2 OXIDANT AT 50% UTILIZATION
75% FUEL UTILIZATION

In addition to operating temperature and pressure, three other major parameters define cell operation characteristics. These parameters include the fuel and oxidant utilizations and the cell performance. Utilization is defined as the ratio of the reactant consumed by the cell to the reactant supplied to the cell. Reactant utilizations determine the variation in reactant partial pressure over the cell and therefore the ideal cell voltage and driving forces for reactant diffusion at each point in the cell. This is an important determinant of cell performance. Because CO is shifted to H_2 and consumed in the molten carbonate cell, fuel utilization is defined as the ratio of the H_2 consumed in the cell to the total H_2 plus CO supplied in the cell.

Fuel and oxidant utilization are subject to optimization on a system level. Cell performance is a measure of the degree of development of the carbonate cell. The unit of performance for fuel cells is the design power density per square foot of active cell area. Cell power density is the product of the voltage measured across the electrodes of each cell and the current density of the cell at that voltage. This unit of performance is analogous to the horsepower to weight ratio for gas turbines. Since the capital cost of the cell stack is proportional to total cell area, high power densities provide lower cost.

At the time of the ECAS study (Ref. 2.1-14), cell performance was estimated to be as shown in Fig. 2.1.1.2-3. For the current DOE development program the cell performance goal is shown in Fig. 2.1.1.2-4. A comparison shows that the slope of the curve has been reduced to approximately midway between the 1976 data and that projected for a demonstration unit in the ECAS study. Table 2.1.1.2-1 gives the operating conditions for the current program.

As mentioned earlier, fuel and oxidant utilization is a subject for system integration. For the carbonate cell, the effect of reactant partial pressures on cell performance is difficult to portray because of the participation of CO at the anode due to the water gas shift reaction and consumption of both O_2 and CO_2 at the cathode. The effect of fuel utilization is shown in Fig. 2.1.1.2-5 (Ref. 2.1-5). The composite effect of fuel and oxidant utilization is shown in Fig. 2.1.1.2-6 (Ref. 2.1-13). Because of the number of variables involved, both fuel and oxidant side compositions, these curves are only tpical and a cell model is necessary to conduct the necessary system optimization.

The effects of impurities on the carbonate cell are not completely defined. Because sulfur is harmful in very low ($\leq$ 1 ppm) concentrations, designs based on a current understanding of carbonate cell technology must reduce sulfur concentrations to that level. In the process, acids such as HCl that are known to be harmful to the cathode will be removed by a water wash prior to low-temperature desulfurization.

As with the acid cell, careful integration of the cell and other system components is necessary to produce an attractive system.

FIG. 2.1.1.2–3

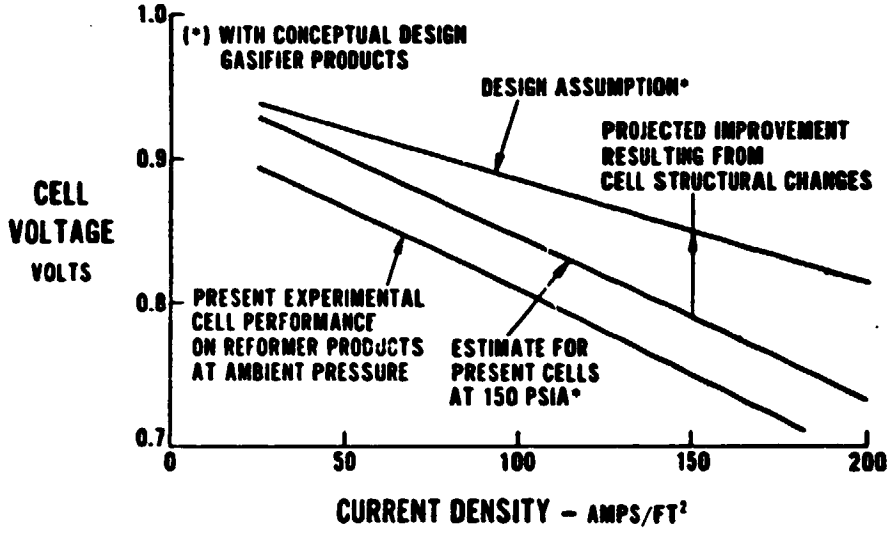

ECAS CELL PERFORMANCE

FIG. 2.1.1.2–4

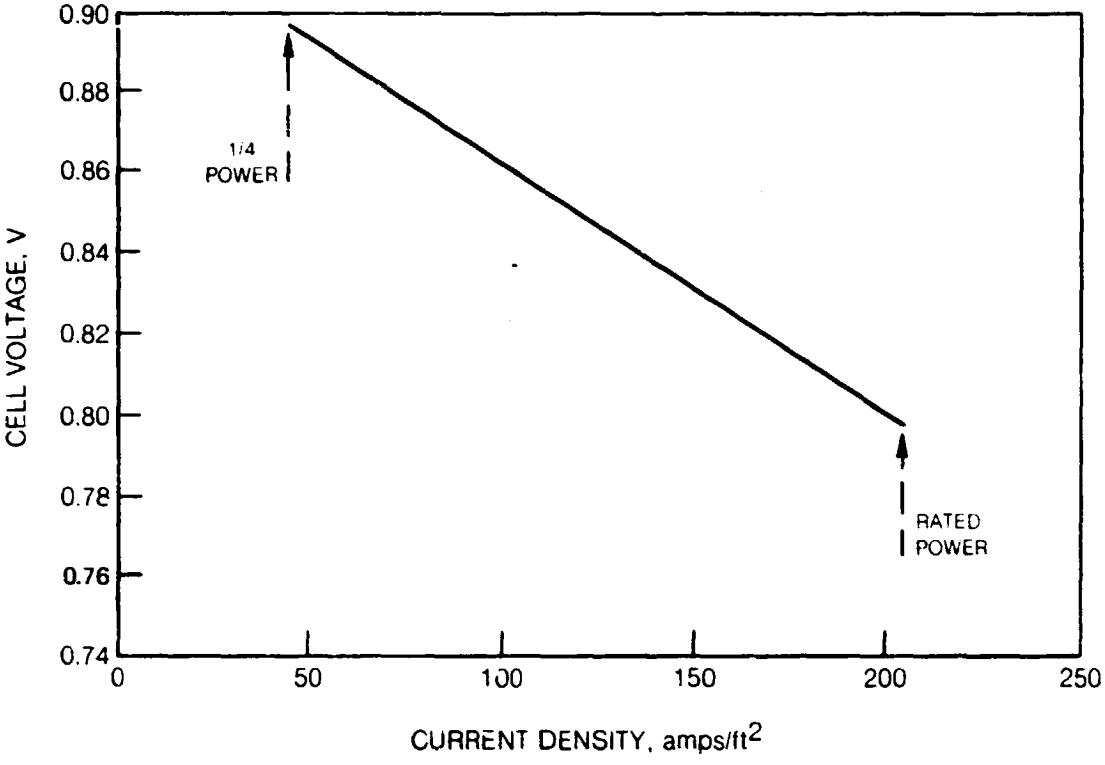

MOLTEN CARBONATE CELL DESIGN PERFORMANCE

81–3–100–5

TABLE 2.1.1.2-1

CELL STACK FLOW CONDITIONS AT RATED POWER

Stream	Anode		Cathode	
	Inlet	Exit	Inlet	Exit
Total Flow (Wet)				
Pounds	0.79	1.97	14.8	13.6
Mols	0.043	0.062	0.51	0.48
Composition (vol% dry)				
H_2	38.3	5.57	--	--
CO	56.0	3.84	--	--
CH_4	0.1	0.07	--	--
CO_2	4.83	90.1	19.6	15.7
N_2	0.7	0.4	70.5	76.3
O_2	--	--	9.9	8.0
H_2O/Dry Gas (vol/vol)	0.755	0.702	0.27	0.29
Temperature (^oF)	1100	1220	1100	1300
Pressure (psia)	150	149	150	149
Utilization	85%		25%	

FIG. 2.1.1.2-5

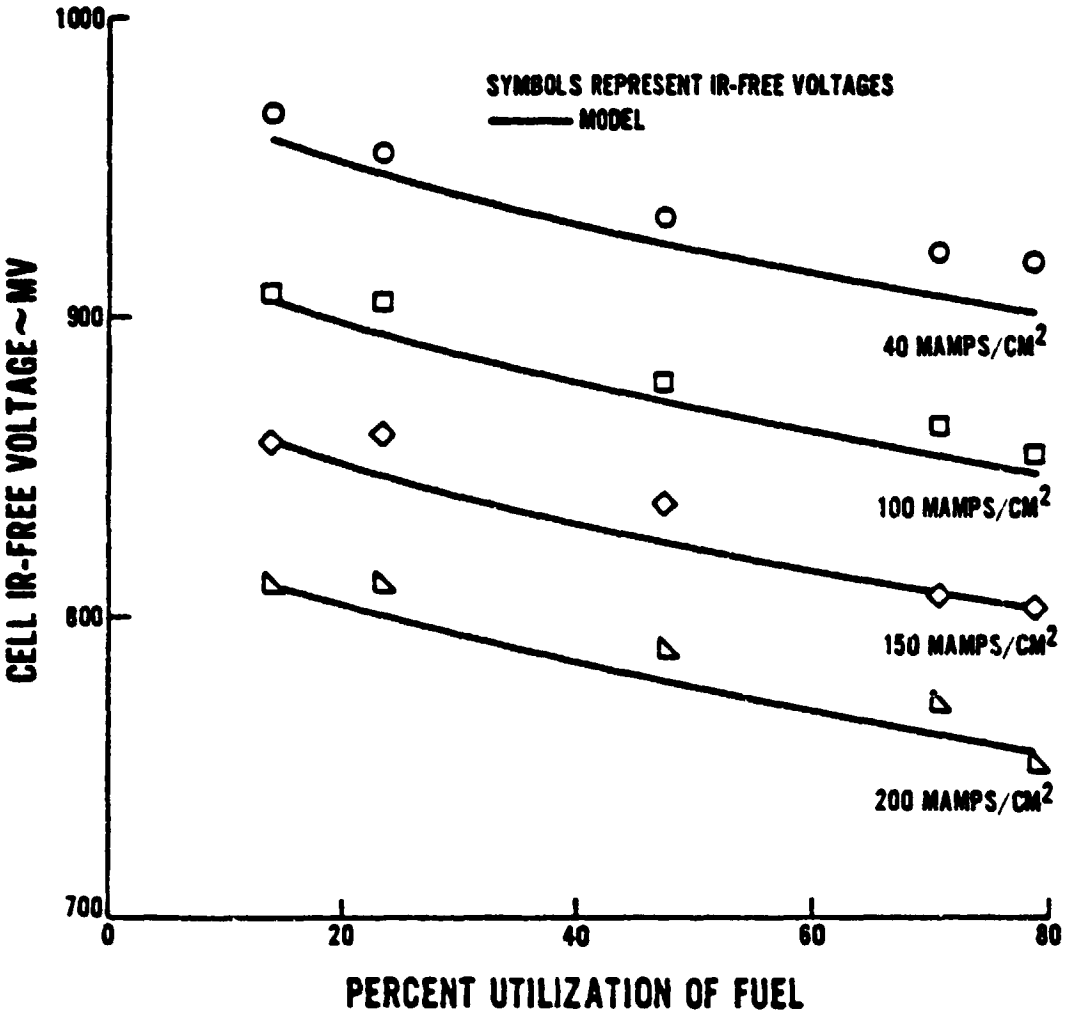

CELL PERFORMANCE AS A FUNCTION OF FUEL UTILIZATION

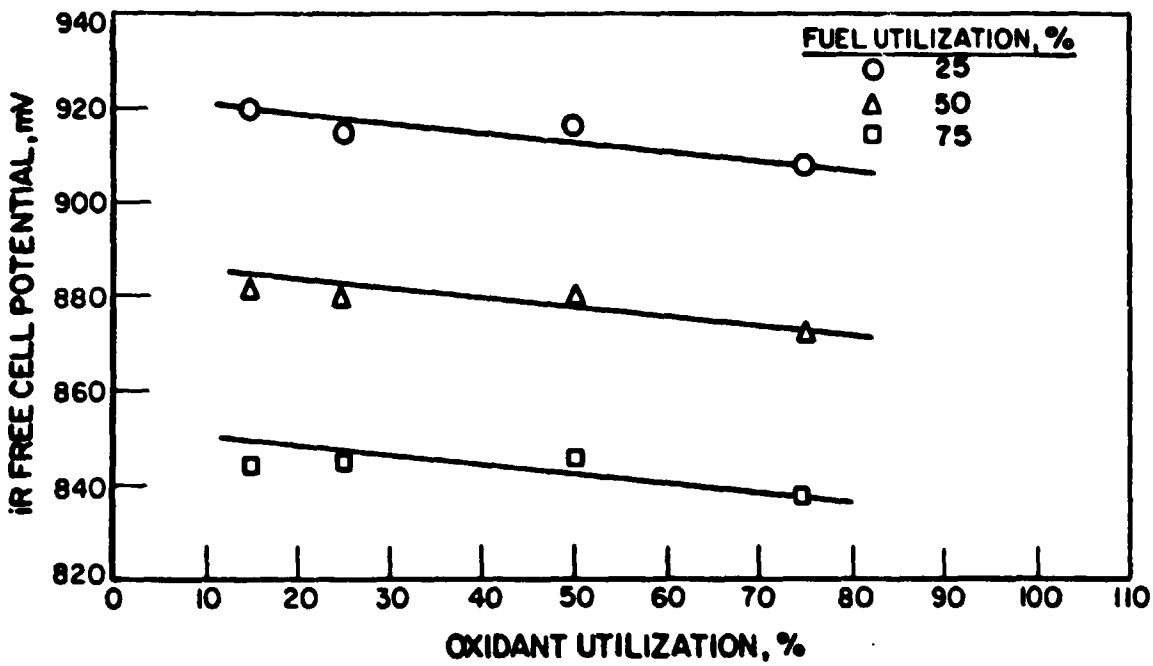

EFFECT OF REACTANT UTILIZATION ON MOLTEN CARBONATE FUEL CELL PERFORMANCE

1 Atm, 200 mA/CM^2, 70 Mol % AIR/30 Mol % CO_2 OXIDANT

SIMULATED REFORMED METHANE FUEL

2.1.2 System/Subsystem Designs

In this section the potential variations in system design and the optimization of the operating parameters are discussed. As mentioned earlier, because of its low operating temperature and requirement for operation on hydrogen alone, the acid cell offers little if any opportunity for variation in its configuration regardless of the gas supply. Therefore discussion in this section is limited to the carbonate cell. Work done at UTC (Ref. 2.1-9) formed the basis for that discussion. For the acid cell, the FCG-1 is typical of future designs and is described in Section 2.1.3.

Integration studies focused on the assessment of the impact on power plant efficiency of the following fuel cell configuration and operating parameters:

- Cell Operating Pressure
- Carbon Formation Criteria
- Cell Cooling Mode
- Cell Performance Technology Level
- Fuel Utilization
- Cell Stack Process Air Coolant Temperature Gradient
- Cooling Recycle Loop Pressure Drop

These studies indicate trends in power section subsystem design options for further study with different gasifiers, and provide the basis for selection of a baseline power section system concept and a baseline set of cell operational parameters.

The power block is defined to include the fuel cell, bottoming cycle, and other conversion and associated equipment downstream of fuel gas cleanup. For these studies, the power block was assumed to be coupled with an oxygen-blown entrained-flow gasifier with physical solvent acid gas cleanup and zinc oxide sulfur polishing similar to that described in Ref. 2.1-15. The fuel gas quality available to the fuel cell, the gasification section operating conditions, and steam and electrical requirements are also based on that study. The schematic of the power plant configuration is shown in Fig. 2.1.2-1. While the basic configuration uses a cathode recycle for heat removal, the anode recycle configuration option is shown as a dashed line. The steam bottoming cycle is not depicted; however, the schematic indicates locations of heat exchangers providing steam to the bottoming cycle or for process reheat. Care was taken to assure that the heat was of sufficient quality for high pressure steam generation, superheating, and/or steam reheat.

Important parameters impacting power plant performance and selection of the baseline power plant system concept are the fuel cell operating pressure, carbon formation criteria, and fuel cell cooling mode. Both anode recycle and fuel gas steam resaturation are design options that were studied to prevent carbon deposition. Three cooling modes were considered: cathode recycle cooling (RR = 0), anode recycle cooling (no cathode recycle), and dual recycle cooling utilizing small anode recycles to reduce the fuel gas resaturation requirements.

FIG. 2.1.2-1

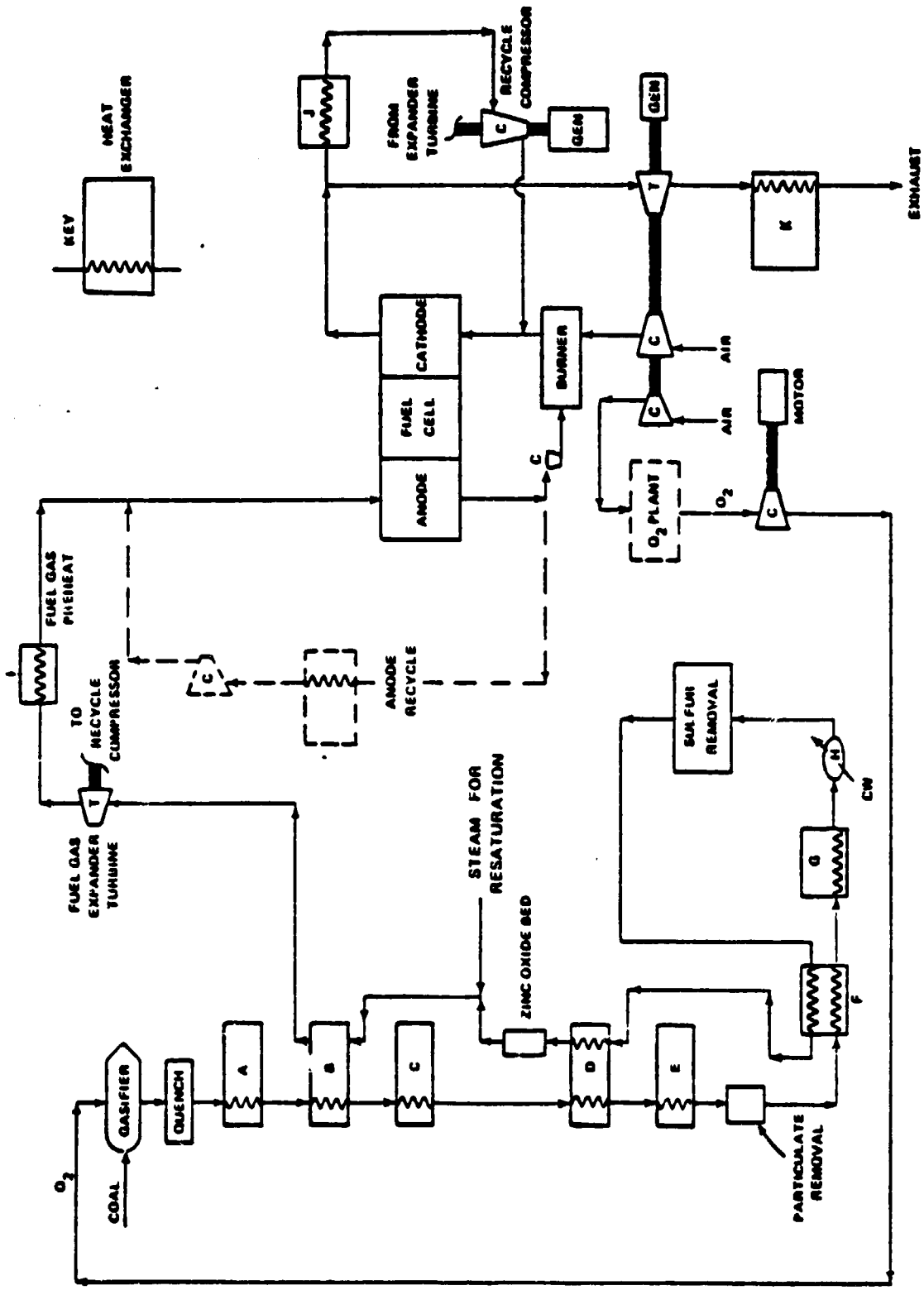

GAS FLOW SCHEMATIC

Initial studies focused on design requirements to prevent carbon deposition over a range of pressures. Based on UTC cell tests and literature data, full C-H-O fuel gas equilibrium has been assumed for the carbon laydown criterion; i.e., at a given temperature and pressure carbon (graphite) deposition will not occur unless thermodynamically favored based on shift and reform equilibria at those conditions. However, for purposes of assessing the impact associated with more stringent design requirements, a second carbon deposition criterion was also investigated. This criterion, defined as partial C-H-O fuel gas equilibrium, assumes carbon (graphite) deposition will not occur unless favored thermodynamically based on shift equilibrium only (frozen methane).

Figure 2.1.2-2 indicates the impact on overall power plant efficiency of the three parameters. The results are normalized for constant cell power density (implies constant $/kW gross dc power) utilizing a performance model with a technology projection similar to that in the ECAS (Ref. 2.1-14) study (Fig. 2.1.1.2-3).

Trends indicated by these parameter studies are as follows:

- Maximum system efficiency is at about 150 psia irrespective of carbon criterion and cooling mode, however, higher pressures have only a small negative impact on efficiency, based on the full C-H-O equilibrium carbon criterion.

- Carbon criterion has a significant impact on efficiency, especially at high pressures.

- Carbon criterion defines the preferred cooling mode. With full C-H-O equilibrium, water resaturation with cathode recycle cooling is the preferred approach, while with partial C-H-O equilibrium, anode cooling is indicated.

Another important parameter influencing the power plant efficiency is the cell performance technology level. Assuming a nearer-term level of performance results in a significant drop in efficiency, as illustrated in Fig. 2.1.2-3. Power plant efficiency again maximizes at ∿ 150 psia, independent of cell performance level.

The above studies assumed the following operational power section parameters to be constant:

- Fuel utilization = 85%
- Cell stack process coolant temperature gradient (ΔT) = 200°F
- Recycle pressure drop (ΔP) = 5 psia

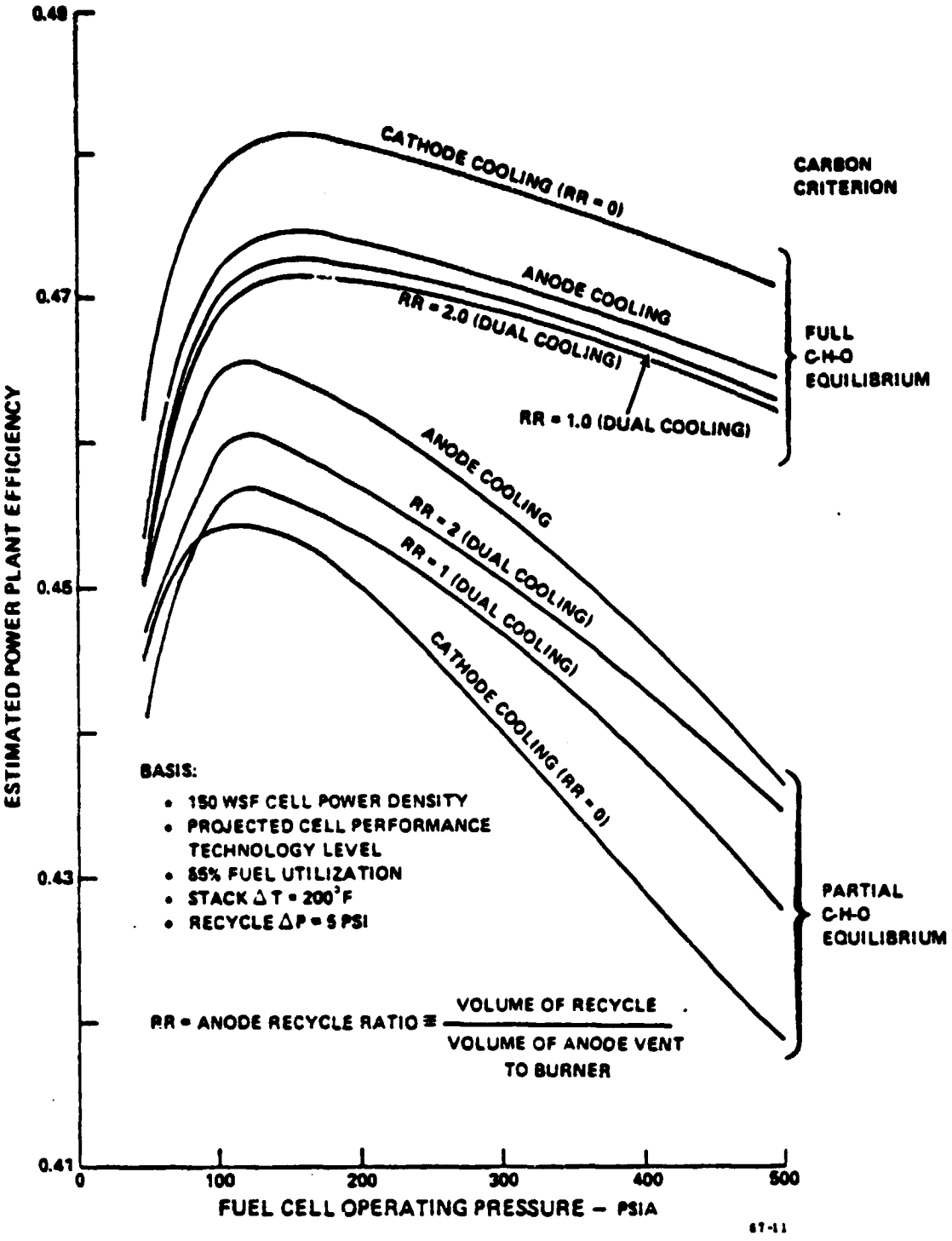

FUEL CELL OPERATING PRESSURE EFFECT ON ESTIMATED POWER PLANT EFFICIENCY

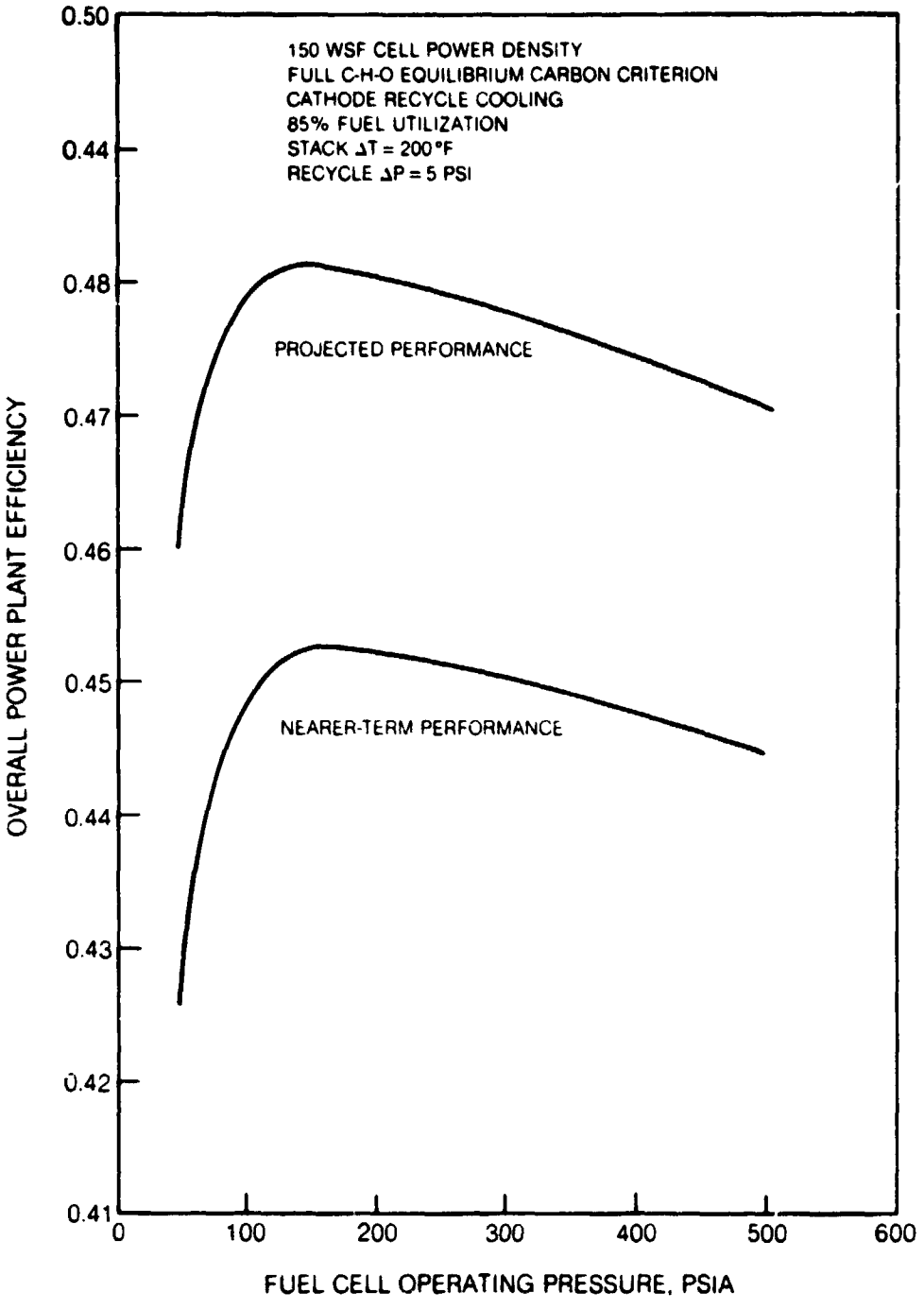

FUEL CELL PRESSURE AND PERFORMANCE LEVEL EFFECT ON OVERALL POWER PLANT EFFICIENCY

81-3-100-4

The impact on efficiency of varying the above parameters are shown in Figs. 2.1.2-4, 2.1.2-5 and 2.1.2-6 respectively. The following summarizes the results of these operational parameter studies.

- Fuel gas utilization has a significant impact on system efficiency. System efficiency increases at high fuel utilization due to the higher efficiency of the fuel cell as compared to the (steam) bottoming cycle.

- Higher stack temperature gradients for cooling increase system efficiency due to reduced compressor parasite requirements.

- Lower recycle pressure drops increase efficiency for the same reason. Alternatively, higher ΔP's tend to flatten the optimum peak, making power plant efficiency insensitive to operating pressure in the high range.

2.1.3 Description of System Baseline Technology

In this section, the systems representative of both the phosphoric acid cell technology and molten carbonate cell technology are described. The acid cell description is based on existing technology while further development is required for the carbonate cell as described in previous sections.

2.1.3.1 Phosphoric Acid Cell Technology

The 4.8-MW fuel cell demonstration unit, while not a commercial prototype, is representative of future plants. To enter widespread commercial service, it will be necessary to reduce the cost of the powerplant and increase its durability. At its inception, the 4.8-MW demonstrator was one module of the larger FCG-1 power plant. Currently, while similar in layout and operation, the FCG-1 design is based on more advanced cell technology and is designed for higher temperature and pressure operation.

In improving operating conditions, current density has been kept constant and efficiency has been improved. The difference in operating conditions was shown in Fig. 2.1.1.1-1. Current cells operate at low (3 atm) pressure and nominally 375 F. Advanced cells, such as would be used in a commercial plant would operate at approximately 6 atm and 400 F. A specification for the FCG-1 is given in Ref. 2.1-16.

The dc module is the heart of the power plant. Its purpose is to convert hydrocarbon fuel and air into direct current. The major functional components of the dc module are shown schematically in Fig. 2.1.2-7. The module consists of fuel and air processing subsystems shown at the left in the figure, a fuel cell power section in the center, and a thermal management subsystem at the upper right. For simplicity, the schematic omits a number of valves and heat exchangers needed for flow and temperature control.

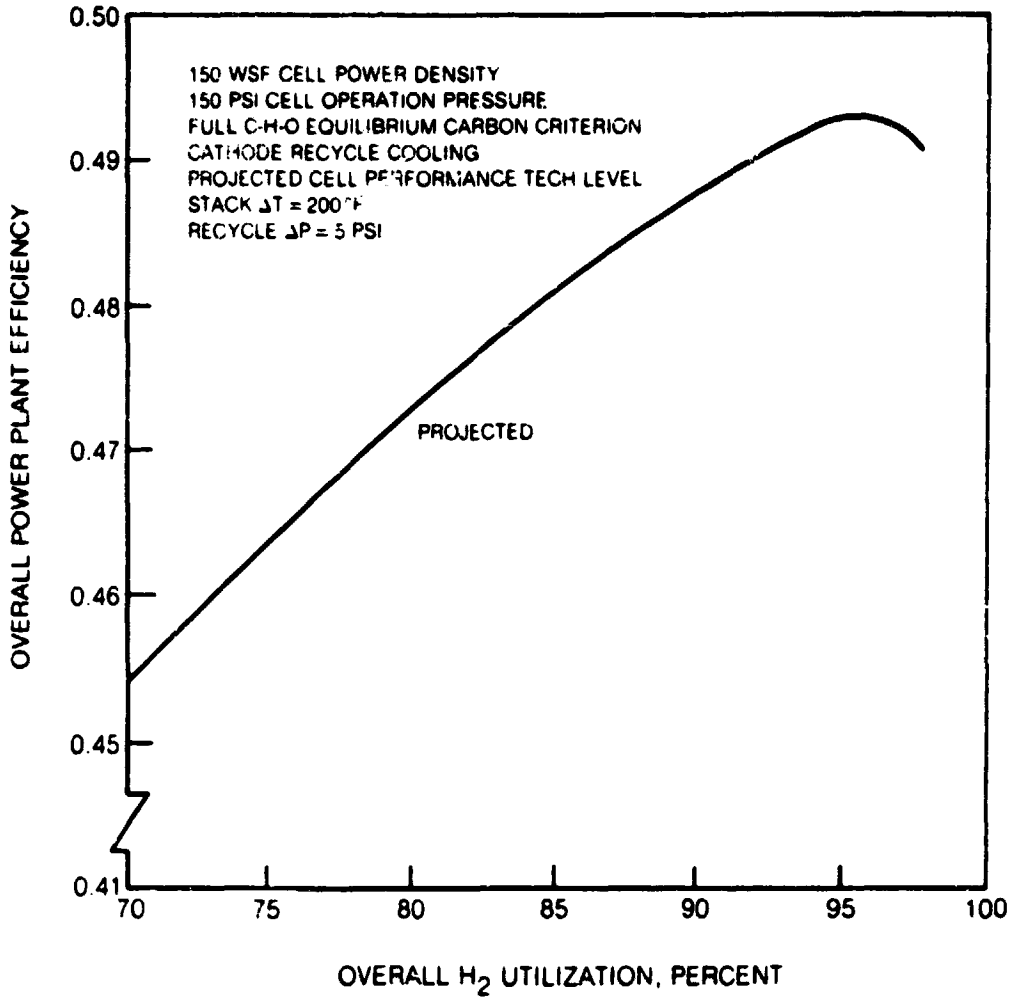

OVERALL H_2 UTILIZATION EFFECT ON OVERALL POWER PLANT EFFICIENCY

81-3-100-3

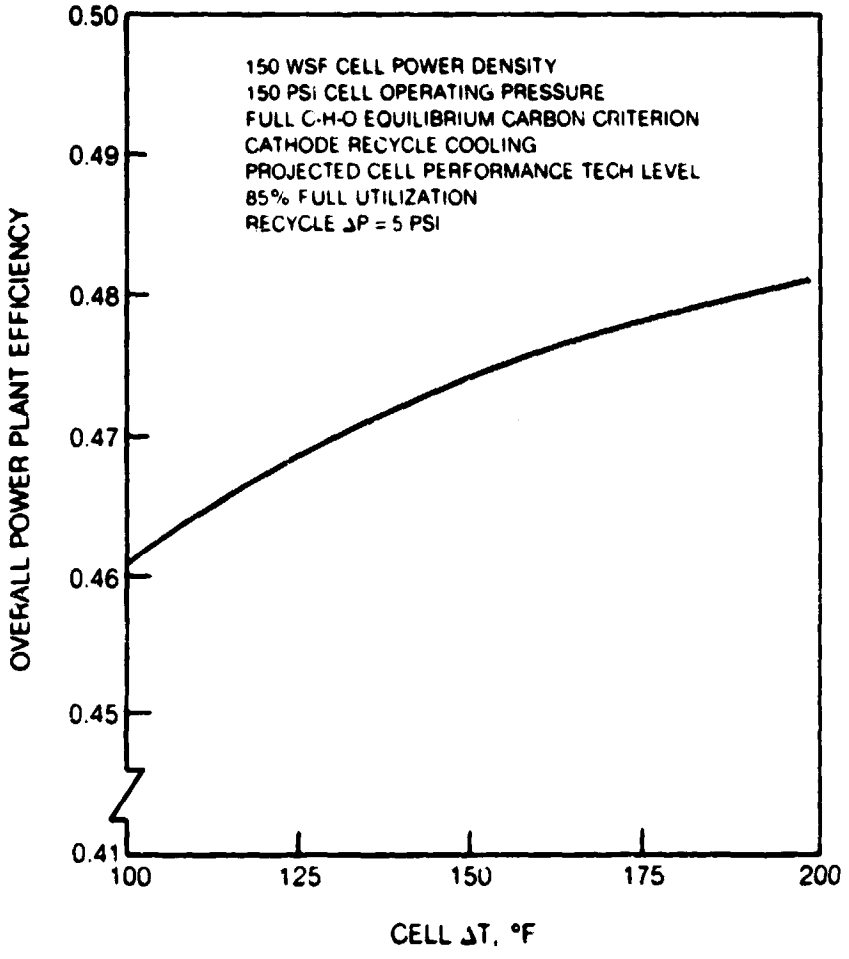

CELL STACK TEMPERATURE GRADIENT EFFECT ON OVERALL POWER PLANT EFFICIENCY

81-3-100-2

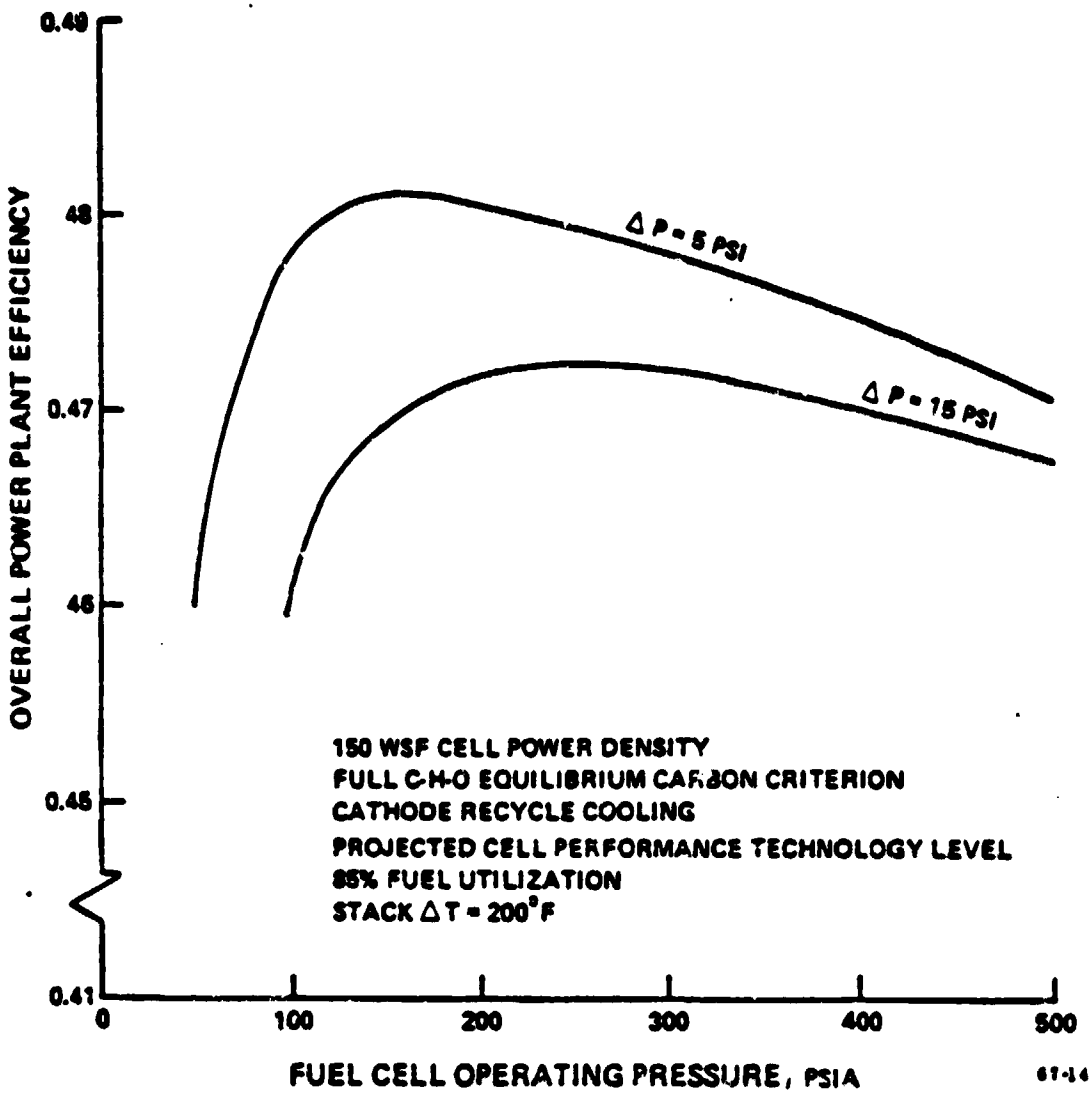

RECYCLE PRESSURE DROP AND CELL OPERATING PRESSURE EFFECT ON OVERALL POWER PLANT EFFICIENCY

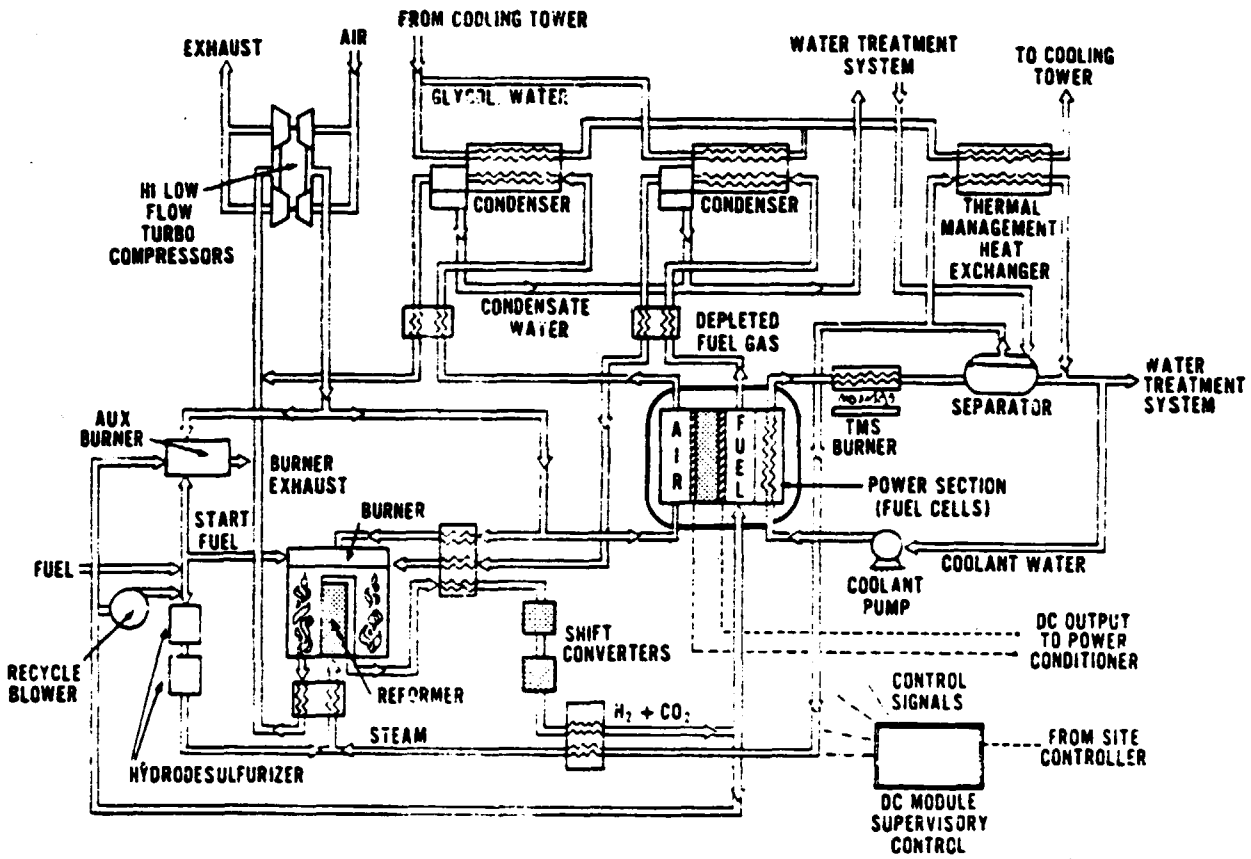

DC MODULE SYSTEM SCHEMATIC

C.2

During demonstrator module operation, air enters one of the compressors, shown at the upper left in the schematic, and is compressed to 35 psig. The low-flow turbocompressor will normally be used below 35 percent of rated power, and the high-flow unit at all other powers. This pressurized air stream is then divided by valves and controls into three streams. The main stream is directed to the cell cathodes to supply the oxygen required for the fuel cell reaction. The fuel cell reaction produces heat and water. Most of this product water evaporates into the air stream flowing through the cathode gas space. This hot, moist, cathode-effluent stream then passes through a regenerator and a liquid-cooled condenser where it is cooled sufficiently to condense the water required for use in the fuel processing subsystem. The cathode exhaust stream, combined with the hot reformer-burner effluent, provides the energy to drive the turbine of the turbocompressor unit.

Power plant process fuel is sometimes burned in the auxiliary burner to add energy to the gas stream before it enters the turbine. The system components are matched such that, at power plant rated output power, the energy in the gas stream is sufficient to power the turbine. As the powerplant output level is reduced, the energy available in the gas stream decreases. Since the turbine requires a near-constant energy input as the output power is reduced, process fuel is burned to make up the small energy deficit at part power.

At the bottom left of the schematic, naphtha fuel, which has been pressurized by a pump, is mixed with hydrogen-rich gas from the fuel processor exit stream. The mixture passes through a hydrotreater (hydrodesulfurizer) where sulfur compounds are converted to hydrogen sulfide and absorbed in a zinc oxide bed. Any halogens in the fuel are absorbed in a guard bed. The clean fuel is then mixed with steam made by power section waste heat. The fuel-steam mixture passes into the reformer. There it is processed to a mixture of hydrogen, carbon dioxide, carbon monoxide, and water vapor. The carbon monoxide and water are then further converted to hydrogen and carbon dioxide in two shift converters operating at successively lower temperatures. The low temperature shift converter reduces the carbon monoxide concentration to less than one percent. The processed fuel next flows to the anode cavities in the fuel cell power section where hydrogen is extracted for the electrochemical reaction. The anode effluent gas stream passes through a regenerator and condenser where it is cooled to condense additional water for power section cooling and steam generation. The anode exhaust stream then enters the reformer burner where the dilute hydrogen is burned to provide heat for the reforming process. Then, as described above, the burner gas stream is combined with the cathode exhaust stream before entering the turbine.

In the power section, cells are stacked in a series-parallel arrangement to produce 3000-volt direct current which is fed to the power conditioner. Power section temperature is controlled by a thermal management subsystem. Steam is generated from condensed water using power section waste heat. As shown at the upper right quadrant of the schematic, cooling water enters the fuel cell coolers, is partially converted to steam, and continues on to the separator where the steam is removed. Part of

the steam is sent to the reformer; the remainder is condensed to maintain the power section at the proper temperature. Water from storage is introduced into the thermal management loop to maintain its inventory. The cooling water is pumped back to the power section. A heat exchanger combined with a burner serves as a source of heat during powerplant startup and standby operation. Excess heat from the dc module is rejected to the dry air cooling towers via a liquid loop. This heat could also be used to provide steam for industrial processes or hot water for space heating or washing.

2.1.3.2 Molten-Carbonate Fuel Cell Technology

A schematic of a molten-carbonate power system developed by UTC for use with an oxygen-blown Texaco gasifier is shown in Fig. 2.1.3.2-1. A combination of Selexol cleanup followed by a zinc oxide bed is used to reduce sulfur to tolerable levels. The system was fully integrated and gave an overall efficiency of 47.9% from coal (HHV) to electricity.

Clean fuel gas enters a Fuel Gas Expander 50-1-EX-2, which drives the Anode Recycle Compressor 50-1-C-2. The fuel gas serves as makeup gas to the anode recycle loop at the discharge of the Anode Recycle Compressor 50-1-C-2. The anode recycle gas stream continuously circulates through the anode side of the 50 parallel fuel cells to supply fuel and to remove the heat of reaction. The 1300°F anode recycle exhaust gas from the fuel cells is cooled in the two pressurized Heat Recovery and Steam Generation units connected in series. The first unit contains Steam Reheater 51-1-E-4 and Superheater 51-1-E-3 as internal coils. The second unit contains HP Boiler 51-1-E-2 and BFW Preheater 51-1-E-1 as internal coils. The cooled anode recycle gas then enters the Anode Recycle Compressor 501-1-C-2 at 1096°F for recompression and recycle. This whole anode recycle loop is designed to operate with a total pressure drop of 5.4 psi.

A portion of the anode effluent at 1300°F combines with inlet air and enters Catalytic Burners 51-1-V-1A&B for combustion. The exit flue gas then flows to the cathode side of the 50 parallel fuel cells. The cathode exhaust gas flows to Exhaust Gas Expander 50-1-EX-1, which drives Air Compressors 50-1-C-1 and 11-1-C-1, and Generator 50-1-G-1.

The gas stream from Exhaust Gas Expander 50-1-EX-1 flows through several economizers including BFW Preheater 51-1-E-5 and Condensate Preheater 51-1-E-7 for recovery of waste heat before discharging to the atmosphere at 250°F.

System performance is summarized in Table 2.1.3.2-1. The nominal cell conditions selected for this study were 150 psia and 1200°F. In this study, process fuel gas cooling was selected to provide for fuel cell thermal management and transfer the rejected heat of reaction to the bottoming cycle via an anode recycle loop. This approach assures that the fuel gases entering the anode are thermodynamically stable with regard to methanation and carbon deposition. However, the kinetics of these reactions may permit less stringent design criteria than was assumed in this study.

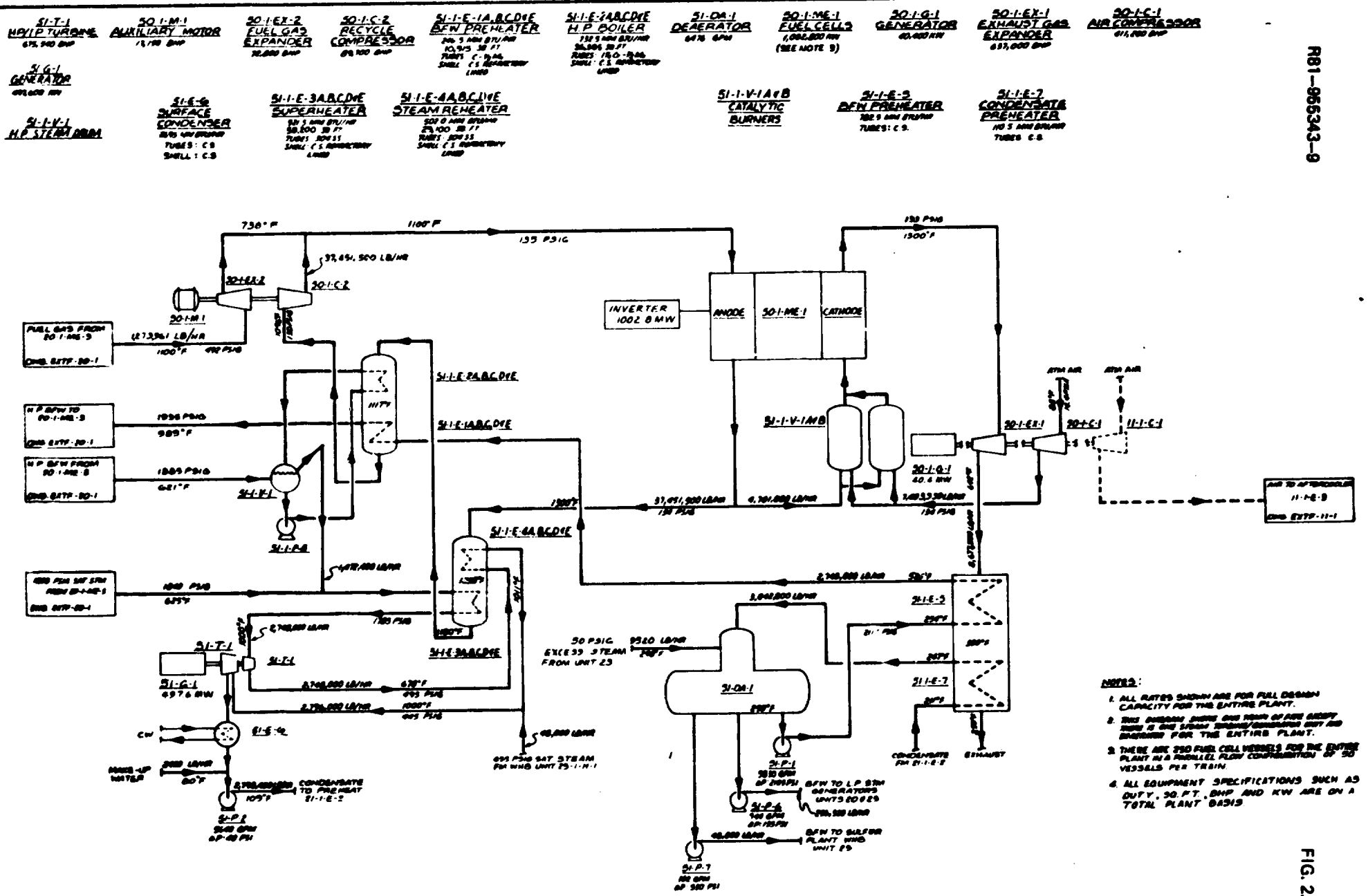

MOLTEN CARBONATE POWER SYSTEM

FIG. 2.1.3.2-1

TABLE 2.1.3.2-1

SUMMARY OF SYSTEM PERFORMANCE FOR
OXYGEN-BLOWN TEXACO GASIFIER/MOLTEN-CARBONATE FUEL CELL

Gasification And Gas Cleaning System	
Coal Feed Rate, lbs/hr (m.f.)	798,333
Oxygen*/Coal Ratio, lbs/lb m.f.	0.858
Oxidant Temperature, °F	300
Steam/Coal Ratio, lbs/lb m.f.	0
Slurry Water/Coal Ratio, lbs/lb m.f.	0.503
Gasification Section Average Pressure, psig	600
Crude Gas Temperature, °F	2,300-2,600
Crude Gas HHV (dry basis), Btu/SCF**	281.1
Temperature of Fuel Gas to Fuel Cell Loop °F	738
Temperature of Fuel Gas to Zinc Oxide Beds	700
Gaseous Sulfur Emission, lb SO_2 Equivalent/10^6 Btu Coal	0.009
Power System	
Air Compression Pressure Ratio (50-1-C-1)	10.4:1
Fuel Cell Inlet Temperature, °F	1,100
Fuel Cell Exhaust Temperature, °F	1,300
Steam Conditions, psia/°F/°F	1800/1000/1000
Condenser Pressure, Inches Hg abs	2.5
Anode Recycle Loop Pressure Drop, psi	5.4
Stack Temperature, °F	250
Fuel Cell Power#, MW	1,002.8
Steam Turbine Power#, MW	497.6
Exhaust Expansion Turbine Power#, MW	40.4
Total Power Consumed, MW	110.8
Net System Power, MW	1,430.0
Overall System	
Process and Deaerator Makeup Water, gpm/1000 MW	445
Cooling Tower Makeup Water, gpm/1000 MW	4,480
Cooling Water Circulation Rate, gpm/MW	208
Cooling Tower Heat Rejection, % of Coal HHV	29.0
Air Cooler Heat Rejection, % of Coal HHV	7.6
Net Heat Rate, Btu/kWh	7,130
Overall System Efficiency (Coal → Power), % of Coal HHV	47.9

*Dry basis, 100 percent O_2

**Excluding the HHV of H_2S, COS and NH_3

#At generator terminals

As discussed in the previous section, improved performance is possible with steam injection and cathode recycle. In addition to operating temperature and pressure, other major parameters defining cell performance and efficiency are cell voltage, and the fuel and oxidant utilizations. Utilizations define the ratio of the reactant consumed by the cell to the reactant supplied to the cell. For a given set of reactant compositions, utilization determines the reactant partial pressure and therefore the maximum ideal cell voltage. Because CO is shifted to H_2 and consumed in the molten carbonate cell, fuel utilization is defined as the ratio of the H_2 consumed in the cell to the total H_2 plus CO supplied to the cell. Fuel utilization and cell voltage are measures of prime cycle system efficiency since they indicate the percentage of CO and H_2 in the fuel gas that is consumed electrochemically and the efficiency of that electrochemical conversion process. A preliminary cost and efficiency trade-off study set the cell voltage at 0.75 volts per cell, and overall fuel utilization at 90 percent. The oxidant air flow rate was set to maintain a two to one ratio between carbon dioxide and oxygen partial pressures on the cathode, a value that optimizes cathode performance. A summary of fuel cell design parameters is given in Table 2.1.3.2-2.

Other cell design conditions that affect overall power plant characteristics are heat losses and cell operating life. The cells are thermally insulated and cell stack heat losses were calculated to be two percent of the design gross power output. For purposes of defining base case economics, cell useful life was assumed to be 40,000 operating hours. This is a goal that has been set for the nearer term acid cells and appears to be a reasonable goal for molten carbonate cells as well. It should be pointed out that after 40,000 hours of operation, the cell with continue to operate, however, at a slightly reduced performance level than assumed for this study. Thus, a utility may choose to replace the fuel cells at this time or it may choose to continue to run the plant with the existing cells, but at a somewhat reduced power level or efficiency.

The fuel cell module produces dc power which is converted to ac in the inverter system. The inverter operates at 96 percent efficiency at rated load, and outputs 60 Hz, 3-phase ac power. Included in Table 2.1.3.2-2 is the power output summary from the inverters. The inverters selected utilize solid-state, self-commutated technology. An important characteristic of utilizing self-commutated technology is that both real and reactive power can be dispatched. Thus, the power factor may be operated over the range of 0.0 to 1.0 within the MVA rating of the inverters, precluding the need for power factor correction capacitors.

The inverters are modular and are designed to be factory fabricated and rail transportable. Each inverter module consists of three inverter bridges connected in parallel to the dc bus. Output voltage harmonics up to 17 times the fundamental are cancelled in harmonic reduction transformers. Any single harmonic voltage

TABLE 2.1.3.2-2

FUEL CELL DESIGN PARAMETERS

Cell Voltage ~ Volts	0.75
Fuel Utilization ~ % *	50
Oxidant Utilization ~ %	58
Gross dc Power Density ~ Watts/Ft^2	148

DC Module Operating Characteristics

Dc Module Output ~ MW	4.18
Number of dc Modules	250
Total dc Output to Inverter ~ MW	1044.6

*Per pass utilization includes anode recycles. Overall utilization for each case is 90 percent

output is limited to less than one percent of the fundamental. Series reactors are inserted between the bridge output and the harmonic cancelling transformers of each inverter module to provide an inductive impedance to the utility line for control purposes and for buffering the bridge from line transients. The 60 Hz, three-phase output from the inverter modules is then combined in an inverter transformer for step-up to an intermediate ac paralleling voltage.

The remaining components in the prime cycle system are the catalytic burners and the turbocompressors and auxiliary generator equipment. The catalytic burners oxidize hydrogen, carbon monoxide, and methane in the fuel anode vent. Adiabatic oxidation temperature is quite low, approximately 1158 F. Kinetic studies indicate that catalytic combustion in these temperature regimes yields very low nitrogen oxide and carbon monoxide emission levels. The catalytic burners utilize a precious metal catalyst supported on a ceramic material, and are enclosed in insulated carbon steel pressure vessles. Design life for the units is two years with replacement of the catalyst bed after this period.

2.1.4 References

2.1-1 United Technologies Corporation: Improved FCG-1 Cell Technology. EPRI Report No. EM1566, October 1980.

2.1-2 Kunz, H. R.: The State-of-the-Art Hydrogen-Air Phosphoric Acid Electrolyte Fuel Cells. Proceedings of the Symposium on Electrode Materials and Processes for Energy Conversion and Storage, Vol. 77-6, 607 (1977).

2.1-3 United Technologies Corporation: Advanced Technology Fuel Cell Program, EPRI Report EM-576, South Windsor, Conn., 1977.

2.1-4 Szymanski, S. T., Gruver, G. A., Katz, M. and Kunz, H. R.: Effect of Ammonia on Hydrogen-Air Phosphoric Acid Cell Performance. Paper presented at Electrochemical Society Meeting, Pittsburgh, October 1978.

2.1-5 United Technologies Corporation: Advanced Technology Fuel Cell Program, EPRI Report EM-335, South Windsor, Conn., 1976.

2.1-6 United Technologies Corporation: Advanced Technology Fuel Cell Program. EPRI Report No. EM-956, December 1978.

2.1-7 Institute of Gas Technology: Fuel Cell Research on Second-Generation Molten Carbonate Systems. Final Report, DOE Contract 31-109-38-3552, 1977.

2.1-8 General Electric Co.: Development of Molten Carbonate Fuel Cells for Power Generation. DOE Report No. SRD-80-055, April 1980.

2.1-9 United Technologies Corporation: Development of Molten Carbonate Fuel Cell Power Plant Technology. Quarterly Report No. 1, DOE-FCR-2026, March 1980.

2.1-10 United Technologies Corporation: Development of Molten Carbonate Fuel Cell Power Plant Technology. Quarterly Report No. 2, DOE-FCR-2268, August 1980.

2.1-11 General Electric Co.: Development of Molten Carbonate Fuel Cell Power Plant. Quarterly Progress Report, DOE/ET/17019-1, April 1980.

2.1-12 General Electric Co.: Development of Molten Carbonate Fuel Cell Power Plant. Quarterly Progress Report, DOE/ET/17019-2, July 1980.

2.1-13 Institute of Gas Technology: Handbook of Fuel Cell Performance. DOE-COO-1545-T1, May 1980.

2.1-14 United Technologies Corporation: Energy Conversion Alternatives Study. NASA-CR-134955, FCR-0237, October 1976.

2.1.4 References (Cont'd)

2.1-15 Fluor Engineers and Constructors, Inc.: An Economic Comparison of Molten Carbonate Fuel Cells and Gas Turbines in Coal Gasification-Based Power Plants. EPRI Report No. AP-1543, September 1980.

2.1-16 United Technologies Corporation: FCG-1 Power Plant Model Specification. DOE/EPRI Report No. FCS-2062, March 1980.

3.1 Evaluation of Coal-Derived Fuels for Advanced Fuel Cell Power Systems

The objective of this task is to determine the overall power plant efficiency of a fuel cell system using medium-Btu gas delivered to the power plant via pipeline. The properties of the gas delivered to the power plant will be obtained and any further processing, if necessary, will be identified. Based upon the fuel gas characteristics, the performance of the fuel cell power plant will be described.

3.1.1 Definition of Fuel Gas Requirements

As discussed in Sections 1 & 2 both the phosphoric acid and molten carbonate type cells are susceptible to degradation from impurities in the fuel. Preliminary fuel specifications have been established for the FCG-1 Power Plant (Ref. 3.1-1). These are presented in Tables 3.1.1-1, 2 & 3. The gaseous fuels of interest here are covered by Table 3.1.1-1. While that specification allows a sulfur level of 100 ppm, the system includes a zinc oxide bed to achieve nearly complete sulfur removal prior to entering the reformer and water gas shift sections of these fuel processing system. While the acid cell can tolerate some H_2S, it appears to have a synergistic effect when accompanied by CO. Since it will not be possible to shift all the CO to H_2, it appears prudent to remove all the sulfur even if catalyst poisoning could be overcome.

In the case of the carbonate cell, allowable sulfur levels have yet to be established. However, it appears likely that these levels will be less than 1 ppm. Cell tolerance to other impurities have been estimated (Ref. 3.1-2) and are presented in Table 3.1.1-4. For purpose of this study it was assumed that low levels (<1%) of C_2 hydrocarbons would act as a diluent and not affect cell performance.

The oxygen-blown Texaco and British Gas Corp. (BGC) slagging gasifiers were selected as the gasifiers to provide medium-Btu fuel gas for transport in pipeline to the power generation site. Properties of the fuel gas from each of these gasifiers, based upon Ref. 3.1-3, are given in Table 3.1.1-5. The total sulfur content of 100 ppm H_2S + COS is that agreed upon by NASA and the Contractor (Ref. 3.1-4) as being typical of pipeline quality fuel gas.

TABLE 3.1.1-1

GASEOUS FUEL SPECIFICATION

Gaseous fuels shall consist of various combinations of saturated hydrocarbon compounds, hydrogen, carbon monoxide and inerts, with the following chemical composition limits:

COMPOSITION LIMITS

Impurity	Upper Limit
Sulfur, ppm vol	100
Nitrogen, vol %	10.0*
Oxygen, vol %	0.1
Olefins, vol %	3.0

* Limit applies only for gases containing hydrocarbons.

Acceptable gaseous fuels include:

Coal Gases from Entrained Flow, Fluidized Bed, or Moving Bed Processes.
Natural Gas
Synthetic Natural Gas
Propane
Hydrogen
Anaerobic Digestor Gases
Some Industrial Byproducts

TABLE 3.1-1

LIQUID FUEL SPECIFICATION

Liquid fuels shall consist of saturated hydrocarbon compounds with the following chemical composition and physical property limits:

COMPOSITION LIMITS

Impurity	Upper Limit
Aromatics, vol %	12.0
Olefins, vol %	3.0
Sulfur, ppm wt.	500.0
Chlorine, ppm wt.	3.0
Lead, ppm wt.	1.0

PHYSICAL PROPERTY LIMITS

Reid Vapor Pressure, Maximum, lb	12.5
Final Boiling Point, Maximum, ^{o}F	420

Acceptable liquid fuels include:

Light Petroleum Distillates
Light Coal Liquids

TABLE 3.1.1-3

ALCOHOL FUEL SPECIFICATION

Alcohol fuels shall consist primarily of methyl, ethyl, isopropyl and isobutyl alcohol, or mixtures thereof, with the following chemical composition limits:

COMPOSITION LIMITS

Impurity	Upper Limit
Sulfur, ppm wt.	0.1
Chlorine, ppm wt.	0.1
Lead, ppm wt.	1.0

Methyl and isopropyl alcohols may be used as denaturants.

TABLE 3.1.1-4

ESTIMATED MAXIMUM ALLOWABLE IMPURITY LEVELS
FOR PHOSPHORIC ACID FUEL CELLS

Impurity	Maximum Limit
CO_2	diluent
CH_4	diluent
N_2	diluent
CO	1%
H_2S, COS	100 ppm
C_2^+	100 ppm
Cl^-	1 ppm
NH_3	1 ppm
Metal ions (Fe, Cu, etc.)	nil

TABLE 3.1.1-5

GAS COMPOSITIONS

	Texaco Gas	BGC Gas
Element	Vol. %	Vol. %
CH_4	0.1	8.4
H_2	35.6	30.6
CO	52.4	58.5
CO_2	10.8	1.9
H_2S) + COS	100 ppm	100 ppm
N_2	0.8	0.5
Ar	0.2	0
H_2O	0.1	0.1
	100.0	100.0
Heating Values, LHV		
LHV, Btu/scf	267.5	349.1
LHV, Btu/lb	4949	6825

Fuel delivery pressure is dictated by the combined cycle of Section 3.2 in which the combustor operates at 175 psia. Allowing for fuel handling, a pressure of at least 250 psia would be required at delivery. It is anticipated that the Texaco and BGC gasifiers would be operated at pressures well beyond this value. Since the fuel cells operate at lower pressures it may be possible to recover some of the compressor work with an expander.

Fuel delivery temperature is not critical unless it is low enough to allow condensation. For the moisture content given in Table 3.1.1-5, temperatures should be above 75 F. An average temperature of 86 F has been assumed.

The required flow rate of fuel gas is a function of heating value and output power levels. For the carbonate systems, flows were selected that provided a heat input comparable to the integrated systems which were sized for a nominal 500 MW output. The flow rate is 527,310 lb/hr for the Texaco gas and 453,190 lb/hr for the BGC gas. In the case of the phosphoric acid cells, flows were made to be compatible with the FCG-1 module.

3.1.2 - Identification of Power Generation Facility

3.1.2.1 Phosphoric Acid Cell

The basic generating system arrangement has been described in Section 2.1.3. The plant, while initially intended for use on light distillate fuel, is designed for fuel flexibility. The fuel processor can be adapted to various gaseous and liquid fuels including those under consideration here.

For operation on naptha, a system schematic and flow sheet are shown in Fig. 3.1.2.1-1 and Table 3.1.2.1-1 (Ref. 3.1-5). For use with either of the gases being considered here, minor changes are required. These will be discussed using the naptha fueled plant as a baseline to describe fuel processor and fuel cell operation.

Referring to Fig. 3.1.2.1-1, naptha with no sulfur (Stream 1) enters the system and passes through the hydrodesulfurizer and zinc oxide bed prior to entering the reformer.

Fuel containing sulfur would be mixed with hydrogen rich gas prior to entering the hydrodesulfurizer. With the medium-Btu gases being considered here, the sulfur has already been combined with hydrogen and can be sent directly to the zinc oxide beds located just downstream of the hydrodesulfurizer. Removal of 100 ppm of sulfur from the gas puts a burden on the zinc oxide bed. The cost of desulfurization by the zinc oxide is on the order of 1 mill per kWh.

FIG. 3.1.2.1-1

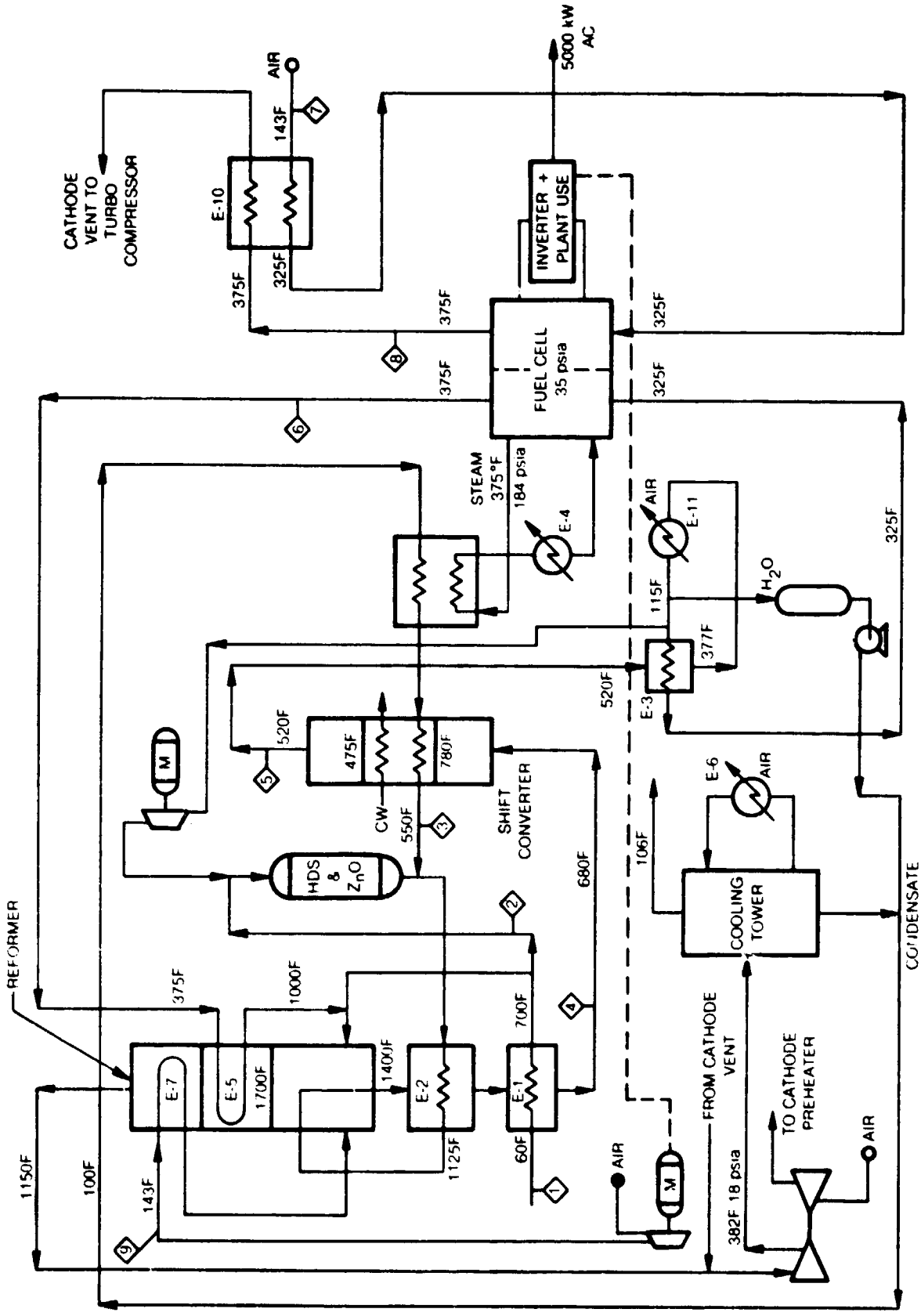

PHOSPHORIC ACID FUEL CELL POWER SYSTEM

81-3-100-7

TABLE 3.1.2.1-1

MASS AND ENERGY BALANCE FOR SYSTEM
FOR PHOSPHORIC ACID FUEL POWER SYSTEM

STREAM (lb-mol/hr)

Stream No.	1	2	3	4	5	6	7	8	9
Component									
H_2	--	--	--	326.2	378.0	37.8	--	--	--
CO	--	--	--	55.6	3.7	3.7	--	--	--
CO_2	--	--	--	65.9	117.7	117.7	--	--	--
H_2O	--	--	491.7	298.5	246.7	26.4	--	340.3	--
CH_4	--	--	--	1.4	1.4	1.4	--	--	--
O_2	--	--	--	--	--	--	378.0	207.9	89.8
N_2	--	--	--	--	--	--	1422.3	1422.3	337.0
TOTAL	--	--	491.7	747.6	747.6	187.1	1800.3	1970.5	426.8
lb/hr	2,250	1,356	8,851	10,608	10,608	5,858	29,082	29,763	12,334

Exchangers	E-1	E-2	E-3	E-4	E-5	E-6	E-7	E-9	E-10	E-11	E-12	E-13
Duty, MMBtu/hr	1.09	3.47	0.85	5.48	1.21	8.22	2.24	9.30	2.28	4.18	0.94	0.66

Following desulfurization, the gas is mixed with steam (Stream 3) and sent to the reformer where the hydrocarbons are converted to hydrogen along with some carbon monoxide, carbon dioxide and methane (Stream 4). These gases are cooled and sent to the shift converter where most of the CO along with a corresponding amount of H_2O is shifted to make H_2 and CO_2 (Stream 5). In the case of the Texaco gas, the reformer can be bypassed and the desulfurized gas sent directly to the shift converter. However, because of the high CO level (52%) in the gas it is necessary to add two high-temperature shift converters with associated heat exchangers to reduce the CO concentration to a level typical of a steam reformer product. The gas can then be processed in the normal shift converter.

In the BGC gas, methane, while only 8% by volume, accounts for 23 percent of the heating value. Therefore, to avoid the loss of that energy, the BGC gas must be processed in the reformer. Because of the low methane concentration and the exothermic shift reactions that will also occur in the reformer, little heat is required. For the BGC gas, no change in the basic fuel processor arrangement is required. However, the size of the low-temperature shift converter must be increased.

After shifting, the fuel gas is cooled and most of the water vapor is condensed and removed for re-use in the reformer. It is then sent to the anode side of the cell. In the fuel cell, 10 percent of the hydrogen is consumed. The remainder, along with residual CO and CH_2, is combined with incoming fuel to provide heat for the reformer.

A comparison of the performance of the phosphoric acid power plant using naptha, the Texaco gas and the BGC gas is given in Table 3.1.2.1-2. As can be seen, there is little change in either heat rate or the availability of low-grade heat as the system is changed from one fuel to the other.

The operation of the FCG-1 power plant on medium-Btu gas both with and without methane is the subject of a study being performed for TVA (Ref. 3.1-6). The final report of that work will not be available for several months. However, it will include a more detailed description of the operation of the cell than is possible at this time.

3.1.2.2 Molten Carbonate Cell

The basic generating system arrangement has been discussed in Section 2.1.3. The carbonate cell, by virtue of its high operating temperature is well suited for integrated operation with the gasifer. However, in the over-the-fence configuration it also exhibits a low heat rate. The system arrangement is shown in Fig. 3.1.2.2-1. It is the same for use with either the Texaco or BGC gas. Table 3.1.2-2 summarizes performance for both gases. For the Texaco gas, a heat and mass balance is given in Table 3.1.2.2-3 and stream compositions are given in Table 3.1.2.2-3. For the BGC gas, the corresponding tables are 3.1.2.2-4 and 3.1.2.2-5 respectively.

TABLE 3.1.2.1-2

SUMMARY OF COAL-DERIVED FUEL IMPACT

11.3-MWAC Net Power Rating

Fuel	Texaco	BGC
Variation from Basic Power Plant	Add 2-Stage Shift Converter Increase Low-Temperature Shift Converter Size	Increase Low-Temperature Shift Converter Size
Rated-Power Heat Rate, Btu/kWh	8350	8360
Recoverable Heat, 10^6 Btu/h		
High Grade, STEAM	4.2	6.2
Low Grade, 160 F WATER	37	37
Overall Energy Utilization, % (Based on HHV)	85	86

FIG. 3.1.2.2-1

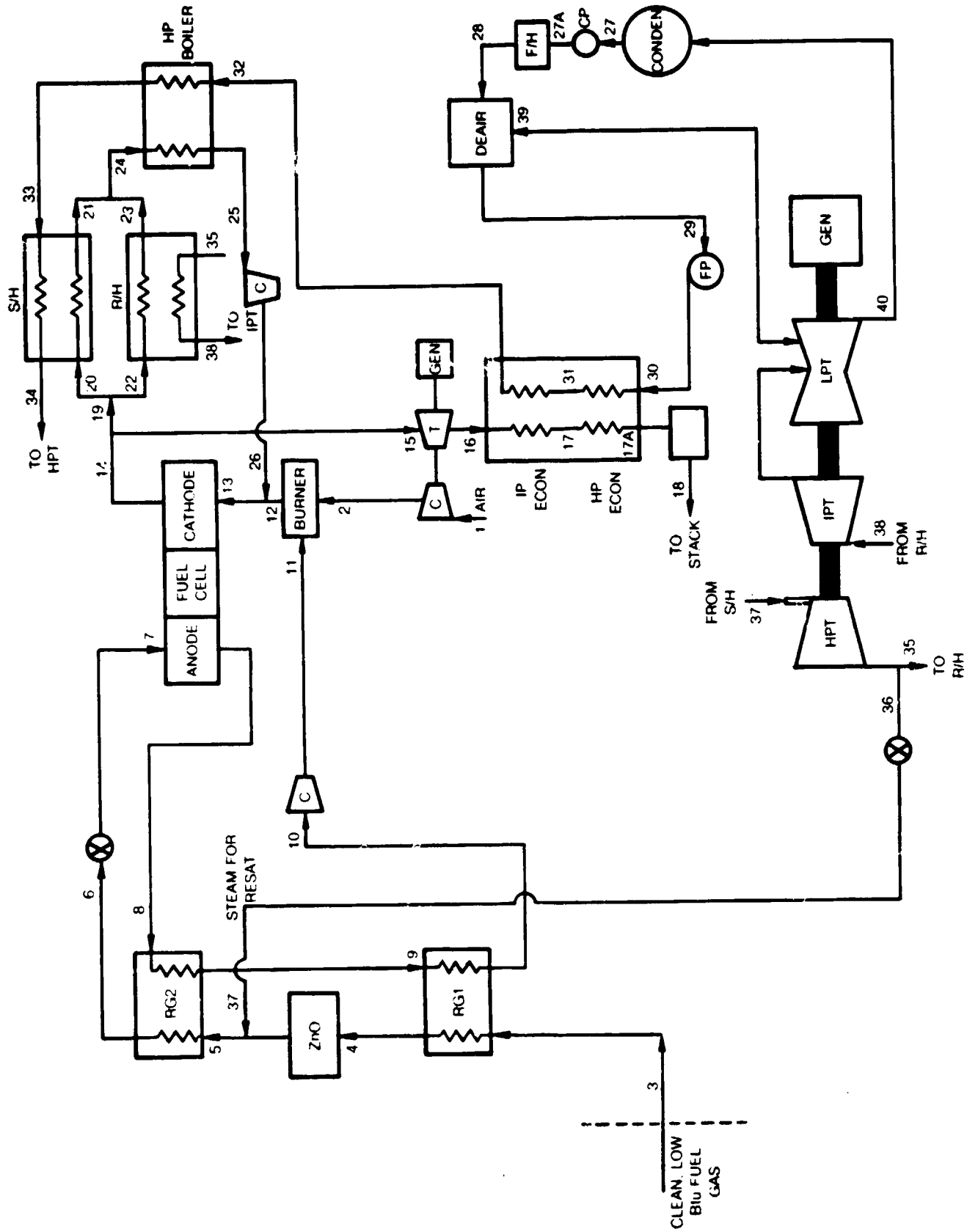

MOLTEN CARBONATE FUEL CELL POWER SYSTEM

81-3-100-9

TABLE 3.1.2.2-1

PERFORMANCE SUMMARY FOR MOLTEN CARBONATE POWER SYSTEMS
AND MEDIUM-BTU FUEL GAS

Fuel Gas:		
Gasification Process	Texaco	BGC
Flow Rate, lb/hr	527310	453190
Lower Heating Value, Btu/lb	4949	6826
Performance:		
Fuel Cell Power, MW	346.0	330.4
Gas Turbine Power, MW	100.3	107.5
Steam Turbine Power, MW	52.0	119.2
Utilities(1), MW	30.8	29.2
Total Net Power, MW	485.5	527.9
Heat Rate, Btu/kWh(2)	5375	5860
Overall Efficiency, %(2)	63.5	58.2

(1) Includes fuel compressors and 3% for plant requirements

(2) Based on lower heating value of gas.

TABLE 3.1.2.2-2

HEAT AND MASS BALANCE FOR MOLTEN CARBONATE POWER SYSTEM
AND TEXACO FUEL GAS

Station Number	Temperature (°F)	Pressure (psia)	Flow (lb/sec)(1)
1	59	14.7	754.4
2	595	150.8	754.4
3	80	275.0	146.5
4	700	270.0	146.5
5	656	260.8	246.9
6	1100	256.1	246.9
7	1100	150.0	246.9
8	1220	150.0	568.4
9	981	147.5	568.4
10	809	145.0	568.4
11	820	150.8	568.4
12	988	150.0	1322.8
13	1100	150.0	3944.5
14	1300	150.0	3622.9
15	1300	150.0	1001.2
16	659	16.2	1001.2
17	480	14.7	1001.2
17A	363	14.7	1001.2
18	300	14.7	1001.2
19	1300	150.0	2621.7
20	1300	150.0	2162.0
21	1213	150.0	2162.0
22	1300	150.0	459.7
23	1213	150.0	459.7
24	1213	150.0	2621.7
25	1140	145.1	2621.7
26	1154	150.0	2621.7
27	108	1.23	159.8
27A	108	30.0	159.8
28	218	30.0	159.8
29	250	30.0	165.0
30	255	2837.0	165.0
31	446	2553.2	165.0
32	662	2400.0	165.0
33	662	2400.0	165.0
34	1000	2400.0	165.0

(1) All flow values are for one engine.

TABLE 3.1.2.2-2 (Cont'd)

HEAT AND MASS BALANCE FOR MOLTEN CARBONATE POWER SYSTEM
AND TEXACO FUEL GAS

35	653	600.0	64.6
36	653	600.0	100.4
37	611	260.8	100.4
38	1000	540.0	64.6
39	405	34.0	5.2
40	108	1.23	57.4

TABLE 3.1.2.2-3

MATERIAL BALANCE FOR MOLTEN CARBONATE
POWER SYSTEM USING TEXACO FUEL GAS

Station Number		1-2		3-4		5-7		8-11		12	
Comp.	M.W.	Lb/Hr	Mols/Hr	Lb/Hr	Mols/Hr	Lb/Hr	Mols/Hr	Lb/Hr	Mols/Hr	Lb/Hr	Mols/Hr
CH_4	16.04	--	--	417	26	417	26	417	26	--	--
H_2	2.016	--	--	18507	9180	18507	9180	4167	2067	--	--
CO	28.01	--	--	378499	13513	378499	13513	37477	1338	--	--
CO_2	44.01	--	--	122040	2773	122040	2773	1506814	34238	--	35601
H_2S	34.08	--	--	--	--	--	--	--	--	--	--
COS	60.07	--	--	--		--	--	--	--	--	--
O_2	32.00	625696	19553	--		--	--	--	--	569600	17800
N_2	28.02	2036746	72689	5912	211	5912	211	5912	211	2042658	72900
A	39.94	36465	913	1478	37	1478	37	1478	37	37943	950
H_2O	18.02	37247	2067	469	26	361896	20083	490090	27197	545375	30265
Total		2736154	95222	527322	25766	888749	45823	2046355	65114	4762376	157516

TABLE 3.1.2.2-3 (Cont'd)

MATERIAL BALANCE FOR MOLTEN CARBONATE
POWER SYSTEM USING TEXACO FUEL GAS

Station Number		13		14		15-18		19-26		27-40	
Comp.	M.W.	Lb/Hr	Mols/Hr	Lb/Hr	Mols/Hr	Lb/Hr	Mols/Hr	Lb/Hr	Mols/Hr	Lb/Hr	Mols/Hr
CH_4	16.04	--	--	--	--	--	--	--	--	--	--
H_2	2.016	--	--	--	--	--	--	--	--	--	--
CO	28.01	--	--	--	--	--	--	--	--	--	--
CO_2	44.01	3446467	78311	2597514	59021	717847	16311	1879667	42710	--	--
H_2S	34.08	--	--	--	--	--	--	--	--	--	--
COS	60.07	--	--	--	--	--	--	--	--	--	--
O_2	32.00	1252960	39155	944352	29511	260992	8156	683360	21355	--	--
N_2	28.02	7391396	263790	7391396	263790	2042658	72900	5348738	190890	--	--
A	39.94	137354	3439	137354	3439	37943	950	99411	2489	--	--
H_2O	18.02	1973370	109510	1973370	190510	545375	30265	1428031	79247	575433	31933
Total		14201547	494205	13043986	465271	3604815	128582	9439207	336691	575433	31933

TABLE 3.1.2.2-4

HEAT AND MASS BALANCE FOR MOLTEN CARBONATE POWER SYSTEM
AND BGC FUEL GAS

Station Number	Temperature (°F)	Pressure (psia)	Flow (lb/sec)(1)
1	59	14.7	865.4
2	595	150.8	865.4
3	80	275.0	125.9
4	700	270.0	125.9
5	649	260.8	236.3
6	1100	256.1	236.3
7	1100	150.0	236.3
8	1220	150.0	532.1
9	969	147.5	532.1
10	808	145.0	532.1
11	819	150.8	532.1
12	1375	150.0	1397.6
13	1100	150.0	3759.9
14	1300	150.0	3464.1
15	1300	150.0	1101.8
16	655	16.2	1101.8
17	485	14.7	1101.8
18	300	14.7	1101.8
19	1300	150.0	2362.3
20	1300	150.0	1763.9
21	1115	150.0	1763.9
22	1300	150.0	598.5
23	1115	150.0	598.5
24	1115	150.0	2362.3
25	924	145.1	2362.3
26	937	150.0	2362.3
27	108	1.23	251.0
28	108	30.0	251.0
29	250	30.0	286.3
30	255	2837.0	286.3
31	446	2553.0	286.3
32	602	2400.0	286.3
33	662	2400.0	286.3
34	1000	2400.0	286.3
35	648	600.0	175.9
36	648	600.0	110.4
37	604	260.8	110.4
38	1000	540.0	175.9
39	385	34.0	35.3
40	108	1.23	140.6

(1) All flow values are for one engine.

TABLE 3.1.2.2-5

MATERIAL BALANCE FOR MOLTEN CARBONATE
POWER SYSTEM USING BGC FUEL GAS

Station Number		1-2		3-4		5-7		8-11		12	
Comp.	M.W.	Lb/Hr	Mols/Hr	Lb/Hr	Mols/Hr	Lb/Hr	Mols/Hr	Lb/Hr	Mols/Hr	Lb/Hr	Mols/Hr
CH_4	16.04	--	--	31535	1966	31535	1966	31535	1966		
H_2	2.016	--	--	14473	7179	14473	7179	3997	1983		
CO	28.01	--	--	383709	13699	383709	13699	32183	1149		
CO_2	44.01	--	--	20069	456	20069	456	1353440	30753	1490531	33368
H_2S	34.08	--	--	--				--			
COS	60.07	--	--	--				--			
O_2	32.00	717824	22432	--				--		541888	16934
N_2	28.02	2336616	83391	2942	105	2942	105	2942	105	2339558	83496
A	39.94	41857	1048	--	--	--				41857	1048
H_2O	18.02	19660	1091	414	23	398008	22082	491640	37383	617870	34288
Total		2115957	107962	453142	23428	850736	45492	1915737	63239	5031704	169634

TABLE 3.1.2.2-5 (Cont'd)

MATERIAL BALANCE FOR MOLTEN CARBONATE
POWER SYSTEM USING BGC FUEL GAS

Station Number		13		14		15-18		19-26		27-40	
Comp.	M.W.	Lb/Hr	Mols/Hr	Lb/Hr	Mols/Hr	Lb/Hr	Mols/Hr	Lb/Hr	Mols/Hr	Lb/Hr	Mols/Hr
CH_4	16.04	--	--	--	--	--	--	--	--	--	--
H_2	2.016	--	--	--	--	--	--	--	--	--	--
CO	28.01	--	--	--	--	--	--	--	--	--	--
CO_2	44.01	3011868	68436	2230867	50690	709529	16122	1521338	34568	--	--
H_2S	34.08	--	--	--	--	--	--	--	--	--	--
COS	60.07	--	--	--	--	--	--	--	--	--	--
O_2	32.00	1094976	34218	811040	25345	257952	8061	553088	17284	--	--
N_2	28.02	7356091	262530	7356091	262530	2339558	83496	5016421	179030	--	--
A	39.94	131562	3294	131562	3294	41857	1048	89745	2247	--	--
H_2O	18.02	1942736	107810	1942736	107810	617870	34288	1324830	73520	903955	50164
Total		13537233	476288	12472296	449669	3966766	143015	8505422	306649	903955	50164

Referring to Fig. 3.1.2.2-1, fuel gas is received at pressure but must be heated prior to use in the cell. This is done by heat exchange with the anode exhaust gas. When the incoming gas reaches 700F, it is withdrawn from the heat exchanger and sent to a zinc oxide bed for complete sulfur removal. The clean gas is mixed with steam to prevent carbon deposition and then returned to the exchanger where it is heated to 1100F which has been specified as the anode inlet temperature.

In the cell, fuel utilization is 85 percent. That is, 85 percent of the total moles of H_2 + CO are consumed in the cell. For each moles of fuel used, one mole of CO_2 and one of H_2O are released to the gas stream. Thus the mass flow out of the cell is greatly increased over the inlet flow rate. The gas leaves the cell at 1220F and the composition corresponds to the water gas shift equilibrium at that temperature.

As noted above the anode exhaust gas is used to heat the incoming fuel gas. Because of the high mass flow rate of the exhaust gas, it is only cooled to approximately 800F before entering a blower which directs the very low-Btu gas to a catalytic burner. Here the gas is burned and the products diluted with air from the turbocompressor. The resultant gas (Stream 12) is mixed with recycle gas from the anode that has been cooled to maintain proper cell temperature. The mixture is sent to the cathode where the utilization of CO_2 and O_2 is approximately 25 percent. Gas leaves the cathode at 1300F. Part of it is cooled by raising high pressure steam and providing superheat and reheat for the steam cycle. That part is recirculated to the cathode by the recycle compressor. The other part of the stream is expanded through a turbine which drives the compressor and a generator adding to the gross power output.

Heat recovered from the turbine exhaust is used for economizing in the steam bottoming cycle. As mentioned earlier boiling and superheating are accomplished in the cathode recycle stream.

3.1.3 References

3.1-1 Handley, L. M.: FCG-1 Power Plant Specifications. Supported by DOE Contract No. EX-76-C-01-2102, March 1980.

3.1-2 Benjamin, T. G., E. H. Camara, and L. G. Marianowski: Handbook of Fuel Cell Performance. Supported by DOE Contract No. EC-77-C-03-1545, May 1980.

3.1-3 Crawford, C. D., R. P. Dawkins, and J. R. Joiner: An Economic Comparison of Molten Carbonate Fuel Cells and Gas Turbines in Coal Gasification - Based Power Plants. EPRI AP-1543, September 1980.

3.1-4 Interim Project Briefing, NASA-MSFC, Huntsville, Alabama, December 17/18, 1980.

3.1-5 Arthur D Little: Assessment of Fuels for Power Generation by Electric Utility Fuel Cells. EPRI EM-695, 1978.

3.1-6 Johnson, W. H.: Study on Phosphoric Acid Fuel Cells Using Coal-Derived Fuels. Ongoing Program Supported by TVA Contract No. TV-53900A.

4.1 Evaluation of Integrated Gasification Fuel Cell Power Systems

The objective of this task is to evaluate the performance of fuel cell systems when integrated with coal gasification and cleanup systems. The gasifiers to be considered are the oxygen-blown Texaco and the BGC slagger. Gasification and gas cleanup systems are the same as reported in Ref. 4.1-1.

Because of their low operating temperature, the phosphoric acid fuel cells do not lend themselves to integration with gasification systems. The more likely use of the acid cell is as a dispersed generator which would have the performance characteristics described in Section 3.1.2. For that reason, this section deals only with gasification systems integrated with the molten carbonate fuel cell.

4.1.1 Identification of Fuel Cell Power Plant with Texaco Gasifier

The fuel cell system with steam bottoming cycle described in Section 2.1.3 will be used as the basis for the integrated power plant. Cell operating conditions are as described in Section 2.1.3 but actual cell output varies with gas compositions and steam cycle arrangement has been changed to fully utilize the heat available in each configuration. A schematic for the Texaco-based system is shown in Fig. 4.1.1-1. A brief description of the system follows.

In the Texaco system coal is mixed with water and the resultant slurry (Stream 5) is pumped up to gasifier pressure. In the gasifier it reacts with oxygen to produce a high temperature (>2300F) medium-Btu gas. At the gasifier exit, a portion of the gas is drawn off to remove the bulk of entrained ash from the main stream. That gas is quenched with water to remove the ash and rejoin the mainstream at the particulate scrubber. Prior to entering the high-pressure boiler, the main gas stream is quenched to below the ash fusion temperature to solidify the ash and minimize heat exchanger fouling. The gas is then cooled by raising high-pressure steam, transferring heat to the clean gas, raising low pressure steam and finally by evaporation in the particulate scrubber. The gas leaves the scrubber fully saturated at 352F. Because it is saturated, there is a large amount of heat available at temperatures below 352F. After reheating the clean gas to 300F and heating the boiler feedwater to 250F, the remaining heat is rejected to ambient and the gas enters the Selexol System at 105F. Following desulfurization, the clean gas is reheated against the raw fuel gas in a series of three heat exchangers. At 700F, the clean gas is removed from the heat exchanger and sent through a zinc oxide bed to guarantee complete sulfur removal. Following this, steam is added to prevent carbon deposition and the gas is reheated to 1100F. At this point the pressure is reduced to the fuel cell operating level by expansion through a turbine.

The remainder of the system is virtually the same as that of the over-the-fence case described in Section 3.1. The cell operates at 185 amps per sq ft with an output voltage of 0.81V.

FIG. 4.1.1-1

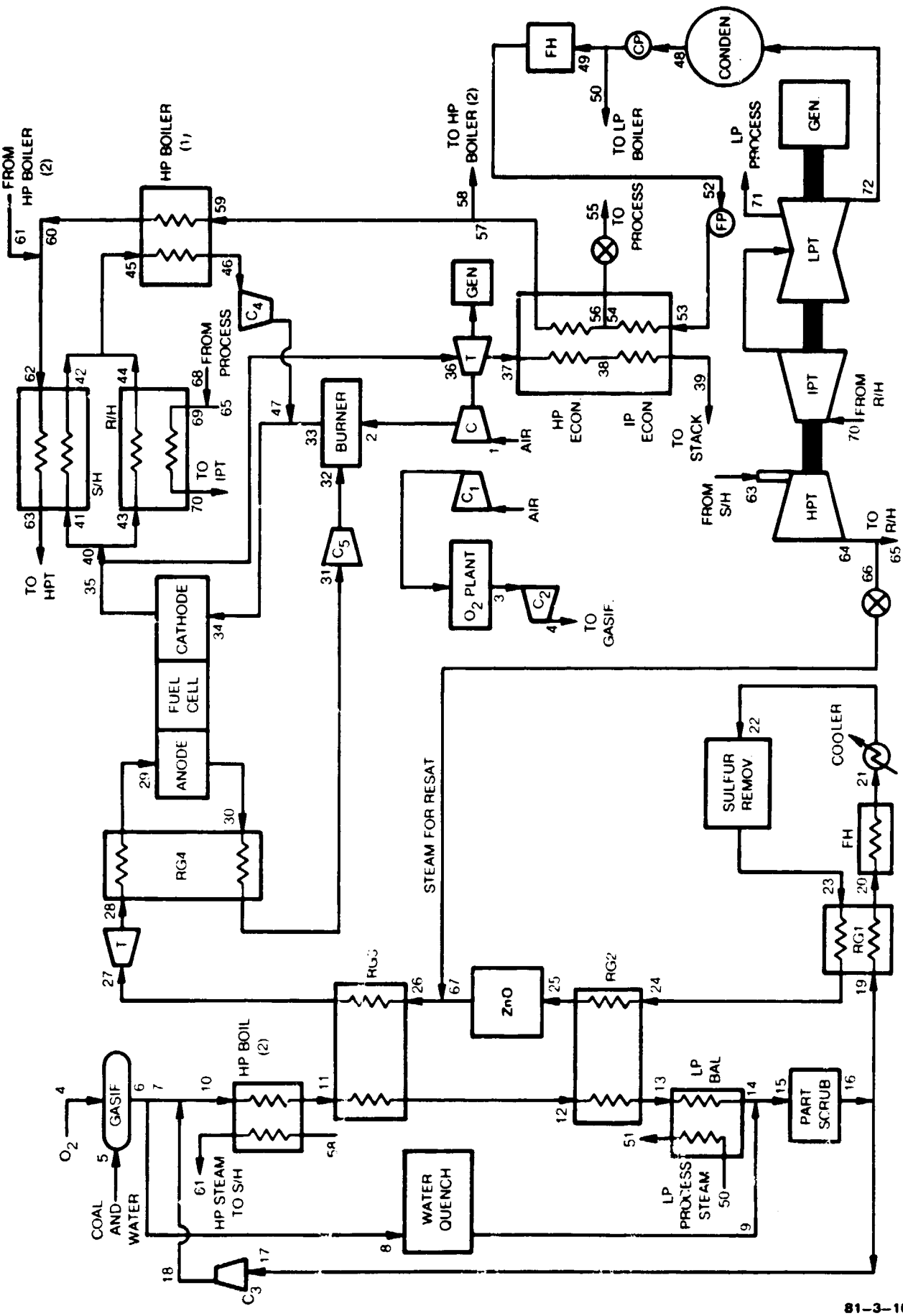

TEXACO OXYGEN– BLOWN GASIFIER/MOLTEN CARBONATE FUEL CELL

81-3-100-8

In the steam cycle, feedwater is sent to the fuel processing equipment where both low- and reheat-pressure steam is raised.

Performance of the system is summarized in Table 4.1.1-1, a heat and mass balance is given in Table 4.1.1-2 and stream compositions in Table 4.1.1-3.

4.1.2 Identification of Fuel Cell Power Plant with BGC Gasifier

The fuel cell system with steam bottoming cycle described in Section 2.1.3 will be used as the basis for the integrated plant. Cell operating conditions are as described in Section 2.1.3 but actual cell output varies with gas composition and steam cycle arrangement has been varied to fully utilize the available waste heat. A schematic for the BGC-based system is shown in Fig. 4.1.2-1.

The major factor in the gasification process that affect the power plant and result in basic differences between the BGC and Texaco based systems are:

1. The Texaco slurry feed and high temperature makes it less efficient than the BGC.

2. BGC raw gas must be water quenched to remove condensible hydrocarbons and the sensible heat is loss to the power plent.

3. BGC product gas contains a significant amount of methane (approx 22 percent of HHV) which cannot be used in the fuel cell.

The primary effect of these differences in terms of the Fig. 4.1.2-1 schematic is the loss of the ability to use heat from the raw gas to reheat the clean gas leaving the Selexol system. Instead, the heat needed to preheat the fuel gas must be taken from the anode exhaust stream. As a result, the fuel cell part of the system is virtually the same as in the over-the-fence case which has been described earlier.

Because of the gasifier steam requirements, the steam cycle is somewhat different than in the Texaco case. Steam for the gasification process is taken from three sources. Gasifier jacket heat provides approximately 60 percent of the total, 25 percent is raised in the sulfur recovery plant and 15 percent is raised in the sulfur recovery plant and 15 percent extracted from the intermediate pressure turbine. Other steam is extracted from the low pressure turbine to supply process needs at both 50 and 100 psig.

Performance of the system has been summarized in Table 4.1.1-1. A heat and mass balance is given in Table 4.1.2-1 and stream compositions are given in Table 4.1.2-2.

TABLE 4.1.1-1

PERFORMANCE SUMMARY FOR INTEGRATED GASIFICATION/
FUEL CELL POWER PLANTS

Gasification System:	Texaco	BGC
Oxident	Oxygen	→
Coal Rate, TPD	3566.6	→
Output:		
Fuel Cell Power, MW	365.3	330.5
Gas Turbine Power, MW	93.2	106.3
Steam Turbine Power, MW	106.0	100.7
Expander Power, MW	35.6	18.0
Gross Output, MW	600.1	555.5
Utilities:		
Selexol Power Consumption, MW	3.3	3.4
Air Compressor Power, MW	45.4	24.8
Oxygen Compressor Power, MW	15.6	7.9
Recirculation Compressor Power, MW	14.8	12.2
Other Utilities Power, MW	16.6	13.3
Total Utilities, MW	95.7	61.6
Total Net Output, MW	504.4	493.9
Heat Rate, Btu/kWh	7223	7362
Overall Efficiency, %	47.2	46.4

TABLE 4.1.1-2

HEAT AND MASS BALANCE FOR INTEGRATED TEXACO GASIFICATION/FUEL CELL POWER PLANT

Station Number	Temperature (°F)	Pressure (psia)	Flow (lb/sec)(1)
1	59	14.7	722.0
2	595	150.8	722.0
3	90	17.0	69.4
4	300	734.7	69.4
5			82.6
6	2400	588.0	180.6
7	2400	588.0	162.5
8	2400	588.0	18.1
9	400	564.5	25.5
10	1850	588.0	227.4
11	1200	582.1	227.4
12	742	576.3	227.4
13	522	570.5	227.4
14	404	570.5	227.4
15	403	570.5	252.9
16	352	570.5	259.1
17	352	570.5	64.9
18	360	588.0	64.9
19	352	570.5	194.2
20	334	570.5	183.2
21	199	558.5	154.5
22	105	541.8	152.0
23	70	530.9	126.3
24	300	530.9	126.3
25	700	525.6	126.3
26	665	515.1	220.0
27	1100	510.0	220.0
28	751	155.2	220.0
29	1100	150.0	220.0
30	1220	150.0	541.8
31	1039	145.0	541.8
32	1051	150.8	541.8
33	1113	150.0	1263.8
34	1100	150.0	3936.4
35	1300	150.0	3614.6
36	1300	150.0	942.0

(1) All flow values are for one engine.

TABLE 4.1.1-2 (Cont'd)

HEAT AND MASS BALANCE FOR INTEGRATED TEXACO
GASIFICATION/FUEL CELL POWER PLANT

Station Number	Temperature (°F)	Pressure (psia)	Flow (lb/sec)[1]
37	658	16.3	942.0
38	537	14.7	942.0
39	300	14.7	942.0
40	1300	150.0	2672.6
41	1300	150.0	1959.5
42	1154	150.0	1959.5
43	1300	150.0	713.1
44	1154	150.0	713.1
45	1154	150.0	2672.6
46	1080	145.0	2672.6
47	1094	150.0	2672.6
48	108	1.23	267.1
49	108	30.0	257.8
50	108	30.0	9.3
51	338	115.0	9.3
52	250	30.0	257.8
53	255	2836.0	257.8
54	486	2837.0	257.8
55	486	600.0	6.1
56	486	2837.0	251.7
57	592	2400.0	251.7
58	592	2400.0	129.2
59	592	2400.0	122.5
60	662	2400.0	122.5
61	662	2400.0	129.2
62	662	2400.0	251.7
63	1000	2400.0	251.7
64	649	600.0	251.7
65	649	600.0	158.0
66	649	600.0	93.7
67	634	515.0	93.7
68	486	600.0	6.1
69	644	600.0	164.1
70	1000	540.0	164.1
71	626	115.0	13.0
72	108	1.23	151.1

TABLE 4.1.1-3

MATERIAL BALANCE FOR INTEGRATED TEXACO GASIFIER/FUEL CELL POWER SYSTEM

Station Number		1-2		3-4		5 Coal Only		6		7		8	
Comp.	M.W.	Lb/Hr	Mols/Hr	Lb/Hr	Mols/Hr	Lb/Hr	Mols/Hr	Lb/Hr	Mols/Hr	Lb/Hr	Mols/Hr	Lb/Hr	Mols/Hr
CH_4	16.04	--	--	--	--	--	--	417	26	369	23	48	3
H_2	2.016	--	--	--	--	--	--	18815	9333	16934	8400	1881	933
CO	28.01	--	--	--	--	--	--	380460	13583	342394	12224	38038	1358
CO_2	44.01	--	--	--	--	--	--	125737	2857	113150	2571	12587	286
H_2S	34.08	--	--	--	--	--	--	11144	327	10020	294	1125	33
COS	60.07	--	--	--	--	--	--	961	16	841	14	120	2
O_2	32.00	598880	18715	245472	7671	--	--	--	--	--	--	--	--
N_2	28.02	1949407	69572	2662	95	--	--	6220	222	5604	200	616	22
A	39.94	34908	874	1797	45	--	--	1797	45	1598	40	200	5
H_2O	18.02	16398	910	--	--	297217	--	103831	5762	93452	5186	10380	576
Total		2599593	90071	249931	7811	297217	--	649382	32171	584362	28952	64995	3218

TABLE 4.1.1-3 (Cont'd)

MATERIAL BALANCE FOR INTEGRATED TEXACO GASIFIER/FUEL CELL POWER SYSTEM

Station Number		9		10-14		15		16		17-18		19	
Comp.	M.W.	Lb/Hr	Mols/Hr	Lb/Hr	Mols/Hr	Lb/Hr	Mols/Hr	Lb/Hr	Mols/Hr	Lb/Hr	Mols/Hr	Lb/Hr	Mols/Hr
CH_4	16.04	48	3	513	32	545	34	545	34	144	9	417	26
H_2	2.016	1881	933	23216	11516	25099	12450	25099	12450	6284	3117	18815	9333
CO	28.01	38038	1358	469448	16760	507513	18119	507513	18119	127053	4536	380460	13583
CO_2	44.01	12587	286	155135	3525	167722	3811	167722	3811	4199	954	125737	2857
H_2S	34.08	1125	33	13734	403	14859	436	14859	436	3715	109	11144	327
COS	60.07	120	2	1201	20	1322	22	1322	22	300	5	961	16
O_2	32.00	--	--	--	--	--	--	--	--	--	--	--	--
N_2	28.02	616	22	7677	274	8294	296	8294	296	2073	74	6220	222
A	39.94	200	5	2197	55	2396	60	2396	60	599	15	1797	45
H_2O	18.02	37337	2072	144574	8023	181912	10095	204221	11333	51123	2837	153098	8496
Total		91952	4714	817695	40608	909662	45323	931971	46561	195490	11656	698649	34905

TABLE 4.1.1-3 (Cont'd)

MATERIAL BALANCE FOR INTEGRATED TEXACO GASIFIER/FUEL CELL POWER SYSTEM

Station Number		20		21		22		23-25		26-29		30-32	
Comp.	M.W.	Lb/Hr	Mols/Hr	Lb/Hr	Mols/Hr	Lb/Hr	Mols/Hr	Lb/Hr	Mols/Hr	Lb/Hr	Mols/Hr	Lb/Hr	Mols/Hr
CH_4	16.04	417	26	417	26	417	26	401	25	401	25	401	25
H_2	2.016	18815	9333	18815	9333	18815	9333	18721	9286	18721	9286	4175	2071
CO	28.01	380460	13583	380460	13583	380460	13583	376062	13426	376062	13426	37421	1336
CO_2	44.01	125737	2857	125737	2857	125737	2857	51404	1168	51404	1168	1433054	32562
H_2S	34.08	11144	327	11144	327	11144	327	--	--	--	--	--	--
COS	60.07	961	16	961	16	961	16	--	--	--	--	--	--
O_2	32.00	--	--	--	--	--	--	--	--	--	--	--	--
N_2	28.02	6220	222	6220	222	6220	222	6192	221	6192	221	6192	221
A	39.94	1797	45	1797	45	1797	45	1757	44	1757	44	1757	44
H_2O	18.02	113184	6281	9983	554	973	54	54	3	337533	18731	467547	25946
Total		658735	32691	555534	26963	546524	26463	454591	24173	792070	42901	1950547	62205

TABLE 4.1.1-3 (Cont'd)

MATERIAL BALANCE FOR INTEGRATED TEXACO GASIFIER/FUEL CELL POWER SYSTEM

Station Number		33		34		35		36-39		40-47		48-72	
Comp.	M.W.	Lb/Hr	Mols/Hr	Lb/Hr	Mols/Hr	Lb/Hr	Mols/Hr	Lb/Hr	Mols/Hr	Lb/Hr	Mols/Hr	Lb/Hr	Mols/Hr
CH_4	16.04	--	--	--	--	--	--	--	--	--	--	--	--
H_2	2.016	--	--	--	--	--	--	--	--	--	--	--	--
CO	28.01	--	--	--	--	--	--	--	--	--	--	--	--
CO_2	44.01	1492951	33923	3318178	75396	2468609	56092	643338	14618	1825227	41473	--	--
H_2S	34.08	--	--	--	--	--	--	--	--	--	--	--	--
COS	60.07	--	--	--	--	--	--	--	--	--	--	--	--
O_2	32.00	542752	16961	1206336	37698	897472	28046	233888	7309	663584	20737	--	--
N_2	28.02	1955600	69793	7503756	267800	7503756	267800	1955572	69792	5548240	198010	--	--
A	39.94	36665	918	140669	3522	140669	3522	36665	918	104004	2604	--	--
H_2O	18.02	522148	28976	2003464	111180	2003464	111180	522148	28976	1481388	1481388	961781	53373
Total		4550116	150571	14172403	495596	13013970	466640	3391611	121613	9622443	345032	961781	53373

FIG. 4.1.2-1

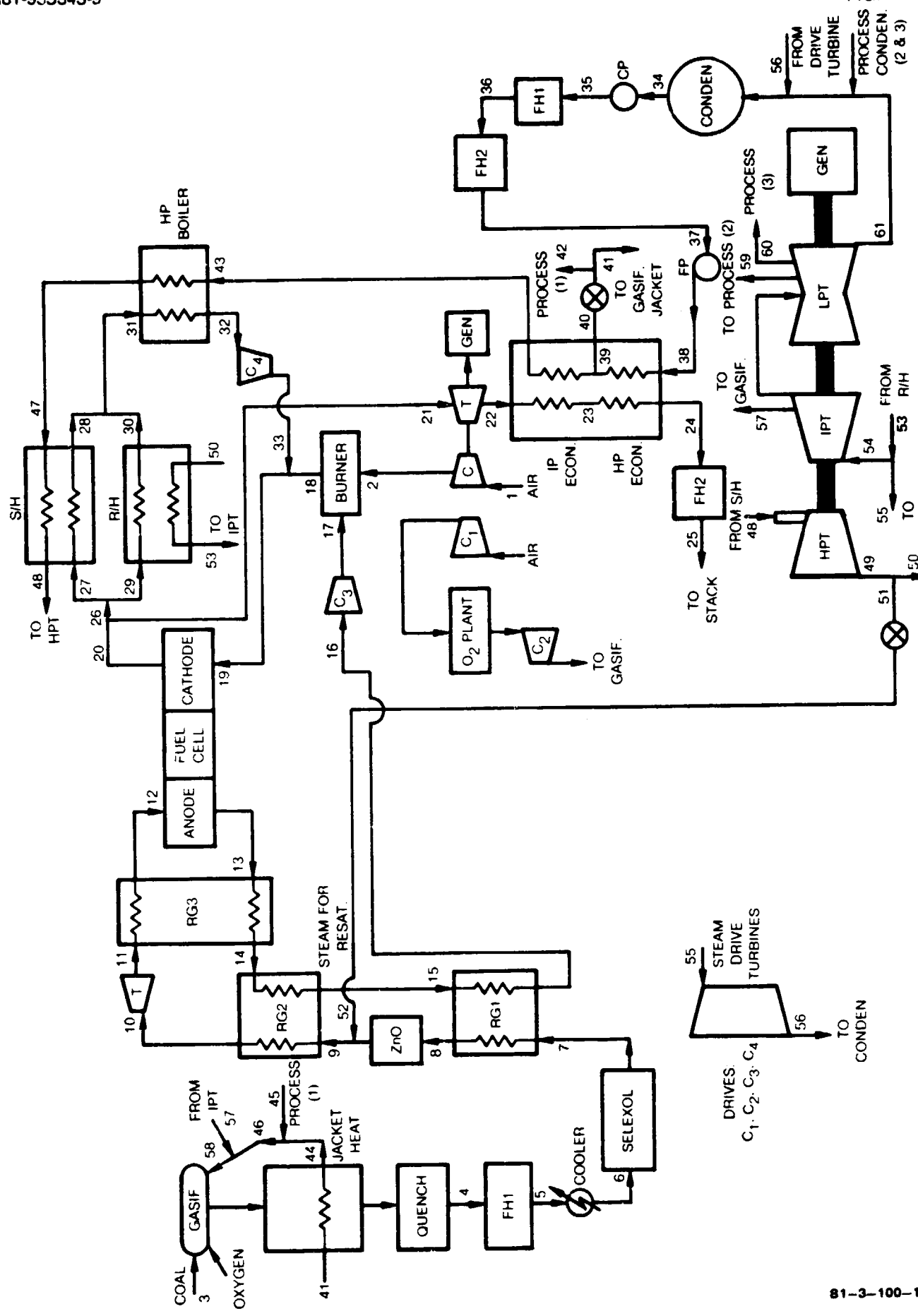

BGC SLAGGER GASIFIER/MOLTEN CARBONATE FUEL CELL

81-3-100-10

TABLE 4.1.2-1

HEAT AND MASS BALANCE FOR INTEGRATED BGC GASIFICATION/
FUEL CELL POWER PLANT

Station Number	Temperature (°F)	Pressure (psia)	Flow (lb/sec)(1)
1	59	14.7	860.0
2	595	150.8	860.0
3			82.6
4	282	325.0	154.0
5	163	320.0	134.2
6	105	306.0	132.6
7	70	296.0	122.4
8	1100	291.0	122.4
9	650	281.1	231.6
10	939	276.2	231.6
11	775	152.0	231.6
12	1100	150.0	231.6
13	1220	150.0	527.3
14	1039	148.0	527.3
15	877	146.0	527.3
16	712	144.1	527.3
17	724	150.8	527.3
18	1341	150.0	1387.3
19	1100	150.0	3756.0
20	1300	150.0	3460.3
21	1300	150.0	1091.6
22	655	16.2	1091.6
23	491	14.7	1091.6
24	300	14.7	1091.6
25	250	14.7	1091.6
26	1300	150.0	2368.7
27	1300	150.0	1780.7
28	1126	150.0	1780.7
29	1300	150.0	588.0
30	1126	150.0	588.0
31	1126	150.0	2368.7
32	945	145.1	2368.7
33	958	150.0	2368.7
34	108	1.23	292.8
35	108	30.0	292.8

(1) All flow values are for one engine.

TABLE 4.1.2-1 (Cont'd)

HEAT AND MASS BALANCE FOR INTEGRATED BGC GASIFICATION/
FUEL CELL POWER PLANT

Station Number	Temperature (°F)	Pressure (psia)	Flow (lb/sec)[1]
36	200	30	292.8
37	250	30	292.8
38	255	2837	292.7
39	446	2553	292.7
40	446	2553	20.6
41	448	415	14.5
42	448	415	6.1
43	603	2400	272.2
44	448	415	14.5
45	448	415	6.1
46	448	415	6.1
47	662	2400	272.2
48	1000	2400	272.2
49	648	600	272.2
50	648	600	162.9
51	648	600.0	109.2
52	608	281.1	109.2
53	1000	540.0	162.9
54	1000	540.0	63.6
55	1000	540.0	99.3
56	108	1.23	99.3
57	937	415.0	4.0
58	510	415.0	24.6
59	611	100.0	39.8
60	475	50.0	4.8
61	108	1.23	15.0

TABLE 4.1.2-2

STREAM COMPOSITIONS FOR INTEGRATED BGC
GASIFIER/FUEL CELL POWER SYSTEM

Station Number		1-2		3		4		5		6	
Comp.	MW	Lb/Hr[1]	Mols/Hr	Lb/Hr	Mols/Hr	Lb/Hr	Mols/Hr	Lb/Hr	Mols/Hr	Lb/Hr	Mols/Hr
CH_4	16.04	--	--	--	--	33235	2072	33235	2072	33235	2072
H_2	2.016	--	--	--	--	14560	7222	14560	7222	14560	7222
CO	28.01	--	--	--	--	386118	13785	386118	13785	386118	13785
CO_2	44.01	--	--	--	--	20245	460	20245	460	20245	460
H_2S	34.08	--	--	--	--	11144	327	11144	327	11144	327
COS	60.07	--	--	--	--	841	14	841	14	841	14
O_2	32.00	713312	22291	--	--	--	--	--	--	--	--
N_2	28.02	2321933	82867	--	--	8994	321	8994	321	8994	321
A	39.94	41578	1041	--	--	160	4	160	4	160	4
H_2O	18.02	19534	1084	297217	--	78675	4366	7154	397	1586	88
Total		3096357	107283	297217	--	553972	28571	482451	24602	476883	24293

(1) All values based on one engine.

TABLE 4.1.2-2 (Cont'd)

STREAM COMPOSITIONS FOR INTEGRATED BGC
GASIFIER/FUEL CELL POWER SYSTEM

Station Number		7-8		9-12		13-17		18		19	
Comp.	M.W.	Lb/Hr	Mols/Hr	Lb/Hr[1]	Mols/Hr	Lb/Hr	Mols/Hr	Lb/Hr	Mols/Hr	Lb/Hr	Mols/Hr
CH_4	16.04	31615	1971	31615	1971	31615	1971	--	--	--	--
H_2	2.016	14505	7195	14505	7195	3998	1983	--	--	--	--
CO	28.01	382981	13673	382981	13673	32155	1148	--	--	--	--
CO_2	44.01	8318	189	8318	189	1340149	30451	1477416	33570	2989291	67934
H_2S	34.08	--	--	--	--	--	--	--	--	--	--
COS	60.07	--	--	--	--	--	--	--	--	--	--
O_2	32.00	--	--	--	--	--	--	537120	16785	1086752	33961
N_2	28.02	2942	105	2942	105	2942	105	2324875	82972	7369540	263010
A	39.94	160	4	160	4	160	4	41737	1045	132281	3312
H_2O	18.02	180	10	393413	21832	487351	27045	613617	34052	1945079	107940
Total		475477	23147	833934	44969	1898370	62707	4994765	168424	13522943	476146

(1) All values based on one engine.

TABLE 4.1.2-2 (Cont'd)

STREAM COMPOSITIONS FOR INTEGRATED BGC
GASIFIER/FUEL CELL POWER SYSTEM

Station Number		20		21-25		26-33		34-61	
Comp.	M.W.	Lb/Hr	Mols/Hr	Lb/Hr	Mols/Hr	Lb/Hr(1)	Mols/Hr	Lb/Hr	Mols/Hr
CH_4	16.04	--	--	--	--	--	--	--	--
H_2	2.016	--	--	--	--	--	--	--	--
CO	28.01	--	--	--	--	--	--	--	--
CO_2	44.01	2208642	50185	696766	15832	1511876	34353	--	--
H_2S	34.08	--	--	--	--	--	--	--	--
COS	60.07	--	--	--	--	--	--	--	--
O_2	32.00	802976	25093	253312	7916	549664	17177	--	--
N_2	28.02	7369540	263010	2324875	82972	5044721	180040	--	--
A	39.94	132281	3312	41737	1045	90544	2267	--	--
H_2O	18.02	1945079	107940	613617	34052	1331462	73888	1054224	58503
Total		12458518	449540	3930307	141817	8528267	307725	1054224	58503

(1) All values based on one engine.

4.1.3 Comparison of Performance

The differences between the Texaco and BGC performance shown in Table 4.1.1-1 are due primarily to gasifier efficiency (the slurry feed makes the Texaco less efficient than the BGC), the loss of raw gas sensible heat (in the case of the BGC) and the presence of methane in the BGC gas that cannot be used in the fuel cell but whose energy improves the steam cycle in that system.

Because of the lower oxygen and steam (water) requirements of the BGC gasifier the cold gas efficiency of that unit is much higher than the Texaco units (93% and 77% respectively). However, this difference is offset by the amount of methane in the BGC off-gas. Nearly 24% of the heating value of that gas is attributed to methane and other hydrocarbons that cannot be utilized in the fuel cell. They are, however, used at steam cycle efficiency.

The low exit temperature of the BGC gasifier results in a significant amount of condensibles in the off-gas. As a result, it is not practical to attempt to remove the sensible heat from the stream. Instead, it must be water quenched and the heat is availible at less(than 282N.

Referring to Table 4.1.1-1, the effects of these differences can be seen. Fuel cell power is some 10% less in the BGC case. This is a direct result of the difference in the quantity of hydrogen and carbon monoxide in the product gas of each. If only those two gases were considered in calculating cold gas efficiency, it would be 70% for the BGC and 77% for the Texaco gasifier.

Gas turbine power is higher in the BGC system due to the increased flow associated with combustion of methane in the cathode loop. The combustion of methane also raises the steam cycle output. Despite the loss of gasifier raw gas sensible heat in the BGC-based system, steam power is almost the same in both cases. Expander power differs due to the difference in pressure at which each gasifier operates.

While total output of the Texaco system is some 8% higher, net output differs by only 2%. This is due primarily to the air compressor for the oxygen plant and the oxygen compressor. The former is lower in the BGC system since oxygen requirements are 44% lower than for the Texaco gasifier. Oxygen compressor power differs due to the lower flow and also due to the lower pressure to which it must be compressed in the BGC system.

4.1.4 Off-Design Operation of Gasification/Molten Carbonate Power Plants

The integration of a molten carbonate fuel cell with a gasification system yields a very complex plant. The ability to operate such a plant can only be demonstrated in an actual installation. Simulation of the plant is possible, however, this has not been done to date. Consequently, it is necessary to infer from existing data the probable part-load capability of an integrated gasification/molten carbonate fuel cell power system.

In Ref. 4.1-2 the plant operation and control of an integrated gasifier/molten carbonate fuel cell was discussed. Two modes of operation at part power were advanced.

The first mode takes advantage of the fact that the powerplant consists of independent gasifier-fuel cell trains operated in parallel. In each train, coal is converted to fuel cell power and the waste heat from all trains is available to a single steam bottoming cycle. Any train can be shut down independently of the others; this reduces the fuel cell output. Shutting down a single gasifier-fuel cell train lowers the amount of steam available to the bottoming cycle, thus lowering its output power. This modular unit shutdown approach to turndown has the disadvantage of slow response time to power turnup. It takes two hours or less to bring a hot unit on line. If it has been off line longer than 48 hours and allowed to cool down, it takes a minimum of 12 hours. The second turndown mode has quick response times and infinitely variable power levels. In this mode, all units remain online and power is reduced by changing the inverter controls and reducing the coal flow to the gasifiers.

The total startup time from cold for the powerplant is limited to heat up of the fuel cell and gasifier sections and requires a minimum of 12 hours. A hot restart of the powerplant is expected to take about two hours or less due to the fact that hot components stay near nominal operating temperatures for up to 48 hours following shutdown.

Both complete or partial shutdown of the plant may be accomplished. For partial shutdown to cold condition, the inverters associated with individual fuel cell islands are automatically shut off and disconnected on both the dc and ac sides. Simultaneously, both the coal and air feed to the appropriate gasifiers are stopped causing a halt in the production of synthesis gas. Steam from auxiliary boilers is fed to the gasifiers to control cooling rate. Residual combustible gases in the gasification system and gases formed during the cool down process are burned and vented through the flare stack. After the gasification vessels have cooled sufficiently, they may be depressurized. Residual coal and ash remaining in the vessels is removed through the ash hoppers and carried off through the ash slurry system. Upon removal of the electrical load, the fuel

cells which are being shut down revert to open circuit conditions. Waste heat is no longer being produced and the cathode recycle loop can be shut down. The turbocompressors are shut off and the cells are allowed to cool slowly by natural convection. If faster cooling of the cells is required, the fuel cell turbocompressor may be operated using its auxiliary burner to provide cooling air to the cells. When the entire plant is to be shut down, the steam bottoming cycle must be removed from the line. Since the steam plant is unfired, it depends on the fuel cell waste heat for process steam production. When the fuel cells are shut down, steam production stops. Residual steam may be either vented to the atmosphere or passed to the turbine condenser unit.

4.1.5 References

4.1-1 Crawford, C. D., R. P. Dawkins, and J. R. Joiner: An Economic Comparison of Molten Carbonate Fuel Cells and Gas Turbines in Coal Gasification-Based Power Plants. EPRI AP-1543, September 1980.

4.1-2 King, J. M.: Energy Conversion Alternatives Study - Intergrated Coal Gasifier/Molten Carbonate Fuel Cell Power plant Conceptual Design and Implementation Assessment. NASA CR 134955, October 1976.

1.2 Assessment of Combined Cycle Systems Technology Status

Although the first application of gas turbines in power generating systems occurred in Switzerland in the 1950's, it was not until the late 1940's that utilities in the U.S. began to use the gas turbine. By the end of 1977, there were 47,736 MW of gas turbine capacity installed, approximately 8.6 percent of the total U.S. utility capacity. By the end of 1980, an additional 4700 MW was added.

The vast majority of the installed gas turbine capacity is used in the simple-cycle mode as peaking units, i.e., units used less than 1200 hr/yr. In locations where low cost clean fuel is available, simple-cycle units may be used for longer periods, perhaps even as base-load units. There are nearly 5000 MW of combined cycle systems installed or under construction in the United States. These units are usually operated in mid-ranges (1500-3000 hr/yr) although several industrial cogeneration applications are base loaded.

1.2.1 Assessment of Combined Cycle Technology Readiness Development Status

Before projections of future gas turbine system technology can be presented, it is necessary to identify the characteristics of current commercial installations and define the technology readiness and development status of gas turbines.

It is instructive to review, at this point, several basic aspects of gas turbine operation. The simple-cycle gas turbine operates on the Brayton cycle (Fig. 1.2.1-1). As with any thermodynamic cycle, the most important parameter is the peak cycle temperature, i.e., Carnot's law states that the efficiency of a heat engine is a function of the peak cycle temperature and the temperature at which the cycle heat is rejected. In the limit this becomes

$$\eta_t = 1 - \frac{T_r}{T_p}$$

where η_t = theoretical Carnot efficiency
T_r = heat rejection temperature
T_p = peak cycle temperature

A second important parameter is the cycle pressure ratio, i.e., the compressor outlet pressure/compressor inlet pressure. There exists a relationship between pressure ratio and turbine inlet temperature which allows selection of the optimum operating characteristics.

In its basic form, a gas turbine consists of compressor, combustor, and turbine components. Typically, the compressor is constructed with one, two or

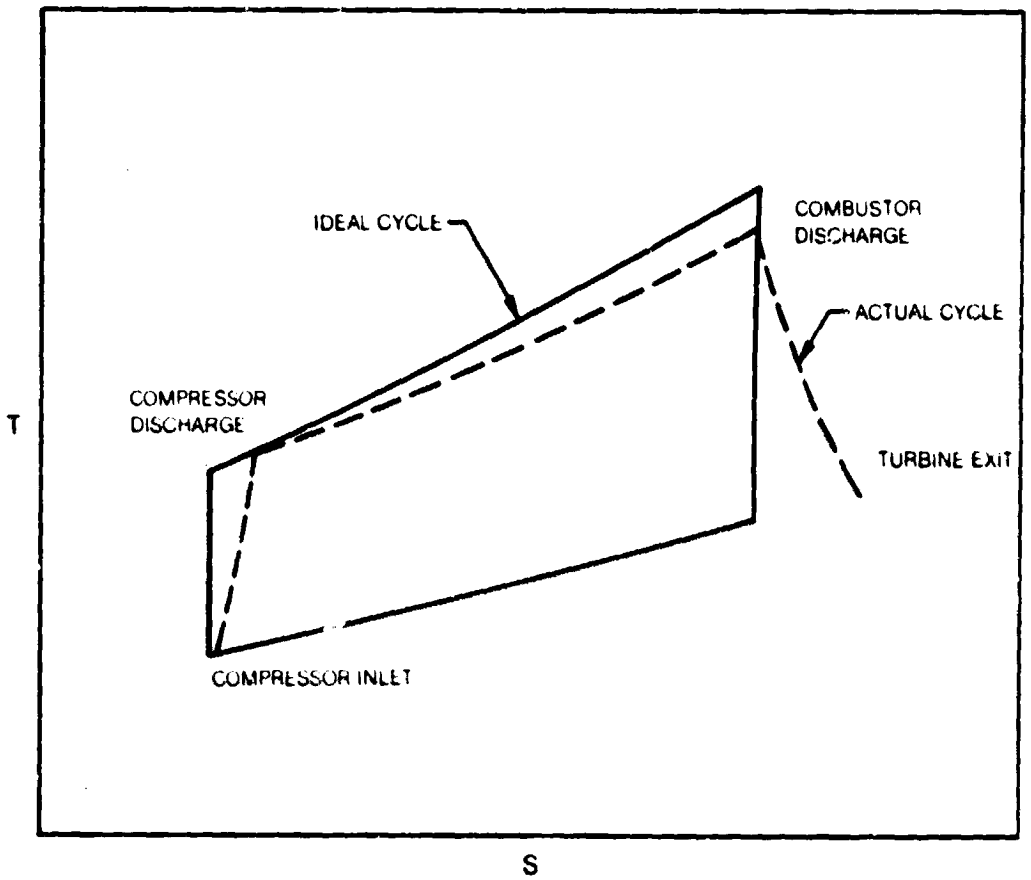

TEMPERATURE-ENTROPY DIAGRAM FOR A BRAYTON CYCLE

more spools (shafts), depending on overall compression ratio and desired characteristics for engine starting and part-load performance. The combustor is usually designed for compact, high heat release characteristics so that mounting directly on the engine structure is possible. The use of coal-derived gaseous fuels, however, has led to other combustor configurations which will be discussed in later sections. The turbine component produces shaft work, approximately one-half to two-thirds is used to drive the compressor with the remainder available to drive the load, i.e., the electric generator. The electric generator may be coupled to the same shaft as the compressor turbine (single-shaft version) or it may be driven by a free power turbine (two-shaft version) aerodynamically coupled to the upstream gas generator.

In the combined-cycle mode, a waste heat boiler would be installed in the hot exhaust stream from the gas turbine. Steam raised in this boiler would be used in a steam turbogenerator to produce electrical power. The use of the steam bottoming system reduces the heat rejection temperature from that associated with the gas turbine exhaust to a value associated with the steam condenser. The result is a significant increase in efficiency. The theory of combined cycle operation is treated in Appendix A.2. A more detailed discussion of the steam bottoming cycle is included in the discussions of the system technology readiness.

The following sections discuss currently available and state-of-the-art gas turbines and combined-cycle systems from the viewpoint of their performance and technology readiness. The development trends in turbomachinery components and materials from the current machine through the state of the art to potential future machines are then described.

1.2.1.1 Technology Readiness - Commercially Available Equipment

The present generation of commercially available simple-cycle gas turbines of interest for utility power generation range in size from approximately 10 MW to nearly 150 MW. These machines have compression ratios ranging from 8.1 to 14.1 and firing temperatures from 1600 F to 2100 F. They are capable of attaining heat rates as low as 10,500 Btu/kWh (32.5 percent thermal efficiency). A typical method of presenting performance for a gas turbine is shown in Fig. 1.2.1.1-1 for the FT4C, a nominal 30-MW gas turbine manufactured by United Technologies Corporation.

The actual heat rates incurred by currently installed gas turbines display a wide divergence. This is due to several operating variations, e.g., a machine with many startups and shutdowns will have a high heat rate since the fuel consumption is high compared to the power generated. Also, several utilities use some of their turbines as synchronous condensers, therefore, essentially no power is generated although fuel is being consumed.

FIG. 1.2.1.1-1

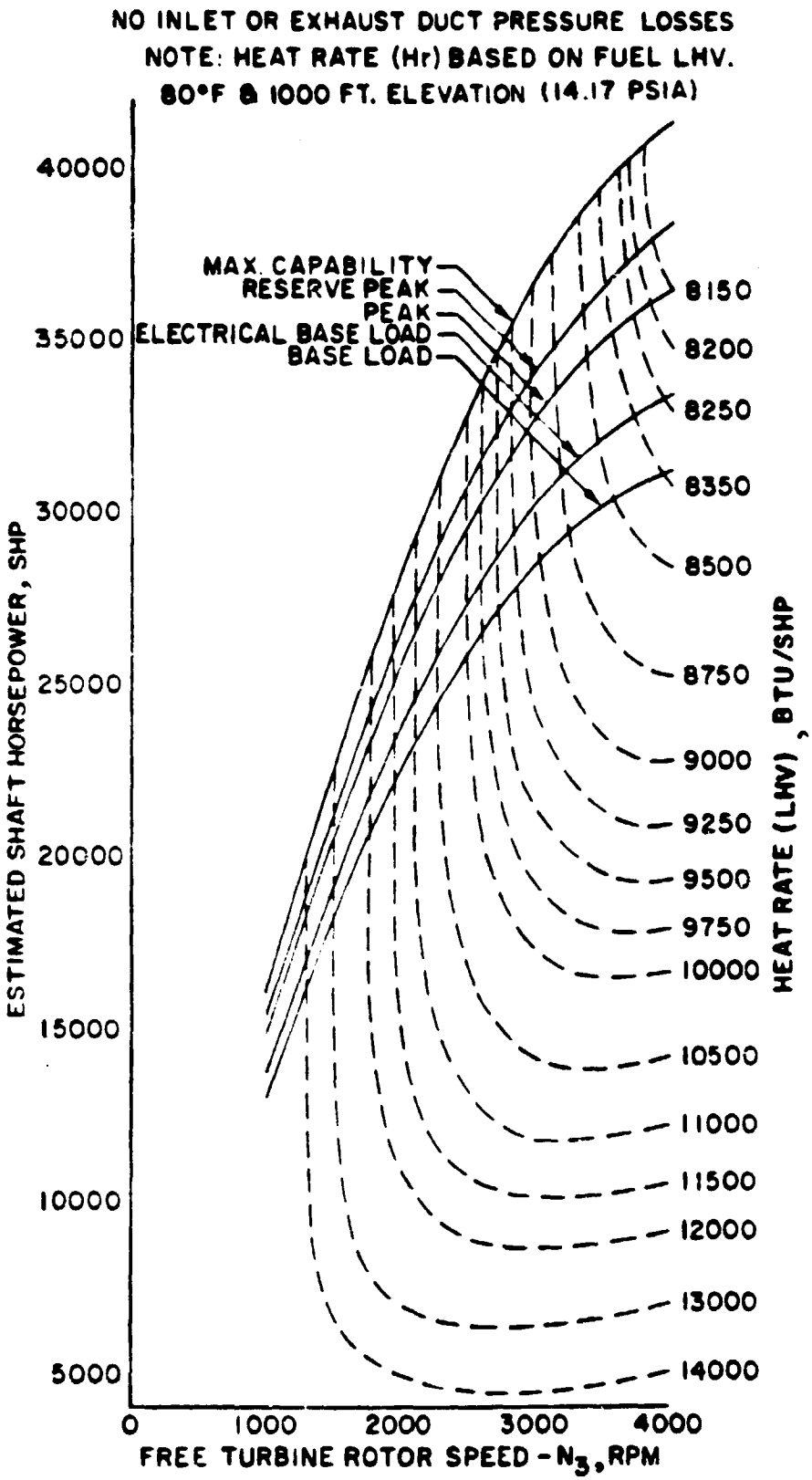

PERFORMANCE OF FT4C

The current offerings of combined-cycle systems vary from slightly over 14.5 MW to approximately 675 MW. The lower ratings are for single gas turbine/steam turbine combinations while the higher ratings are for multiple gas turbines (up to eight) and one steam turbine. The heat rates range from 7500 Btu/kWh to 9500 Btu/kWh (45.5 percent and 35.9 percent, respectively).

The foregoing performance values are based on the use of clean fuels. Use of such fuels is necessary to preserve the lifetime of combustor and turbine (hot section) components. All gas turbine manufacturers agree that natural gas is the best currently available fuel where long life of hot section parts is desired. It is recognized that in most areas of the country natural gas is a limited use fuel and for most utility installations is usually available, at best, only on an interruptable basis. Natural gas costs vary considerably, e.g., $\$1.00/10^6$ Btu in Texas to $\$4.50/10^6$ Btu in Illinois.

Next to natural gas, the best fuels for gas turbines are those used in aircraft applications. These are the kerosene fuels, JP4, JP5, and ASTM GT No. 1 also known as Jet A or Jet B fuels. These kerosene-base fuels, although providing good combustion characteristics in gas turbines, are more expensive than natural gas or more plentiful, lower grade fuels. Jet fuel is approximately $\$7.00/10^6$ Btu. Below the kerosene-base fuels in acceptability to gas turbine applications are fuels known as diesel No. 2 and home heating No. 2. This latter fuel is widely used by the electric utilities as gas turbine fuel. Residual oil is sometimes used, but requires pretreatment. Even with this treatment, residual oil is not a satisfactory fuel for long-term use. The cost of GT-2 (No. 2 oil) varies from $\$1.90/10^6$ Btu in Texas to $\$6.50/10^6$ in Delaware. Residual oil (No. 6) varies from \$2.30 to $\$4.65/10^6$ Btu.

Another important aspect to be considered in the design of a gas turbine system is the characteristic of the load to which the system will be subjected. Where the unit is used for short periods at high powers with frequent starts and stops, it is important to have a clear understanding of the number of planned starts and stops in addition to the power level expected during this operation. In addition, it is necessary to know the rate at which the load is to be applied. If it is possible to load the machine at a relatively low rate and still meet requirements, the least deterioration of the equipment over a given operating period will result. If, however, a fast start is required with quick loading, it may be necessary to reduce the length of the overhaul period on the machine.

For a continuously operating installation where loads will be maintained relatively constant, it is desirable to derate the gas turbine to power levels below those needed for peaking applications. Customarily, the base-load or continuous-load power level of an industrial gas turbine installation is approximately 80 percent of the maximum capability of the machine; however, where high ambient temperature are expected year-round, it may be advisable to decrease this to 70 percent or 75 percent in order to stay within desirable turbine temperature levels.

Records compiled from the hundreds of gas turbine installations throughout the U.S. and the world show that the starting reliability of these machines range from 96 percent to 99 percent and overhaul cycle times from 8,000 to 40,000 hours. As might be expected, those engines which have come up to 40,000 hours of operation have normally been found to be lightly loaded.

1.2.1.1 Technology Readiness - State-of-the-Art Gas Turbines

The next generation of gas turbines is already in the testing phase. Generally speaking these turbines have a larger power output and are of heavier duty than the present generation. A joint design by United Technologies and Stal-Laval (Sweden) completed in the mid-1970's, is representative of just such as engine. Known as the UTC FT50 or the Stal Laval GT200, the engine appeared in prototype form in 1975. At the present time only the GT200 is in production although several FT50 prototypes were built and run at the conditions equivalent to 90 MW with a heat rate of 10,000 Btu/kWh. The FT50 and the GT200 have identical gas generators and differ only in that the power turbines operate at 3600 rpm (60 Hz) and 3000 rpm (50 Hz), respectively. This engine could evolve into a 100 MW-plus power plant with heat rates in the 9500 Btu/kWh range.

FT50/GT200

The FT50 is a high performance industrial gas turbine consisting of a twin-spool gas generator and a free turbine driving the output shaft. Nominal rotating speeds are 3520 rpm for the low compressor spool, 4200 rpm for the high compressor spool, and 3600 rpm for the power (free) turbine shaft. The two gas generator spool systems are concentric to each other, yet mechanically independent. Each compressor is driven by its own single-stage reaction turbine. The hot gases from the gas generator drive the two-stage free turbine. The free turbine converts the heat and kinetic energy of the gas generator exhaust to useful work energy in the form of shaft horsepower without the use of additional mechanical devices.

The FT50/GT200 was designed as the state-of-the-art gas turbine for use in simple cycle applications such as peaking or mid-range duty. It was designed to handle clean fuels, i.e., natural gas or distillate oil. The engine pressure ratio is 16:1 and it operates at approximately 2100 F with a heat rate of slightly over 10,000 Btu/kWh.

The engine represents the ultimate in adapting aircraft engine technology to industrial applications. The multi-spool design allows each compressor and turbine section to operate at optimum efficiency while the use of the free turbine allows efficient operation at either 50 Hz or 60 Hz.

Because of the multiple shaft design, it is necessary to have a number of bearings, some operating in the hot section. To facilitate engine maintenance, the FT50/GT200 was designed in modular fashion (Fig. 1.2.1.1-2) which would allow the engine to be dismantled, new or rebuilt parts installed and the engine reassembled in ten working days for the longest maintenance item, combustor replacement. This compares to several months for other large industrial machines.

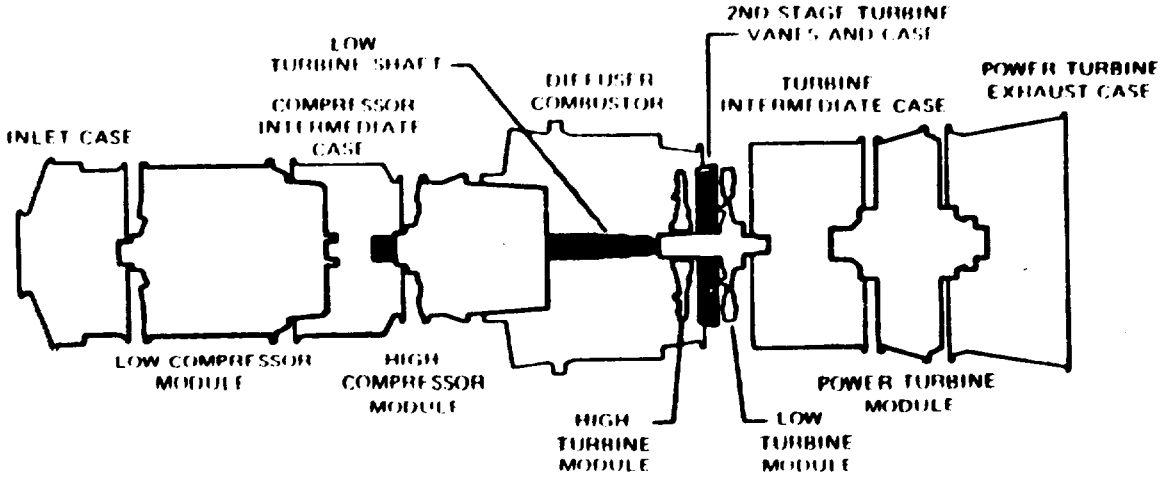

MODULE	WEIGHT (LB)	TIME TO REPLACE (HOURS)
LOW COMPRESSOR	33,200	12
HIGH COMPRESSOR	20,100	23
HIGH TURBINE	4,300	34
LOW TURBINE	5,100	28
POWER TURBINE	33,700	31

ALL MODULE DIMENSIONS ARE LESS THAN 11 FEET

MODULAR CONSTRUCTION OF FT50

In addition to the modular construction, the FT500/GT200 uses aircraft type turbine cooling technologies. (The following section on Development Trends will cover cooling in some detail, therefore, only a brief description is included here.) The technique used in this engine is known as film cooling. Cooling air is circulated within the blade prior to ejection of some portion through holes in the blade leading edge (called showerhead cooling). A film of air is then formed around the blade keeping metal temperatures to the 1500-1600 F range while operating in a 2000 F plus environment. Cooling of this type requires clean fuels since the cooling holes can be plugged by carryover of combustion ash or corrosive components.

The GT200 has run successfully on the grid of the Swedish Power Grid and the engine is now offered commercially by Stal-Laval. They also offer a combined cycle based upon this design with an output of 228 MW using two GT200 engines and one turbine. The estimated heat rate for this system (on natural gas) is 7420 Btu/kWh. The estimated output and heat rate for the FT50/GT200 are given in Figs. 1.2.1.1-3 and 4.

V84.3

A second, and entirely different state-of-the-art approach to the large industrial gas turbine is represented by another UTC joint effort, this one with KraftWork Union (KWU) of West Germany. In general, European turbine designs have differed from the US designs in that they tended to be less highly stressed both aerodynamically and physically and usually operated at much lower temperatures, i.e., 1350-1600 F, and thus, did not required turbine cooling. These machines generally were designed for base-load (5000 hr/yr or greater) applications.

A typical conservatively designed European machine is the KWU 94 series, a 100-MW plus machine with a single shaft and front-end drive. The exhaust is ducted directly out the rear of the machne making combined-cycle application easier. The method of construction results in a shaft that is extremely stiff and is supported by only two bearings. Rather than the on-line combustion cans used by US manufactures, the KWU combustion system consists of two large externally-mounted silos. These combustors have proven to be extremely durable and are readily adaptable to a variety of fuels, including crude oil, residual and heavy synthetic liquids. The silo construction is also very well suited for low-Btu gas or pressurized fluidized bed cycles, where air must be extracted for the process. The general component arrangement for the KWU gas turbine and auxiliaries can be seen in Fig. 1.2.1.1-5.

United Technologies and KraftWork Union have completed a preliminary design study as part of a potential joint venture, the object of which is to apply advanced UTC technology in compressor, combustor and turbine development to the KWU overall design. The result of such a venture would be an engine design based on the V94 gas turbine but with improved cost per kilowatt, heat rate and emissions

GENERATOR EFFICIENCY = 98.7%

ALTITUDE = SEA LEVEL (PAM = 14.7 PSIA)

3600 RPM

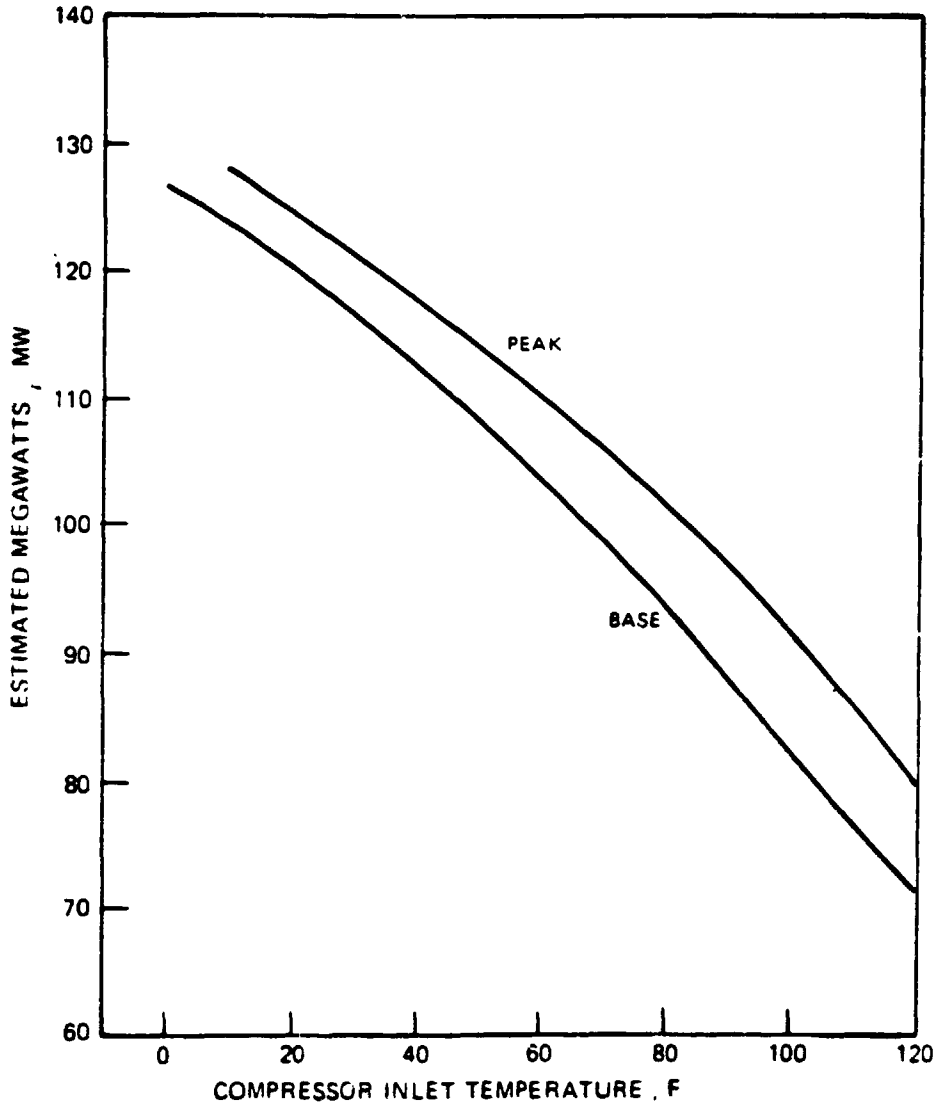

ESTIMATED OUTPUT OF FT50

FIG. 1.2.1.1-4

GENERATOR EFFICIENCY = 98.7%
ALTITUDE = SEA LEVEL (PAM = 14.7 PSIA)
3600 rpm

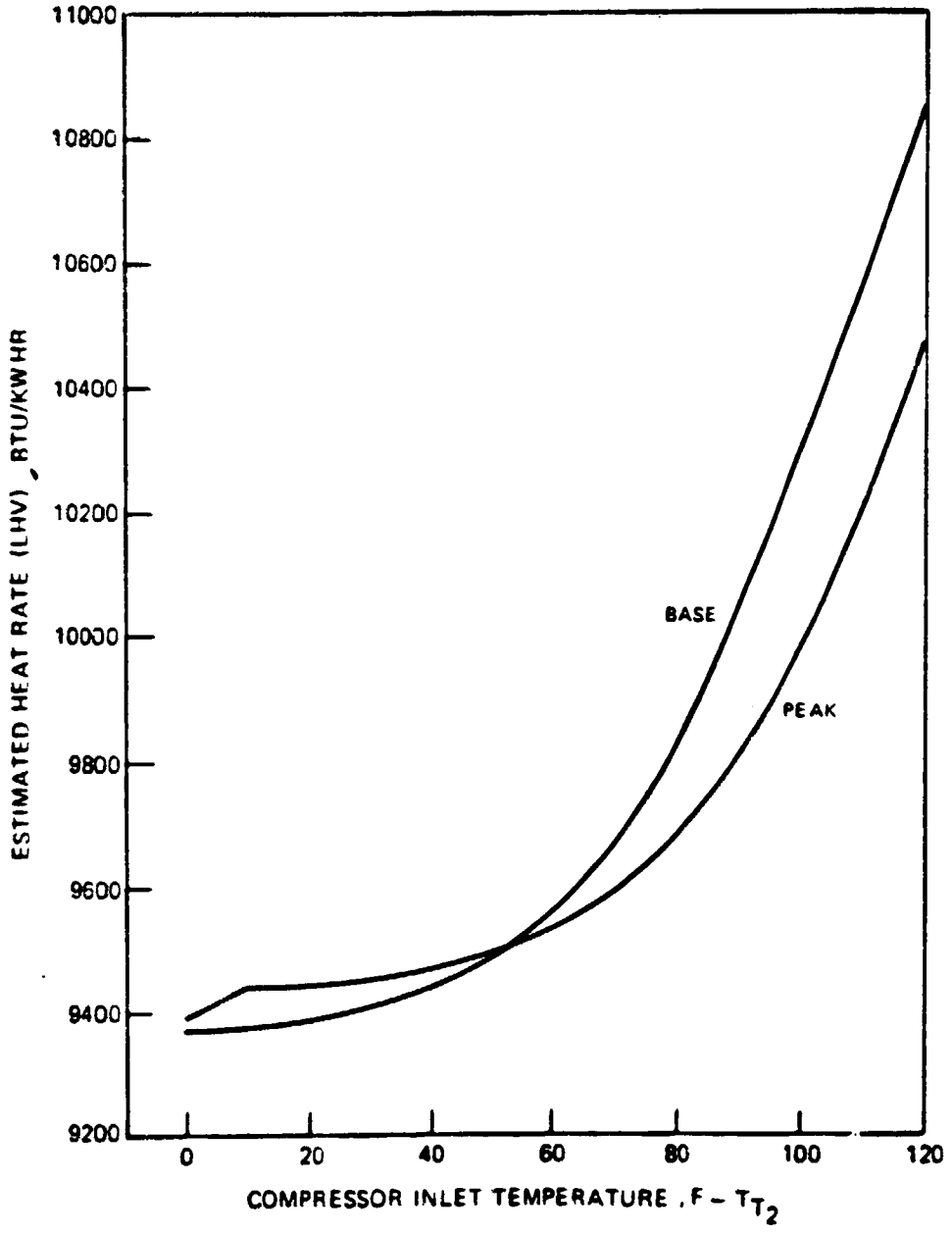

ESTIMATED HEAT RATE OF FT50

FIG. 1.2.1.1-5

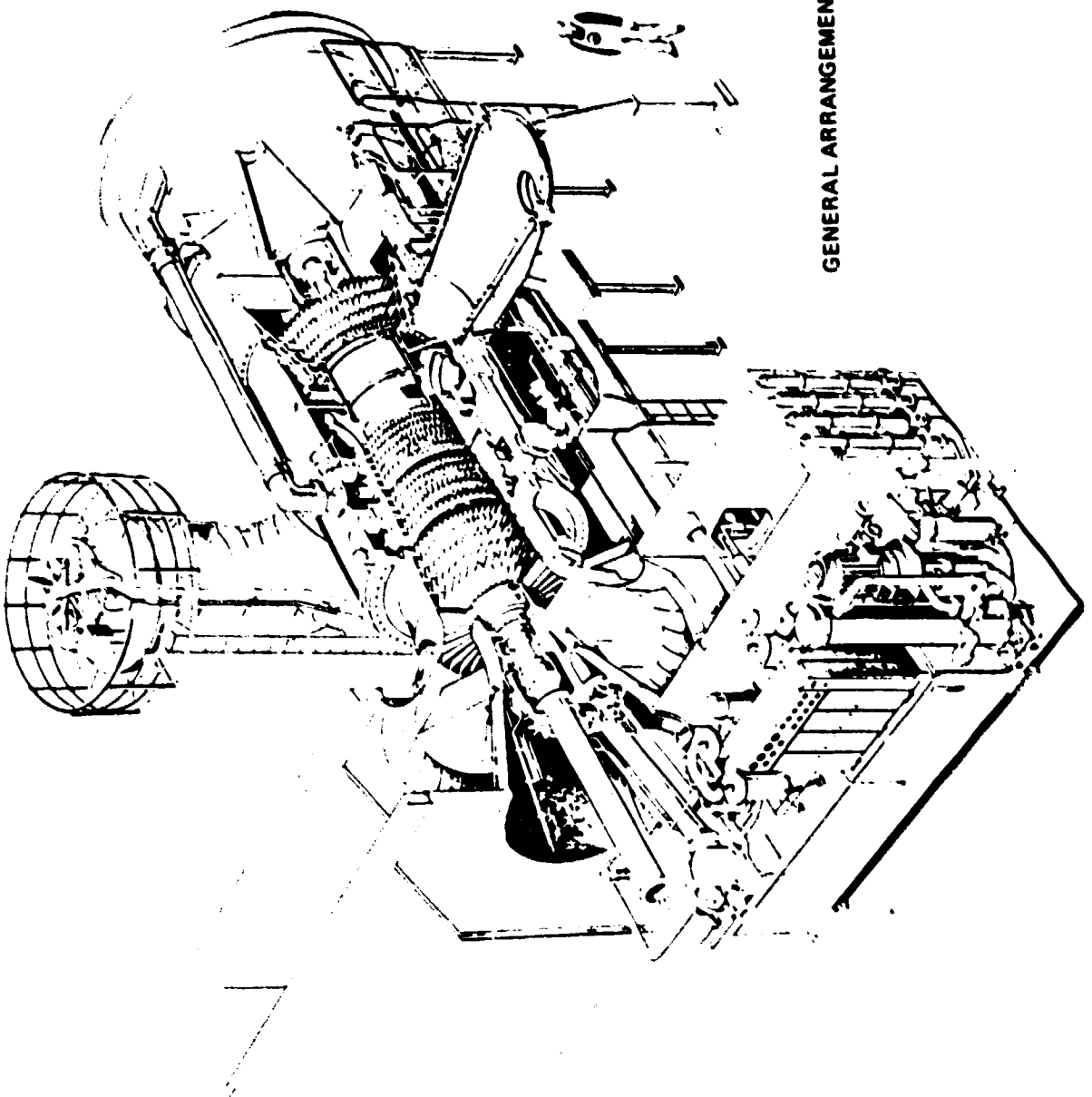

GENERAL ARRANGEMENT

KWU GAS TURBINE AND AUXILIARIES

performance while retaining the excellent durability that KWU has experienced. Performance estimates of the current V94 and advanced state-of-the-art V94 and V84.3 (60 Hz) are given in Table 1.2.1.1-1.

Other Engines

At this time, there are no other industrial gas turbines which have reached the state of technology of the FT50/GT200. However, several manufacturers have uprated versions of their current commercial equipment which could now be ordered. For example, General Electric is offering an uprated version of the Frame 7 with a projected output of nearly 79 MW at a pressure ratio of 11.5 and an estimated turbine inlet temperature of 2100 F. Westinghouse presently offers an uprated version of the W501, the W501D, with a rated output of 104 MW at a pressure ratio of 14.2 and a turbine inlet temperature estimated to be 2066 F.

The technology readiness state of gas turbine and combined cycle systems can be described as mature. A number of manufacturers, U.S. and foreign, offer both simple- and combined-cycle power systems burning natural gas or distillate with satisfactory performance. State-of-the-art machines are beginning to appear and could be offered widely on a commercial basis by 1984. These machines could offer an approximate 10 percent increase in size with a five to eight percent reduction in heat rate.

1.2.1.2 Development Trends in Operating Parameters

The following section describes the development trends in gas turbine and combined-cycle technology and briefly discusses the major ongoing R&D programs on turbine technology.

Compressors

Technological advances in aircraft gas turbine compressor design have resulted in substantial improvements in cycle pressure ratios, increasing from about 4:1 in the early English (National Gas Turbine Establishment) centrifugal compressors of the 1940's to present twin-spool axial-flow compressors (see Fig. 1.2.1.2-1). A spool is commonly considered to be a compressor and connected turbine. The compressor or turbine may have one or more stages. Thus, twin-spool compressors consist of two tandem compressors with their respective turbines that form two rotor systems which are mechanically independent but related aerodynamically. These configurations facilitate proper compressor-stage matching for relatively high pressure ratio designs as an alternative solution to single-spool compressors that would have to incorporate variable geometry stator vanes.

The technology is available that has permitted the introduction of machines with pressure ratios exceeding 30:1. Proportionate increases in the number of axial compressor stages to meet these pressure ratio requirements have been

TABLE 1.2.1.1-1

PERFORMANCE OF LARGE INDUSTRIAL ENGINES

	Commercially Available (KWU)	State of the Art (UTC/KWU)	
Model	V94.2	V94.3	V84.3
Rotor Speed, RPM	3000	3000	3600
Output, MW	110	161	112
Heat Rate, Btu/kWh	12000	11140	11140
First Commercial Appearance	1979	1984	1984

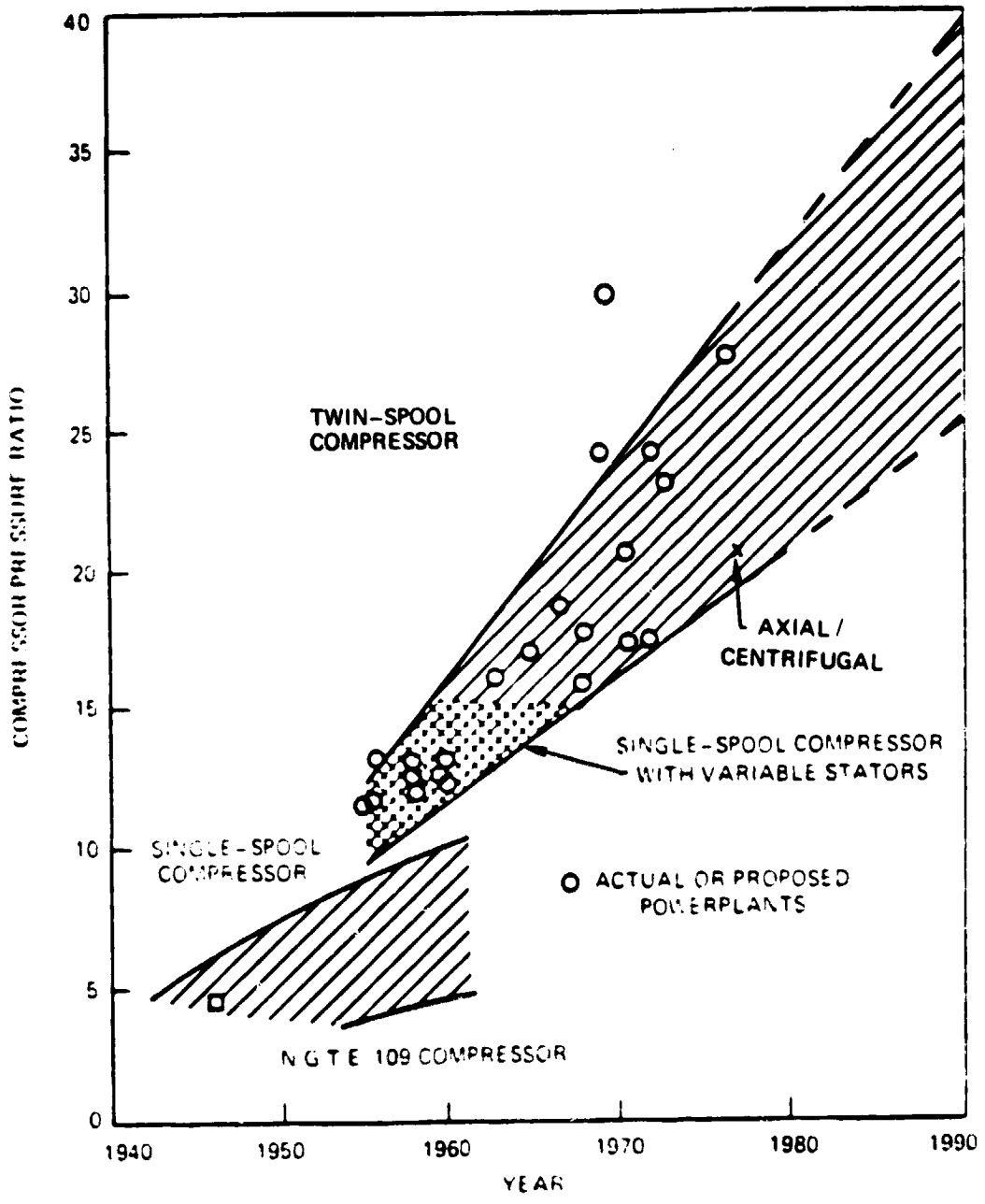

COMPRESSOR TECHNOLOGY PROGRESSION

avoided through intensive research and development efforts to increase stage pressure ratios. For example, it is presently possible to achieve single stage pressure ratio of 1.2 to 1.4 while still maintaining stage efficiencies of 90 percent or more. These stage performance levels have been extended to multistage aircraft compressor designs and permit the attainment of average stage pressure ratios on the order of 1.2 to 1.3 with associated polytropic efficiencies of approximately 90 percent or greater. Further improvements in polytropic efficiency to peak values of 90 to 93 percent within the next generation of engines appear feasible. In fact, the LP compressor of the state-of-the-art FT50/GT200 has achieved 90 percent and the HP compressor, 89 percent.

Principal factors which influence stage pressure ratio are rotor tip speed and aerodynamic loading. Rotor tip speeds of 1100 to 1200 ft/sec are attainable with current advanced lightweight compressor designs, and values as high as 1400 ft/sec are forecast for the early 1980's. Although lightweight fan stages are in aircraft operation at tip speeds of 1500 ft/sec and above, high stress limits and supersonic Mach number operation will limit compressors to the aforementioned levels.

A measurement of the aerodynamic loading is the airfoil diffusion factor (D_f), a parameter which includes a factor reflecting the overall change in relative velocity across the blade row and a term proportional to the conventional lift coefficient. High values of D_f are desirable since they result in a reduction in the number of compressor stages; values of 0.40 and 0.45 are currently obtainable. The present limit in D_f is due primarily to excessive secondary flow or endwall losses and to compressor surge margins that are dangerously low. Further improvements in tip speed and diffusion factor will result from aircraft compressor research and development programs.

The specific flow (lb/sec per unit flow area) of axial aircraft compressors varies from approximately 33 to 40 lb/sec/ft^2 of frontal area. Increases in this parameter result in more compact designs (smaller cross-sectional area); however, for a given wheel speed (U_m) and work coefficient, high specific flows and, alternatively, higher axial velocities (C_x) reflect high flow coefficients (C_x/U_m) and correspondingly lower compressor efficiency.

Adaptation of these developments to industrial units has been slow because of the lack of incentives to undertake parallel costly development programs for long-life stationary gas turbine power plants. Consequently, present industrial gas turbine axial compressors incorporate moderate blade loadings and tip speeds of only 650 to 750 ft/sec, and achieve average stage pressure ratios only on the order of 1.1 to 1.15. As a result, as many as 15 to 17 compressor stages are required to produce cycle pressure ratios above 10:1. Thus, high thermal efficiency performance cannot be easily achieved with these designs. The FT50 which typifies the advanced technology engines achieves a 16:1 pressure ratio with a 7-stage low compressor and a 10-stage high compressor.

Turbines

Increases in turbine inlet operating temperatures through the use of improved materials and cooling techniques represent the principal means of improving the performance and increasing the output potential of future gas turbine designs. Although historically most of this effort was directed primarily toward aircraft propulsion systems, some ot the advances were eventually used to improve industrial designs. This trend is evident by an inspection of Fig. 1.2.1.2-2 which shows the progression of maximum operating cycle temperatures with time for gas turbines designed for various aircraft, industrial, and electric power generation applications.

The data indicate that turbine inlet temperatures up to 2000 F are currently being used in gas turbine electric power plants, and temperatures several hundred degrees higher are being used in commercial and military aircraft. Prior to mid-1960's, advances in materials technology traditionally accounted for a respectable 20 to 40 F increase per year in turbine inlet temperature. From the mid-1960s to early 1970's, however, significant increases in turbine inlet temperature approaching 70 to 80 F per year, were achieved through substantial improvements in turbine cooling techniques in combination with newer materials. Turbine inlet gas temperatures as high as 2200 F for continuous cruise operation and 2600 F for take-off are now experienced by the engines utilized in today's 747 and DC10 jumbo jets.

The projections shown in Fig. 1.2.1.2-2 indicate that the industrial engines would follow the trends of aircraft engine turbine inlet temperatures, i.e., increse at 50-75 F/yr. However, the rapid increase in fuel costs since 1974 have dramatically slowed progress in industrial engine design. This is simply due to a sharp decrease in turbine sales. Because of the combination of rapid fuel cost increases and confused fuel policies, the utility industry essentially stopped purchasing gas turbines. As sales declined, R&D efforts were reduced by the manufacturers and emphasis was placed on reducing inventories and meeting environmental goals rather than on increasing performance. Thus, turbine inlet temperatures have been essentially constant for several years. The projected increases shown in Fig. 1.2.1.2-2 are based on government or utility industry funded R&D programs aimed at increased performance turbines for use with coal gasification. These programs will be discussed later.

Improvements in turbine performance resulting from technological advances in aircraft turbine designs have paralleled those for the compressor, with turbine isentropic efficiency increasing from about 85 percent in early 1950 designs to over 90 percent in current designs; efficiencies of 92 to 93 percent are feasible in the near future, particularly in high output designs. The design philosophy of turbines for industrial turbine designs will incorporate a higher degree of impulse staging than exists in most present designs to achieve a relatively large gas temperature drop in the nozzle, thus avoiding high gas temperatures with corresponding high cooling flows in the rotor. The stage work for aircraft turbines varies from a low of 20 Btu/lb in the last stage of low pressure ratio

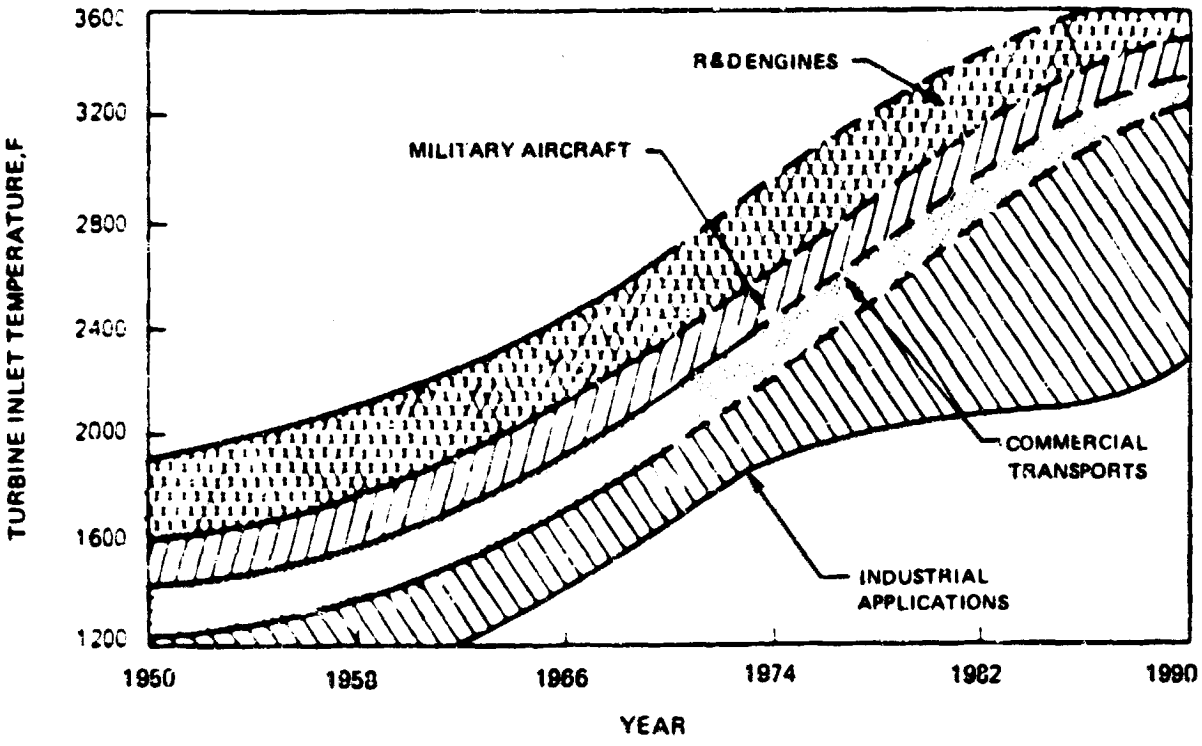

TURBINE TECHNOLOGY PROGRESSION

units to a maximum of about 130 Btu/lb in the high pressure ratio stage of current production units; technology presently exists to increase this value to about 200 Btu/lb without sacrificing turbine efficiency.

High stage work in itself does not cause aerodynamic problems, but when associated with high efficiency it requires high wheel speeds which become limited by structural considerations. Turbine tip speeds in current twin-spool aircraft designs vary from 900 to 1000 ft/sec in the low pressure ratio stages to as high as 1500 to 1600 ft/sec in the high pressure ratio stages. These tip speeds can be achieved in future industrial-type designs that utilize the improved turbine materials and cooling techniques described in the following section.

Problems in Advancing Gas Turbine Technology

The most important future technological challenge to the use of open-cycle gas turbines for generating electric utility power is the need to develop engines capable of economical intermediate- or base-load service on coal-based fuels. Gas turbines operating with steam bottoming cycle offer the greatest potential for attaining this objective.

The most important factor limiting the application of gas turbines to intermediate- and base-load services has been the modest thermal efficiencies attained in comparison with conventinal steam sytems. Efficiency and specific power for simple, open-cycle systems are critically dependent on gas turbine firing temperature (Fig. 1.2.1.2-3). The figure indicates that higher turbine inlet temperatures given higher efficiencies. The specific power term indicates the amount of power which can be obtained from a certain size gas turbine unit and is, indirectly, a guide to cost, i.e., a machine with high specific power will generally have a lower cost in $/kW than a machine of lower specific power.

Further significant improvements in specific power and thermal efficiency for gas turbine power plants can be an achieved only by increasing the turbine inlet temperature accompanied by an increase in the pressure ratio. Any increase in performance due to improvement in aerodynamic efficiencies will be small since these values have reached a relatively high level due to the 30 years of extensive research in compressor and turbines for aircraft propulsion. Thus, the major improvements in performance will result from advances in turbine cooling and materials.

Turbine Cooling Techniques

Only first stage vanes and disks of industrial gas turbines operating at 1600 to 1700 F turbine inlet gas temperatures are cooled. For long life, base-load operation at turbine inlet temperatures of 1800 F and above, successive

FIG. 1.2.1.2-3

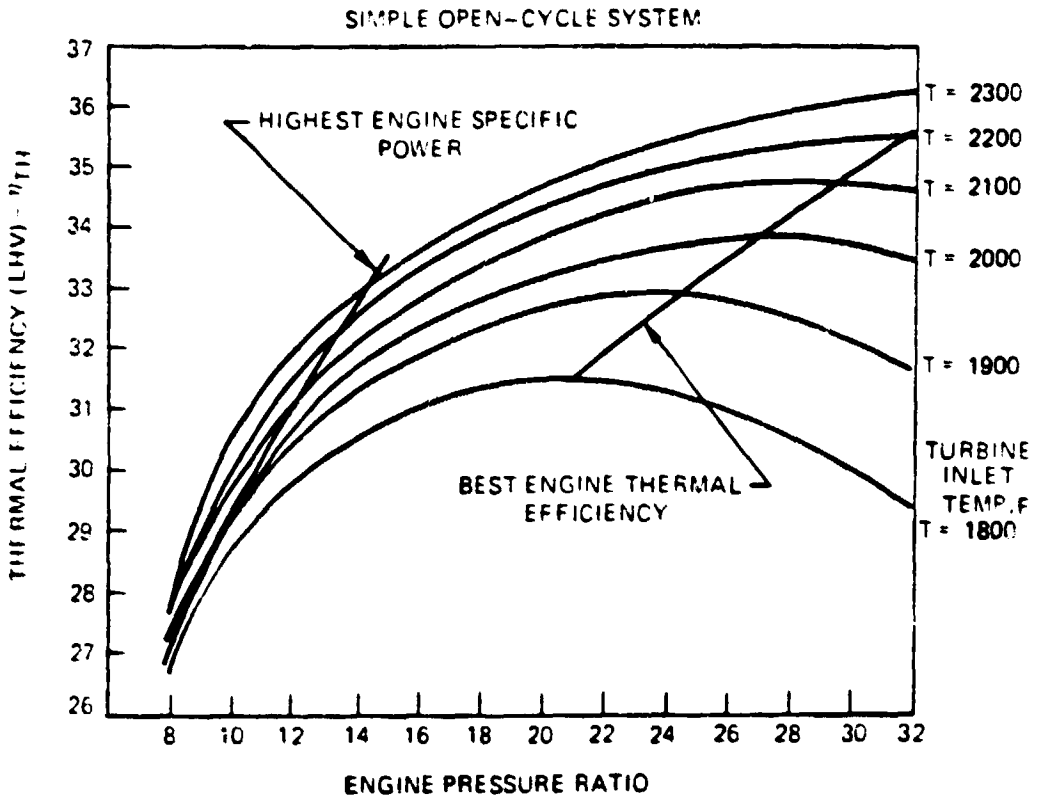

PARAMETRIC PERFORMANCE

stages of turbine blades also require cooling. Cooling is necessary for two reasons, strength and corrosion resistance. With current materials, metal temperatures of 1500 F-1600 F appear to be good compromise between long life and excessive cooling penalty. Turbine cooling can be accomplished with coolants such as air, water, or liquid metals, but because of the complex cooling system designs and mechanical problems associated with liquid systems, air has been used exclusively as the coolant in all aircraft propulsion systems and for all commercially available stationary applications.

Air Cooling

Turbine cooling systems in current aircraft engines have progressed from single convective cooling configurations incorporating cast, round, radial passages, for vanes (Fig. 1.2.1.2-4) and single cavities for blades to advanced convective heat transfer designs utilizing impingement cooling of the inside surface of the leading edge (Fig. 1.2.1.2-5) to film cooled designs where a layer of coolant is injected in hollow blades through radial slots to form an insulating air blanket for the outside blade surface (Fig. 1.2.1.2-6). These designs were used in the state of the art FT50/GT200.

In transpiration cooled blades, coolant is bled through a porous material which may be formed by a series of small drilled holes along the airfoil surface or a mesh-like material may be used for blade construction. These designs are in the early stages of development and, when applied to 1990 time period turbines, could offer operation at turbine inlet temperatures approaching 2600 F-2800 F.

Another advanced cooling concept currently being demonstrated in test rigs involves the construction of turbine blades and vanes from many thin wafers. A series of radial wafers is fabricated with complex cooling holes (see Fig. 1.2.1.2-7 for a vane and Fig. 1.2.1.2-8 for a blade) glued together to form an aerodynamic shape. The complex cooling passages allow very effective cooling.

Each of the cooling concepts have advantages and drawbacks. For the concepts outlined above, these are as follows:

Radial Holes

- Low cost
- Low effectiveness due to difficulty in accurate hole placement
- Poor low-cycle fatigue life due to poor distribution of coolant

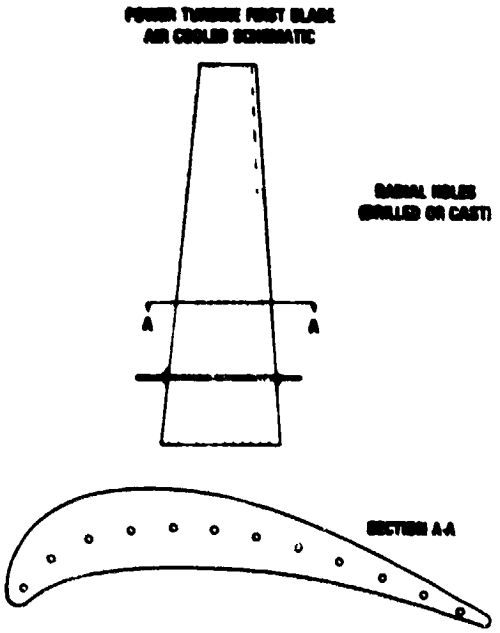

VANE CONVECTIVE COOLING

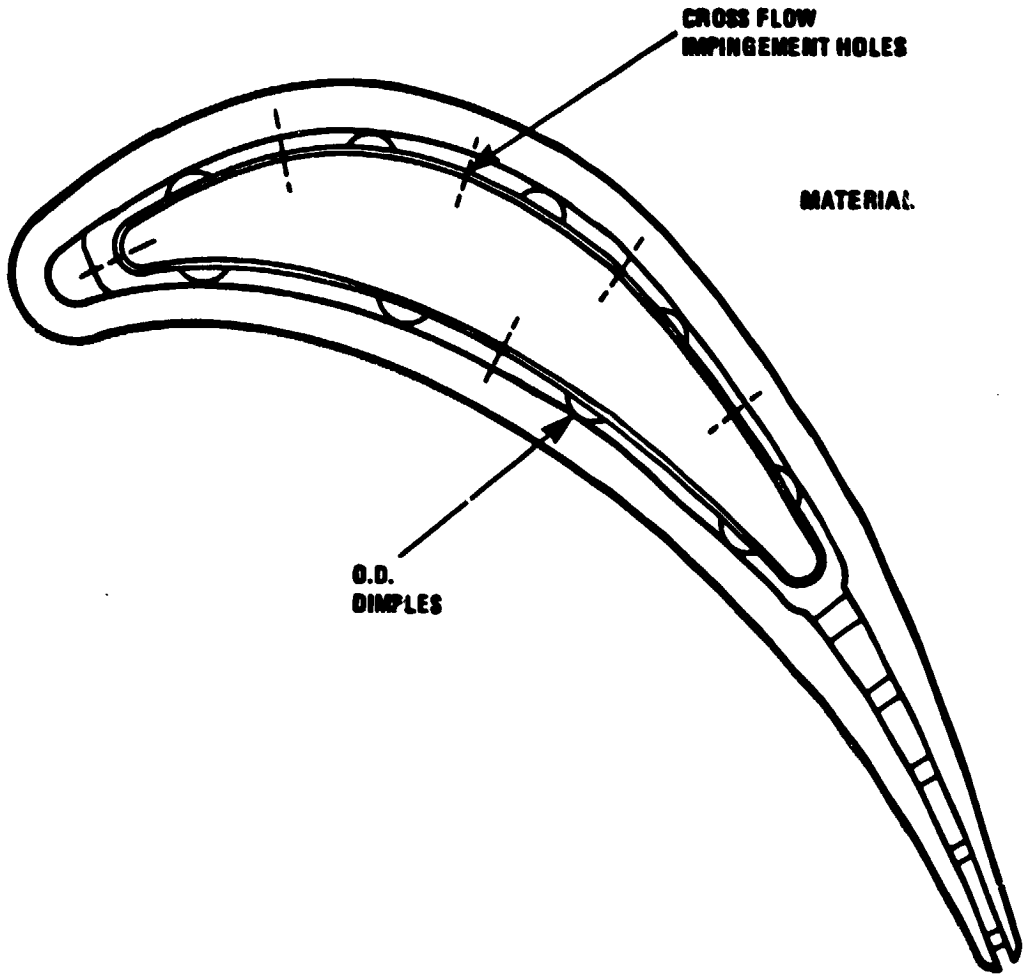

CONVECTIVE IMPINGEMENT COOLING

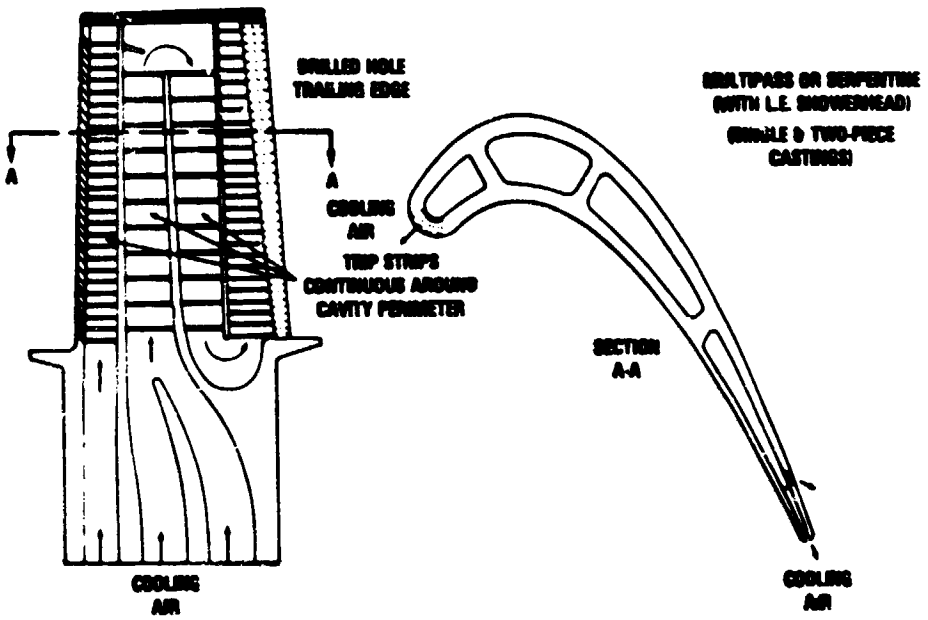

FILM COOLING

FIG.1.2.1.2-7

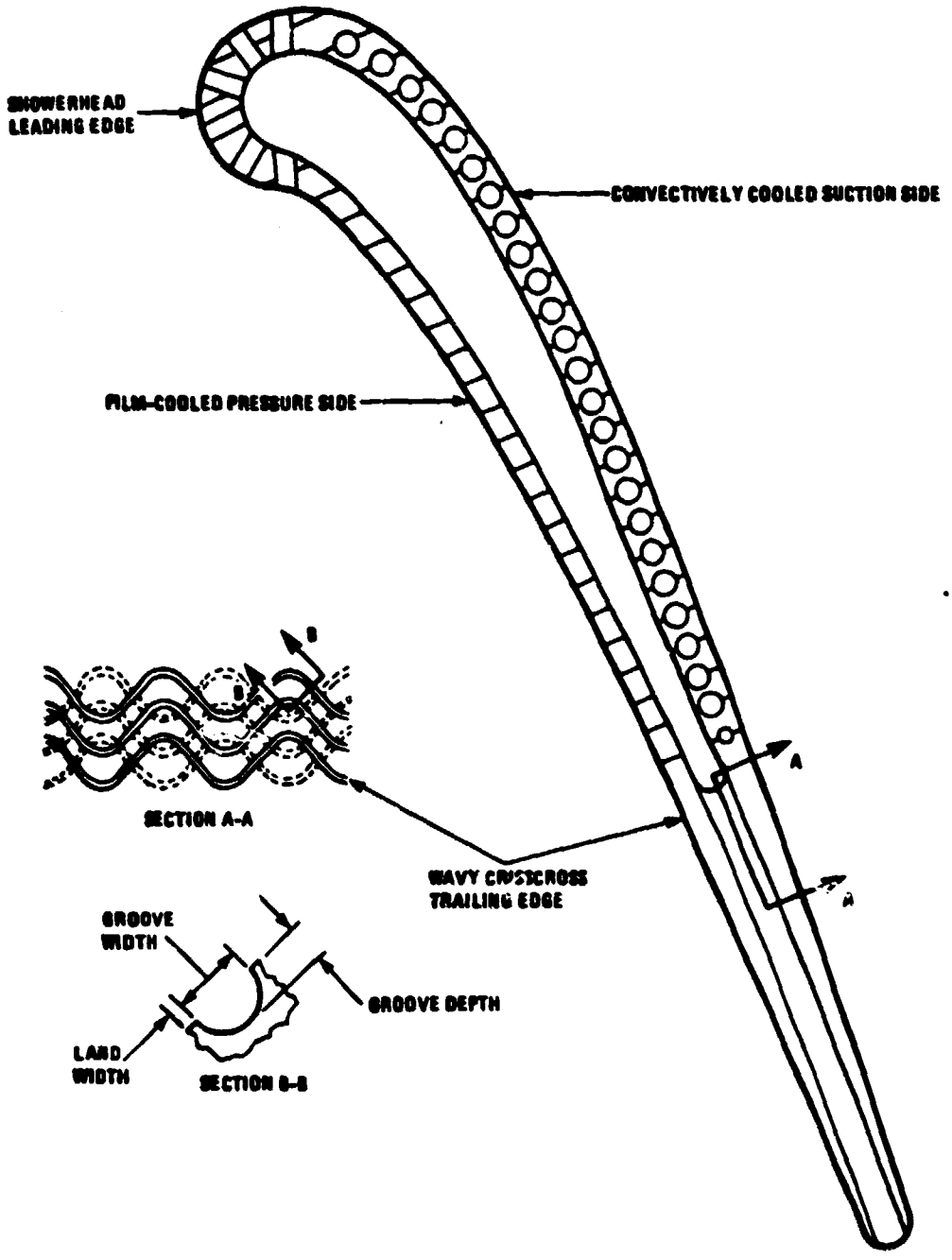

RADIAL WAFER COOLING–VANE

FIG. 1.2.1.2-8

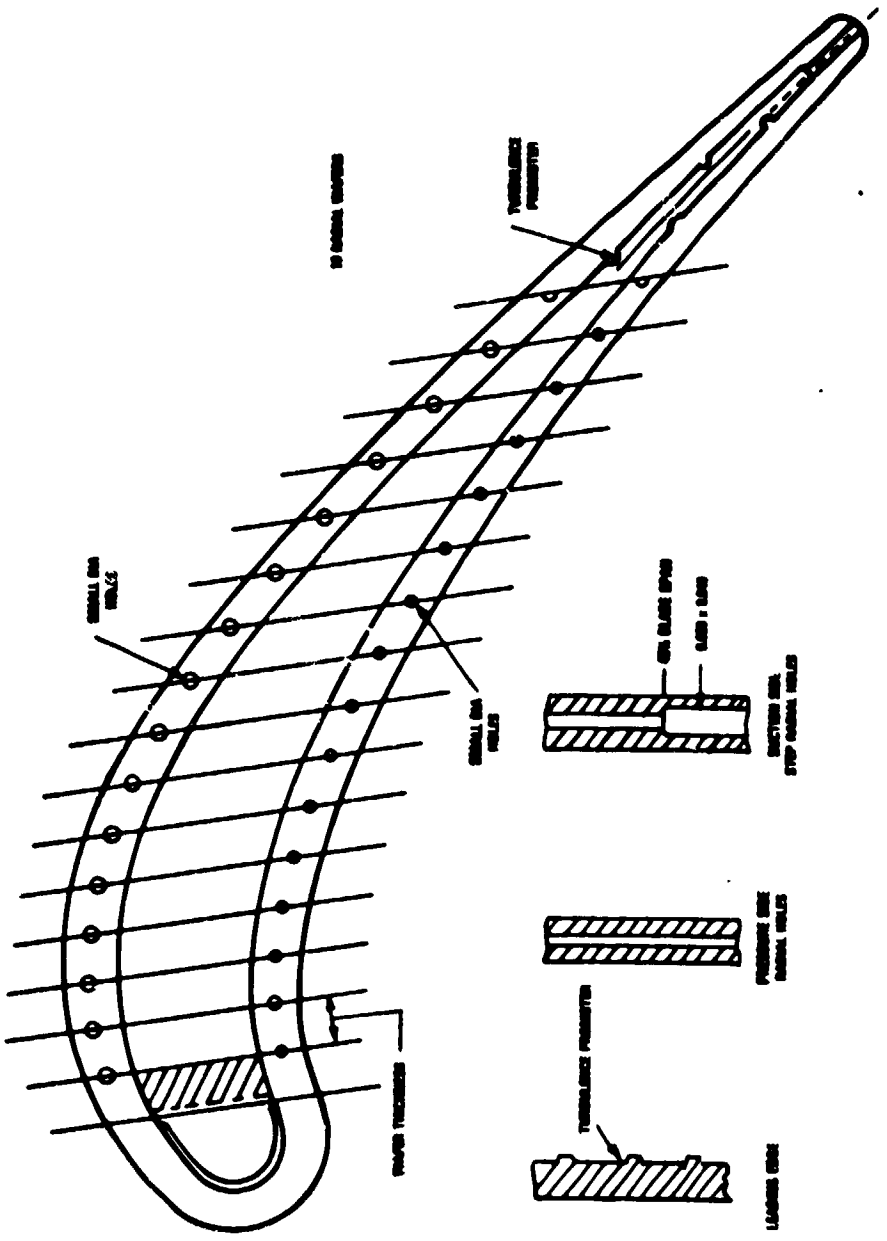

RADIAL WAFER COOLING–BLADE

Convective Multipass

. Moderate to low cost

. Moderate effectiveness

. For high temperature (2000 F plus) applications, showerhead or impingement cooling required for leading edge.

Impingement

. Moderate cost

. Moderate effectiveness

. Manufacturing problems

. Tube insert subject to failure

Transpiration

. High cost

. High effectiveness

. Poor structural properties

. Reduced aerodynamic performance

Wafer Blade

. Moderate cost

. Allows design of intricate cooling scheme

. Subject to cold rib problems

. High effectiveness

The optimum design will probably be a combination of techniques and fabrication methods.

In aircraft engines, the air used to cool the turbine blades and vanes is at an elevated temperature, 800 to 1200 F, even before it is introduced into the turbine, since it is bled from the compressor discharge airstream.

Precooling the compressor bleed air to fairly low levels before it is used to cool the turbine has not been a general practice in these aircraft applications because the added cooling system weight detracts from the potential gains in performance that might otherwise be achieved by reducing the turbine cooling flow. However, as industrial turbine inlet temperatures and compressor pressure ratios continue to rise and approach the limits established for proven turbine blade cooling techniques, precooling of the compressor bled air to 400 F or lower will be considered.

For stationary industrial power plants, air-, water-, or even possibly fuel-cooled heat exchangers could be used to reduce the temperature or compressor discharge cooling air to fairly low levels since in these stationary applications weight is not an important criteria. Therefore, with this technique it should be possible to achieve desirable gas temperature levels on a continuous basis in base-load plants with presently available combinations of impingement-convection cooling techniques.

Water Cooling

The high effectiveness of water cooling turbine components greatly reduces the cooling air requirements for the gas turbine and offers an opportunity for overall cycle efficiency improvement. If all the turbine airfoils and static structures are water cooled, only a very small percentage of engine airflow will be needed to cool other components such as disks and seals.

There are two types of water cooling to be considered for stationary and rotating components, namely the use of supercritical water and subcooled boiling water as coolants (Fig. 1.2.1.2-9). Cooling by subcooled boiling water will be accomplished in a closed loop. Therefore, the heat transferred in cooling the turbine can be used in the steam portion of the combined cycle. Initially, supercritical water cooling of the blades will not be a closed loop system. There will be a high recirculation rate in the blade and a small amount of steam exiting from the blade trailing edge. However, this will have a negligible performance impact. Further development of the system may produce a closed-loop cooling scheme with water recovery; however, the recovered water must be cleaned before being reused as a coolant.

Materials

The improvements in the temperature capability of turbine materials, with time, for aircraft gas turbines is shown in Fig. 1.2.1.2-10. The gains have been most significant for the nickel-base alloys, with an improvement of more than 200 F in temperature capability over the past decade. Presently, nickel-base cast blade alloys, such as Inconel 718, B1900, and IN-100, have in some aircraft turbine designs replaced forged Udimet 700 (U-700) for high-temperature applications and, at the same time, decreased thermal fatigue failures by a factor of five.

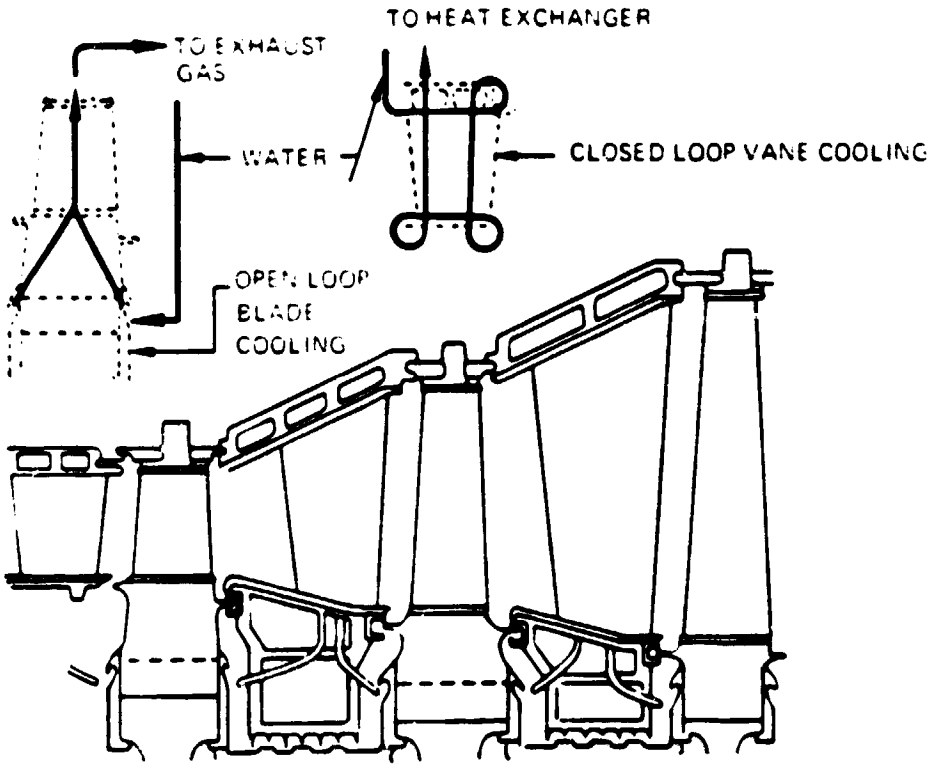

WATER COOLING

FIG.1.2.1.2-10

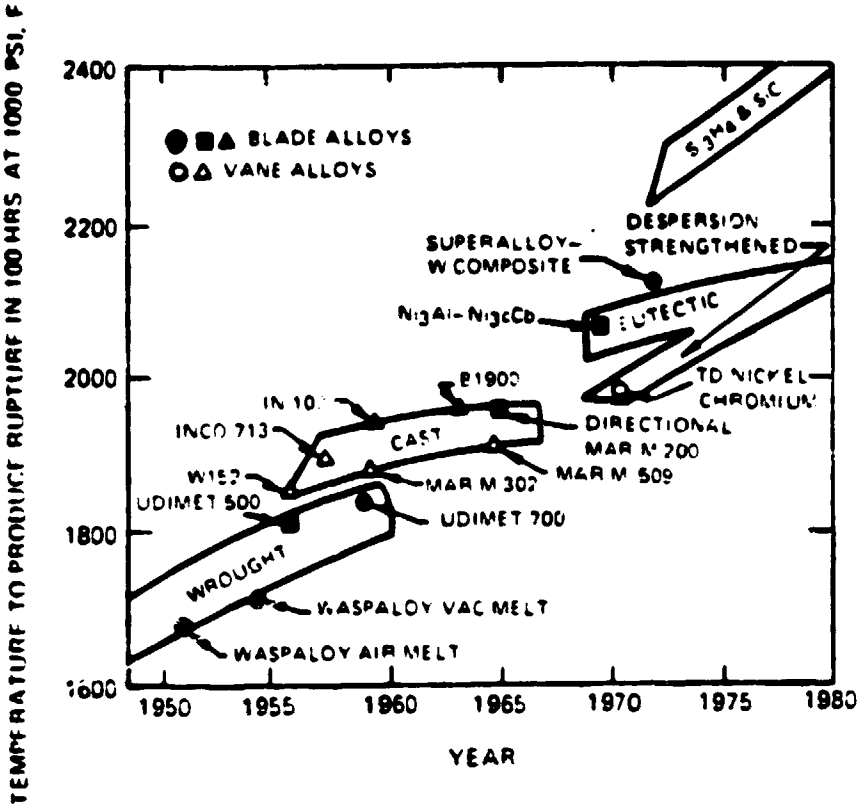

AIRCRAFT MATERIALS TEMPERATURE IMPROVEMENTS

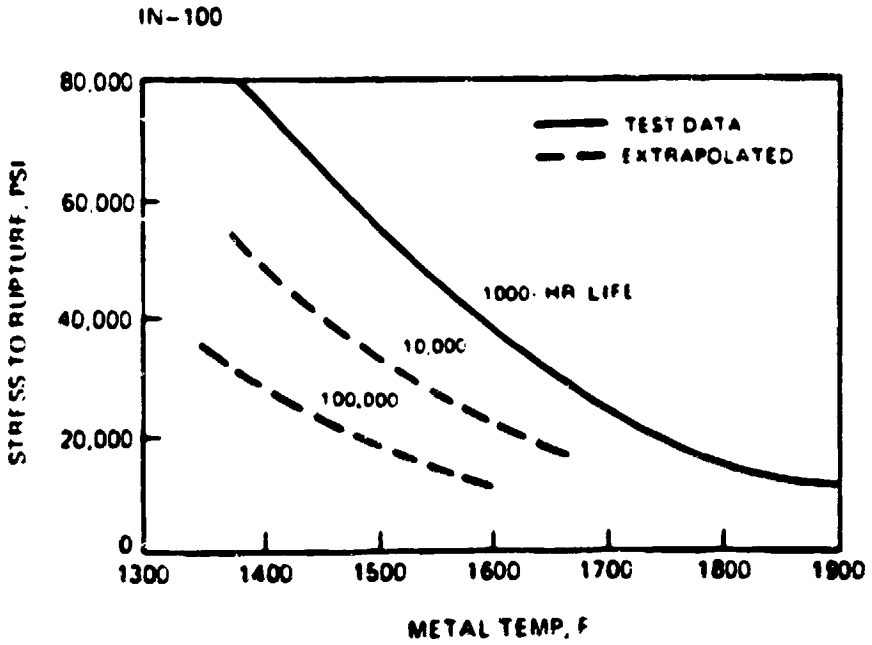

STRESS–TEMPERATURE RELATIONSHIP

Figure 1.2.1.2-11 shows the stress-to-rupture strength of the nickel-base alloy IN-100 for a range of material temperatures. Curves for 1000-, 10,000-, and 100,000-hr lifetimes are shown and illustrate the sharp reduction in allowable stress as the desired operating time is increased. The 1000-hr life curve is based on experimental data while the 10,000- and 100,000-hr curves are extrapolated data from short duration test results. Although these materials were developed initially for relatively short time (1000 hr) high-strength aircraft turbine applications, modifications to the heat treatment cycle have permitted their use for long time operation (approaching 100,000 hr) as required in base-load power generation. It is anticipated that similar modifications for the aforementioned high-temperature nickel-base alloys will allow the eventual replacement of such alloys as wrought Udimet 5000 and M252 presently used in industrial turbines and, thus, permit high operating temperature.

Turbine blade materials for industrial designs anticipated by the 1990's will be the superalloys currently under development for advanced aircraft gas turbines; these include unidirectionally solidified eutectic alloys such as Nk_3Al-Ni_3Cb and particle or fiber dispersion-strengthened metals. On the basis of efforts currently underway it is reasonable to expect a continuation of at least 20 F-per-year improvement in material temperature. Chromium-base alloys, for instance, with potential firing temperatures to 2000 F, are being investigated. While recent breakthroughs in the ability to coat columbium-base alloys also offer a possibility for the use of these alloys, it is currently felt that advanced cooling schemes could, however, allow relatively low metal temperatures which, in turn, could allow the use of current, less expensive materials.

Ceramic materials such as silicon nitride and silicon carbide composites are under intensive study for automotive gas turbine applications and offer firing temperatures on the order of 2500 to 2600 F. The quality and reliability of ceramic materials have been greatly improved during the past decade. The benefits of ceramics include intrinsically low cost, abundant material, low density, corrosion resistance, and high temperature strength. Both silicon nitride and silicon carbide are being studied. The use of ceramics in gas turbines can be expected when the industry's design systems can accommodate materials that exhibit low ductility, large thermal expansion differences, and when stress concentrations can be eliminated by design and subsequent fabrication.

Coatings

Coatings have been developed which provide adequate oxidation-corrosion resistance for blades and vanes in aircraft turbines. These coatings are aluminide types, applied by pack or slurry techniques. These coatings have eliminated intergranular oxidation attack (which could cause a thermal fatigue failure) and have provided some protection against sulfidation attack (corrosion

due to the presence of sodium sulfate compounds in the combustion products of distillate fuels). However, coating life decreases rapidly with increases in allowable metal temperatures. For instance, at a metal temperature of approximately 1500 F, a coating life of 50,000 hr may be achieved. A 200 F increase in metal temperature reduces coating life to less than 10,000 hr. Consequently, coating life rather than creep strength properties as determined by peak temperatures in the first-stage turbine vanes will be an important criterion used to specify turbine inlet gas temperature for different power plant operating mode. Adequate coating life could be especially critical when the fuel used in the engine contains quantities of ash, metals, or sulfur that could cause erosion and corrosion problems. Natural gas or low heating value coal gas, in this respect, would be ideal fuel for high performance gas turbines. Meanwhile, new coating materials and application techniques including nondiffusion-type coatings are being developed which, when applied in sufficient thicknesses, should provide uninterrupted service for period exceeding 25000 hr.

Ceramics

Ceramics will offer the advantage of large reductions in cooling heat load throughout the turbine system as reliable methods in incorporating brittle materials are developed. Early application would include stationary structures such as vanes, platforms and outer air seals. Because of the requirement in industrial machinery for long life, low cost systems, maximum metal temperatures must be kept low. While development of advanced cooling schemes will make this possible, additional advantage can result to the cycle if the heat loss could be avoided in part by the use of materials with higher surface temperature capability. Ceramics of various types offer this potential.

The fundamental problem to solve in realizing this potential is adapting design procedures to an unforgiving brittle material. Two approaches have been followed in recent years to use ceramics in gas turbines: (1) the use of insulating graded ceramic coatings bonded to metal members which carry the structural loads, and (2) the use of bulk ceramics as high-temperature structural members. The problem in the first approach is to develop bonding methods and cooling systems which ensure that large differential thermal strains do not occur throughout the operating range. These strains could impose excessive stresses on the ceramic or its bond, resulting in spalling of the coating or crack propagation into the substrate metal. The successful application of such ceramic coatings have used sprayed or sintered powder ceramics bonded to the metal substrate through a ceramic/metal intermediate layer which is graded form pure ceramic at the interface with the ceramic surface layer to pure metal at the substrate interface.

While bulk ceramics potentially offer minimum performance penalty and low cost, the problems to be overcome are: (1) obtaining uniformity of material properties, and (2) developing design technology to provide transmittal of

loading throughout the ceramic and from the ceramic-to-metal structure without excessive stresses, even locally. A fundamental of brittle material design is that failure initiated at a point of weakness or stress concentration is not absorbed by ductile flow but leads to a fracture. Considerable progress has been made toward acquiring the required materials strengths and design technology, however, the appearance of bulk ceramics is expected to be several years after that of graded ceramics.

Combustors

All of the currently offered large industrial gas turbines from U.S. manufacturers have the in-line, can-type combustor (see Fig. 1.2.1.2-12). This combustor has a long history of development in aircraft use and has many advantages: high volumetric heat release, ease of cooling, and low cost, for example. These advantages, however, are dependent on burning clean, high calorific value fuels such as natural gas or distillate. Several European manufacturers such as Stal-Laval, Brown Boveri and KWU use off-base combustors. They are usually tall cylindrically shaped devices sometimes called silos (Fig. 1.2.1.2-13). The requirement to burn coal-derived fuels, both liquid and gaseous, and to meet new stringent environmental regulations (discussed in Task 2) has led to development of alternative burner configurations.

The major problem to be faced is that of reducing the emissions of nitrogen oxides (NO_x). There are two types of NO_x emissions, thermal NO_x due to the fixation of atmospheric nitrogen during high-temperature combustion; and fuelbound nitrogen caused NO_x due to combustion of fuel containing nitrogen bearing compounds. Unfortunately, there is not a simple way to handle both problems.

Thermal NO_x production is a strict function of combustion temperature (Fig. 1.2.1.2-14). By modifying the combustion process to reduce peak temperature, thermal NO_x can be reduced. One method of doing this is to premix fuel and air to the desired stoichiometric ratio prior to combustion, i.e., burn lean (ϕ = 0.6-0.7 for example). This type of combustor modification affects only the combustor "head" and can be used with any type of combustor. A significant amount of testing on the fuel gas from a Texaco gasifier has been carried out by UTC using a modified can-type burner using a premix combustor head (Fig. 1.2.1.2-15). This premixed type burner has shown that it can easily meet NO_x standards using coal-derived fuel gases.

To reduce fuel-bound nitrogen caused emissions, a different type of modification is required. By burning rich (ϕ>1), the formation of NO_x from fuel-bound nitrogen is suppressed. The resulting partially burned mixture is then quickly cooled by mixing with excess air and the combustion completed at a reduced temperature to ensure low thermal NO_x emissions. Testing of this rich-burn/quick quench burner (shown schematically in Fig. 1.2.1.2-16), again by UTC, has shown great promise.

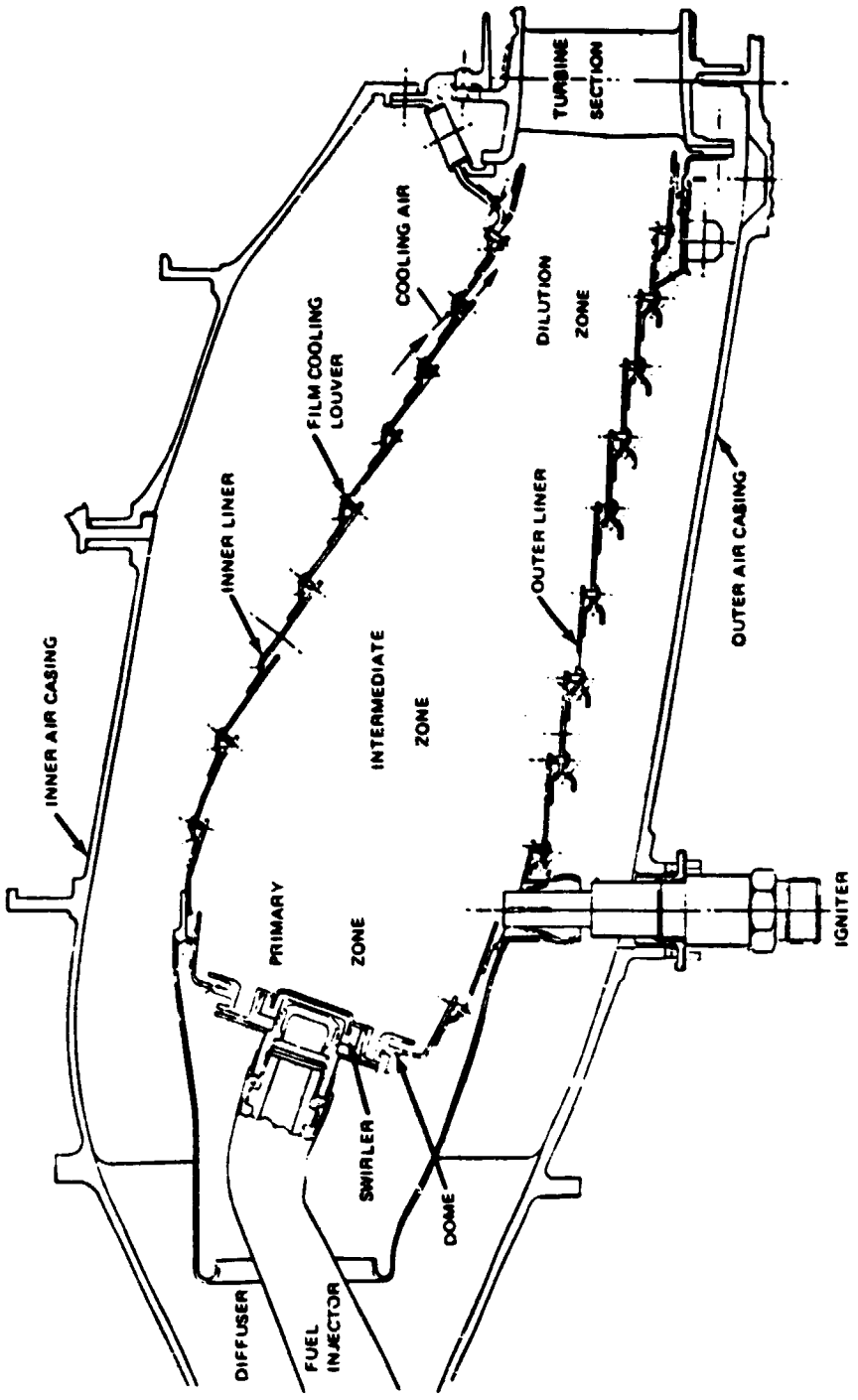

TYPICAL IN-LINE COMBUSTOR

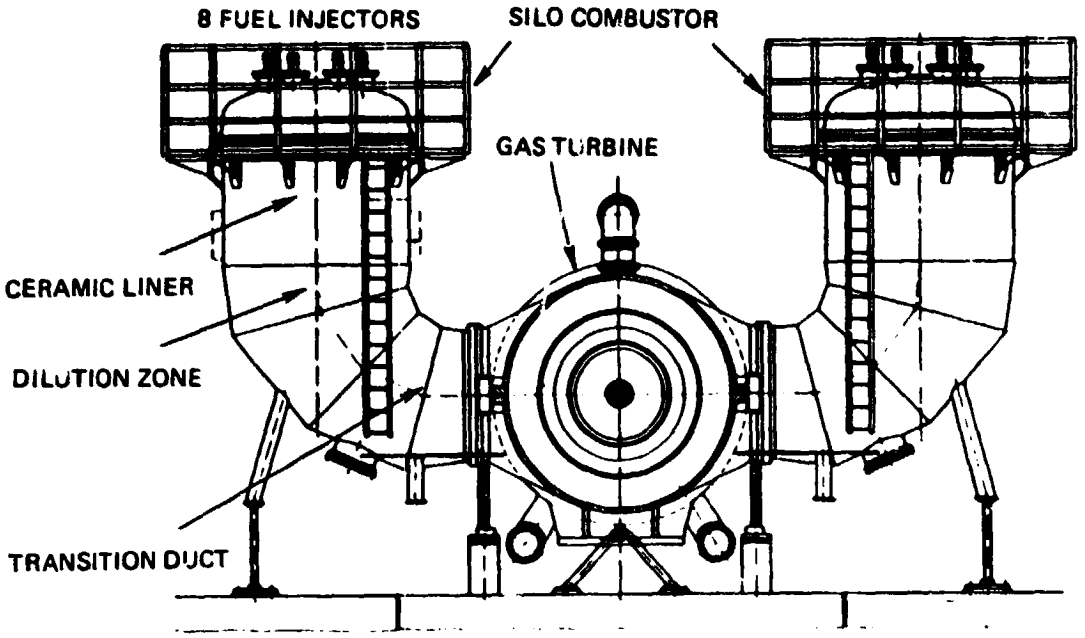

SILO COMBUSTOR ARRANGEMENT

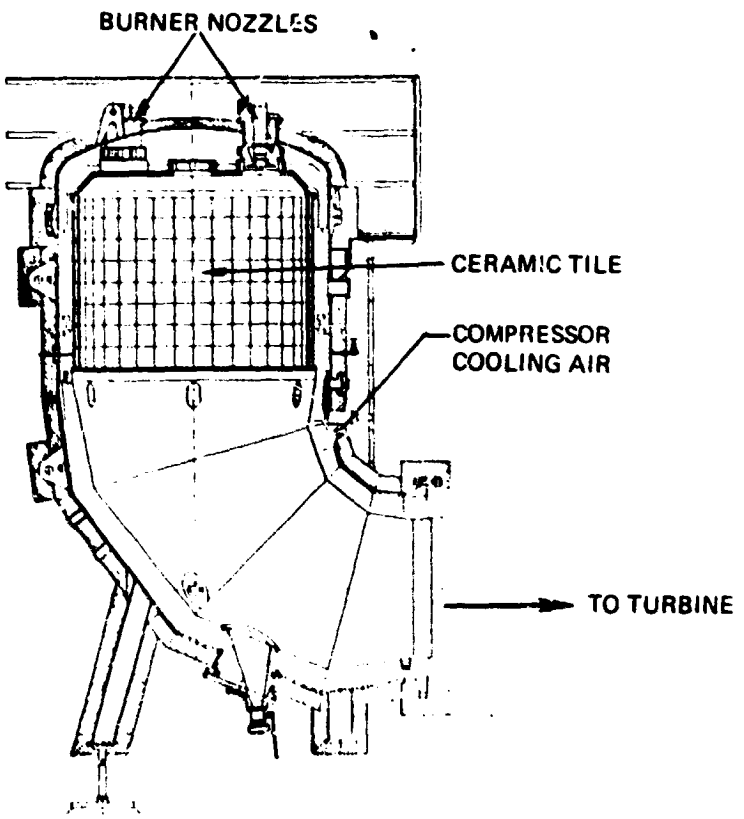

CROSS-SECTION OF SILO COMBUSTOR

FIG. 1.2.1.2-14

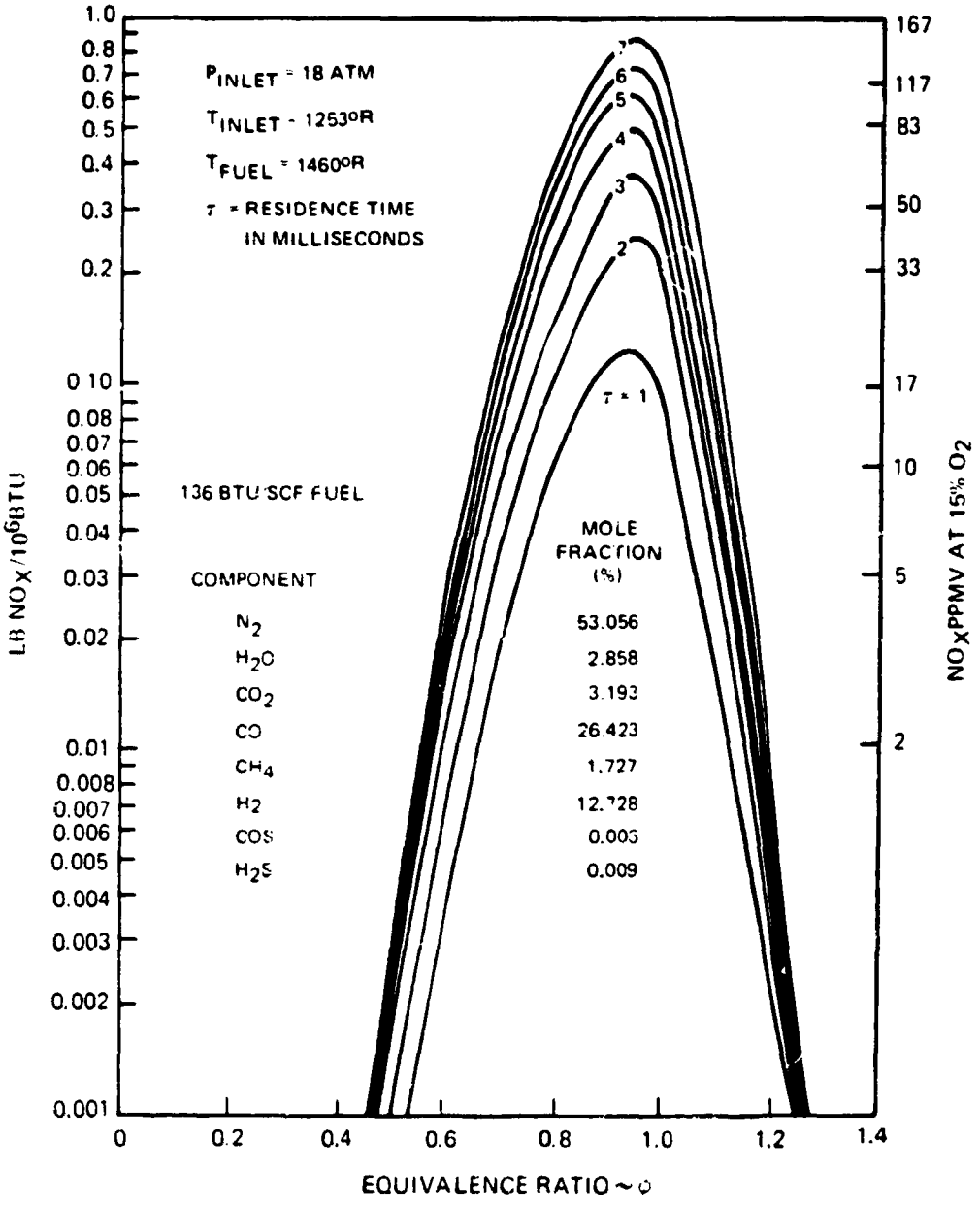

EQUIVALENCE RATIO EFFECT ON NO_X EMISSIONS

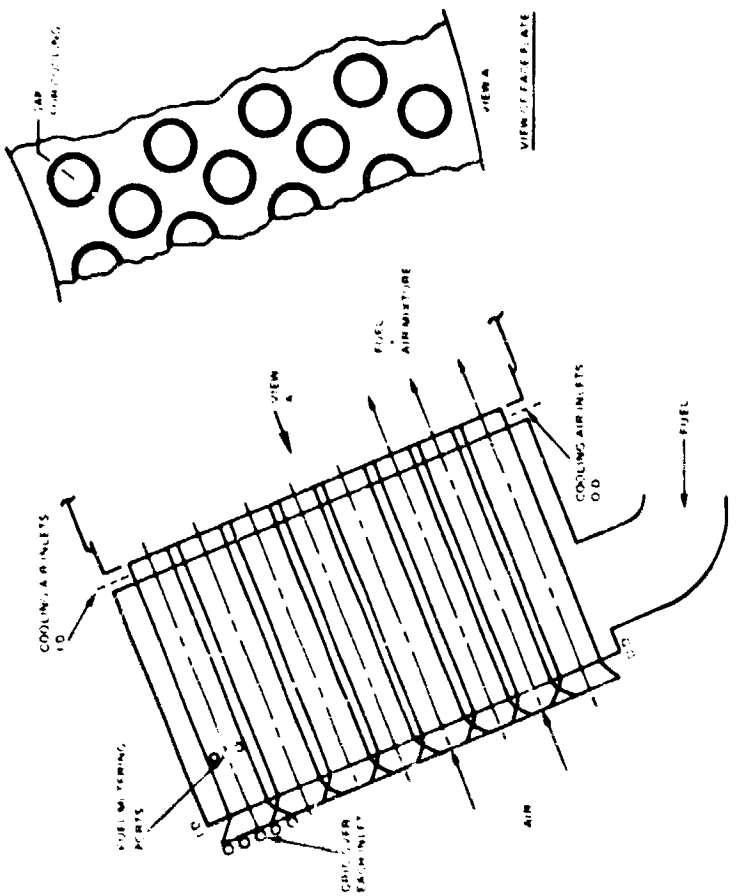

PREMIX COMBUSTOR HEAD

FIG. 1.2.1.2-16

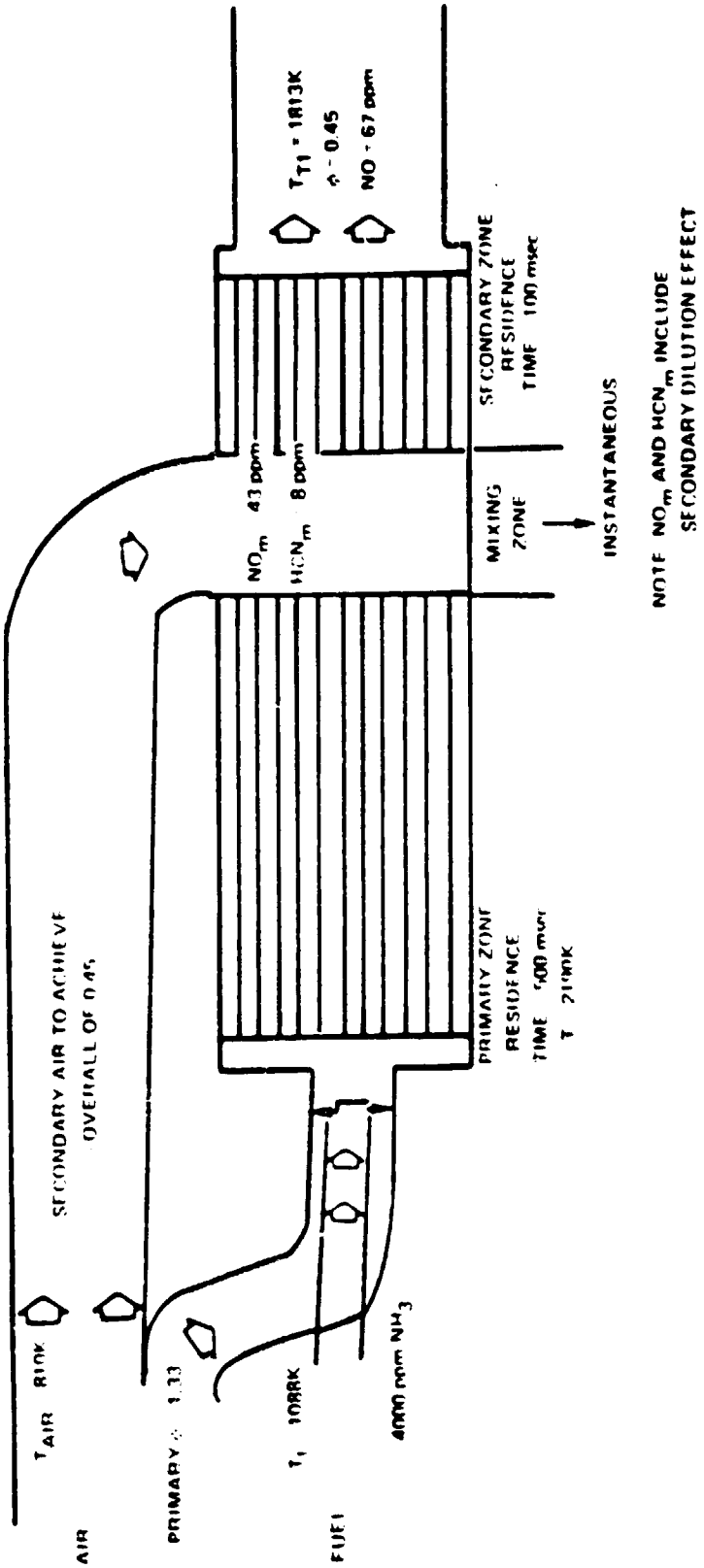

SCHEMATIC OF RICH-BURN QUICK-QUENCH COMBUSTOR

The major development trend in combustor technology is, then, the low pollution burner. A second consideration is the reduction of maintenance and increased component lifetime. The use of the off-base, silo-type burner appears to be a method of attaining this goal. The large size means that the volumetric heat release is reduced, thereby reducing the cooling necessary to maintain reasonable combustor wall temperature. The use of ceramic liners, usually segmented into tiles or other smaller shapes, further reduces burner wall cooling requirements. The large volume also ensures complete combustion of low heating valve fuels. The shape is also conducive to two-stage burning, i.e., the rich burn/quick quench approach. The major disadvantage is the increased manufacturing and erection costs.

Steam System Development

To this point, the steam system technology has been essentially ignored. This is because the steam systems used with combined cycles have generally lower operating parameters than the large central station systems. For example, nearly all of the fossil-fired steam stations installed in the past two decades operate at 1000 F and 2400 psi or higher throttle conditions with reheat to 1000 F. There is no single combined-cycle operating level although most are limited by gas turbine exhaust temperatures to throttle conditions of 800-900 F with a corresponding pressure of 1450 psi or less.

As turbine inlet temperatures increase, there is a corresponding increase in exhaust temperature and, thus, steam conditions will increase. One way of indicating the trend in steam cycle equipment is to examine the relationship between turbine exhaust temperature and amount of heat transferred to the steam system. This is usually done through the use of temperature-heat or T-Q curves. In Fig. 1.2.1.2-17, a T-Q curve for a combined cycle system using a typical currently available bottoming steam system is shown. A minimum pinch (smallest temperature difference between the gas side and the steam side) of 50 F is usually deemed reasonable and a maximum stack temperature of 300 F is desirable. While this type of combined cycle is attractive, system efficiency can be increased by better utilizing the turbine exhaust heat. For example, a dual-pressure system (Fig 1.2.1.2-18) which has a high-pressure and a low-pressure boiler section allows more steam turbine power to be generated while meeting the various pinch temperature constraints.

As turbine inlet temperatures increase, and the turbine exhaust temperatures become higher, it is possible to use steam cycle technology comparable to that used in central stations. In Fig. 1.2.1.2-19, a 2400 psi, 1000 F/1000 F steam system is shown. This would bottom a gas turbine having a turbine inlet temperature over 2400 F (the exact value is a function of engine pressure ratio).

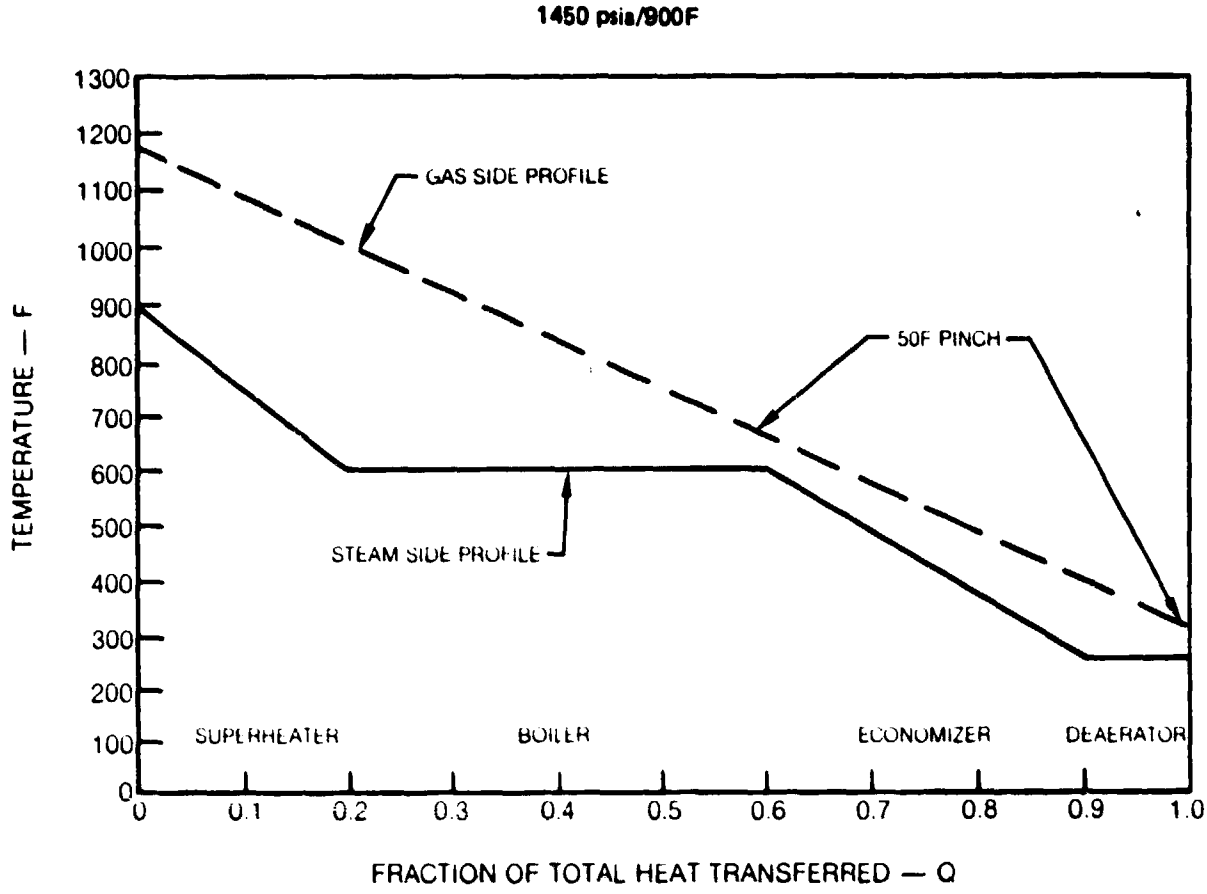

COMBINED–CYCLE WASTE–HEAT BOILER T–Q CURVE FOR NONREHEAT STEAM CYCLE

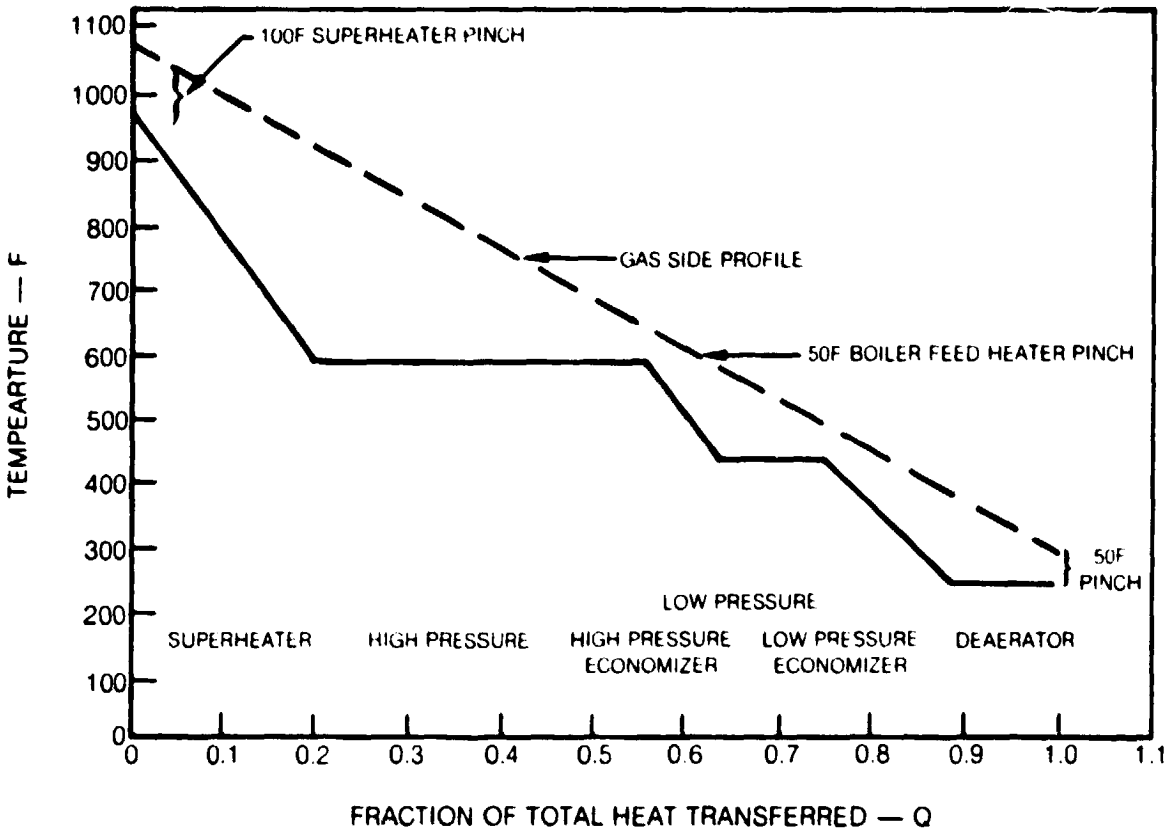

COMBINED–CYCLE WASTE–HEAT BOILER T–Q CURVE FOR DUAL–PRESSURE STEAM CYCLE

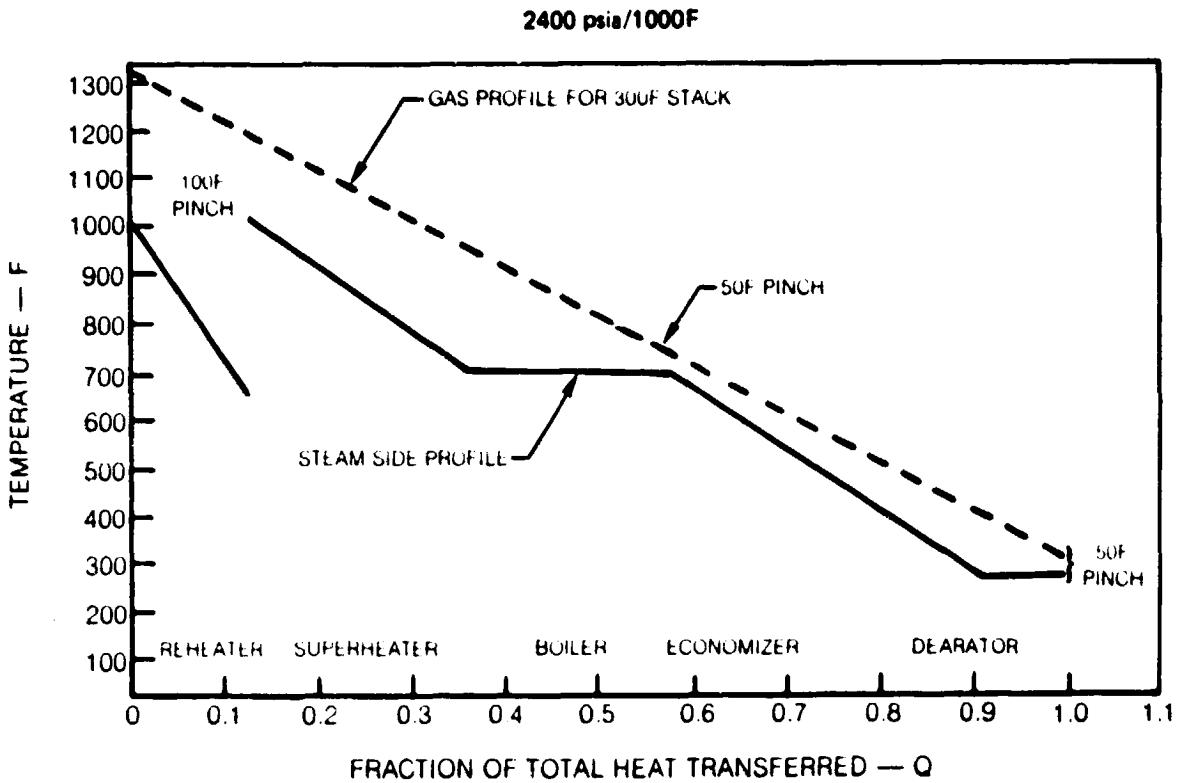

COMBINED-CYCLE WASTE-HEAT BOILER T-Q CURVE FOR REHEAT STEAM CYCLE

The trend in steam equipment is such that no new technology need be developed. However, variations on waste heat boiler design will be necessary.

Current Research and Development Efforts

Several research and development programs are currently underway on turbine cooling and materials for advanced gas turbines. The two major sponsoring agencies are the U.S. Department of Energy (DOE), and the Electric Power Research Institute (EPRI), the central research organization of the U.S. electric utility industry.

DOE Programs

The major DOE-sponsored program currently underway is the "High-Temperature Turbine Technology Program." This program has as the objective, the development and demonstration of the technology to allow operation at a turbine inlet temperature of 2600 F on a coal-derived fuel, specifically low calorific value gas. Although the technology demonstration does not have to be at full scale, all technology must be applicable to machines of a nominal 100-MW capacity.

This program has three phases. Phase I, which commenced in June 1976, defined an overall power plant concept and identified the approach to attaining the 2600 F goal. In Phase II, a two-year program started in September 1977, testing of components and cooling schemes in rig scale units was to be carried out. The third and final phase, which was originally scheduled to last from September 1979 to September 1982, would result in the demonstration of a turbine hot section (combustor, diffusers, vanes and blades) operating on gasified coal. The third phase has not yet been sent to procurement.

The four major U.S. gas turbine manufacturers, Curtis Wright, General Electric, United Technologies and Westinghouse participated in Phase I. Their proposed schemes are as follows:

Curtis Wright - transpiration cooling of both vanes and blades by air
General Electric - water cooling of both vanes and blades
United Technologies - water cooling of static structures and vanes with air cooled blades (film cooling)
Westinghouse (with the assistance of the Allison Division of General Motors) - transpiration and film cooling by air of vanes and blades

Only the first two manufacturers were refunded in Phase II; a new competition will be held for Phase III contractors. The results to date in these programs will be discussed in Section 1.2.2.2, Demonstration Engine Characteristics.

A second program currently being carried out under DOE sponsorship which has applications to advanced gas turbines is the so-called "Fireside Corrosion" program being performed by General Electric and Babcock & Wilcox. The objective of this program is to identify the corrosion characteristics of a variety of materials suitable for use in gas turbines and in boilers when exposed to the combustion products of coal or coal-derived fuels.

Under DOE sponsorship, the United Technologies Corporation developed a technology for a low-cost, high performance gas turbine for peaking services. This machine of nominal 10-MW capacity uses a combined axial/centrifugal compressor, patented diffuser concepts and a "wafer" blade turbine operating in the 2200-2400 F range.

Specific goals for this program were to demonstrate the turbine cooling and high-pressure compressor technologies required to achieve thermal efficiencies of 34 to 36 percent simple cycle while reducing the number of compressor and turbine parts 80 percent over state-of-the-art units. Heat transfer cascade testing of the first-stage turbine wafer airfoil cooling designs has exceeded design goals (1500 F maximum metal temperatures at 2500 F combustor exit temperature) and demonstrated cooling effectiveness levels higher than current production aircraft engine airfoils. Additionally, the all-convective cooling design eliminates the leading edge showerhead holes which would be susceptable to plugging in an industrial fuel environment.

The advanced single-spool compressor employs low aspect ratio axial compressor blading and a centrifugal back end stage to achieve 18:1 pressure ratio at 90 percent polytropic efficiency in only 7 stages. The compressor rig tests results were expected during the last half of 1980.

ARPA Programs

The major program on advanced non-metallic materials for gas turbines was that carried out under the sponsorship of the Advanced Projects Research Agency (ARPA) of the U.S. Government. A multiyear program was carried out by Westinghouse and the Ford Motor Company on the development of ceramic turbine components. Westinghouse was to develop ceramic stators for large industrial engines while Ford was to develop ceramic components for automatic gas turbine applications.

Although Westinghouse developed the technology to fabricate large ceramic vanes, successful long term application has not been demonstrated. The major difficulty appears to be the dissimilar thermal growth of the ceramic vane end of the metallic mounts holding the vanes. Failure occurs after only a few cycles.

Ford, however, appears to have developed the technology required to fabricate smaller ceramic components and utilize them successfully in the several hundred horsepower-size engines.

Currently, Garrett Air Research is continuing this program with the objective of developing ceramic technology for industrial turbines of 2 to 10 MW.

EPRI Programs

Additional research efforts have also been carried out under the sponsorship of EPRI. A multiyear program beginning in 1975 on water cooling of static and rotating turbine parts has been performed by General Electric. This program has as its goal, the development of gas turbines able to operate at 2800 to 3000 F on coal-derived liquid fuels. A small rotating test rotor with blades operating at 2800 F has been demonstrated by General Electric during this program.

A test program on erosion/corrosion of turbine materials in coal combustion products and particulate-laden streams is being carried out by United Technologies under EPRI funding.

The latest research program supported by EPRI is the "High Reliability Gas Turbine Combined Cycle Development" program. Recognizing the benefits offered by the gas turbine for future utility power plants, EPRI has asked the gas turbine manufacturers to create a new engine design especially tailored to fill that role. It is envisioned that the gas turbine can be used advantageously in combined-cycle power plants to satisfy base/intermediate-load generating requirements. This represents a shift in emphasis from the current use of gas turbines principally for peakers; and, it presents a more demanding set of requirements. The gas turbine of the next generation must be designed primarily to operate dependably and reliably. The new design must do this while fulfilling the overall need to produce electric power at a low cost and exhibit increased reliability over the current market offering as a preeminent requirement. This is to be achieved with minimum use of hardware development process. Rather, the new high reliability machine must represent the application of perfected and credible analytical design procedures. Westinghouse and UTC was funded by EPRI for this program. At this time, no release has been made of Westinghouse results.

The program has been mated with the joint venture design study that is being considered by UTC and the Kraftwork Union Company of West Germany. This new 60-cycle engine design, designated the V84.3 is an improved version of the KWU production model V94.2. The changes to the compressor section include an optional variable inlet guide vane for improved combined-cycle part-load performance. The first four stages were redesigned for a 10 percent increase in airflow and a 20 percent increase in pressure ratio. The turbine hot section was also redesigned

by increasing the turbine diameter, increasing the firing temperature and reducing the airfoil metal temperatures. These changes significantly increased the turbine output while improving the hot section durability. This program was funded through the end of 1980 with most of the effort devoted to the evaluation of the UTC/KWU engine design.

1.2.2 Develop Data Base on Commercial and Demonstration/Pilot Systems

A data base on commercially available gas turbines and combined-cycle systems is presented for the major U.S. and foreign turbine manufacturers. A second set of data is presented for state-of-the-art systems that are proposed for operation within the next several years.

1.2.2.1 Commercially Available Systems

Data on commercially available gas turbine and combined cycles systems are given in Tables 1.2.2.1-1 and 1.2.2.1-2, respectively. Only turbines of 10,000 kW or larger are listed. Machinery from Eastern-bloc countries have been omitted.

1.2.2.2 Demonstration/Pilot Systems

Projections of operating characteristics of advanced gas turbines which could result from various DOE- and EPRI-sponsored programs are given in Table 1.2.2.2-1. Also included are the characteristics of an advanced Westinghouse turbine which is to be offered commercially in 1981-82.

1.2.3 Evaluate Requirements for Operational System/Subsystem Development and Testing

The technology required for the advanced gas turbine is already under development. Both DOE- and EPRI-sponsored efforts previously discussed will provide component technologies which could be used in advanced turbines. A brief description of the status of these programs follows.

1.2.3.1 High Temperature Turbine Technology Program

The High Temperature Turbine Technology Program (HTTTP) is a three-phased program initiated in 1976 to develop to a technology readiness state the requisite hot section,i.e., combustor or turbine, components needed to operate at 2600 F and above. The three major U.S. turbine manufacturers plus Curtis Wright were awarded Phase I contracts. In the fall of 1977, Curtis Wright and General Electric were selected to carry out Phase II development and testing.

C-3

TABLE 1.2.2.1-1 OPERATING CHARACTERISTICS OF COMMERCIALLY AVAILABLE GAS TURBINES

U. S. Manufacturers

Model	Year First Appearance	Base Load Output	Base Load Heat Rate Btu/kWh	Peak Load Output	Peak Load Heat Rate Btu/kWh	Pressure Ratio	Flow Rate lb/sec	Speed rpm	Temperature °F Turbine Inlet	Temperature °F Exhaust
Curtiss-Wright Power Systems										
Mod-Pod 20HE1	1973	20,000 kW	9,800	20,000 kW	9,795	18.0	144	3600/3000	2150 est.	888
Mod-Pod 25	1974	24,900 kW	11,850	26,00 kW	11,770	11.0	236	3600/3000	1990 est.	995
Mod-Pod 50	1974	49,800 kW	11,850	53,400 kW	11,770	11.0	472	3600/3000	1990 est.	995
General Electric GT Division										
G3142	1949	10,200 kW	13,540	----	----	7.2	113	6,500	1730	979
G3132R	1951	9,750 kW	10,520	----	----	7.2	113	6,500	1750	668
G5261	1958	18,900 kW	13,400	----	----	8.1	213	5,100	1720	955
G5341	1958	24,700 kW	12,230	----	----	10.2	261	5,105	1730	901
PG5341	1961	24,110 kW	12,450	26,050 kW	12,340	10.2	261	5,105	1805	955
G7851	1971	61,750 kW	10,920	----	----	9.7	529	3,600	1850	944
PG7851	1970	60,000 kW	11,130	66,300 kW	11,030	9.7	527	3,600	1960	1018
G7101	1977	75,000 kW	10,590	----	----	11.5	590	3,600	1985	977
PG7101	1976	72,900 kW	10,790	78,800 kW	10,750	11.5	587	3,600	2085	1045
G9141	1976	105,600 kW	10,700	----	----	9.6	760	3,000	1955	953
PG9141	1976	102,700 kW	10,900	111,300 kW	10,860	9.6	753	3,000	2055	1020
LM2500	1979	20,100 kW	9,800	----	----	18.0	144	3,600	2167	940
PG6501	1978	34,850 kW	11,310	38,000 kW	11,190	11.5	302	5,105	2085	1055
G6501	1978	35,650 kW	11,170	----	----	11.5	302	5,105	1985	989
UTC Power Systems										
FT4C-3F	1974	29,820 kW	10,880	32,180 kW	10,760	13.8	306	3,600	1970 est.	877
TP4-2(C3F)	1974	59,950 kW	10,820	64,700 kW	10,700	13.8	611	3,600	1970 est.	877
Westinghouse Combustion Turbine Systems Division										
W251B 60 Hz	1974	38,850 kW	11,980	41,960 kW	11,845	12.0	363	5,015	2066 est.	1111
W251B 50 Hz	1974	38,850 kW	11,980	41,960 kW	11,845	12.0	363	5,011	2066 est.	1111
W501D 60 Hz	1975	96,440 kW	10,660	104,200 kW	10,580	14.2	773	3,600	2066	1026
W501D 50 Hz	1981	95,250 kW	10,800	102,880 kW	10,720	14.2	794	3,000	2066	1026

TABLE 1.2.2.1-1 OPERATING CHARACTERSTICS OF COMMERCIALLY AVAILABLE GAS TURBINES (Cont.)

Foreign Manufactures

Model	Year First Appearance	Base Load Output	Base Load Heat Rate Btu/kWh	Peak Load Output	Peak Load Heat Rate Btu/kWh	Pressure Ratio	Flow Rate lb/sec	Speed rpm	Temperature °F Turbine Inlet	Temperature °F Exhaust	Comments
ACEC											
W-251	1979	38,160 kW	11,564	41,510 kW	11,247	10.0	360	5,000	1940	966	Westinghouse License
W-1101	1979	92,980 kW	11,438	100,430 kW	11,334	12.0	868	3,000	2070	1026	
Alsthom-Atlantique											
G5341	1958	25,350 kW	12,020	----	----	10.0	269	5,100	1730	901	
PG5341	1961	24,500 kW	12,310	25,500 kW	12,310	10.0	266	5,100	1730	905	General Electric License
PG6441	1978	35,700 kW	11,178	38,800 kW	11,120	11.5	300	5,705	1985	991	
G9111	1976	87,400 kW	10,820	----	----	---	760	3,000	1840	945	
PG9111	1976	84,700 kW	11,050	93,900 kW	10,930	---	752	3,000	1940	950	
G9141	1978	107,500 kW	10,620	----	----	---	876	3,000	1955	953	
PG9141	1978	104,500 kW	10,820	113,300 kW	10,790	---	868	3,000	1955	958	
BBC Brown, Boveri & Co Ltd Brown, Boveri & Cie AG Brown Boveri Turbomachinery Inc											
Type 9	1970	34,500 kW	12,016	37,500 kW	11,890	8.8	355	4473/4485	1850(est)	1013	
Type 11	1971	72,300 kW	10,766	78,900 kW	10,664	11.0	639	3,600	1950(est)	1022	
Type 13	1970	81,000 kW	10,868	88,200 kW	10,749	11.6	818	3,000	1900(est)	919	
Fiat TTG											
TG7	1964	8,200 kW	14,840	8,950 kW	14,520	6.0	134	6,000	1350(est)	831	
TG16	1968	18,200 kW	13,175	19,500 kW	12,975	7.0	267	4,850	1400(est)	786	
TG20	1971	37,850 kW	11,590	41,180 kW	11,310	11.0	355	4,920	1750(est)	1000	
TG50	1975	92,600 kW	11,090	100,000 kW	10,990	12.0	851	3,000	1800(est)	995	
GEC Gas Turbines											
EM85	1960	6,750 kW	15,950	----	----	6.0	100	5100/6300	1481	860	
EM610	1975	74,000 kW	12,030	80,600 kW	11,860	9.6	792	3,000	---	---	
EAS-133	1965	11,300 kW	13,240	14,580 kW	12,390	9.5	168	6,500	1652	848	
EAS-134	1975	12,780 kW	13,040	15,960 kW	12,390	9.8	168	6,500	1787	913	
EAS-135/1	1977	13,970 kW	12,920	17,020 kW	12,420	9.5	170	6,500	1827	947	Rolls Royce Avon gas generator
EAS-135/2	1979	14,190 kW	12,780	17,560 kW	12,040	9.5	170	6,500	1827	937	
ESP-1	1980	11,200 kW	10,800	13,230 kW	10,410	---	---	6,500	---	---	Rolls Royce Spey gas generator
ERB-124	1980	20,350 kW	10,480	22,600 kW	10,270	20.0	---	6,500	---	---	Rolls Royce RB-211 gas generator
EO-1C	1972	23,350 kW	11,300	27,900 kW	11,020	11.0	242	3000/3600	1990	995	Rolls Royce Olympus-3 C gas erator
DEO-1C	1972	46,700 kW	11,300	55,800 kW	11,020	11.0	484	3000/3600	1990	995	generator, two Olympus-3 C
ELM-125/2	1979	18,820 kW	9,971	20,650 kW	9,910	17.2	143	6,500	2160(est)	942	General Electric LM2500 gas generator
ELM-125/6	1978	20,060 kW	9,452	21,890 kW	9,424	17.2	143	6000/3600	2180(est)	922	
ELM-150	1979	31,000 kW	9,437	36,090 kW	9,280	30.0	272	3000/3600	----	783	General Electric LM5000 gas generator two LM5000
DELM-150	1979	62,000 kW	9,437	72,180 kW	9,280	30.0	544	3000/3600	----	783	
EO-2	1969	29,400 kW	13,260	41,000 kW	12,300	10.9	484	3000/3600	1735	896	two Olympus-3 gas generator
DEO-2	1976	58,800 kW	13,260	82,000 kW	12,300	10.4	968	3000/3600	1735	896	two Olympus-3 gas generator

TABLE 1.2.2.1-1 OPERATING CHARACTERISTICS OF COMMERICALLY AVAILABLE GAS TURBINES (Cont'd)

Foreign Manufacturers

Model	Year First Appearance	Base Load Output	Base Load Heat Rate Btu/kWh	Peak Load Output	Peak Load Heat Rate Btu/kWh	Pressure Ratio	Flow Rate lb/sec	Speed rpm	Temperature, °F Turbine Inlet	Temperature, °F Exhaust	Comments
Hitachi											
G3142	1966	10,200 kW	13,540	----	----	7.1	116	6,500	----	----	
G5341	1967	24,050 kW	12,310	25,950 kW	12,180	10.0	261	5,105	1805	954	General Electric Licenses
G6441	1981	31,800 kW	11,250	----	----	11.0	304	5,105	----	----	
G7821	1972	60,000 kW	10,960	66,300 kW	10,860	9.7	530	3,600	1950	1016	
G7981	1981	74,290 kW	10,700	80,300 kW	10,660	11.5	591	3,600	2085	1038	
G9111	1980	85,200 kW	10,990	94,400 kW	10,870	9.6	760	3,000	1950	1015	
G9141	1981	105,600 kW	10,790	----	----	9.6	760	3,000	1955	953	
PG5341	1967	23,450 kW	12,490	25,300 kW	12,370	10.2	258	5,105	1805	958	
PG6441	1981	31,100 kW	11,380	34,000 kW	11,310	11.0	301	5,105	1950	967	
PG7821	1972	58,500 kW	11,130	64,600 kW	11,030	9.7	524	3,600	1950	1023	
PG7981	1981	72,900 kW	10,790	78,800 kW	10,750	11.5	599	3,600	2085	1045	
PG9111	1980	82,600 kW	11,210	91,600 kW	11,090	9.6	753	3,000	1950	1020	
PG9141	1981	102,700 kW	10,900	111,300 kW	10,860	9.6	753	3,000	2055	1020	
Hitachi Zosen											
GT35	1979	12,300 kW	11,960	14,000 kW	11,780	12.0	185	3,000/3,600	1560	750	Stal-Laval G735
Ishikawajima-Harima Heavy Industries											
IM1500	1968	10,000 kW	14,000	11,000 kW	13,760	12.6	161	3,000/3,600	1700 (est)	842	
IM2500	1976	20,000 kW	9,580	21,800 kW	9,550	18.1	149	3,000/3,600	2140 (est)	986	General Electric LM2500 gas generator
IM5000	1978	35,400 kW	9,210	38,100 kW	9,080	28.8	289	3,000/3,600	2120 (est)	824	General Electric LM5000 gas generator
Type 7	1976	10,050 kW	14,200	----	----	7.5	137	6,400	1700 (est)	896	
John Brown Engineering											
G3142J	1949	10,450 kW	13,320	----	----	7.1	115	6,500	1730	979	
G5341P	1958	25,350 kW	12,020	----	----	10.1	269	5,105	----	----	General Electric Licenses
PG5341P	1961	24,500 kW	12,310	26,450 kW	12,220	10.1	266	5,105	1805	955	
G6441A	1978	32,450 kW	11,150	----	----	11.5	304	5,100	----	----	
PG6441A	1978	31,750 kW	11,280	34,750 kW	11,210	11.5	301	5,100	1950	967	
G7101E	1976	76,400 kW	10,510	----	----	11.5	604	3,600	----	----	
PG7101E	1976	74,400 kW	10,690	80,500 kW	10,640	11.5	599	3,600	2085	1045	
G9141E	1979	107,500 kW	10,620	----	----	11.4	876	3,000	----	----	
PG9141E	1979	104,500 kW	10,830	113,300 kW	10,790	11.4	868	3,000	2055	1020	
LM2500	1978	21,100 kW	9,725	----	----	18.9	144	3,600	2139	922	
Kraft Work Union											
V93.2	1971	74,460 kW	11,790	81,300 kW	11,730	10.0	763	3,000	1800	985	
V94.2	1974	116,470 kW	11,064	122,300 kW	10,962	10.0	1072	3,000	1800	955	

TABLE 1.2.2.1-1 OPERATING CHARACTERISTICS OF COMMERCIALLY AVAILABLE GAS TURBINES (Cont'd)

Foreign Manufacturers

Model	Year First Appearance	Base Load Output	Base Load Heat Rate Btu/kWh	Peak Load Output	Peak Load Heat Rate Btu/kWh	Pressure Ratio	Flow Rate lb/sec	Speed rpm	Temperature, °F Turbine Inlet	Temperature, °F Exhaust	Comments
Kvaerner Brug											
G5341	1958	24,700 kW	12,230	26,500 kW	----	10.2	266	5,105	1805	955	General Electric License
PG5341	1961	24,000 kW	12,460	25,900 kW	12,350	10.2	266	5,105	1805	955	
G6001	1979	31,800 kW	11,250	33,300 kW	----	11.5	300	5,100	1950	967	
G9001	1979	105,600 kW	10,700	114,000 kW	10,860	9.6	868	3,000	2055	1020	
PG9001	1979	102,700 kW	10,900	11,300 kW	10,860	9.6	868	3,000	2055	1020	
LM2500	1978	20,100 kW	9,800	----	----	18.0	144	3,600	---	---	
LM2500	1978	19,730 kW	9,990	----	----	18.0	144	3,000	---	---	
Mitsubishi Heavy Industries											
MW-101L	1968	8,710 kW	14,960	9,250 kW	14,640	8.0	145	6,000	1450(est)	806	Westinghouse License
MW-191	1963	17,790 kW	13,440	19,100 kW	13,220	7.0	269	4,912	1475(est)	784	
MW-251	1964	36,840 kW	11,830	39,980 kW	11,520	12.0	347	4,984	2050(est)	1008	
MW-501B	1973	83,620 kW	10,850	90,600 kW	10,720	12.0	782	3,600	2000(est)	952	
MW-501D	1980	99,870 kW	10,470	107,900 kW	10,400	14.0	779	3,600	2060(est)	1029	
MW-701B	1976	90,830 kW	11,160	97,780 kW	11,070	11.0	863	3,000	2064(est)	937	
Mitsui Engineering & Shipbuilding											
SB-90C	1969	17,500 kW	13,020	19,300	12,750	9.4	175	5,475	1940	1060	
Nuovo Pignone											
MS 3142	1949	10,200 kW	13,540	----	----	7.2	115	6,500	1730	980	General Electric License
MS 5001	1958	24,700 kW	12,230	26,600 kW	12,180	10.2	269	5,100	1805	950	
MS 6001	1979	32,450 kW	11,150	34,700 kW	11,190	11.5	304	5,100	1950	952	
MS 7001	1970	75,000 kW	10,590	80,240 kW	10,670	11.5	604	3,600	2085	1035	
MS 9001	1976	105,600 kW	10,700	113,300 kW	10,770	9.6	876	3,000	1950	1010	
Pratt & Whitney Aircraft Canada											
CFT4C-3F	1976	29,820 kW	10,880	32,180 kW	10,760	13.8	306	3,600	1970	877	
P&WC	1978	59,950 kW	10,820	64,700 kW	10,700	13.8	611	3,600	1970	877	

TABLE 1.2.2.1-1 OPERATING CHARACTERISTICS OF COMMERCIALLY AVAILABLE GAS TURBINES (Cont'd)

Foreign Manufacturers

Model	Year First Appearance	Base Load Output	Base Load Heat Rate Btu/kWh	Peak Load Output	Peak Load Heat Rate Btu/kWh	Pressure Ratio	Flow Rate lb/sec	Speed rpm	Temperature °F Turbine Inlet	Temperature °F Exhaust	Comments
Rolls-Royce Industrial and Marine											
Spey	1976	11,900 kW	10,240	13,800 kW	10,050	19.0	128	----	----	----	
Avon 1533	1964	12,000 kW	12,490	15,600 kW	11,650	10.0	180	----	----	----	
Avon 1534	1970	15,600 kW	11,770	17,400 kW	11,480	10.0	180	----	----	----	
Avon 1535	1975	16,300 kW	11,790	18,200 kW	11,540	10.0	181	----	----	----	
RB 211	1974	23,800 kW	9,840	----	----	19.2	207	----	----	----	
Olympus	1962	26,100 kW	11,040	28,000 kW	10,980	11.0	240	3000/3600	1990 est.	1024	
SK30	1977	26,100 kW	11,040	28,000 kW	10,980	11.0	----	3000/3600	----	986	
SK60	1977	52,200 kW	11,040	56,000 kW	10,980	11.0	----	3000/3600	----	986	
FS80	1964	74,600 kW	12,470	78,000 kW	12,450	----	----	3000	----	900	
Stal-Laval Turbin											
GT35B	1968	12,550 kW	11,930	14,450 kW	11,500	12.0	186	3000/3600	1560	740	
PP3-Avon 1533	1966	14,300 kW	12,220	15,400 kW	12,200	10.0	180	3000/3600	1560	860	
GT120C	1959	70,000 kW	11,960	75,000 kW	11,780	15.0	790	3000	1530	635	
GT200	1977	75,000 kW	10,300	85,000 kW	10,120	16.0	770	3000	----	----	
Sulzer Brothers											
Type 3	1976	5,300 kW	12,640	5,550 kW	12,545	8.1	62	10,000	1750	918	
Type R3	1976	5,150 kW	10,340	5,400 kW	10,155	8.3	62	10,000	1750	920	
Type 7	1970	10,580 kW	13,485	11,100 kW	13,380	7.5	137	6,400	1700	496	
Type R7	1970	10,020 kW	11,190	10,530 kW	10,970	7.6	137	6,400	1700	900	
PRIMO 12	1978	12,200 kW	12,275	----	----	10.0	168	6,500	1650 est.	758	
PRIMO 14	1978	13,700 kW	12,140	----	----	10.0	167	6,500	1775 est.	925	
PRIMO 15	1978	14,900 kW	12,015	----	----	10.0	169	6,500	1850 est.	870	
PRIMO 21	1979	21,000 kW	10,215	----	----	20.0	196	6,500	----	887	
Thomassen Holland											
G3142J	1949	10,450 kW	13,320	----	----	7.2	115	6,500	1730	979	
G3142R	1951	10,000 kW	10,370	----	----	7.2	115	6,500	1730	668	
G5341P	1958	25,350 kW	12,020	----	----	10.2	269	5,100	1730	901	
PG5341P	1961	24,500 kW	12,310	26,450 kW	12,220	10.2	266	5,100	1805	955	
PG6441A	1979	31,750 kW	11,280	34,750 kW	11,210	11.1	301	5,100	1850	901	
PG6441B	1981	34,140 kW	11,280	36,900 kW	11,250	11.5	301	5,100	1950	967	General Electric License
G7101E	1979	76,400 kW	10,510	----	----	11.5	604	5,100	2085	1041	
PG7101E	1979	74,400 kW	10,690	80,500 kW	10,640	11.5	699	3,600	1985	977	
G9141E	1979	107,500 kW	10,620	----	----	9.6	876	3,000	1955	953	
PG9141E	1979	104,500 kW	10,820	113,390 kW	10,790	9.6	868	3,000	2055	1020	
Toshiba											
Type 9	1970	34,500 kW	12,010	37,500 kW	11,890	8.9	348	4473/4485	----	535	
Type 11	1971	72,500 kW	10,760	78,900 kW	10,660	11.0	626	3600	----	546	Brown Boveri License
Type 13	1970	79,400 kW	11,370	86,900 kW	11,220	10.4	799	3000	----	505	
Westinghouse											
W191G	1960	18,040 kW	13,220	19,350 kW	13,010	7.9	273	4912	1450	773	
W191PG	1966	17,700 kW	13,390	19,000 kW	13,210	7.0	270	4912	1450	773	
W191PG Super	1980	19,250 kW	12,930	----	----	8.6	297	4912	1450	758	
W301G	1961	32,300 kW	13,060	34,400 kW	12,870	6.8	438	3600	1450	800	
W301G Super	1978	35,125 kW	12,600	----	----	7.5	481	3600	1450	785	

TABLE 1.2.2.1-2 OPERATING CHARACTERISTICS OF COMMERCIALLY AVAILABLE COMBINED CYCLE PLANTS

Model	Year First Appearance	Base Load Output	Base Load Heat Rate Btu/kWh	Peak Load Output	Peak Load Heat Rate Btu/kWh	Output Frequency	Boiler Type	Turbine Size	Steam	Engine No. and Type
CUCY 50	1979	51,000 kW	8,520	54,400 kW	8,470	50 Hz	non-fired	36,500 kW	14,600 kW	one W251
CUCY 100	1977	94,500 kW	8,640	99,200 kW	8,410	50 Hz	non-fired	67,000 kW	27,500 kW	two W251
CUCY 130	1977	128,300 kW	7,990	134,700 kW	7,770	50 Hz	non-fired	91,300 kW	37,000 kW	one W1101
CUCY 140	1979	143,000 kW	7,440	153,000 kW	7,430	50 Hz	non-fired	91,700 kW	51,300 kW	one W1101
Alsthom-Atlantique										
VEGA 105P	1976	33,100 kW	8,850	36,000 kW	8,570	50/60 Hz	non-fired	22,400 kW	10,700 kW	one PG5341
VEGA 205P	1976	69,000 kW	8,575	----	---	50/60 Hz	non-fired	47,350 kW	22,100 kW	two PG5341
VEGA 206P	1978	102,300 kW	8,030	----	---	50/60 Hz	non-fired	72,800 kW	30,200 kW	two PG6441
VEGA 209P	1976	237,000 kW	7,900	----	---	50 Hz	non-fired	168,900 kW	70,000 kW	two PG9111
VEGA 209E	1978	290,000 kW	7,791	----	---	50 Hz	non-fired	209,400 kW	87,500 kW	two PG9141
VEGA 109E	1978	144,200 kW	7,845	----	---	50 Hz	non-fired	104,700 kW	40,000 kW	one PG9141
BBC Brown, Boveri & Co. Ltd Brown, Boveri & Cie AG Brown Boveri Turbomachinery Inc.										
KA9-1	1977	51,100 kW	8,105	55,690 kW	8,025	50/60 Hz	non-fired	31,870 kW	19,230 kW	one Type 9
KA9-2	1977	103,990 kW	7,955	113,350 kW	7,875	50/60 Hz	non-fired	63,740 kW	40,250 kW	two Type 9
KA9-3	1979	157,210 kW	7,915	171,350 kW	7,835	50/60 Hz	non-fired	95,610 kW	61,600 kW	three Type 9
KA9-4	1979	209,980 kW	7,880	228,870 kW	7,805	50/60 Hz	non-fired	127,480 kW	82,500 kW	four Type 9
KA11-1	1979	104,790 kW	7,435	114,200 kW	7,360	60 Hz	non-fired	68,400 kW	36,390 kW	one Type 11
KA11-2	1979	211,550 kW	7,355	230,600 kW	7,285	60 Hz	non-fired	136,800 kW	74,750 kW	two Type 11
KA11-3	1979	317,320 kW	7,350	345,880 kW	7,280	60 Hz	non-fired	205,200 kW	112,120 kW	three Type 11
KA11-4	1979	426,380 kW	7,305	464,700 kW	7,235	60 Hz	non-fired	273,600 kW	152,780 kW	four Type 11
KA13-1	1979	113,660 kW	7,700	123,880 kW	7,630	50 Hz	non-fired	77,160 kW	36,500 kW	one Type 13
KA13-2	1979	228,350 kW	7,670	248,900 kW	7,600	50 Hz	non-fired	154,320 kW	74,030 kW	two Type 13
KA13-3	1979	344,050 kW	7,635	375,000 kW	7,565	50 Hz	non-fired	231,480 kW	112,570 kW	three Type 13
KA13-4	1979	459,800 kW	7,615	501,200 kW	7,545	50 Hz	non-fired	308,640 kW	151,160 kW	four Type 13
Curtiss-Wright Power Systems										
TEC 150	1978	150,000 kW	9,100	165,000 kW	9,000	50/60 Hz	non-fired	89,000 kW	61,000 kW	four
TEC 200	1978	210,000 kW	9,300	230,000 kW	9,200	50/60 Hz	non-fired	89,000 kW	121,000 kW	four
Fiat TTG										
CC 50	1978	53,700 kW	8,115	----	----	50/60 Hz	non-fired	36,300 kW	17,400 kW	one TG.20
CC 100	1978	107,400 kW	8,115	----	----	50/60 Hz	non-fired	72,600 kW	34,800 kW	two TG.20
CC 150	1978	126,000 kW	8,035	----	----	50 Hz	non-fired	86,000 kW	38,000 kW	one TG.50
CC 250	1978	252,000 kW	8,035	----	----	50 Hz	non-fired	176,000 kW	76,000 kW	two TG.50
GEC Gas Turbines										
EM610	1975	118,200 kW	7,790	----	----	50 Hz	non-fired	----	----	one EM610
General Electric GT Div										
STAG 109E	1979	140,400 kW	7,940	----	----	50 Hz	non-fired	----	----	one MS9001E
STAG 209E	1979	282,300 kW	7,890	----	----	50 Hz	non-fired	----	----	two MS9001E
STAG 309E	1979	423,800 kW	7,890	----	----	50 Hz	non-fired	----	----	three MS9001E
STAG 409E	1979	564,700 kW	7,890	----	----	50 Hz	non-fired	----	----	four MS9001E

TABLE 1.2.2.1-2 OPERATING CHARACTERISTICS OF COMMERCIALLY AVAILABLE COMBINED CYCLE PLANTS (Cont'd)

Model	Year First Appearance	Base Load Output	Base Load Heat Rate Btu/kWh	Peak Load Output	Peak Load Heat Rate Btu/kWh	Output Frequency	Boiler Type	Turbine Size	Steam	Engine No. and Type
Stal-Laval Turbin										
Gasteam 125	1977	113,000 kW	7,500	122,000 kW	7,420	50 Hz	non-fired	80,000 kW	34,000 kW	one GT200
Gasteam 250	1977	228,000 kW	7,420	246,000 kW	7,340	50 Hz	non-fired	160,000 kW	70,000 kW	two GT200
Sulzer Giothers										
Turbotur 305	1974	16,300 kW	8,210	----	----	50/60 Hz	non-fired	10,600 kW	5,700 kW	two Type 3
Turbotur 210	1974	17,000 kW	8,340	----	----	50/60 Hz	non-fired	10,580 kW	6,420 kW	One Type 7
Turbotur 310	1974	34,000 kW	8,330	----	----	50/60 Hz	non-fired	21,160 kW	12,840 kW	Two Type 7
Turbotur 214	1978	20,400 kW	8,030	----	----	50/60 Hz	non-fired	13,700 kW	6,700 kW	One PRIMO 14
Turbotur 314	1978	41,000 kW	8,010	----	----	50/60 Hz	non-fired	27,400 kW	13,600 kW	Two PRIMO 14
Turbotur 225	1978	39,300 kW	7,320	----	----	50/60 Hz	non-fired	25,400 kW	13,900 kW	One Olympus
Turbotur 325	1978	78,800 kW	7,300	----	----	50/60 Hz	non-fired	50,800 kW	28,000 kW	Two Olympus
Thomassen Holland										
STEG 105P	1972	33,400 kW	8,740	----	----	50/60 Hz	non-fired	----	----	One PG5341
STEG 205P	1972	67,200 kW	8,720	----	----	50/60 Hz	non-fired	----	----	Two PG5341
STEG 106B	1980	47,800 kW	8,120	----	----	50 Hz	non-fired	----	----	One PG6441
STEG 206B	1980	95,900 kW	8,100	----	----	50 Hz	non-fired	----	----	Two PG6441
STEG 107E	1979	99,300 kW	7,700	----	----	60 Hz	non-fired	----	----	One PG7891
STEG 207E	1979	198,800 kW	7,660	----	----	60 Hz	non-fired	----	----	Two PG7891
STEG 109E	1979	140,400 kW	7,940	----	----	50 Hz	non-fired	----	----	One PG9141
STEG 209E	1979	282,100 kW	7,890	----	----	50 Hz	non-fired	----	----	Two PG9141
UTC Power Systems										
TSP-2	1980	81,150 kW	8,385	----	----	60 Hz	non-fired	57,250 kW	23,900 kW	Two FT4C
TSP-4	1980	162,950 kW	8,350	----	----	60 Hz	non-fired	114,500 kW	48,450 kW	Four FT4C
TSP-8	1977	326,580 kW	8,335	----	----	60 Hz	non-fired	229,000 kW	97,580 kW	eight FT4C
Westinghouse Canada										
Mini Pace	1987	53,445 kW	9,800	----	----	50/60 Hz	bunker	34,244 kW	18,200 kW	Two W191 both gas
Westinghouse Combustion Turbine Systems Div.										
PACE 2511	1981	55,200 kW	8,300	----	----	50/60 Hz	non-fired	36,800 kW	18,400 kW	one W251B
PACE 2512	1981	110,400 kW	8,300	----	----	50/60 Hz	non-fired	73,500 kW	36,900 kW	two W251B
PACE 2513	1981	165,600 kW	8,300	----	----	50/60 Hz	non-fired	110,300 kW	55,300 kW	three W251B
PACE 2514	1981	220,800 kW	8,300	----	----	50/60 Hz	non-fired	147,100 kW	73,700 kW	four W251B
PACE 5011	1981	134,700 kW	7,630	----	----	50/60 Hz	non-fired	93,800 kW	40,900 kW	one W501D
PACE 5012	1981	269,400 kW	7,630	----	----	50/60 Hz	non-fired	187,500 kW	81,900 kW	Two W501D
PACE 5013	1981	404,100 kW	7,630	----	----	50/60 Hz	non-fired	281,300 kW	122,800 kW	three W501D
PACE 5014	1981	538,800 kW	7,630	----	----	50/60 Hz	non-fired	375,000 kW	163,800 kW	four W501D
PACE 5015	1981	673,600 kW	7,630	----	----	50/60 Hz	non-fired	468,800 kW	204,800 kW	five W501D

TABLE 1.2.2.1-2 OPERATING CHARACTERISTICS OF COMMERCIALLY AVAILABLE COMBINED CYCLE PLANTS (Cont'd)

Model	Year First Appearance	Base Load Output	Base Load Heat Rate Btu/kWh	Peak Load Output	Peak Load Heat Rate Btu/kWh	Output Frequency	Boiler Type	Turbine Size	Steam	Engine No. and Type
STAG 406P	1977	138,400 kW	8,700	---	---	50/60 Hz	non-fired	---	---	four MS5001P
STAG 206B	1979	96,200 kW	8,070	---	---	50/60 Hz	non-fired	---	---	two MS6001B
STAG 406B	1979	192,400 kW	8,070	---	---	50/60 Hz	non-fired	---	---	four MS6001B
STAG 107E	1977	99,300 kW	7,700	---	---	60 Hz	non-fired	---	---	one MS7001E
STAG 407E	1979	396,700 kW	7,650	---	---	60 Hz	non-fired	---	---	four MS7001E
STAG 607E	1979	595,600 kW	7,630	---	---	60 Hz	non-fired	---	---	six MS7001E
Hitachi										
HITSTAG205	1980	68,300 kW	9,110	74,400 kW	8,930	50/60 Hz	non-fired	46,000 kW	22,300 kW	two PG5341
HITSTAG107B	1980	86,000 kW	8,430	97,000 kW	8,230	60 Hz	non-fired	59,000 kW	27,000 kW	one PG7821
HITSTAG207B	1980	174,000 kW	8,350	195,000 kW	8,150	60 Hz	non-fired	117,000 kW	57,000 kW	two PG7821
HITSTAG307B	1980	262,000 kW	8,350	291,000 kW	8,150	60 Hz	non-fired	176,000 kW	86,000 kW	three PG7821
HITSTAG407B	1980	351,000 kW	8,290	393,000 kW	8,110	60 Hz	non-fired	235,000 kW	116,000 kW	four PG7821
HITSTAG107E	1980	106,000 kW	8,050	115,000 kW	7,940	60 Hz	non-fired	73,000 kW	33,000 kW	one PG7981
HITSTAG207E	1980	214,000 kW	7,980	233,000 kW	7,850	60 Hz	non-fired	147,000 kW	67,000 kW	two PG7981
HITSTAG307E	1980	323,000 kW	7,920	352,000 kW	7,800	60 Hz	non-fired	220,000 kW	103,000 kW	three PG7981
HITSTAG407E	1980	430,000 kW	7,920	469,000 kW	7,800	60 Hz	non-fired	293,000 kW	137,000 kW	four PG7981
HITSTAG109B	1980	123,000 kW	8,410	138,000 kW	8,210	50 Hz	non-fired	83,000 kW	40,000 kW	one PG9111
HITSTAG209B	1980	248,000 kW	8,350	278,000 kW	8,130	50 Hz	non-fired	165,000 kW	83,000 kW	two PG9111
HITSTAG309B	1980	373,000 kW	8,330	418,000 kW	8,110	50 Hz	non-fired	248,000 kW	125,000 kW	three PG9111
John Brown Engineering										
SCOTSTAG 103	1979	14,500 kW	9,180	---	---	50/60 Hz	non-fired	10,000 kW	4,500 kW	one Frame 3
SCOTSTAG 105	1978	33,685 kW	8,746	---	---	50/60 Hz	non-fired	23,550 kW	10,135 kW	one Frame 5
SCOTSTAG 106	1980	41,890 kW	8,322	---	---	50/60 Hz	non-fired	30,440 kW	11,450 kW	one Frame 6
SCOTSTAG 109	1979	128,600 kW	7,246	---	---	50 Hz	non-fired	83,800 kW	44,800 kW	one Frame 9
Kraftwerk Union										
GUD 17.14	1977	170,000 kW	7,588	---	---	50 Hz	non-fired	*116,470 kW	60,310 kW	one
GUD 35.24	1977	340,000 kW	7,587	---	---	50 Hz	non-fired	*232,940 kW	120,620 kW	two
GUD 70.44	1977	680,000 kW	7,586	---	---	50 Hz	non-fired	*465,880 kW	241,240 kW	four
Nuovo Pignone										
CC-205N	1977	75,000 kW	8,350	75,000 kW	8,350	50 Hz	gas-fired	50,000 kW	25,000 kW	two G5341
CC-209B	1977	248,300 kW	7,850	248,300 kW	7,850	50 Hz	non-fired	169,800 kW	78,500 kW	two G9001
Pratt & Whitney Aircraft Canada										
TSP-2	1980	81,150 kW	8,385	---	---	60 Hz	non-fired	57,250 kW	23,900 kW	two CFT4C-3F
TSP-4	1980	162,950 kW	8,350	---	---	60 Hz	non-fired	114,500 kW	48,450 kW	four CFT4C-3F
TSP-8	1980	326,580 kW	8,335	---	---	60 Hz	non-fired	229,000 kW	97,580 kW	eight CFT4C-3F
Prvni Brnenska Strojirna										
STGT 9	1974	11,700 kW	8,100	11,700 kW	8,100	50 Hz	gas-fired	7,000 kW	4,700 kW	one ST9
Rolls-Royce Industrial and Marine										
SK30-CS	1977	17,800 kW	7,650	---	---	50/60 Hz	non-fired	25,400 kW	12,400 kW	one Olympus
SK40-CS	1977	75,600 kW	7,650	---	---	50/60 Hz	non-fired	50,800 kW	24,800 kW	two Olympus

TABLE 1.2.2.2.-1

PROJECTED OPERATING CHARACTERISTICS OF DEMONSTRATION ENGINES

Mfg.	Time of Appearance	Output	Heat Rate Btu/kWh	Pressure Ratio	Flow lb/sec	Temperature Turbine Inlet	Temperature Exhaust	Comments
Curtis Wright	1988+	130 MW	9800 (est)	17	470	3000	1300 (est)	Based on DOE High Temperature Turbine Technology Program - Aircooled (Transpiration) Vanes and Blades
General Electric	1988+	73 MW	10200 (est)	12.1	301	2600	1273	Based on DOE High Temperature Turbine Technology Program - Water Cooled Vanes and Blades
UTC	1988+	140 MW	10600 (est)	12	860	2400	1150	Based on Uprate of EPRI Reliable Engine Program - Aircooled (Convective) Vanes and Blades
Westinghouse								
W501D	1981	95.3 MW	10800	14.2	794	2066 (est)	1026	50 Hz Version of W501
W1101D/701D	1981	118.6 MW	10800	14.2	970	2066 (est)	1024	Based on a 50 Hz scaled-up version of 501

Curtis Wright

The technology path chosen by Curtis Wright uses the transpiration cooling by air of both blades and vanes to achieve operating temperatures of 2600 F and above.

A two-shaft, 17:1 pressure ratio engine with free turbine (Fig. 1.2.3.1-1), a scaled version of the C-W 6515 turbine was selected for the basic layout. Cooling air from the compressor discharge is used to cool the turbine blade and vanes (Fig. 1.2.3.1-2). The air foils (Fig. 1.2.3.1-3) consist of a structural spar with spanwise radial channels to which are electron beam welded porous metal skins. Cooling air from the hub is fed through each of the channels and then through the skin. The structural spars are kept to reasonable temperatures (1300 F - 1500 F) and the skin, which is non-load carrying, is protected by a film of relatively cool air.

Tests to date have demonstrated the capability to operate at 2600 F to 3000 F. These tests have been carried out using test cascades (not full engine configurations) for limited times. Only clean, liquid fuels have been used, although a blended fuel gas resembling low-Btu gas will be tested.

The results to date have been encouraging as far as the capability of attaining high temperature operation is concerned. Problems with over temperature on structural members has been resolved.

The combustor arrangement anticipated for use with the multi-spool engine is annular wrap-around combustor (Fig. 1.2.3.1-4). (An annular configuration resembles a torous. There are no individual cans, just a continuous section.) Cooling air keeps the wall temperatures to a 1600 F maximum level. No significant testing has been done on this combustor concept using low-Btu fuel.

General Electric

The technology path chosen by G.E. is the use of water to cool the vanes and blades to achieve operating temperature of 2600 F.

A single shaft 12.1:1 pressure ratio engine approximately the same size as the current Frame 6 was selected for the basic layout (Fig. 1.2.3.1-5). Cooling water is circulated in a closed loop for vane cooling. Water enters the vane from the bottom (Fig. 1.2.3.1-6) and exits at the top after making one more downward pass.

FIG. 1.2.3.1-1

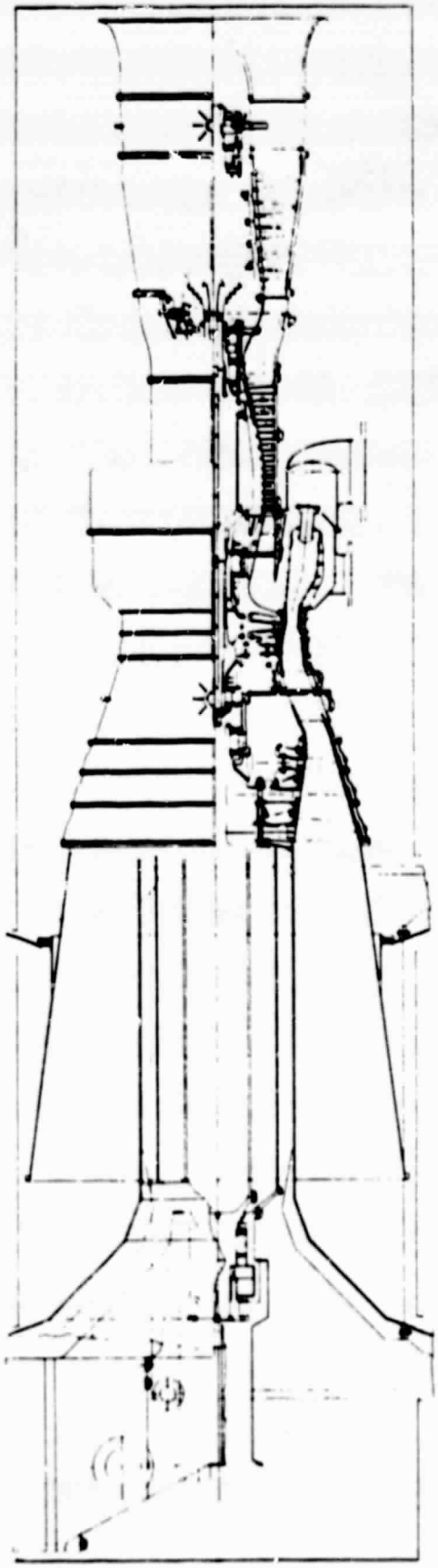

CURTIS WRIGHT 130-MW GAS TURBINE CONFIGURATION

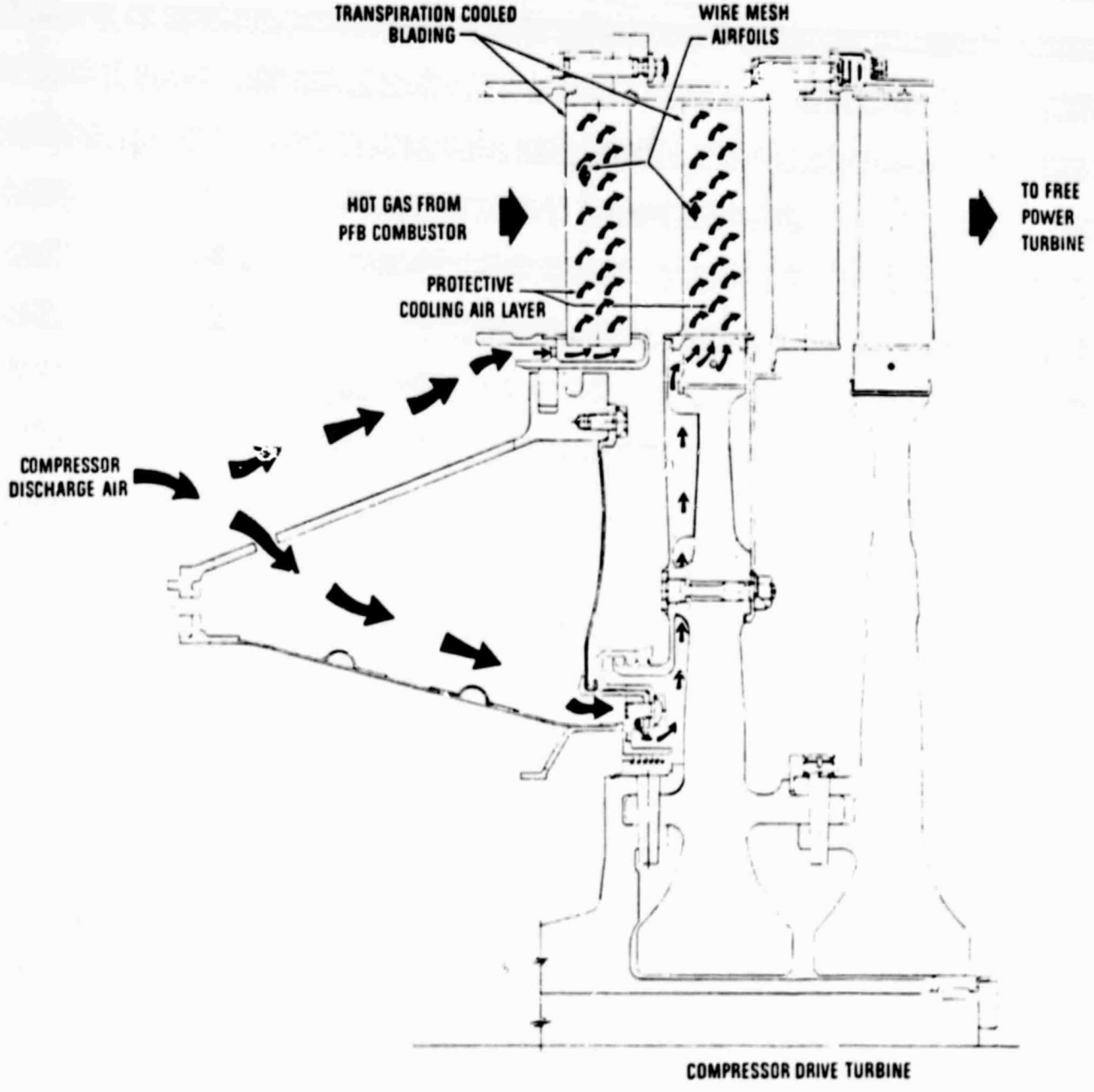

COOLING CONFIGURATION FOR HIGH TEMPERATURE TURBINE

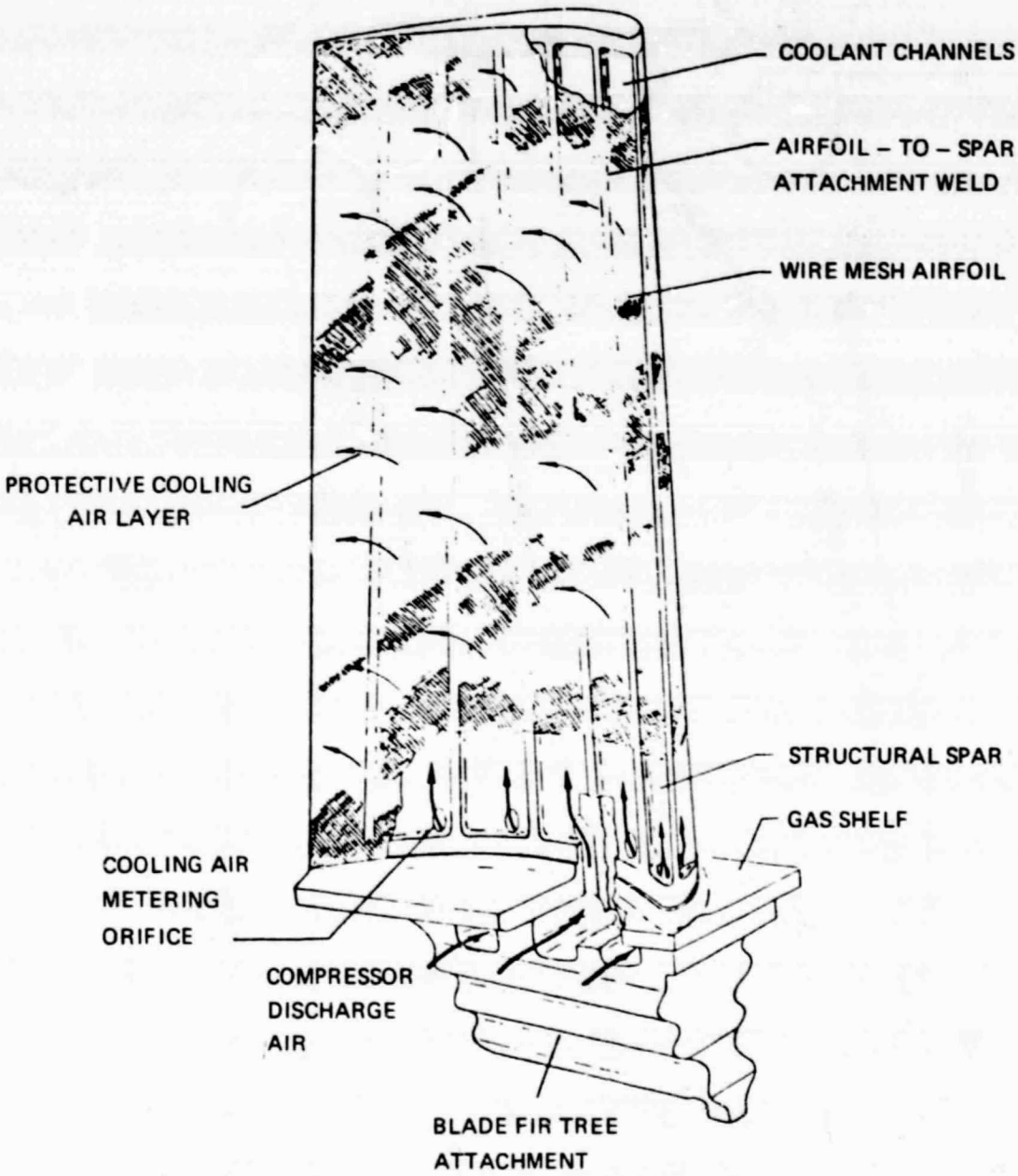

TRANSPIRATION AIR-COOLED TURBINE BLADE

FIG. 1.2.3.1-4

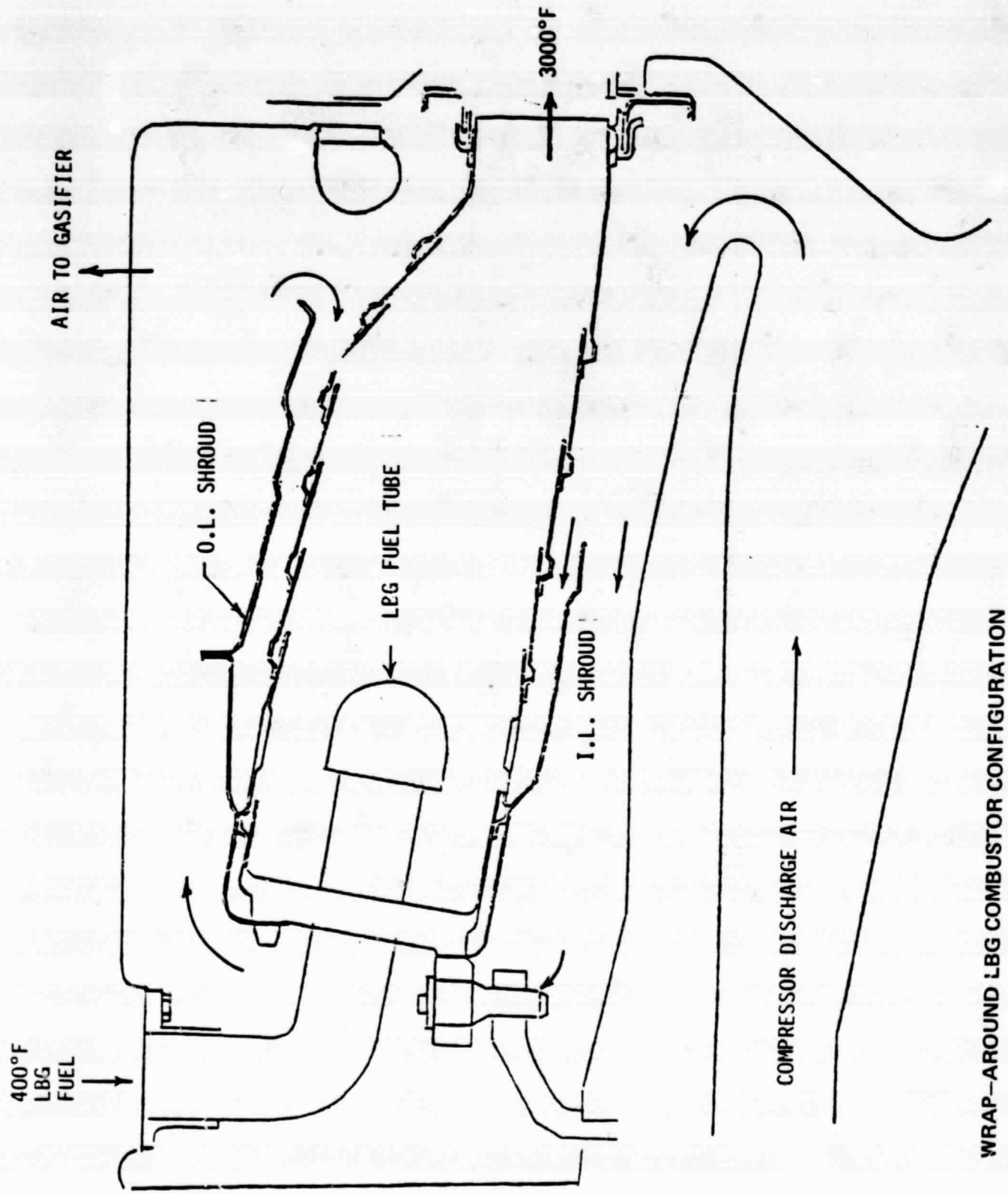

WRAP-AROUND LBG COMBUSTOR CONFIGURATION

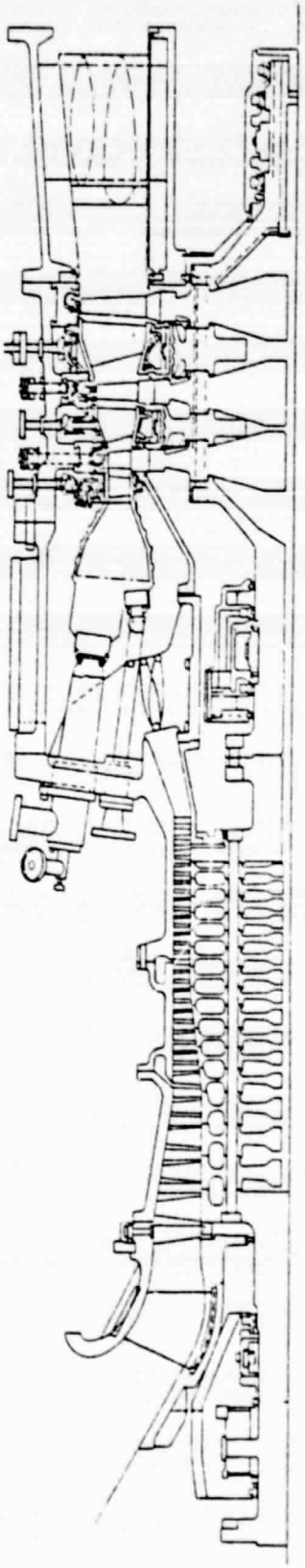

GENERAL ELECTRIC HIGH-TEMPERATURE MACHINE CROSS SECTION

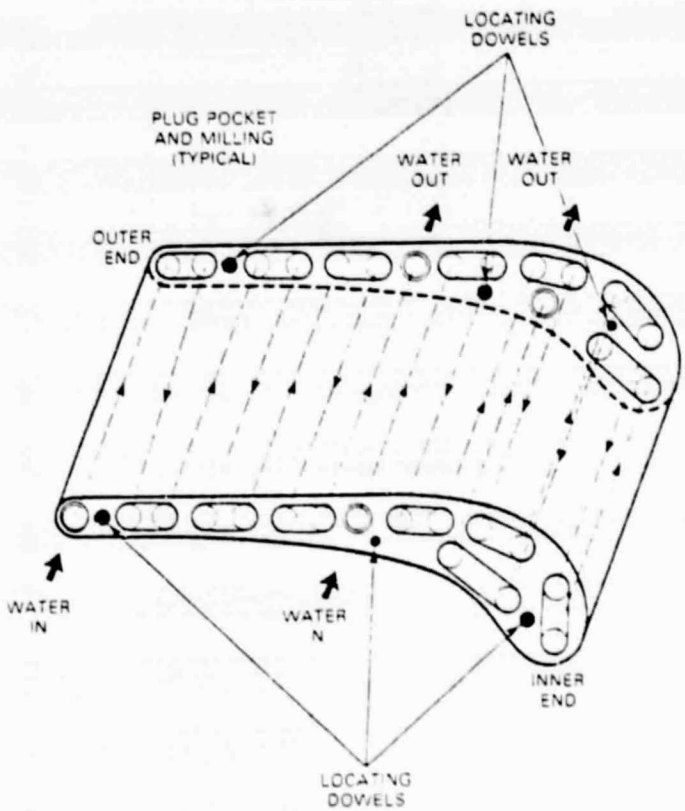

NOZZLE COOLING CIRCUITS

The airfoils are of two different constructions. The initial vane and blade are of composite construction (Fig. 1.2.3.1-7 shows the first-stage blade) using copper alloy inserts with nickel alloy skins. Coolant flows through nickel alloy tubes. The copper alloy inserts are supported by nickel alloy spars. This use of the copper is to assure even heat transfer through the blade/vane.

The blades and vanes for the second stage and beyond are of monolithic structure and are being considered as a backup for the composite first-stage vanes (Fig. 1.2.3.1-8). Water flows up the blade under the influence of a centrifugal field. Approximately 65 percent of the blade coolant is dumped overboard.

A sectoral combustor has been selected by G.E. (Fig. 1.2.3.1-9). This type of combustor is a compromise between the can-type and full annular combustor in that the torus is made up of a number of sectors, each with its own fuel system. In the G.E. system, the combustor is equipped with oil nozzle for startup and part load assistance.

General Electric has had good success with the water cooling. The vanes present no problems from the cooling view point although there have been structure problems. Water cooling of the blades has been demonstrated, but it appears that the monolithic structure is structural superior to the composite structure. Water purity requirements are high (deionized boiler feed water) and the water is lost overboard. None of these are unsurmountable problems.

1.2.3.2 High Reliability Gas Turbine Program

The High Reliability Gas Turbine Program (HRGT) was initiated by EPRI in 1978 with the objectives of defining those areas in gas turbine and combined-cycle design that have had poor records for reliability and identifying design changes to increase the system reliability to levels as least as good as steam turbine system. Three contractors, GE, United Technologies and Westinghouse, were selected. This program is an ongoing program, and no reports have been released by EPRI to date. Discussion centers on the UTC contribution.

The engine selected as the starting point of the HRGT program was the V84.3, the engine which would result from the UTC/KWU joint venture. This engine is a single shaft, two bearing engine with a pressure ratio of 12:1 (Fig. 1.2.3.2-1). In line with the EPRI philosophy of high reliability through extension of state-of-the-art technology, the turbine rotor inlet temperature of this machine would be 2120 F (combustor exit 2210 F) and the output will be 120 MW. Compressor discharge air is used to convectively cool the vanes and blades. The first stage vane cooling is shown in Fig. 1.2.3.2-2. The leading edge of the blade is cooled by air flowing radially in a channel formed by an

FIG. 1.2.3.1–7

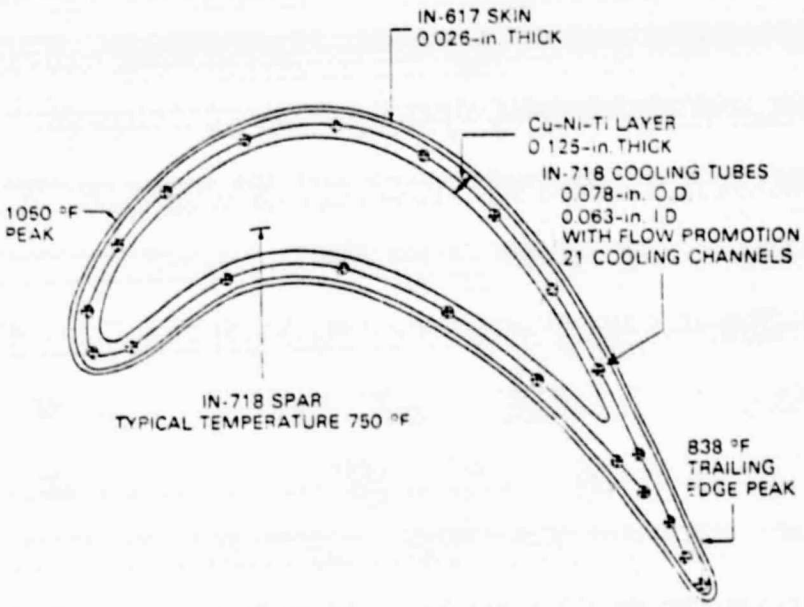

FIRST–STAGE COMPOSITE BLADE SECTION

FIG. 1.2.3.1-8

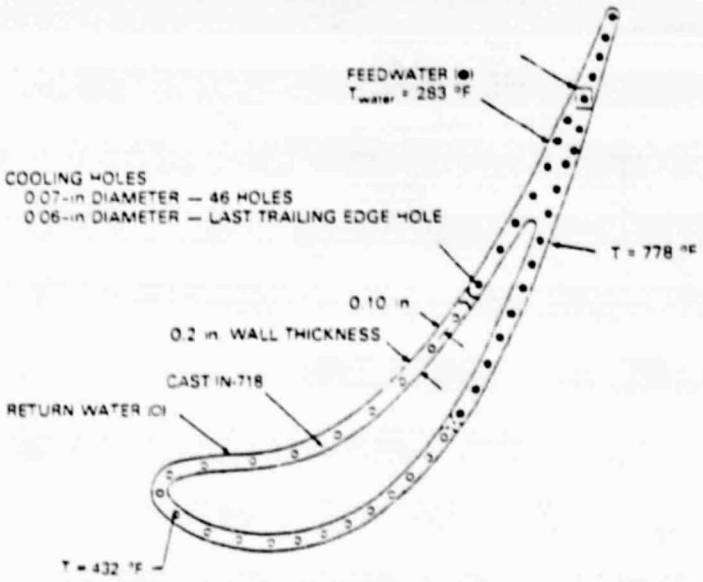

SECOND-STAGE MONOLITHIC VANE SECTION

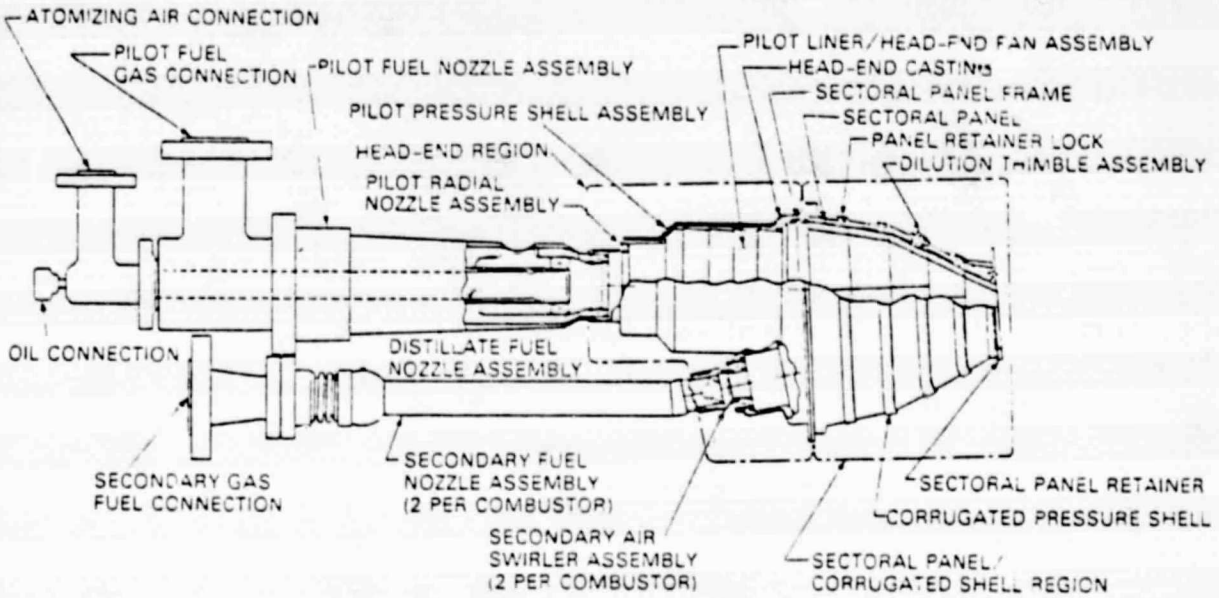

GENERAL ELECTRIC LOW-BTU GAS SECTORAL COMBUSTOR

FIG. 1.2.3.2-1

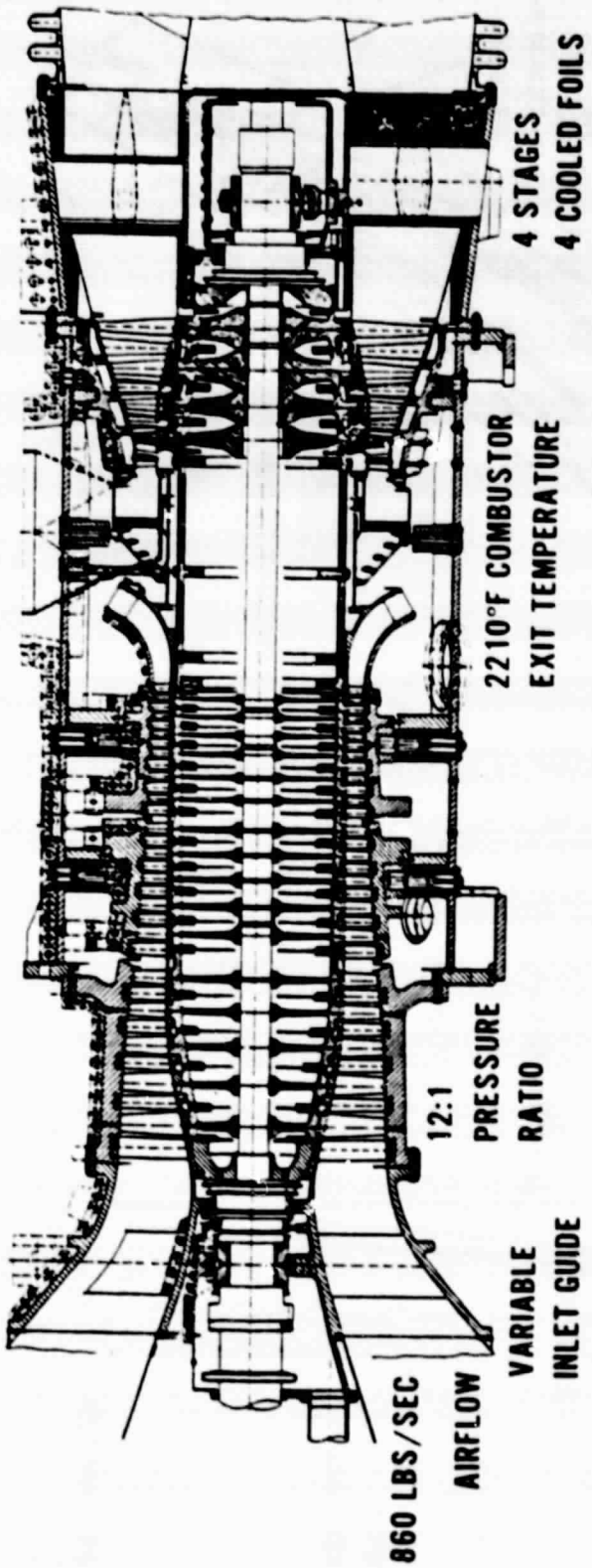

V84.3 GAS TURBINE

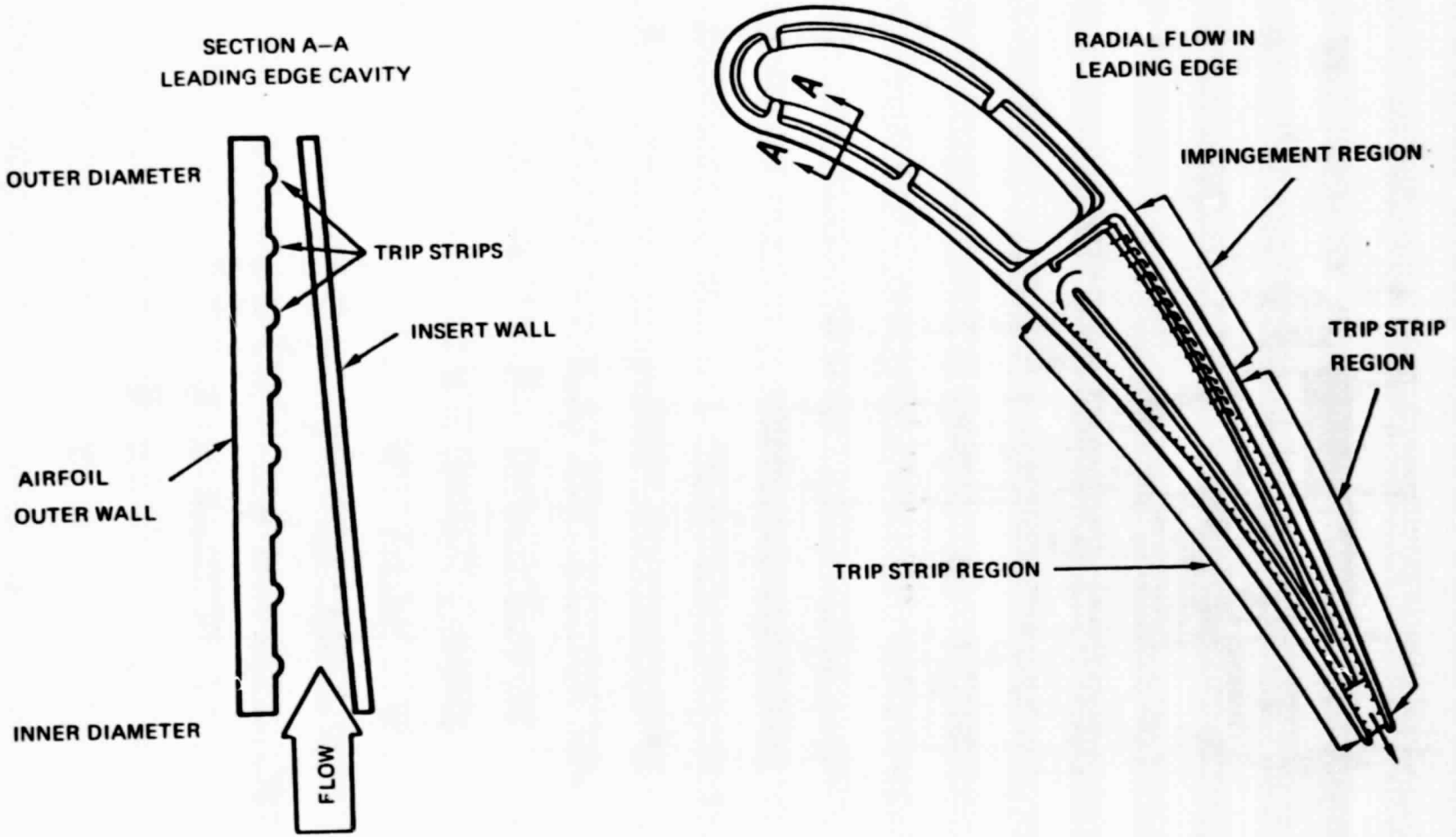

FIRST VANE COOLING CONFIGURATION

insert and the airfoil wall. Trip strips enhance the heat transfer. The trailing section of the blade is cooled on the suction side in the same manner except the flow is chordwise. The pressure side is cooled partially by impingement and partially by channel flow. There are no holes in the blade to plug up due to dirty fuels. The first stage blade is also convectively cooled by radially flowing air (Fig. 1.2.3.2-3).

Two types of combustors have been considered for this engine; the conventional (by U.S. standards) in-line can-type combustor and the off-base silo-type combustor. The silo-type combustor (Fig. 1.2.3.2-4), while initially more expensive offers advantages of high reliability, both for the combustor and for downstream elements and ease of tailoring for different fuels and for emission control.

All the elements of the HRGT program are either state-of-the-art or limited extensions thereof. These design features could be incorporated into engines which could appear in the 1984-85 time frame.

1.2.3.3 Potential Problem Areas

The major problem facing the use of gas turbines for base-load utility systems is a perceived lack of reliability. Thus, programs aimed at quantum jumps in technology may not achieve their goal of producing technology acceptable to the market. It must be understood that it is the market, and not technology, which will make the concept of advanced power systems a reality. Unless the industry accepts the product and furnishes enough money through purchases to amortize the hundreds of millions of dollars required to develop technology, the rate of progress will be very slow.

This problem is excebated by the fact that the quantum jumps in technology do not necessarily result in quantum jumps in performance. For example, Fig. 1.2.3.3-1 shows the performance for three levels of technology. The 2400 F and 3000 F performance levels differ by less than two percent; however, the 2400 F level of technology is only a modest extension of the state-of-the-art whereas the 2600 F/3000 F technology, as currently structured, requires quantum advances.

The combined -cycle systems using advanced technology gas turbines will compete against conventional steam stations with flue gas desulfurization (FGD) having performance levels of 35 percent or less, and against nuclear plants having performance of 32-33 percent. Thus, extracting the last bit of performance out of the system at the expense of very high R&D costs and potential reliability problems does not appear an attractive scenario.

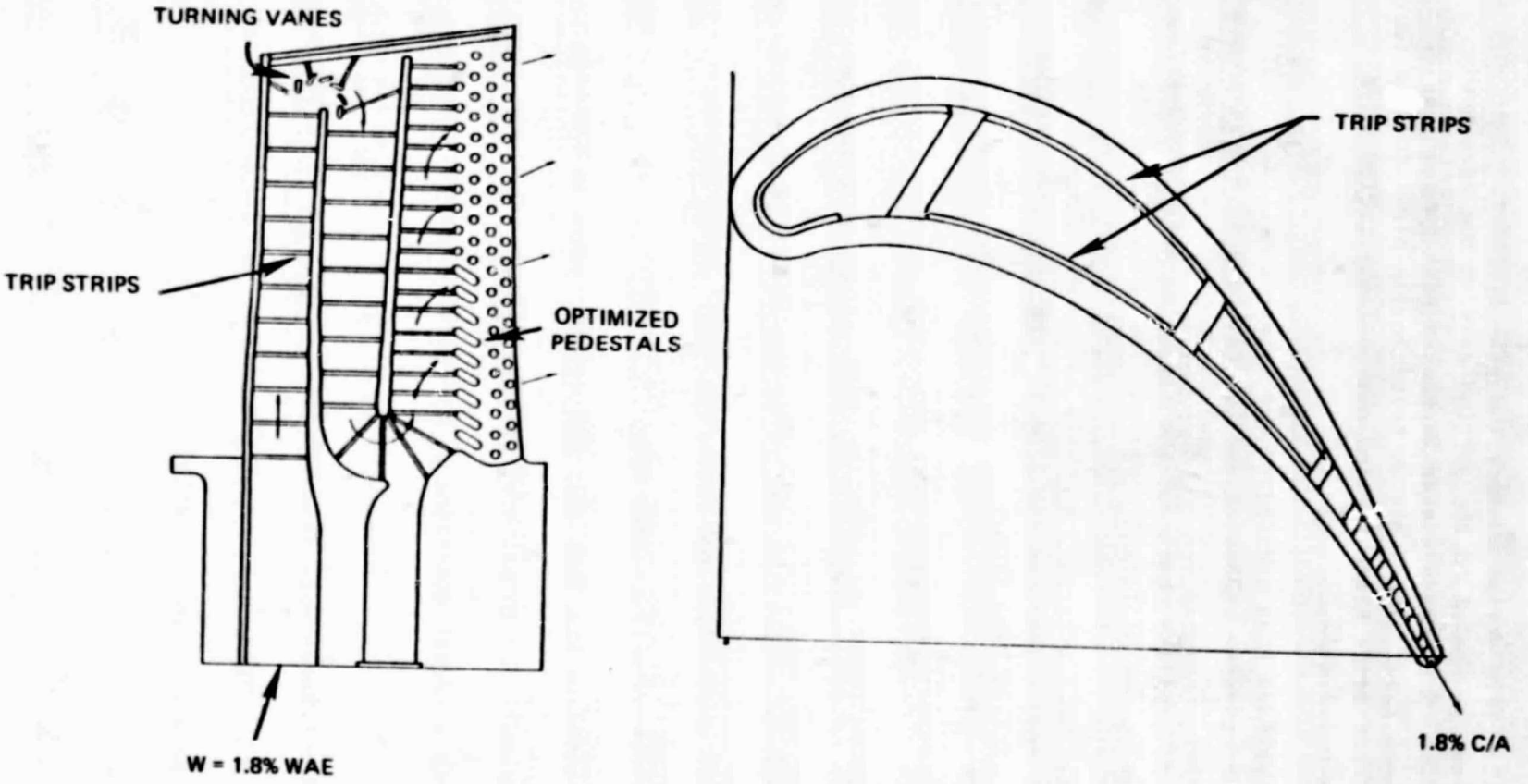

V84.3 FIRST STAGE BLADE COOLING SCHEME

FIG. 1.2.3.2-3

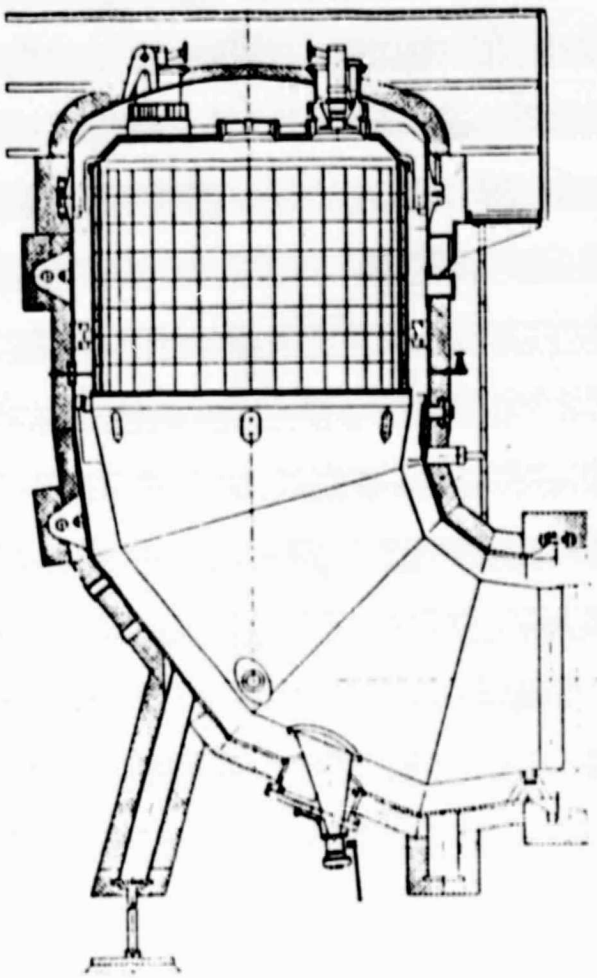

COMBUSTION CHAMBER CROSS SECTION

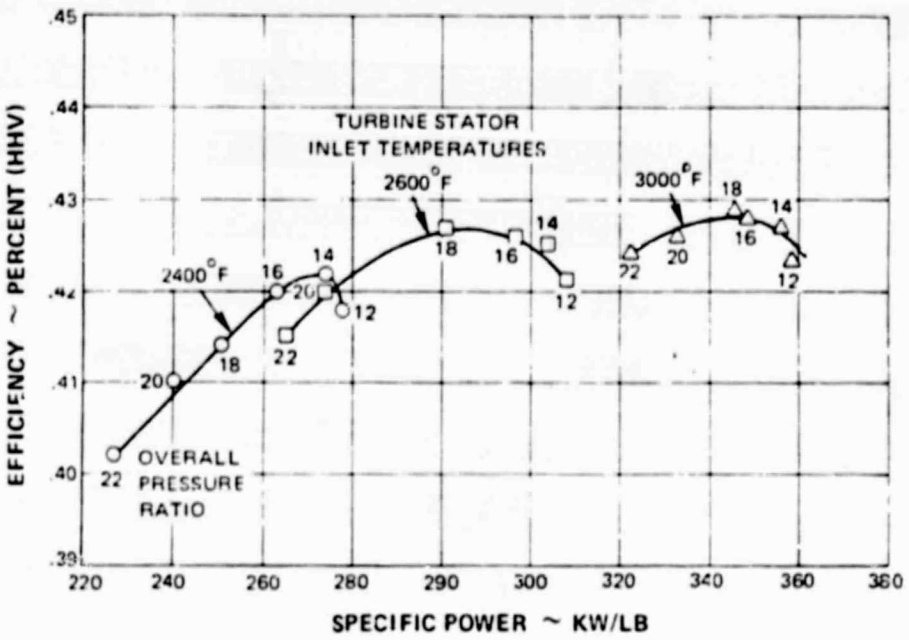

TURBINE INLET TEMPERATURE EFFECT ON PERFORMANCE

The path appearing most attractive would increase turbine temperatures through modest extensions of state-of-the-art techniques. Thus, one could envision air-cooled 2200 F turbines in the 1984-85 time frame followed by air-cooled 2400 F turbines in the 1988 time frame and, ultimately, air-cooled 2600 F turbines in the 1995 time frame. The use of air cooling throughout would allow updating of already installed machines at relatively low cost. The substitution of a different cooling medium would increase any retrofit costs substantially.

1.2.4 Bibliography

1.2-1 Blecher, W. A. and F. L. Robson: Assessment of Fuel Gas Cleanup Systems. Final Report to Morgantown Energy Technology Center. (To be published)

1.2-2 Curtis Wright Corp.: High Temperature Turbine Technology Program, Phase II, Technology Test and Support Studies. Technical Program Reports (Quarterly), January 1978 through March 1980. Department of Energy.

1.2-3 Day, W. H. and H. Maghon: Combustion Turbines with High Durability for Baseload Power Generation. Presented to Association of Edison Illuminating Companies, February 13, 1980.

1.2-4 Electrical Week: Utility Fuel Costs, McGraw Hill, November 24, 1980.

1.2-5 EPRI: Technical Assessment Guide. EPRI PS-1201-SR, July 1979.

1.2-6 Gas Turbine World 1980-1981 Handbook. Pequot Publishing, Inc., September 1980.

1.2-7 General Electric Co.: Development of High Temperature Turbine Subsystem Technology to a Technology Readiness Status, Phase II. Quarterly Reports, January 1978 through March 1980. Department of Energy.

1.2-8 MITRE Corp.: Coal Combined Cycle System Study. Report on DOE Contract ET-78-C-01-3189, April 1980.

1.2-9 National Research Council: Assessment of Technology for Advanced Power Systems, Ad-Hoc Committee on Advanced Power Systems. National Academy of Sciences, 1978.

1.2-10 Robson, F. L. and W. A Blecher: Gasification/Combined-Cycle Power Generation: Environmental Assessment of Alternative Systems. ANL/ECT-7, November 1978.

1.2-11 Schweitzer, J. K. and B. T. Brown: ERDA/P&WA Program for Demonstration of Advanced Industrial Gas Turbine Cooling and High Pressure Compressor Technology. Proceedings of 12th Annual IECEC, August 1977.

1.2-12 United Technology Corporation: High Temperature Turbine Technology Program, Phase I Final Report. Department of Energy, April 1977.

1.2-13 United Technologies Corporation: 300 Btu Gas Combustor Development Program - Phase 1. EPRI AF-1144, August 1979.

1.2-14 Westinghouse Electric Corporation: Gasification Combined-Cycle Plant Configuration Studies. EPRI AP-1393, June 1980.

2.2 Description of Advanced Combined-Cycle Systems

The operating characteristics of advanced gas turbine systems and combined-cycle systems are described and, where pertinent, system design schemes presented. The baseline technology to be used in subsequent tasks is described.

2.2.1 Establish Operational Characteristics

The operational characteristics of commercially available and projected engines have been tabulated in Section 1.2. In addition to these characteristics, the requirements for fuel in terms of cleanliness will be presented and the environmental standards which currently have to be met by gas turbines will be discussed.

2.2.1.1 Gas Turbine/Combined Cycle Operational Characteristics

Based upon the results of Task 1.2, the ranges of probable operating characteristics for advanced gas turbine and combined cycle power plants are given in Table 2.2.1.1-1.

The operation of combined-cycle systems is routinely accomplished with no hazards beyond those associated with rotating machinery and high-temperature steam. Potential air pollution problems can be avoided by meeting the EPA standards for gas turbine operation described in Section 2.2.1.3.

2.2.1.2 Fuel Requirements

The gas turbine has often been touted as being able to run on nearly any fuel from peanut oil to blast furnace gas. While it is true that these fuels may be burned, the reliability and lifetime of the turbine are direct consequences of fuel characteristics.

Because of severe corrosion problems encountered when alkali metals, vanadium, sulfure, etc., are present in the fuel, there are strict requirements for fuel cleanliness. Erosion due to ash or other particulate carryover can also be a problem and thus, there is a limit on particulates.

Specifications for liquid and gaseous fuels are given in Tables 2.2.1.2-1 and -2, respectively. It must be noted that there are no actual specifications for coal-derived gaseous fuels. The values in Table 2.2.1.2-2 are based upon extrapolation of high Btu requirements or maximum allowable concentrations to meet pollution regulations.

2.2.1.3 Emission Standards for Gas Turbines

The emission standards for gas turbines are given in Table 2.2.1.3-1. Included for comparison are the steam station regulations. Combined-cycle plants must meet

TABLE 2.2.1.1-1

RANGE OF OPERATING CHARACTERISTICS OF ADVANCED
GAS TURBINE AND COMBINED CYCLE SYSTEMS

Gas Turbine	
Output, MW	75 - 140
Flow rate, lb/sec	300 - 900
Pressure ratio	12 - 17
Turbine Inlet Temp, F	2200-3000
Metal Temp., F	1100 - 1600
Exhaust Temp., F	1000 - 1150
Heat Rate, Btu/kWh	9500-10500
Steam Turbine	
Output, MW	100 - 400(1)
Pressure, psi	1000 - 2400(2)
Temp., F	850 - 1000
Type	Reheat, multi-pressure
Combined Cycle	
Output, MW	300 - 1000(3)
Heat Rate, Btu/kWh	6200 - 7500(4)

(1) Not limited by technology. One to four gas turbines will provide waste heat to generate steam for one steam turbine.

(2) Pressure level fixed by optimizing overall system.

(3) Multiple engines and one steam turbine.

(4) Based on clean fuel delivery to gas turbine.

TABLE 2.2.1.2-1

LIQUID FUEL SPECIFICATIONS

Property	Distillate[1]	Heavy Oil[2]
Net Heating Value, Btu/lb	18400	18400
Sulfur, wt %	1[3]	1[3]
Metal Contaminants, ppm		
Vanadium	0.5	0.5
Sodium plus Potassium	1.0	1.0
Calcium	2.0	2.0
Lead	1.0	1.0
Initial Ash Sticking Pt., F	1652	1652
Ash, ppm	50	50
Carbon-Hydrogen Ratio	No Limit[4]	No Limit[4]

(1) All JP-type fuels, diesel 1 and GT-1, diesel 2 and GT-2, GT-3 and distillate-type cuts of coal derived liquid fuels.

(2) GT-3, residual No. 5 and 6, Bunker C and heavy cracks or heavy oil-type cuts of coal derived liquid fuels.

(3) Air pollution requirements reduce this to a maximum of 0.8% S content.

(4) The lowest C/H ratio is recommended.

TABLE 2.2.1.2-2

GASEOUS FUEL SPECIFICATIONS

Property	High Btu[1]	Low Btu[2]
Heating Value, Btu/ft^3	950 - 1200	100-350[3]
Sulfur	1.8 mol. %[4]	< 0.075 mol % or less than amount required to form 0.6 ppm alkali metal sulfates[5]
Metals		
Vanadium	< 0.2 ppm (wt)	< 0.03 ppm
Sodium plus	< 0.6 ppm (wt)	See sulfur spec.
Calcium	< 0.1 ppm (wt)	< 0.012 (wt)
Lead	< 0.1 ppm (wt)	< 0.012 (wt)
Copper	< 0.2 ppm (wt)	< 0.025 (wt)
Particulates	< 0.08 lb/10^6 ft^3	0-3μ <0.025 gr/ft^3
		4-5μ <0.03 gr/ft^3
		>5μ <0.0036 gr/ft^3

(1) P&WA Specification 527

(2) There are no definitive specifications for low-Btu fuel gas. The values listed are suggested values based upon extrapolation from natural gas or other considerations.

(3) Fuel gas with heating values less than 100 Btu/ft^3 and greater than 350 Btu/ft^3 have been successfully combusted. The range listed encompasses the majority of coal-delivered fuels.

(4) Does not meet pollution requirement of 0.45 mol %.

(5) Based on typical 150 Btu/ft^3 fuel.

TABLE 2.2.1.3-1

EMISSIONS REGULATIONS

Pollutant	Gas Turbine	Coal-Fired Steam
Sulfur	0.015 mol % SO_2 (0.9 lb $SO_2/10^6$ Btu) or 0.8% (wt) S in fuel	1.2 lb $SO_2/10^6$ Btu max with 90% reduction over uncontrolled level
Nitrogen Oxides	0.0075 to 0.0125 mol % 0.31 to 0.52 $lb/10^6$	0.5 $lb/10^6$ Btu for sub-bituminous or coal-derived fuels; 0.6 $lb/10^6$ Btu for other coals
Particulates	No standard	0.03 $lb/10^6$ Btu

the gas turbine regulations unless the steam portion is supplementally fired. Then the gas turbine must meet the turbine specifications while the steam portion must be treated as a fired system and meet the required regulations for oil- or gas-fired steam stations.

2.2.2 Summarize System/Subsystem Design

The gas turbine-based combined-cycle power system is shown in schematic form in Fig. 2.2.2-1. A range of operating parameters is included in Fig. 2.2.2-1 corresponding to the values given in Table 2.2.1.1-1.

Subsystem drawings for the gas turbines have been shown in Section 1.2.3, while a front view giving combustor details is shown in Fig. 2.2.2-2. A subsystem drawing of the steam bottoming cycle is shown in Fig. 2.2.2-3 while details of the steam turbine are shown in Fig. 2.2.2-4.

2.2.3 Describe System Baseline Technology

The data presented in Tasks 1 and 2 on gas turbines and combined-cycle systems have a wide range from which to select a baseline technology. There are, however, guide lines for selection which can be used. These are:

- date of appearance
- likelihood of technology attainment
- acceptance by utility market place

All of these are interrelated and are, unfortunately, subjective in nature.

The advanced gas turbines are being developed, for the most part, as power systems for use with coal-derived fuels. While there will continue to be a market for petroleum-fired systems in several parts of the world, the major manufacturing nations are anticipating the need for synthetic fuels. At this time, only one demonstration combined-cycle plant using coal-derived fuels is in operation although several more are planned. Thus, it appears that it will be the end of the 1980 decade before there will be a market for these engines.

With a target date of 1988, it is possible that the goals of the HTTTP will be met, i.e., turbine inlet temperatures of 2600 F or higher will have been demonstrated. Given, however, the state of the present government and industry R&D funding and the state of the marketplace, it is improbable that such technologies will be deemed commercial. This means that there could be demonstration plants (or units) operating at these advanced levels but no deliveries of equipment with warranted performance.

According to the R&D path being followed by EPRI, the most important requirement for utility acceptance of gas turbine is reliability. The utility industry

FIG. 2.2.2-1

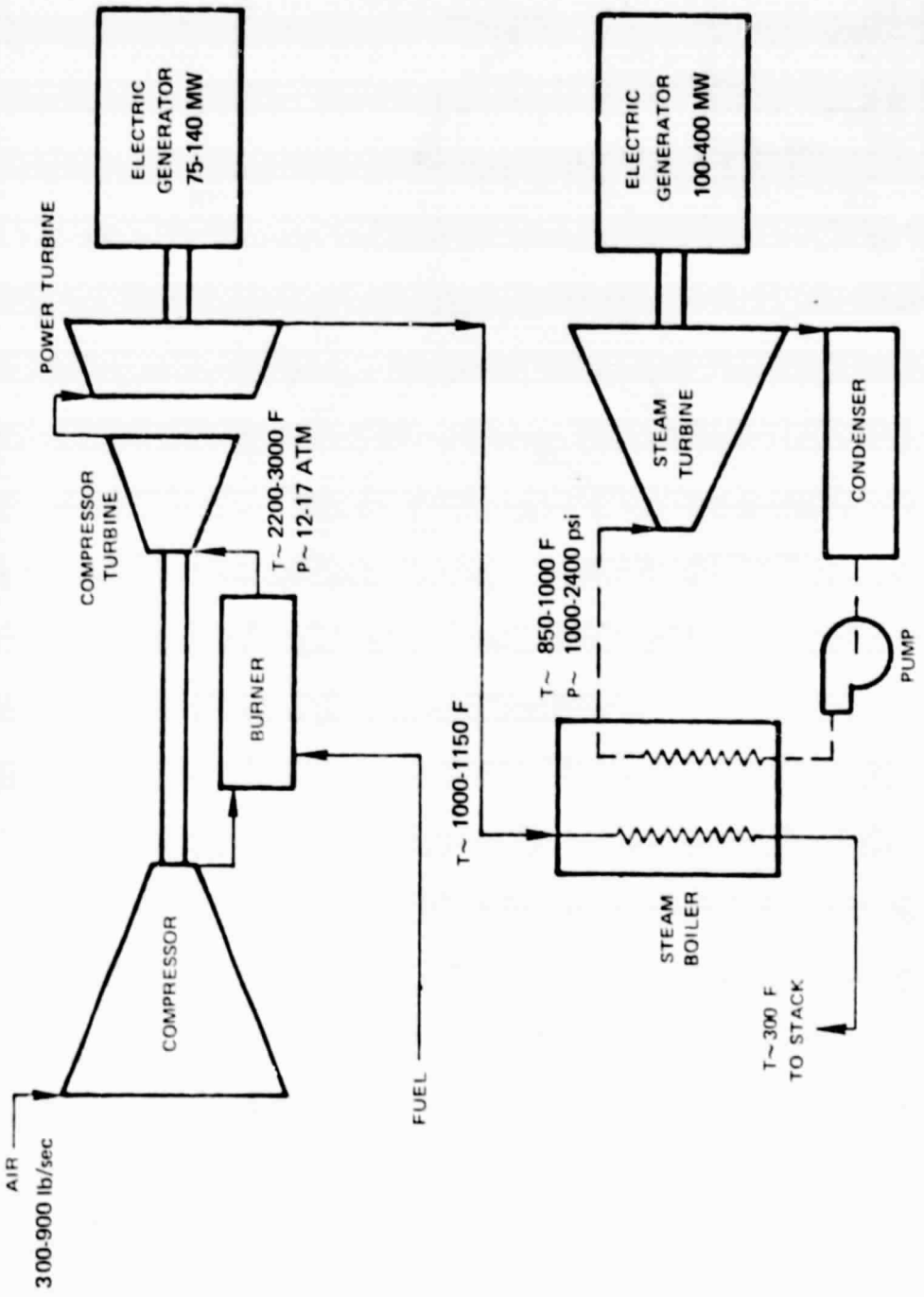

TYPICAL WASTE-HEAT COMBINED GAS AND STEAM TURBINE SYSTEM

FIG. 2.2.2-2

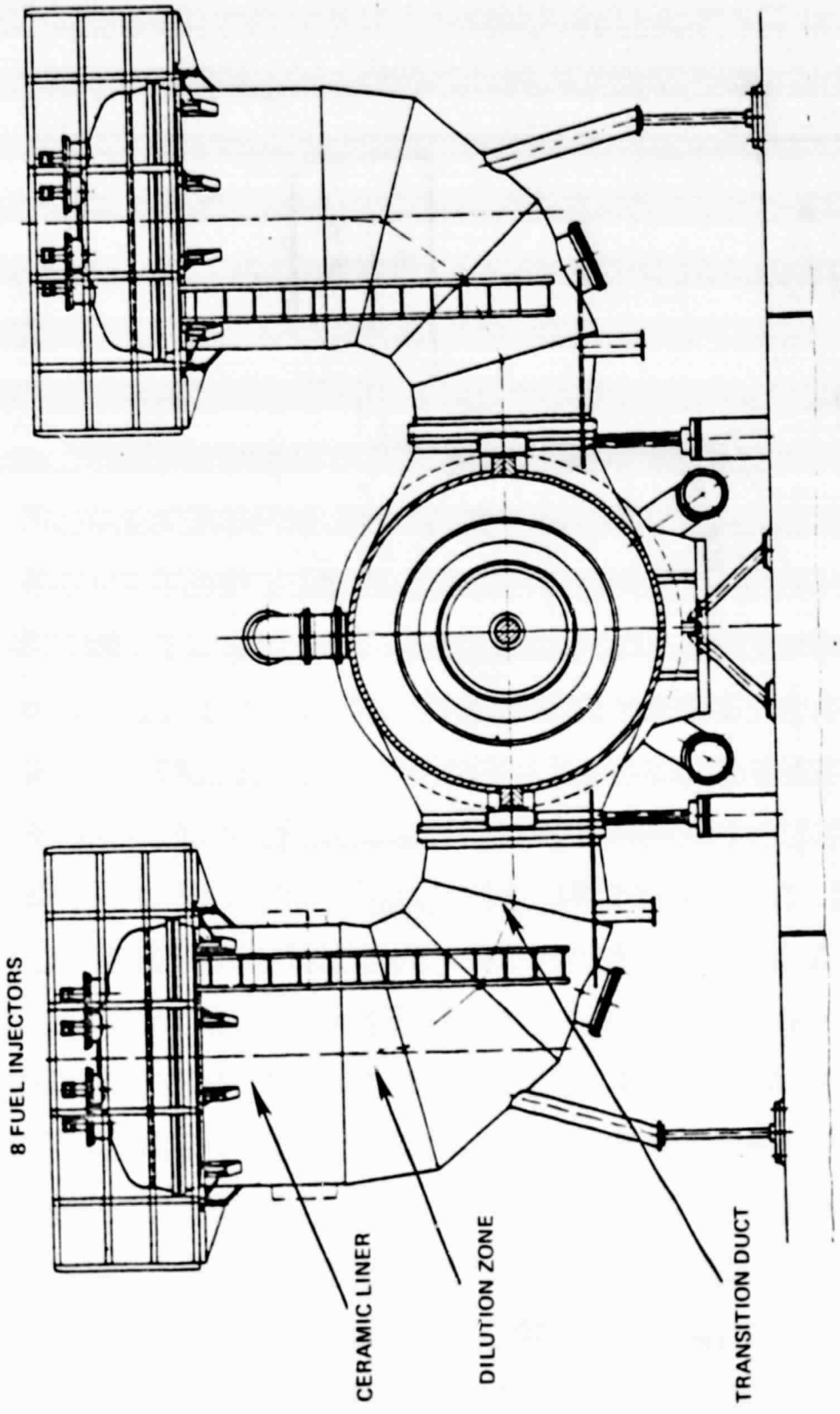

FRONT ELEVATION OF V 84.3

FIG. 2.2.2-3

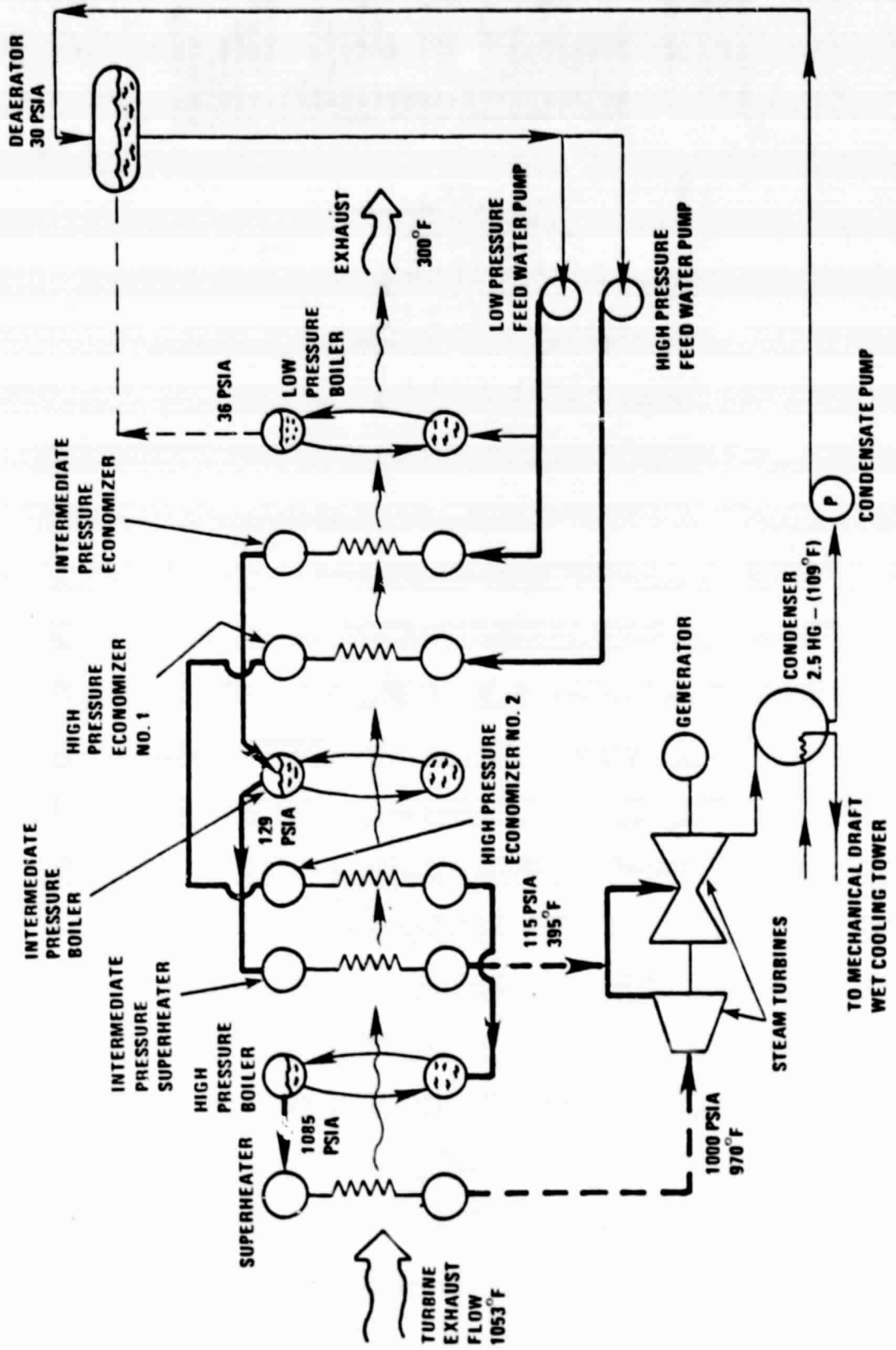

SCHEMATIC OF STEAM BOTTOMING CYCLE

FIG. 2.2.2-4

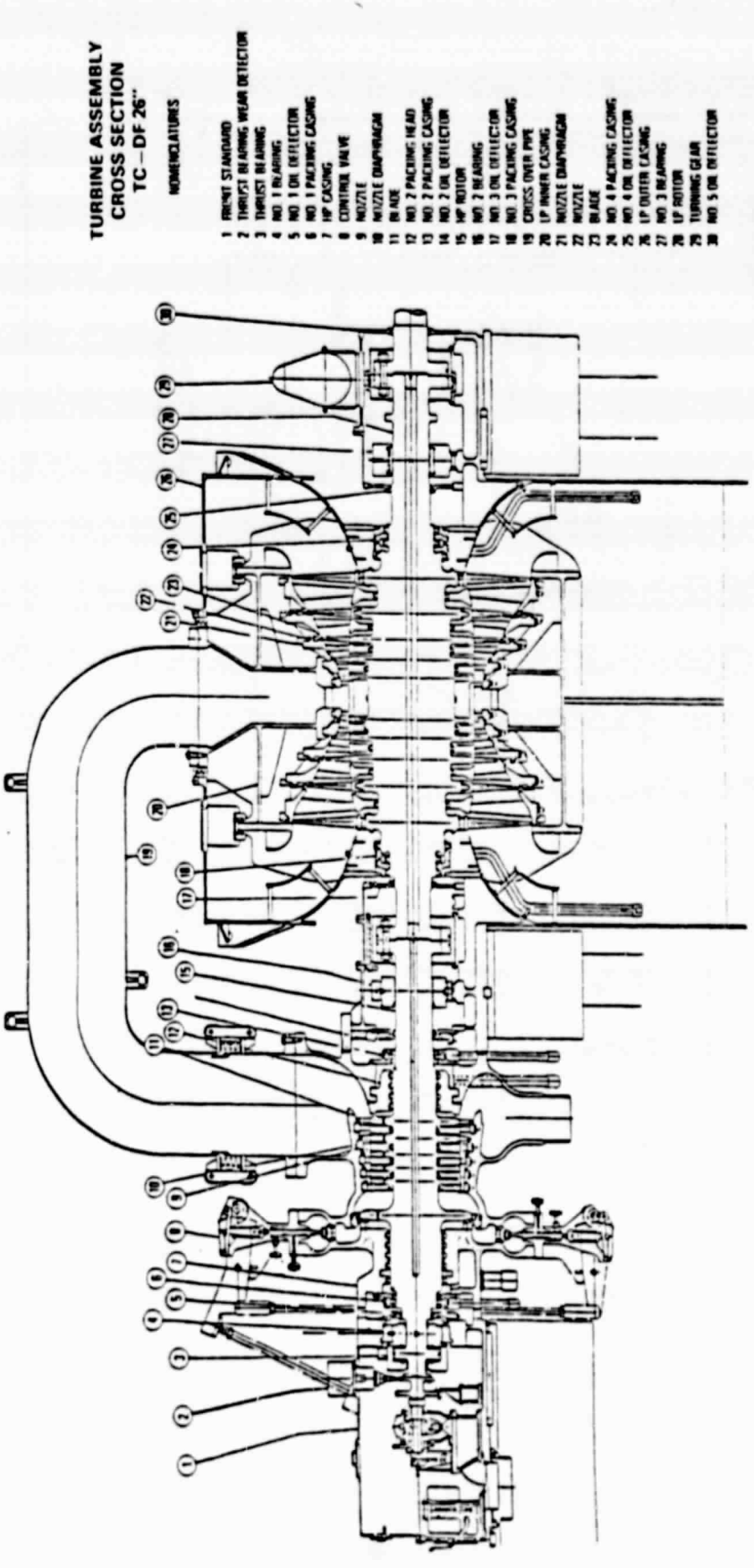

TYPICAL STEAM TURBINE GENERATOR

appears convinced that combined-cycle power plants could offer superior performance compared to conventional alternatives. Their widespread acceptance, however, even at modest technology levels is predicated on the demonstration of reliability similar to that of alternative plants.

With the foregoing discussions in mind, it would appear that the selection of technology for the gas turbine should be a compromise between the HTTTP levels and the EPRI HRGT levels. This would be an engine using technology which is a logical progression from that in the HRGT towards that possible in the HTTTP. Based on this, an uprated version of the UTC engine proposed for the EPRI HRGT program has been projected. The operating characteristics of this engine are:

Flow rate - 860 lb/sec
Pressure ratio - 12
Turbine inlet - 2400 F
Power output - 140 MW (nominal)

To achieve these operating characteristics will require an increase in the turbine cooling effectiveness previously discussed in Section 1.2.3.2. It will also require a low-emission combustor to meet stringent NO_x emission levels.

2.2.3.1 Compressor

The compressor will consist of 16 stages giving an overall pressure ratio of 12:1. Variable inlet guide vanes will be used to allow good start up and part-load operation.

2.2.3.2 Combustor

The silo-type combustor will be utilized. In order to meet the requirements for low-NO_x emissions, the combustor head will be redesigned to use the rich-lean burn concept. This concept meets NO_x regulation without the use of water injection. As applied to gaseous fuels, the concept is shown in Fig. 2.2.3-1. Because of the large size of the silo-burner, it is relatively easy to achieve a tailored combustion pattern.

2.2.3.3 Turbine

A four-stage turbine would be used. The major change required is in the type of blade/vane cooling. Rather than the monolithic blade with internal cooling passages, a bonded blade would be used (Fig. 2.2.3-2). The use of the multi-piece blade will allow much closer control over coolant channel dimensions and locations, thus allowing metal temperatures to remain at the desired level at higher firing temperatures but with no appreciable increase in cooling flow.

FIG. 2.2.3-1

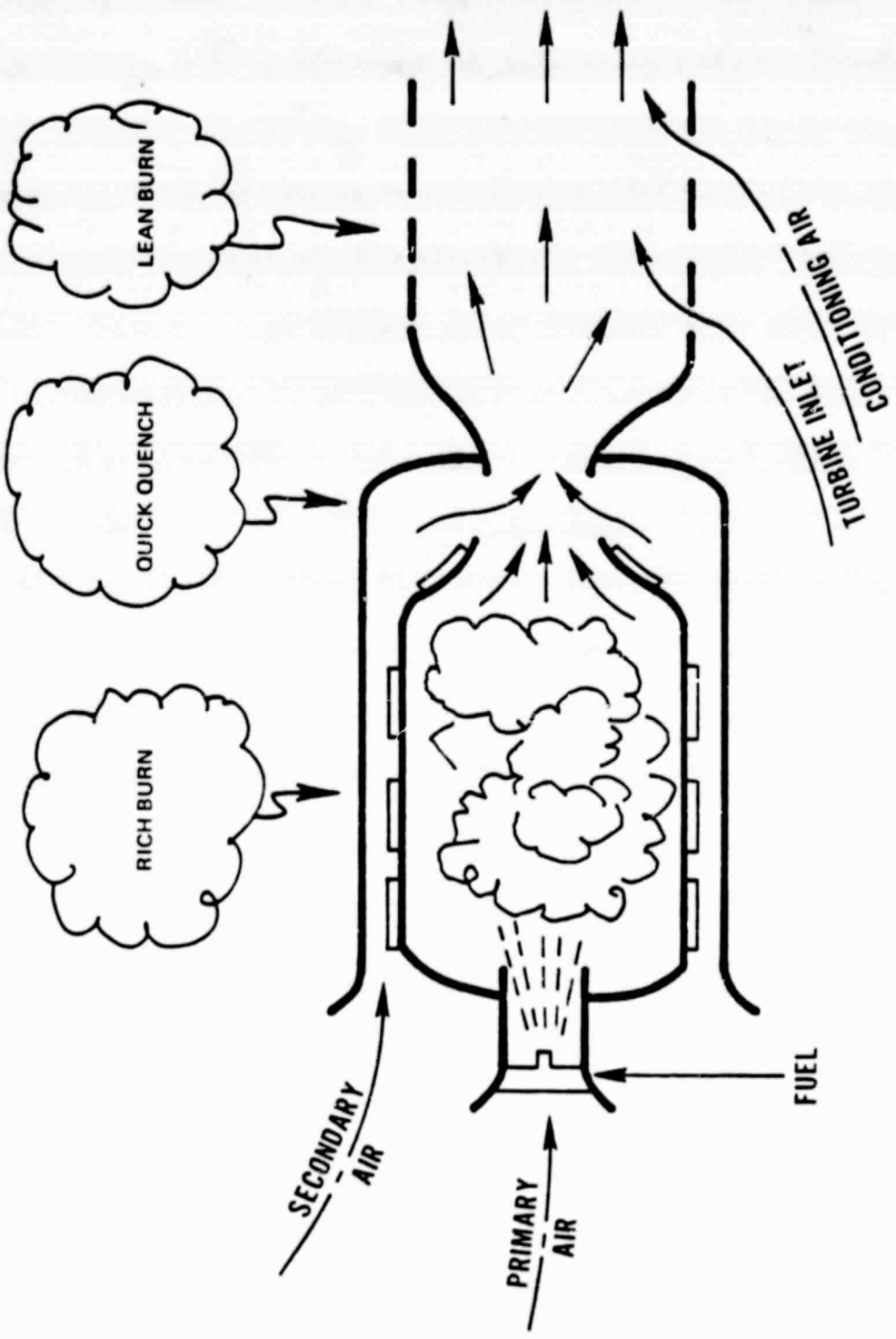

RICH/LEAN COMBUSTOR CONCEPT

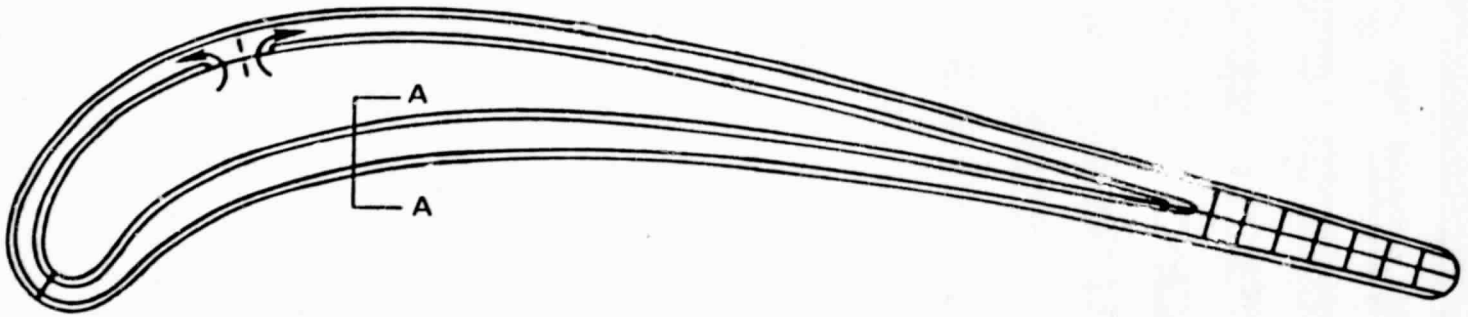

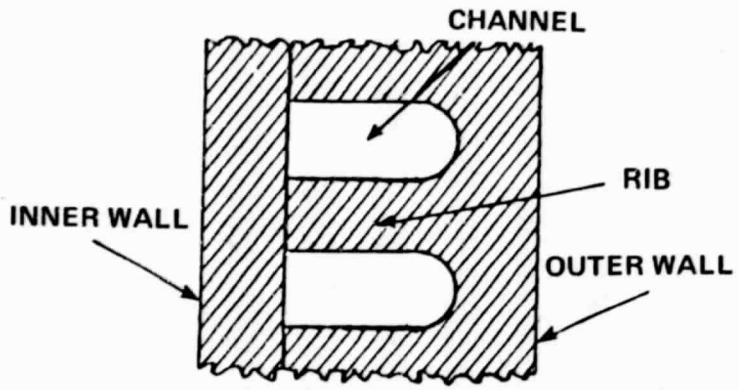

SECTION A–A

- ALL CONVECTIVE COOLING
- INTERNAL AREA AUGMENTATION
- THIN WALL
- INTERNAL HEAT TRANSFER MATCHED TO EXTERNAL HEAT LOAD

BONDED AIRFOIL FIRST VANE FOR V84.3 GROWTH MODEL

2.2.3.4 Combined Cycle System

A schematic of the baseline combined-cycle system is shown in Fig. 2.2.3-3. The operating characteristics and estimated performance are given in this figure. A two engine module has been selected for presentation. Any multiple of engines may be used. Each would have its own heat recovery steam generator feeding into a central steam turbine.

FIG. 2.2.3-3

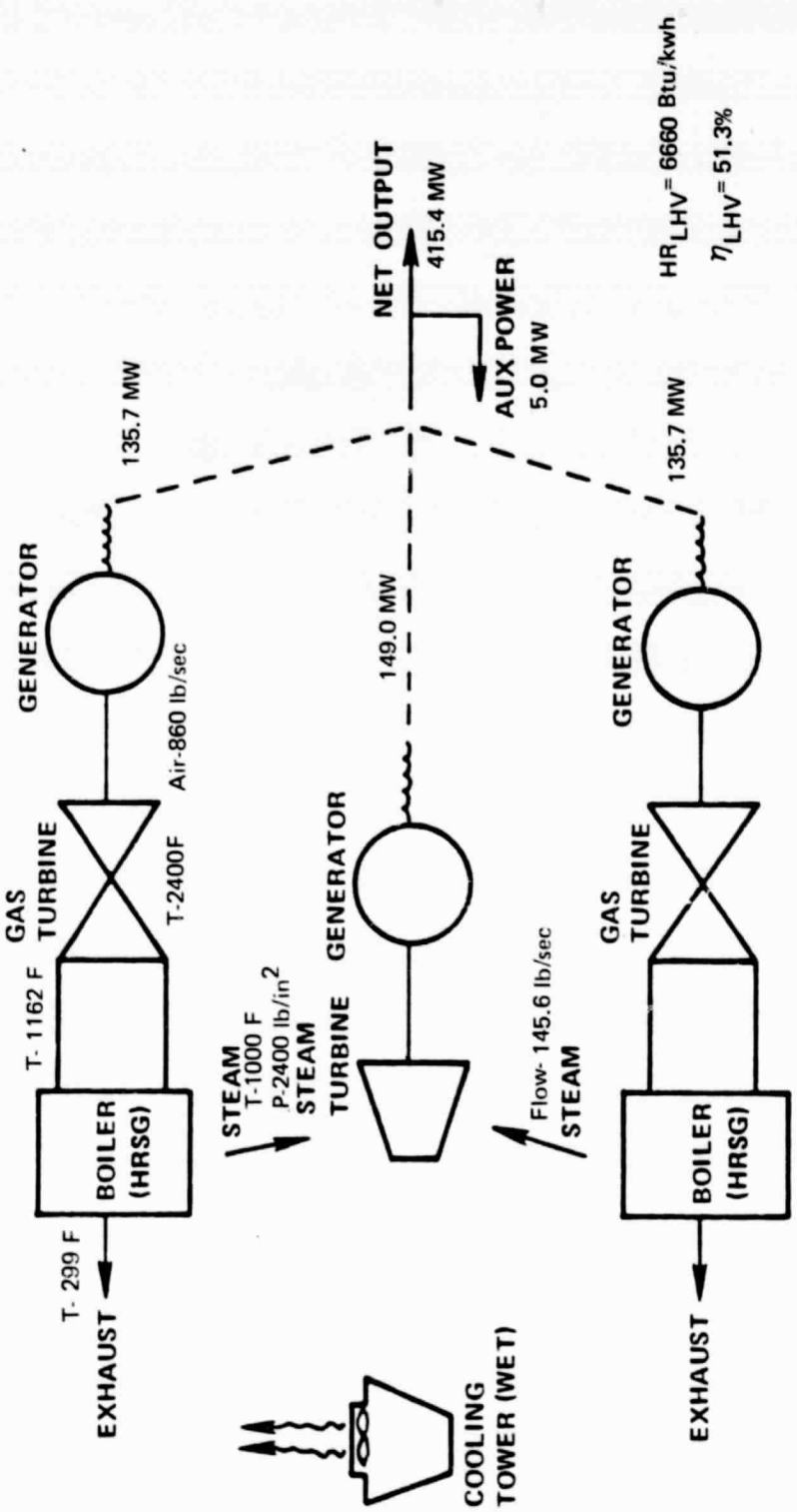

OVERALL PLANT SYSTEM CONCEPT

3.2 Evaluation of Coal-Derived Fuels for Advanced Combined-Cyle Power Systems

The objective of this task is to determine the overall power plant efficiency of a combined gas turbine and steam turbine (combined-cycle) system using medium-Btu gas delivered to the power plant via pipeline. The properties of the gas delivered to the power plant will be obtained and any further processing, if necessary, will be identified. Based upon the fuel gas characteristics, the performance of the combined cycle power plant will be described.

3.2.1 Definition of Fuel Gas Requirements

A description of the suggested fuel gas properties for coal-derived gases was prepared as part of Task 2.2.1 and presented in Table 2.2.1.2-2. As mentioned in the description, the allowable quantities of alkali metals and other heavy metals must be quite low. This should not pose a problem, because these low levels are attained during the low-temperature cleanup associated with sulfur removal (Refs. 3.2.-1 and -2.).

The oxygen-blown Texaco and British Gas Corp. (BGC) slagging gasifiers were selected as the gasifiers to provide medium-Btu fuel gas for transport in pipelines to the power generation site. Properties of the fuel gas from each of these gasifiers, based upon Ref. 3.2.-3, are given in Table 3.2.1-1. The total sulfur content of 100 ppm (H_2S + COS) is that agreed upon by NASA and the Contractor (Ref. 3.2-4) as being typical of pipeline quality fuel gas.

The combustor pressure is 175 psia so that the fuel delivery pressure at the power plant boundary must be 175 psia plus that required for the fuel control system. For medium-Btu fuel gases, an overall pressure drop of 75 psi between the power plant boundary and the combustor is adequate. Thus, a pressure of at least 250 psia would be required at delivery. It is anticipated that the Texaco and BGC gasifiers would be operated at pressures well beyond this value.

Fuel delivery temperature is not critical unless it is low enough to allow condensation. For the moisture content given in Table 3.2.1-1, temperatures should be above 75 F. An average temperature of 86 F has been assumed. An upper limit on temperature is set by the valves and seals in the fuel controls and is well beyond any value typically associated with pipeline delivery of gas.

The required flow rate of fuel gas is a function of heating value and engine power levels. For a single engine at design point operations (nominally 150 MW), the flow rate for gas from the Texaco gasifier would be 309,850 lb/hr while that from the BGC would be 215,550 lb/hr.

3.2.2 Identification of Power Generation Facility

The combined-cycle power system has been described in Section 2.2.3. The use of medium-Btu fuel gas does not require any additional equipment although individual equipment will vary in size and output depending on the fuel. A general schematic for the combined cycle power plant is given in Fig. 3.2.2-1. In brief, the operation is as follows:

Air (Steam 1 in Fig. 3.2.2-1) is compressed to approximately 175 psia in the gas turbine compressor. Upon exiting the compressor, a small fraction of the air is sent to the turbine for turbine vane/blade cooling while the remainder is used for combustion. The combustion products are expanded and the exhaust steam (3) is split into two streams and used to superheat steam (4) and to reheat steam (5). The exhaust streams are rejoined (6) in the boiler, pass through an economizer, the boiler for deaeration steam, and finally exit through the stack (9).

Condensate (10) is pumped to a low-pressure deaerator, and then pumped to boiler pressure before entering the economizer (16). From the economizer, the high-pressure water enters the boiler where it is changed to saturated steam (18). The steam is superheated, expanded to an intermediate pressure (20) and then reheated (21) prior to complete expansion in the intermediate- and low-pressure turbines (22).

The flow conditions (heat and mass) vary for each type of fuel gas. A heat and mass balance for the Texaco fuel gas system, based on one engine, is given in Table 3.2.2-1 while that for the BGC system is given in Table 3.2.2.-2. Material balances corresponding to these are given in Table 3.2.2-3 and 3.6.2-4 for the Texaco and BGC systems, respectively.

Because of the modularity of the combined-cycle system, an actual power plant could consist of a number of gas and steam turbines. However, the basic building block would be two gas turbines with two waste heat boilers generating steam for one steam turbine. The nominal output of the module would be 450 MW.

The estimated performance for this basic module for both fuel gas types is given in Table 3.2.2-5. The estimated performance of a distillate-fueled system is given for comparisons. The performance levels for all three fuels are comparable at approximately 50 percent. The differences are mainly due to the differences in mass flow rate through the engines. The fuel flow for the distillate fuel represents approximately 2.5 percent of inlet flow; for the Texaco, 10 percent; and for the BGC, 7 percent.

TABLE 3.2.1-1

GAS COMPOSITIONS

	Texaco Gas		BGC Gas	
Element	Moles/hr	Vol. %	Moles/hr	Vol. %
CH_4	15.0	0.1	935	8.4
H_2	5394	35.6	3414	30.6
CO	7940	52.4	6515	58.5
CO_2	1629	10.8	217	1.9
H_2S + COS	--	100 ppm	--	100 ppm
N_2	124	0.8	50	0.5
Ar	22	0.2	<1	0
H_2O	15	0.1	11	0.1
	15139	100.0	11142	100.0

Heating Values, LHV

LHV, Btu/scf	267.5	349.1
LHV, Btu/lb	4949	6825

FIG. 3.2.2-1

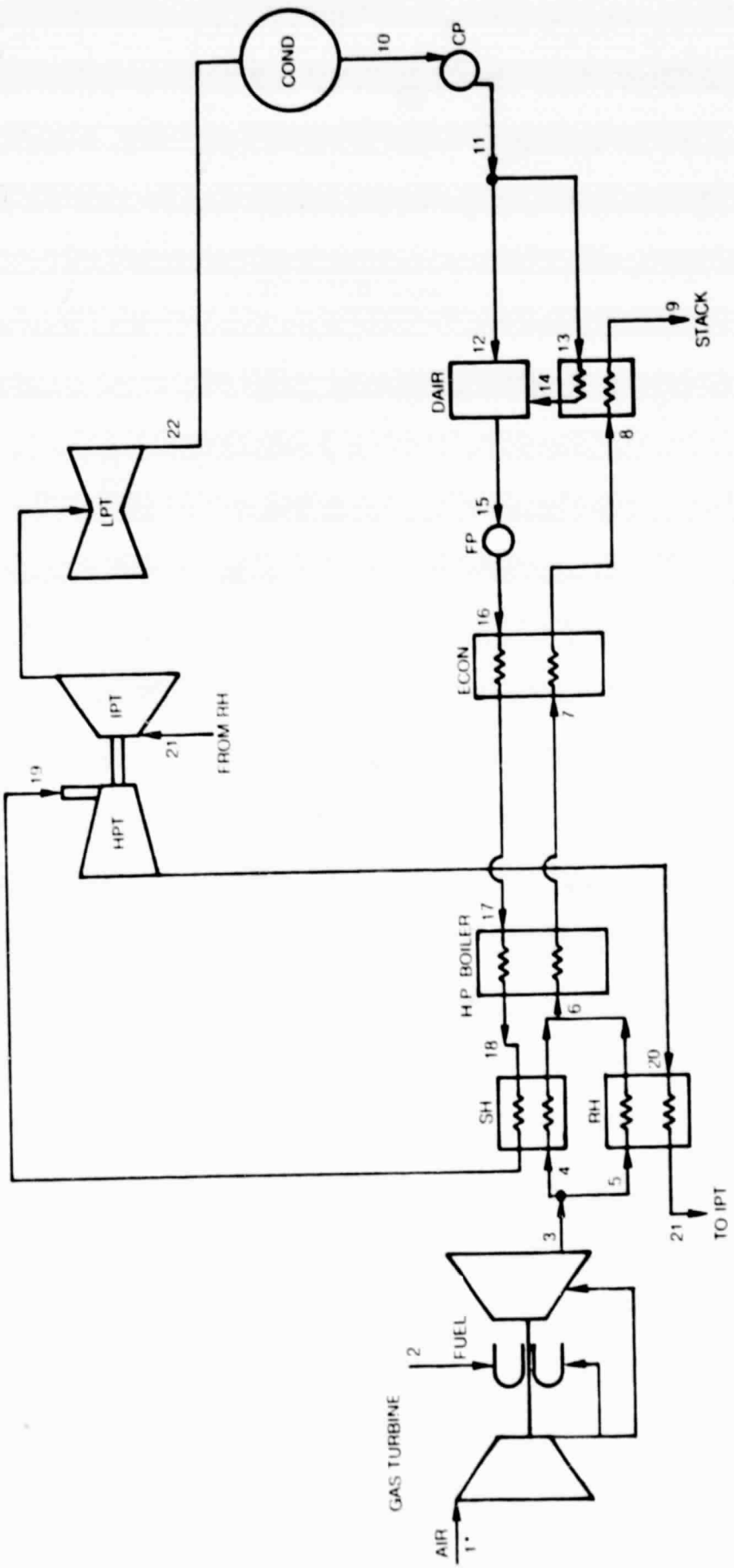

COMBINED CYCLE POWER SYSTEM

(BASED ON V84.3 GAS TURBINE)

*REFERS TO STATION NUMBERS

81-1-46-1

TABLE 3.2.2-1

HEAT AND MASS BALANCE FOR COMBINED CYCLE
POWER SYSTEM USING TEXACO COAL-DERIVED FUEL

Station Number	Temperature (°F)	Pressure (Psia)	Flow (lb/sec)(1)
1	59	14.7	860.0
2	100	175.0	86.1
3	1191	14.8	946.1
4	1191	14.8	620.0
5	1191	14.8	326.1
6	907	14.8	946.1
7	716	14.8	946.1
8	447	14.8	946.1
9	364	14.8	946.1
10	101	1.2	132.4
11	101	30.0	132.4
12	101	30.0	114.3
13	101	30.0	18.1
14	101	30.0	18.1
15	250	30.0	132.4
16	255	2844.0	132.4
17	666	2474.0	132.4
18	666	2474.0	132.4
19	1000	2400.0	132.4
20	656	600.0	132.4
21	1000	540.0	132.4
22	106	1.2	132.4

(1) All flow values are for one engine.

TABLE 3.2.2-2

HEAT AND MASS BALANCE FOR COMBINED CYCLE POWER SYSTEM USING BGC COAL-DERIVED FUEL

Station Number	Temperature (°F)	Pressure (Psia)	Flow (lb/sec)(1)
1	59	14.7	860.0
2	100	175.0	59.9
3	1179	14.8	919.9
4	1179	14.8	603.5
5	1179	14.8	316.4
6	902	14.8	919.9
7	716	14.8	919.9
8	454	14.8	919.9
9	373	14.8	919.9
10	101	1.2	125.3
11	101	30.0	125.3
12	101	30.0	108.1
13	101	30.0	17.2
14	101	30.0	17.2
15	250	30.0	125.3
16	255	2644.0	125.3
17	666	2474.0	125.3
18	666	2474.0	125.3
19	1000	2400.0	125.3
20	657	600.0	125.3
21	1000	540.0	125.3
22	106	1.2	132.4

(1) All flow values are for one engine.

TABLE 3.2.2-3

MATERIAL BALANCE FOR COMBINED CYCLE POWER SYSTEM USING TEXACO COAL-DERIVED FUEL

Station Number		1		2		3		4		5		6	
Comp.	M.W.	Lb/Hr[1]	Mols/Hr	Lb/Hr	Mols/Hr	Lb/Hr	Mols/Hr	Lb/Hr	Mols/Hr	Lb/Hr	Mols/Hr	Lb/Hr	Mols/Hr
CH_4	16.04		-	241	15.0		-		-		-		-
H_2	2.016		-	10874	5394		-		-		-		-
CO	28.01		-	222399	7940		-		-		-		-
CO_2	44.01		-	71692	1629	421792	9584	276427	6281	145365	3303	421792	9584
H_2S	34.08		-	-	-		-		-		-		-
COS	60.07		-	-	-		-		-		-		-
O_2	32.00	713312	22291	-	-	499008	15594	327040	10220	171968	5374	499008	15594
N_2	28.02	2321933	82867	3474	124	2325408	82991	1523980	54389	801400	28601	2325380	82990
A	39.94	41578	1041	879	22	42456	1063	27838	697	14618	366	42456	1063
H_2O	18.02	19534	1084	270	15	117544	6523	77017	4274	40509	2248	117526	6522
Total		3096357	107283	309829	15139	3406208	115755	2232302	75861	1173860	39892	3406162	115753

(1) All values based on one engine.

TABLE 3.2.2-3 (Cont'd.)

MATERIAL BALANCE FOR COMBINED CYCLE
POWER SYSTEM USING TEXACO COAL-DERIVED FUEL

Station Number		7		8		9		10		11		12	
Comp.	M.W.	Lb/Hr[1]	Mols/Hr	Lb/Hr	Mols/Hr	Lb/Hr	Mols/Hr	Lb/Hr	Mols/Hr	Lb/Hr	Mols/Hr	Lb/Hr	Mols/Hr
CH_4	16.04												
H_2	2.016												
CO	28.01												
CO_2	44.01												
H_2S	34.08												
COS	60.07												
O_2	32.00												
N_2	28.02												
A	39.94												
H_2O	18.02	------	------	------	------	------	------	476737	26456	476737	26456	411469	22834
Total		3406162	115753	3406162	115753	3406162	115753	476737	26456	476737	26456	411469	22834

TABLE 3.2.2-3 (Cont'd.)

MATERIAL BALANCE FOR COMBINED CYCLE
POWER SYSTEM USING TEXACO COAL-DERIVED FUEL

Station Number		13		14		15		16		17		18	
Comp.	M.W.	Lb/Hr[1]	Mols/Hr	Lb/Hr	Mols/Hr	Lb/Hr	Mols/Hr	Lb/Hr	Mols/Hr	Lb/Hr	Mols/Hr	Lb/Hr	Mols/Hr
CH_4	16.04												
H_2	2.016												
CO	28.01												
CO_2	44.01												
H_2S	34.08												
COS	60.07												
O_2	32.00												
N_2	28.02												
A	39.94												
H_2O	18.02	65268	3622	65268	3622	476737	26456	476737	26456	476737	26456	476737	26456
Total		65268	3622	65268	3622	476737	26456	476737	26456	476737	26456	476737	26456

TABLE 3.2.2-3 (Cont'd.)

MATERIAL BALANCE FOR COMBINED CYCLE
POWER SYSTEM USING TEXACO COAL-DERIVED FUEL

Station Number		19		20		21		22	
Comp.	M.W.	Lb/Hr[1]	Mols/Hr	Lb/Hr	Mols/Hr	Lb/Hr	Mols/Hr	Lb/Hr	Mols/Hr
CH_4	16.04								
H_2	2.016								
CO	28.01								
CO_2	44.01								
H_2S	34.08								
COS	60.07								
O_2	32.00								
N_2	28.02								
A	39 94								
H_2O	18.02	476737	26456	476737	26456	476737	26456	476737	26456
Total		476737	26456	476737	26456	476737	26456	476737	26456

TABLE 3.2.2-4

MATERIAL BALANCE FOR COMBINED CYCLE
POWER SYSTEM USING BGC COAL-DERIVED FUEL

Station Number		1		2		3		4		5		6	
Comp.	M.W.	Lb/Hr(1)	Mols/Hr	Lb/Hr	Mols/Hr	Lb/Hr	Mols/Hr	Lb/Hr	Mols/Hr	Lb/Hr	Mols/Hr	Lb/Hr	Mols/Hr
CH_4	16.04			14997	935								
H_2	2.016			6883	3414								
CO	28.01			182485	6515								
CO_2	44.01			9550	217	337469	7668	221370	5030	116098	2638	337469	7668
H_2S	34.08				-		-						
COS	60.07				-		-						
O_2	32.00	713312	22291		-	494624	15457	324480	10140	170144	[illegible]17	494624	15457
N_2	28.02	2321933	82867	1401	50	2323334	82917	1524148	54395	799186	285[illegible]	2323334	82917
A	39.94	41578	1041		-	41578	1041	27279	683	14299	358	41578	1041
H_2O	18.02	19534	1084	198	11	114932	6378	75396	4184	39536	2194	114932	6378
Total		3096357	107283	215514	11142	3311937	113461	2172673	74432	1139263	39029	3311937	113461

(1) All values based on one engine.

TABLE 3.2.2-4 (Cont'd.)

MATERIAL BALANCE FOR COMBINED CYCLE
POWER SYSTEM USING BGC COAL-DERIVED FUEL

Station Number		7		8		9		10		11		12	
Comp.	M.W.	Lb/Hr[1]	Mols/Hr	Lb/Hr	Mols/Hr	Lb/Hr	Mols/Hr	Lb/Hr	Mols/Hr	Lb/Hr	Mols/Hr	Lb/Hr	Mols/Hr
CH_4	16.04												
H_2	2.016												
CO	28.01												
CO_2	44.01												
H_2S	34.08												
COS	60.07												
O_2	32.00												
N_2	28.02												
A	39.94												
H_2O	18.02							451185	25038	451185	25038	389412	21610
Total		2172673	74432	2172673	74432	2172673	74432	451185	25038	451185	25038	389412	21610

TABLE 3.2.2-4 (Cont'd.)

MATERIAL BALANCE FOR COMBINED CYCLE
POWER SYSTEM USING BGC COAL-DERIVED FUEL

Station Number		13		14		15		16		17		18	
Comp.	M.W.	Lb/Hr[1]	Mols/Hr	Lb/Hr	Mols/Hr	Lb/Hr	Mols/Hr	Lb/Hr	Mols/Hr	Lb/Hr	Mols/Hr	Lb/Hr	Mols/Hr
CH_4	16.04												
H_2	2.016												
CO	28.01												
CO_2	44.01												
H_2S	34.08												
COS	60.07												
O_2	32.00												
N_2	28.02												
A	39.94												
H_2O	18.02	61773	3428	61773	3428	451185	25038	451185	25038	451185	25038	451185	25038
Total		61773	3428	61773	3428	451185	25038	451185	25038	451185	25038	451185	25038

TABLE 3.2.2-4 (Cont'd.)

MATERIAL BALANCE FOR COMBINED CYCLE
POWER SYSTEM USING BGC COAL-DERIVED FUEL

Station Number		19		20		21		22	
Comp.	M.W.	Lb/Hr(1)	Mols/Hr	Lb/Hr	Mols/Hr	Lb/Hr	Mols/Hr	Lb/Hr	Mols/Hr
CH_4	16.04								
H_2	2.016								
CO	28.01								
CO_2	44.01								
H_2S	34.08								
COS	60.07								
O_2	32.00								
N_2	28.02								
A	39.94								
H_2O	18.02	451185	25038	451185	25038	451185	25038	451185	25038
Total		451185	25038	451185	25038	451185	25038	451185	25038

TABLE 3.2.2-5

PERFORMANCE ESTIMATES FOR COMBINED-CYCLE SYSTEMS

Fuel Type:	Distillate	Coal Derived	
	No. 2 Oil	Texaco	BGC
Gas Turbine:			
Flow Rate, lb/sec	860	860	860
Pressure Ratio	12	12	12
Combustor Exit Temp., ^{o}F	2400	2400	2400
Exhaust Temp., ^{o}F	1162	1192	1179
Stack Temp., ^{o}F	387	364	374
Turbine Area, in^2	483	521	506
Fuel System:			
Flow Rate, lb/hr/engine	74758	309850	215550
Heating Value, Btu/lb (LHV)	18476	4948	6826
Combined Cycle Performance*:			
Gas Turbine Output, MW (2 engines)	271.4	306.8	292.8
Steam Turbine Output, MW (1 turbine)	143.6	165.4	156.2
Utility Losses, MW (per engine)	6.2	7.1	6.7
Total Net Power, MW	402.2	458	435.6
Heat Rate, Btu/kWh (LHV)	6865	6696	6755
Efficiency, %	49.7	51.0	50.5

* Steam System: Single pressure, 2400 psia/1000^{o}F/1000^{o}F
Condenser Pressure = 2.5 in.

The additional flow rate due to the large amount of medium-Btu fuel could require modifications to the gas turbine to ensure that no mismatch between the turbine and compressor occurs. Usually, if flow area differences are less than 10 percent of the design basis (the distillate case), the changes can be accommodated by adjustment of turbine components. Larger differences could require redesign of the turbine. The turbine areas listed in Table 3.1.2-5 indicate that no redesign would be necessary.

3.2.3 References

3.2-1 Robson, F. L., W. A. Blecher and V. A. May: Fuel Gas Environmental Impact. EPA 600/7-78-088, June 1978.

3.2-1 Blecher, W. A. and F. L. Robson: Assessment of Fuel Gas Cleanup Systems. Contract DE-AC21-79MC12050 with METC, November 1980.

3.2-3 Fluor Engineers and Constructors: An Economic Comparison of Molten Carbonate Fuel Cells and Gas Turbines in Coal Gasification-Based Power Plants. EPRI AP-1543, Sept. 1980.

3.2-4 Interim Project Briefing, NASA-MSFC, Huntsville, Alabama, December 17/18 1980.

4.2 Evaluation of Integrated Gasification Combined-Cycle Power Systems

The objective of this task is to determine the overall power plant efficiency of an integrated gasification combined-cycle (IGCC) power plant. Two types of gasifiers will be considered and the performance of the two resulting IGCC power plants will be compared. Flow sheets for the gasifiers, the oxygen-blown Texaco and British Gas Corp. slagging types, are those previously developed by the contractor as agreed upon by NASA and the contractor (Ref. 4.2-1).

4.2.1 Identification of IGCC Power Plant with Texaco Gasifier

The combined-cycle power system identified in Section 2.2.3 will be used as the basis of the IGCC power plant. The operating conditions are the same but the equipment output differs because of differing steam loads in the IGCC power plant. A schematic for the Texaco-based IGCC is given in Fig. 4.2.1-1.

In brief, the operation is as follows. Similar to the conventional combined-cycle plant of Section 2.2.3, air (Steam 1 in Fig. 4.2.2-1) is compressed to approximately 175 psia in the gas turbine compressor. Upon exiting the compressor, a small fraction of the air is sent to the turbine for turbine vane/blade cooling while the remainder is used for combustion. The combustion products are expanded and the exhaust stream (30) is split into two streams and used to superheat steam (31) and to reheat steam (32). The exhaust streams are rejoined (33) in the boiler. They then pass through economizers and the deaerator finally exiting through the stack (37).

Both the steam system and the fuel system differ from the conventional plant. Water from the condenser (38) is pumped to a low pressure and split into two streams. Stream 40 is further pumped and heated against the fuel gas stream (Q_1) to furnish process steam for use in the cleanup system. The other condensate stream (43) is heated aainst the fuel gas stream, then used to deareate the remaining flow prior to final pumping to boiler inlet pressure before the fist of two economizers (47). After this economizer, the stream is again split with a small stream being used to raise LP steam for process use while the majority passes through the second economizer (54). This stream is then split, some going to the waste heat boiler behind the gas turbine (55) and some to the heat recovery boiler in the fuel gas stream (56). These streams rejoin, pass through the superheater and are expanded in the high-pressure steam turbine. After reheating the steam is sent to the intermediate pressure turbine (67) with a side stream being separated to drive the air and oxygen compressors in the air separation plant (66). After full expansion in the low-pressure turbine, the steam enters the condenser (70).

FIG. 4.2.1-1

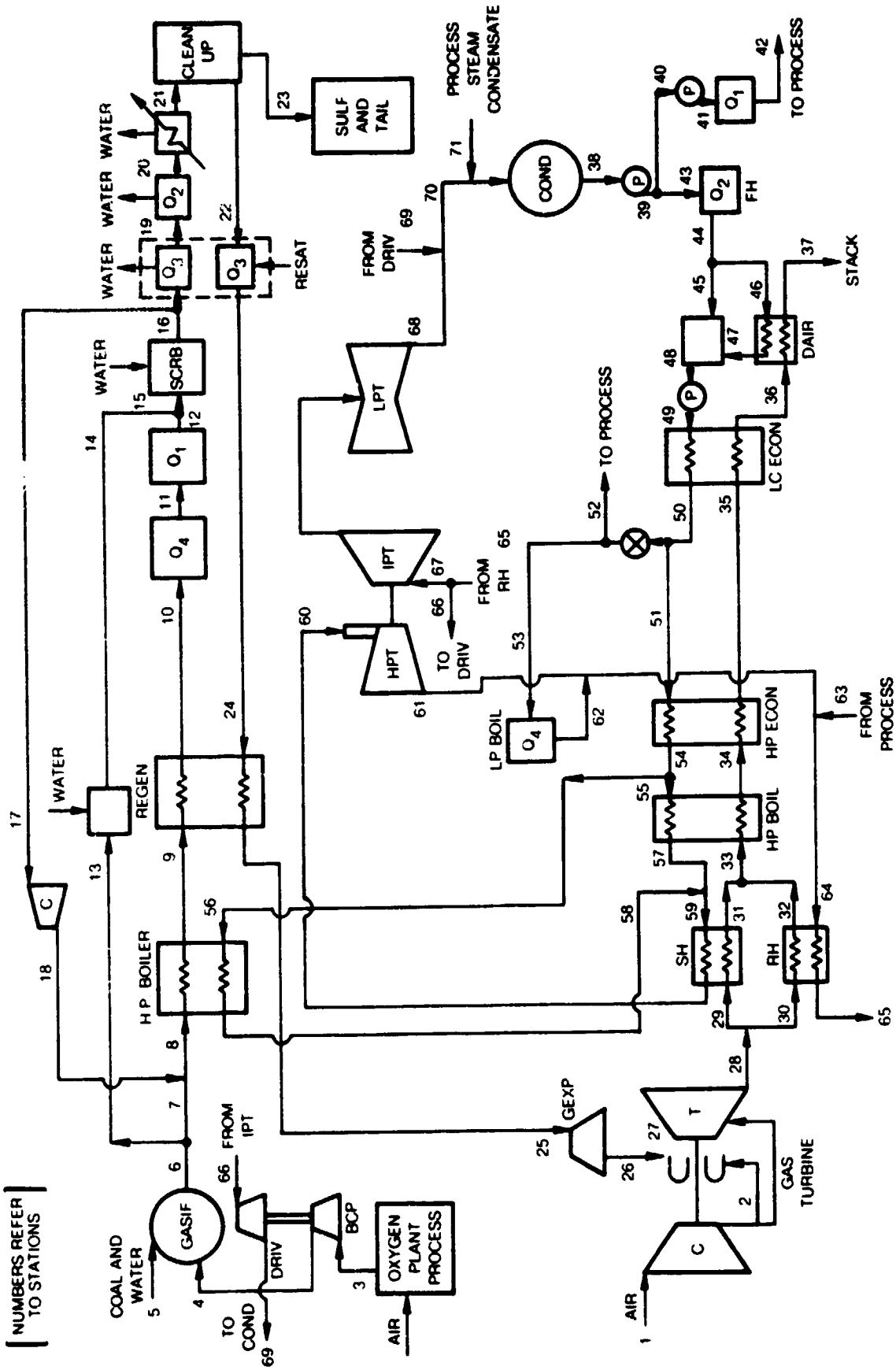

81-2-3-1

The fuel gas starts as a coal-water slurry (5) and oxygen (4) feeds to the gasifier. After gasification, the fuel gas stream is split, one stream being water quenched (13) to remove slag while the other passes through a boiler (8), then a fuel gas regenerator. Prior to going through the boiler, the hot gas temperature is moderated by a recycle stream of cool gas (18). The fuel gas is subsequently cooled, sulfur removed and then resaturated and reheated prior to expansion in a turboexpander (25) down to combustor pressure.

The heat and mass balance for the Texaco-based IGCC is given in Table 4.2.1-1 (flow is for one engine). Material balances are given in Table 4.2.1-2 (again based on one engine)

Because of the modularity of the combined-cycle system, an actual power plant could consist of a number of gas and steam turbines. However, the basic building block would be two gas turbines with two waste heat boilers generating steam for one steam tubine. The nominal output of the module would be 475 MW.

The coal gasification system is costly and benefits from scale and replication, thus, it is probable that the 475-MW module would be the minimum size plant. A more typical plant would probably consist of two such modules, i.e., four gas tubines and waste heat boilers feeding one steam turbine. Such a system would require ten gasifiers (two spares). The estimated performance for such an IGCC plant is given in Table 4.2.1-3.

4.2.2 Identification of IGCC Power Plant with British Gas Corporation Gasifier

The IGCC power plant using the BGC gasifier is similar to that using the Texaco gasifiers (Fig. 4.2.2-1 shows a schematic) except for variations in the steam raising sections.

Because of the lower exit temperature from the gasifier and the need to remove tars and solid carryover, there is no waste heat recovery boiler in the gasifier exit stream (stream 41 - Fig. 4.2.2-1). Rather, the heat removed from this stream prior to desulfurization is used to resaturate the fuel gas after cleanup. All the steam for power generation and process use is raised in the gas turbine exhaust, with the exception of a small amount of process steam raised in the gasifier jacket.

A heat and mass balance for the IGCC powerplant with the BGC gasifier is given in Table 4.2.2-1 and a material balance is given in Table 4.2.2-2. The performance of this system is given in Table 4.2.1-3.

TABLE 4.2.1-1

HEAT AND MASS BALANCE FOR GAS TURBINE COMBINED CYCLE POWER PLANT
USING TEXACO OXYGEN-BLOWN GASIFICATION SYSTEM

Station Number	Temperature (°F)	Pressure (psia)	Flow (lb/sec) (1)
1	59	14.7	860.0
2	655	175	723.5
3	60	17	39.3
4	300	588	39.3
5	140	588	70.2
6	2400	588	102.2
7	2400	588	92.0
8	1850	588	128.7
9	1200	567	128.7
10	729	567	128.7
11	515	567	128.7
12	407	567	128.7
13	2400	588	10.2
14	400	567	14.4
15	406	567	143.1
16	352	567	146.8
17	352	567	36.7
18	361	588	36.7
19	283	567	93.4
20	121	552	86.1
21	105	552	86.0
22	70	541	80.1
23	105	552	6.0
24	300	536	90.3
25	1000	528	90.3
26	748	225	90.3
27	2400	165	813.8
28	1194	16.3	950.3
29	1194	14.7	580.7
30	1194	14.7	369.6
31	818	14.7	580.7
32	818	14.7	369.6
33	818	14.7	950.3
34	721	14.7	950.3
35	542	14.7	950.3
36	357	14.7	950.3
37	300	14.7	950.3
38	108	1.2	191.0

(1) All flow values are for one engine

TABLE 4.2.1-1 (Cont'd)

HEAT AND MASS BALANCE FOR GAS TURBINE COMBINED CYCLE POWER PLANT
USING TEXACO OXYGEN-BLOWN GASIFICATION SYSTEM

39	108	30	191.0
40	108	30	4.8
41	108	115	4.8
42	108	115	4.8
43	108	30	186.2
44	178	30	186.2
45	178	30	172.8
46	178	30	13.4
47	250	30	13.4
48	250	30	186.2
49	255	2837	186.2
50	485	2837	186.2
51	485	2553	168.3
52	485	600	3.1
53	485	600	14.8
54	662	2400	168.3
55	662	2400	68.0
56	662	2400	100.4
57	662	2400	68.0
58	662	2400	100.4
59	662	2400	168.3
60	1000	2400	168.3
61	653	600	168.3
62	485	600	14.8
63	485	600	3.1
64	634	600	186.2
65	1000	540	186.2
66	1000	540	70.3
67	1000	540	115.9
68	108	1.2	115.9
69	108	1.2	70.3
70	108	1.2	186.2
71	485		3.1

TABLE 4.2.1-2

MATERIAL BALANCE FOR TEXACO GASIFICATION/COMBINED CYCLE POWER PLANT

Station Number		1		2		3		4		5 Coal Feed		6 Fuel Gas	
Comp.	M.W.	Lb/Hr[1]	Mols/Hr	Lb/Hr	Mols/Hr	Lb/Hr	Mols/Hr	Lb/Hr	Mols/Hr	Lb/Hr	Mols/Hr	Lb/Hr	Mols/Hr
CH_4	16.04											321	20
H_2	2.016											10632	5274
CO	28.01											215201	7683
CO_2	44.01											71208	1618
H_2S	34.08											6305	185
COS	60.07											541	9
O_2	32.00	713312	22291	599392	18731	138880	4340	138880	4340				
N_2	28.02	2321933	82867	1951117	69633	1681	60	1681	60			3699	132
A	39.94	41578	1041	34948	875	799	20	799	20			799	20
H_2O	18.02	19534	1084	19534	1084	-	-	-	-			58763	3261
Total		3096357	107283	2604991	90323	141360	4420	141360	4420	168250		367469	18202

(1) All values based on one engine.

TABLE 4.2.1-2 (Cont'd)

MATERIAL BALANCE FOR TEXACO GASIFICATION/COMBINED CYCLE POWER PLANT

Station Number		7		8-12		13		14		15		16	
Comp.	M.W.	Lb/Hr[1]	Mols/Hr	Lb/Hr	Mols/Hr	Lb/Hr	Mols/Hr	Lb/Hr	Mols/Hr	Lb/Hr	Mols/Hr	Lb/Hr	Mols/Hr
CH_4	16.04	289	18	385	24	32	2	24	2	417	26	417	26
H_2	2.016	9570	4747	13116	6506	1062	527	1062	527	14181	7034	14181	7034
CO	28.01	193661	6914	265479	9478	21512	768	21512	768	286990	10246	286990	10246
CO_2	44.01	64123	1457	87888	1997	7130	162	7130	162	94974	2158	94974	2158
H_2S	34.08	5657	166	7770	228	613	18	613	18	8418	247	8418	247
COS	60.07	481	8	661	11	60	1	60	1	721	12	721	12
O_2	32.00	-	-	-	-	-	-	-	-	-	-	-	-
N_2	28.02	3334	119	4567	163	364	13	364	13	4932	176	4932	176
A	39.94	719	18	999	25	80	2	80	2	1078	27	1078	27
H_2O	18.02	52889	2935	81991	4550	13020	326	20957	1163	102948	5713	116301	6454
Total		330723	16382	462856	22982	43873	1819	51802	2656	514659	25639	528012	26380

(1) All values based on one engine.

TABLE 4.2.1-2 (Cont'd)

MATERIAL BALANCE FOR TEXACO GASIFICATION/COMBINED CYCLE POWER PLANT

Station Number		17-18		19		20		21		22		23	
Comp.	M.W.	Lb/Hr(1)	Mols/Hr	Lb/Hr	Mols/Hr	Lb/Hr	Mols/Hr	Lb/Hr	Mols/Hr	Lb/Hr	Mols/Hr	Lb/Hr	Mols/Hr
CH_4	16.04	96	6	305	19	305	19	305	19	305	19		
H_2	2.016	3548	1760	10632	5274	10632	5274	10632	5274	10600	5288	32	16
CO	28.01	71818	2564	215201	7683	215201	7683	215201	7683	213800	7633	1401	50
CO_2	44.01	23765	540	71208	1618	71208	1618	71208	1618	59061	1342	12147	276
H_2S	34.08	2113	62	6305	185	6305	185	6305	185	511	15	5794	170
COS	60.07	180	3	541	9	541	9	541	9	360	6	180	3
O_2	32.00												
N_2	28.02	1233	44	3699	132	3699	132	3699	132	2186	78	1514	54
A	39.94	280	7	799	20	799	20	799	20	799	20		
H_2O	18.02	29102	1615	27048	1501	865	48	541	30	360	20	180	10
Total		132135	6601	335738	16441	309555	14988	309231	14970	309050	14391	21248	579

(1) All values based on one engine

TABLE 4.2.1-2 (Cont'd)

MATERIAL BALANCE FOR TEXACO GASIFICATION/COMBINED CYCLE POWER PLANT

Station Number		24-26		27		28-37 GT Exhaust Gas		38-71 Steam	
Comp.	M.W.	Lb/Hr(1)	Mols/Hr	Lb/Hr	Mols/Hr	Lb/Hr	Mols/Hr	Lb/Hr	Mols/Hr
CH_4	16.04	305	19						
H_2	2.016	10600	5258						
CO	28.01	213800	7633						
CO_2	44.01	59061	1342	395826	8994	395826	8994		
H_2S	34.08	511	15	511	15	5..1	15		
COS	60.07	360	6	360	6	360	6		
O_2	32.00			391904	12247	505824	15807		
N_2	28.02	2186	78	1953302	69711	2324119	82945		
A	39.94	799	20	35706	844	42376	1061		
H_2O	18.02	37247	2067	152215	8447	152215	8447	687661	38161
Total		345937	16438	2929824	100314	3421231	117275	687661	38161

(1) All values based on one engine.

TABLE 4.2.1-3

PERFORMANCE SUMMARY FOR IGCC POWER PLANTS

	Texaco	BGC
Gas Turbine		
Number of turbines	4	4
Air flow/turbine, lb/sec	860	860
Pressure Ratio	12	12
Combustor exit temp., F	2400	2400
Exhaust temp., F	1194	1177
Stack temp., F	300	335
Steam Turbine		
Throttle reheat temperature, F	1000	1000
Throttle pressure, psia	2400	2400
Condenser pressure, in. Hg	2.5	2.5
Overall System		
Gas turbine power, MW	630.4	605.6
Steam turbine power, MW	324.8	244.4
Net total power, MW	946.4(1)	819.2
Net heat rate, Btu/kWh(2)	8716	8400
Coal rate, tons/day (as received)	8076	6752

(1) Includes fuel gas expander.

(2) Coal in-to-kW out at busbar.

FIG. 4.2.2-1

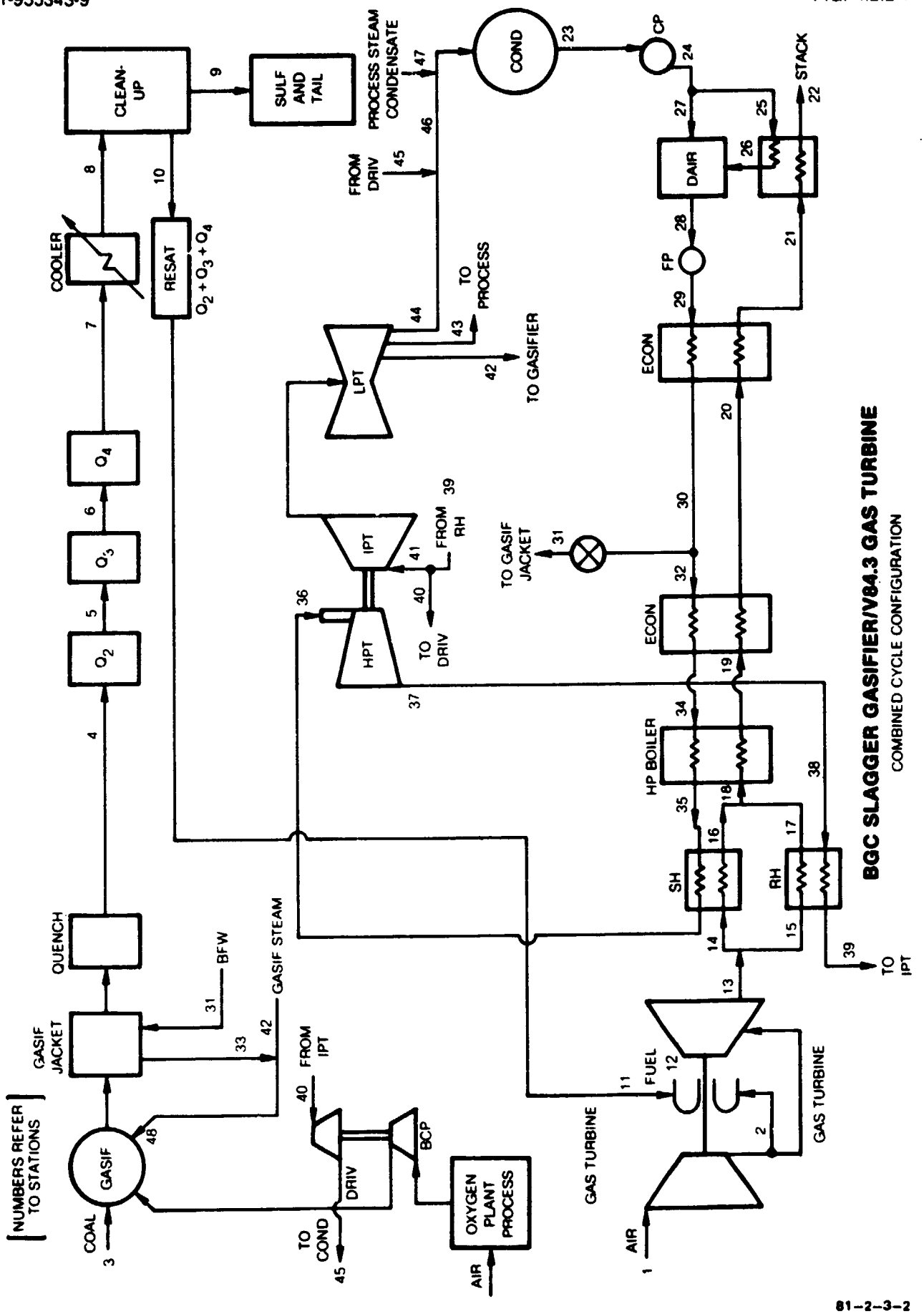

81-2-3-2

TABLE 4.2.2-1

HEAT AND MASS BALANCE FOR GAS TURBINE COMBINED CYCLE POWER PLANT USING BGC GASIFICATION SYSTEM

Station Number	Temperature (°F)	Pressure (psia)	Flow (lb/sec)(1)
1	59	14.7	860.0
2	655	175	723.5
3			39.1
4	282	325	72.9
5	262	320	70.1
6	250	320	68.5
7	202	315	64.8
8	105	305	62.8
9	70	305	2.7
10	70	295	59.9
11	242	290	65.2
12	2400	167	788.7
13	1176	16.2	925.2
14	1176	16.2	601.9
15	1176	16.2	323.3
16	894	14.7	601.9
17	894	14.7	323.3
18	894	14.7	925.2
19	702	14.7	925.2
20	559	14.7	925.2
22	335	14.7	925.2
23	108	1.2	137.6
24	108	30	137.6
25	108	30	18.0
26	250	30	18.0
27	108	30	119.6
28	250	30	137.6
29	255	2837	137.6
30	485	2837	137.6
31	448	415	6.9
32	485	2837	130.8
33	448	415	6.9
34	662	2400	130.8
35	662	2400	130.8
36	1000	2400	130.8
37	657	600	130.8
38	657	600	130.8

(1) All flow values are for one engine.

TABLE 4.2.2-1 (Cont'd)

HEAT AND MASS BALANCE FOR GAS TURBINE COMBINED CYCLE POWER PLANT
USING BGC GASIFICATION SYSTEM

Station Number	Temperature (°F)	Pressure (psia)	Flow (lb/sec)(1)
39	1000	540	130.8
40	1000	540	31.9
41	1000	540	98.9
42	935	415	4.8
43	602	100	7.4
44	108	1.2	86.7
45	108	1.2	31.9
46	108	1.2	118.5

(1) All flow values are for one engine.

TABLE 4.2.2-2

MATERIAL BALANCE FOR BGC GASIFICATION/COMBINED-CYCLE POWER PLANT

Station Number		1		2		3		4		5		6	
Comp.	M.W.	Lb/Hr[1]	Mols/Hr	Lb/Hr	Mols/Hr	Lb/Hr Coal Feed	Mols/Hr	Lb/Hr	Mols/Hr	Lb/Hr	Mols/Hr	Lb/Hr	Mols/Hr
CH_4	16.04							15735	981	15735	981	15735	981
H_2	2.016							6893	3419	6893	3419	6893	3419
CO	28.01							182793	6526	182793	6526	182793	6526
CO_2	44.01							9594	218	9594	218	9594	218
H_2S	34.08							5282	155	5282	155	5282	155
COS	60.07							420	7	420	7	420	7
O_2	32.00	713312	22291	599392	18731			--	--	--	--	--	--
N_2	28.02	2321933	82867	1951117	69633			4259	152	4259	152	4259	152
A	39.94	41578	1041	34948	875			80	2	80	2	80	2
H_2O	18.02	19534	1084	19534	1084			37247	2067	26868	1491	21354	1185
Total		3096357	107283	2604991	90323	140724		262303	13527	251924	12951	246410	12645

(1) All values based on one engine

TABLE 4.2.2-2 (Cont'd)

MATERIAL BALANCE FOR BGC GASIFICATION/COMBINED-CYCLE POWER PLANT

Station Number		7		8		9		10		11		12	
Comp.	M.W.	Lb/Hr[1]	Mols/Hr	Lb/Hr	Mols/Hr	Lb/Hr	Mols/Hr	Lb/Hr	Mols/Hr	Lb/Hr	Mols/Hr	Lb/Hr	Mols/Hr
CH_4	16.04	15735	981	15735	981	176	11	15559	970	15559	970	--	--
H_2	2.016	6893	3419	6893	3419	8	4	6885	3415	6885	3415	--	--
CO	28.01	182793	6526	182793	6526	392	14	182401	6512	182401	6512	--	--
CO_2	44.01	9594	218	9594	218	1320	30	8274	188	8274	188	337557	7670
H_2S	34.08	5282	155	5282	155	4873	143	409	12	409	12	--	--
COS	60.07	420	7	420	7	126	2	300	5	300	5	--	--
O_2	32.00	--	--	--	--	--	--	--	--	--	--	378464	11827
N_2	28.02	4259	152	4259	152	2858	102	1401	50	1401	50	1952518	69683
A	39.94	80	2	80	2	--	--	80	2	80	2	34987	876
H_2O	18.02	8217	456	757	42	685	38	72	4	19119	1061	135150	7500
Total		233273	11916	225813	11502	10432	344	215381	11158	234428	12215	2098676	97556

(1) All values based on one engine.

TABLE 4.2.2-2 (Cont'd)

MATERIAL BALANCE FOR BGC GASIFICATION/COMBINED-CYCLE POWER PLANT

Station Number		13-22 GT Exhaust Gas		23-47 Steam	
Comp.	M.W.	Lb/Hr[1]	Mols/Hr	Lb/Hr	Mols/Hr
CH_4	16.04				
H_2	2.016				
CO	28.01				
CO_2	44.01	337557	7670		
H_2S	34.08				
COS	60.07				
O_2	32.00		15387		
N_2	28.02	492384	82917		
A	39.94	41657	1043		
H_2O	18.02	135150	7500		27504
Total		3330082	114517		27504

(1) All values based on one engine.

4.2.3 Comparison of Performance

The performance estimates in Table 4.2.1-3 indicates that the IGCC power plant using the BGC gasifier would be 1.4 percentage points or approximately 3.5 percent more efficient than the Texaco-based IGCC power plant (40.6 versus 39.2 percent). The major contributor to this performance difference is the efficiency of the gasifier.

A review of Tables 4.2.1-1 and 4.2.2-1 show that the amounts of oxygen and steam used by the BGC gasifier are 26 and 50 percent lower than the oxygen and water used by the Texaco gasifier. The lower the oxygen and steam requirement, the more efficient the gasifer. A second benefit is that the oxygen plant and the boost compressor for the BGC-based system requires less power.

4.2.4 Off-Design Operation of IGCC Power Plants

The performance estimates presented thus far are for design point operation, i.e., full load at 59 F, 1000 ft (ISO) conditions. While the efficient power plants such as the IGCC power plants would be used as base-load plants (5000 h/yr or more) operating at full load, even these plants must follow load and be able to drop load, start, etc.

The IGCC power plant is a very complex plant having the characteristics of a chemical plant superimposed upon a power plant. The ability to successfully operate such a plant can only be demonstrated in an actual installation. It is possible, however, to simulate the part-load and transient behavior of this type of plant. Examples of this can be found in the literature (Refs. 4.2.-2 and -3) and have been the subject of a recent UTC in-house investigation (Ref. 4.2-4). The pertinent results of these studies are discussed below.

There are two modes of IGCC control: gasifier-lead in which coal/oxident flow to the gasifier is used to control load; and turbine-lead in which the turbine fuel controls are used to control load. Either control mode can be used successfully, i.e., either can meet the usual load ramp rates expected of large central station power systems. These load variations include the gradual changes for daily load following (4 percent/min from 80 percent of full load to full load and back) to rapid changes for tie line thermal backup (20-percent step change).

In transient and part-load operation, there are several critical operating parameters that must be observed, these involve the sulfur removal system and the heat exchangers. The Selexol absorber is a well proven process that operates unattended in some applications. However, in transient and part load operation, it is important to maintain the sulfur removal level so that emissions are within prescribed limits. To do this, the pressure control point for the overall systems should be directly downstream of the Selexol unit. This will allow close control of the pressure in the absorber during all operations.

As load is changed, the turbine inlet temperature and the exhaust temperature also change. The fuel gas temperature from the gasifier, however, remains essentially constant. Steam temperature from the waste heat boiler located in the fuel gas stream remains constant but the pinch temperature (minimum approach) between the exhaust gas and the steam in the superheater and reheater changes. It is necessary to balance the flows so that an adequate temperature difference is maintained, i.e., the steam is always cooler than the exhaust gases. The pinch temperature at the HP and LP boilers (see Fig. 4.2.1-1) are shown in Table 4.2.4-1.

Of particular interest is the performance at part load. Combined-cycle systems have excellent part-load efficiencies and the IGCC systems continue to display this characteristic. The part-load heat rate for the IGCC plant is shown in Fig. 4.2.4-1. Here it can be seen that at 70-percent load, the heat rate has increased by only 8.9 percent. Also shown in Fig. 4.2.4-1 is the relationship between steam turbine output and load. As indicated in Table 4.2.4-1, reduction in load reduces throttle conditions and, thus power.

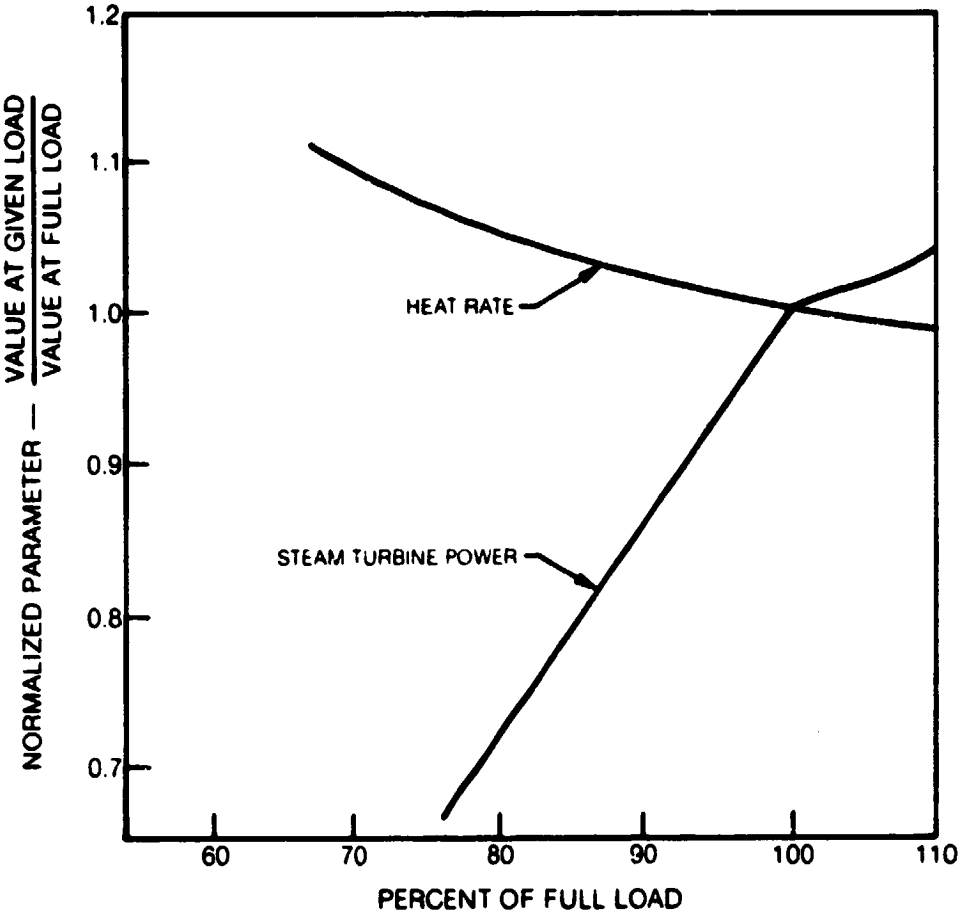

PART-LOAD PERFORMANCE OF IGCC POWERPLANTS

TABLE 4.2.4-1

PINCH TEMPERATURE IN TEXACO IGCC POWER PLANT

	Pinch Temp., F		Throttle Conditions	
Load, Percent	LP	HP	Temp.,F	Press., psia
100	40	40	1000	2400
90	45	31	935	2157
80	50	22	864	1911
70	54	14	785	1664

4.2.5 References

4.2-1 Interim Project Briefing, NASA-MSFC, Huntsville, Alabama, December 17/18 1980.

4.2-2 Carlson, N. G.: High Temperature Turbine Technology Program, UTC Final Report FE-2292-19, April 1977.

4.2-3 Fluor Engineers and Constructors: Entrained Gasification Combined-Cycle Control Study - Vol. I. EPRI AP 1422, June 1980.

4.2-4 Lehman, S. J.: Off-Design Performance Variation of an Advanced Combined Cycle Power Plant Using the V84.3 Gas Turbine and the Texaco Entrained Flow Gasifier. UTRC Report R80-752717-1, December 22, 1980.

1.3 Assessment of MHD Technology Status

Magnetohydrodynamics (MHD) is a branch of physics which deals with phenomena arising from the motion of electrically conducting fluids in the presence of electric and magnetic fields. This covers a broad area ranging from astrophysics to a number of technological applications including power generation, propulsion, pumping, flow measurement and magnetic - confinement thermonuclear fusion. The types of conducting fluids include liquid metals, electrolytic solutions and ionized gases or "plasmas."

This assessment is restricted to the application of MHD to the production of electric power by utilizing an ionized gas as the conducting fluid. There are basically two categories of cycles for MHD power generation; open-cycle and closed-cycle. In open-cycle MHD power generation, the ionized gas flows through an MHD generator channel and is ultimately exhausted to the atmosphere after treatment to make it environmentally acceptable. In closed-cycle MHD power generation, the ionized gas is continuously recirculated through the MHD channel in much the same manner as the gas in a closed-cycle gas-turbine system. The assessment is further restricted to consideration of open-cycle MHD power generation because it is in a more advanced state of development and appears to be much closer to commercial application. Also, the majority of the financial support for MHD power generation programs in the U.S., provided by the U.S. Department of Energy and the Electric Power Research Institute, are primarily directed towards open-cycle MHD power generation.

1.3.1 Assessment of MHD Technology Readiness Development Trends

The basic principles of the phenomena involved in MHD power generation have been known since experiments in electrodynamics were performed by Michael Faraday in the nineteenth century. However, the only electrically conducting fluids which were practical at that time were liquid metals and electrolytes. Developments in this century in high temperature technologies led to interest in gases as conducting fluids. Experiments with gaseous MHD power generation were conducted between 1938 and 1944 by Westinghouse, with unsatisfactory results. However, as the technologies associated with high temperature fluid dynamics advanced, interest was again aroused in MHD power generation. Experiments were conducted in several industrial research laboratories in the late 1950's and early 1960's. These experiments have yet to lead to commercially available equipment. A review of selected efforts, however, will establish the current technology base.

1.3.1.1 Technology Readiness - Earlier Programs

In 1959 a test was conducted at Avco-Everett Research Laboratory in which 11.5 kW of electric power was generated for a period of 10 seconds. In 1960, a 10-kW MHD generator was operated at Westinghouse for a period of over one hour. General Electric Co. was also active in MHD during this period. These early tests produced only small amounts of power, but the demonstrated the possibility of

generating power by MHD and considerable interest was displayed by industry, government, and universities, both in this country and in several other countries.

In 1965, Avco-Everett Research Laboratory performed a test in which 32 MW of electric power was produced in an MHD generator for a period of one minute. The duration was limited by the capabilities of the test facility rather than by failure of the generator. Another generator built by Avco produced 18 MW for one minute in 1966. Long duration testing at Avco was conducted on a much smaller scale. One Avco long duration test facility had accumulated over 2000 hours of operation by 1966 at a power level of several kW.

Another development in the 1960's which has had a significant impact on the potential for MHD power generation is the progress made in constructing superconducting magnets. This field was in its infancy in 1961. Considerable progress in superconducting magnet development has been made because of its applicability to high energy physics experiments, controlled thermonuclear fusion and other areas as well as MHD power generation.

MHD programs have been initiated in several other countries. France, The Federal Republic of Germany and Great Britain developed strong programs, but they eventually declined as these countries shifted emphasis to nuclear energy. However, MHD programs have continued to grow in many other countries, including the U.S.S.R., Japan, China, the Netherlands, Poland, India, Australia and Italy. Today, the U.S.S.R. has the largest MHD program in the world. In 1965, they completed construction of their U-02 facility which has a thermal power input capacity of 5 MW. In 1971 they completed construction of their U-25 facility which has a thermal power input capacity of 300MW.

In the decade of the 1970's, the MHD program in the United States has grown considerably, with a shift in emphasis towards coal as a fuel. Funding of MHD by the Department of the Interior's Office of Coal Research was at a level of several million dollars per year in the early 1970's. Funding has steadily increased as the MHD program came under the jurisdiction of the Energy Research and Development Administration and, later, under the Department of Energy. The DOE appropriations for the MHD program were 79 million dollars in fiscal year 1980 and 67 million dollars for FY 81.

Great strides in MHD have been made in the past decade. An MHD channel has been operated at a power level of several hundred kWe for two continuous 250-hour runs Although this channel is small compared to that required for a commercial power plant, the local conditions at the electrodes of the channel were comparable to those anticipated for a commercial-scale channel. In the U.S.S.R., a channel has been operated for 250 hours at a power level of several MWe. In other tests, electric power was successfully delivered to the Moscow electrical network on a small scale.

No MHD power plants have been constructed to date which produce electric power specifically for utility use. The earliest date by which such a plant could be built in the U.S.S.R. is probably 1985. The earliest date by which such a plant could be built in the U.S. is probably 1990. The construction of an MHD power plant in the U.S. could probably be substantially accelerated by retrofitting an existing steam power plant by the addition of an MHD generator as a topping unit. The actual dates of implementation of MHD for the production of electric power depend, of course, upon further technological advancement and upon the support given to research and development by government and industry.

1.3.1.2 Technology Readiness - Projected Commercial Plant

A general summary of the major characteristics of a projected commercial MHD power plant is indicated in Table 1.3.1.2-1. Since no such power plants have been constructed, these characteristics are based upon conceptual designs, anticipated technological developments and extrapolation of test data. The power plant would be a combined MHD/steam power plant with a net output in the range of 500 to 2000 MW-electrical. Approximately one half of this power would be produced by the MHD generator and the remainder by the steam-turbine driven generator. The large size of the plant is desired because of the tendency for the efficiency of an MHD generator to increase significantly with size. The increase in efficiency as size (and hence the volume to surface-area) increases is due to the fact that the power generating phenomenon is a volumetric effect while the thermal, viscous and electrical losses are surface effects. The overall power plant efficiency from the coal pile to the utility grid is projected to be in the vicinity of 50%. This is the major reason for the interest being expressed in MHD power generation at the present time.

Emission levels from the plant are projected to be below the environmental limits. The collection of flyash and K_2SO_4 result in adequate control of particulate matter and sulfur-oxide emissions. Nitrogen oxides and carbon monoxide emissions can also be controlled in an MHD power plant by control of combustion conditions and the MHD generator exhaust gas cooling rate. Due to the high power plant efficiency, the heat rejection rate is less than that of conventional plants which have overall efficiencies of 40% or less.

Another attractive feature of an MHD power plant is the capability it has for direct utilization of coal as a fuel. Coal can be injected directly into the combustor and the resulting combustion products can be tolerated by the MHD generator. Problems which are typical of conventional coal fired plants do arise, but the presence of coal ash is not highly detrimental to the MHD generator itself.

Table 1.3.1.2-2 presents a summary of projected MHD/steam power plant performance results and cost estimates based upon several recent investigations. The investigations are the Energy Conversion Alternatives Study (ECAS) completed in 1975 (Ref. 1.3-1) and the Parametric Study of Potential Early Commercial MHD

TABLE 1.3.1.2-1

PROJECTED CHARACTERISTICS OF A
COMMERCIAL-SCALE MHD/STEAM POWER PLANT

Size Range

500 - 2000 MWe

Efficiency

50%

Environmental Control

Low SO_x, NO_x, CO, Particulate and Thermal Discharges

Fuel Capability

Coal (direct-fired)

Cost of Electricity

Competitive

TABLE 1.3.1.2-2

SUMMARY OF PROJECTED MHD/STEAM POWER PLANT
PERFORMANCE AND COST ESTIMATES

Source of Data	ECAS	PSPEC
Type of Plant	Direct-Fired Air Preheater	Oxygen-Enriched Air
Net Electrical Power Output (a.c.)	1932 MWe	931 MWe
MHD Generator Electrical Power Output (a.c.)	1406 MWe	512 MWe
Overall Efficiency	48.3 %	43.4 %
Year of Cost Basis	mid-1975	mid-1978
Plant Capital Cost	$718 per kW	$646 per kW
Cost of Electricity	31.8 mills/kWhr	32.5 mills/kWhr

Power Plants (PSPEC) completed in 1979 (Ref. 1.3-2). The cost estimates shown for these studies are given in 1975 and 1978 dollars, respectively. The basis for the ECAS design is an MHD power plant utilizing advanced or "second generation" technology projected to be available for commercial orders in the mid to late 1990's. The basis for the PSPEC design is an MHD power plant utilizing near term or "first generation" technology projected to be available for commerical orders in the early 1990's.

1.3.1.3 Trends in Operating Parameters

Figure 1.3.1.3-1 shows a simplified sketch of an MHD generator. The generator consists of a duct with two electrode walls and two insulating walls with a magnetic field applied perpendicular to the duct axis. When an ionized gas flows through the duct, electrical energy is extracted directly from the kinetic and thermal energy of the gas due to its interaction with the magnetic field. The current in the gas is carried almost entirely by electrons. The net current generated may pass through a single load as indicated in Fig. 1.3.1.3-1 or through a set of multiple loads, depending on the type of electrode interconnections.

The MHD generator essentially behaves as an electromagnetic "turbine", being thermodynamically equivalent to a gas turbine. Both types of machines can be most efficiently utilized for production of electric power when operating in a Brayton topping cycle over a conventional Rankine-cycle steam power plant. MHD generators, however, operate at much higher temperatures (2300 to 2800°K or 3700 to 4600°F), lower pressures (6 to 10 atm) and are considered to be most efficient at very large sizes (500 MWe).

Plasma Properties

The plasma properties of primary interest in MHD power generation are the electrical conductivity σ and the Hall parameter $\omega\tau$ of the gas. The plasma is essentially electrically neutral and the conduction of electricity in the plasma is carried out primarily by electrons. The Hall parameter relates to the effect of the magnetic field on the electrical conduction process.

In order to conduct electricity, the gas must be partially ionized, meaning that some of the atoms in the gas are stripped of one or more of their electrons, as occurs at high temperatures. If an alkali metal is added to the gas, sufficient ionization may occur at a reasonable temperature because of the metal's low ionization potential. Table 1.3.1.3-1 indicates the ionization potential of several materials. The process of adding an alkali metal to a gas to achieve the desired degree of ionization is referred to as "seeding". The primary candidate seed materials for use in MHD power generation are potassium (K) and cesium (Cs).

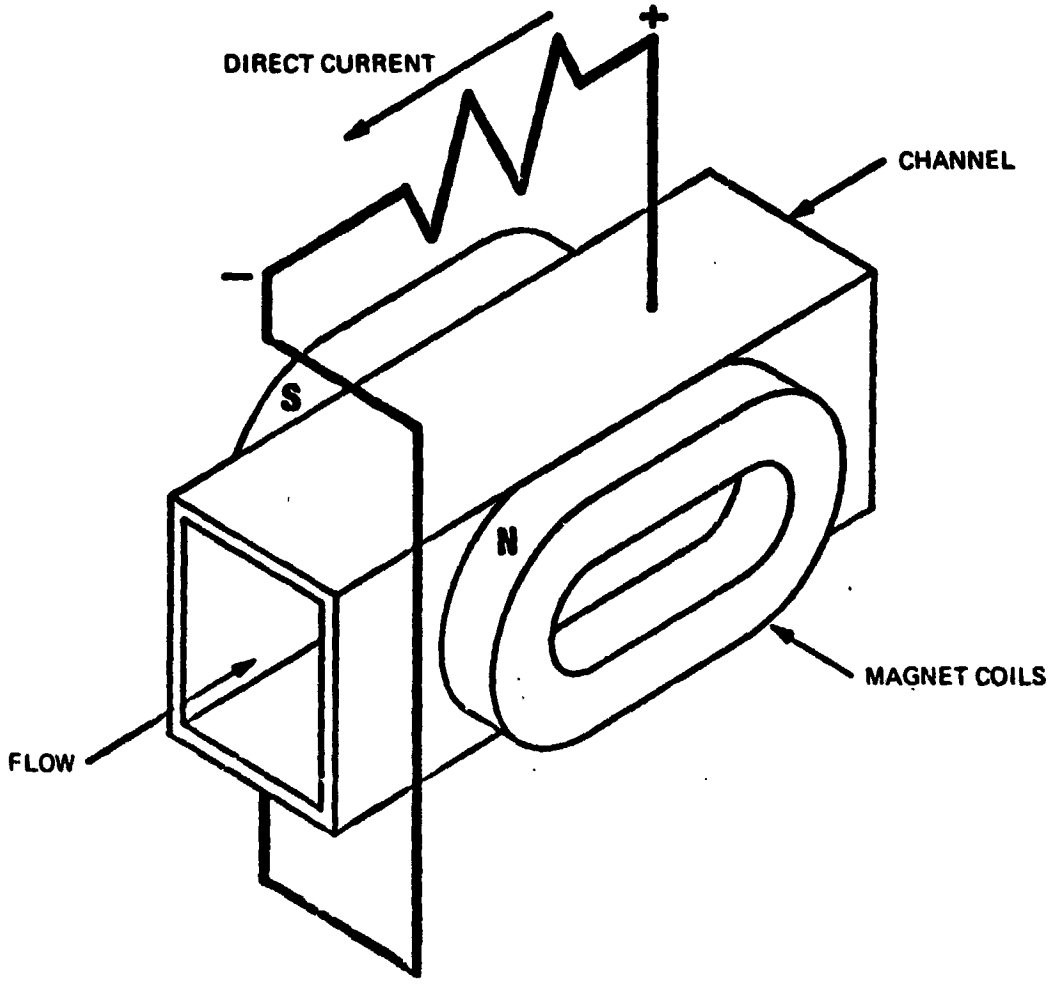

GENERATION OF D.C. ELECTRIC POWER BY MAGNETOHYDRODYNAMICS

TABLE 1.3.1.3-1

IONIZATION POTENTIAL OF METAL VAPORS

Metal	Ionization Potential (electron-volts)
Lithium	5.363
Sodium	5.12
Aluminum	5.96
Potassium	4.318
Calcium	6.09
Rubidium	4.16
Cesium	3.87
Barium	5.19
Mercury	10.39

The electrical conductivity of the plasma depends upon the composition, temperature and pressure of the gas. Figure 1.3.1.3-2 shows the variation of electrical conductivity with temperature and pressure for a specific seed concentration and gas composition. For economical power production in an MHD generator, conductivity requires very high combustion temperatures. In combustion gases, the presence of the OH radical introduces the posibility of electron attachment, forming OH^-, and reduction of electrical conductivity. Therefore, fuels with high carbon content are preferred over fuels with high hydrogen content. In general, however, it is difficult to predict plasma conductivities with a great degree of precision.

The Hall effect arises because of the tendency for charged particles to take on circular or spiral trajectories in a magnetic field. The cyclotron frequency ω of an electron of charge e and mass m_e in a magnetic field of strength B is given by:

$$\omega = \frac{eB}{m_e}$$

Collisions between free electrons and other molecules and atoms in the gas prevent the electrons from continuing to spiral indefinitely and cause the electrons to migrate in a direction dependent upon the relative strengths and directions of the electric and magnetic fields present. The Hall parameter is a dimensionless parameter equal to the product of the electron cyclotron frequency and mean time τ between collisions of electrons with other particles:

$$\text{Hall Parameter} = \omega\tau$$

The Hall parameter is proportional to the magnetic field strength and is dependent upon the gas composition, pressure and temperature.

MHD Channel Phenomena

In the following paragraphs, the basic relations are developed for a simplified model of an MHD generator. This is a "zero-dimensional" model in which the variables (such as velocity, conductivity, electric field strengths, etc.) do not vary with respect to location within the generator. Although this is unrealistic, the model is useful for illustrating basic problems.

Figure 1.3.1.3-3 is an elementary diagram showing the electrode walls of an MHD duct (channel) with a connected external electrical load (shown simply as a resistor). The magnetic field is perpendicular to the diagram, directed away from the reader. The motion of the ionized gas induces an electric field across the duct in the direction from the anode to the cathode. The magnitude of this induced electric field is equal to the product of the velocity, u, and the magnetic field strength, B.

FIG. 1.3.1.3-2

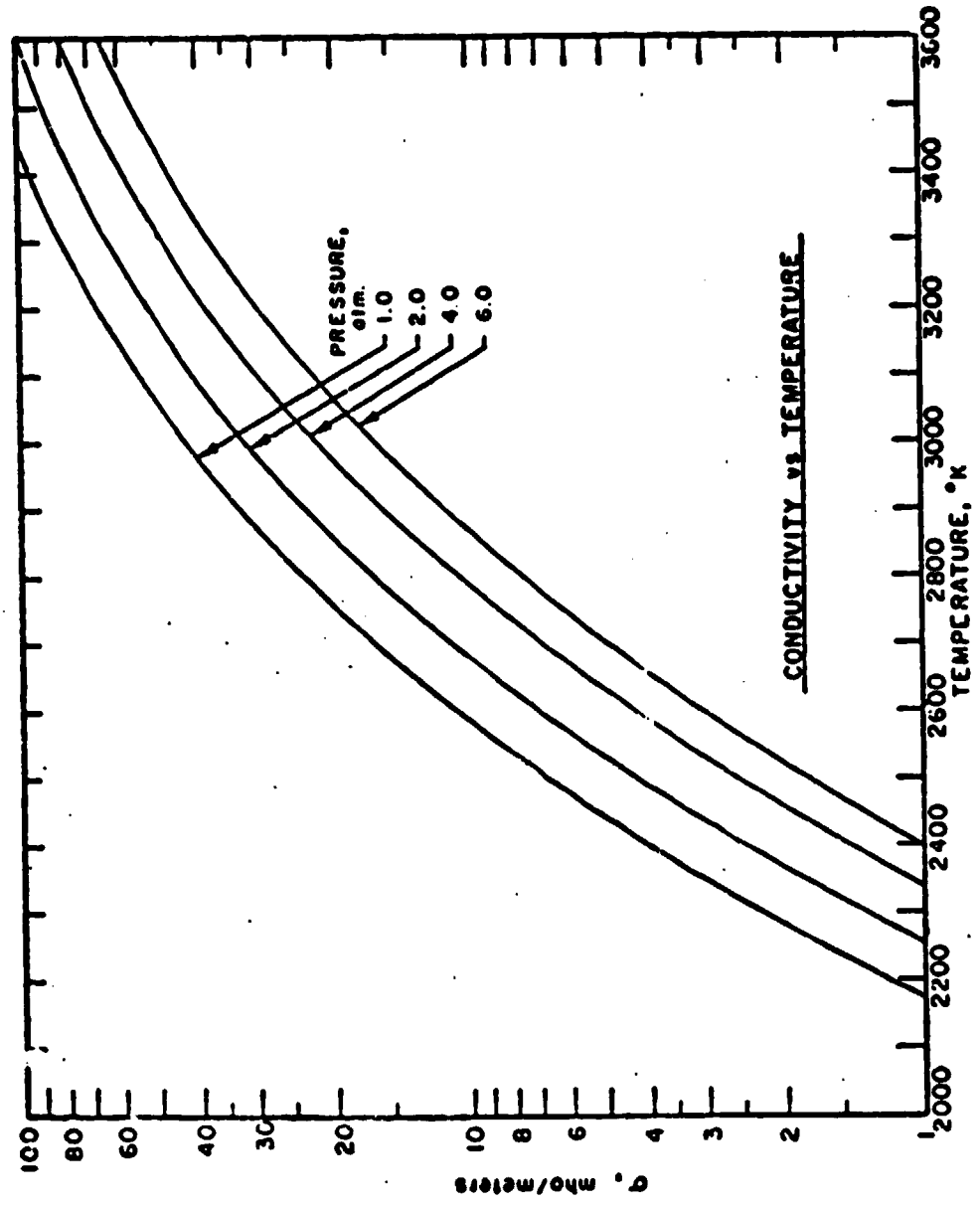

ELECTRCAL CONDUCTIVITY OF COMBUSTION GASES

FIG. 1.3.1.3-3

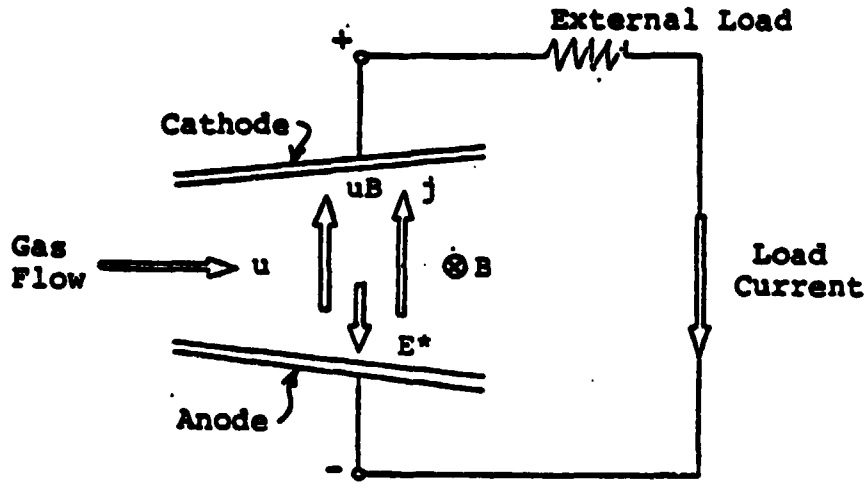

MHD DUCT WITH CONTINUOUS ELECTRODES WITHOUT HALL EFFECT

$$E_{induced} = uB$$

If the velocity has units of meters per second and the magnetic field strength has units of tesla (1 tesla - 10,000 gauss), the electric field will have units of volts per meter.

This induced field tends to make the cathode positive in voltage with respect to the anode. Thus if an external load is connected between the terminals on the electrodes, an electric current would pass through this load in the direction from the cathode to the anode. A corresponding electric current would pass through the gas in the duct in the direction from the anode to the cathode. This is shown in Fig. 1.3.1.3-3, where the current inside the duct is indicated as a "current density", j, which has the units of current per unit area (amp per square meter).

The magnitude of the voltage difference between the electrodes depends upon the magnitude of the external electrical load connected to the terminals as well as upon the induced field, uB. The occurrence of this voltage difference induces an electrostatic field in the gas opposite in direction to the magnetically induced field uB. Thus the net electric field is:

$$E = E_{induced} - E^*$$

$$= uB - E^*$$

where E* is the "electrostatic" field arising from the potential difference between the electrodes. The directions of these field components are shown in Fig. 1.3.1.3-3.

The electric current density, j, will be proportional to the electrical conductivity, σ, of the gas, which is expressed in units of mhos per meters (where a mho is the reciprocal of an ohm). If there is no "Hall effect", the electric current will be parallel to the net electric field and is given by the expression:

$$j = \sigma (uB - E^*)$$

The electric power P generated per unit volume is equal to the product of the current density and the electric field through E*. Thus,

$$P = jE^* = \sigma E^* (uB - E^*)$$

The Hall effect results from the combined tendency for electrons to spiral around the lines of magnetic flux and to interact with other particles. Thus, when an ionized gas is the presence of both a magnetic field and an electric field, the electric current is not parallel to the electric field. As shown in Fig. 1.3.1.3-4, there is an angle, θ, between the electric field direction and the current direction. In terms of the dimensionless "Hall parameter", $\omega\tau$, the "Hall angle" is

$$\theta = \tan(\omega\tau)$$

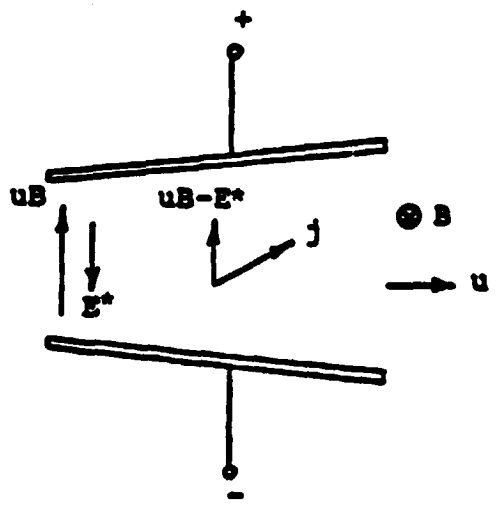

MHD DUCT WITH CONTINUOUS ELECTRODES WITH HALL EFFECT

where $\omega\tau$ is directly proportional to the magnetic field strength as previously indicated. Typically, θ would be in the range of 45 to 75 degrees.

If the electrodes are continuous (that is, if they are continuous walls of constant electrical potential), the electric field and electric current directions are as shown in Fig. 1.3.1.3-4. The fact that the electric current traverses diagonally across the MHD duct results in a reduction in the power output of the generator. The magnitude of the reduction in power compared to the power which would be generated with no Hall effect is equal to the factor

$$1 + (\omega\tau)^2$$

In order to counteract this detrimental effect, the channel can be constructed by "segmenting" the electrode walls, as shown in Fig. 1.3.1.3-5. To make the current traverse the duct in the direction perpendicular to the flow direction, each opposing pair of electrodes is connected to an individual external load. For this case, the electric field is directed diagonally across the duct, and the power output is equivalent to that which would occur with no Hall effect. This configuration is referred to as a segmented "Faraday" generator.

The disadvantage of this arrangement is that there must be a large number of individual loads. A commercial-scale duct would require approximately 1000 segments. However, an alternate method for making connections between electrode pairs which can reduce the number of loads is illustrated in Fig. 1.3.1.3-6. This is referred to as a "diagonal generator." Each electrode segment on the anode wall is connected to a corresponding electrode segment on the cathode wall through a short circuit. The load is then connected between the farthest upstream and farthest downstream electrode pairs. If the diagonal lines between interconnected electrodes (shown as dashed lines in Fig. 1.3.1.3-6) correspond to lines of constant electrostatic potential for the segmented Faraday configuration of Fig. 1.3.1.3-5, then the directions of the electric field and electric current are the same as that for the ideal case. The advantage of this configuration is that there is only one load. But once the interconnections have been made, the ideal power extraction can only occur at the corresponding value of the Hall parameter, $\omega\tau$. If the Hall parameter should happen to deviate from the design value, the generator performance will diminish.

The equations presented in this section were developed on the basis of a "zero-dimensional" model of the MHD channel. In reality, even though the magnetic field strength, velocity, conductivity and other parameters vary throughout the channel, the equations are applicable locally at any point within the channel. Figure 1.3.1.3-7 from Ref. 1.3-3 shows how the values of the parameters (averaged over the channel cross section) vary along the direction of the axis of the channel.

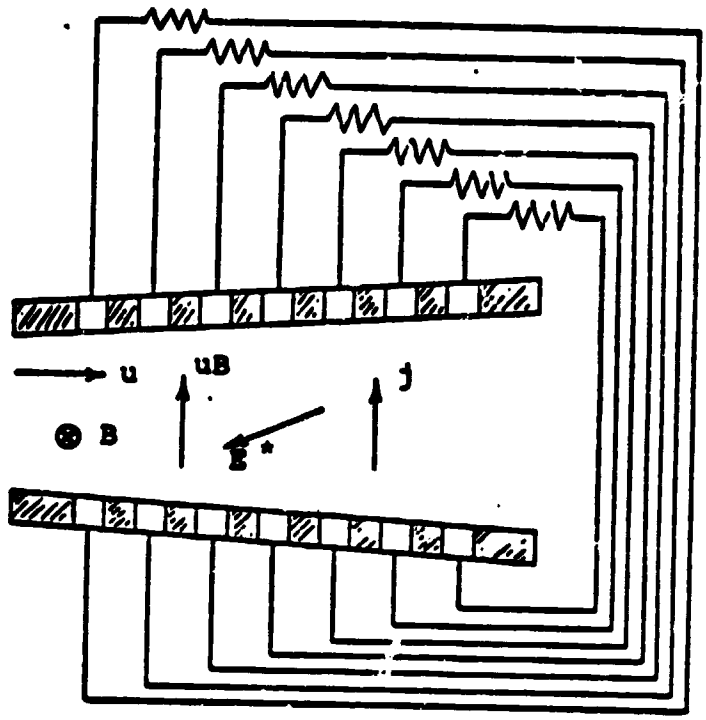

SEGMENTED FARADAY GENERATOR

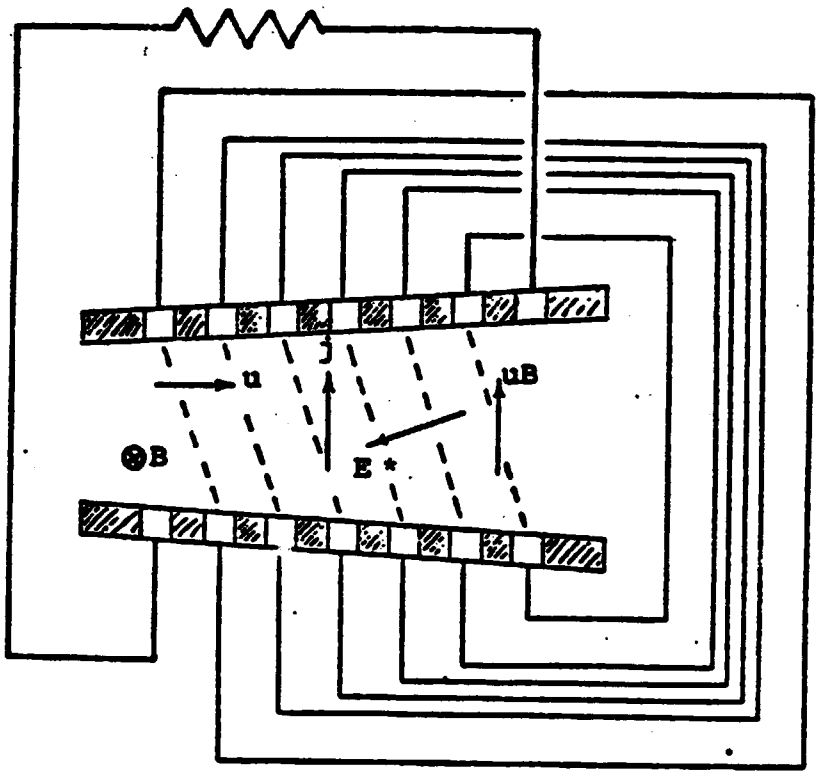

DIAGONAL GENERATOR

C-4

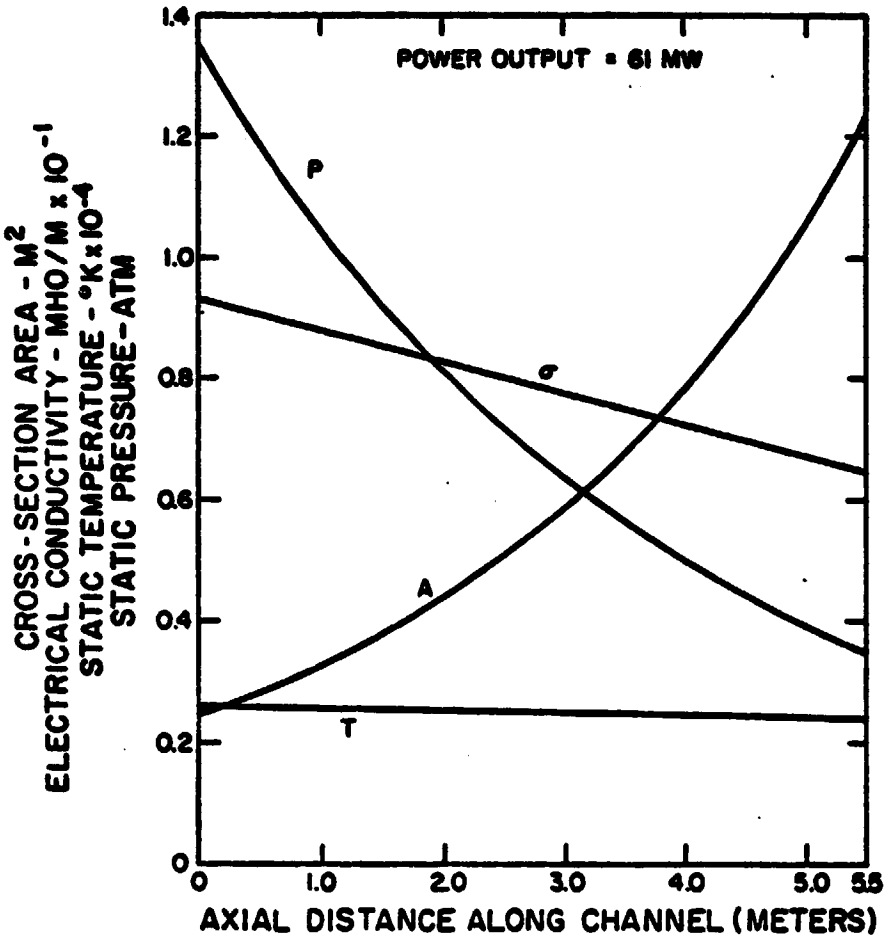

VARIATION OF PARAMETERS ALONG AXIS OF MHD CHANNEL

Channel Construction and Materials

There are a number of alternate means of constructing the MHD channel in order to meet design requirements. The channel construction approach which has been proposed by Avco-Everett Research Laboratory for the MHD Engineering Test Facility (Ref. 1.3-4) has been selected. Both the Faraday and Diagonal modes of interelectrode interconnection will be considered.

Three variations of the Faraday MHD channel concept are shown schematically in Figs. 1.3.1.3-8(a), 8(b) and 8(c) from Ref. 1.3-4. The differences between the three are in the design of the insulator wall. The insulating walls have the requirement of preventing electric current from flowing along the walls in a direction perpendicular to the direction of the electrostatic field, E*. There are three ways to achieve this requirement: a continuous insulating wall, a peg-wall configuration, or a diagonal-bar configuration. The continuous insulating wall is simple in principle but puts a severe restriction on the choice of material of construction. The material must be a good electrical insulator and, of course, must be able to maintain its structural integrity and its insulating property during operation.

Figure 1.3.1.3-8 illustrates the multiple-load Faraday design using metallic peg wall construction. The wall is constructed of metal "pegs" which are insulated from one another, thus minimizing the flow electric current along the wall. However, heat can be conducted away from the surface of the wall to cooling water. In general, the segmentation of the pegs is about equal to that of the electrodes. Square pegs are illustrated but polygon cross sections can be and have been used. An all-ceramic side wall and peg wall are approximate electrical equivalents, but the feasibility of ceramic walls for long duration has not yet been demonstrated. In contrast, several promising peg wall schemes have been evolved and tested.

The advantage of the peg-wall Faraday channel is that its performance is generally considered to be the best of all possible channel types. Its disadvantage is associated with the mechanical complexity and the question of long term reliability of a peg wall. The number of pegs is large. Provision for adequate and reliable cooling can be a formidable design problem, given the mechanical and electrical stress conditions present in an MHD generator.

Figure 1.3.1.3-8 shows another Faraday type channel in which the insulator wall is constructed of long bars rather than pegs. Some segmentation of the bars may be incorporated to control gap voltages and current densities. The bars are oriented along the equi-potentials predicted for the free-stream plasma. The gross performance of the Fig. 1.3.1.3-8(b) channel is equivalent to that of the peg wall type of Fig. 1.3.1.3-8(a), at the full load or design point. The advantage of a bar wall is the mechanical simplicity and reliability of this kind of construction. Its disadvantage is in part-load (or off-design) operation where the fixed bars will be at an incorrect angle. The resulting circulation of Hall current is likely to make performance less than that of a part-load, peg wall design.

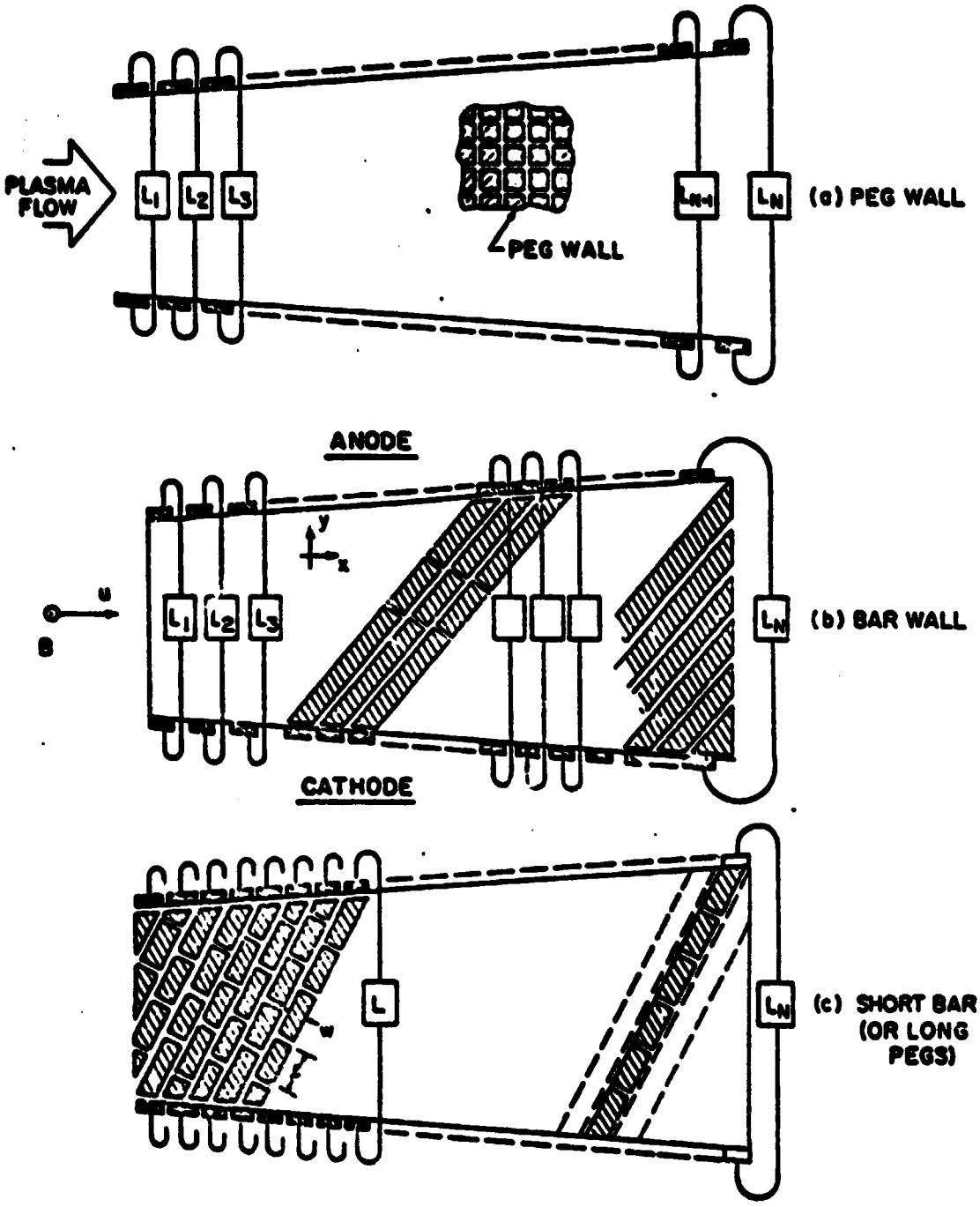

MHD CHANNELS WITH FARADAY INTERCONNECTION AND ALTERNATE INSULATING WALL STRUCTRURES

A possible compromise for side wall construction is depicted in Fig. 1.3.1.3-8(c). In this concept the bars are highly segmented but the segmentation is not as great as that of a peg wall. The approach here is to approximate a peg wall design with its good part-load performance, and yet retain some of the mechanical simplicity of bar wall construction. This concept needs further investigation within the context of part-load performance requirements.

Variations of the basic single-load diagonal channel are illustrated in Figs. 1.3.1.3-9(a) and 9(b) from Ref. 1.3-4. Figure 1.3.1.3-9(a) shows the "window frame" design in which each electrode/bar pair is an integral unit; no external connections are necessary. The window frame technique appears to represent a simple and low cost type of construction. However, window frames may have a serious fault in that severe current concentrations tend to exist on the bars near the corners. These current concentrations cause unacceptable long term damage as has been observed in experiments. To alleviate this difficulty, the current path is interrupted by separating the bars from the electrodes, and each bar is split into at least two elements. The electrode pair previously connected by virtue of the window frame technique must now be connected by external wires. This arrangement is shown in Fig. 1.3.1-9(b). In this design the window frame technique cannot be used, but the basic mechanical simplicity of a diagonal channel is retained.

There are two disadvantages to the single load diagonal channel concept. First, ideal single load diagonal channel performance will be less than that of the multiloaded Faraday machines because the loading cannot be adjusted to an arbitrary distribution along the channel's length. Secondly, part-load performance may be significantly less than that of any of the Faraday options. Multiple loading offsets these disadvantages. Two multiple loading schemes are depicted on Figs. 1.3.1.3-10(a) and 10(b) from Ref. 1.3-4. These apply to either window frames or split bar designs.

The design of the electrodes and insulators and the selection of materials of construction are determined by the requirements for efficiency and material durability and the severity of the environment to which they are exposed and the electrical phenomena occurring in the immediate vicinity of the walls. The high temperature of the plasma dictates that a means be provided to cool the wall elements, but not to such an extent that large heat transfer losses occur. From the viewpoint of phenomena occurring in the ionized gas itself, it is desirable to have the gas-side surfaces of the wall elements at high temperature. The wall elements must be able to withstand corrosion and erosion by oxidation and by electrolytic action as well as damage by arcing phenomena. Consideration must also be given to efficient transfer of electric current from the plasma to the external load through the elements and compatibility of materials with one another and with their environment.

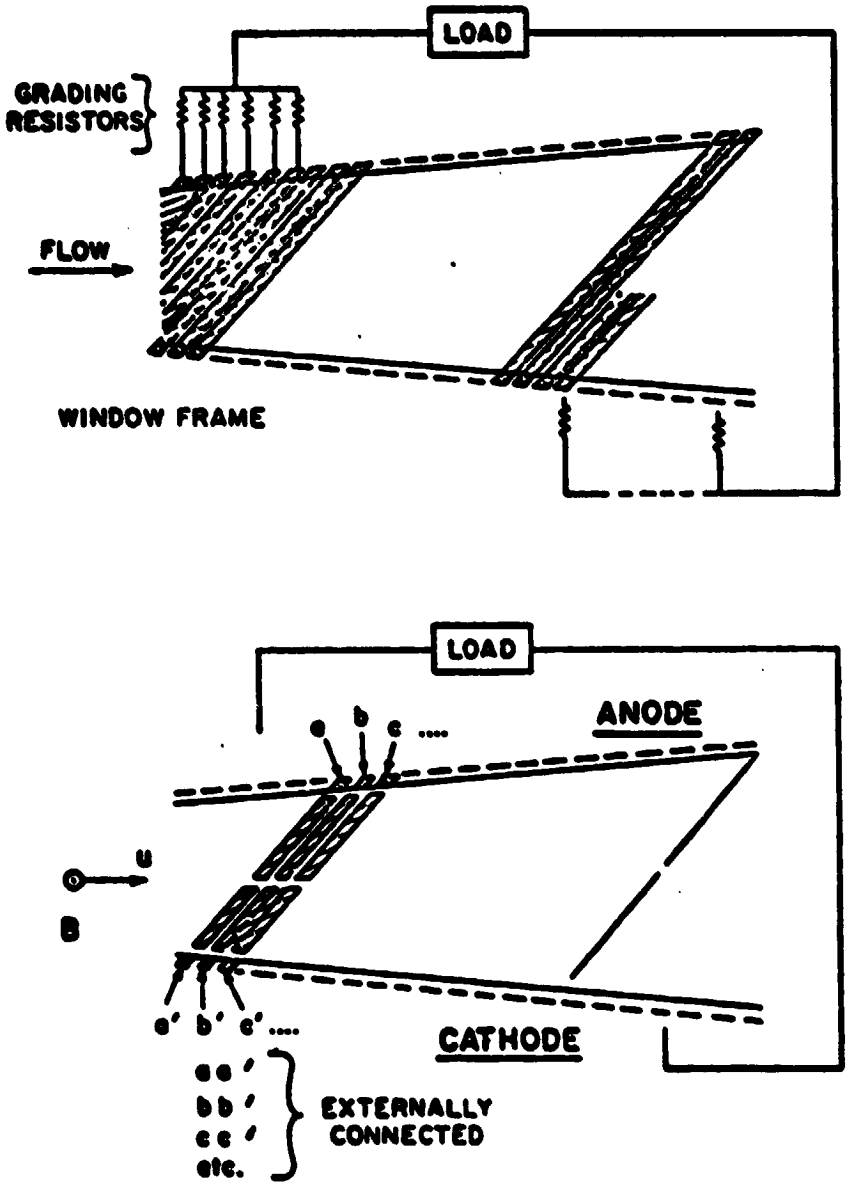

MHD CHANNELS WITH ALTERNATE TYPES OF DIAGONAL INTERCONNECTION

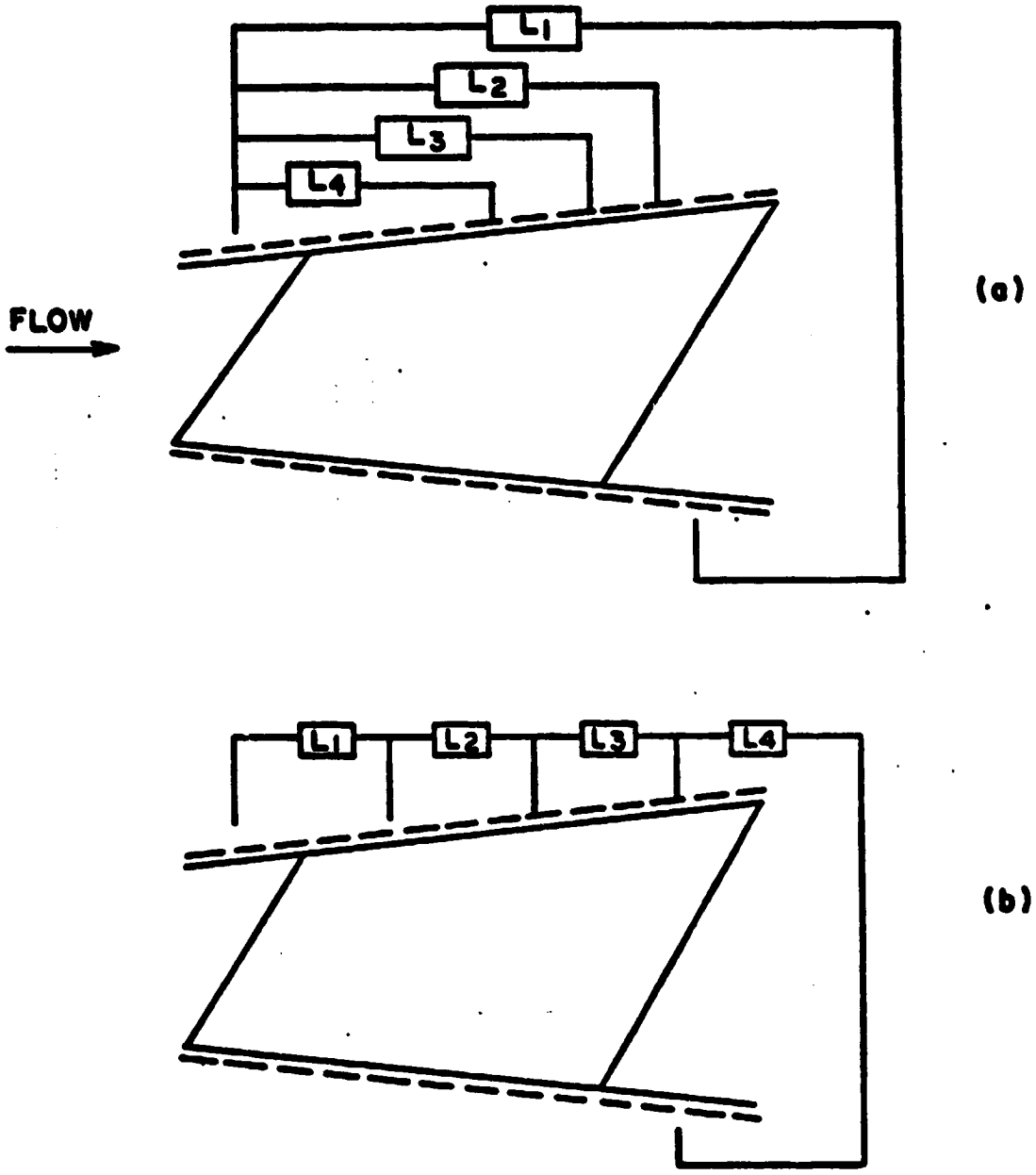

DIAGONAL MHD CHANNELS WITH MULTIPLE LOADS

An approach which has been established in the U.S. is to employ the principle of channel wall protection by deposition of a maintenance material on the interior surfaces of the channel. In the early 1960's, MHD channels were built and tested in which zirconia was injected into the gas stream to form a protective coating. The principle was to establish an equilibrium state in which the rate of erosion of this coating would equal the rate of deposition. More recently, coal slag has been utilized as the maintenance material since it is naturally present in the products of combustion in a direct coal-fired MHD plant. Experiments with coal-slag deposition have indicated that this is a feasible approach and is not detrimental to MHD generator performance or operation. Figure 1.3.1.3-11 schematically shows a channel in which the electrode walls are covered by a protective coating of a material which is continually eroded and replenished. Figure 1.3.1.3-12 schematically shows the various regions of the channel including the plasma and the electrode wall elements. Figure 1.3.13-13 from Ref. 1.3-5 illustrates a number of electrode system design configurations showing the different types of materials required in each design in order to fulfill the numerous requirements of the electrodes.

A specific electrode design, which has evolved at Avco after extensive testing over a period of several years with deposition of maintenance materials simulating the properties of coal slag, is illustrated in Figs. 1.3.1.3-14 for an insulating peg-wall design and 1.3.1.3-15 for an insulating bar-wall design. The basic electrode design is a water-cooled copper bar, clad with a thin layer of oxidation resistant material over vulnerable surfaces. Cladding materials under consideration include platinum, paladium, gold, silver, inconel and nickel. Extensive long duration testing is necessary to determine which materials are best, considering both technical performance and cost. The plasma-side surface of the electrode has grooves, prefilled with ceramic (e.g., zirconia), to provide attachment points for the deposited slag and thereby facilitate development of a slag layer. The high thermal conductivity and high thermal diffusivity of the copper substrate makes it more suitable as an electrode than other materials. Specifically, the local high heating associated with arcing phenomena is more readily dissipated in copper. Arc damage is thereby alleviated or avoided. Boron nitride (BN) hard spacers are employed as insulators since BN is a good thermal conductor, is resistant to thermal shock, and is not wetted by coal slag.

The design for insulator walls is the same as that for the electrodes, and essentially for the same reasons. Namely, water cooled copper peg or bar-segments are used, with grooves on the gas side surface to facilitate slag layer development. Dense aluminum oxide spacers may be used as gap insulators rather than BN to minimize cost. The various erosion difficulties are not as severe on insulator walls compared to electrode walls. But in the special case of a peg wall, experimental evidence indicates that BN is necessary. BN's capability to be better cooled than Al_2O_3, and its good resistance to thermal shock affords better protection of the numerous O-ring seals associated with a peg wall.

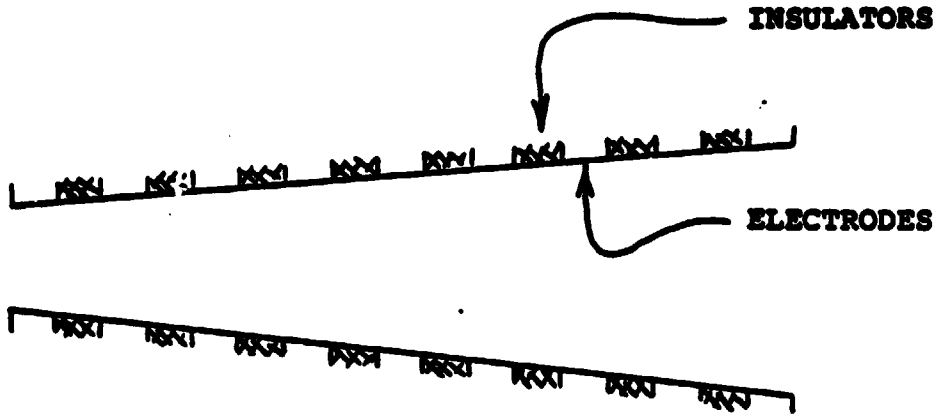

(a) CLEAN-FUEL SYSTEM

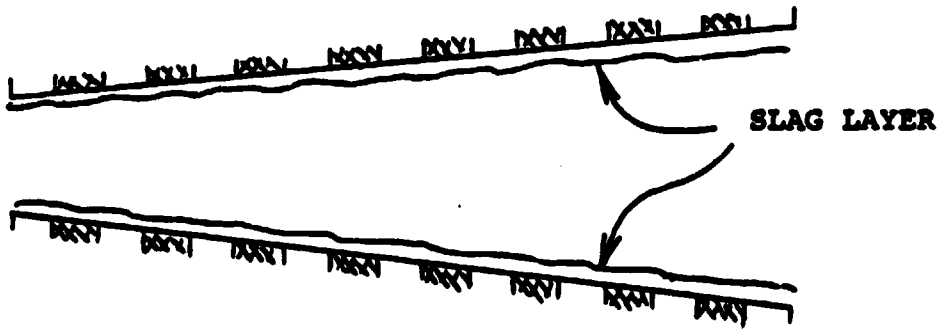

(b) COAL-FIRED SYSTEM

MHD CHANNELS WITH AND WITHOUT MAINTENANCE LAYERS

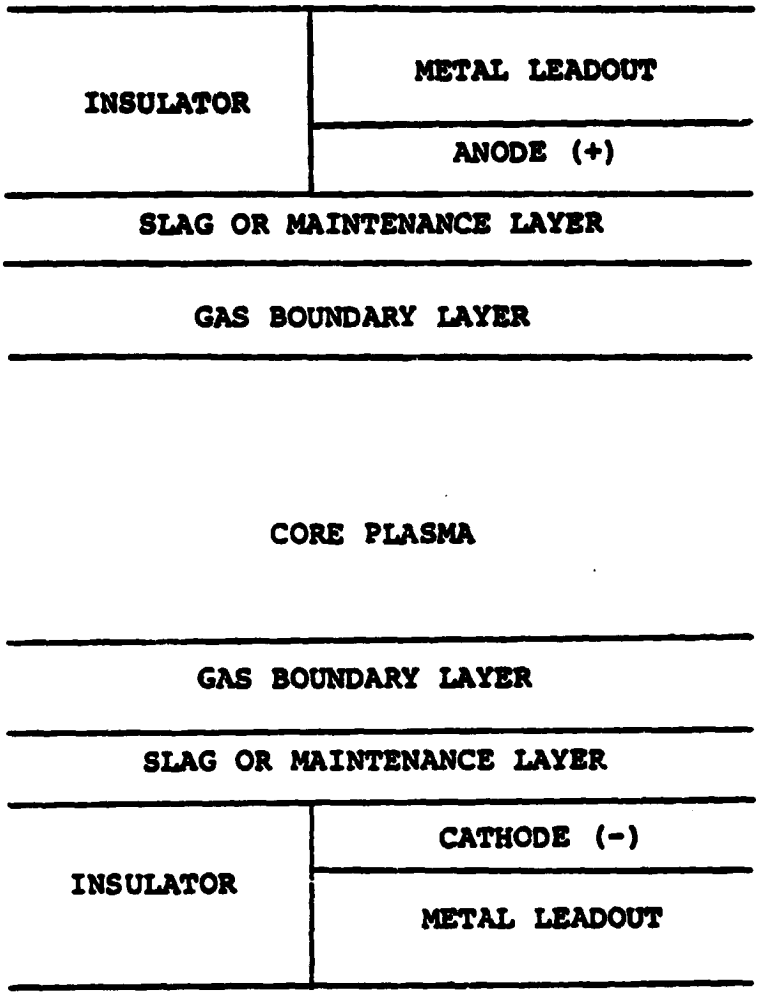

REGIONS OF ELECTRODE/ PLASMA SYSTEM

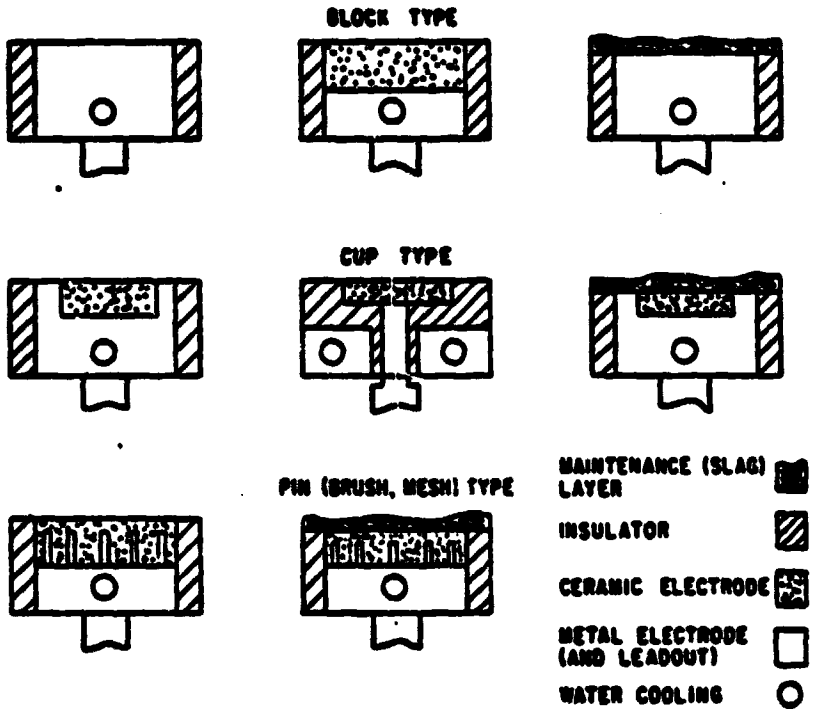

ELECTRODE SYSTEM CINFIGURATIONS

FIG. 1.3.1.3.-14

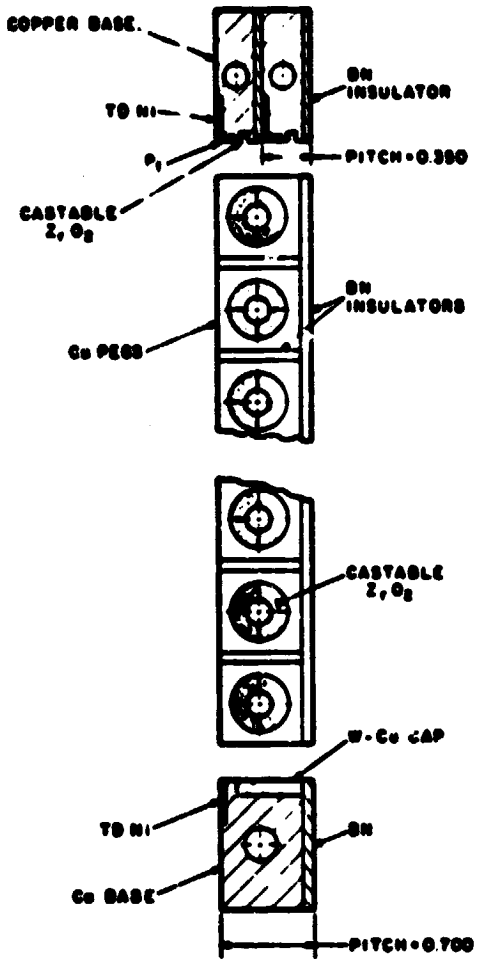

CATHODES

ELECTRODE AND PEG WALL DESIGN

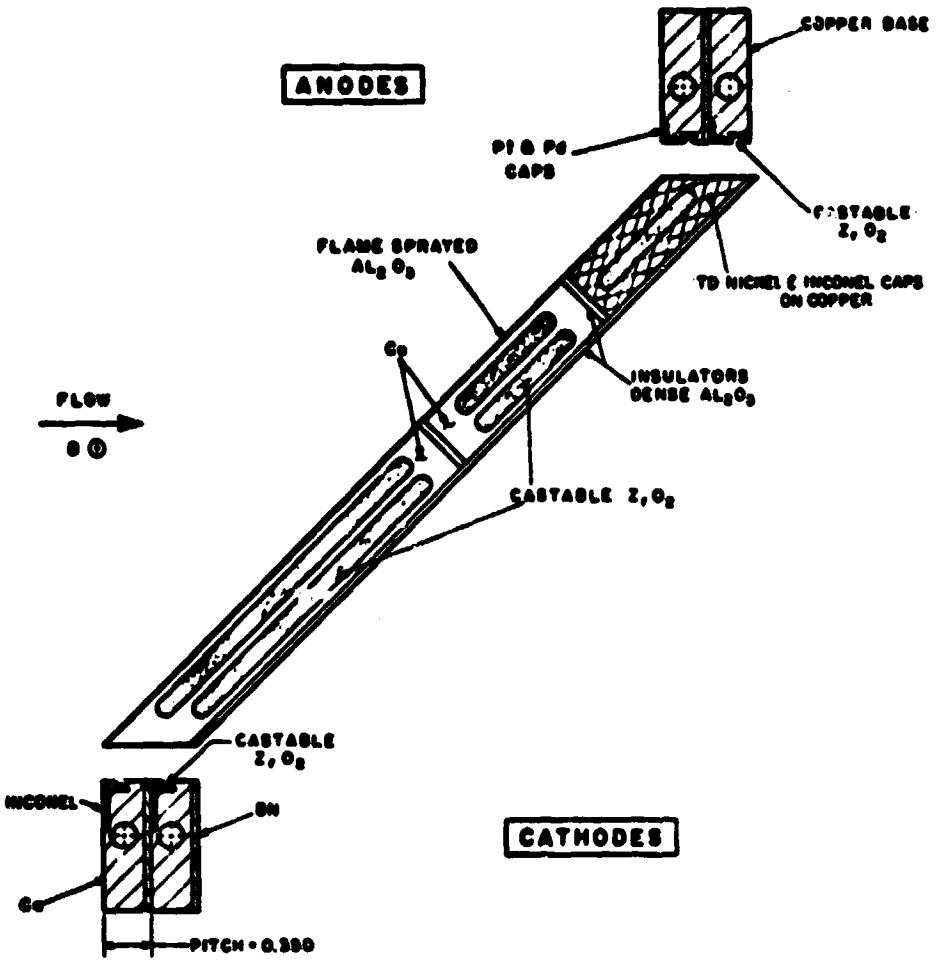

ELECTRODE AND BAR WALL DESIGN

1.3.2 Develop Data Base For MHD Programs

Because MHD systems are far from commercialization, there is no operational data base. It is possible, however, to review the development programs currently underway. An MHD power plant will include a number of components which require further research and development before they can perform satisfactorily. These include the MHD channel, superconducting magnet, inverter system, combustor, air preheater system, heat and seed recovery system and the seed regeneration system. In general, each of these components and systems must be scaled up to larger sizes than those which have been tested to date. Their performances in general require improvement and longer lifetimes must be demonstrated. In most cases, the performance is expected to improve as the components are scaled up. Further advances in system integration are also required as very few facilities presently exist in which all of the major components have been tested together as a unified system.

1.3.2.1 Major Test Facilities

A number of facilities exist in the U.S. for testing of specific MHD components at various scales. Two major facilities are now under construction for larger scale testing and for integration of components. These are the Coal Fired Flow Facility (CFFF) at the University of Tennessee Space Institute and the Component Development and Integration Facility (CDIF) in Butte, Montana. The objective of both facilities is to provide test data for long-duration operation at significant scales. Another major facility is the High Performance Demonstration Experiment (HPDE) facility at the Arnold Engineering and Development Center (AEDC).

The CFFF is a new facility which will initially have the capacity for a 20-MW thermal input and later will be increased to a 50-MW thermal level. Three test bays will be installed which will give the facility the capability for testing various combustor, channel and magnet configurations. Downstream equipment will be installed for testing steam bottoming plant components and recovery of seed from the gas stream. The CDIF will also be a coal-fired facility and will have a 50-MW thermal input capacity. Emphasis will be upon testing of MHD flow train components under conditions of low slag carryover (approximately 10 percent) into the channel. Both facilities are scheduled for initial startup in 1981.

The HPDE at AEDC is designed for short-duration operation (10 to 20 seconds) and began operation in 1979. Tests were performed in 1979 and 1980. The channel is now undergoing modification and will be started up again in 1981.

1.3.2.2 MHD Channel Technology

The principal design problems associated with the MHD channel are power extraction and durability. The electric power must be extracted from a multitude of electrodes and it must be controlled, conditioned and inverted to alternating current. The walls of the channel must resist a unique combination of electrochemical, electrodynamic, thermal and aerodynamic stresses. Effective power

extraction from MHD channels has been demonstrated at power levels up to 32 MW_e in the U.S. and up to 20 MW_e in the U.S.S.R. The results have given researchers confidence that large sized channels can perform according to expectations.

Long duration testing has been conducted at lower, yet significant, power levels. A U.S. channel has been operated by Avco for two continuous 250-hour test runs with a power output of several hundred kilowatts. Ash was injected into the combustor to simulate coal firing. Local electrical conditions near the electrode were comparable to conditions which would be anticipated in a larger scale channel. Testing of a channel with direct coal firing in the combustor has been achieved at the University of Tennessee Space Institute. In the U.S.S.R. a channel has been operated for 250 hours with the power output ranging from 3 to 11 MW_e.

The major organizations involved in MHD channel design, construction, testing or analysis include Avco-Everett Research Laboratory, University of Tennessee Space Institute (UTSI), Modern Electric Power Products and Services Company (MEPPSCO), Reynolds Metals Company (RMC) and STD Research Corporation. Avco has built and tested numerous generators including the largest tested to date. They have recently delivered a channel to CDIF site, along with a combustor of Avco's design. UTSI has built and extensively tested small channels utilizing coal as the fuel. Upon completion of the CFFF, UTSI capabilities will be greatly expanded. RMC is presently operating an MHD generator test facility. MEPPSCO has designed several very large generators, including the channel for the HPDE and a channel for the U-25 facility in the U.S.S.R. STD has developed extensive computer programs for analysis of MHD channel phenomena and behavior.

1.3.2.3 Superconducting Magnet

Superconducting magnet technology has experienced advances because of the wide application of large superconducting magnets. A magnet for an MHD plant requires a nearly uniform magnetic field of approximately 6 Tesla across an elongated channel. This is most effectively achieved by means of a saddle-shaped coil. The largest MHD superconducting magnet constructed to date is one which was manufactured in the U.S. and tested in the U.S.S.R. The magnet system weighed approximately 40 tons, produced a field of 5 tesla and had a stored energy capacity of 34 megajoules. The magnet has been operated successfully and reliably.

For commercial application in a 1000-MW_e power plant, the magnet would have to be scaled up to approximately a 5000 megajoule stored energy capacity. The major difficulties anticipated in scaling up to this level is in the area of structural integrity in the presence of very large magnetic forces, construction techniques for the coils and keeping the magnet cost within reason. This is viewed as a design problem rather than a technology problem as no technological breakthroughs are required.

The DOE MHD superconducting magnet programs are being conducted under management of the Francis Bitter National Magnet Laboratory at MIT. Organizations which have built or are building magnets for MHD facilities include Argonne National Laboratories, Magnetic Corporation of America and G.E.

1.3.2.4 Inverter Systems

Inverter technology is another area in which advances have been made without assistance from the MHD program. Application of inverters in MHD systems has been very limited to date. In most of the experiments, the generated electrical power is dissipated in a resistive load. In the U-25 facility in the U.S.S.R., MHD power has been fed to the Moscow grid by means of inverters. The cumulative time over which this has occurred to date is more than 800 hours.

Inverter equipment is presently available. The major area in which development is required is in designing an inverter system to meet the requirements of an MHD channel. The Electric Power Research Institute (EPRI) is playing a major role in the inverter program for MHD. EPRI is responsible for the procurement of the inverter system which will be installed in the Component Development and Integration Facility in Butte, Montana. Avco-Everett Research Laboratory, Westinghouse, General Electric Company and the University of Tennessee Space Institute are engaged in work on MHD inverter systems.

1.3.2.5 Combustors

MHD combustors must provide a very high temperature gas with a rather uniform flow with uniform mixing of seed to the MHD channel. Combustor operating pressures must be in the range of five to ten atmospheres. A major criterion for combustor performance is minimum heat loss through the walls of the combustor. When coal is used as a fuel, the coal slag must be handled, as well. One major coal-fired combustor approach is to remove up to 90 percent of the slag from the combustor. Another major approach is to allow all of the slag to be carried over into the MHD channel.

A combustor utilizing clean fuel with a thermal power input of 250 MW has been successfully operated in the U.S.S.R. Combustors utilizing coal as the fuel have been operated in the U.S. inlcuding an 8-MW_t combustor without slag removal and a 5-MW_t combustor which achieved 95-percent slag removal. Future development programs are aimed at scaling up present-day combustor designs and reducing heat losses.

The Pittsburgh Energy Technology Center is responsible for the DOE MHD combustor programs. Avco, TRW and Rockedyne Division of Rockwell International have all developed combustor designs and have built and tested them at the 20-MW_t level.

1.3.2.6 Air Preheater Systems

Regenerative air preheater systems of the type required for MHD power plants have been utilized in the steel industry for many years. Their temperature of operation, however, is below that required for MHD systems. Regenerative air preheaters for MHD have been constructed and tested. Preheaters operating on clean fuels have been tested in the U.S. for over 100 hours with air outlet temperatures over 3000°F. In the U.S.S.R., separately fired air preheaters have operated as part of an MHD pilot plant, with air preheat temperatures up to 2240°F.

Scaling up separately-fired high temperature air heaters to commercial power plant size appears to be achievable provided clean fuels are utilized. The challenge is in the area of developing a coal combustion system which can provide sufficiently clean combustion products to fire the heaters. Direct fired air preheaters represent a greater benefit in terms of plant efficiency as well as a greater challenge in terms of development. Materials capable of withstanding the severe seed/slag environment of a direct-fired air preheater system are currently being investigated. Extensive testing programs and materials analysis programs are in progress. Air preheating elements have undergone over 800 hours of testing in a slag/seed environment at temperatures up to 2780°F. Substantial programs on high temperature air preheater development have been undertaken by FluiDyne Engineering Corporation, Avco and G.E.

1.3.2.7 Heat Recovery/Seed Recovery Systems

The heat recovery system includes the heat transfer surfaces which transfer heat from the hot gas flow stream to the steam bottoming plant boiler feedwater and produce steam for driving the steam turbines. The seed recovery system includes the surfaces and equipment which contribute to the removal of seed compounds from the hot gas flow stream. Basically, these systems are comprised of conventional steam plant boiler equipment and particulate removal systems such as electrostatic precipitators. However, the seed-laden environment presents a considerable challenge in terms of prevention of corrosion, erosion and plugging as well as designing the system to optimize the collection of seed.

Testing programs to simulate MHD plant gas compositon an flow conditions in heat recovery equipment are being conducted at Mississippi State University and Argonne National Laboratory. The Department of Energy has issued a contract to Babcock and Wilcox Company for the design, construction and installation of a larger heat-recovery/seed-recovery system at the Coal Fired Flow Facility at the UTSI site.

1.3.2 Seed Regeneration Systems

Conversion of K_2SO_4 recovered from the exhaust gases into K_2CO_3 for purposes of recycling seed to the combustor can be accomplished by a number of chemical processes. The challenge to the MHD program is to select or develop a seed

regeneration system which is economical in terms of capital equipment costs, operating costs and energy consumption. A process referred to as the "Formate" process was used in Europe for the production of K_2CO_3. The Pittsburgh Energy Technology Center has proposed a more economical process for seed regeneration which also separates ash from the seed compounds. Testing has been performed on the bench-scale level. Further testing at larger scales is required in order to evaluate the economic feasibility of this scheme.

1.3.3 Characteristics of MHD Systems

Several comprehensive open-cycle MHD power plant parametric studies and conceptual designs have been conducted in the U.S. over the past five years. The purposes of these investigations have been primarily to assess the potential economic benefits to be gained from developing MHD technology, determine the optimum MHD power plant configurations for both early commercial and second generation technologies, and to establish a basis for planning and evaluating government-sponsored MHD research and development programs. These investigations have been funded by the Energy Research and Development Administration (ERDA), the Department of Energy (DOE) and the Electric Power Research Institute (EPRI).

The first of these comprehensive studies was the Energy Conversion Alternatives Study (ECAS), which was administered and managed by the National Aeronautics and Space Administration (NASA) - Lewis Research Center and supported by ERDA and the National Science Foundation (NSF). The purpose of this study was to develop estimates on power plant costs and energy production costs for a number of advanced coal-fueled electric energy conversion technologies including gas turbines, combined cycles, MHD, fuel cells, etc. The two major prime contractors were General Electric Co. and Westinghouse Electric Corporation. Avco-Everett Research Laboratory assisted GE with the MHD power plant analysis as a subcontractor. The ECAS program was conducted in two phases, beginning in 1975. In the first phase, both GE and Westinghouse examined several MHD power plant configurations with a number of variations in major design parameters. In the second phase, GE developed a conceptual design and analyzed costs and performance for the most promising MHD power plant configuration. MHD was not included by Westinghouse in the second phase.

Two investigations were conducted under EPRI sponsorship following the completion of ECAS. The emphasis of these investigations was directed towards several optional configurations not considered in ECAS and towards a technology base which was considered to be less advanced than that of ECAS. The two prime contractors in these investigations were Westinghouse and STD Research Corporation.

The most recent comprehensive comparative MHD study is the Parametric Study of Potential Early Commercial MHD Power Generation (PSPEC). Contracts for the PSPEC program were awarded by NASA-Lewis Research Center to GE and Avco-Everett Research Laboratory and a grant was awarded to the University of Tennessee Space Institute (UTSI). As the name implies, the emphasis in the PSPEC program was on

"first generation" commercial MHD technology rather than on the more advanced technology status assumed in ECAS. Work on the PSEC MHD power plant concepts is being extended through a program called the Conceptual Design Study of Potential Early Commercial MHD Power Generation (CSPEC). NASA has awarded contracts for the CSPEC program to GE and Avco.

1.3.3.1 MHD Power Plant Design Variations

A large number of variations of MHD power plant configurations were considered in the ECAS, EPRI and PSPEC investigations. These variations are indicated in Table 1.3.3.1-1. In addition to varying the plant configurations, major plant parameters were also varied in order to determine the optimum plant designs and to determine the characteristics of each configuration. Parameters which were varied included:

- air preheat temperature
- oxygen enrichment level
- ash carryover into channel
- seed concentration in channel
- combustor pressure and temperature
- extent of coal drying
- magnetic field strength
- channel loading parameter

The plants ranged in size from approximately 600 MWe to 2000 MWe for the ECAS program and from approximately 400 to 1000 MWe for the PSPEC and the EPRI programs.

1.3.3.2 Descriptions of Selected MHD Cycles

Several of the configurations considered in the ECAS and PSPEC investigations will be described in this section because of the insights revealed and their relevance to the selection of an MHD power plant configuration to be considered for use with over-the-fence gasified coal and with an integrated coal gasifier.

Integrated Low-Btu Gasifier Cycle

The only cycle which included the use of a clean low Btu gas as a fuel for the MHD combustor was one which was investigated by Westinghouse in Phase 1 of the ECAS program, (Ref. 1.3-6). Figure 1.3.3.2-1 is a schematic diagram of this cycle. The gasifier is a Westinghouse fluidized bed gasifier incorporating high-temperature desulfurization. The gasifier is integrated into the MHD cycle, in that the gasifier air is bled from the MHD compressor discharge after being preheated by the MHD exhaust gas. The clean product fuel gas is also preheated by the MHD exhaust gas. Steam is also supplied to the gasifier from the steam bottoming plant. A schematic diagram of the Westinghouse fluidized bed gasifier is shown in Fig. 1.3.3.2-2 (Ref. 1.3-7).

TABLE 1.3.3.1-1

VARIATIONS IN MHD POWER PLANT CONFIGURATIONS

Type of Fuel

- Illinois No. 6 coal
- Montana Rosebud coal
- North Dakota lignite
- Solvent refined coal (SRC)

Types of Seed Material

- Potassium
- Cesium

Fuel Utilization by MHD Combustor

- Direct coal firing
- Integrated low Btu cleanup
  - with fuel gas cleanup
  - without fuel gas cleanup
- Char from air-preheater carbonizer

Combustor Type

- Single stage
- Multiple stage

MHD Channel Interconnection

- Faraday
- Diagnoal

Oxidizer

- Preheated air (high temperature)
- Oxygen enriched air

Air Preheat Mode

- Direct-fired high temperature air heater (DFHTAH)
- Separately-fired high temperature air heater (SFHTAH)
  - atmospheric pressure
  - pressurized

TABLE 1.3.3.1-1 (Cont'd)

VARIATIONS IN MHD POWER PLANT CONFIGURATIONS

Fuel Source for SFHTAH

- Direct coal firing with slagging combustor
- Vapor from coal carbonizer
- Integrated low Btu gasifier
- Chemically active pressurized fluidized bed

Oxygen Supply

- Over-the-fence purchase
- On-site high-purity air separation plant
- On-site low-purity air separation plant

Bottoming Plant

- Air turbine
- Subcritical steam plant with reheat
- Supercritical steam plant with reheat

Nitrogen Oxide Control Method

- Combustion control with homogenous decomposition
- Supplemental ammonia injection
- Supplemental catalytic decomposition
- Scrubbing for maximum HNO_3 production

Sulfur Recovery Method

- Seed regeneration
- Conventional flue gas desulfurization
- Low Btu Fuel Gas Desulfurization
- Combined sulfur recovery with HNO_3 production

Seed Regeneration Method

- PETC (i.e., PERC or USBM) process
- Formate process

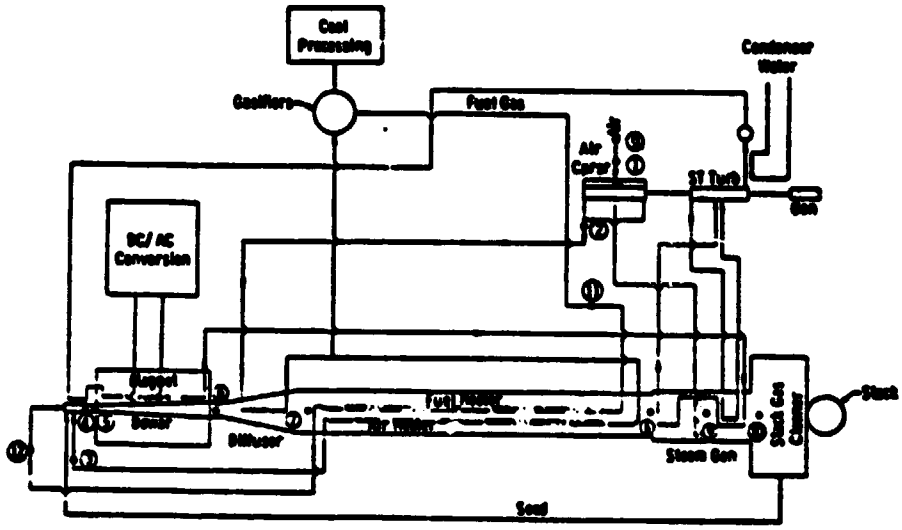

MHD POWER PLANT CYCLE WITH INTEGRATED LOW BTU GASIFIER

FIG. 1.3.3.2-2

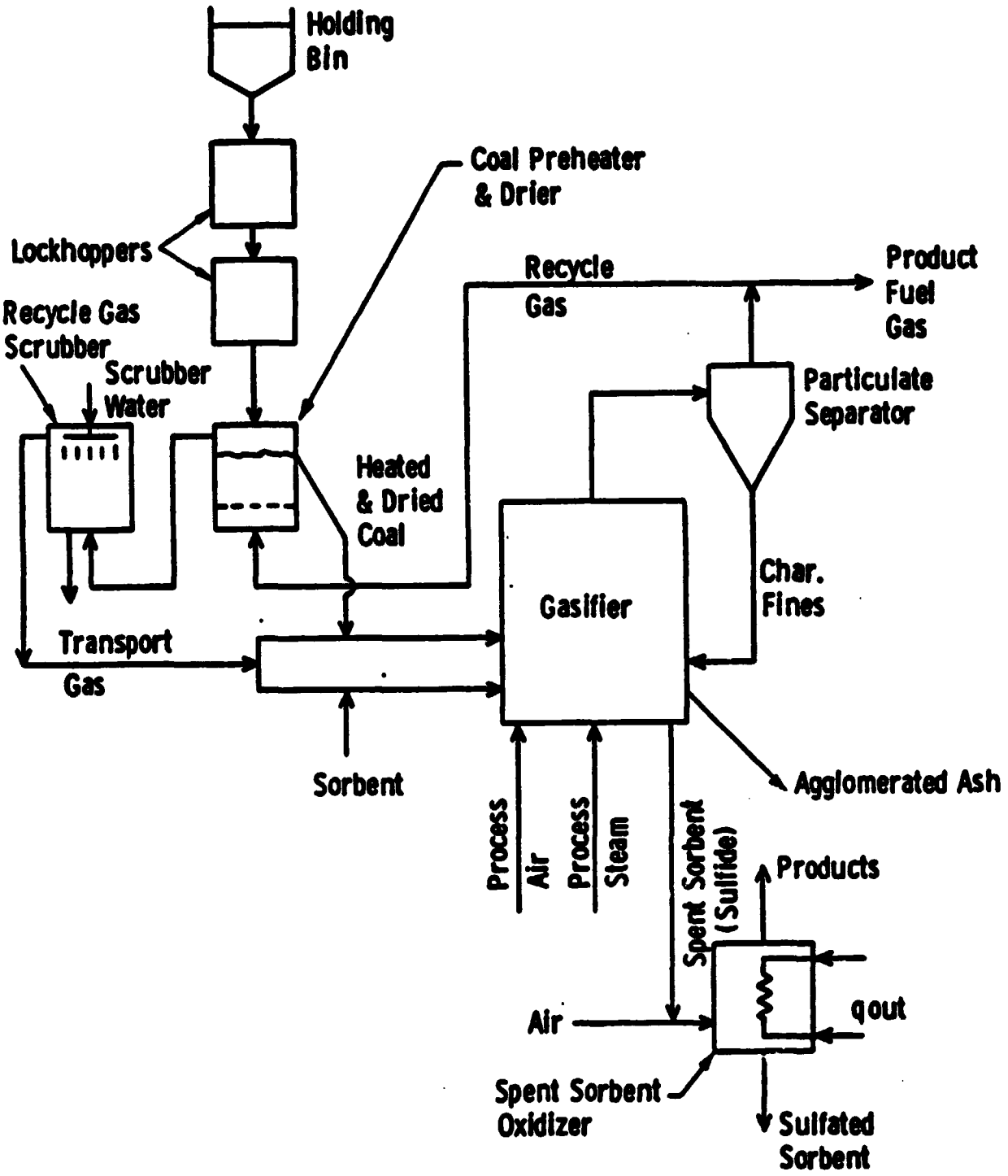

FLUIDIZED BED GASIFICATION PROCESS WITH HIGH TEMPERATURE SULFUR AND PARTICULATE REMOVAL

This cycle employs a direct-fired high temperature air heater. No oxygen is added to the air. The seed material is cesium. Since the sulfur removal is performed prior to combustion, the seed is recovered primarily in the form of cesium carbonate and recycled directly to the combustor along with additional seed to make up for losses. The steam bottoming plant employs a supercritical single-reheat steam cycle. For a nominal power plant output of 2000 MWe, the plant efficiency was estimated to be in the range of 48 to 54 percent, depending upon design conditions. This efficiency compares favorably with other ECAS configurations considered by Westinghouse, but the cost of electricity was estimated to be higher than those of the other configurations.

Direct Coal Fired Plant With Direct Air Preheating

The MHD cycle which was selected in Phase I of the ECAS program as the most economical cycle was a direct coal-fired MHD power plant with a direct-fired high temperature air heater. This is the cycle for which GE conducted a conceptual design study in Phase 2 of the ECAS program (Ref. 1.3-1). A simplified schematic diagram of the GE cycle is shown in Fig. 1.3.3.2-3.

In this cycle, the oxidizer is air which is preheated by the MHD exhaust gas. The seed is potassium, which is recovered from the exhaust gas primarily as K_2SO_4 and converted to K_2CO_3 for recycle to the combustor. The seed regeneration process is the "PERC" process which requires a synthesis gas such as that produced by a medium-Btu coal gasifier. The steam bottoming plant employs a supercritical single-reheat steam cycle. For a power plant output of 1932 MWe, the overall efficiency is estimated to be 48.3 percent. The gross MHD generator output is 1406 MWe. The gross steam plant electric power output is 587 MWe and the plant auxiliary electric load is 61 MWe. The compressor power requirement is 372 MW, which is provided by steam-turbine mechanical drive.

Figure 1.3.3.2-4 is a more detailed schematic diagram of this cycle. It illustrates the extent of integration of the MHD topping cycle, the MHD bottoming cycle and the seed regeneration system. Boiler feed water for the steam plant is heated in cooling passages in the walls of the combustor, MHD channel and diffuser; the air compressor is driven mechanically by a steam turbine; air for MHD combustion and air for seed reprocessing are preheated by the MHD exhaust gas which is also used for coal drying.

Direct Coal Fired Plant With Indirect Air Preheating

Both of the cycles described thus far in this section employ direct-fired high temperature air preheating. Although these cycles lead to high power plant efficiency, the direct-fired high temperature air heater is a component which requires significant advancement in the current state-of-the-art in order to attain commercial feasibility. It appears that the practical approach to early commercial MHD power generation is to employ a separately-fired high temperature air heater (SFHTAH) or to utilize a cycle which is based upon oxygen enrichment of the air.

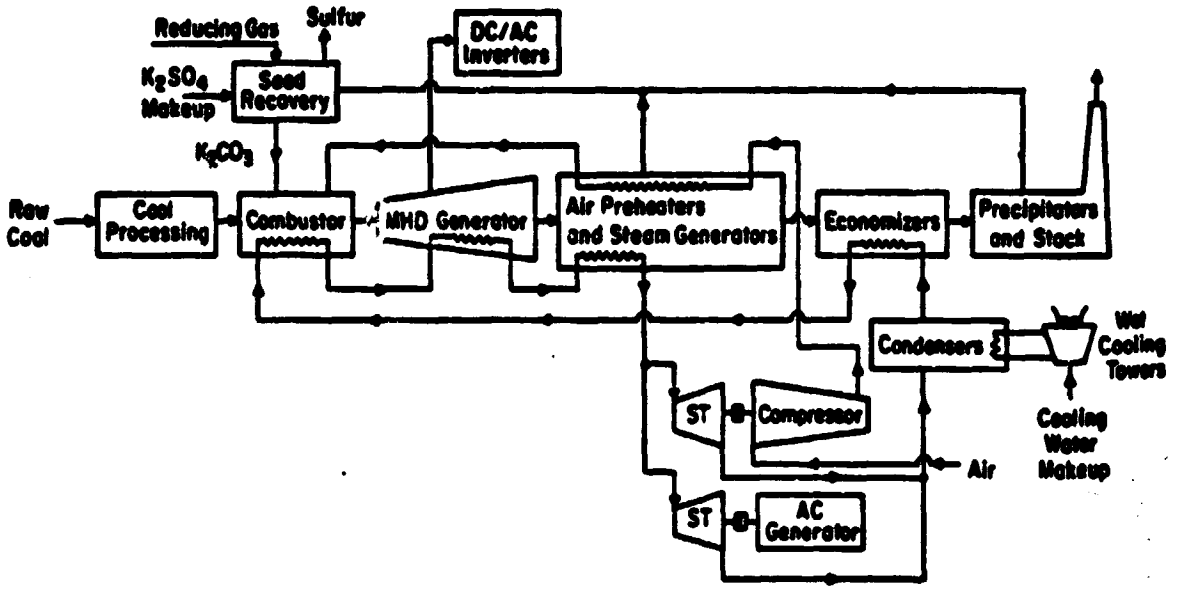

MHD POWER PLANT CYCLE WITH DIRECT–FIRED HIGH TEMPERATURE AIR PREHEATER

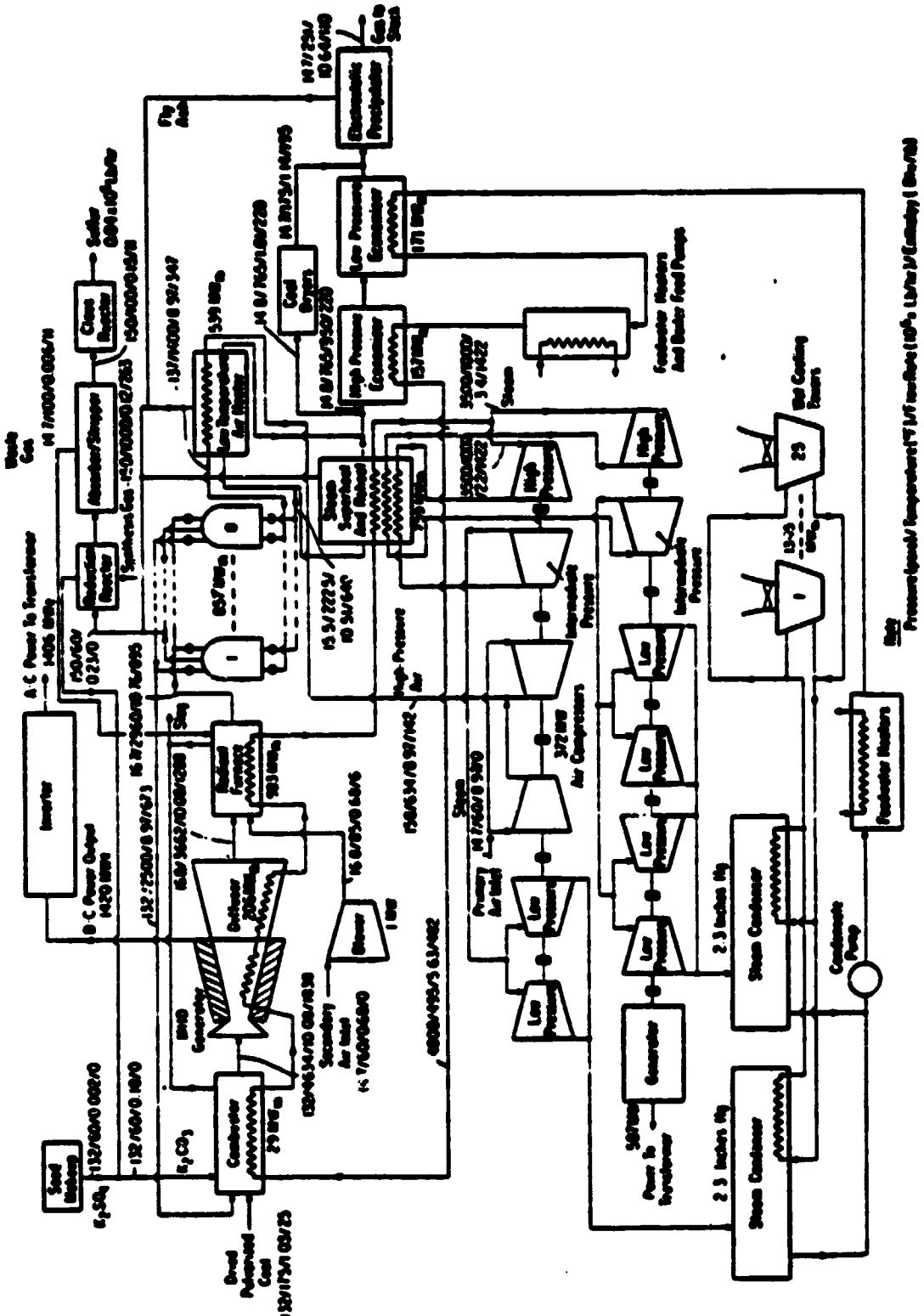

MHD POWER PLANT CYCLE WITH DIRECT-FIRED HIGH TEMPERATURE AIR PREHEATER

Figure 1.3.3.2-5 is a schematic diagram of one of the SFHTAH cycles investigated by Avco in the PSPEC program (Ref. 1.3-2). The MHD combustor is directly fired with coal. However, the SFHTAH, which is more susceptible to plugging due to ash, is fired with a low Btu gas produced from coal in a series of Wellman-Galusha fixed bed gasifier units. All of the fuel gas produced in the gasifier is cleaned of particulate matter, but only part (approximately one half) undergoes sulfur removal (low temperature), as shown in Fig. 1.3.3.2-6. The fuel gas is preheated by MHD exhaust gas prior to burning in the SFHTAH combustors. The products of combustion from the SFHTAH units are mixed with the MHD exhaust gas stream prior to discharge to allow additional sulfur removal in conjunction with seed recovery. The MHD exhaust gas is also utilized for coal drying.

MHD power plants of this configuration were investigated in the size range of approximately 400 to 900 MWe net power output. Estimated efficiencies ranged from 41.4 to 43.2 percent, depending upon various design parameters. For a typical case with a net power output of 936.1 MWe, the MHD generator d.c. power output is 495 MWe and the steam plant output is 611.6 MW, including electrical power generated and mechanical steam drives for compressors and pumps. The compressor-drive power requirement is 113 MW and the total auxiliary load and related losses is 57.5 MW, resulting in a net plant power output of 936.1 MWe with an efficiency of 42.5 percent.

The seed regeneration method proposed by Avco for this cycle is the formate process. This process requires a gas rich in CO. The proposed source of CO is a coke gasifier. The formate process produces $CaSO_4$ which requires disposal. Heat from the MHD combustor channel and diffuser is used to heat boiler feedwater. The steam plant is a subcritical cycle with single reheat.

Direct Coal-Fired Plant With Oxygen Enrichment

Figure 1.3.3.2-7 is a schematic diagram of the oxygen-enriched-air cycle investigated by Avco in the PSPEC program (Ref. 1.3-2). The MHD combustor is directly fired with coal and the oxidizer is preheated to moderate temperature (within the current state-of-the-art) by the MHD exhaust gas. The oxygen is provided by an on-site air separation plant which is integrated with the steam bottoming plant by utilizing steam-turbine drives for the air separation plant compressors. The air separation plant produces oxygen of 80-percent purity to provide a total oxygen content of the combustion gas of 29.2 to 39.1 percent by volume. The proposed seed regeneration method is the formate process utilizing a coke gasifier to provide the required CO. As in the previous cycle, $CaSO_4$ from the seed regeneration system must be discarded; MHD combustor and channel cooling provide boiler feedwater heating; the air compressor is steam-turbine driven and coal drying is accomplished with MHD exhaust gas. The steam plant is a subcritical cycle with single reheat.

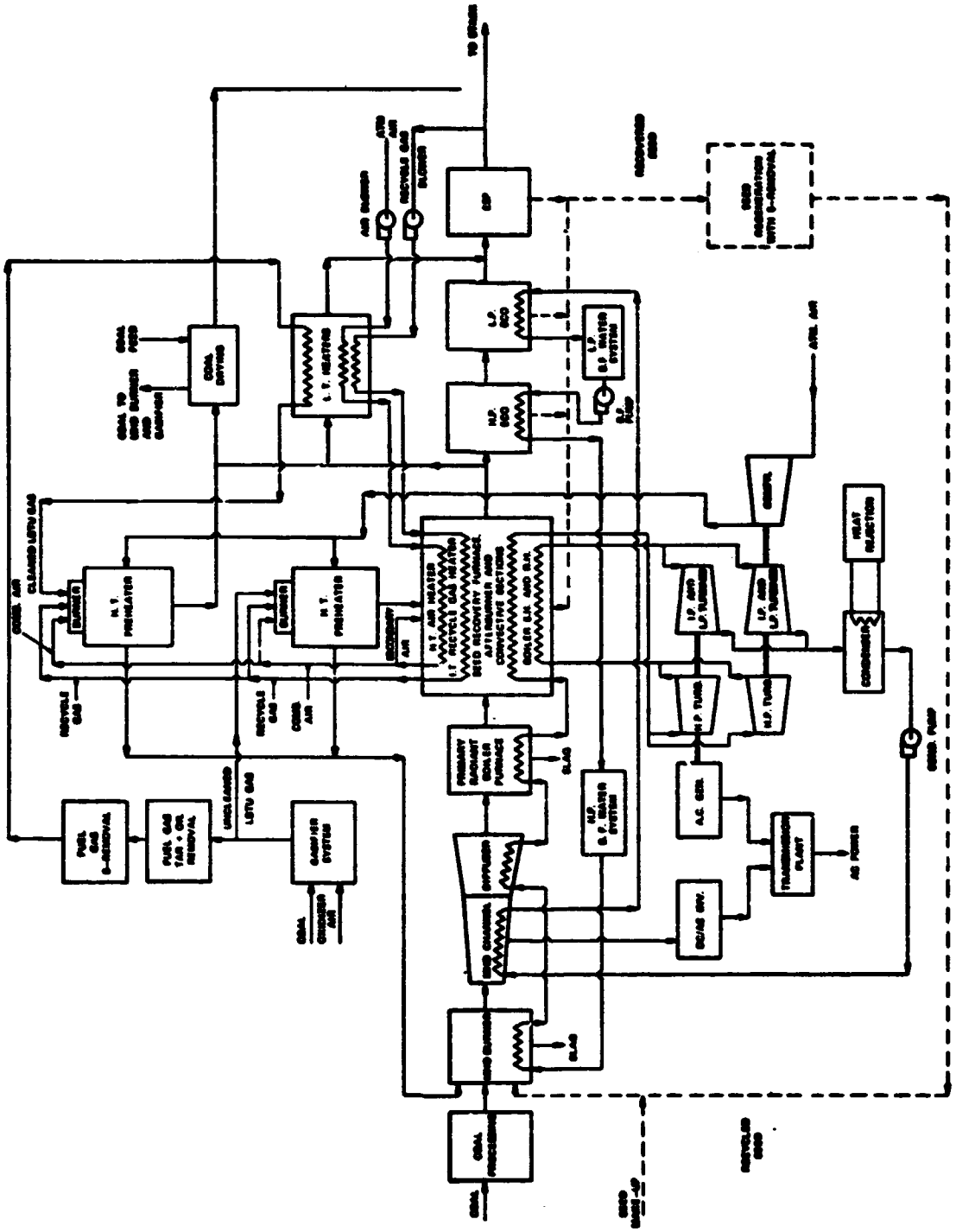

MHD POWER PLANT CYCLE WITH SEPARATELY-FIRED HIGH TEMPERATURE AIR PREHEATER

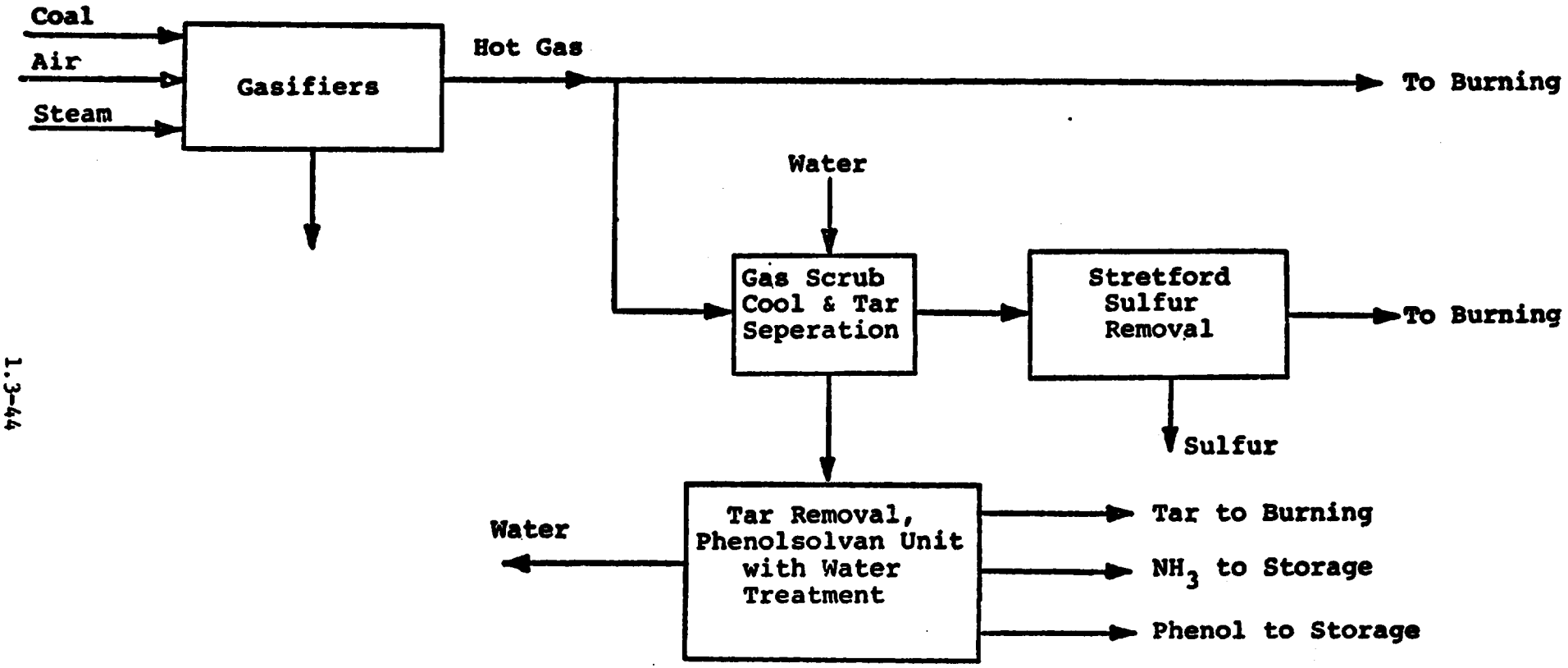

GASIFIER SYSTEM FOR SEPARATELY–FIRED HIGH TEMPERATURE AIR HEATER PREHEATER

FIG. 1.3.2-6

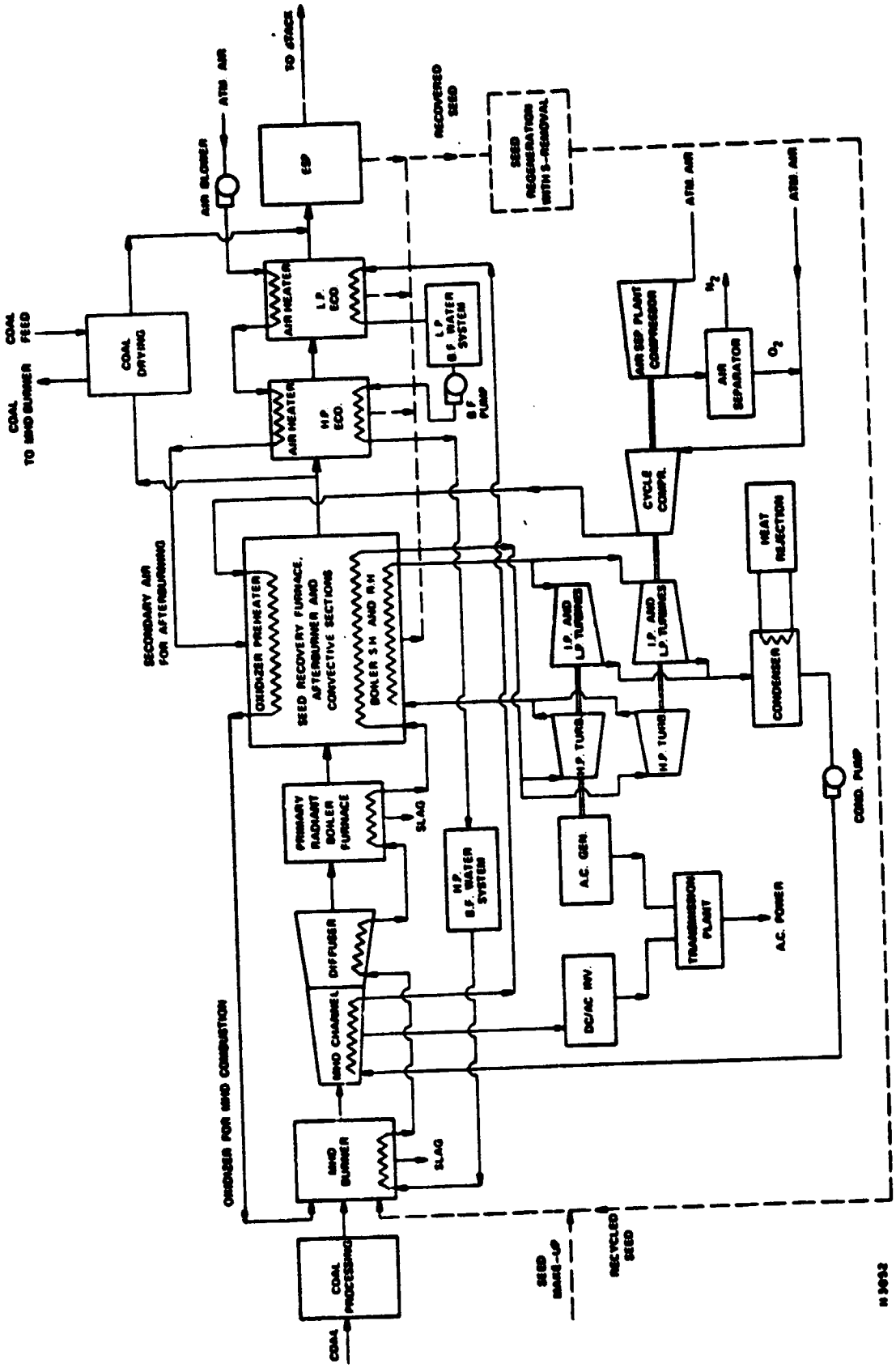

MHD POWER PLANT CYCLE WITH OXYGEN ENRICHMENT

MHD power plants of this configuration were investigated in the size range of approximately 600 to 900 MWe net power output. Estimated efficiencies ranged from 42.9 to 44.4 percent, depending upon various design parameters. For a typical case, with a net power output of 930.7 MWe, the MHD generator d.c. power output is 523 MWe and the steam plant output is 636.3 MW including electrical power generated and mechanical steam drives for compressors and pumps. The compressor-drive power requirement is 175.5 MW and the total auxiliary load and related losses is 53.1 MW, resulting in a net plant power output of 930.7 MWe with an efficiency of 43.4 percent.

1.3.3.3 Other MHD Configurations

A number of other investigations have been conducted in recent years which have a bearing on the selection of a configuration for the combination of a coal gasifer and an MHD power plant. The emphasis in the U.S. is on direct coal-fired MHD power generation. The program in the U.S.S.R. has been primarily directed towards the use of natural gas as a fuel. Although MHD experiments have been conducted in the U.S.S.R. with the combustion of coal, it is anticipated that the first Soviet large-scale MHD power plant will be fired with natural gas. The only countries which have recently conducted investigations involving low or medium Btu gas as a fuel for the MHD combustor are India, Poland and Sweden.

India has considerable reserves of coal with high ash content. The government of India is presently supporting an MHD research and development program which is aimed at developing an MHD plant using low Btu gas as a fuel. An investigation was conducted during the early stages of this program to compare the potential suitability of various gasification processes for MHD application (Ref. 1.3-8). The processes considered were Lurgi, blue water, Koppers-Totzek and producer gas. The primary criteria for comparison were the theoretical flame temperature and the electrical conductivity of the plasma under various conditions of air preheat temperature and oxygen enrichment. All of the gases except producer gas were determined to be acceptable, with Lurgi gas being the most promising. A pilot plant is presently under construction which will utilize blue water gas as a fuel because of its availability at the selected site.

The MHD research and development program in Poland is aimed at direct coal firing. Theoretical investigations have been conducted in Poland regarding MHD with coal gasification, but information on these investigations is not presently available. A study was recently conducted in Sweden of an MHD cycle in which coal is gasified by use of the exhaust gas from the MHD generator (Ref. 1.3-9). Figure 1.3.3.3-1 is a schematic diagram of this cycle. Investigations of this concept have previously been conducted in several countries, including the U.S. The concept leads to a very efficient power plant, but it is in a relatively primitive stage of development compared to conventional coal gasification techniques.

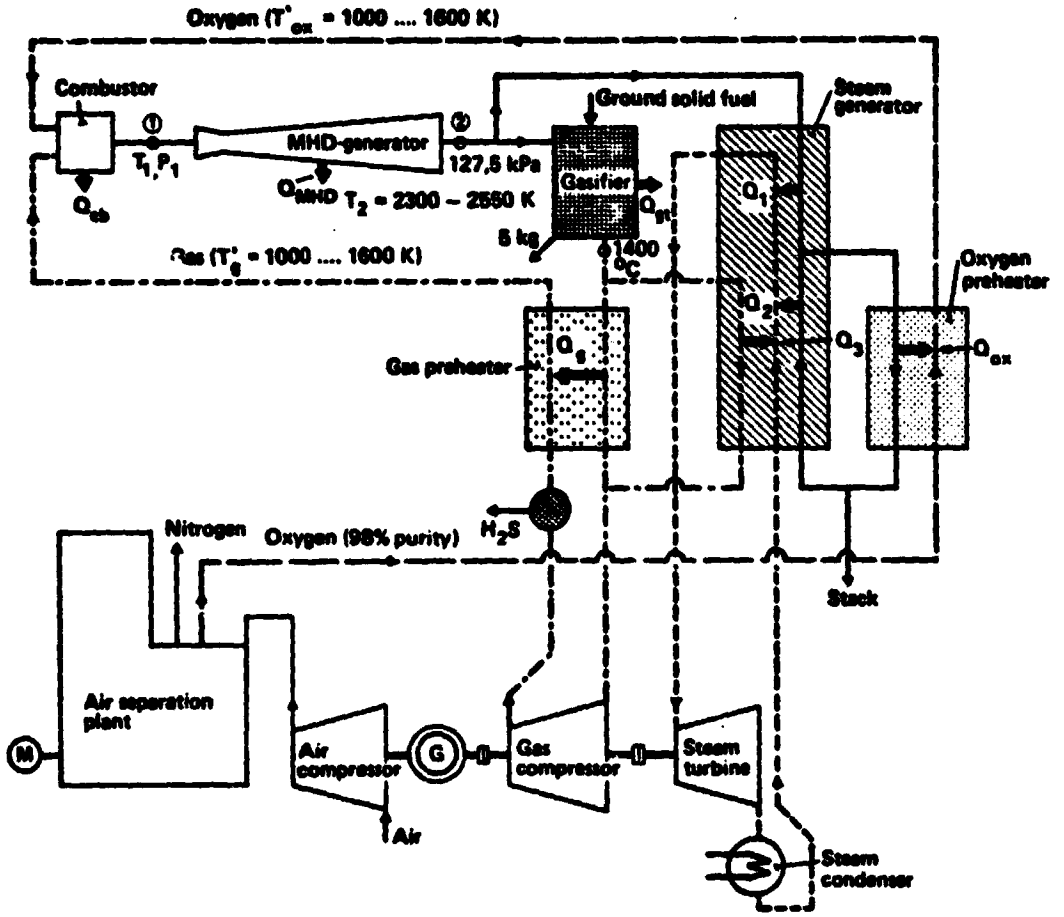

MHD POWER PLANT CYCLE WITH TAIL GASIFICATION

A major program in the U.S. is the Engineering Test Facility (ETF) program. This is a facility which is presently in the planning stage. The ETF is an MHD pilot plant with a net power output of several hundred MWe and is conceived to be the next major step between facilities now under construction and the first commercial scale MHD power plant. The ETF program was initiated with the award by ERDA of contracts to GE, Westinghouse and Avco for extensive ETF conceptual design studies. Upon completion of these studies, further work on MHD ETF design criteria and facility definition has been conducted under program management by NASA-Lewis Research Center. The importance of this work lies in the fact that decisions being made with regard to the MHD ETF configuration will largely determine the direction of current MHD research and development programs.

1.3.4 References

1.3-1 Harris, L. P., Shah, R. P., Energy Conversion Alternatives Study (ECAS), General Electric Phase II Final Report, NASA CR-134949, Vol. II, Part 3, 1976.

1.3-2 Hals, F. A., Avco-Everett Research Laboratory, Inc., Parametric Study of Potential Early Commerical MHD Power Plants, DOE/NASA/0051-79/1, NASA CR-159633, December 1979.

1.3-3 Avco-Everett Research Laboratory, Fifty MW Experimental MHD Power Plant - Phase I Final Report, April 1971.

1.3-4 Avco-Everett Research Laboratory, Engineering Test Facility Conceptual Design Final Report, DOE REport FE-2614-2, June 1978.

1.3-5 Petrick, M., Shumyatsky, B. Ya., Open Cycle Magnetohydrodynamic Electrical Power Generation, A Joint U.S.A./U.S.S.R. Publication, Argonne National Laboratory, 1978.

1.3.-6 Hoover, D. Q., et al., Energy Conversion Alternatives Study (ECAS), Westinghouse Phase I Final Report, NASA CR-134941, Vol. VIII, 1976.

1.3-7 Hamm, J. R., et al., Energy Conversion Alternatives Study (ECAS), Westinghouse Phase I Final Report, NASA CR-134941, Vol. III, 1976.

1.3-8 Ramaprasad, V. R., Pilot Plant in the Indian MHD Research Complex, Seventh International Conference on MHD Electrical Power Generation, M.I.T., 1980.

1.3-9 Braun, J., Pudlik, W., An Evaluation of MHD Coal Cycles with Tail Gasification of Coal and Oxygen as Oxidizer, Seventh International Conference on MHD Electrical Power Generation, M.I.T., 1980.

2.3 Description of Advanced Combined MHD/Steam Power Plant

2.3.1 Establish Operational Characteristics

As indicated in the equations presented in the previous section, it is necessary for the plasma to have a high electrical conductivity, a high velocity and the strength of the imposed magnetic field must be high in order to extract electrical power economically. The desired order of magnitude of the electrical conductivity is approximately 10 ohm^{-1} m^{-1}; the Mach number is typically in the high subsonic range and the magnetic field strength should be in the range of 5 to 7 tesla (where 1 tesla is equal to 10,000 gauss).

Figure 2.3.1-1 indicates the means by which the desired levels of conductivity, velocity and magnetic field strength are achieved. A gas becomes electrically conducting when free electrons are present in the gas. The free electrons are introduced into the gas when one or more of the constituents of the gas become ionized. This requires elevating the gas to a high temperature and introducing a "seed" material (a compound containing potassium or cesium) which can more readily be ionized at temperatures which can be achieved by practical means. The high temperature is achieved by combustion of a fuel and air. However, the combustion temperatures, which are attainable from combustion of fossil fuels in air are typically in the vicinity of 2200°K (3500°F) which is inadequate for obtaining the desired electrical conductivity. In order to achieve a temperature in the vicinity of 2800°K (4600°F) which is desired for MHD, the combustion air must be preheated or the oxygen content of the air must be increased. Figure 2.3.1-2 from Ref. 2.3-1 shows the effects of air preheat temperature and oxygen enrichment on combustion temperature.

The desired velocity in the MHD channel corresponds to Mach numbers ranging from slightly subsonic to slightly supersonic. The velocity level is readily achieved by compressing the combustion air to pressures in the range of 5 to 10 atmospheres. Expansion of the combustion products through a subsonic or supersonic nozzle connecting the combustion chamber to the MHD channel provides the required velocity.

Magnetic field strengths as high as 5 to 7 tesla are attainable by the use of a superconducting magnet. This type of magnet consists of coils of special materials which completely lose their electrical resistivity when cooled to a very low temperature. Superconducting magnet systems for MHD operate at the temperature of liquid helium at atmospheric pressure which is 4.2°K. The only power requirements for the magnet are for initial energizing of the coils and for refrigeration to keep the temperature at the desired level.

METHODS FOR ACHIEVING HIGH ELECTRICAL CONDUCTIVITY, VELOCITY AND MAGNETIC FIELD STRENGTH

FIG. 2.3.1-2

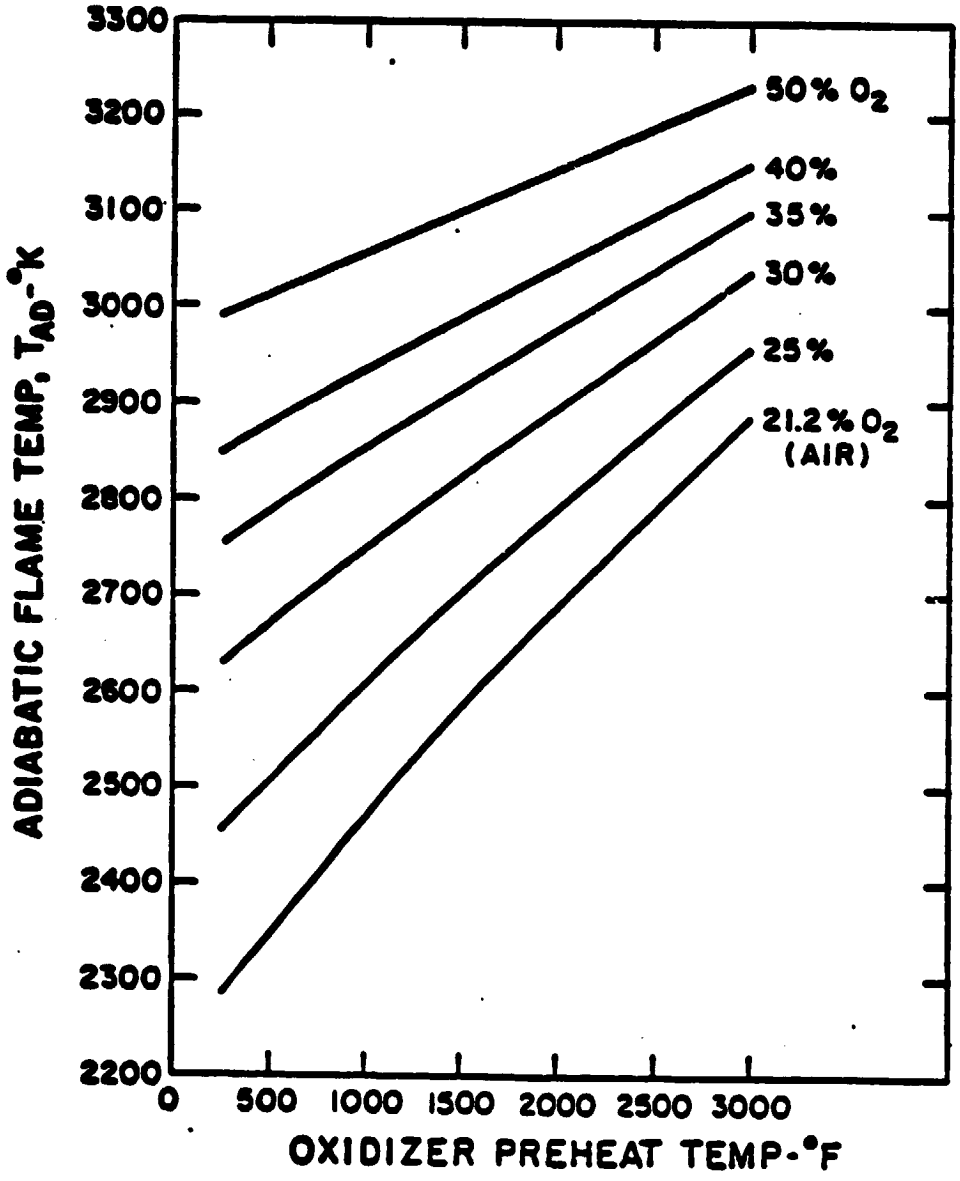

ADIABATIC FLAME TEMPERATURE

2.3.2 Basic MHD Power Plant Configurations

Based upon the requirements for obtaining the desired levels of electrical conductivity, velocity and magnetic field strength, two basic minimum MHD power generating plant configurations are shown in Fig. 2.3.2-1. One utilises oxygen enrichment and the other utilizes an air preheater. Typical preheat requirements are 1650 to 1900°K (2500 to 3000°F) with no oxygen enrichment or 850°K (1100°F) with an overall oxygen concentration of 30 to 40 percent by volume. In either case, the oxidants are fed under compression to the combustor along with fuel and a seed material. The conducting gases which flow through the MHD channel consist of the products of combustion and the seed material. The seed material is injected into the combustor as a potassium or cesium compound such as K_2CO_3 (potassium carbonate). At the high temperature attained in the combustor, the seed compound vaporizes and potassium ions are formed, providing free electrons.

The temperature of the gas decreases as it passes through the channel due to extraction of energy in the form of electricity. When the gas temperature decreases to approximately 2300°K (3700°F), the conductivity is too low to produce further electrical power economically. This limits the electric power which can be extracted from the MHD generator. The MHD generator configurations shown, however, can be used as topping units in conjunction with a steam bottoming cycle.

The electrical power output of the MHD channel is in the form of direct current. This may be suitable for certain industrial applications such as aluminum production. However, for electric utility applications feeding into an existing grid system, an inverter system is required for changing the direct current output to alternating current, as shown in Fig. 2.3.2-1.

One means of attaining a higher efficiency is by utilizing the high temperature exhaust gas from the MHD generator channel to preheat the air prior to combustion as shown in Fig. 2.3.2-2. This is referred to as direct-fired air preheating. However, the technology of achieving such high air temperatures with a gas which contains seed materials is beyond the present state of the art. At the present time, an upper limit of air temperature for direct-fired preheating is in the 1100 to 1300°K (1500 to 1900°F) temperature range.

Full utilization can be made of the MHD generator exhaust gas by adding a steam bottoming plant to the system discussed previously. A simple version of such a combined MHD/steam power plant cycle is shown in Fig. 2.3.2-3. The heat from the gas leaving the air preheater produces steam which drives a steam turbine connected to a conventional electric generator. The a.c. output of this generator is combined with the a.c. output of the MHD generator inverter system to provide power to an electric utility network or to an industrial plant. For air preheat temperatures in the vicinity of 2500°F, an overall power plant efficiency of nearly 50 percent is projected.

FIG. 2.3.2-1

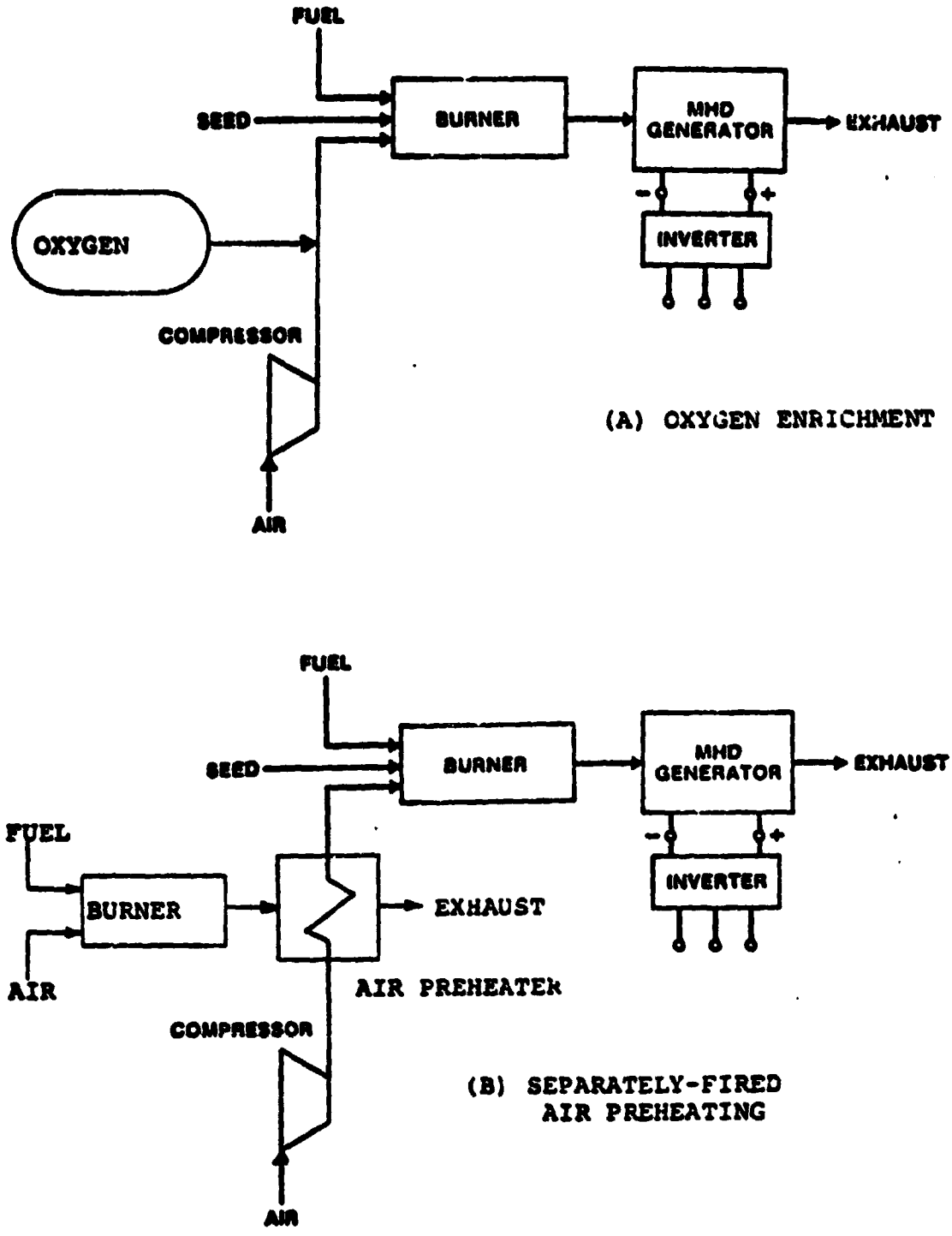

BASIC MHD POWER GENERATION SYSTEMS UTILIZING (A) OXYGEN ENRICHMENT AND (B) SEPARATELY-FIRED AIR PREHEATING

FIG. 2.3.2-2

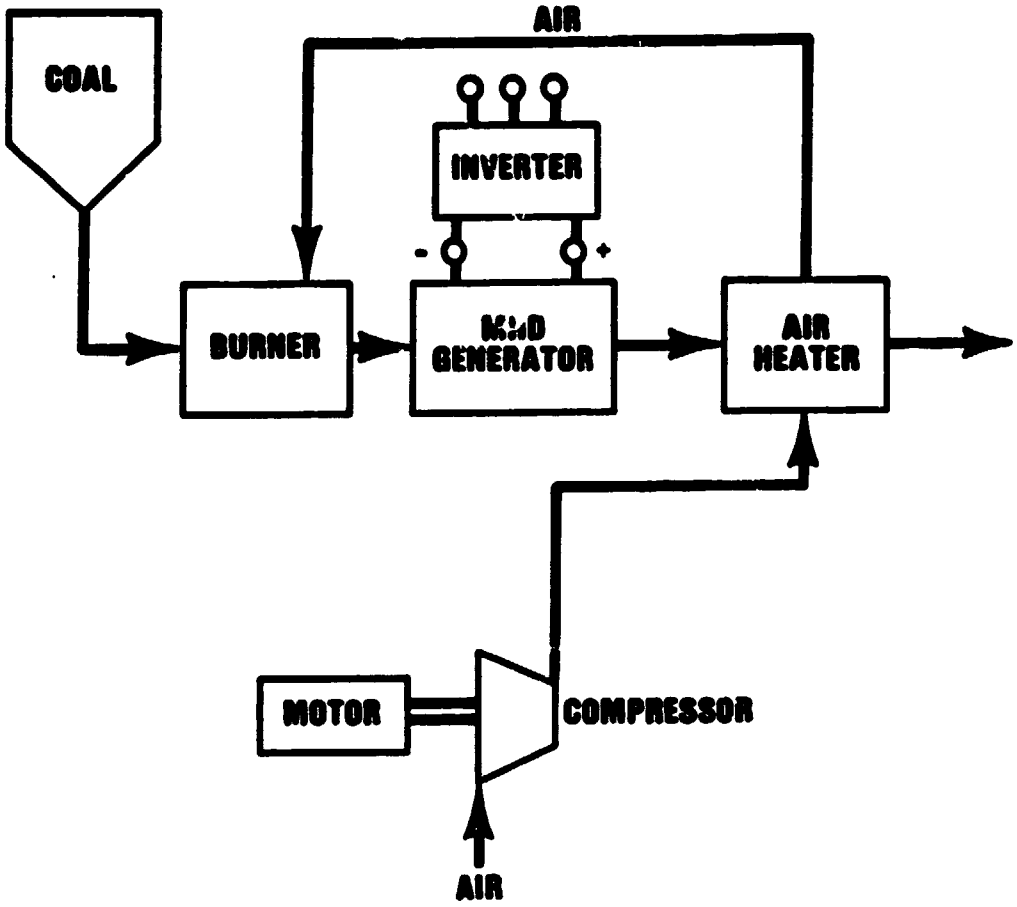

BASIC MHD POWER GENERATION SYSTEM UTILIZING DIRECT-FIRED AIR PREHEATING

FIG. 2.3.2-3

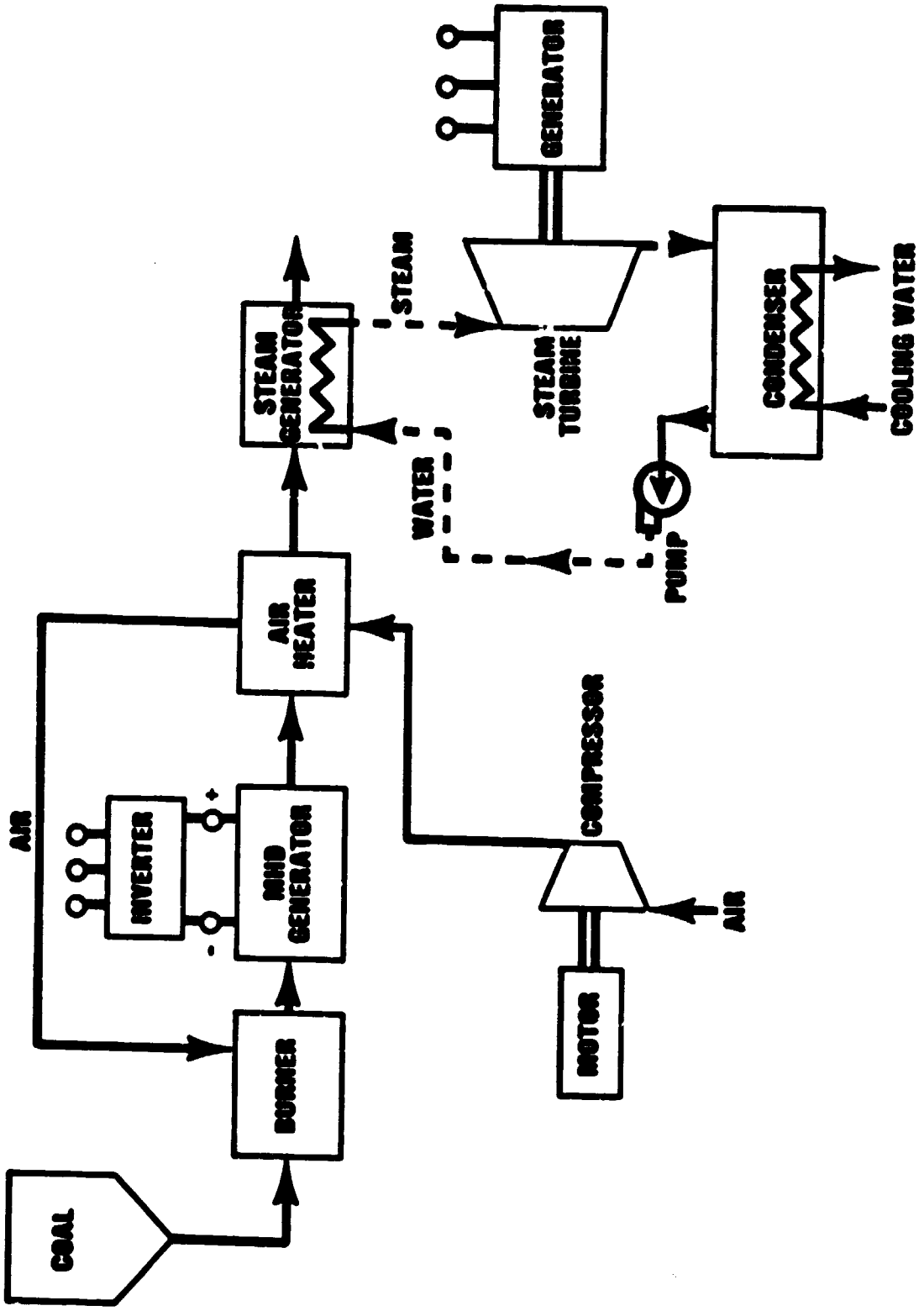

MHD/STEAM COMBINED – CYCLE POWER GENERATION SYSTEM

Figure 2.3.2-4 shows the combined MHD/steam cycle with the addition of systems for cleaning the exhaust gas prior to emission from the stack and for processing the seed for recyling to the combustor. The gas clean-up system consists of a particulate removal system such as a bag filter system or an electrostatic precipitator which is capable of collecting fine particles. This serves the dual prupose or recovering the seed material and reducing pollutant emission levels. By the time the exhaust gas has reached the gas clean-up system, it has been cooled to the point at which seed compounds have first condensed and then solidifed and formed primarily K_2CO_3 and K_2SO_4. There is a strong tendency for the formation of K_2SO_4 which limits the amount of sulfur oxides which enter the atmosphere without the need for a flue-gas desulfurization system. The gas clean-up system removes both flyash and seed compounds from the gas stream. If the fuel contains negligible sulfur, the collected seed compound would be primarily K_2CO_3 which can be recycled directly to the combustor. If the fuel does contain a significant amount of sulfur, the seed compounds include K_2SO_4 which must be converted into K_2CO_3 before recycling to the combustor in order to meet environmental regulations on stack emissions of sulfur oxides. This conversion is accomplished in a chemical processing system which may be located at the plant site.

2.3.3 MHD Power Plant Components and Subsystems

The MHD power plant can be considered to be subdivided into three categories:

- MHD Power Train
- Heat Recovery Seed Recovery System
- Balance of Plant

The MHD power train includes the combustor, channel, diffuser, magnet and inverter. The channel has been described previously. The combustor, magnet and inverter are described in later sections. The diffuser is a diverging duct located at the downstream end of the channel. Its function is to efficiently reduce the velocity of the gas before it enters the remainder of the plant.

The heat recovery seed recovery (HRSR) system includes the equipment through which the gas flows after leaving the diffuser. The functions of the HRSR are to cool down the gas while transferring heat from the gas to the boiler feedwater, steam and air and to remove seed compounds and ash from the gas. All other components and subsystems may be classified as balance-of-plant equipment. These include the steam turbine-generator, compressors, pumps, fans, piping, electrical equipment, etc., as well as equipment which may be unique to an MHD power plant such as the seed regeneration system.

FIG. 2.3.2-4

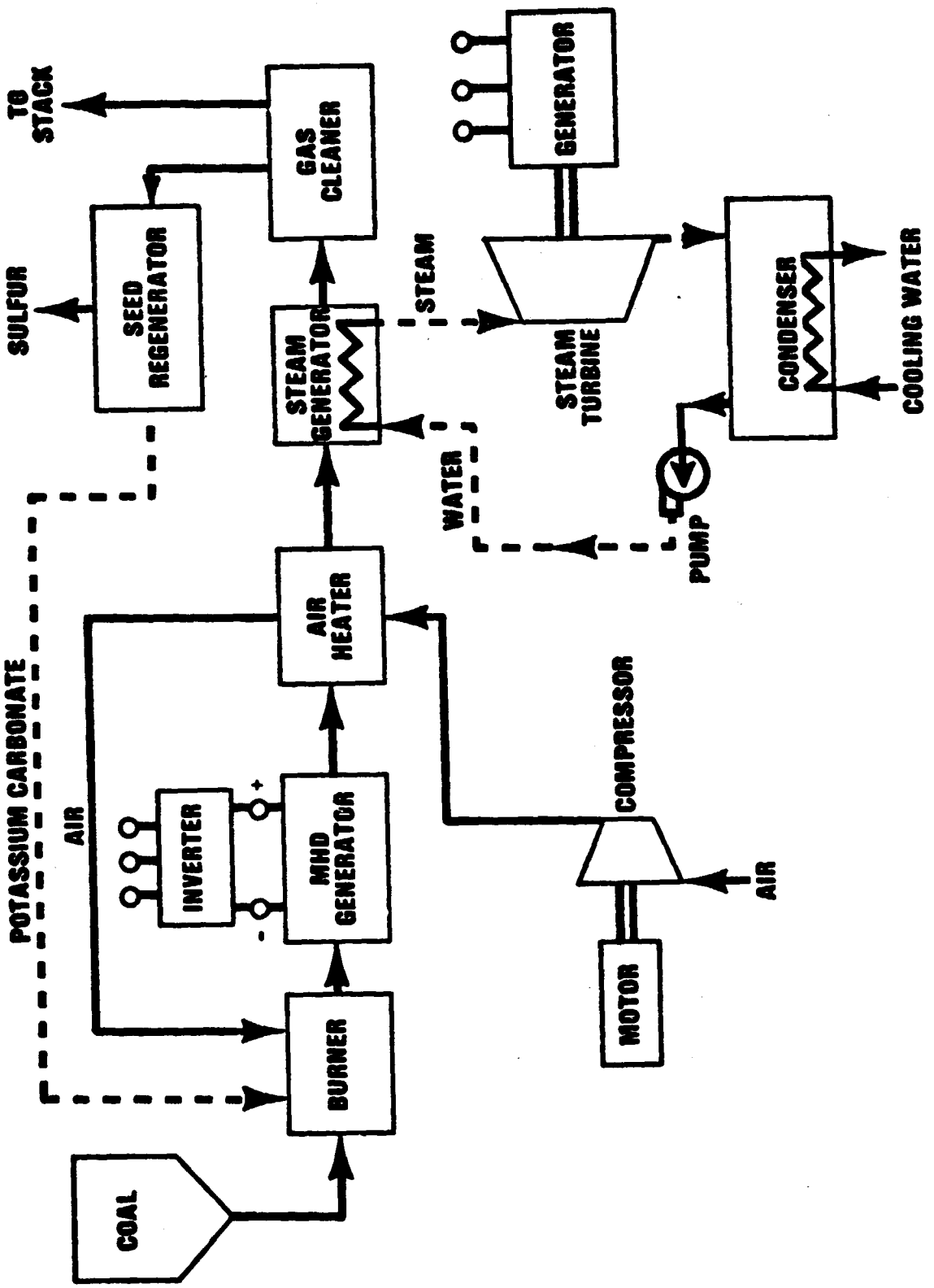

MHD/STEAM COMBINED-CYCLE POWER GENERATION SYSTEM INCLUDING GAS CLEAN-UP, SEED RECOVERY AND SEED RECYCLING

2.3.3.1 Coal Processing and Combustion

There are several proposed approaches to the utilization of coal as the fuel for the MHD generator. Three approaches are illustrated schematically in Fig. 2.3.3.1-1. As indicated previously, the MHD generator can be designed to operate in the presence of coal slag. Thus, the direct-firing of coal in the combustor is a viable option. However, the slag has been observed to absorb seed material when the slag and seed cool down as the as flows through the components downstream of the MHD generator. The seed absorbed by the slag is very difficult to recover. The amount of seed absorbed is found to be unacceptable unless approximately ninety percent of the slag is removed either in the combustor, as in Fig. 2.3.3.1-1(a) or immediately downstream of the diffuser as in Fig. 2.3.3.1-1(b). The third method of coal utilization is to gasify the coal prior to combustion as indicated in Fig. 2.3.3.1-1(c). This can be done with or without fuel-gas sulfur removal since sulfur removal can be accomplished downstream of the MHD generator in conjunction with seed recovery and regeneration.

Several combustor designs have been developed for MHD systems which are capable of extracting large amounts of ash from the combustion products. One method is to use a two-stage combustor in which the temperature of combustion in the first stage is controlled by delivering less air to it. The slag is removed from the first stage and the remainder of the air is added to the second stage. Removal of over 90 percent of the slag from a two-stage combustor has recently been demonstrated at the U.S. Department of Energy's Pittsburgh Energy Technology Center with a two-stage combustor as illustrated in Fig. 2.3.3.1-2. Another two-stage combustor design which has been proposed by TRW is shown in Fig. 2.3.3.1-3. A single-stage combustor, designed by Avco-Everett Research Laboratory for achieving high slag removal, is shown in Fig. 2.3.3.1-4.

2.3.3.2 Systems for Control of Pollutant Emissions

Nitrogen Oxides

The very high temperatures occurring in the combustor of an MHD power plant are conducive to the production of nitrogen oxides through the fixation of nitrogen which is present in both the air and the fuel. Unless precautions are taken in the design of the plant, NO_x emissions will exceed allowable environmental limits. Figure 2.3.3.2-1 illustrates schematically the design features which are instituted to reduce NO_x emissions to acceptable levels. The amount of air delivered to the combustor is maintained at approximately 95 percent of the stoichiometric requirements in order to reduce the initial production of nitrogen oxides. However, the incomplete combustion which thereby occurs results in production of excessive amounts of carbon monoxide. This makes it necessary to add additional air at a location where the gas has cooled to the point that the oxidation of nitrogen is no longer significant. This should be done in the 2400°F to 2900°F

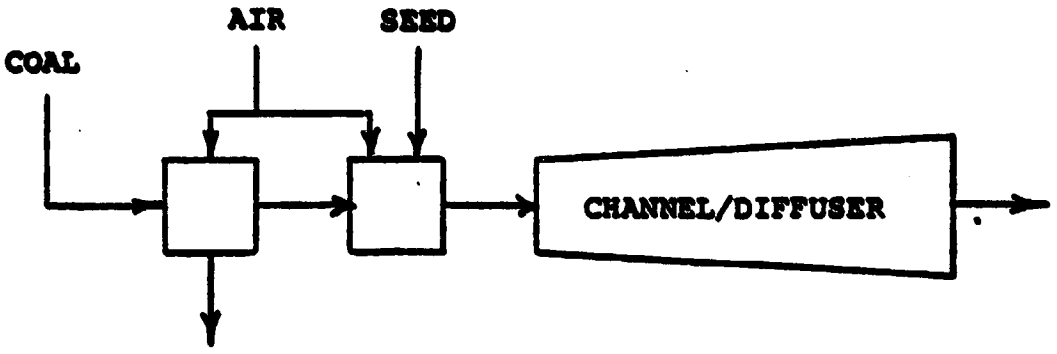

(A) 10% SLAG CARRYOVER UTILIZING A TWO-STAGE COMBUSTOR

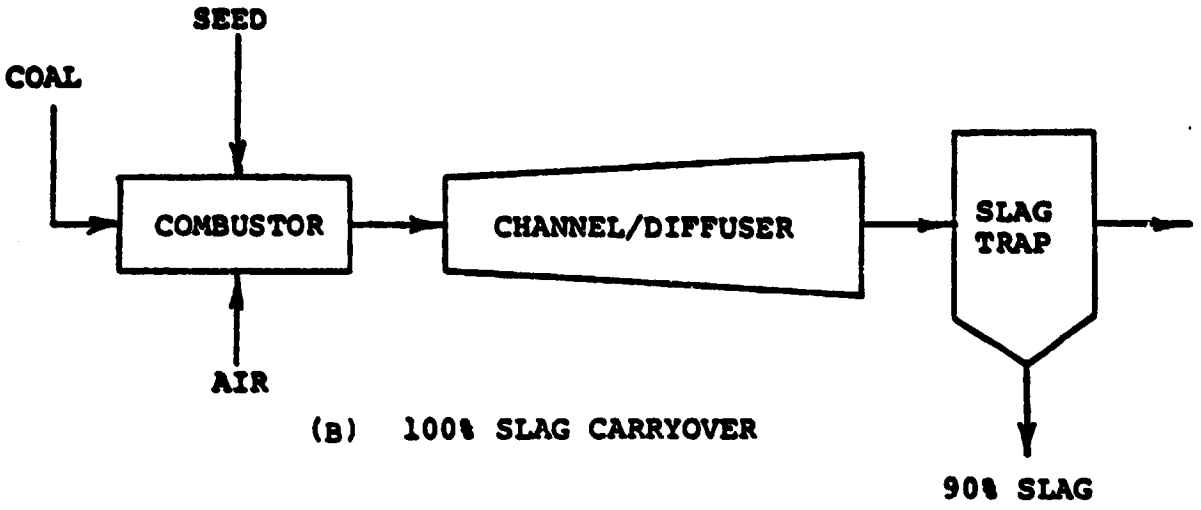

(B) 100% SLAG CARRYOVER

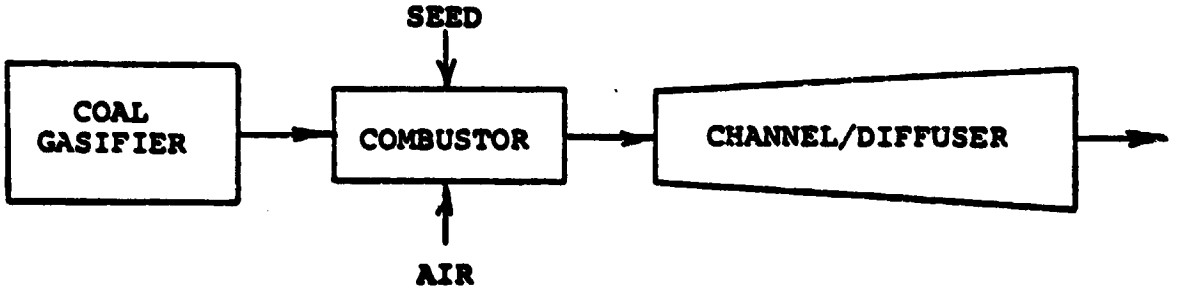

(C) CLEAN FUEL FROM COAL GASIFIER

SLAG REMOVAL SCHEMES IN COAL-FIRED MHD POWER PLANTS

FIG. 2.3.3.1-2

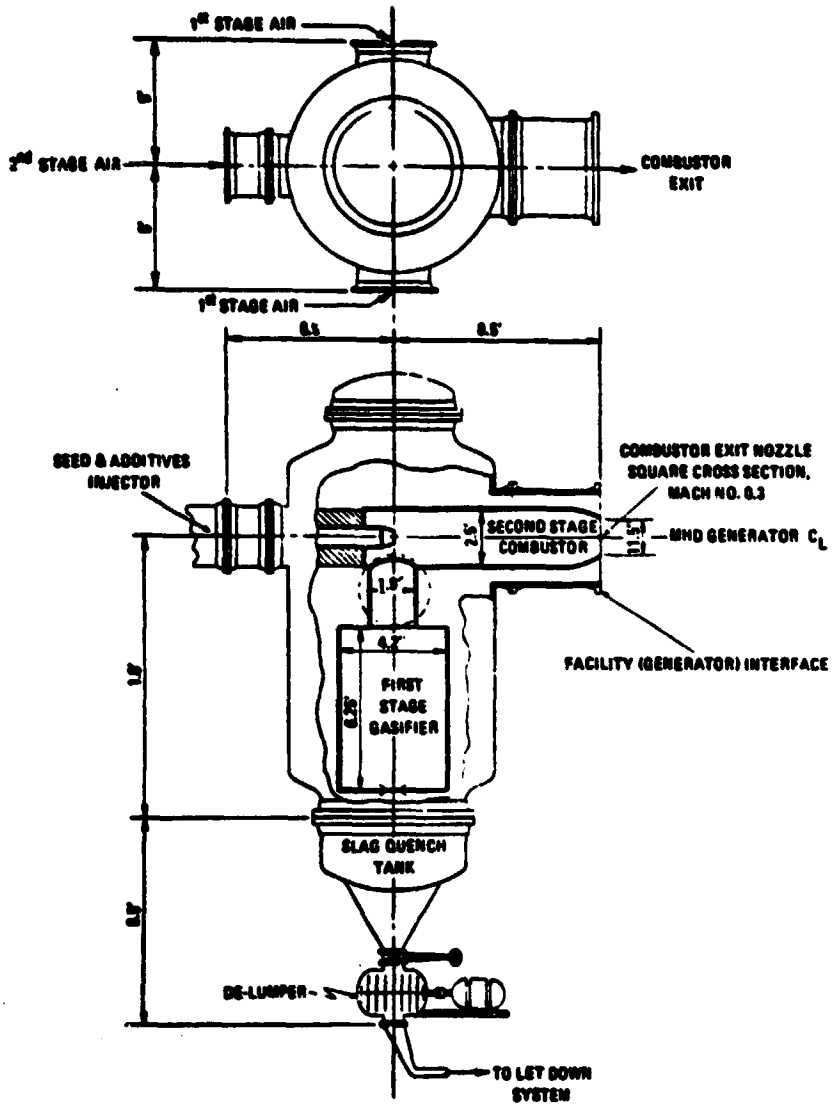

TWO-STAGE DIRECT COAL-FIRED MHD COMBUSTOR DESIGN

FIG. 2.3.3.1-3

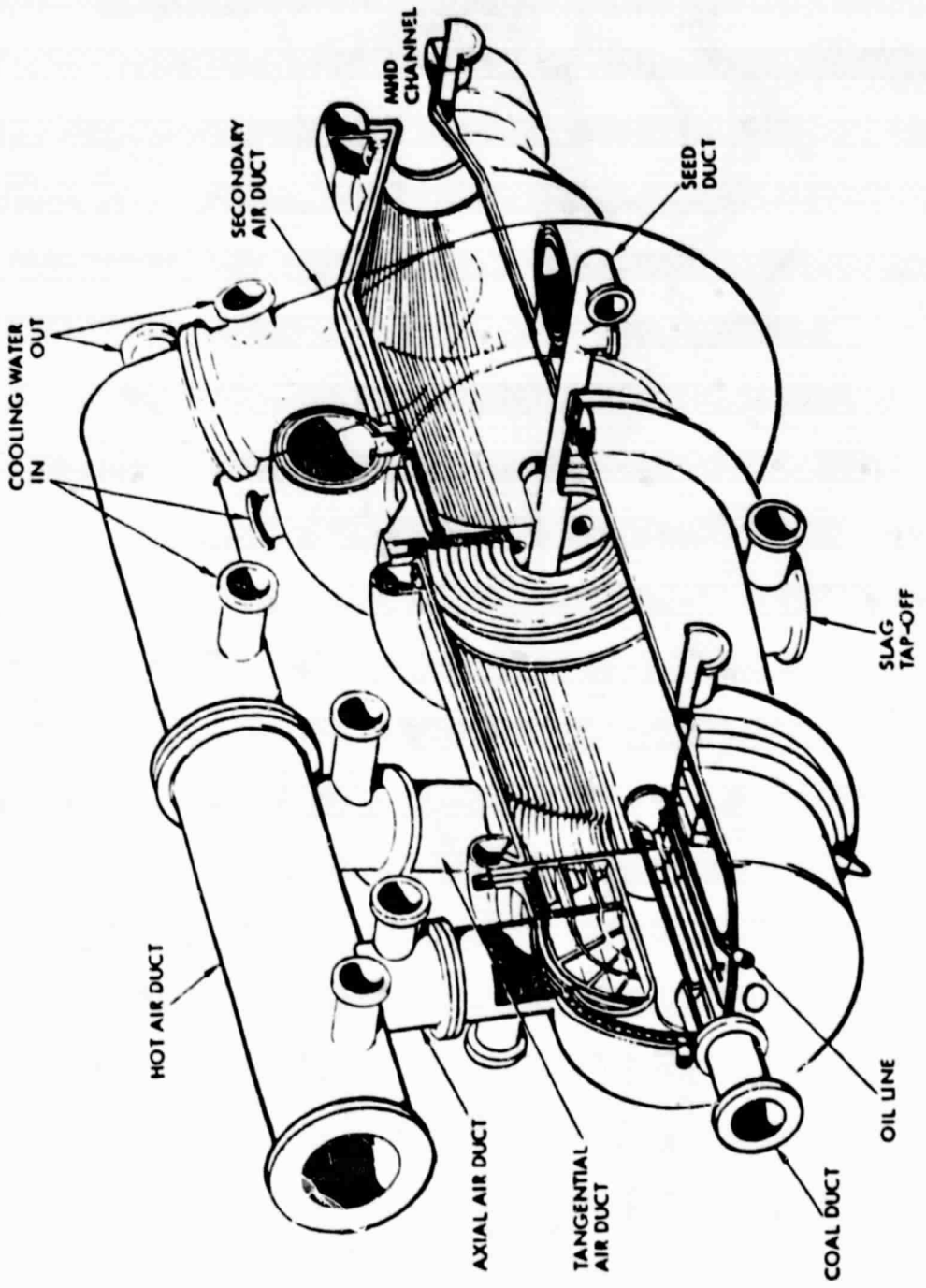

TWO-STAGE DIRECT COAL-FIRED MHD COMBUSTOR

FIG. 2.3.3.1-4

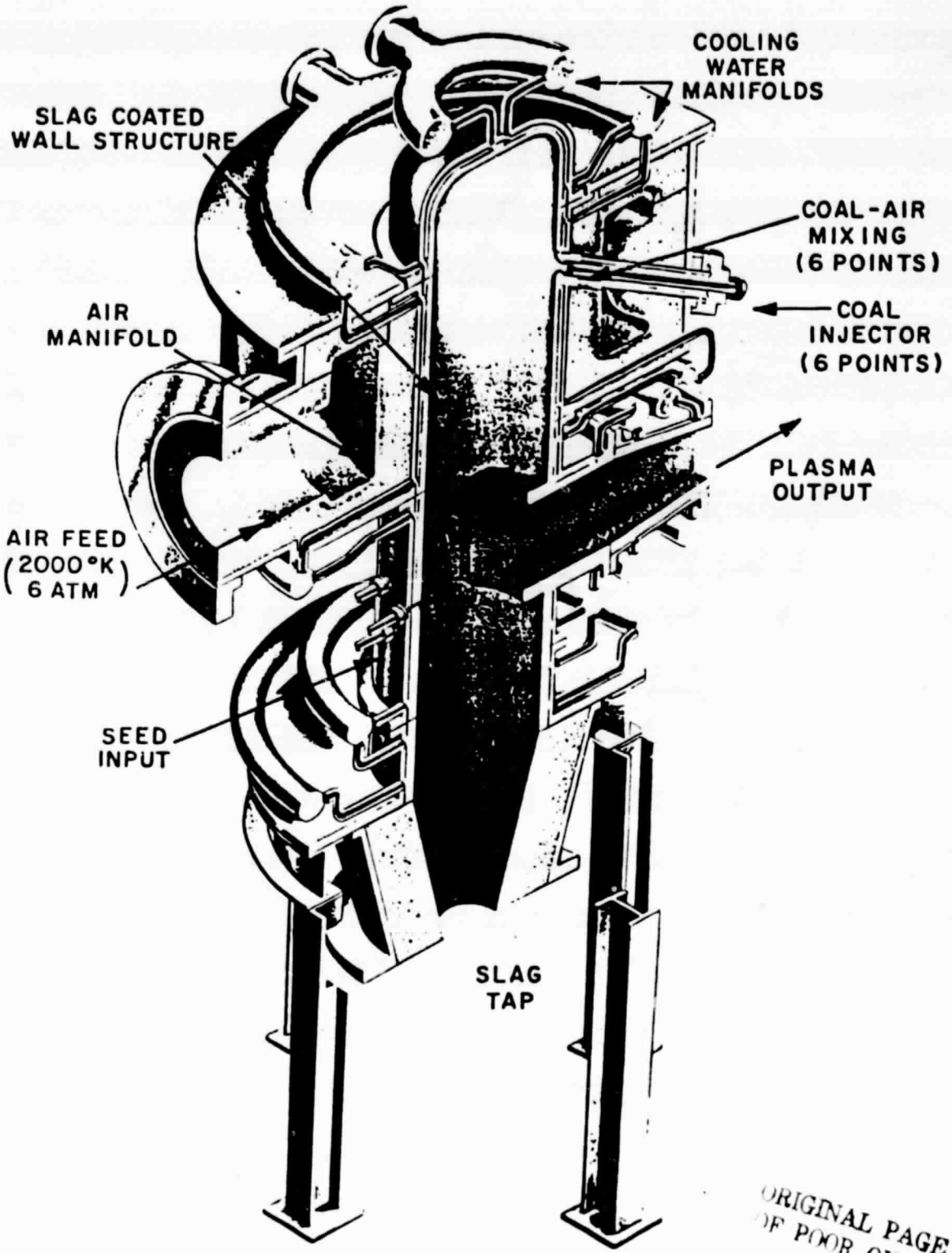

SINGLE-STAGE DIRECT COAL-FIRED MHD COMBUSTOR

FIG. 2.3.3.2-1

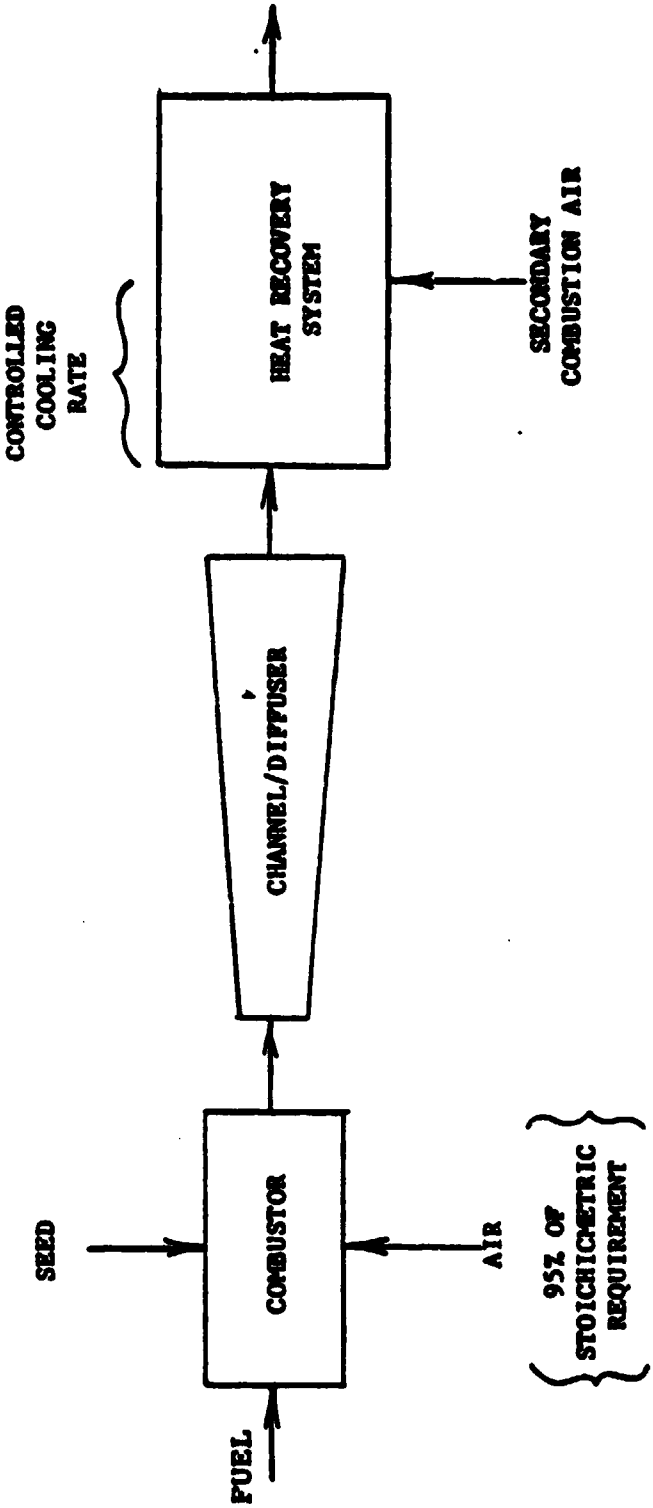

CONTROL OF NITROGEN OXIDES IN MHD POWER PLANTS

temperature range. Additional decomposition of NO_x is achieved by control of the cooling rate of the gas as it passes through the critical temperature range of 3300°F to 2900°F. This is achieved by ensuring sufficient residence time in the components immediately downstream of the diffuser. For example, a radiant boiler at this location would provide the required cooling rate for the gas.

Particulates

The particulate matter in the exhaust gas includes ash and compounds of potassium. Typical potassium compounds may incude:

K_2SO_4
K_2CO_3
KOH
KO
$KHCO_3$
K_2S
$K_2S_2O_7$
$KHSO_4$

For fuels with high sulfur content, the predominant compound at low temperatures is K_2SO_4. For fuels with low sulfur content, the predominant compound at low temperatures is K_2CO_3.

Condensed or solidified materials adhere to surfaces of components in the equipment downstream of the generator or are entrained in the gas stream and carried further downstream. Liquid or solid materials are continually or intermittently removed from the surface (for example, by sootblowers) to prevent excessive build-up and seed loss. The materials removed from the surfaces are either collected at the bottoms of the various components or entrained in the gas stream. Particles which are carried in the gas stream are collected by either a baghouse filter or an electrostatic precipitator to prevent excessive pollutant emissions as well as for the purpose of recovering seed.

Sulfur Oxides

As discussed previously, the mechanism most frequently proposed for sulfur emissions control in an MHD power plant is by means of the formation of K_2SO_4 and its subsequent removal from the MHD exhaust stream by means of baghouse filters or electrostatic precipitators. The potassium is required for MHD to enhance the electrical conductivity of the gas. For fuels with moderate-to-low sulfur content, the amount of seed required for achieving adequate gas conductivity is more than is required to extract sulfur from the gas. For fuels with high sulfur content, the potassium which must be added for sulfur extraction may be

only slightly greater than that required for conductivity. Due to the cost of potassium, it is necessary to recover as much of it as possible to re-use in the combustor. Thus there is no added penalty associated with the removal of sulfur oxides from the gas stream. However, the recovered K_2SO_4 must be converted to K_2CO_3 before recycling. It has been projected that approximately 95 percent of the potassium must be recovered for economic reasons.

Seed Regeneration

The amount of seed required to achieve adequate electrical conductivity of the ionized gas is equal to approximately 15 percent of the mass of fuel when the fuel is coal. It is estimated that at least 95 percnet of this seed must be recovered and recylced to make the plant operating cost acceptable. When low sulfur fuels are used, the seed is collected primarily as K_2CO_3 with small amounts of K_2SO_4. Sufficient K_2SO_4 must be converted to K_2CO_3 before recycling to the combustor to meet environmental regulations. When high sulfur fuels are used, most of the collected seed is in the form of K_2SO_4 and a large percentage of it must be converted to K_2CO_3 before recycling. The regeneration process includes separation of ash from the seed as well as conversion of potassium sulfate to potassium carbonate.

A seed regeneration process which has been investigated at the Pittsburgh Energy Technology Center involves two stages with the following reactions:

Reduction:

$$K_2SO_4 + 4\ CO \rightarrow K_2S + 4\ CO_2$$

$$K_2SO_4 + 4\ H_2 \rightarrow K_2S + 4\ H_2O$$

Regeneration:

$$K_2S + CO_2 + H_2O \rightarrow K_2CO_3 + H_2S$$

In this process, coal is supplied as a fuel to provide a $CO-H_2$ producer gas for the process and the hydrogen sulfide is converted to elemental sulfur in a Claus plant. This process is presently in the "bench-scale" stage of development.

An alternate regeneration process is the Formate process based upon the chemical reaction

$$K_2SO_4 + Ca\ (OH)_2 + 2\ CO \rightarrow 2\ KCOOH + CaSO_4$$

This process was used commercially for production of K_2CO_3 from K_2SO_4, but has since been abandoned as it became more economical to produce K_2CO_3 from other feedstocks. In an MHD power plant, the steps in the process would be:

1. Gasification to produce carbon monoxide (CO);
2. Dissolving of recovered seed (K_2SO_4) and slurrying of lime ($Ca(OH)_2$);
3. Reaction of CO, K_2SO_4 and $Ca(OH)_2$ to produce soluble potassium formate (KCOOH) and insoluble calcium sulfate ($CaSO_4$);
4. Filtration of $CaSo_4$;
5. Evaporation of water from KCOOH;
6. Recycle of KCOOH to combustor.

2.3.3.3 Heat Recovery-Seed Recovery System

There are a number of alternate ways in which the heat recovery components downstream of the diffuser can be arranged. The heat recovery-seed recovery (HRSR) components include steam generating equipment, superheater, reheater, air preheater(s), economizer(s), a bag-house filter or electrostatic precipitator, an induced-draft fan and a stack. A portion of the gas stream may be diverted for the purpose of drying the coal. Figure 2.3.3.3-1 shows one possible arrangement.

The system depicted in Fig. 2.3.3.2-1 employs a direct-fired high-temperature air heater. The first component through which the MHD generator diffuser exhaust gas flows is a radiant boiler. This component is placed here primarily because of the need for high gas residence time to allow slow cooling through a critical temperature range to enhance the decomposition of nitrogen oxides. The secondary air for completion of combustion may be added before or after the gas flows through the high-temperature air heater depending upon the temperature drop of the gas through the radiant boiler section. The steam superheater and steam reheater sections of the plant follow the high-temperature air heater and these, in turn, are followed by a low-temperature air heater.

The reason for splitting the air heater into a high-temperature and a low-temperature section is due to materials considerations. The low-temperature air heater would be a recuperative type of heat exchanger of metallic construction. The upper limit of this type of heat exchanger would be an air outlet temperature in the vicinity of 1100°K (1500°F) due to the presence of seed materials in the gas. The high-temperature air preheater would be of the regenerative type. The outlet temperature of the air from the high-temperature air heater is highly dependent upon advances in the state of the art. Figure 2.3.3.3-1 also shows an economizer located downstream of the low-temperature air heater. The economizer brings the gas temperature down to a range which is suitable for an electrostatic precipitator or a bag filter system.

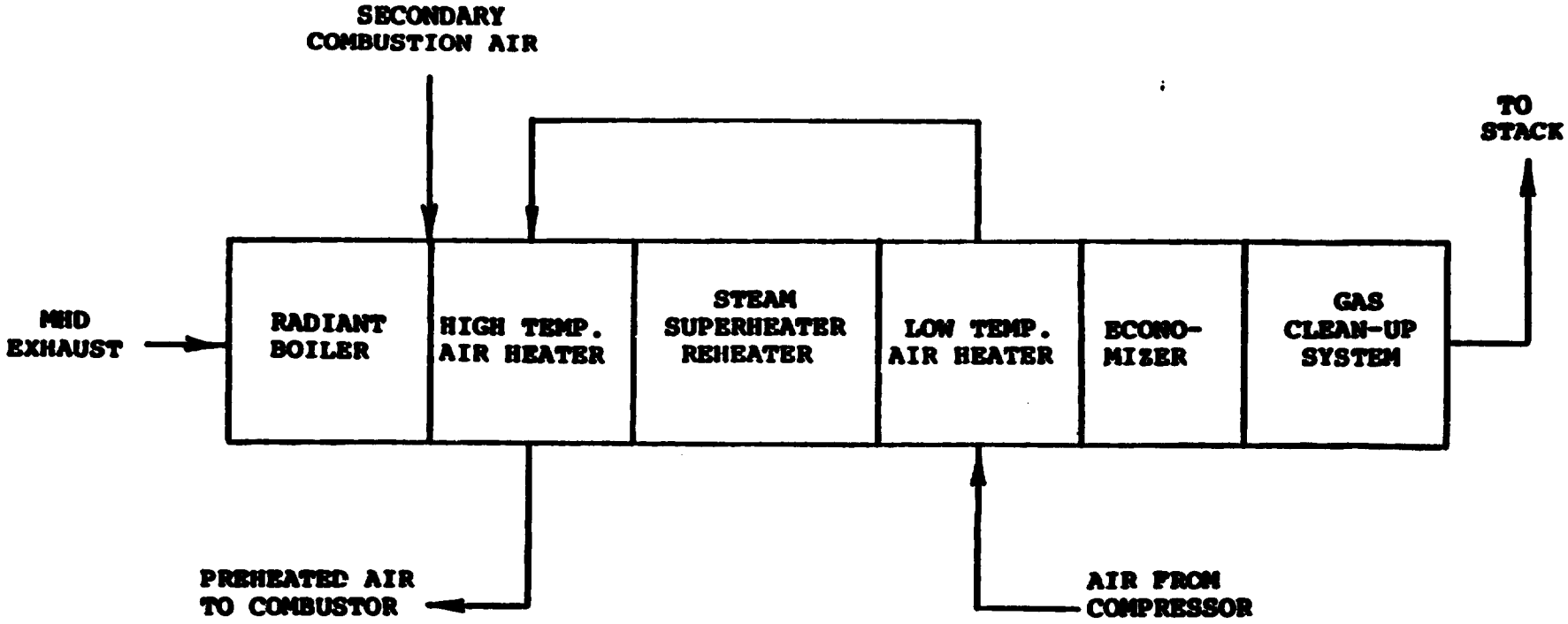

TYPICAL HEAT RECOVERY SYSTEM FLOW TRAIN ARRANGEMENT WITH DIRECT-FIRED HIGH TEMPERATURE AIR HEATER

Several alternate heat recovery system flow train arrangments are shown in Fig. 2.3.3.3-2. Each is based upon a different means of achieving a high air preheat temperature. Arrangement A shows a direct fired air preheater. Arrangements B, C and D show separately-fired arrangements. Arrangement B utilizes clean fuel fired at atmospheric pressure. Arrangement C utilizes clean fuel fired at high pressure with the combustion gases driving a turbine after preheating the air. Arrangement D utilizes low-Btu gas provided by a coal devolatilizer.

Figure 2.3.3.3-3 is a schematic diagram of the condensate, feedwater and steam flow system in the steam bottoming plant. A single deaerating feedwater heater is shown. Additional feedwater heaters may or may not be necessary due to the substantial thermal energy which can be picked up from the MHD exhaust gas and the cooling system for the combustor, MHD channel and the diffuser. The cooling of the MHD flow train is achieved by means of secondary flow loops. The air compressor is steam-turbine driven. This requires a substantial amount of power. For example, a plant with a net electrical power output of 1000 MW may utilize as much as 150 MW of mechanical drive power for the air compressor systems. The main steam turbine shown is a single reheat turbine.

2.3.3.4 High-Temperature Air Preheating

The highest air preheat temperatures can be achieved by the intermittently-operating regenerative type of air preheater. This type consists of several vessels, each encasing a matrix of ceramic refractory materials. The matirx is alternately heated by the hot gas and cooled by the air, thereby tranferring heat from the gas to the air. Multiple vessels in parallel and switchover valves are employed to deliver a continuous supply of preheated air. Figures 2.3.3.4-1 and -2 are simplified diagrams showing a vessel cross-section with a matrix consisting of hexagonal-shaped cored bricks with internal flow passages. As many as 10 to 20 vessels may be required. Maximum air preheat temperatures in excess of 3000°F have been achieved with minimum deterioration of matrix materials utilizing a clean gas as a heat source. Air preheaters utilizing, as a heat source, gases containing slag or seed are not yet capable of sustained operation at temperatures high enough for economical operation of an MHD/steam power plant.

2.3.3.5 Superconducting Magnet

Magnetic field strengths of 5 to 7 teslas are required over volumes of several hundred cubic meters in order to obtain the overall efficiency advantages of MHD power generation. These field strengths are much greater than the 2-tesla field strengths that can be provided by a water-cooled conductor, iron pole magnet of medium power. The power requirements of a 6-tesla magnet using water-cooled conductors would exceed the power output of the generator. Therefore, large-volume superconducting magnets are required for efficienct MHD power generation. The only power continuously consumed by a superconducting-magnet system is that which is required for refrigeration to maintain the magnet coils at liquid helium temperatures.

FIG. 2.3.3.3-2

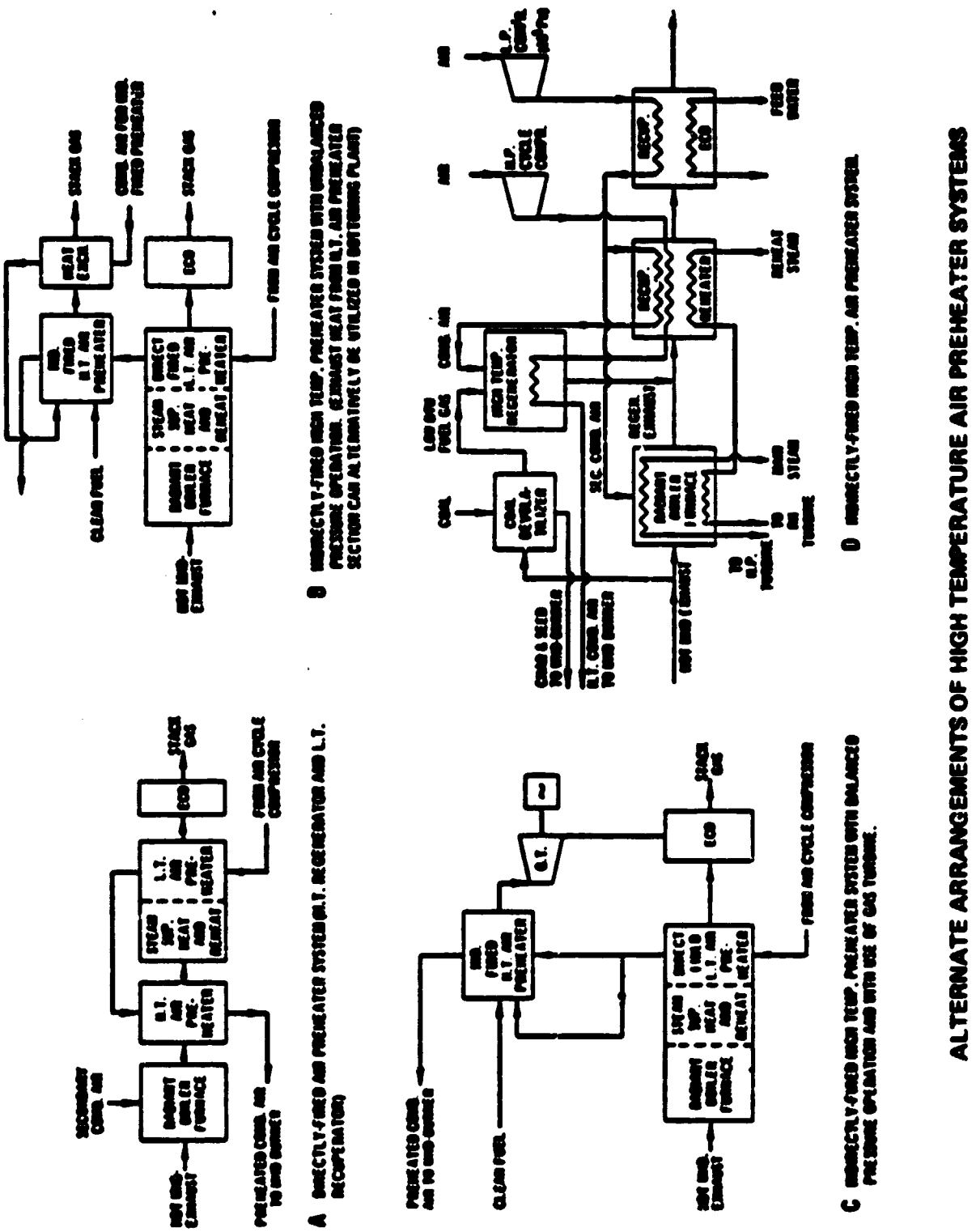

ALTERNATE ARRANGEMENTS OF HIGH TEMPERATURE AIR PREHEATER SYSTEMS

FIG. 2.3.3.3-3

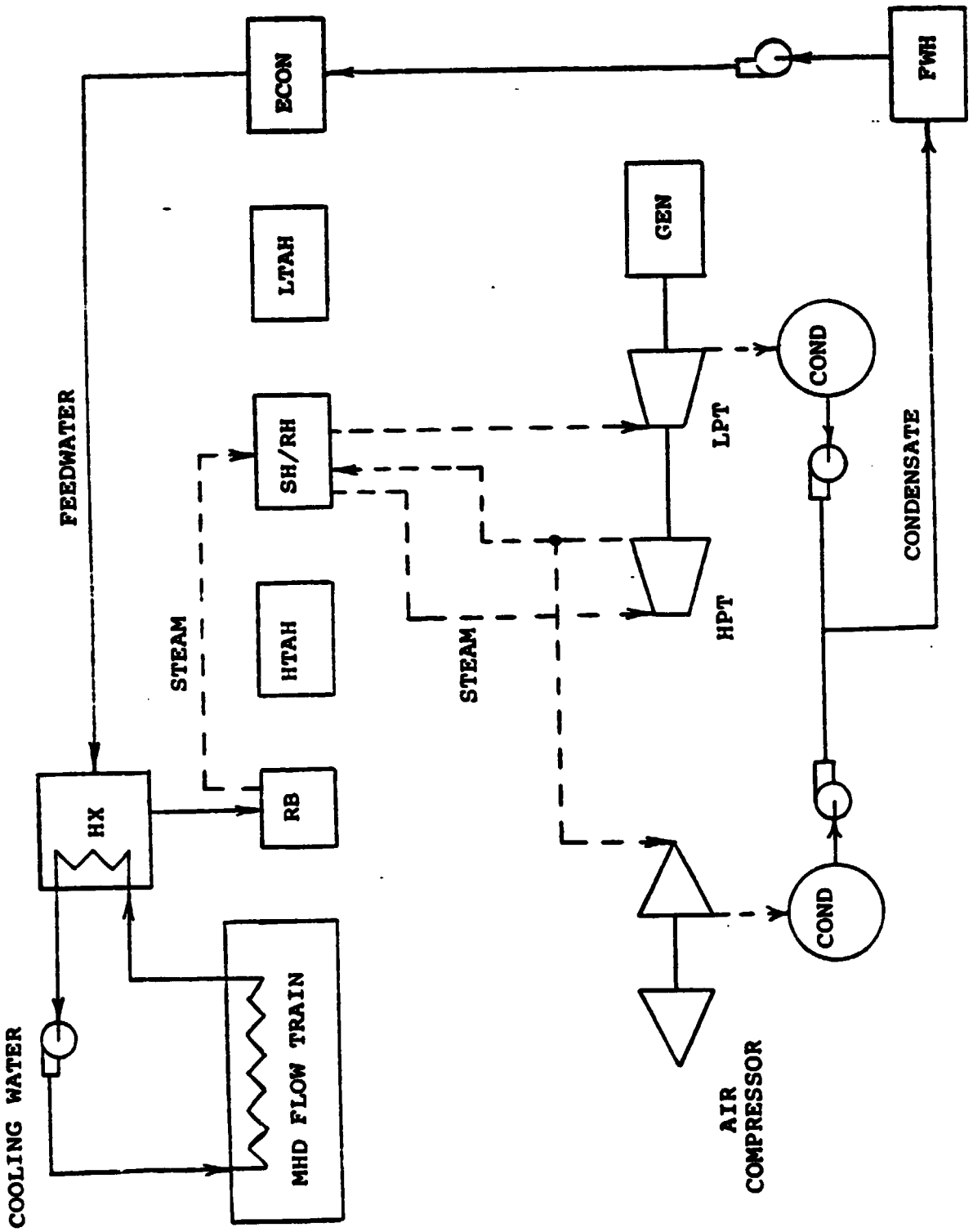

CONDENSATE, FEEDWATER AND STEAM FLOW SYSTEMS FOR MHSD/STEAM POWER PLANT

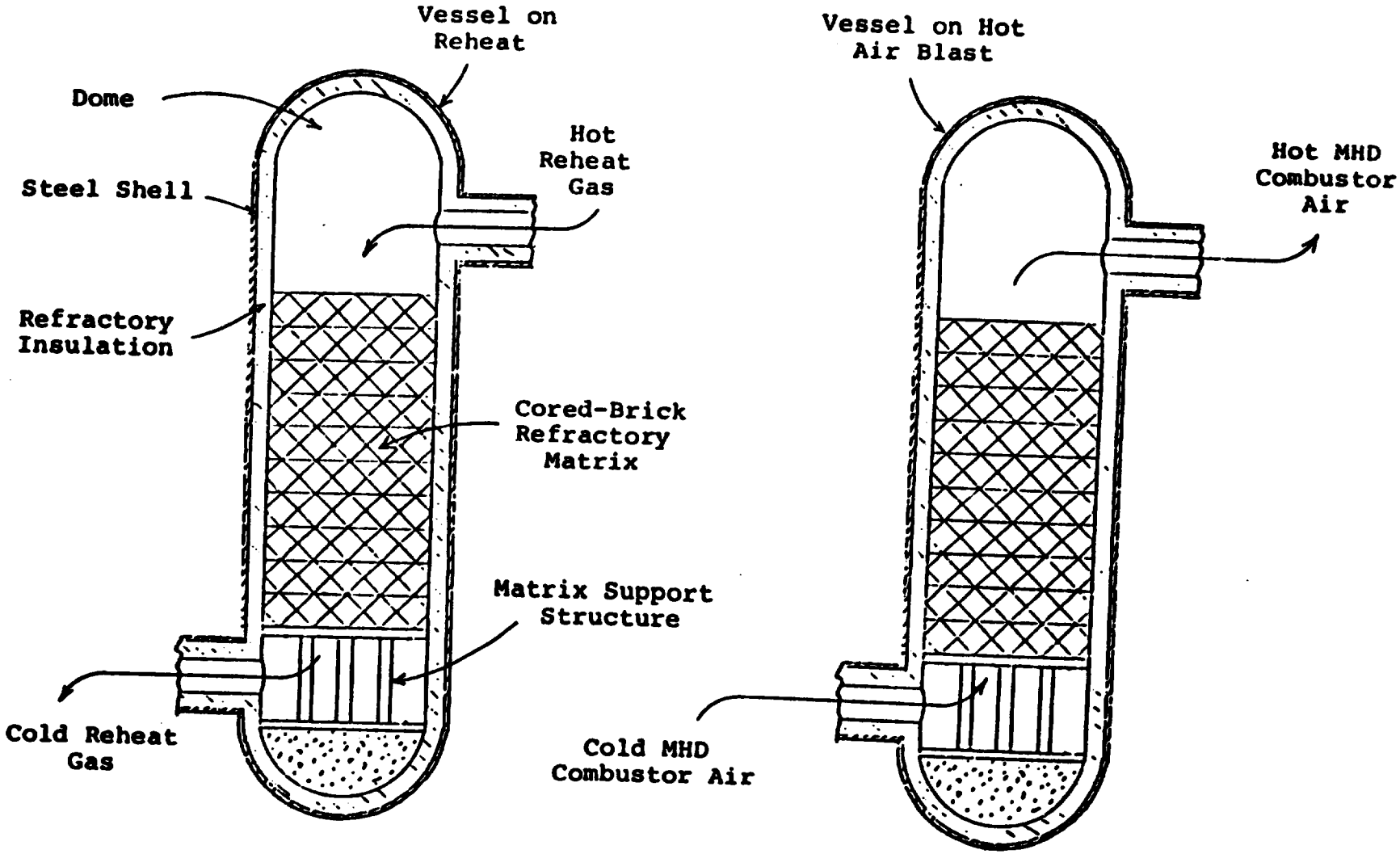

DIAGRAM OF REGENERATIVE HTAH SYSTEM

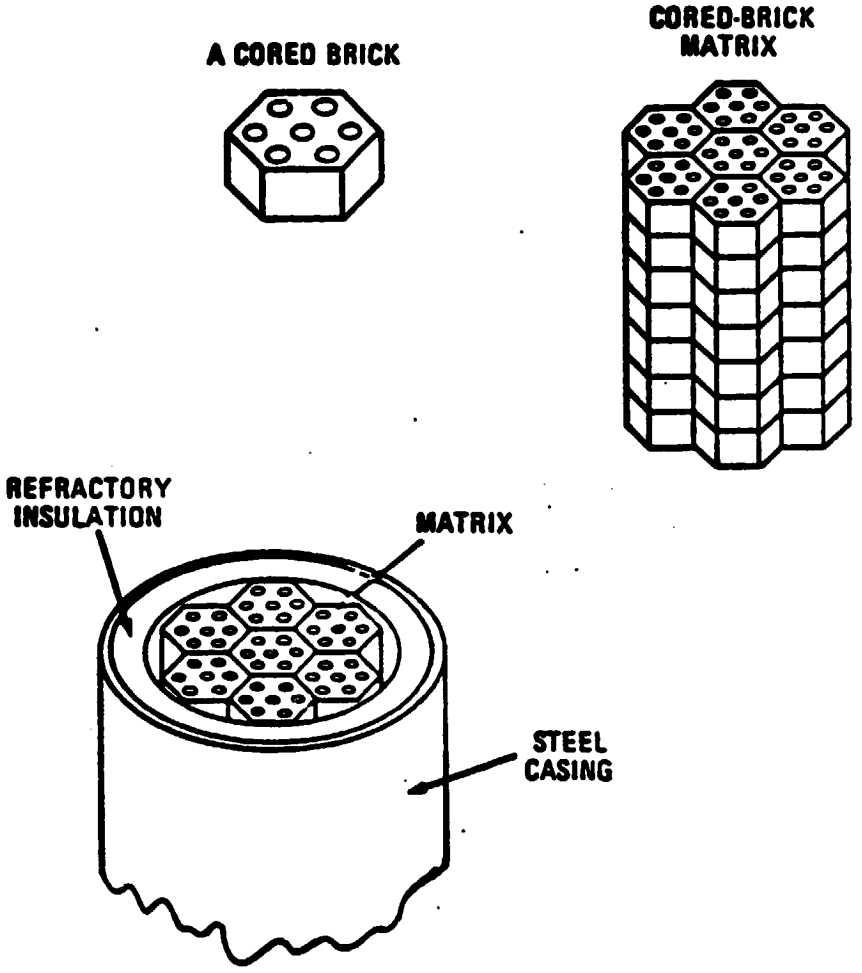

SECTION OF REGENERATIVE HIGH TEMPERATURE AIR HEATER VESSEL AND CORED BRICK

The superconducting material being considered for MHD application is niobium-titanium (NbTi) which is a superconductor at the temperature of liquid helium ($4.2^{o}K$). In order to maintain the material in a superconducting state it is necessary to "stabilize" the superconductor. Stability is achieved by constructing the coils with NbTi imbedded in a copper substrate. This prevents the entire coil from reverting to its "normal" (non-superconducting) state when small local temperature excursions cause a small region of the coil to temporarily go normal.

The most efficient configuration for an MHD magnet is the "saddle coil" illustrated schematically in Fig. 2.3.3.5-1 from Ref. 2.3-2. The coils must be cooled by circulation by liquid helium and the entire magent structure must be thermally insulated from the channel in the bore of the magnet as well as from the surroundings. The extremely high electric currents and magnetic field strengths existing in the magnet generate very large stresses which tend to distort the magnet. A very substantial structure is required to restrain these forces. Figure 2.3.3.5-2 from Ref. 2.3-3 illustrates a superconducting magnet which is currently under construction or in the initial stages of construction for the Component Development and Integration Facility. Figure 2.3.3.5-3 from Ref. 2.3-4 is a block diagram of the cryogenic support system required for maintaining the magnet coils at liquid-helium temperature.

2.3.3.6 Inverter Systems

The MHD generator produces direct current electricity which must be converted to alternating current for electric utility utilization. The inverter system which converts d.c. power to a.c. power must meet the unique requirements of an MHD generator. For the Faraday type of MHD channel configuration the d.c. electric power is extracted from the channel via a very large number of individual electrode parts. It is necessary to consolidate these individual outputs in conjuction with the inverter system. Figure 2.3.3.6-1 from Ref. 2.3-1 illustrates a consolidation network for combining the electrical output of twelve individual electrodes. Figure 2.3.3.6-2 also from Ref. 2.3.-1 illustrates, schematically, the manner of consolidating the outputs for either a Faraday or Diagonal type of channel. Although the inverter network for MHD application is unique, the equipment required for the inverter system is not unique for MHD.

2.3.4 Recommendations for Selection of MHD Power Plant Baseline Technology

Several alternate MHD power plant configurations were identified and described in the preceding sections of this report. The selection of one or more of these configurations depends upon the guidelines and selection criteria which are established. The major guidelines followed in selecting an MHD power plant configuration are that the MHD power plant be of a type which is:

- suitable for "early commercial" operation by a utility company
- economically attractive compared to alternate configurations
- currently receiving support under the U.S. Government MHD program.

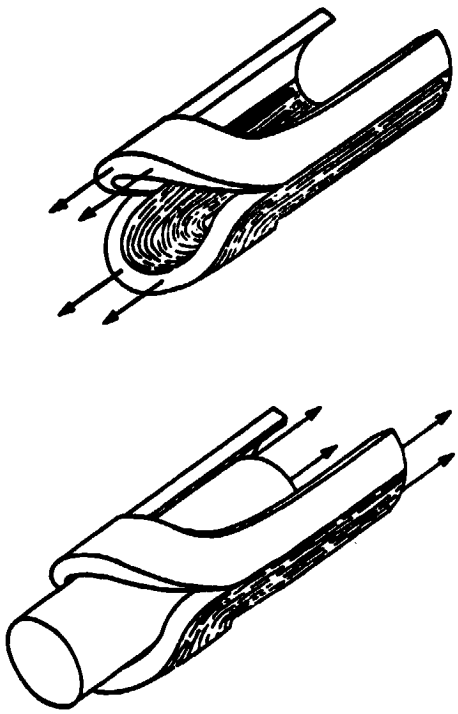

Circular End Turn Saddle

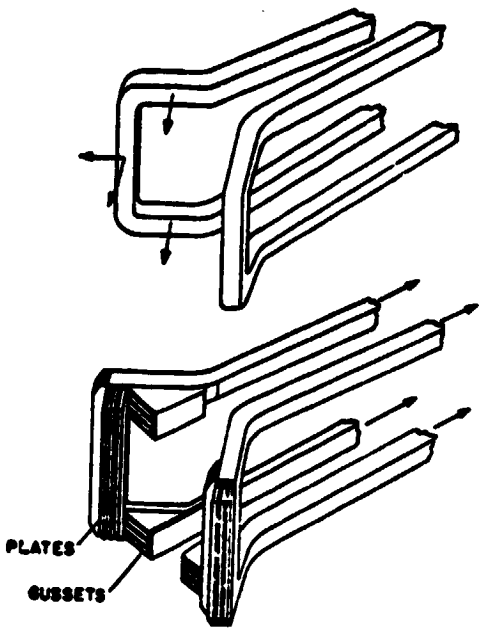

Rectangular Saddle

MHD MAGNET SADDLE COIL CONFIGURATIONS

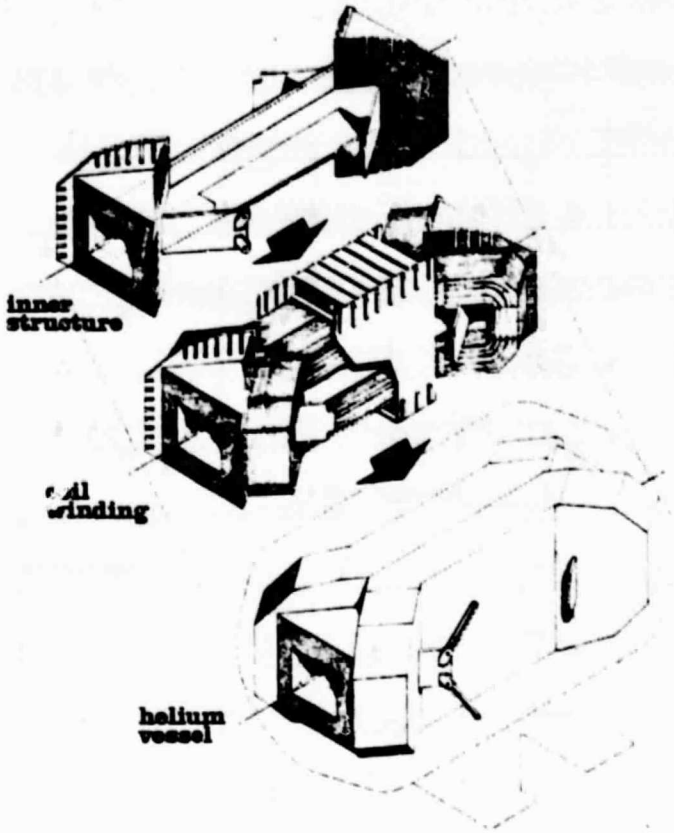

CDIF Superconducting Magnet

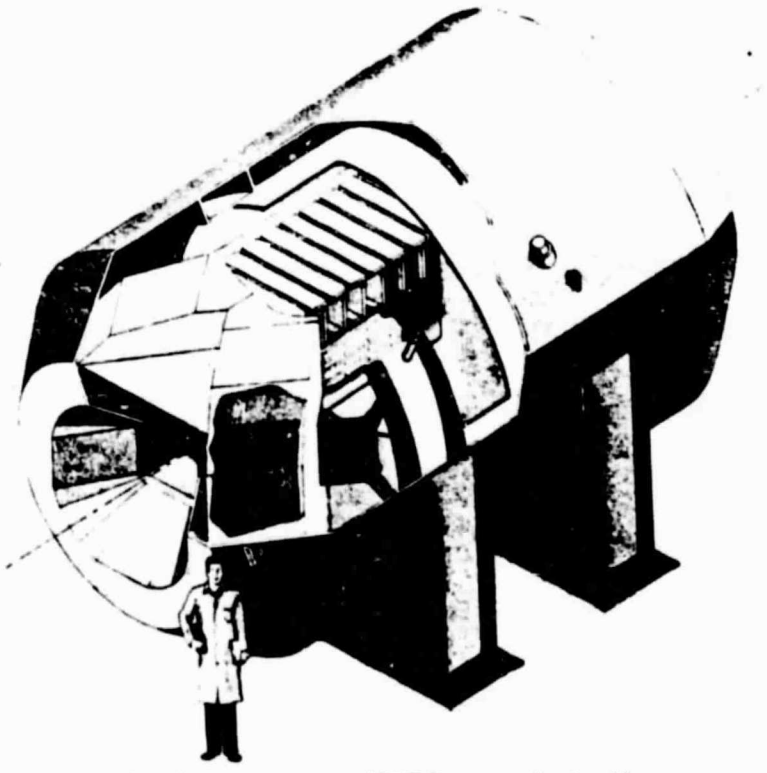

Interior Arrangement, CDIF Superconducting Magnet

SUPERCONDUCTING MAGNET DESIGN FOR MHD COMPONENT DEVELOPMENT AND INTEGRATION FACILITY

FIG. 2.3.3.5-3

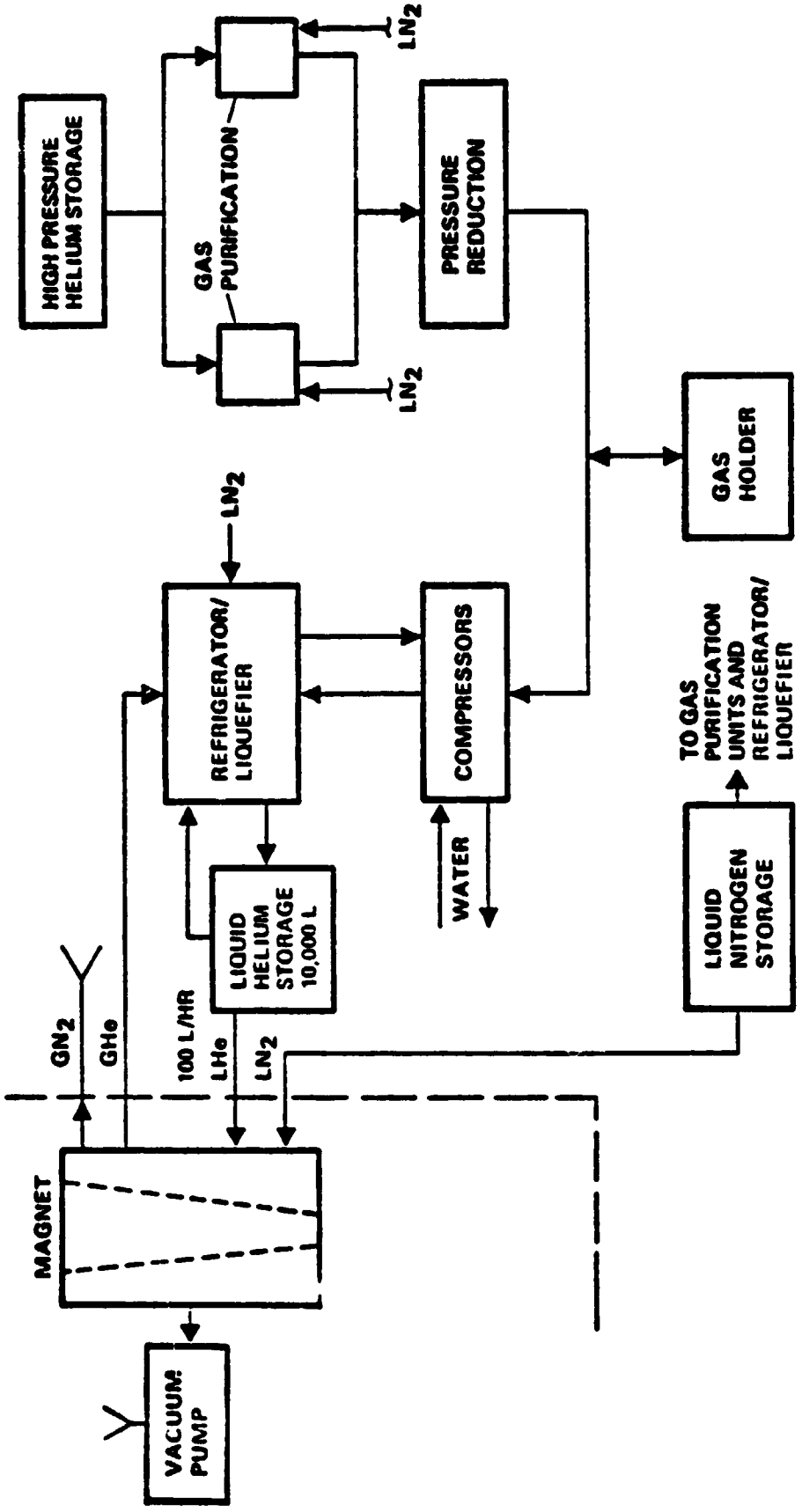

SCHEMATIC DIAGRAM OF CRYOGENIC SUPPORT SYSTEM FOR SUPERCONDUCTING MAGNET

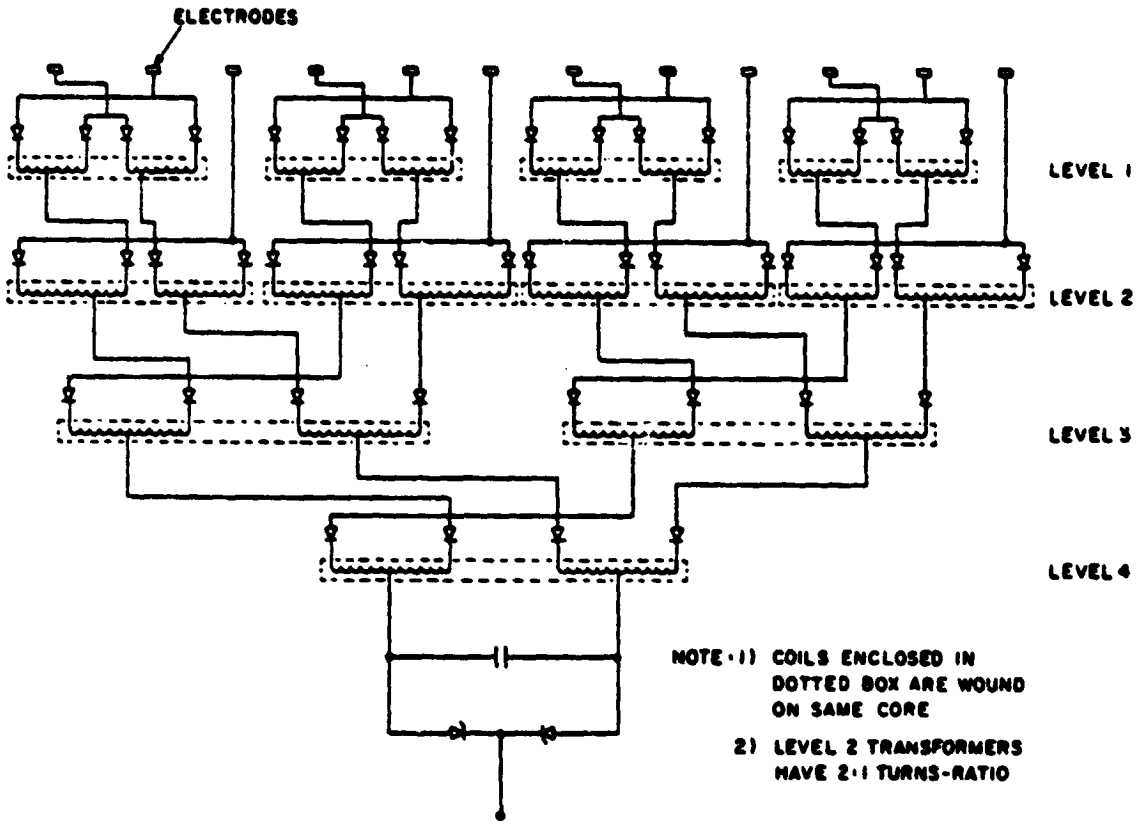

CONSOLIDATION NETWORK FOR 12 ELECTRODES

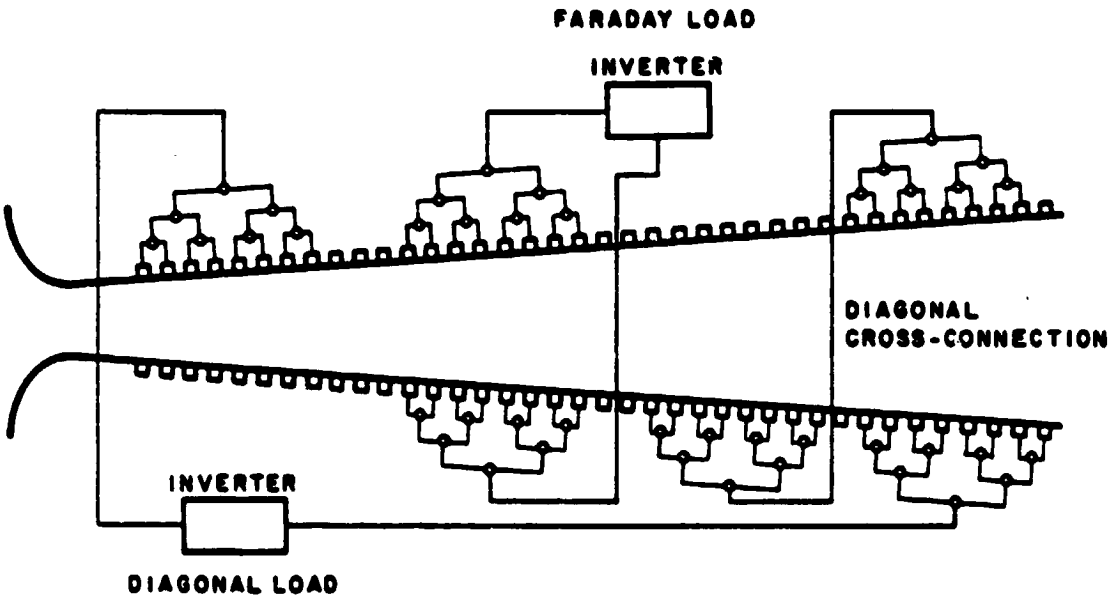

CONSOLIDATION SCHEMES FOR FARADAY AND DIAGONAL CHANNELS

The first guideline narrows the choice to cycles which employ separately-fired high temperature air heaters or oxygen enrichment since directly-fired high temperature air heaters require considerably more development. The second criterion favors the oxygen enrichment cycle since it appears to have a slight economic edge over the separately-fired high temperature air heater case. The third criterion also favors the oxygen enrichment case since a "decision was made by the Director of the DOE Office of MHD in August 1979 to select the oxygen enrichment option for use in the ETF and the target commercial plant," according to a recent report (Ref. 2.3-5).

On this basis, the oxygen enrichment option has been selected for the present investigation and the specific configuration and design parameters of the oxygen enriched cycle investigated by Avco in the PSPEC program have been selected as a reference plant. The baseline technology characteristics are given in Table 2.3.4-1.

TABLE 2.3.4-1

BASELINE TECHNOLOGY FOR COAL-FIRED MHD COMBINED CYCLE POWER PLANT

Illinois No. 6 Coal

MHD		
Oxidizer Flow,	lb/sec (34% O_2)	1008
Combustion Temperature,	F	4675
Pressure Ratio		9.1
Magnet Strength,	Tesla	6
Power Output,	MW(dc)	554
Steam System		
Throttle/Reheat Temperature,	F/F	1000/1000
Throttle/Reheat Pressure,	psi/psi	2400/444
Throttle/Reheat Flow,	lb/sec/lb/sec	974/735
Power Output	MW	684
Overall Plant		
Total Power,	MW	1238
Net Power,	MW	978.5
Heat Rate,	Btu/kWh	7828

2.3.5 References

2.3-1 Avco-Everett Research Laboratory, Engineering Test Facility Conceptual Design Final Report, DOE Report FE-2614-2, June 1978.

2.3-2 Marston, P. G., Thome, R. J., "The U.S. Department of Energy National Program of Magnet Technology for MHD," Seventh International Conference on MHD Electrical Power Generation, M.I.T., 1980.

2.3-3 U.S. Department of Energy, Fossil Energy Program Report, 1 October 1977 - 30 September 1978, DOE/FE-0001/1, December 1979.

2.3-4 General Electric Co., MHD-ETF Program Final Report, DOE Report FE-2613-6, March 1978.

2.3-5 Bercaw, R. W., Seikel, G. R., "Engineering Test Facility Design Definition," Seventh International Conference on MHD Electrical Power Generation, M.I.T., 1980.

3.3 Evaluation of Coal-Derived Fuels for MHD Power Generation Systems

The objective of this task is to determine the overall power plant efficiency of an open-cycle MHD power plant using medium-Btu MBa gas delivered to the power plant via pipline. The properties of the gas delivered to the power plant will be established and any further processing, if necessary, will be identified. Based upon the fuel gas characteristics, the performance of the MHD power plant will be described.

The major emphasis in the Department of Energy MHD program is on direct coal-fired (DCF) open-cycle MHD power generation. This emphasis is based upon the results of a number of comparative investigations in which direct coal-firing has been judged to be the most economical approach. As a result, a large amount of data has been developed on cycle performance and plant costs for DCF MHD. The only comprehensive investigation currently being conducted in MHD power generation utilizing coal-derived gas as a fuel is in India (Ref. 3.3-1).

In the investigation reported herein, a DCF MHD plant is selected as a reference case. Modifications due to using MBG as a fuel are identified and the changes in performance are calculated. This procedure takes advantage of the considerable amount of recently-developed estimates of DCF MHD power plant performance (Ref. 3.3-2).

3.3.1 Definition of Fuel Gas Requirements

One of the most critical parameters of an MHD generator is the electrical conductivity of the plasma. The plasma acquires its electrical conductivity as the seed material ionizes at very high temperature. For a given amount of seed material in the products of combustion, the electrical conductivity is very sensitive to the temperature, so that special measures are taken to achieve high flame temperature. These measures include enrichment of the combustion air with oxygen and preheating the enriched air and, possibly, the fuel. For a given fuel and a given oxidizer (enriched air), the conductivity at a given temperature depends strongly on the composition of the products of combustion.

A complete determination of the suitability of a coal-derived gaseous fuel for application in an MHD power plant and the optimum fuel conditions requires the determination of the electrical conductivity of the products of combustion over a range of fuel and oxidizer conditions. Because an accurate determination of the electrical conductivity of candidate fuels is beyond the scope of the present investigation. The approach taken herein is to determine the conditions which are necessary for attaining the same levels of electrical conductivity as are projected for the DCF MHD power plant reference case.

The oxygen-blown Texaco and British Gas Corporation (BGC) slagging gasifiers were selected as the gasifiers to provide medium-Btu fuel gas for transport in pipelines to the power generation site. Properties of the fuel gas from each of these gasifiers, based on Ref. 3.3-3, are given in Table 3.3.1-1. Since the conductivity of the products of combustion were not determined directly, it was ascertained whether or not the flame temperatures are sufficiently high for achieving adequate conductivity. Thus flame temperatures were determined for combustion of the two types of fuel gas with several different oxidants under several sets of conditions. The results of the flame temperature calculations are given in Table 3.3.1-2. Oxidizer compositions investigated include unenriched air (20.74 percent O_2 by volume) and enriched air with oxygen concentrations of 28 percent and 35 percent. In all cases, the oxidizer was considered to be preheated to 1100°F. The fuel gas was considered to be preheated to 1100°F or to be delivered to the combustor at the pipeline temperature of 68°F. The pressures considered were 6 atmospheres and 8 atmospheres.

As seen in Table 3.3.1-2, the flame temperatures determined range from a minimum of 4207°F for the combustion of the Texaco fuel gas with unenriched air at 8 atmospheres to a maximum of 4870°F for the combustion, at a pressure of 8 atmospheres, of the BGC slagging gasifier fuel gas with air enriched to 35 percent O_2 by volume with both the oxidizer and the fuel gas preheated to 1100°F. The acutal stagnation temperature at the inlet to the MHD generator will be less than the estimated flame temperature due to heat loss to the walls of the combustor and heat absorption due to vaporization and ionization of the seed.

In the DCF MHD reference plant, the MHD generator inlet stagnation temperature is in the 4650 to 4800°F range. Achieving an MHD generator inlet stagnation temperature in this range for the MBG-fired MHD plant is estimated to require an adiabatic flame temperature in the 4750°F to 4900°F range. It is observed in Table 3.3.1-2 that the lower end of this range can be achieved with the Texaco MBG at a pressure of 8 atmospheres utilizing air enriched with oxygen to 35 percent by volume if the oxidizer and the MBG are preheated to 1100°F. Under the same conditions, the adiabatic flame temperature for combustion of BGC medium-Btu gas approaches the upper end of this range. The MBG is delivered to the plant site at pressures well in excess of the required pressure and at a temperature above 75°F to prevent condensation of moisture. No further conditioning of the fuel gas is required except for preheating to achieve the necessary flame temperature. The exhaust gas from the MHD generator will be utilized to preheat the MBG as well as the oxidizer.

TABLE 3.3.1-1

GAS COMPOSITIONS

Element	Texaco Gas Vol. %	BGC Gas
CH_4	0.1	8.4
H_2	35.6	30.6
CO	52.4	58.5
CO_2	10.8	1.9
H_2S + COS	100 ppm	100 ppm
N_2	0.8	0.5
Ar	0.2	0
H_2O	0.1	0.1
	100.0	100.0
Heating Values, LHV		
LHV, Btu/scf	267.5	349.1
LHV, Btu/lb	4949	6825

TABLE 3.3.1-2

ADIABATIC FLAME TEMPERATURES FOR COMBUSTION OF MEDIUM-BTU GASES

Fuel Gas Type	Oxidizer Oxygen Content, Vol%	Combustion Pressure, atm	Oxidizer Preheat Temperature, °F	Fuel Gas Preheat Temperature, °F	Adiabatic Flame Temperature, °F
Texaco	20.74	8	1100	1100	4207
Texaco	28.00	6	1100	68	4402
Texaco	28.00	6	1100	1100	4539
Texaco	28.00	8	1100	68	4434
Texaco	28.00	8	1100	1100	4575
Texaco	35.00	6	1100	68	4578
Texaco	35.00	6	1100	1100	4710
Texaco	35.00	8	1100	68	4616
Texaco	35.00	8	1100	1100	4753
BGC	20.74	8	1100	1100	4344
BGC	28.00	6	1100	68	4522
BGC	28.00	6	1100	1100	4630
BGC	28.00	8	1100	68	4555
BGC	28.00	8	1100	1100	4668
BGC	35.00	6	1100	68	4719
BGC	35.00	6	1100	1100	4825
BGC	35.00	8	1100	68	4760
BGC	35.00	8	1100	1100	4870

3.3.2 Identification of Power Generation Facility

The direct coal-fired MHD power plant configuration which has been selected as a reference plant is the conceptual design for an oxygen-enriched MHD power plant investigated by Avco-Everett Research Laboratory in the Parametric Study of Potential Early Commercial (PSPEC) MHD Power Plants (Ref. 3.3-2). A schematic diagram of the cycle configuration for this reference plant is shown in Fig. 3.3.2-1. A schematic diagram of its steam and feedwater cycle configuration is shown in Fig. 3.3.2-2.

This reference plant configuration was investigated in the PSPEC MHD study over a range of sizes and parameters. The base case is a 931-MWe plant utilizing enriched air with 35 percent oxygen by volume preheated to 1100°F by the MHD generator exhaust gas. The fuel is Montana Rosebud coal. Variations investigated included power plant size reduction to 614 MWe, oxygen enrichment levels ranging from 29 percent to 39 percent, oxidizer preheat levels ranging from 1000°F to 1400°F and utilization of Illinois No. 6 coal as an alternate fuel.

The oxygen for enriching the air is provided on an on-site air separation plant which produces oxygen with a purity of 80 percent. The air separation plant compressor-drive turbines are driven by steam from the MHD power plant bottoming cycle. Steam from the bottoming cycle also drives the compressors for the combustion air. The steam bottoming plant boiler feedwater is used for cooling the combustor, MHD generator and diffuser. The steam turbine is a subcritical unit operating at 2400 psia/1000°F inlet conditions with 1000°F single reheat. Stack gas from the steam bottoming plant is used for drying the coal. Extensive coal drying is required in order to maximize the flame temperature and the plasma electrical conductivity. The recovered seed is converted from K_2SO_4 to K_2CO_3 by means of the formate seed regeneration process which produces $CaSO_4$ as a by-product which requires disposal. The formate process also requires fuel gas produced from an on-site coal gasifier.

The performance of the MBG-fired MHD plant is determined by identifying the differences between the MBG-fired MHD power plant and the reference plant. These differences arise from the fuel and fuel characteristics. For the DCF MHD plant, there is need for coal handling and processing and means must be provided for dealing with the coal ash and sulfur. The MBG is essentially free of ash and sulfur and has different chemical composition and heating value. The differences between the two types of MHD power plant may be categorized as differences in plant configuration, operational differences and performance differences.

The change in fuel means the elimination of facilities and equipment for delivery, storage drying, pulverizing, pressurization and injection of coal. These

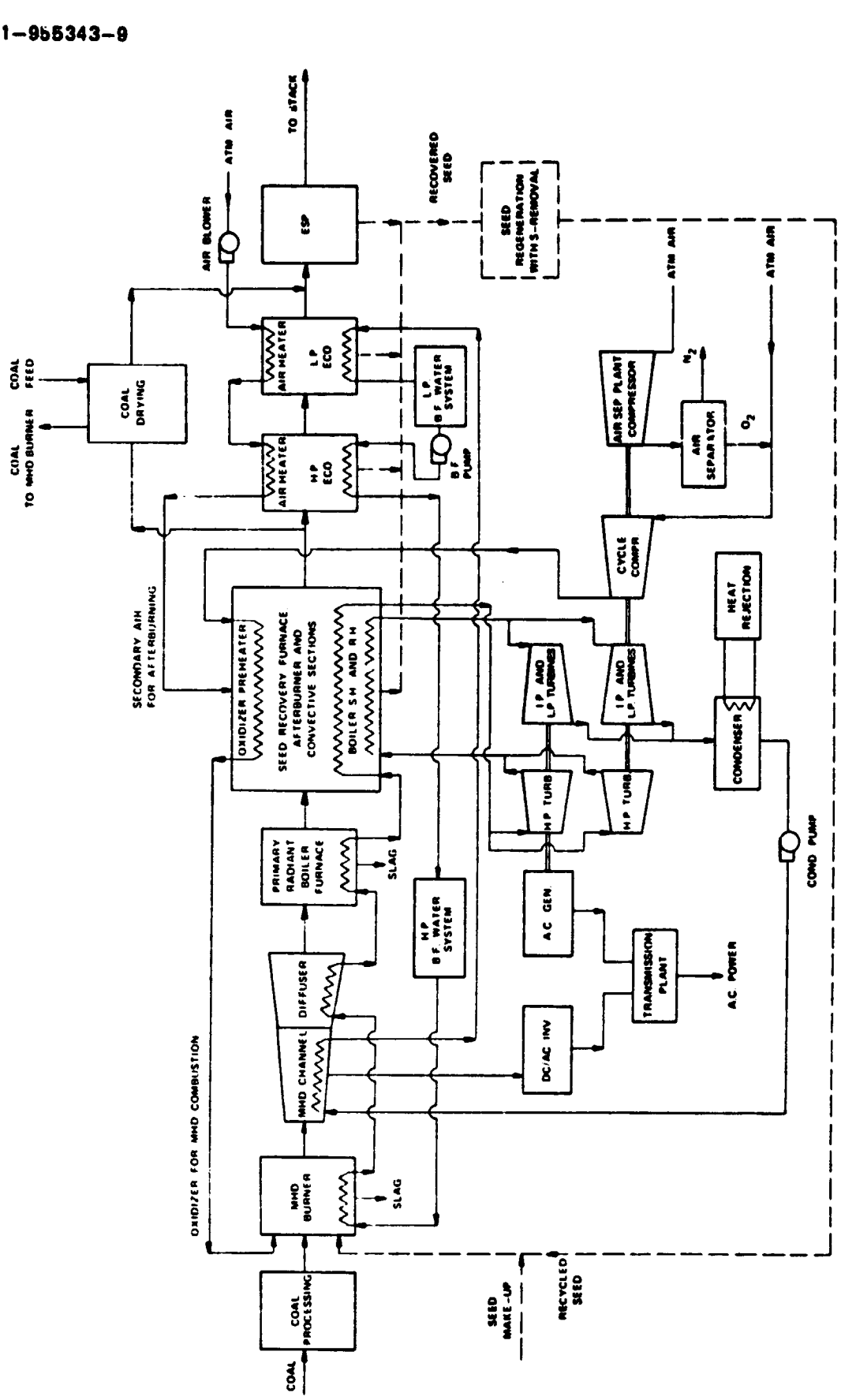

CYCLE CONFIGURATION FOR DIRECT COAL–FIRED MHD REFERENCE PLANT

FIG. 3.3.2-2

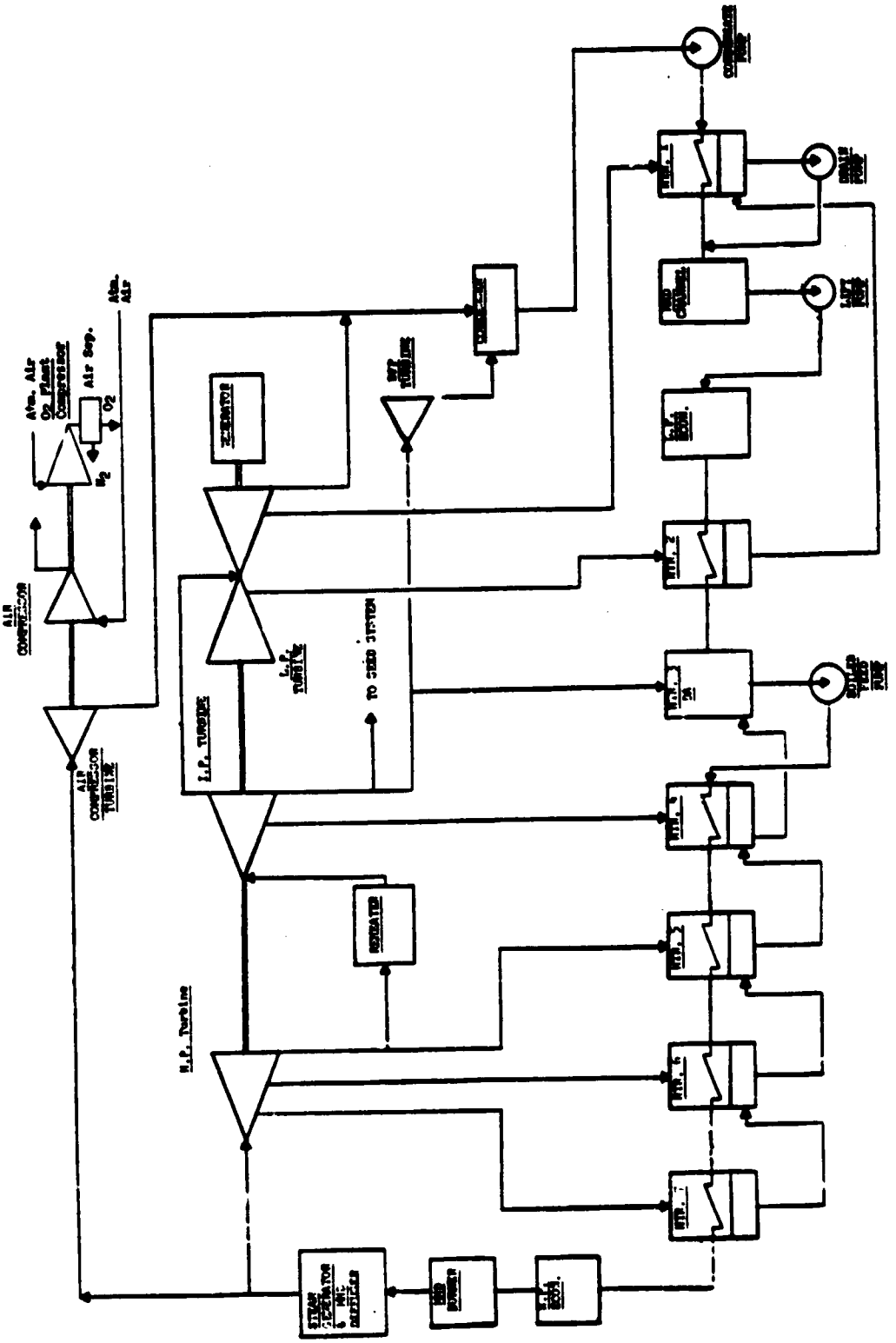

STEAM AND FEED WATER CYCLE CONFIGURATION FOR DIRECT COAL-FIRED MHD REFERENCE POWER PLANT

items are replaced with medium-Btu gas piping and flow controls. An additional heat exhanger is required for preheating the MBG prior to combustion.

The absence of coal ash in the MBG fuel has several implications. The combustor is considerably simplified since it is not necessary to remove slag from the combustor. There will be no build-up of a slag layer on the walls of the MHD generator. This entails a considerable change in MHD channel design which is related more to channel lifetime and materials selection than to channel performance. The equipment downstream of the MHD generator will be relieved from problems associated with slag, including deposits, corrosion, fouling, seed absorption and ash removal. There is also no requirement for facilities and equipment for ash handling and disposal.

The absence of sulfur in the MBG fuel introduces the possibility of several modifications in MHD power plant configuration.* Since the seed does not need to play a role in sulfur emissions control, the amount of seed injected into the combustor is the optimum amount required for achieving high plasma electrical conductivity, rather than the amount required to achieve the necessary sulfur emissions control. Furthermore, the option becomes available of injecting the seed into the combustor in the form of K_2SO_4 instead of a sulfur-free compound. The need for a seed regeneration system is eliminated since the fuel is virtually sulfur-free. This not only eliminates the seed regeneration facility itself, but also the associated coal gasifier, the CaO delivery and handling system and the $CaSO_4$ disposal system.

The changes in configuration of the heat recovery seed recovery system (HRSR) include the addition of a heat exchanger to transfer heat from the MHD generator exhaust gas to the MBG fuel and the elimination of the need to divert some of the stack gas to the coal drying system. The elimination of design constraints due to the absence of ash and sulfur in the gas stream introduce additional flexibility in certain design details which may lead to small improvements in performance and reductions in cost. A major change in balance-of-plant systems arise from elimination of ash and $CaSO_4$ disposal. Figure 3.3.2-3 is a schematic diagram of the cycle configuration for the MBG-fired MHD plant based upon the cited modifications of the DCF MHD plant.

The overall performance of each of the MBG-fired MHD power plants is determined by estimating the performance modifications for each component and subsystem and

---

* In the DCF MHD power plant, sulfur is captured by the seed material and collected from the gas stream in the process of recovering the seed. Sulfur is removed external to the cycle in a seed regeneration system and the seed is recycled to the combustor in a sulfur-free form.

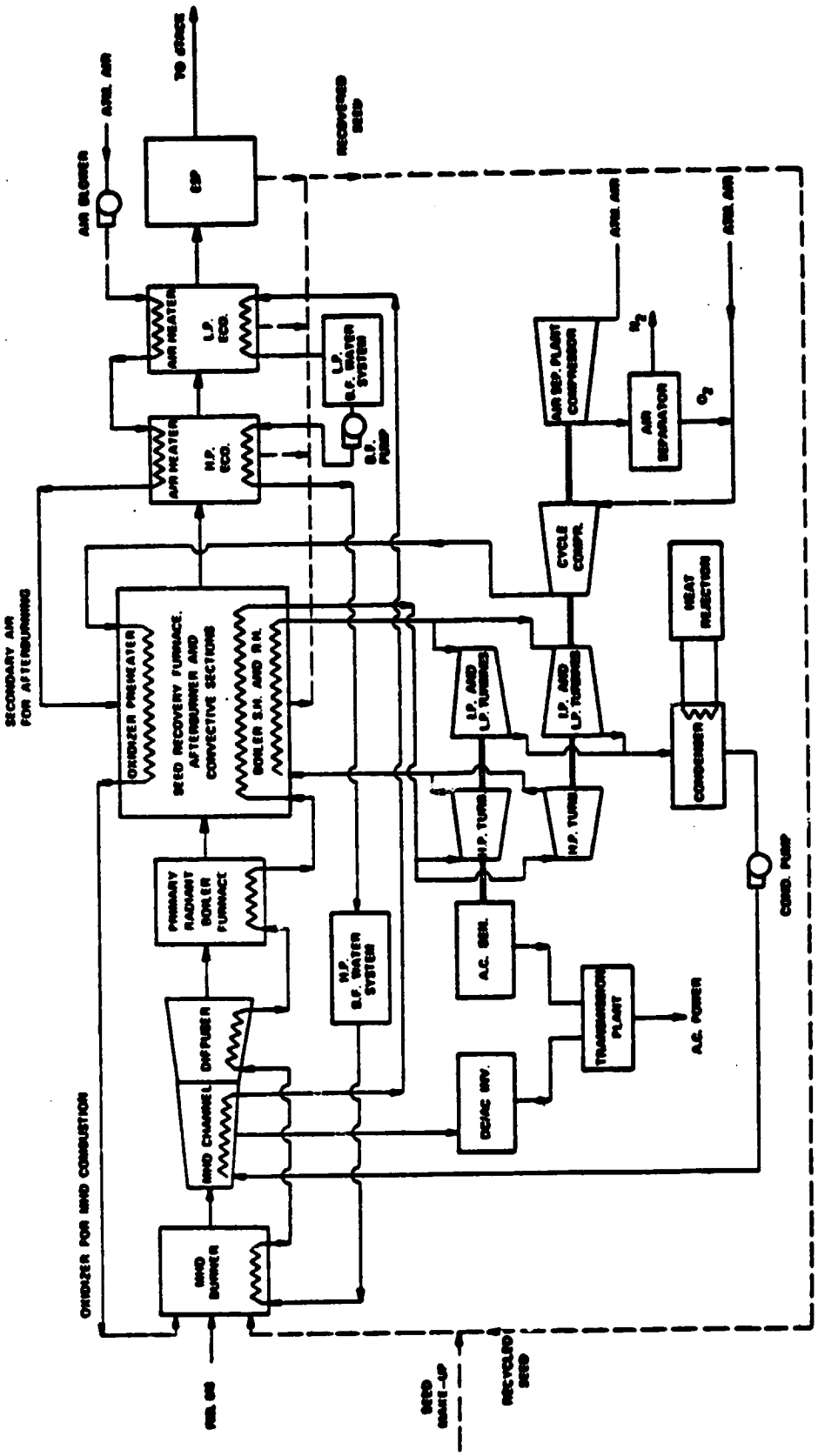

CYCLE CONFIGURATION FOR MEDIUM-BTU GAS FIRED MHD POWER PLANT

determining their cumulative effects. The component and subsystem performance modifications are determined by making direct comparisons between the MBG-fired MHD power plants and the DCF MHD power plant. The thermal input to the MBG-fired MHD power plants is taken to be the same as the thermal input to the MHD combustor of the reference plant, based upon the fuel higher heating value. This input is 2174 Mwt (7420 x 10^6 Btu/hr).

The operating conditions such as magnetic field strength and steam throttle conditions for the MBG-fired MHD power plants are generally taken to be the same as for the DCF MHD reference plant. However, combustor pressures for the MBG cases are taken to be greater than that for the DCF case. The reason for this is that the selection of the pressure is based upon a trade-off between MHD generator output and the power consumption of the oxidizer compressor, both of which increase with increasing pressure. Since the oxidizer flow rates for the MBG cases are less than that for the DCF case, it is advantageous to operate at higher pressure. This helps to compensate for the lower combustion temperatures of the plasma for the Texaco MBG case.

The MHD generator output will be lower for the Texaco MBG case, due primarily to the lower combustion temperature, and, hence, lower conductivity. The heat loss for the MBG-fired MHD combustors are less than that of the DCF MHD because of the requirement for slag removal from the combustion products for the DCF combustor. The MHD channel and diffuser heat loss for the DCF is less than that for the MBG cases because of the insulating effect of the slag layer in the DCF case. However, the heat losses from the combustor, channel and diffuser are picked up by boiler feedwater for the steam bottoming plant.

The compressor power consumption for the oxidizer for the MBG cases is reduced relative to that for the DCF case due to the lower oxidizer flow rates for the MBG-fired power plants. The air separation plant power consumption for the MBG cases is also lower than that for the DCF case because of the reduction in oxygen demand.

The oxidizer preheating requirement is also reduced for the MBG cases because of the lower oxidizer flow rates. However, this advantage is more than offset by the necessity to preheat the medium-Btu gas itself in order to achieve high combustion temperatures. The requirements for coal drying energy and fuel for seed reprocessing are eliminated for the MBG cases.

The estimated performance for the two MBGF MHD power plants are given in Table 3.3.2-1. The performance levels for the Texaco and BGC gas fuels are 43.4 and 44.6 percent, respectively, based upon fuel higher heating value. The efficiencies based upon lower heating values are listed, respectively, as 46.3 and 47.6 percent, for comparison with the fuel cell and combined cycle cases. The lower performance of the plant utilizing Texaco MBG is due primarily to the lower MHD generator output resulting from the lower electrical conductivity associated with lower combustion temperature.

TABLE 3.3.2-1

PERFORMANCE ESTIMATES FOR MHD SYSTEMS

	Texaco	BGC
Fuel System:		
Flow Rate (lb/sec)	390.4	282.7
Heating Value, HHV (Btu/lb)	5282	7290
MHD Generator:		
Oxygen Enrichment (% by Vol.)	35	35
Oxidizer Flow Rate (lb/sec)	652	693
Oxidizer Preheat Temp. (^{o}F)	1100	1100
Fuel Preheat Temp. (^{o}F)	1100	1100
Seed (% K by Wt.)	1.0	1.0
Pressure Ratio (Compressor)	11.5	10.5
Combustor Exit Temp. (^{o}F)	4650	4750
Magnet Strength (Tesla)	6	6
MHD Gen. Output, dc (MW)	510	560
Steam Cycle:		
Throttle/Reheat Temp. (^{o}F/^{o}F)	1000/1000	1000/1000
Throttle/Reheat Pres. (psi/psi)	2400/444	2400/444
Throttle/Reheat Flow (lb/sec/lb/sec)	913/689	886/668
Power Output (MW)	641	622
Overall Plant:		
Total Power (MW)	1151	1182
Net Power (MW)	944	969
Heat Rate, HHV - basis (Btu/kwh)	7864	7652
Heat Rate, LHV - basis (Btu/kwh)	7368	7164
Efficiency, HHV - basis (%)	43.4	44.6
Efficiency, LHV - basis (%)	46.3	47.6

3.3.3 References

3.3-1 Sharma, R., et al.: An Appraisal of MHD Generator Performance With Coal Based Fuels and Aqueous Seed Injection. Seventh International Conference on MHD Electrical Power Generation, M.I.T, 1980.

3.3-2 Hals, F.A.: Parametric Study of Potential Early Commercial MHD Power Plants, DOE/NASA/0051-79/1, NASA CR-159633, December 1979.

3.3-3 Fluor Engineers and Constructors: An Economic Comparison of Molten Carbonate Fuel Cells and Gas Turbines in Coal Gasification - Based Power Plants. EPRI AP-1543, September 1980.

Task 4.3 Evaluation of Integrated Gasification MHD Power Systems

The objective of this task is to determine the overall power plant efficiency of an integrated gasification MHD (IGMHD) power plant. Two types of gasifiers will be considered and the performance of the two resulting IGMHD power plants will be compared. Flow sheets for the gasifiers, the oxygen-blown Texaco and British Gas Corp. slagging types, are those previously developed by the contractor as agreed upon by NASA and the contractor.

4.3.1 Identification of IGMHD Power Plant with Texaco Gasifier

The MHD power system described in Section 3.3.2 utilizing medium-Btu gas (MBG) derived from the oxygen-blown Texaco gasifier will be used as the basis for the IGMHD power plant. The operating conditions are the same but the equipment output differs because of different steam loads in the power plant and power consumption by the gasification system. Figure 4.3.1-1 is a schematic for the interfacing between the gasification plant and the MHD power plant. Figures 4.3.1-2 and 4.3.1-3 are schematic diagrams of the MHD plant.

The fuel gas leaving the gasifier (1) is split, one stream being water quenched (2) to remove slag while the other passes through a high-pressure boiler (3). Prior to going through the boiler, the hot gas temperature is moderated by a recycle stream of cool gas (9). The steam raised in the high-pressure boiler (19) is superheated in the MHD boiler and then goes to the high-pressure turbine in the steam cycle of the MHD power plant. The fuel gas from the high-pressure boiler goes to a fuel gas regenerator (4), an intermediate-pressure boiler (5) and a low-pressure boiler (6).

The steam from the intermediate-pressure boiler (20) is combined with steam from the sulfur plant boiler. It is superheated by means of the exhaust gas from the MHD generator and goes to the intermediate pressure turbine of the MHD plant. Steam from the low pressure boiler is split into two streams. One stream is used for the gasification process and the other is fed to a feedwater heater (HTR.2) in the MHD steam bottoming cycle. This reduces the amount of extraction steam from the steam plant turbines and raises the turbine output.

The fuel gas is scrubbed (7) and passes through a fuel gas regenerator (9) to a feedwater heater (10), allowing further reduction in the extraction steam required from the MHD plant steam turbines. This feedwater heater allows elimination of HTR which had appeared in the Fig. 3.3.2-2. Additional heat exchangers are needed to reduce the gas temperature prior to sulfur removal.

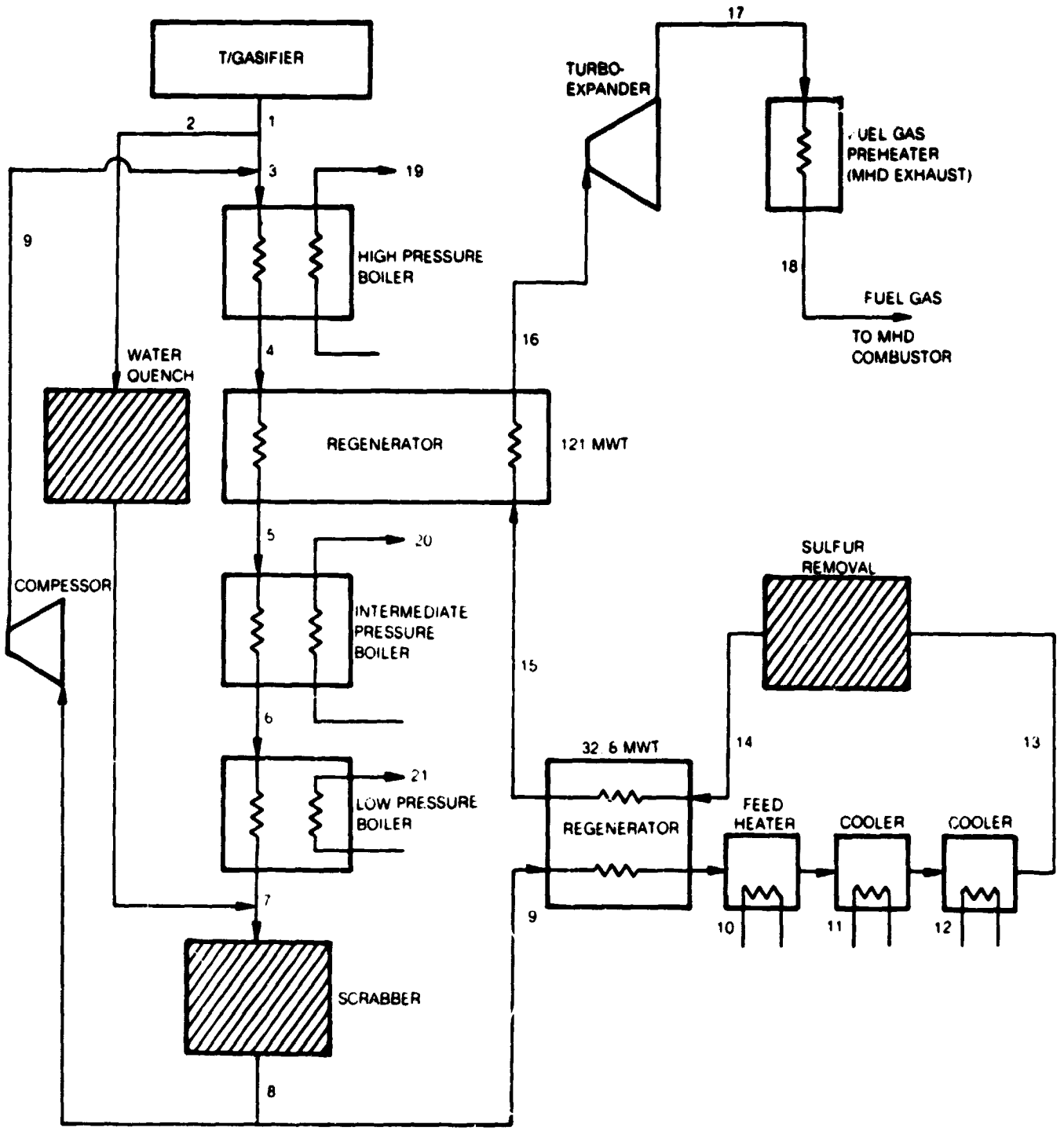

INTEGRATED TEXACO GASIFICATION/MHD POWER PLANT

81-3-154-2

FIG. 4.3.1-2

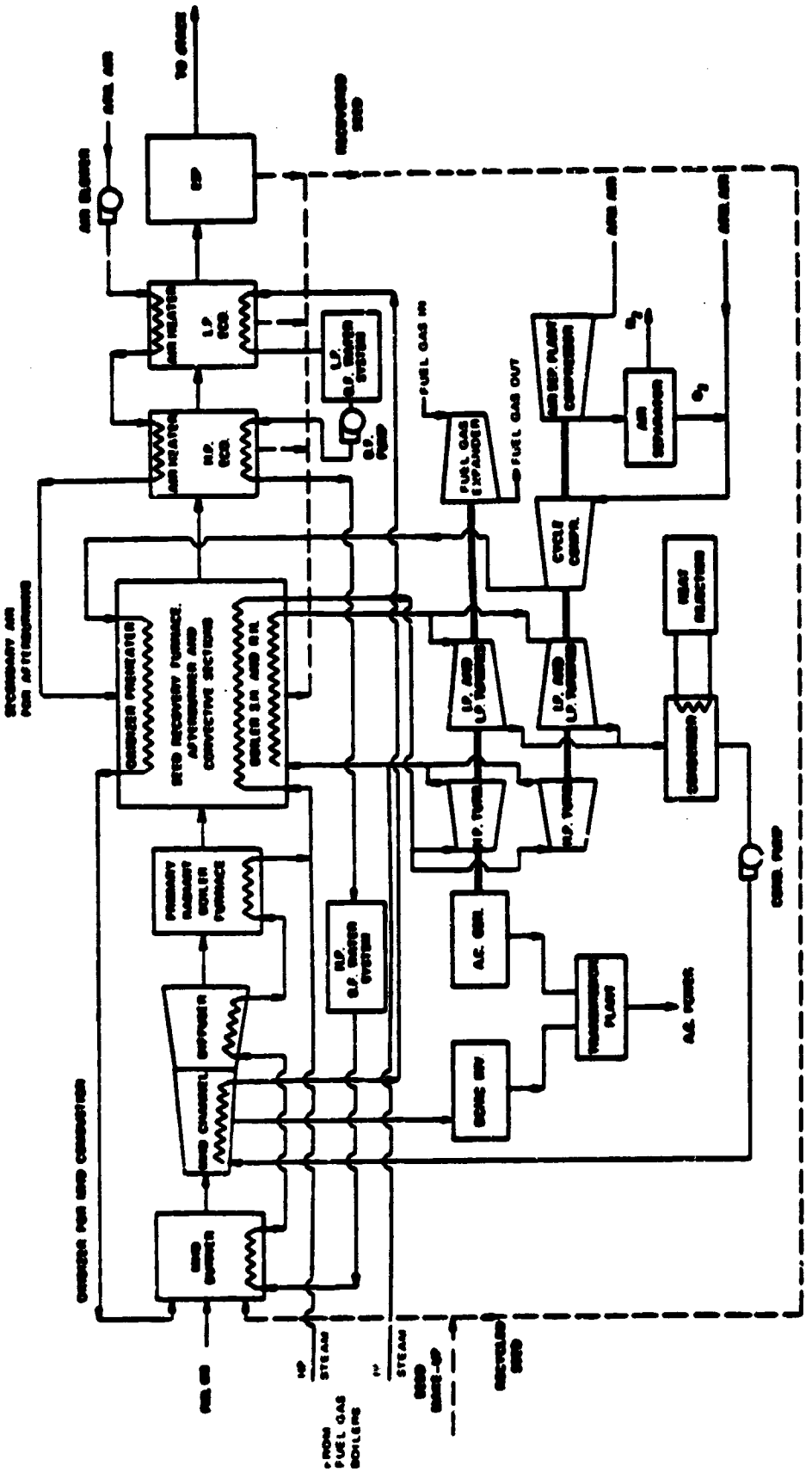

CYCLE CONFIGURATION FOR INTEGRATED TEXACO GASIFICATION/MHD POWER PLANT

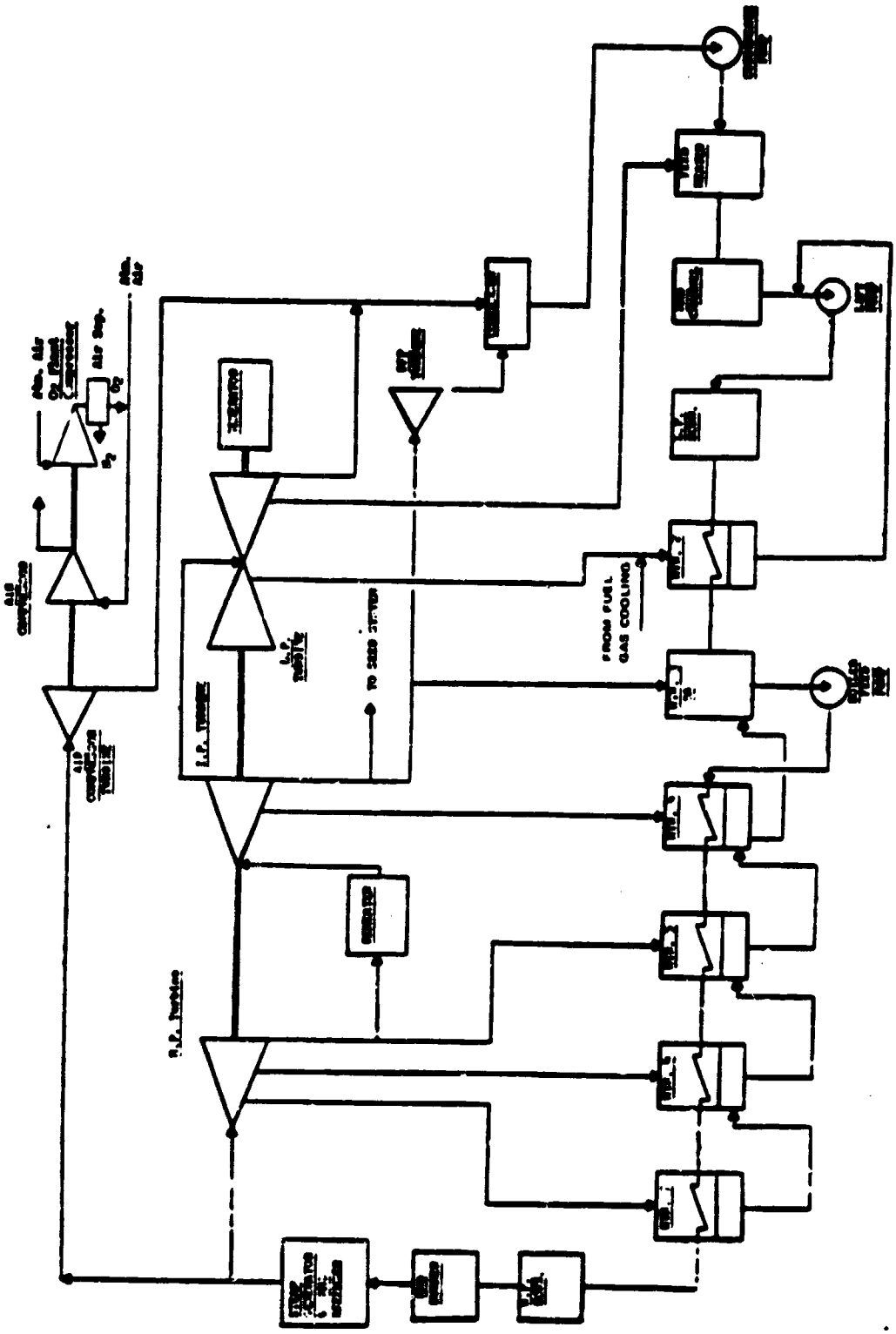

STEAM AND FEED WATER CYCLE CONFIGURATION FOR INTEGRATED TEXACO GASIFICATION/MHD POWER PLANT

Following desulfurization, the low-temperature fuel gas passes through the two regenerators (14, 15) to raise the temperature of the fuel gas to 1100 F at the inlet to the fuel-gas expander (16). The expander lowers the fuel gas pressure to the level required for injection into the MHD combustor and provides additional shaft power. Since the expansion also reduces the temperature, additional heat is provided from the MHD exhaust flow (17, 18) to bring the fuel gas temperature up to 1100 F, which is required to produce a combustion temperature adequate to achieve high electrical conductivity of the plasma. The estimated performance for the Texaco-based IGMHD plant is given in Table 4.3.1-1.

4.3.2 - Identification of IGMHD Power Plant with BGC Gasifier

The MHD power system described in Section 3.3.2 utilizing medium-Btu gas (MBG) derived from the oxygen-blown BGC gasifier will be used as the basis for the IGMHD power plant. The operating conditions are the same but the equipment output differs because of interchanges of flows and energy between the gasifier and the power plant. Figure 4.3.2-1 is a schematic for the interfacing between the gasification plant and the MHD power plant. Figures 4.3.2-2 and 4.3.2-3 show the corresponding schematics for the MHD plant.

The fuel gas leaving the gasifier undergoes a quench (1) and transfers heat for feedwater heating (2) prior to sulfur removal (3). The heating of the MHD steam bottoming cycle feedwater reduces the amount of extraction steam from the steam plant turbines eliminating HTR.1 (shown in Fig. 3.3.2-2) and raising the turbine output. Heat is provided to the clean fuel gas (4) from the MHD exhaust gas, raising the fuel gas to 1100 F at the inlet to the fuel gas expander (5). The expander lowers the fuel gas pressure to the level required for injection into the MHD combustor and provides additional shaft power. Since the fuel gas temperature drops as it goes through the expander, additional heat is provided from the MHD exhaust gas to raise the temperature back up to 1100 F. The estimated performance for the BGC-based IGMHD plant is given in Table 4.3.1-1.

4.3.3 Comparison of Performance

The performance estimates in Table 4.3.1 indicate that the IGMHD power plants using the Texaco and BGC gasifiers would be 34.4 and 37.2 percent, respectively, based upon the fuel higher heating value. The corresponding efficiencies based upon the fuel lower heating value would be 35.9 and 38.9 percent. The higher efficiency of the BGC-based case results from both the higher efficiency of the BGC gasifier and the higher MHD power plant efficiency when BGC medium-Btu gas is the fuel.

TABLE 4.3.1-1

PERFORMANCE ESTIMATES FOR IGMHD SYSTEMS

	Texaco	BGC
Fuel System:		
Coal Rate (tons/day)	9414	7968
Heating Value, HHV (Btu/lb)	12,235	12,235
MHD Generator:		
Oxygen Enrichment (% by Vol.)	35	35
Oxidizer Flow Rate (lb/sec)	652	693
Oxidizer Preheat Temp. (^{o}F)	1100	1100
Fuel Preheat Temp. (^{o}F)	1100	1100
Seed (% K by Wt.)	1.0	1.0
Pressure Ratio (Compressor)	11.5	10.5
Combustor Exit Temp. (^{o}F)	4650	4750
Magnet Strength (Tesla)	6	6
MHD Gen. Output, dc (MW)	510	560
Steam Cycle:		
Throttle/Reheat Temp. (^{o}F/^{o}F)	1000/100	1000/1000
Throttle/Reheat Pres. (psi/psi)	2400/444	2400/444
Throttle/Reheat Flow (lb/sec/lb/sec)	1152/992	886/648
Power Output (MW)	664	539
Overall Plant:		
Total Power (MW)	1174	1099
Net Power (MW)	967	886
Heat Rate, HHV - basis (Btu/kWh)	9925	>174
Heat Rate, LHV - basis (Btu/kWh)	9498	8773
Efficiency, HHV - basis (%)	34.4	37.2
Efficiency, LHV - basis (%)	35.9	38.9

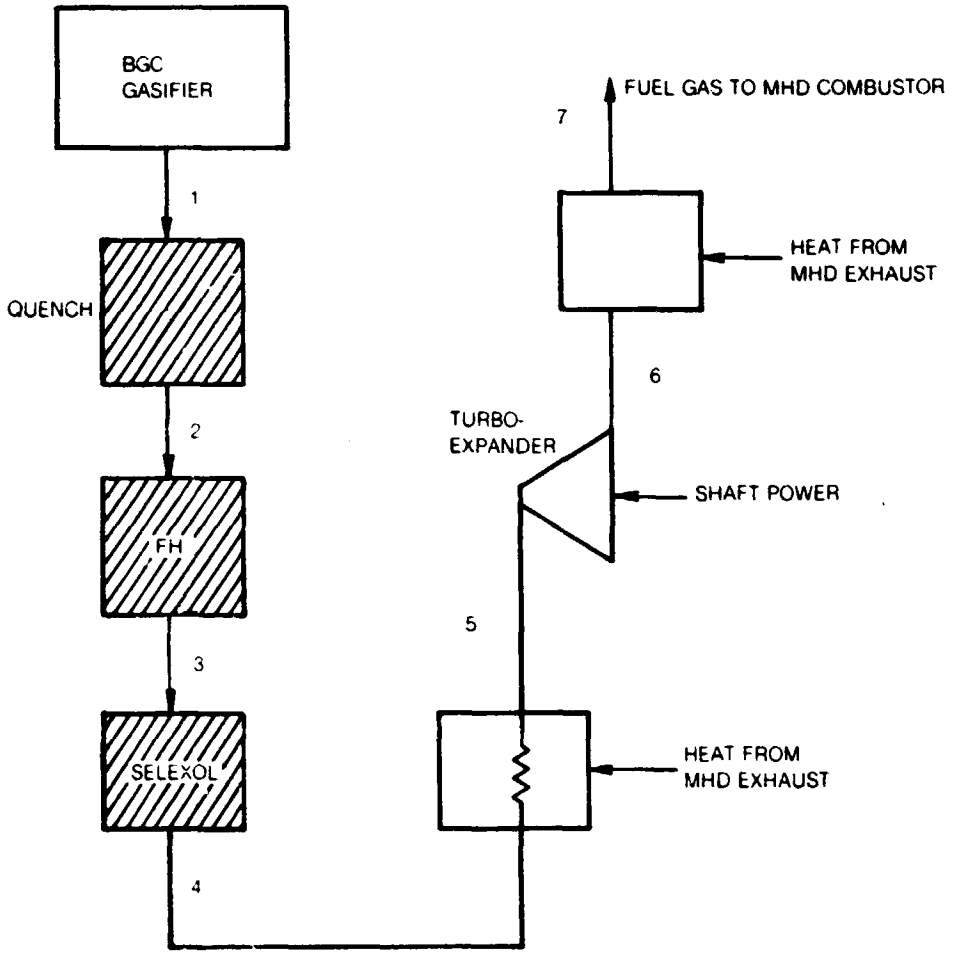

INTEGRATED BGC GASIFICATION/MHD POWERPLANT

81-3-154-1

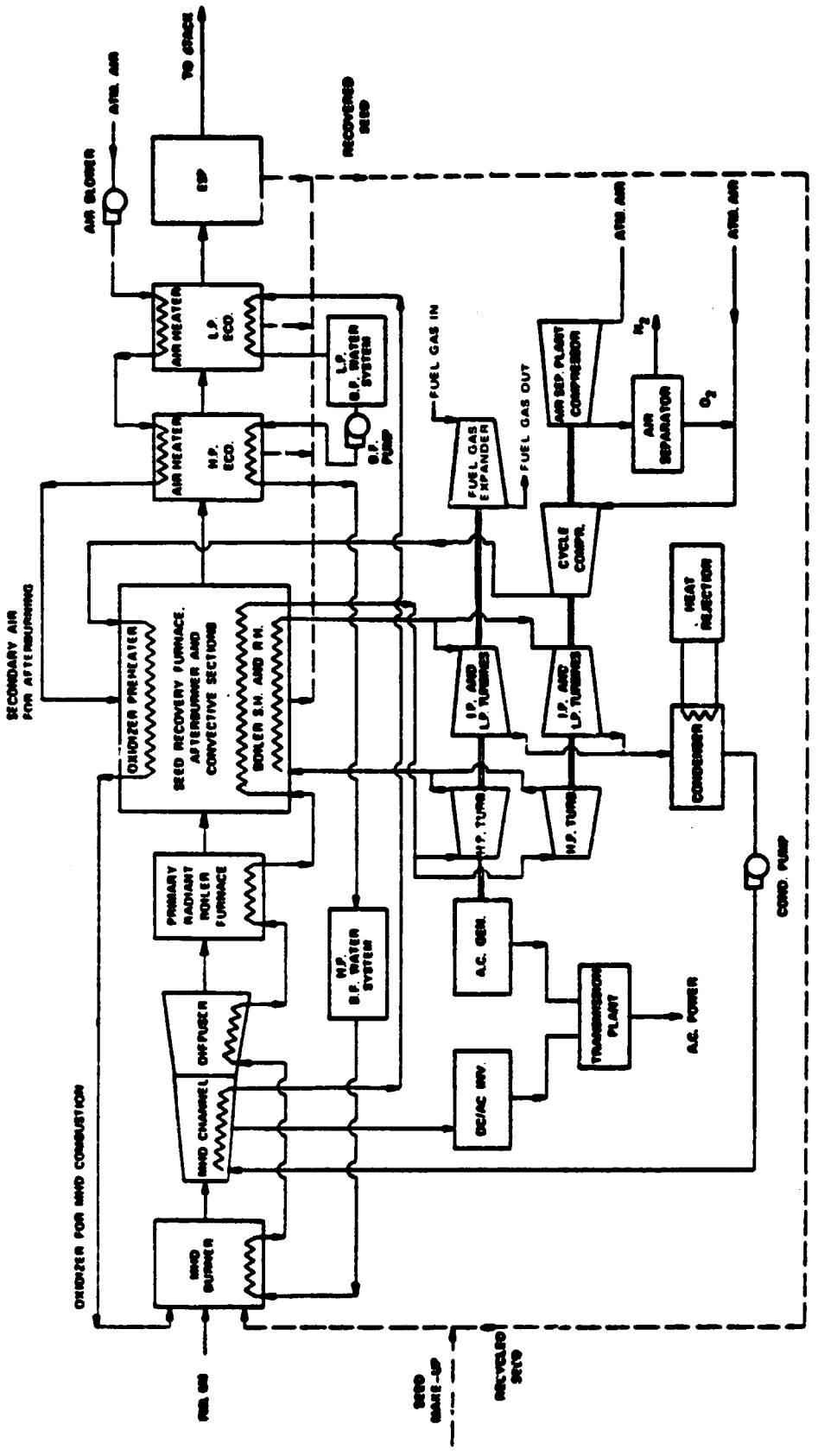

CYCLE CONFIGURATION FOR INTEGRATED BGC GASIFICATION/MHD POWER PLANT

FIG. 4.3.2-3

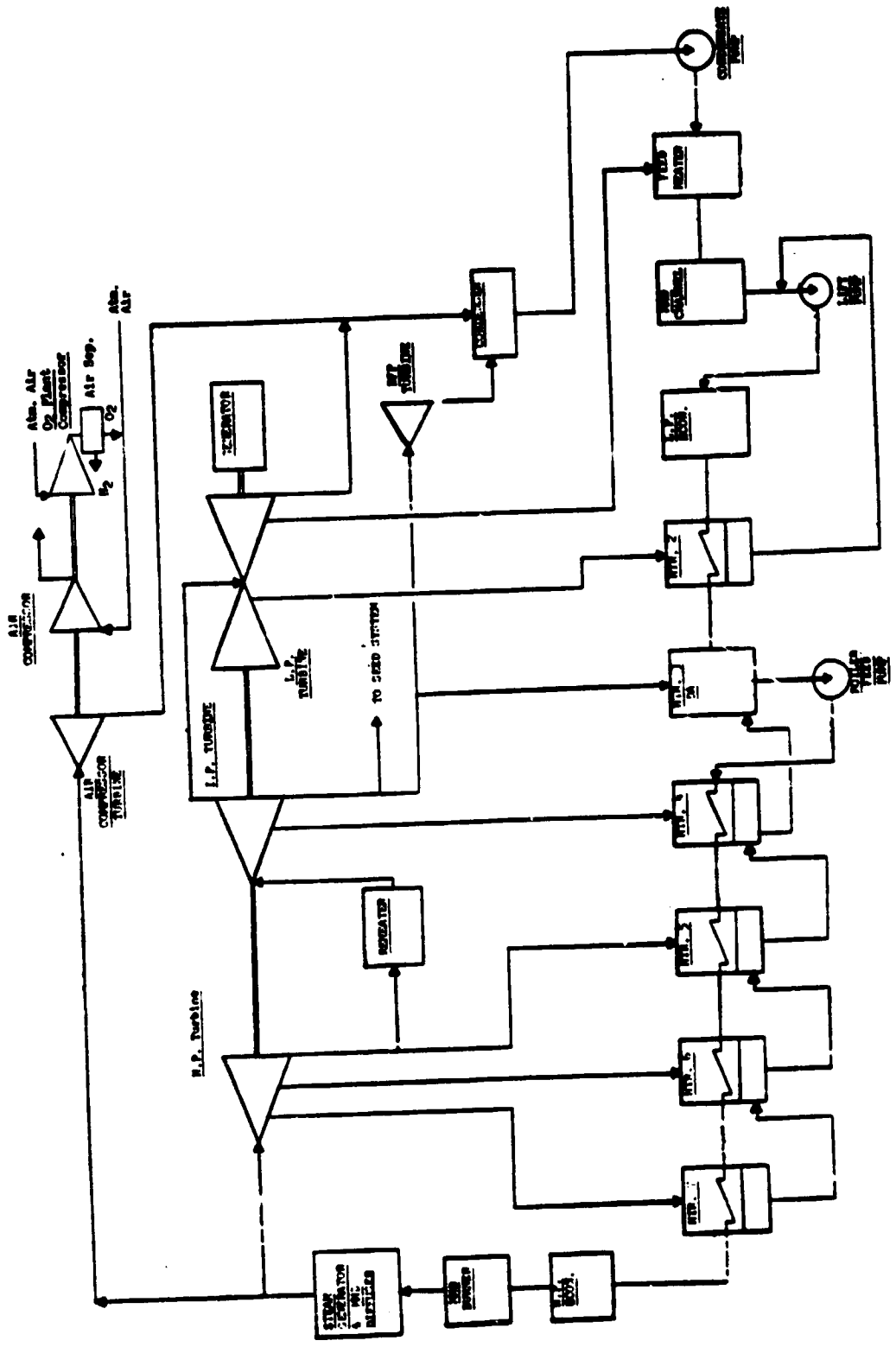

STEAM AND FEED WATER CYCLE CONFIGURATION FOR INTEGRATED BGC GASIFICATION/MHD POWER PLANT

4.3.4 Load Following Capabilities of IGMHD Power Plants

The capability of an MHD power plant to respond to rapid load changes is determined by the response characteristics of the steam bottoming plant and gasifier plant since the MHD generator itself has very fast response characteristics. In fact, MHD generators have been proposed for applications which require rapid pulsed power output. On the basis of response-time capability, the IGMHD power plants are, therefore, estimated to be able to meet electric utility response time requirements.

An estimate of part load performance of MHD power plants indicates that at 70 percent of rated load, the efficiency of an MHD power plant to 96 percent of its full load efficiency. At 50 percent of rated load, the efficiency was estimated to decrease to 83 percent of its full load efficiency.

A.1 Fuel Cell Electrochemical Fundamentals

Fuel cells are electrochemical energy conversion devices, defined as electrochemical cells that can directly and continuously transform the chemical energy of a fuel and oxidant to electrical energy by an isothermal process involving an essentially invariant electrode-electrolyte system. Unlike a battery, a fuel cell in theory does not require recharging rather it will operate as long as both fuel (H_2 from a hydrocarbon fuel) and an oxidant (O_2 from air) are supplied to the electrodes. The electrodes act as reaction sites where the electrochemical transformation of the fuel and oxidant occurs, producing d.c. power. This electrochemical transformation is isothermal; that is, the fuel cell directly uses the available free energy in the fuel at its operating temperature. Thus, it is not Carnot-cycle limited and can yield a high fuel-to-d.c. power conversion efficiency.

To comprehend the operation of a fuel cell, it is necessary to understand the basic electrochemical relationships which incorporate the parameters of primary importance in the determination of fuel cell performance. Because the primary parameters in these relationships do effect performance, an understanding of them will also provide an explanation for the thrust for the fuel cell development activity.

The following presents a brief introduction to the electrochemistry of fuel cells. This presentation has drawn upon the presentation of Ref. A.1-1 which provided a commentary at the appropriate level of detail for appreciating the discussion advanced in the current study. A more exhaustive treatment of electrochemical theory can be obtained from Refs. A.1-2 through A.1-9.

A.1.1 Reversible (Equilibrium) Electrode

Consider an oxidation-reduction reaction such as in Eq. A.1.1-1 occurring at an electrode:

$$aA + ne^- \rightleftarrows bB \qquad \text{(A.1.1-1)}$$

At equilibrium, there is no net reaction, but there is a difference in potential between the electrode and electrolyte. Based on the following thermodynamic relatio ships:

$$\Delta G = -nFE \qquad \text{(A.1.1-2)}$$

$$\Delta G = \Delta G^o + RT \ln K \qquad \text{(A.1.1-3)}$$

where: ΔG = free energy change

n = number of electrons transferred in a reaction

F = Faraday constant

E = fuel cell equilibrium potential

ΔG^o = standard free energy change

R = universal gas constant

T = absolute temperature

K = equilibrium constant

Nernst developed an equation relating the equilibrium potential, E, to the activities of the species involved in the reaction. In general, the Nernst equation is written as:

$$E = E^o + \frac{RT}{nF} \ln \frac{[\text{product of the activity of reactant species}]}{[\text{product of the activity of product species}]} \qquad \text{(A.1.1-4)}$$

where E^o is the standard potential when all the species involved are at unit activity. The standard potential, E^o, is related to the standard free energies of the species by:

$$\Delta G^o = -nFE^o \qquad \text{(A.1.1-5)}$$

For the acid fuel cell, the overall reaction is given in the following equation:

$$H_2 + 1/2\ O_2 \rightleftarrows H_2O \qquad \text{(A.1.1-6)}$$

At the normal operating temperature of 190 C and $E^o = 1.14$ volts, the Nernst equation is:

$$E = 1.14 + \frac{RT}{2F} \ln \frac{[P_{H_2}]\ [P_{O_2}]^{1/2}}{[P_{H_2O}]} \qquad \text{(A.1.1-7)}$$

The molten carbonate reactions are given in the following equations:

$$H_2 + CO_3^{=} \rightleftarrows H_2O + CO_2 + 2e^- \qquad \text{(A.1.1-8)}$$

$$CO_2 + 1/2\ O_2 + 2e^- \rightleftarrows CO_3^{=} \qquad \text{(A.1.1-9)}$$

Because CO_2 is fed to the cathode and produced at the anode, the concentrations are not necessarily equal, so the overall reaction is written as:

$$H_2 + [CO_2]_c + 1/2\ O_2 \rightarrow [CO_2]_a + H_2O \qquad \text{(A.1.1-10)}$$

At a normal operating temperature of 650 C and $E^o = 1.02$ volts, the Nernst equation can be written as:

$$E = 1.02 + \frac{RT}{2F} \ln \frac{[P_{H_2}]}{[P_{CO_2}]_a[P_{H_2O}]} + \frac{RT}{2F} \ln [P_{CO_2}]_c[P_{O_2}]^{1/2} \qquad \text{(A.1.1-11)}$$

The fuel cell equilibrium potential, E, can be less or greater than the standard potential, E^o, depending on the sign and magnitude of the logarithmic, concentration-dependent terms of Eqs. A.1.1-7 and A.1.1-11.

Current is related to the electrochemical reaction rate by:

$$i = nFr \qquad \text{(A.1.1-12)}$$

where r is the reaction rate, i/nF. At equilibrium, the forward and reverse reaction rates of Eq. A.1.1-1 are equal. They produce currents equal in magnitude but opposite in sign. The magnitude of the currents is called the equilibrium exchange current density, i_o. High exchange current density indicates that the electrochemical reaction rate is high and good fuel cell performance is possible.

A.1.2 Non-Equilibrium Electrodes - Polarization

Chemical and physical factors associated with various elements of the cell when current is flowing limit the processes described above. This results in a reduction in voltage from the expected reversible potential, E, (Fig. A.1.2-1). Knowledge of these limitations, called polarizations, overpotentials, or overvoltages, η, is useful when attempting to calculate efficiencies.

$$\eta = E - V \qquad \text{(A.1.2-1)}$$

where V is the cell voltage.

The total polarization of the electrode is the sum of the factors which effect efficiency.

A.1.2.1 Activation Polarization - Tafel Equation

Most chemical reactions involve an energy barrier that must be overcome by the reacting species. This activation energy results in activation polarization, η_{act}. Activation polarization is the energy loss which occurs as the fuel or oxidizer is transformed into a state suitable for reaction. This energy loss is the sum of the heat of chemisorption on the catalyst and the heat of formation of the active ion. It is related to the current, i, by the Tafel equation:

$$\eta_{act} = a + b' \log i \qquad \text{(A.1.2.1-1)}$$

This can also be written as:

$$i = i_o \exp (2.3\eta_{act}/b') \qquad \text{(A.1.2.1-2)}$$

where a and b' are empirical and b' is referred to as the Tafel slope obtained from plots of log i versus η. The exchange current can be determined experimentally by extrapolating plots of log i versus η to $\eta = 0$. Equation A.1.2.1-2 describes either the fuel cell anode or the cathode when the appropriate values for i_o, η, and b' are used.

Activation polarization is related to the slow step in the reaction sequence. The slow step could be adsorption of reactant onto the surface, electron transfer, desorption of product, or any other step in the reaction sequence.

Since the required reaction rate for chemisorption and ion formation are both proportional to the current density and a greater potential is needed to maintain a high reaction, the activation polarization loss increases with current density. Porous electrodes of large internal surface area are used to increase the number of "active sites" for chemisorption and, thus, to decrease the potential required for a given over-all reaction rate. An other approach to decreasing activation polarization is to increase temperature.

A.1.2.2 Concentration Polarization - The Limiting Current

Concentration polarization occurs when the electrode reaction is hindered by mass transport effects. The controlling process in the case of concentration polarization may be slow diffusion in the gas phase through the pores of the electrode, solution/dissolution of reactants/products into/out of the electrolyte, or diffusion through the electrolyte to a reaction site. As practical current densities, the latter predominates. When the electrode is completely governed by diffusion processes because of low reactant concentration

in the feed gases or because of conversions approaching 100 percent (reactants depleted), the limiting current, i_L is reached. This situation is characterized by a rapid drop in cell voltage, with increasing current density, as shown in Fig. A.1.2.2-1.

The limiting current, i_L, can be calculated from the diffusion coefficient of the reacting ions, D, the bulk concentration of the reacting ions, C_B, and the thickness of the diffusion layer, X, by applying Fick's Law:

$$i_L = \frac{DnFC_B}{X} \qquad \text{(A.1.2.2-1)}$$

For an electrode free from activation polarization (that is, the reaction is fast), the concentration overpotential is X:

$$\eta_{conc} = \frac{RT}{nF} \ln \left(1 - \frac{i}{i_L}\right) \qquad \text{(A.1.2.2-2)}$$

It should be noted that it is possible to properly design a fuel cell so that the concentration polarization effect on cell voltage is negligible.

A.1.2.3 Total Electrode Polarization

The total overpotential, η, is the sum of the activation and concentration polarizations.

$$\eta = \eta_{act} + \eta_{conc} \qquad \text{(A.1.2.3-1)}$$

In Eq. A.1.2.3-1, E_e is not the Nernst potential for a complete cell (Eqs. A.1.1-7 or A.1.1-11), but is the Nernst potential of either the oxidation or reduction half-cell reaction, as measured against an inert reference electrode.

The signs of the quantities in Eq. A.1.2.3-1 are always such that $V_e \leq E_e$ so that the equation is applicable to both anode and cathode.

A.1.2.4 Ohmic Polarization - iR Losses

When an anode and cathode are connected to an external load, the circuit is complete and current flows. Resistance to conduction of ions through the electrolyte, electrons through the electrodes and current collectors, and by contact resistances (between components) causes ohmic or iR polarization. Because both fuel cell electrodes and the electrolyte obey Ohm's Law, it is easy to calculate the voltage gradient (and loss) required to force ionic and electronic conduction:

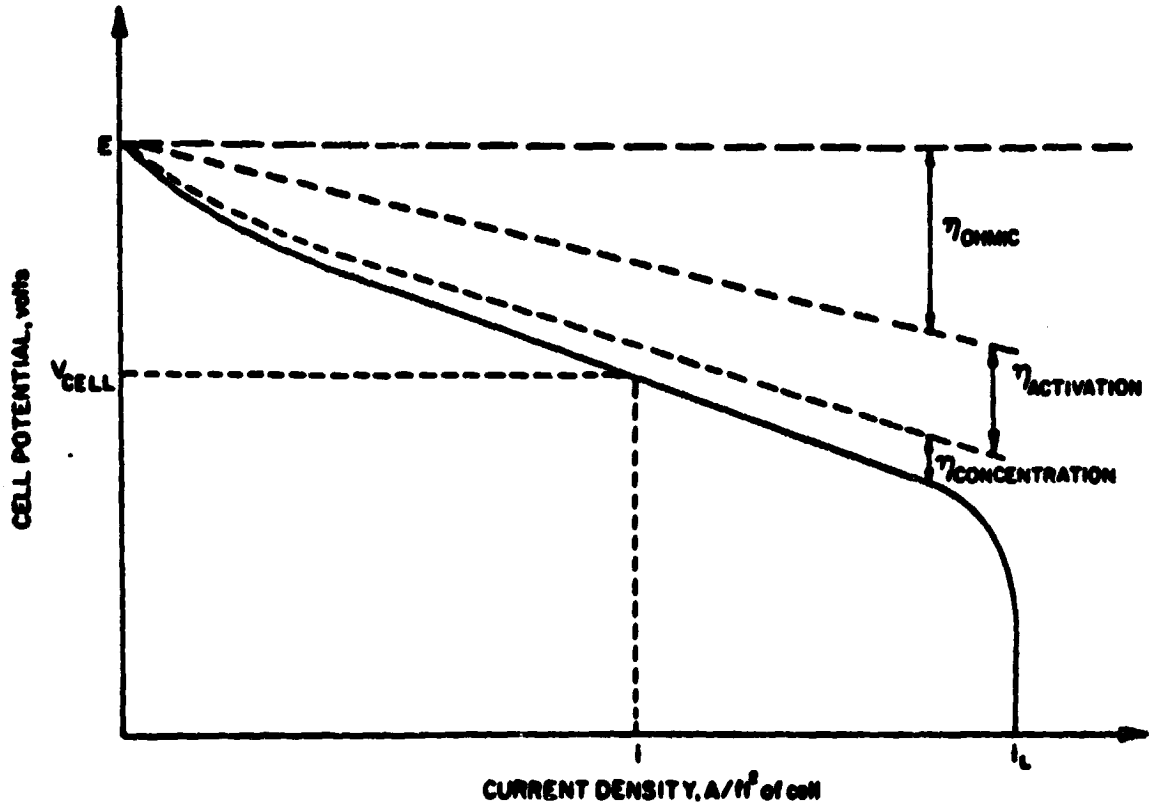

FUEL CELL POLARIZATION CURVE

$$\eta_{ohm} = iR \qquad \text{(A.1.2.4-1)}$$

where R is the total cell resistance including electronic, ionic, and contact resistances.

A.1.3 Cell Performance

Both anodic and cathodic reactions contribute to the cell voltage, and the internal resistance of the cell reduces the available voltage. Therefore,

$$V_{cell} = V_{anode} + V_{cathode} - iR \qquad \text{(A.1.3-1)}$$

where V_{anode} and $V_{cathode}$ are determined experimentally or by Eq. I.A.2-7.

Polarization cannot be eliminated, but can be minimized by cell design. The iR loss can be reduced by using thin electrolytes and be efficient contacts between electrode and leads. Temperature and electrolyte composition also influence the cell resistance.

Concentration polarization is dependent on the mass transport properties of the system. Mass transfer is a function of temperature, pressure, concentration, and the physical properties of the system. In a fuel cell, the reactants must diffuse through the tortuous paths of the porous electrode. This makes electrode structure important. The electrochemical reaction rate is a function of the concentration of the reacting species so, as the conversion increases, the concentration polarization becomes more severe.

Activation polarization depends upon the fundamental electrochemical reaction rate, which is also a function of temperature, pressure, and concentration. However, because the fuel cell reactions under consideration are catalytic, the activation polarization can be changed by using different catalysts.

A.1.4 References

A.1-1 Benjamin, T. G., E. H. Camara, and L. G. Marianowski: Handbook of Fuel Cell Performance. DOE Contract No. EC-77-C-03-5145, May 1980.

A.1-2 Angrist, S. W.: Direct Energy Conversion. Allyn and Bacon, Boston, Mass., 1965.

A.1-3 Williams, K. R., Ed.: An Introduction to Fuel Cell. Elsevier, New York, 1966.

A.1-4 McDougall, A.: Fuel Cells. John Wiley, New York, 1976.

A.1-5 Fontana, M. G., and N. D. Greene: Corrosion Engineering, McGraw-Hill, New York, 1967.

A.1-6 Bockris, J. O'M. and A. K. Reddy: Modern Electrochemistry. Plenum Press, New York, 1970.

A.1-7 Bockris, J. O'M. and S. Srinivasan: Fuel Cells: Their Electrochemistry. McGraw-Hill, New York, 1969.

A.1-8 Sutton, C. W., Ed.: Direct Energy Conversion. McGraw-Hill, New York, 1966.

A.1-9 Soo, S. L.: Direct Energy Conversion. Prentice-Hall, Englewood Cliffs, New Jersey, 1968.

B.1 Potential Fuel Cell Power Generation System Advantages

Electric power plants containing a fuel cell power generation system would have many characteristics which could be attractive to electric utilities. Among the more important characteristics are:

1) high fuel efficiency at both design rating and over the plant's operating range,

2) low environmental emissions,

3) rapid response to load-demand changes,

4) waste heat recovery potential, and

5) little effect of size on efficiency.

The following commentary elaborates on the potential benefits which could occur to an electric utility from these characteristics.

B.1.1 Fuel Cell Efficiency

Because a fuel cell is not a thermal machine, it is not limited by the Carnot cycle. It therefore offers the potential for higher conversion efficiencies and greater fuel conversion than conventional thermal generators are likely to achieve. First-generation fuel cells, (phosphoric acid) would have efficiencies of 38-40 percent, second-generation (molten carbonate and advanced phosphorus acid), 45 percent. In contrast, the efficiency of conventional fossil-fueled generators is in the range of 28-38 percent. As cell technology advances, these efficiencies are bound to increase. Also, since fuel cell efficiency is related to individual cell performance rather than generator size, small power plants will be just as efficient as larger ones (Ref. B.1-1).

Besides being more efficient than conventional generators, fuel cell power plants maintain their efficiency over a wide range of loads. This characteristic is displayed in Fig. B.1.1-1 where part-load heat rate is plotted for seven power plants including two fuel cell power plants. Whereas conventional power generation equipment is more efficient at rated power and markedly less efficient at part power, the fuel cell power plant is nearly constant in efficiency from 25 to 100 percent of its rated power output.

The high part-load efficiency could permit the fuel cell plant to be used in the load-following mode (Ref. B.1-2). By operating the fuel cell power plant in a load-following mode to provide for the variation in power demand a utility need not vary the output from their conventional intermediate or peaking units. This will then permit them to be operated at their most efficient output, 100 percent of rated power.

C-5

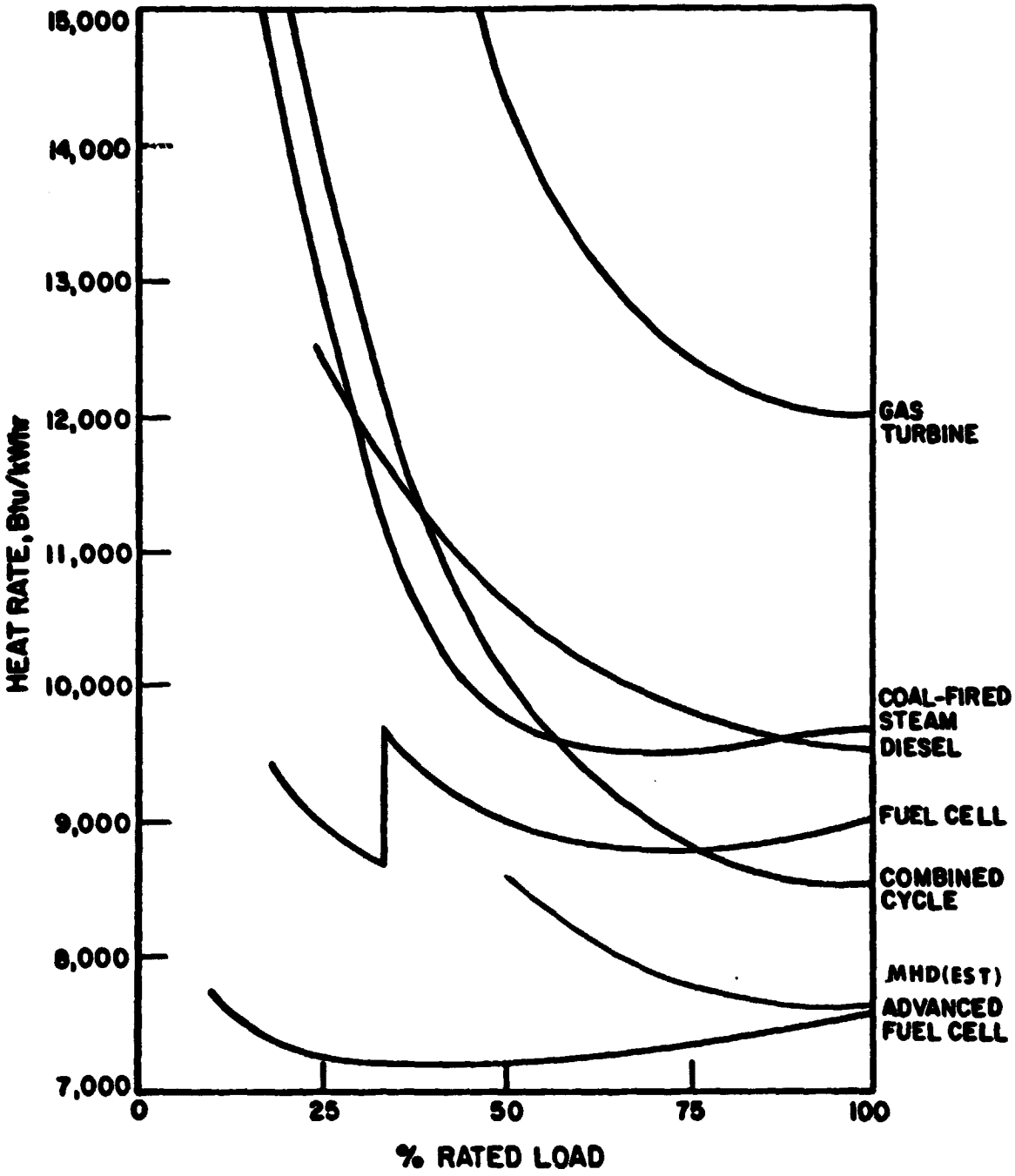

COMPARISON OF POWER SYSTEM EFFICIENCIES

B.1.2 Environmental Emissions

The fuel cell does not operate on a combustion cycle, consequently emission levels other than carbon dioxide, air, and water, such as nitrogen oxides (NO_x), carbon monoxide (CO), and unburned hydrocarbons (UHC), are not high. The emission of sulfur oxides (SO_x) are also not high because the sulfur content of the fuel stream must be reduced to attain long fuel cell life. The NO_x, CO, UHC, and SO_x emissions that do occur originate mainly in the power plant's fuel processor (Ref. B.1-3).

The environmental emissions of fuel cell power plants are expected to be low. Table B.1.2-1 compares Federal Environmental Protection Agency (EPA) requirements with the design goals for the 4.8-MW unit being installed at Con Edison in N.Y. and the measured emissions for a 1-MW test unit using naphtha as fuel. It can be concluded from this table the emission from a fuel cell power plant are expected to be at least an order of magnitude below EPA standards.

In addition, the fuel cell is expected to be quiet. There will be pumps and cooling fans, but the noise level will be appreciably below the level of a fossil steam plant (Ref. B.1-4). Also little or no makeup water or cooling water will be required eliminating the need for cooling ponds.

B.1.3 Response Characteristics

Fuel cells are quick to follow load changes. The load response time for the 4.8-MW demonsttration to be installed in the Con Edison system has a performance specification of minimum power to rated power of 15 seconds and a specification of 35-percent power to rated power of one second (Ref. B.1-3).

If a fuel cell were operated in the load-following mode to take advantage of its quick response, it could be used to reduce mechanical spinning reserve requirements. Mechanical spinning reserve is supplied by a conventional power plant operating in a part-load condition so that it has the capability to match load variations. Operation in this mode is, however, is relatively inefficient due to the poor off-design characteristics of most conventional power plants. Reducing the mechanical spinning reserve by substituting the fuel cell with its rapid response and superior part-load performance characteristics would result in utility production cost savings.

B.1.4 Waste Heat Recovery Potential

Fuel cells because of their elevated operating temperature produce waste heat that can be utilized in the production of hot water or steam. The hot water could be used in a cogeneration application to supply district heat or

TABLE B.1.2-1

FUEL CELL POWER PLANT EMISSIONS
POUNDS PER MILLION BTU ENERGY INPUT
(from Ref. B.1-3)

Emission	EPA Requirement	4.8-MW Design Goal*	1-MW Test Results*
NO_x	0.3	0.02	0.02
SO_x	0.8	0.00003	0.0015
Particulates	-	0.000003	Non-Detectable
Smoke	-	None	None

* At rated power

industrial process heat while the steam could be used in a steam bottoming cycle power plant to produce additional electric power. Utilization of this waste in a cogeneration application could increase overall efficiency to as high as 90 percent (Ref. B.1-1) while the bottoming cycle application of the waste heat could yield overall efficiencies between 50 percent (phosphoric acid) and 75 percent (molten carbonate).

B.1.5 Scaling Effects

The heart of a fuel cell power generation system, the fuel cell stack, consists of a stack of individual fuel cells connected in series to obtain the desired voltage. Since all the individual cells operate essentially identically, the efficiency of the cell stack is comparable to the individual cell. Consequently, for the voltages and the cell stack outputs envisioned for electric utility applications the fuel cell stack efficiency is independent of output.

The lack of a scale effect has numerous advantages. It permits the development of a standard size module in the 5-25 MW range which could be factory-fabricated and mass produced. This would reduce costs and lag time between orders and commissioning to about 24 months (Ref. B.1-1). The standard size modules would allow the utility to tailor their additions to more closely match anticipated load increases. Once installed the presence of many smaller modules would increase system reliability in comparison to one large power plant with the name output. This, in turn, reduces the magnitude of reserve requirement needed to cover for forced outages.

Additional benefits accrue due to the coupling of modularity and low environmental emissions. The tailored power plant can be located near the load center thus reducing transmission losses and costs. The reduced transmission distances will permit easier control of reactive power and voltage. Lastly, easier siting increases the probability of effective waste heat utilization.

B.1.6 References

B.1-1 Fickett, A. P.: Clean Power for the Cities. EPRI Journal, November 1978.

B.1-2 Benjamin, T. G., E. H. Camara, and L. G. Marianowski: Handbook of Fuel Cell Performance. Work Performed Under DOE Contract No. EC-77-C-03-1545, May 1980.

B.1-3 Bell, R. A. and W. A. Messner: Fuel Cells for Electric Utility Use. Proceedings of the 7th Energy Technology Conference, Washington, D.C., March 1980.

B.1-4 Berman, I. M.: Fuel Cells and Coal-Derived Fuels. Power Engineering, October 1980.

C.1 Fuel Cell Historical Overview

The fuel cell concept is an old concept. In 1839, W. Grove, building upon earlier work performed by H. Davy, constructed a chemical battery in which the waterforming reaction of hydrogen and oxygen generated an electric current. Grove used platinum electrodes in contact with dilute sulfuric acid in his device. Fifty years later, L. Mond and C. Langer developed a device they called a fuel cell which had an output of 6 amps/ft^2. The development of the dynamo in the same time period overshadowed this work and the fuel cell remained undeveloped for another fifty years. In the early 1940's Justi started to work with porous metal electrodes. Finally, in 1954, F. Bacon published the results of his high-pressure cell (Ref. C.1-1).

The real impetus for fuel cell development occurred as a result of the NASA-sponsored programs for the Gemini and Apollo spacecraft in the early 1960's. By the mid-1960's some 50 U.S. companies were investigating fuel cells as these companies tried to adapt the fuel cell to non-space applications. By the late 1960's the number of participants had dwindled because most companies were unwilling to make the long-term research and development commitments required to develop the fuel cell for commercial applications (Ref. C.1-2).

One of the companies willing to make the commitment has been United Technologies Corporation (UTC, formerly United Aircraft). Although it may appear somewhat provincial in outlook, it can be stated that this commitment has placed UTC in the forefront of fuel cell activity. It can be further stated that a review of UTC fuel cell activities would essentially cover most of the highlights associated with fuel cell development in the last quarter century.

C.1.1 Early UTC Activity

Energy systems studied at United Technologies in the 1950's indicated that fuel cells would be attractive as a source of on-board power for space vehicles and that they also had potential for many military and commercial applications. A patent license was obtained for the Bacon type of fuel cell which was the most advanced at the time and which was applicable to NASA missions. This patent license took the form of an agreement with National Research and Development Corporation in Britain who was the owner of the Bacon patents and the Patterson-Moos Laboratories (now Leesona Corporation) who held a United States license. Certain obligations of this agreement survive to the present.

C.1.2 NASA Program History

NASA gave early support to the fuel cell program and has continued to fund the application of fuel cells to space craft through the Apollo Program, Space Shuttle Procurements, and many R&D programs.

In March 1962, North American Aviation, prime contractor for the NASA Apollo spacecraft, contracted with Pratt & Whitney Aircraft to develop and produce 1.5 kilowatt fuel cell power plants for lunar missions. After successful development, 61 power plants were manufactured and delivered through 1968. Over 10,000 failure-free hours were experienced in space including all Apollo Lunar, Apollo Sky-Lab, and Apollo-Soyuz missions.

In November 1973, Pratt & Whitney Aircraft was named to develop and produce fuel cell power plants for the NASA Space Shuttle Orbiter under subcontract with Rockwell International Corporation (formerly North American Aviation). The Space Shuttle Orbiter fuel cells have been constructed and have demonstrated the required performance for this contract. Drawing on technology developed since 1962, the Orbiter develops 12 kilowatts of power compared to 1.5 kilowatts for Apollo and has a weight of 201 pounds compared to the Apollo all-up weight of 248 pounds. The Shuttle power plant will have a required lifetime of 2,000 hours (5,000 hours have been demonstrated) compared to the useful life of 450 hours required of the Apollo power plant (Ref. C.1-3).

C.1.3 Other Space and Defense Programs

A contract was received from NASA-Marshall Space Flight Center to deliver a power plant similar to the Shuttle Orbiter fuel cell for Space Tug, an auxiliary spacecraft in the Shuttle Program. NASA-Lewis Research Center has continued to support advanced space fuel cell technology contracts to develop ultra-lighweight fuel cells.

A power plant system including two fuel cell power plants and deep submergence-type fuel tanks was completed and delivered to the Navy for the Deep Submergence Rescue Vehicle. A submersible auxiliary power unit for a classified mission based on this DSRV design was delivered in August 1975. Previous programs with the U.S. Army for portable power supply and with the Air Force for airborne weapons power supplies have lapsed largely because of lack of mission definition in those agencies.

C.1.4 Fuel Cell Program for the Gas Utilities

Columbia Gas became aware of United's interest in fuel cells through the gas turbine pipeline pumping program. They undertook a three year program in 1963 to investigate natural gas fuel cells. Following the test of a 4-kW experimental fuel cell power plant by Columbia Gas Systems in 1966, some thirty gas utilities formed a not-for-profit corporation called TARGET (Team to Advance Gas Energy Transformation) to support fuel cell research at UTC.

During 1971-73, 65 experimental 12.5-kW fuel cell power plants (PC-11 designation), designed and built by UTC in conjunction with TARGET, were

installed and operated by gas and combination utilities in 35 on-site locations to determine the conceptual feasibility of on-site fuel cell electric service. The longest continuous run recorded without major overhaul in these tests was 4,000 hours; 10,560 hours was the longest run on any single power plant with overhaul; and a total of 200,000 hours was logged in the program. This testing, conducted by gas industry personnel at gas industry expense, provided service experience with the real impurities of natural gas and water supplies, furnished actual market acceptance and public relations experience, and demonstrated that gas personnel can be trained to install and operate fuel cell type equipment. Many mechanical problems were experienced early in the program but by the end of the program a failure rate of less than one unscheduled shutdown per thousand hours was experienced, which is comparable to industrial gas turbine experience. This experimental power plant identified a number of system requirements which provided the objectives and direction for the continuing effort.

In 1976, a 40-kW experimental unit (PC-18) reflecting lessons learned from the previous comprehensive field tests, successfully demonstrated electrical generating efficiency of 40-percent and the availability of power plant waste heat at useful temperatures. The combined output of electrical and thermal energy exceeded 80 percent overall natural gas utilization in contrast to about 30-percent utilization for electrical power plants and 60-percent utilization for space and water heating.

An even higher utilization level was achieved in testing involving a simulated 16-unit apartment building located in New England. Winter conditions were simulated and a heat pump was included with the heat recovery system. The results produced indicated that less gas energy would be used to provide the total energy requirements of the building -- electrical and thermal -- than was needed by a conventional gas-fired furnace to provide heat alone.

The successful 18,000 hours of operation of this power plant in United's facility and continuing gas utility and UTC expenditures and advocacy resulted in sponsorship by the Gas Research Institute (GRI, the sucessor to TARGET) and DOE of a 40-kW development program which was initiated in 1977. This program incorporated recent technological improvements in the development of an improved 40-kW design suitable for precommercial field test.

In the near future, field tests of some fifty 40-kW fuel cell systems will be conducted at some 25 sites by a similar number of utilities. In parallel with these tests, it is proposed that the utilities examine proposed business scenarios for commercial service, and the Federal Government and GRI determine what incentives are required, if any, to encourage commercialization. These actions would provide the basis for establishing the detailed plans and actions required for commercialization (Ref. C.1-4).

C.1.5 Fuel Cell Program for the Electric Utilities

In 1971 the Edison Electric Institute (EEI), and a group of electric utilities began evaluating the fuel cell. Significant benefits were identified, and in 1972 the Fuel Cell Generator-1 (FCG-1) program was mounted by United and nine utilities. The goal of the program was the development of a 26-MW, power plant for commercial service by 1980. Operational targets included a capital cost of $350/kW in 1980 dollars (the stated goal was $185/kW in 1972 dollars), a heat rate of 9000-9300 Btu, a 40,000-hour stack life, and the ability to run on naphtha (Ref. C.1-2).

A 1-MW pilot FCG-1 plant was demonstrated successfully in 1976-1977 for more than 1,000 hours generating about 700,000 kWh (Ref. C.1-5). The plant, while not in the packaged, modular form these plants will ultimately take, confirmed that a naphtha-fueled unit could provide electricity to a utility bus, while meeting heat rate, loading-following, emissions, and other operational requirements established by the utilities.

In 1976 ERDA (now DOE) and the Electric Power Research Institute (EPRI) joined the FCG-1 effort, resulting in a program to design, fabricate, and test one 4.5-MW a.c. module of the FCG-1 power plant in 1979-1980. Consolidated Edison Company of New York, was chosen as the host utility, and a downtown site in New York City was selected for the demonstration. The 4.5-MW demonstrator is expected to exhibit the suitability of the fuel cell for utility service. Unlike the 1-MW plant, the 4.5-MW unit will be fully packaged, with virtually all components organized into modules. After fuel cell stack installation in 1981 an acceptance test of 200 hours will commence. This will be followed by a 2000-hour validation test (Ref. C.1-5). Plugged into Consolidated Edison's grid, the demonstrator will be operated by utility personnel. The plant's downtown location is expected to verify the fuel cell's emissions, and noise levels. In addition, general acceptability to its neighbors will be evaluated. Economic advantages in the form of transmission savings, voltage control, load following, and system reliability will be determined. The program will also verify the FCG-1's operational claims, including those on heat rate, power quality, transient response, and startup-shutdown characteristics (Ref. C.1-2).

C.1.6 Summary

A chronological summary of the fuel cell activity mentioned above is provided in Table C.1.6-1.

TABLE C.1.6-1

CHRONOLOGY OF UTC FUEL CELL ACTIVITIES

1959 - Bacon Patent Licence Obtained
- U. S. Army Regenerative Cell Contract

1961 - NASA 250-W Fuel Cell Contract
Columbia Gas 500-W Cell Contract

1962 - Apollo Development Contract

1963 - Columbia Gas Hydrocarbon-Air Cell Contract

1966 - 3.75-kW Natural Gas Powerplant Delivered to Columbia Gas
- First Apollo Fuel Cell Flight

1967 - TARGET Gas Utility Program Initiated

1969 - TARGET 12.5-kW Powerplant Tested
- First Apollo Lunar Mission

1970 - Navy Deep Submergence Contract

1972 - Electric Utility Development Initiated

1974 - Space Shuttle Orbiter Contract

1975 - TARGET 40-kW Powerplant Tested

1976 - ERDA (DOE) and EPRI Contract

1977 - DOE and GRI Contract
- PCG-1 Pilot Power Plant Tested

1981 - DOE/EPRI 4.8-MW Demonstrator Installed
- Possible DOE/GRI 40-kW Field Tests

C.1.7 References

C.1-1 Angrist, S. W.: Direct Energy Conversion. Allyn and Bacon, Inc., Boston, Massachusetts, 1965.

C.1-2 Fickett, A. P.: Clean Power for the Cities. EPRI Journal, November 1978.

C.1-3 Been, J. F.: The Role of Fuel Cells in NASA's Space Power Systems. Proceedings of the 14th IECEC Boston, Massachusetts, August 1979.

C.1-4 Larson, E.: Fuel Cells in the Gas Industry. Proceedings of the 14th IECEC, Boston, Massachusetts, August 1979.

C.1-5 Bell, R. A. and W. A. Messner: Fuel Cells for Electric Utility Use. Proceedings of the 7th Energy Technology Conference, Washington, D.C., March 1980.

A.2 Theory of Combined-Cycle Operations

In the simplified integrated gasification combined-cycle system, the turbine exhaust gas is used directly to raise steam in an unfired boiler. Additional heat from the fuel gas stream is also used to raise steam. The performance of such a system can be estimated from the following equation:

$$\eta_{cc} = \frac{\eta_{gt} + \left[(1-\eta_{gt}) + \frac{W_s}{W_f}\right]\left(\frac{T_{ex}-T_{st}}{T_{ex}-T_a}\right)\eta_s}{1+\frac{W_s}{W_f}} \qquad \text{(A.2-1)}$$

where

η_{cc} = combined cycle efficiency
η_{gt} = gas turbine efficiency
η_s = steam cycle efficiency
T_{ex} = temperature of gas turbine exhaust
T_{st} = temperature of the stack gas
T_a = ambient temperature
W_s = amount of fuel heating value used to raise steam directly
W_f = total fuel heating value

In Equation A.2-1, the ratio W_s/W_f represents the amount of steam raised by heat other than that contained in the gas turbine exhaust. This heat may be the fuel gas sensible heat used to raise steam or, in some configurations, fuel gas may be burned in the turbine exhaust prior to the waste heat boiler to give a higher approach temperature.

For the case where W_s is zero, i.e., the pipeline delivery of fuel gas, the equation A.2-1 simplifies to:

$$\eta_{cc} = \eta_{gt} + \left[(1-\eta_{gt})\left(\frac{T_{ex}-T_{st}}{T_{ex}-T_a}\right)\right]\eta_s \qquad \text{(A.2-2)}$$

These equations point out the importance of gas turbine efficiency and of cycle temperatures on the ability to utilize the gas turbine exhaust heat.

The gas turbine efficiency is a function of pressure ratio, turbine inlet temperature and the mechanical efficiencies of the components. Losses due to internal pressure drops, cooling loads, diffuser losses, etc. must also be accounted for

For the gas turbine used in this study, the efficiency is in the 32 to 34 percent range.

Similarly, the steam turbine cycle efficiency is a function of operating pressure, throttle temperature, cycle configuration (reheat, regeneration and component efficiencies). A fully regenerative single reheat steam cycle operating at modern steam conditions (1800 - 2400 psi, 1000 F/1000 F) would have cycle efficiencies of 40-43 percent. In combined-cycles, however, there is usually no regeneration since gas turbine exhaust heat is used to preheat feed water, deaerate, etc. Steam cycle efficiencies are then of the order of 30-35 percent. The loss of cycle efficiency is more than made up by the reduction in stack temperature of the gas turbine exhaust.

All of the above parameters are very closely interrelated. It is virtually impossible to change one variable without affecting another. For this reason, a very sophisticated computational program must be used to reduce analysis times to reasonable levels. This is especially true when considering the integrated power plant because the operation of the gasifier must be accounted for.